

Insights in cancer immunity and immunotherapy 2022

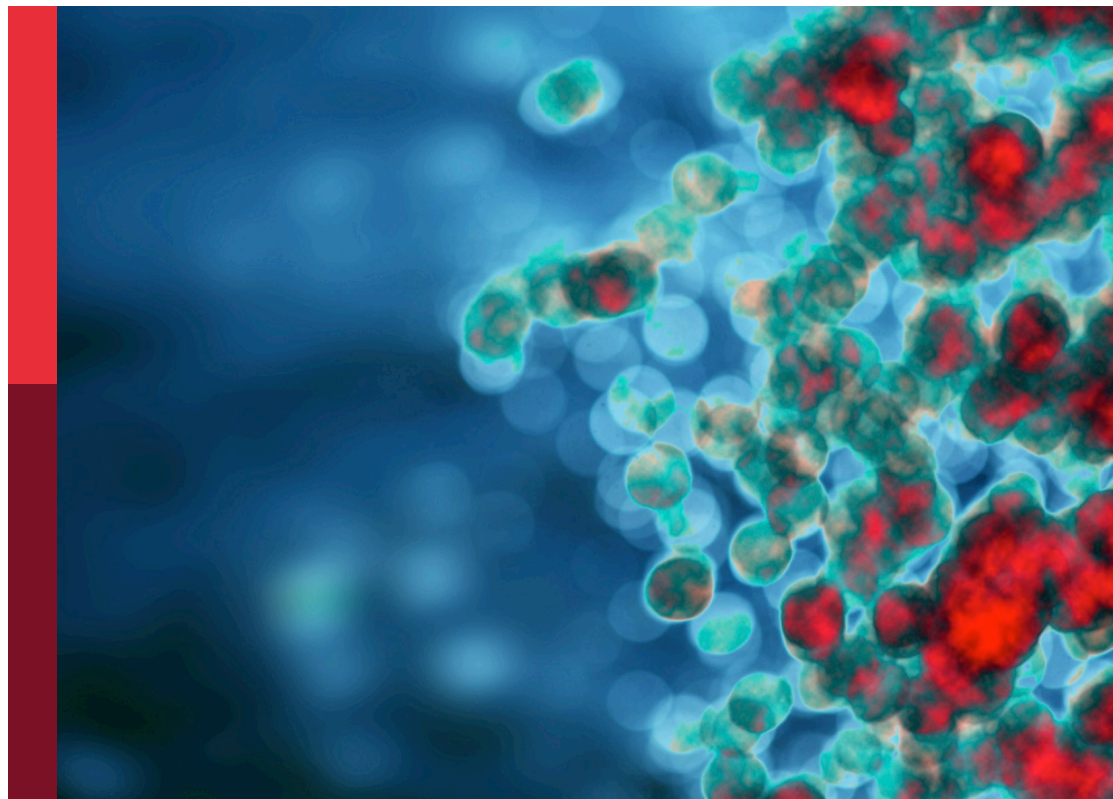
Edited by

Katy Rezvani and Catherine Sautes-Fridman

Published in

Frontiers in Immunology

Frontiers in Oncology



FRONTIERS EBOOK COPYRIGHT STATEMENT

The copyright in the text of individual articles in this ebook is the property of their respective authors or their respective institutions or funders. The copyright in graphics and images within each article may be subject to copyright of other parties. In both cases this is subject to a license granted to Frontiers.

The compilation of articles constituting this ebook is the property of Frontiers.

Each article within this ebook, and the ebook itself, are published under the most recent version of the Creative Commons CC-BY licence. The version current at the date of publication of this ebook is CC-BY 4.0. If the CC-BY licence is updated, the licence granted by Frontiers is automatically updated to the new version.

When exercising any right under the CC-BY licence, Frontiers must be attributed as the original publisher of the article or ebook, as applicable.

Authors have the responsibility of ensuring that any graphics or other materials which are the property of others may be included in the CC-BY licence, but this should be checked before relying on the CC-BY licence to reproduce those materials. Any copyright notices relating to those materials must be complied with.

Copyright and source acknowledgement notices may not be removed and must be displayed in any copy, derivative work or partial copy which includes the elements in question.

All copyright, and all rights therein, are protected by national and international copyright laws. The above represents a summary only. For further information please read Frontiers' Conditions for Website Use and Copyright Statement, and the applicable CC-BY licence.

ISSN 1664-8714
ISBN 978-2-8325-3199-0
DOI 10.3389/978-2-8325-3199-0

About Frontiers

Frontiers is more than just an open access publisher of scholarly articles: it is a pioneering approach to the world of academia, radically improving the way scholarly research is managed. The grand vision of Frontiers is a world where all people have an equal opportunity to seek, share and generate knowledge. Frontiers provides immediate and permanent online open access to all its publications, but this alone is not enough to realize our grand goals.

Frontiers journal series

The Frontiers journal series is a multi-tier and interdisciplinary set of open-access, online journals, promising a paradigm shift from the current review, selection and dissemination processes in academic publishing. All Frontiers journals are driven by researchers for researchers; therefore, they constitute a service to the scholarly community. At the same time, the *Frontiers journal series* operates on a revolutionary invention, the tiered publishing system, initially addressing specific communities of scholars, and gradually climbing up to broader public understanding, thus serving the interests of the lay society, too.

Dedication to quality

Each Frontiers article is a landmark of the highest quality, thanks to genuinely collaborative interactions between authors and review editors, who include some of the world's best academicians. Research must be certified by peers before entering a stream of knowledge that may eventually reach the public - and shape society; therefore, Frontiers only applies the most rigorous and unbiased reviews. Frontiers revolutionizes research publishing by freely delivering the most outstanding research, evaluated with no bias from both the academic and social point of view. By applying the most advanced information technologies, Frontiers is catapulting scholarly publishing into a new generation.

What are Frontiers Research Topics?

Frontiers Research Topics are very popular trademarks of the *Frontiers journals series*: they are collections of at least ten articles, all centered on a particular subject. With their unique mix of varied contributions from Original Research to Review Articles, Frontiers Research Topics unify the most influential researchers, the latest key findings and historical advances in a hot research area.

Find out more on how to host your own Frontiers Research Topic or contribute to one as an author by contacting the Frontiers editorial office: frontiersin.org/about/contact

Insights in cancer immunity and immunotherapy: 2022

Topic editors

Katy Rezvani — University of Texas MD Anderson Cancer Center, United States

Catherine Sautes-Fridman — INSERM U1138 Centre de Recherche des Cordeliers (CRC), France

Citation

Rezvani, K., Sautes-Fridman, C., eds. (2023). *Insights in cancer immunity and immunotherapy: 2022*. Lausanne: Frontiers Media SA.

doi: 10.3389/978-2-8325-3199-0

Table of contents

- 05 **The role of B cells in cancer development**
Rongying Tan, Manhua Nie and Wang Long
- 12 **Ligand-based CAR-T cell: Different strategies to drive T cells in future new treatments**
Alejandro Ramírez-Chacón, Sergi Betriu-Méndez, Ariadna Bartoló-Ibars, Azucena González, Mercè Martí and Manel Juan
- 29 **Corrigendum: Ligand-based CAR T-cell: Different strategies to drive T-cells in future new treatments**
Alejandro Ramírez-Chacón, Sergi Betriu-Méndez, Ariadna Bartoló-Ibars, Azucena González, Mercè Martí and Manel Juan
- 31 **Urinary incontinence as a possible signal of neuromuscular toxicity during immune checkpoint inhibitor treatment: Case report and retrospective pharmacovigilance study**
Yizhang Hu, Wenchao Lu, Borui Tang, Zhixia Zhao and Zhuoling An
- 41 **Engineered cord blood megakaryocytes evade killing by allogeneic T-cells for refractory thrombocytopenia**
Bijender Kumar, Vahid Afshar-Kharghan, Mayela Mendt, Robert Sackstein, Mark R. Tanner, Uday Popat, Jeremy Ramdial, May Daher, Juan Jimenez, Rafet Basar, Luciana Melo Garcia, Mayra Shanley, Mecit Kaplan, Xinhai Wan, Vandana Nandivada, Francia Reyes Silva, Vernikka Woods, April Gilbert, Ricardo Gonzalez-Delgado, Sunil Acharya, Paul Lin, Hind Rafei, Pinaki Prosad Banerjee and Elizabeth J. Shpall
- 55 **Clinical cancer immunotherapy: Current progress and prospects**
Chenglong Liu, Mengxuan Yang, Daizhou Zhang, Ming Chen and Di Zhu
- 77 **SILAC-based quantitative proteomics and microscopy analysis of cancer cells treated with the *N*-glycolyl GM3-specific anti-tumor antibody 14F7**
Paula A. Bousquet, Dipankar Manna, Joe A. Sandvik, Magnus Ø. Arntzen, Ernesto Moreno, Kirsten Sandvig and Ute Krengel
- 91 **Multiple CAR-T cell therapy for acute B-cell lymphoblastic leukemia after hematopoietic stem cell transplantation: A case report**
Lei Deng, Yu Xiaolin, Qian Wu, Xiaochen Song, Wenjun Li, Yixi Hou, Yue Liu, Jing Wang, Jun Tian, Xiaona Zuo and Fang Zhou
- 101 **Case report: Complex paraneoplastic syndromes in thymoma with nephrotic syndrome, cutaneous amyloidosis, myasthenia gravis, and Morvan's syndrome**
Huiqin Liu, Zeqin Dong, Milan Zhang, Rui Pang, Jiajia Xu, Pan He, Wenli Mei, Shuai Zhang, Guanqiao You and Wei Li

- 109 **The frequency of differentiated CD3⁺CD27⁺CD28⁺ T cells predicts response to CART cell therapy in diffuse large B-cell lymphoma**
Nina Worel, Katharina Grabmeier-Pfistershammer, Bernhard Kratzer, Martina Schlager, Andreas Tanzmann, Arno Rottal, Ulrike Körmöcz, Edit Porpaczy, Philipp B. Staber, Cathrin Skrabs, Harald Herkner, Venugopal Gudipati, Johannes B. Huppa, Benjamin Salzer, Manfred Lehner, Nora Saxenhuber, Eleonora Friedberg, Philipp Wohlfarth, Georg Hopfinger, Werner Rabitsch, Ingrid Simonitsch-Klupp, Ulrich Jäger and Winfried F. Pickl
- 126 **The role of histone methylase and demethylase in antitumor immunity: A new direction for immunotherapy**
Yuanling Zhang, Junhao Chen, Hang Liu, Rui Mi, Rui Huang, Xian Li, Fei Fan, Xueqing Xie and Jie Ding
- 142 **Perspectives of ERCC1 in early-stage and advanced cervical cancer: From experiments to clinical applications**
Pei Du, Guangqing Li, Lu Wu and Minger Huang
- 154 **Multi-omics analysis of N6-methyladenosine reader IGF2BP3 as a promising biomarker in pan-cancer**
Pin Chen, Jing Xu, Zihan Cui, Silin Wu, Tao Xie and Xiaobiao Zhang
- 177 **Understanding the squamous cell carcinoma immune microenvironment**
Vahide Saeidi, Nicole Doudican and John A. Carucci
- 188 **A systematic review and meta-analysis evaluating the impact of antibiotic use on the clinical outcomes of cancer patients treated with immune checkpoint inhibitors**
Athéna Crespin, Clément Le Bescop, Jean de Gunzburg, Fabien Vitry, Gérard Zalcman, Julie Cervesi and Pierre-Alain Bandinelli
- 209 **Sequential therapy with supercharged NK cells with either chemotherapy drug cisplatin or anti-PD-1 antibody decreases the tumor size and significantly enhances the NK function in Hu-BLT mice**
Kawaljit Kaur, Po-Chun Chen, Meng-Wei Ko, Ao Mei, Emanuela Senjor, Subramaniam Malarkannan, Janko Kos and Anahid Jewett



OPEN ACCESS

EDITED BY

Catherine Sautes-Fridman,
INSERM U1138 Centre de Recherche
des Cordeliers (CRC), France

REVIEWED BY

Dharmendra Kumar Yadav,
Gachon University, Korea
Sotirios Sotiriou,
University of Thessaly, Greece

*CORRESPONDENCE

Wang Long
longimm1991@outlook.com
Manhua Nie
niemanhua77@csu.edu.cn

[†]These authors share last authorship

[‡]Lead author

SPECIALTY SECTION

This article was submitted to
Cancer Immunity
and Immunotherapy,
a section of the journal
Frontiers in Oncology

RECEIVED 01 June 2022

ACCEPTED 18 July 2022

PUBLISHED 11 August 2022

CITATION

Tan R, Nie M and Long W (2022) The
role of B cells in cancer development.
Front. Oncol. 12:958756.
doi: 10.3389/fonc.2022.958756

COPYRIGHT

© 2022 Tan, Nie and Long. This is an
open-access article distributed under
the terms of the [Creative Commons
Attribution License \(CC BY\)](https://creativecommons.org/licenses/by/4.0/). The use,
distribution or reproduction in other
forums is permitted, provided the
original author(s) and the copyright
owner(s) are credited and that the
original publication in this journal is
cited, in accordance with accepted
academic practice. No use,
distribution or reproduction is
permitted which does not comply with
these terms.

The role of B cells in cancer development

Rongying Tan^{1,2}, Manhua Nie^{1,2*†} and Wang Long^{3*†‡}

¹Clinical Nursing Teaching and Research Section, The Second Xiangya Hospital, Central South University, Changsha, China, ²Department of Kidney Transplantation, The Second Xiangya Hospital of Central South University, Changsha, China, ³Department of Pathology, Nihon University, Tokyo, Japan

B cells play a critical role in adaptive immune responses mainly due to antigen presentation and antibody production. Studies about the tumor-infiltrating immune cells so far demonstrated that the function of B cells in tumor immunity is quite different among various tumor types. The antigen presentation of B cells is mainly anti-tumoral, while the role of antibody production is controversial. Moreover, the immunosuppressive regulatory B cells are detrimental to anti-tumor immunity *via* the secretion of various anti-inflammatory cytokines. This review briefly summarizes the different roles of B cells classified by the primary function of B cells, antigen presentation, antibody production, and immunity regulation. Further, it discusses the potential therapeutic target of B cells in tumor immunity.

KEYWORDS

B cell, tumor, tumor immunity, cancer, immunotherapy, tumor microenvironment

Introduction

Cancer is still a threat to humanity due to its high death rate (1). Various therapies have been developed to treat cancer, including surgery, radiotherapy, chemotherapy, immunotherapy, etc. Among these therapies, immunotherapy has become more and more attractive for researchers, companies, and clinicians in recent years (2). T cell-based immunotherapy is critical and effective in cancer therapy, and the promising outcome of the antibodies targeting immune checkpoints in the treatment of cancer created a grave impact on immunotherapy (2, 3). Though the CD8⁺ T cells have an irreplaceable role in the cytotoxicity in the tumor microenvironment (TME) (4) and immune checkpoint inhibitors (ICIs) are quite efficient in many cancer types, most patients are still resistant to ICIs (5). Increasing studies demonstrated the function of other immune cells in the development of cancer in recent years (6, 7), which might be additional and optimal targets for the treatment of cancer.

B cells are involved in adaptive immunity as the antigen-presenting cells (APCs) and antibody-secreting cells (ASCs), while the function of B cells in cancer immunity is controversial. B cell depletion in mice by anti-IgM treatment from birth showed

resistance to syngeneic fibrosarcoma and reduced incidence of pulmonary metastasis (8). In contrast, the lung adenocarcinoma cell inoculation in μ MT mice failed to show any difference to WT mice (9), yet the μ MT mice had faster tumor growth than WT mice when the tumor cell line was transfected with B cell-specific neoantigen (9). The function of B cells in tumor growth seems to vary among different tumor cell lines. Moreover, antibody production from B cells is not always beneficial. For example, antibody-dependent cellular cytotoxicity (ADCC) is a critical mechanism of the antibody in the anti-tumor effect of B cells (10), while the immune complexes in circulation or TME are correlated with poor clinical outcomes (11).

In this review, we will briefly discuss the immunological mechanism of B cells in cancer immunity to elucidate the controversial phenomenon in various tumor types and potential therapeutic targets of B cells in different tumor types. This review is classified by the basic functions of B cells, but not anti- and pro- tumoral functions of B cells, which is already discussed in other reviews (12).

Antigen-presenting cells

B cells are efficient APCs in T cell-dependent (TD) antigen-induced humoral immunity. TD antigens are recognized and engulfed by B cells through B cell receptor (BCR), degraded in lysosome, and presented to $CD4^+$ cells, resulting in $CD4^+$ T cells and further $CD8^+$ cells activation (13). Several studies demonstrated the antigen presentation of B cells plays a critical role in tumor-specific $CD4^+$ and $CD8^+$ T cell activation. B cells undoubtedly present antigen to induce T cell activation in virus-induced tumor growth (14). In the syngeneic B16 melanoma cell line transfer system, B cell depletion by anti-CD20 antibody treatment resulted in a two-fold bigger tumor volume and impaired interferon- γ (IFN- γ) and tumor necrosis factor (TNF- α) production from $CD4^+$ T cells and $CD8^+$ T cells (15).

A recent study elucidated how antigen presentation of B cells plays a role in tumor immunity. T follicular helper (TFH) cells are involved in B cell maturation and activation. Germinal center (GC) B cells could be activated by TFH-B interaction and further differentiate into short-term living plasma cells, long-term living plasmablasts, and memory B cells. The single-cell RNA sequencing result of tumor-infiltrating lymphocytes in many studies revealed the presence of GC B cells in the TME (9, 16), yet the role of GC B cells is not well known. The study done by Cui et al. in lung adenocarcinoma patients elucidated that GC B cells facilitate the function of $CD8^+$ T cells in anti-tumor immunity *via* the TFH-GC B cell interaction in a neoantigen-dependent manner (9). They utilized a lung adenocarcinoma cell line (KP) with limited somatic mutations, which means that there are few or no neoantigen

expression and weak B/T cell responses so that B cell or T cell depletion doesn't affect the tumor growth. With the transfection of HELLO fusion protein, which contains HEL, GP33, and GP66 that can be recognized by MD4 transgenic BCR, GP33-specific $CD4$ TCR, and GP66-specific $CD8$ TCR, respectively, KP-HELLO cells are able to activate specific B/T cells. The inoculation of KP-HELLO cells in B cell knockout or TFH knockout mice showed much faster tumor growth and weaker $CD8^+$ T cell function compared to tumor growth inoculated in WT mice, suggesting that the GC B cells that recognize the neoantigen and further interact with activated $CD4^+$ T cells are able to support $CD8^+$ T cells function in TME. Further results demonstrated that interaction between neoantigen-specific TFH and GC B cells and interleukin-21 (IL-21) secreted by TFH cells are necessary for the cytotoxicity of $CD8^+$ T cells (9).

Antibody-secreting cells

B cells play an essential role in the adaptive immune responses by producing antibodies (17). At the same time, the role of antibody-secreting B cells is a double-edged sword in tumor immunity. Once the B cells are activated by recognizing the neoantigen, B cells participate in a two-pathway differentiation process that induces both short-lived plasmablasts and long-lived plasma cells and memory B cells (17). Therefore, these plasmablasts, plasma cells, memory B cells, and the secreted antibodies are neoantigen-specific. Both BCR signaling that provides binding to the antigen, and the B-T cell interaction are essential in the TD antigen-involved long-term antibody production (17).

Commonly, the antibodies are thought to be anti-tumoral. Antibodies with high $Fc\gamma R$ affinity and target neoantigens expressed on tumor cell surface induce ADCC, antibody-dependent cellular phagocytosis (ADCP), and complement-dependent cytotoxicity (CDC), which are significant mechanisms of antibody drugs for cancer therapy. For example, the Fc domain of the monoclonal antibody (mAb) has a different affinity to different $Fc\gamma R$ expressed on various immune cells (18), among which natural killer (NK) cell is involved in ADCC and is discussed in many mAb treatments in cancer (10, 19). Several mAbs have been used in the clinic based on their cytotoxicities, such as anti-GD2 mAb for melanoma and neuroblastoma treatment (20–23) and chimeric anti-CD20 mAb and anti-CD22 mAb for leukemia treatment (24–27).

Unfortunately, not all of the antibodies contribute to anti-tumoral immunity. Antibodies bind to various antigens released by tumor cells and form circulating immune complexes (CICs), which correlate with poor outcomes (11). In the squamous cell carcinoma mouse model, CICs accumulate in the dermal stroma of neoplastic tissue, activate $Fc\gamma R$ on residents, and recruit pro-

tumoral and angiogenic myeloid cells (especially mast cells and macrophages) to facilitate tumor cell survival and angiogenesis (28).

Except for IgG, IgA is also a double-edged sword for tumor growth. Many studies have found the accumulation of IgA-producing B cells in TME (29, 30), yet the role of IgA in tumor growth is still controversial. In ovarian cancer patients, tumor-infiltrating B cell-derived IgA dampens tumor growth through the unspecific transcytosis and neoantigen-specific phagocytosis (29). Yet the function of IgA in other cancers is entirely different. Several cancer types have shown that the proportion of IgA-producing cells is highly associated with poor outcomes (31–33). IgA is pro-tumoral in these cases and has the following mechanisms. Firstly, the IgA production is not induced by neoantigen presentation but by the immunosuppressive microenvironment, and the IgA cannot mediate ADCC (34, 35). Secondly, IgA is immunosuppressive in mucosal immunity (36). IgA deficiency leads to a higher risk of inflammation (37–39), and the interaction between IgA and marginal zone B and B1 cell-specific protein (MZB1) may be an important factor (36). What's more, IgA induces anti-inflammatory cytokine interleukin-10 (IL-10) production from monocytes and further inhibits the immune system (40).

Regulatory B cells

The discovery of a population of the suppressive function of B cells can be retrospect to 1974 since B cells could delay hypersensitivity (41, 42). Subsequently, more and more papers found that some B cells inhibit the development of various diseases such as experimental autoimmune encephalomyelitis (EAE) (43), allograft rejection (44, 45), lupus nephritis (LN) (46), type 1 diabetes (T1D) (47, 48), anti-neutrophil cytoplasmic antibody (ANCA)-associated vasculitis (AAV) (49) and so on. These B cells regulate immune responses by secreting anti-inflammatory cytokines such as IL-10 (50–54), IL-35 (55–57), and transforming growth factor- β (TGF- β) (58, 59) to dampen CD4⁺ T cells (60), CD8⁺ T cells (53), antibody production (61) and facilitate regulatory T (Treg) cells (62, 63). These B cells are so-called Breg cells. Breg cells are not restricted to a specific B cell phenotype. Therefore, IL-10-producing B cells, for example, are usually utilized to detect Breg cells. Since Breg cells vary in various phenotypes, those types of B cells all have an inhibitory function in immune responses. The phenotype of Breg cells mainly includes transitional B cells (CD19⁺CD24^{hi}CD38^{hi}) (64) and plasmablasts (CD19⁺CD27^{int}CD38⁺) (65) in human, follicular B cells (CD19⁺CD23⁺CD21^{int}), marginal zone B cells (CD19⁺CD23⁺CD21^{hi}), plasma/plasmablasts (CD19⁺/B220^{lo/-}CD138⁺), transitional B cells and B10 cells (CD19⁺/B220^{lo/-}CD1d⁺CD5⁺) in mice (50).

Breg cells can not only impair immune responses in TME by secreting antibodies as described above but many anti-inflammatory cytokines production and pathways also contribute to immunosuppression in TME. IL-10 is the most important anti-inflammatory cytokine defining the Breg cells, several pathways are involved in IL-10 production (66, 67). For example, IL-10 production is increased from B cells when stimulated with LPS or CpG (68–70), and MyD88, the downstream of TLR, is necessary for IL-10 production from B cells under LPS stimulation (71), suggesting that TLR activation is able to induce Breg cells differentiation. CD40 and BCR signaling are also related to IL-10 production, as anti-CD40 antibody treatment *in vivo* and *in vitro* expands the IL-10⁺ B cells, and antigen-stimulated B cells transfer in the EAE mouse model rescued IL-10 production in a CD40-dependent manner (72, 73). B cell-derived IL-10 is a strong immunosuppressive cytokine in various autoimmune diseases, it is also important in tumor growth. B cell-deficient mice showed slower tumor growth than WT mice when the mice bearing MC38 carcinoma and EL4 thymoma, and this effect is related to the B cell-derived IL-10 (74, 75). IFN- γ production reduced from B cell-knock out splenic cells when cocultured with WT B cells, and IL-10 production from B cells increased after coculturing with irradiated melanoma cells, not sarcoma cells, indicating that Breg cells suppress the anti-tumor immunity to certain tumors (75). IL-10 production from B cells impairs inflammatory cytokines, including TNF- α and IFN- γ , secretion from cytotoxic T cells to promote tumor growth. While in the chemical carcinogenesis of skin, TNF- α is a promoter for tumor growth, IL-10 produced by B cells facilitates tumor growth in a TNF- α -dependent manner (76). Moreover, IL-10-producing B cells are also being found to promote tumor growth in non-Hodgkin B cell lymphoma (77).

TGF- β is another critical anti-inflammatory cytokine secreted by Breg cells. In the breast tumor model, TGF- β is highly expressed on tumor-infiltrating B cells and associated with the conversion of resting CD4⁺ T cells to Treg cells (78, 79). Furthermore, IL-35 produced by Breg cells also plays a promotion role in pancreatic tumor growth (80, 81). Altogether, Breg cells suppress anti-tumor immunity *via* the secretion of anti-inflammatory cytokines such as IL-10, TGF- β and IL-35.

Anti- and pro-tumorigenic factors secreted by B cells

Except for the antibodies and cytokines described above, B cells also secrete some other factors that affect tumor growth. Lymphotoxin α 1 β 2 (LT α 1 β 2) plays a critical role in the

lymphoid organ development and especially in ectopic tertiary lymphoid organs (82–84). Indeed, the presence of B cells in tertiary lymphoid organs is associated with better anti-tumor immunity in lung cancer (85). Though the remodeling of lymphoid organs contributes to the anti-tumor immunity, some studies found that lymphotoxin derived from B cells supports tumor growth. Androgen promotes prostate cancer (CaP) growth by binding to the androgen receptor expressed on both normal and cancerous prostate cancer cells. Androgen ablation by castration induces cell death of cancer cells and lymphocyte infiltration in TME, and it is effective for androgen-dependent CaP patients, while many patients are castration-resistant (CR). B cells are abundant in TME of CaP, and the B cell-derived lymphotoxin in TME activates $\text{IKK}\alpha$, which is involved in nuclear factor κB (NF- κB) signaling and promotes metastasis, and STAT3, leading to CR-CaP and prostate tumor growth (86, 87).

In addition, a recent study found that γ -Aminobutyric acid (GABA) derived from B cells promotes tumor growth by facilitating $\text{IL}10^+$ macrophages in TME (88). In the study of MC38 colon cancer cell line inoculation *in vivo*, which is reported that B cells suppress anti-tumor T cell responses in this cell line (89, 90), and B cells secreted GABA promotes tumor growth by facilitating IL-10 production from macrophages. Though GABA production is not restricted to B cells, GABA production from B cells is much more than other immune cells in draining lymph nodes. In addition, B cell-specific GABA depletion restored anti-tumor immunity (88).

Therefore, the metabolism network of tumor-infiltrating immune cells could be a valuable target for therapy.

Discussion

The function of B cells in cancer development is controversial. Different B cell phenotypes play a different role in various cancer (Figure 1). When the tumor cells express neoantigens containing BCR epitope, B cells can present these neoantigens and interact with neoantigen-activated TFH cells to facilitate the cytotoxicity of $\text{CD}8^+$ T cells. Activated B cells further differentiate into ASCs. The IgG antibodies secreted by ASCs induce ADCC, ADCP, and CDC to promote anti-tumor immunity. Immunosuppressive IgA production in TME supports tumor growth. In addition, CIC accumulation is associated with poor outcomes. $\text{IL}10^+$ IgA-producing B cells could be categorized as a part of Breg cells, which suppress the anti-tumor immunity, other Breg cells such as $\text{TGF-}\beta$ -producing B cells or IL-21-producing B cells also limit anti-tumor immunity. Moreover, B cells-derived lymphotoxin supports lymphoid organ development but promotes tumor growth and relapse by inducing angiogenesis. And GABA produced by B cells in TME impairs tumor growth by supporting $\text{IL}10^+$ macrophages.

Though there are many controversial functions of B cells in tumor immunity, the role of B cells in different tumor types is

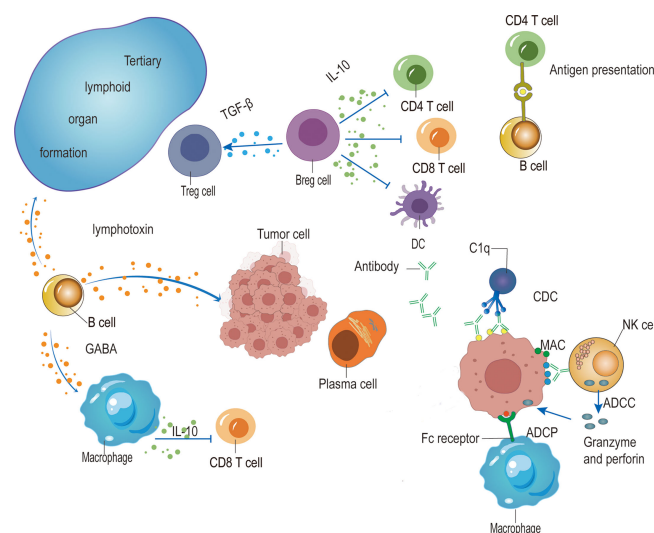


FIGURE 1

The role of B cells in tumor immunity. The antibodies produced by plasma cells induce ADCC mediated by NK cells, ADCP by macrophages, and CDC mediated by C1q, which target and kill tumor cells. IgA-expressing Breg cells dampen anti-tumor immunity by secreting anti-inflammatory cytokines such as IL-10 and $\text{TGF-}\beta$ to suppress $\text{CD}4^+$ T cells, $\text{CD}8^+$ T cells and dendritic cells (DCs), and facilitate Treg cells. B cells also promote anti-tumor immunity by presenting antigen to $\text{CD}4^+$ T cells and further interacting with activated T cells to induce TFH cells, thus promoting the function of $\text{CD}8^+$ T cells. In addition, the production of lymphotoxin from B cells enhances anti-tumor immunity by facilitating tertiary lymphoid organ formation while promoting tumor growth by the induction of angiogenesis. Moreover, B cells produce GABA to impair anti-tumor immunity by facilitating IL-10-producing macrophages.

different. Therefore, it is still possible to look for an adequate B cell-based therapy in some specific tumors. For example, IgA⁺ Breg cells express PDL1, secrete IL-10 in TME and suppress local immune responses in several cancer types, such as human prostate and liver cancer (91, 92). PD-L1/PD-1 blockade can restore the anti-tumor immunity by reactivating CD8⁺ T cells since Breg cells suppress CD8⁺ T cells by producing anti-inflammatory cytokine IL-10. Simply depleting B cells couldn't well demonstrate the function of B cells in a specific tumor cell type, thus, further studies may be needed to elucidate which phenotype of B cells or which mechanism is predominant. Yet, if the depletion of B cells largely impairs tumor growth, it can still be considered a potential treatment. Breg cells play a critical role in suppressing tumor immunity in some cases. Therefore, for these tumor cells, it is valuable to deplete Breg cells. However, since there is no good marker for Breg cells, it is challenging to deplete Breg cells specifically. In the case that B cell deficiency promotes tumor growth, antibody production, and antigen presentation might be essential. Therefore, B cell activation seems feasible in those BCR epitope-containing neoantigen expressing tumor cells. Though STAT3 activation and CD5⁺ B cell proportion are correlated with poor outcomes in B16 skin tumor cell lines (93, 94), adoptive transfer of activated B cells in tumor cell inoculated mice leads to slower tumor growth (95).

In summary, increasing studies found that B cell-targeted therapy could be a prospective candidate in immunotherapy. However, based on the mouse experiment, B cell-targeted therapy may not be as efficient as T cell-based therapy. Therefore, the combination of B cell and T cell-targeted therapy could be promising in cancer therapy.

References

1. Siegel RL, Miller KD, Fuchs HE, Jemal A. Cancer statistics, 2021. *CA Cancer J Clin* (2021) 71(1):7–33. doi: 10.3322/caac.21654
2. Kottschade LA. The future of immunotherapy in the treatment of cancer. *Semin Oncol Nurs* (2019) 35(5):150934. doi: 10.1016/j.soncn.2019.08.013
3. Choi Y, Shi Y, Haymaker CL, Naing A, Ciliberto G, Hajjar J. T-Cell agonists in cancer immunotherapy. *J Immunother Cancer* (2020) 8(2):e000966. doi: 10.1136/jitc-2020-000966
4. Farhood B, Najafi M, Mortezaee K. CD8(+) cytotoxic t lymphocytes in cancer immunotherapy: a review. *J Cell Physiol* (2019) 234(6):8509–21. doi: 10.1002/jcp.27782
5. Hirsch I, Zitvogel L, Eggermont A, Marabelle A. PD-loma: a cancer entity with a shared sensitivity to the PD-1/PD-L1 pathway blockade. *Br J Cancer* (2019) 120(1):3–5. doi: 10.1038/s41416-018-0294-4
6. Long W, Chen J, Gao C, Lin Z, Xie X, Dai H. Brief review on the roles of neutrophils in cancer development. *J Leukoc Biol* (2021) 109(2):407–13. doi: 10.1002/JLB.4MR0820-011R
7. Cendrowicz E, Sas Z, Bremer E, Rygiel TP. The role of macrophages in cancer development and therapy. *Cancers (Basel)* (2021) 13(8):1946. doi: 10.3390/cancers13081946
8. Brodt P, Gordon J. Anti-tumor immunity in b lymphocyte-deprived mice. i. immunity to a chemically induced tumor. *J Immunol* (1978) 121(1):359–62.
9. Cui C, Wang J, Fagerberg E, Chen PM, Connolly KA, Damo M, et al. Neoantigen-driven b cell and CD4 T follicular helper cell collaboration promotes

Author contributions

RT and WL drafted the manuscript. RT generated the figure. MN and WL revised the manuscript. WL designed the outline of the manuscript and revised the manuscript. All authors contributed to the article and approved the submitted version.

Funding

This work is supported by Education Reform Research of Central South University (2022jy147).

Conflict of interest

The authors declare that the research was conducted in the absence of any commercial or financial relationships that could be construed as a potential conflict of interest.

Publisher's note

All claims expressed in this article are solely those of the authors and do not necessarily represent those of their affiliated organizations, or those of the publisher, the editors and the reviewers. Any product that may be evaluated in this article, or claim that may be made by its manufacturer, is not guaranteed or endorsed by the publisher.

anti-tumor CD8 T cell responses. *Cell* (2021) 184(25):6101–18 e13. doi: 10.1016/j.cell.2021.11.007

10. Wang W, Erbe AK, Hank JA, Morris ZS, Sondel PM. NK cell-mediated antibody-dependent cellular cytotoxicity in cancer immunotherapy. *Front Immunol* (2015) 6:368. doi: 10.3389/fimmu.2015.00368

11. Gunderson AJ, Coussens LM. B cells and their mediators as targets for therapy in solid tumors. *Exp Cell Res* (2013) 319(11):1644–9. doi: 10.1016/j.yexcr.2013.03.005

12. Yuen GJ, Demissie E, Pillai S. B lymphocytes and cancer: a love-hate relationship. *Trends Cancer* (2016) 2(12):747–57. doi: 10.1016/j.trecan.2016.10.010

13. Chen XJ, Jensen PE. The role of b lymphocytes as antigen-presenting cells. *Archivum Immunol Et Therapiae Experimentalis* (2008) 56(2):77–83. doi: 10.1007/s00005-008-0014-5

14. Schultz KR, Klarinet JP, Gieni RS, HayGlass KT, Greenberg PD. The role of b cells for *in vivo* T cell responses to a friend virus-induced leukemia. *Science* (1990) 249(4971):921–3. doi: 10.1126/science.2118273

15. DiLillo DJ, Yanaba K, Tedder TF. B cells are required for optimal CD4(+) and CD8(+) T cell tumor immunity: Therapeutic b cell depletion enhances B16 melanoma growth in mice. *J Immunol* (2010) 184(7):4006–16. doi: 10.4049/jimmunol.0903009

16. Hu Q, Hong Y, Qi P, Lu G, Mai X, Xu S, et al. Atlas of breast cancer infiltrated b-lymphocytes revealed by paired single-cell RNA-sequencing and antigen receptor profiling. *Nat Commun* (2021) 12(1):2186. doi: 10.1038/s41467-021-22300-2

17. LeBien TW, Tedder TF. B lymphocytes: how they develop and function. *Blood* (2008) 112(5):1570–80. doi: 10.1182/blood-2008-02-078071
18. Bruhns P. Properties of mouse and human IgG receptors and their contribution to disease models. *Blood* (2012) 119(24):5640–9. doi: 10.1182/blood-2012-01-380121
19. Alderson KL, Sondel PM. Clinical cancer therapy by NK cells via antibody-dependent cell-mediated cytotoxicity. *J BioMed Biotechnol* (2011) 2011:379123. doi: 10.1155/2011/379123
20. Mujoo K, Kipps TJ, Yang HM, Cheresh DA, Wargalla U, Sander DJ, et al. Functional-properties and effect on growth suppression of human neuro-blastoma tumors by isotype switch variants of monoclonal antiganglioside gd2 antibody 14.18. *Cancer Res* (1989) 49(11):2857–61.
21. Handgretinger R, Baader P, Dopfer R, Klingebiel T, Reuland P, Treuner J, et al. A phase-I study of neuroblastoma with the antiganglioside gd2 antibody 14.g2a. *Cancer Immunol Immunother* (1992) 35(3):199–204. doi: 10.1007/BF01756188
22. Frost JD, Hank JA, Reaman GH, Friedrich S, Seeger RC, Gan J, et al. A phase I/IB trial of murine monoclonal anti-GD2 antibody 14.G2a plus interleukin-2 in children with refractory neuroblastoma: a report of the children's cancer group. *Cancer* (1997) 80(2):317–33. doi: 10.1002/(sici)1097-0142(19970715)80:2<317::aid-cnrc21>3.0.co;2-w
23. Handgretinger R, Anderson K, Lang P, Dopfer R, Klingebiel T, Schrappe M, et al. A phase I study of human/mouse chimeric antiganglioside GD2 antibody ch14.18 in patients with neuroblastoma. *Eur J Cancer* (1995) 31A(2):261–7. doi: 10.1016/0959-8049(94)00413-y
24. Cartron G, Dacheux L, Salles G, Solal-Celigny P, Bardos P, Colombat P, et al. Therapeutic activity of humanized anti-CD20 monoclonal antibody and polymorphism in IgG fc receptor FcγRIIIa gene. *Blood* (2002) 99(3):754–8. doi: 10.1182/blood.V99.3.754
25. Romee R, Foley B, Lenvik T, Wang Y, Zhang B, Ankarlo D, et al. NK cell CD16 surface expression and function is regulated by a disintegrin and metalloprotease-17 (ADAM17). *Blood* (2013) 121(18):3599–608. doi: 10.1182/blood-2012-04-425397
26. Goede V, Fischer K, Busch R, Engelke A, Eichhorst B, Wendtner CM, et al. Obinituzumab plus chlorambucil in patients with cll and coexisting conditions. *New Engl J Med* (2014) 370(12):1101–10. doi: 10.1056/NEJMoa1313984
27. Haso W, Lee DW, Shah NN, Stetler-Stevenson M, Yuan CM, Pastan IH, et al. Anti-CD22-chimeric antigen receptors targeting b-cell precursor acute lymphoblastic leukemia. *Blood* (2013) 121(7):1165–74. doi: 10.1182/blood-2012-06-438002
28. Andreu P, Johansson M, Affara NI, Pucci F, Tan T, Junankar S, et al. FcγR activation regulates inflammation-associated squamous carcinogenesis. *Cancer Cell* (2010) 17(2):121–34. doi: 10.1016/j.ccr.2009.12.019
29. Biswas S, Mandal G, Payne KK, Anadon CM, Gatenbee CD, Chaurio RA, et al. IgA transcytosis and antigen recognition govern ovarian cancer immunity. *Nature* (2021) 591(7850):464–70. doi: 10.1038/s41586-020-03144-0
30. Zhong ZW, Nan K, Weng ML, Yue Y, Zhou WC, Wang ZQ, et al. Pro- and anti- effects of immunoglobulin a- producing b cell in tumors and its triggers. *Front Immunol* (2021) 12. doi: 10.3389/fimmu.2021.765044
31. Jia X, Liu H, Xu C, Han S, Shen Y, Miao X, et al. MiR-15a/16-1 deficiency induces IL-10-producing CD19(+) TIM-1(+) cells in tumor microenvironment. *J Cell Mol Med* (2019) 23(2):1343–53. doi: 10.1111/jcmm.14037
32. Bosisio FM, Wilmott JS, Volders N, Mercier M, Wouters J, Stas M, et al. Plasma cells in primary melanoma. prognostic significance and possible role of IgA. *Modern Pathol* (2016) 29(4):347–58. doi: 10.1038/modpathol.2016.28
33. Chiaruttini G, Mele S, Opzoomer J, Crescioli S, Ilieva KM, Lacy KE, et al. B cells and the humoral response in melanoma: The overlooked players of the tumor microenvironment. *Oncoimmunology* (2017) 6(4):e1294296. doi: 10.1080/2162402X.2017.1294296
34. Pinto D, Montani E, Bolli M, Garavaglia G, Sallusto F, Lanzavecchia A, et al. A functional BCR in human IgA and IgM plasma cells. *Blood* (2013) 121(20):4110–4. doi: 10.1182/blood-2012-09-459289
35. Sharonov GV, Serebrovskaya EO, Yuzhakova DV, Britanova OV, Chudakov DM. B cells, plasma cells and antibody repertoires in the tumour microenvironment. *Nat Rev Immunol* (2020) 20(5):294–307. doi: 10.1038/s41577-019-0257-x
36. Xiong E, Min Q, Wang JY. MZB1 promotes the secretion of J chain-containing dimeric IgA and is critical for the suppression of gut inflammation. *Eur J Immunol* (2019) 49:1365–6. doi: 10.1073/pnas.1904204116
37. Fadlallah J, El Kafsi H, Sterlin D, Juste C, Parizot C, Dorgham K, et al. Microbial ecology perturbation in human IgA deficiency. *Sci Transl Med* (2018) 10(439):eaan1217. doi: 10.1126/scitranslmed.aan1217
38. Jorgensen GH, Gardulf A, Sigurdsson MI, Sigurdardottir ST, Thorsteinsdottir I, Gudmundsson S, et al. Clinical symptoms in adults with selective iga deficiency: a case-control study. *J Clin Immunol* (2013) 33(4):742–7. doi: 10.1007/s10875-012-9858-x
39. Koskinen S. Long-term follow-up of health in blood donors with primary selective IgA deficiency. *J Clin Immunol* (1996) 16(3):165–70. doi: 10.1007/BF01540915
40. Pilette C, Detry B, Guisset A, Gabriels J, Sibille Y. Induction of interleukin-10 expression through fc alpha receptor in human monocytes and monocyte-derived dendritic cells: role of p38 MAPKinase. *Immunol Cell Biol* (2010) 88(4):486–93. doi: 10.1038/icb.2009.120
41. Katz SI, Parker D, Turk JL. B-cell suppression of delayed-hypersensitivity reactions. *Nature* (1974) 251(5475):550–1. doi: 10.1038/251550a0
42. Neta R, Salvin SB. Specific suppression of delayed hypersensitivity: the possible presence of a suppressor b cell in the regulation of delayed hypersensitivity. *J Immunol* (1974) 113(6):1716–25.
43. Wolf SD, Dittel BN, Hardardottir F, Janeway CA Jr. Experimental autoimmune encephalomyelitis induction in genetically b cell-deficient mice. *J Exp Med* (1996) 184(6):2271–8. doi: 10.1084/jem.184.6.2271
44. Lal G, Nakayama Y, Sethi A, Singh AK, Burrell BE, Kulkarni N, et al. Interleukin-10 from marginal zone precursor b-cell subset is required for costimulatory blockade-induced transplantation tolerance. *Transplantation* (2015) 99(9):1817–28. doi: 10.1097/TP.0000000000000718
45. Lal G, Kulkarni N, Nakayama Y, Singh AK, Sethi A, Burrell BE, et al. IL-10 from marginal zone precursor b cells controls the differentiation of Th17, tH and tfr cells in transplantation tolerance. *Immunol Lett* (2016) 170:52–63. doi: 10.1016/j.imlet.2016.01.002
46. Yap DYH, Chan TM. B cell abnormalities in systemic lupus erythematosus and lupus nephritis-role in pathogenesis and effect of immunosuppressive treatments. *Int J Mol Sci* (2019) 20(24):6231. doi: 10.3390/ijms20246231
47. Kleffel S, Vergani A, Tezza S, Ben Nasr M, Niewczas MA, Wong S, et al. Interleukin-10+ regulatory b cells arise within antigen-experienced CD4+ b cells to maintain tolerance to islet autoantigens. *Diabetes* (2015) 64(1):158–71. doi: 10.2337/db13-1639
48. Boldison J, Da Rosa LC, Davies J, Wen L, Wong FS. Dendritic cells license regulatory b cells to produce IL-10 and mediate suppression of antigen-specific CD8 T cells. *Cell Mol Immunol* (2020) 17(8):843–55. doi: 10.1038/s41423-019-0324-z
49. Todd SK, Pepper RJ, Draibe J, Tanna A, Pusey CD, Mauri C, et al. Regulatory b cells are numerically but not functionally deficient in anti-neutrophil cytoplasm antibody-associated vasculitis. *Rheumatol (Oxford)* (2014) 53(9):1693–703. doi: 10.1093/rheumatology/keu136
50. Scapini P, Lamagna C, Hu YM, Lee K, Tang QZ, DeFranco AL, et al. B cell-derived IL-10 suppresses inflammatory disease in Lyn-deficient mice. *Proc Natl Acad Sci United States America* (2011) 108(41):E823–E32. doi: 10.1073/pnas.1107913108
51. Knippenberg S, Peelen E, Smolders J, Thewissen M, Menheere P, Cohen Tervaert JW, et al. Reduction in IL-10 producing b cells (Breg) in multiple sclerosis is accompanied by a reduced naive/memory breg ratio during a relapse but not in remission. *J Neuroimmunol* (2011) 239(1–2):80–6. doi: 10.1016/j.jneuroim.2011.08.019
52. Saussine A, Tazi A, Feuillet S, Rybojad M, Juillard C, Bergeron A, et al. Active chronic sarcoidosis is characterized by increased transitional blood b cells, increased IL-10-producing regulatory b cells and high BAFF levels. *PLoS One* (2012) 7(8):e43588. doi: 10.1371/journal.pone.0043588
53. Das A, Ellis G, Pallant C, Lopes AR, Khanna P, Peppas D, et al. IL-10-producing regulatory b cells in the pathogenesis of chronic hepatitis b virus infection. *J Immunol* (2012) 189(8):3925–35. doi: 10.4049/jimmunol.1103139
54. Liu F, Dai W, Li C, Lu X, Chen Y, Weng D, et al. Role of IL-10-producing regulatory b cells in modulating T-helper cell immune responses during silica-induced lung inflammation and fibrosis. *Sci Rep* (2016) 6:28911. doi: 10.1038/srep28911
55. Wang K, Gong H, Chai R, Yuan H, Chen Y, Liu J. Aberrant frequency of IL-35 producing b cells in colorectal cancer patients. *Cytokine* (2018) 102:206–10. doi: 10.1016/j.cyt.2017.10.011
56. Yu CR, Choi JK, Uche AN, Egwuagu CE. Production of IL-35 by bregs is mediated through binding of BATF-IRF-4-IRF-8 complex to il12a and eb13 promoter elements. *J Leukoc Biol* (2018) 104(6):1147–57. doi: 10.1002/jlb.3A0218-071RRR
57. Dambuza IM, He C, Choi JK, Yu CR, Wang R, Mattapallil MJ, et al. IL-12p35 induces expansion of IL-10 and IL-35-expressing regulatory b cells and ameliorates autoimmune disease. *Nat Commun* (2017) 8(1):719. doi: 10.1038/s41467-017-00838-4

58. Tian J, Zekzer D, Hanssen L, Lu Y, Olcott A, Kaufman DL. Lipopolysaccharide-activated b cells down-regulate Th1 immunity and prevent autoimmune diabetes in nonobese diabetic mice. *J Immunol* (2001) 167(2):1081–9. doi: 10.4049/jimmunol.167.2.1081
59. Parekh VV, Prasad DV, Banerjee PP, Joshi BN, Kumar A, Mishra GC. B cells activated by lipopolysaccharide, but not by anti-ig and anti-CD40 antibody, induce anergy in CD8+ T cells: role of TGF-beta 1. *J Immunol* (2003) 170(12):5897–911. doi: 10.4049/jimmunol.170.12.5897
60. Carter NA, Vasconcellos R, Rosser EC, Tulone C, Muñoz-Suano A, Kamanaka M, et al. Mice lacking endogenous IL-10-producing regulatory b cells develop exacerbated disease and present with an increased frequency of Th1/Th17 but a decrease in regulatory T cells. *J Immunol* (2011) 186(10):5569–79. doi: 10.4049/jimmunol.1100284
61. van de Veen W, Stanic B, Yaman G, Wawrzyniak M, Sollner S, Akdis DG, et al. IgG4 production is confined to human IL-10-producing regulatory b cells that suppress antigen-specific immune responses. *J Allergy Clin Immunol* (2013) 131(4):1204–12. doi: 10.1016/j.jaci.2013.01.014
62. Park MJ, Lee SH, Kim EK, Lee EJ, Park SH, Kwok SK, et al. Myeloid-derived suppressor cells induce the expansion of regulatory b cells and ameliorate autoimmunity in the sanroque mouse model of systemic lupus erythematosus. *Arthritis Rheumatol* (2016) 68(11):2717–27. doi: 10.1002/art.39767
63. Mutnal MB, Hu S, Schachte SJ, Lokensgard JR. Infiltrating regulatory b cells control neuroinflammation following viral brain infection. *J Immunol* (2014) 193(12):6070–80. doi: 10.4049/jimmunol.1400654
64. Liu Y, Cheng LS, Wu SD, Wang SQ, Li L, She WM, et al. IL-10-producing regulatory b-cells suppressed effector T-cells but enhanced regulatory T-cells in chronic HBV infection. *Clin Sci (Lond)* (2016) 130(11):907–19. doi: 10.1042/CS20160069
65. Matsumoto M, Baba A, Yokota T, Nishikawa H, Ohkawa Y, Kayama H, et al. Interleukin-10-producing plasmablasts exert regulatory function in autoimmune inflammation. *Immunity* (2014) 41(6):1040–51. doi: 10.1016/j.immuni.2014.10.016
66. Wasik M, Nazimek K, Bryniarski K. Regulatory b cell phenotype and mechanism of action: the impact of stimulating conditions. *Microbiol Immunol* (2018) 62(8):485–96. doi: 10.1111/1348-0421.12636
67. Catalán D, Mansilla MA, Ferrier A, Soto L, Oleinika K, Aguillón JC, et al. Immunosuppressive mechanisms of regulatory b cells. *Front Immunol* (2021) 12:611795. doi: 10.3389/fimmu.2021.611795
68. Yanaba K, Bouaziz JD, Matsushita T, Tsubata T, Tedder TF. The development and function of regulatory b cells expressing IL-10 (B10 cells) requires antigen receptor diversity and TLR signals. *J Immunol* (2009) 182(12):7459–72. doi: 10.4049/jimmunol.0900270
69. Lampropoulou V, Hoehlig K, Roch T, Neves P, Calderon Gomez E, Sweeney CH, et al. TLR-activated b cells suppress T cell-mediated autoimmunity. *J Immunol* (2008) 180(7):4763–73. doi: 10.4049/jimmunol.180.7.4763
70. Barr TA, Brown S, Ryan G, Zhao J, Gray D. TLR-mediated stimulation of APC: Distinct cytokine responses of b cells and dendritic cells. *Eur J Immunol* (2007) 37(11):3040–53. doi: 10.1002/eji.200636483
71. Neves P, Lampropoulou V, Calderon-Gomez E, Roch T, Stervbo U, Shen P, et al. Signaling via the MyD88 adaptor protein in b cells suppresses protective immunity during salmonella typhimurium infection. *Immunity* (2010) 33(5):777–90. doi: 10.1016/j.immuni.2010.10.016
72. Fillatreau S, Sweeney CH, McGeachy MJ, Gray D, Anderton SM. B cells regulate autoimmunity by provision of IL-10. *Nat Immunol* (2002) 3(10):944–50. doi: 10.1038/ni833
73. Blair PA, Chavez-Rueda KA, Evans JG, Shlomchik MJ, Eddaoudi A, Isenberg DA, et al. Selective targeting of b cells with agonistic anti-CD40 is an efficacious strategy for the generation of induced regulatory T2-like b cells and for the suppression of lupus in MRL/lpr mice. *J Immunol* (2009) 182(6):3492–502. doi: 10.4049/jimmunol.0803052
74. Shah S, Divekar AA, Hilchey SP, Cho HM, Newman CL, Shin SU, et al. Increased rejection of primary tumors in mice lacking b cells: inhibition of anti-tumor CTL and TH1 cytokine responses by b cells. *Int J Cancer* (2005) 117(4):574–86. doi: 10.1002/ijc.21177
75. Inoue S, Leitner WW, Golding B, Scott D. Inhibitory effects of b cells on antitumor immunity. *Cancer Res* (2006) 66(15):7741–7. doi: 10.1158/0008-5472.CAN-05-3766
76. Schioppa T, Moore R, Thompson RG, Rosser EC, Kulbe H, Nedospasov S, et al. B regulatory cells and the tumor-promoting actions of TNF-alpha during squamous carcinogenesis. *Proc Natl Acad Sci U S A* (2011) 108(26):10662–7. doi: 10.1073/pnas.1100994108
77. Horikawa M, Minard-Colin V, Matsushita T, Tedder TF. Regulatory b cell production of IL-10 inhibits lymphoma depletion during CD20 immunotherapy in mice. *J Clin Invest* (2011) 121(11):4268–80. doi: 10.1172/JCI59266
78. Olkhanud PB, Damdinsuren B, Bodogai M, Gress RE, Sen R, Wejksza K, et al. Tumor-evoked regulatory b cells promote breast cancer metastasis by converting resting CD4(+) T cells to T-regulatory cells. *Cancer Res* (2011) 71(10):3505–15. doi: 10.1158/0008-5472.CAN-10-4316
79. Zhang Y, Morgan R, Chen C, Cai Y, Clark E, Khan WN, et al. Mammary-tumor-educated b cells acquire LAP/TGF-beta and PD-L1 expression and suppress anti-tumor immune responses. *Int Immunol* (2016) 28(9):423–33. doi: 10.1093/intimm/dxw007
80. Pylayeva-Gupta Y, Das S, Handler JS, Hajdu CH, Coffre M, Koralov SB, et al. IL35-producing b cells promote the development of pancreatic neoplasia. *Cancer Discovery* (2016) 6(3):247–55. doi: 10.1158/2159-8290.CD-15-0843
81. Mirlekar B, Michaud D, Searcy R, Greene K, Pylayeva-Gupta Y. IL35 hinders endogenous antitumor t-cell immunity and responsiveness to immunotherapy in pancreatic cancer. *Cancer Immunol Res* (2018) 6(9):1014–24. doi: 10.1158/2326-6066.CIR-17-0710
82. Shen P, Fillatreau S. Antibody-independent functions of b cells: a focus on cytokines. *Nat Rev Immunol* (2015) 15(7):441–51. doi: 10.1038/nri3857
83. Luther SA, Lopez T, Bai W, Hanahan D, Cyster JG. BLC expression in pancreatic islets causes b cell recruitment and lymphotoxin-dependent lymphoid neogenesis. *Immunity* (2000) 12(5):471–81. doi: 10.1016/S1074-7613(00)80199-5
84. Schrama D, Thor Straten P, Fischer WH, McLellan AD, Brocker EB, Reisfeld RA, et al. Targeting of lymphotoxin-alpha to the tumor elicits an efficient immune response associated with induction of peripheral lymphoid-like tissue. *Immunity* (2001) 14(2):111–21. doi: 10.1016/S1074-7613(01)00094-2
85. Germain C, Gnjatich S, Tamzalit F, Knockaert S, Remark R, Goc J, et al. Presence of b cells in tertiary lymphoid structures is associated with a protective immunity in patients with lung cancer. *Am J Respir Crit Care Med* (2014) 189(7):832–44. doi: 10.1164/rccm.201309-1611OC
86. Ammirante M, Luo JL, Grivennikov S, Nedospasov S, Karin M. B-cell-derived lymphotoxin promotes castration-resistant prostate cancer. *Nature* (2010) 464(7286):302–5. doi: 10.1038/nature08782
87. Luo JL, Tan W, Ricono JM, Korchynskiy O, Zhang M, Gonias SL, et al. Nuclear cytokine-activated IKKalpha controls prostate cancer metastasis by repressing maspin. *Nature* (2007) 446(7136):690–4. doi: 10.1038/nature05656
88. Zhang B, Vogelzang A, Miyajima M, Sugiyama Y, Wu Y, Chamoto K, et al. B cell-derived GABA elicits IL-10(+) macrophages to limit anti-tumour immunity. *Nature* (2021) 599(7885):471–6. doi: 10.1038/s41586-021-04082-1
89. Zhang Y, Morgan R, Podack ER, Rosenblatt J. B cell regulation of anti-tumor immune response. *Immunol Res* (2013) 57(1-3):115–24. doi: 10.1007/s12026-013-8472-1
90. Akrami M, Menzies R, Chamoto K, Miyajima M, Suzuki R, Sato H, et al. Circulation of gut-preactivated naive CD8(+) T cells enhances antitumor immunity in b cell-defective mice. *Proc Natl Acad Sci U S A* (2020) 117(38):23674–83. doi: 10.1073/pnas.2010981117
91. Shalalpour S, Font-Burgada J, Di Caro G, Zhong Z, Sanchez-Lopez E, Dhar D, et al. Immunosuppressive plasma cells impede T-cell-dependent immunogenic chemotherapy. *Nature* (2015) 521(7550):94–8. doi: 10.1038/nature14395
92. Shalalpour S, Lin XJ, Bastian IN, Brain J, Burt AD, Aksenov AA, et al. Inflammation-induced IgA+ cells dismantle anti-liver cancer immunity. *Nature* (2017) 551(7680):340–5. doi: 10.1038/nature24302
93. Zhang C, Xin H, Zhang W, Yazaki PJ, Zhang Z, Le K, et al. CD5 binds to interleukin-6 and induces a feed-forward loop with the transcription factor STAT3 in b cells to promote cancer. *Immunity* (2016) 44(4):913–23. doi: 10.1016/j.immuni.2016.04.003
94. Yang C, Lee H, Pal S, Jove V, Deng J, Zhang W, et al. B cells promote tumor progression via STAT3 regulated-angiogenesis. *PLoS One* (2013) 8(5):e64159. doi: 10.1371/journal.pone.0064159
95. Li Q, Teitz-Tennenbaum S, Donald EJ, Li M, Chang AE. *In vivo* sensitized and *in vitro* activated b cells mediate tumor regression in cancer adoptive immunotherapy. *J Immunol* (2009) 183(5):3195–203. doi: 10.4049/jimmunol.0803773



OPEN ACCESS

EDITED BY

Catherine Sautes-Fridman,
U1138 Centre de Recherche des
Cordeliers (CRC) (INSERM), France

REVIEWED BY

Masakazu Kamata,
University of Alabama at Birmingham,
United States
Kailin Xu,
Xuzhou Medical University, China

*CORRESPONDENCE

Manel Juan
mjuan@clinic.cat

SPECIALTY SECTION

This article was submitted to
Cancer Immunity
and Immunotherapy,
a section of the journal
Frontiers in Immunology

RECEIVED 29 April 2022

ACCEPTED 22 August 2022

PUBLISHED 12 September 2022

CITATION

Ramírez-Chacón A, Betriu-Méndez S,
Bartoló-Ibars A, González A, Martí M
and Juan M (2022) Ligand-based CAR-
T cell: Different strategies to drive T
cells in future new treatments.
Front. Immunol. 13:932559.
doi: 10.3389/fimmu.2022.932559

COPYRIGHT

© 2022 Ramírez-Chacón, Betriu-
Méndez, Bartoló-Ibars, González, Martí
and Juan. This is an open-access article
distributed under the terms of the
[Creative Commons Attribution License](#)
(CC BY). The use, distribution or
reproduction in other forums is
permitted, provided the original
author(s) and the copyright owner(s)
are credited and that the original
publication in this journal is cited, in
accordance with accepted academic
practice. No use, distribution or
reproduction is permitted which does
not comply with these terms.

Ligand-based CAR-T cell: Different strategies to drive T cells in future new treatments

Alejandro Ramírez-Chacón^{1,2}, Sergi Betriu-Méndez^{3,4},
Ariadna Bartoló-Ibars^{3,4}, Azucena González^{3,4,5},
Mercè Martí^{1,2} and Manel Juan^{3,4,5*}

¹Immunology Unit, Department of Cellular Biology, Physiology and Immunology, Universitat Autònoma de Barcelona (UAB), Cerdanyola del Vallès, Spain, ²Laboratory of Cellular Immunology, Institute of Biotechnology and Biomedicine (IBB), Cerdanyola del Vallès, Spain, ³Immunology Department, Hospital Clínic de Barcelona, Centre de Diagnòstic Biomèdic (CDB), Barcelona, Spain, ⁴Immunology Department, Institut d'Investigacions Biomèdiques August Pi i Sunyer (IDIBAPS) – Fundació Clínic per a la Recerca Biomèdica (FCRB) Universitat de Barcelona (UB), Barcelona, Spain, ⁵Immunology Department, Hospital Sant Joan de Déu, Barcelona, Spain

Chimeric antigen receptor (CAR)-based therapies are presented as innovative treatments for multiple malignancies. Despite their clinical success, there is scientific evidence of the limitations of these therapies mainly due to immunogenicity issues, toxicities associated with the infusion of the product, and relapses of the tumor. As a result, novel approaches are appearing aiming to solve and/or mitigate the harmful effects of CAR-T therapies. These include strategies based on the use of ligands as binding moieties or ligand-based CAR-T cells. Several proposals are currently under development, with some undergoing clinical trials to assess their potential benefits. In addition to these, therapies such as chimeric autoantibody receptor (CAAR), B-cell receptor antigen for reverse targeting (BAR), and even chimeric human leukocyte antigen (HLA) antibody receptor (CHAR) have emerged, benefiting from the advantages of antigenic ligands as antibody-binding motifs. This review focuses on the potential role that ligands can play in current and future antitumor treatments and in other types of diseases, such as autoimmune diseases or problems associated with transplantation.

KEYWORDS

T cells, chimeric antigen receptor (CAR), ligands, receptor, antigen, CAAR, BAR

Introduction

Immunotherapy using autologous genetically engineered chimeric antigen receptor (CAR) T (CAR-T) cells is widely emerging as one of the major breakthroughs for treating cancer. The aim of these therapies is focused on driving T-cell cytotoxicity specifically

against tumor antigens in cancer cells (1, 2). However, the identification of suitable targeted tumor-associated antigens (TAAs) remains a challenge nowadays due to life-threatening toxicity derived from off-tumor on-target antigen recognition (3–5).

Various approaches are being proposed for both hematological and non-hematological malignancies (6). Remarkable antitumor responses have been achieved from anti-CD19 CAR-T therapies against B-cell acute lymphoblastic leukemia (B-ALL) and other refractory B-cell malignancies, demonstrated in pivotal clinical trials (7–11). This has led to the approval by Food and Drug Administration (FDA) and/or European Medicines Agency (EMA) of several CD19-directed products, such as tisagenlecleucel (KYMRIA[®], Novartis) (12), axicabtagene ciloleucel (YESCARTA[®], Kite Pharma-Gilead) (13), and lisocabtagene maraleucel (BREYANZI[®], Juno Therapeutics-Celgene-BMS) (14) for treating large B-cell lymphoma and brexucabtagene autoleucel (TECARTUS[®], Kite Pharma-Gilead) (15) for treating relapsed/refractory mantle cell lymphoma. In this context, our group obtained the first European-developed CAR-T approved by the Spanish Agency of Medicine [Agencia Española del Medicamento y Productos Sanitarios (AEMPS)] with the authorization of ARI-0001 (at Hospital Clínic de Barcelona) administration for relapsed or refractory CD19+ B-ALL in adult patients (16). Another CAR-T treatment recently approved by the FDA is idecabtagene vicleucel (ABECMA[®], Celgene-BMS) based on the recognition of B-cell maturation agents (BCMAs) for treating multiple myeloma (MM) (17). Besides approved therapies, ciltacabtagene autoleucel (of CARTITUDE clinical trials, Janssen-Johnson&Johnson) (18) is also a BCMA-directed CAR-T product expected to be authorized for MM treatment.

Despite this range of validated products, researchers are striving to broaden the clinical benefit of CAR-T cells while exploring new cutting-edge applications. Nevertheless, resistance mechanisms, such as T-cell exhaustion, immunosuppression, or antigen loss, carrying to relapse and therapy failure, have been reported during these trials (19, 20). In fact, an estimated 30% of relapses after anti-CD19 therapy were related to antigen loss (20). This highlights the need to improve or fine-tune CAR-T therapies to avoid tumor escape by identifying novel tumor antigen targets, testing various CAR-expressing cells as CAR-Natural killer (NK), and, most importantly, enhancing the CAR molecule itself.

The minimal structure of a CAR consists of an extracellular antigen recognition domain, tethered to a hinge domain followed by a transmembrane region, and an intracellular signaling domain (CD3 ζ). Additionally, different generations can be found according to the number of modular intracellular costimulatory domains (mainly 4-1BB, CD28, or OX-40) (1, 21) (Figure 1).

Autologous T cells expressing CAR molecules are activated upon non-HLA-restricted ligand recognition, subsequent posttranslational phosphorylation of CD3 ζ is produced, and the zeta-chain-associated protein kinase 70 (Zap-70) is recruited, inducing the assembly of downstream proteins. Meanwhile, CAR-costimulatory regions can activate Phosphoinositide 3-kinase (PI3K)/Protein kinase B (AKT), tumor necrosis factor (TNF) receptor-associated factor 2 (TRAF2)/Mitogen-activated protein kinase (p38MAPK), and c-Jun N-terminal kinase (JNK) pathways. Finally, CAR functional domains enable the CAR to integrate all downstream signaling pathways that end up with the expression and activation of transcriptional modulators—Nuclear factor kappa B (NF- κ B), Nuclear factor of activated T-cells (NFAT), Signal transducer and activator of transcription 3 (STAT3), Activator protein 1 (AP-1)—to drive the effector function of CAR-T cells (22, 23).

Largely, the extracellular antigen recognition domain is a single-chain variable fragment (scFv) composed of a variable heavy chain (V_H) and a variable light chain (V_L), which are usually derived from a murine monoclonal antibody (moAb), joined by a linker region (1) (Figure 2). Due to the scFv murine nature, immunogenicity is one of the major issues regarding *in vivo* long-term expression of CAR-T cells (24, 25). Moreover, aggregation and instability can lead to poor persistence and loss of effectiveness (26). Even though the moAb characteristics of scFv allow potential benefits for the CAR-T therapy, cell persistence, antitumor response efficiency, and off-tumor on-target toxicity need to be improved, and thus, innovative approaches can bring improvements in this regard.

Changing the extracellular target-binding region, changing the “CAR” concept to other but similar receptors

Optimized design of every region of a synthetic CAR has been shown to be relevant to its clinical success (27). Different strategies are being developed to increase CAR-T cell response, one of which is proposing a new extracellular target-binding region (28). Given this, non-antibody-based strategies are being proposed as a promising improvement for CAR-T cell therapies based on the interaction of surface receptors with their natural ligands (29). Specifically, ligand-based CAR-T cells take benefit from the receptor-binding domain of soluble molecules, i.e., cytokines, growth factors, immunoglobulin superfamily proteins, or chimeric peptides for targeting TAA to induce the antitumor response (26) (Figure 2). Similar to scFv-based CAR-T cells, the ligand recognition is in an HLA-independent manner. Additionally, the downstream signaling T-cell

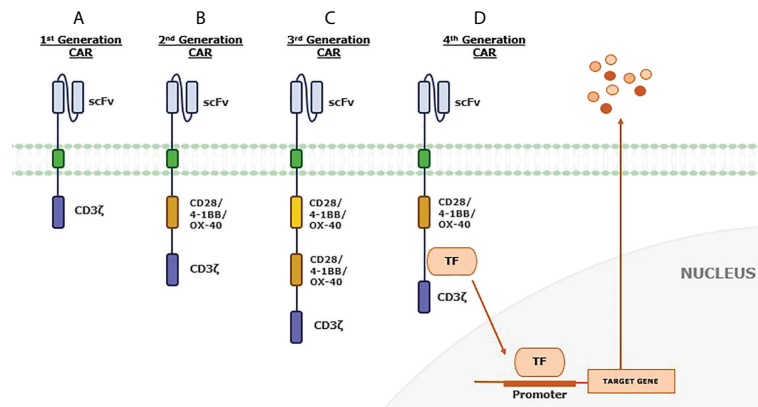


FIGURE 1

Chimeric antigen receptor (CAR) generations. (A) First-generation CAR includes a single-chain variable fragment (scFv) extracellular region and a T-cell activation domain. This minimal structure can recognize the antigen in an HLA-independent manner. By adding a costimulatory domain, (B) second-generation CAR is more able to expand and persist due to this second signal. (C) The third-generation CAR has an additional costimulatory signaling domain to increase proliferation, survival, and activity of engrafted T cells. Recently, (D) the fourth-generation CAR has been developed to include extra genes, such as recognition domains for transcription factors involved in mediating signal transduction. The idea is to modulate the effect of the CAR, facing an immunosuppressive tumor microenvironment by cytokine production or other additional effects.

activation is maintained in the ligand-based CAR-Ts as all four generations can be found, but most approaches use the second- and third-generation CARs (Table 1).

One of the main constraints lies in finding the right ligand for the CAR structure, as the pool of candidates is still limited.

Moreover, its target must be tumor specific or highly expressed while having minimal presence in normal tissues, making it necessary to optimize the proposals as much as possible. Worldwide, a considerable number of preclinical studies have been published and clinical trials are currently ongoing,

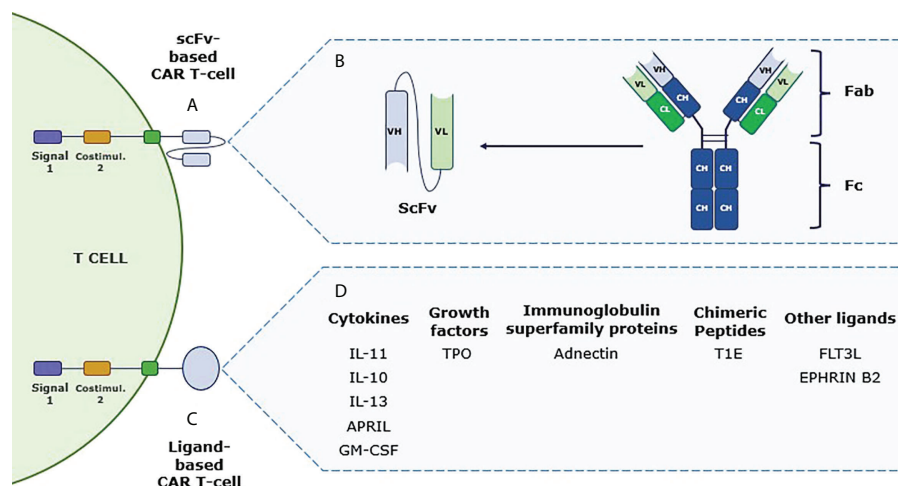


FIGURE 2

Schematic differences between conventional chimeric antigen receptor T (CAR-T) cell and ligand-based CAR-T cell. (A) Second-generation conventional CAR-T cell structure, including T-cell activation domain (signal 1) and costimulatory regions. The recognition domain of this CAR-T is composed of the single-chain variable fragment (scFv) that allows direct interaction with the tumor-associated antigen to trigger the antitumor response. (B) Schematic representation of the different chains that form an antibody and how the scFv domain is obtained from the variable heavy and light chains of a monoclonal antibody to be used in the CAR-T structure. (C) Structure of a second-generation ligand-based CAR-T cell that shares the same domains as mentioned with scFv-based CAR-T cells but incorporating a ligand as a target recognition domain. (D) Immune cytokines, growth factors, immunoglobulin superfamily proteins, and chimeric peptides, among others, are listed as potential molecules to be used as ligand-based CAR-T cell recognition domains (see some abbreviations in Table 1).

validating suitable ligands and elucidating their clinical potential (Table 1).

Ligand-based Chimeric Antigen Receptor (CAR)-T cell preclinical studies

Over the recent years, efforts have been focused on proving CAR-T success against solid tumors, but several difficulties have arisen such as finding a specific TAA, insufficient cell expansion after recognition, tumor penetration, and evasion mechanisms. These obstacles for CAR-T therapies need to be overcome (39–41). Indeed, different approaches are being evaluated, including ligand-based strategies.

IL-11-based CAR-T cell

The IL-11/IL-11R α signaling pathway is involved in several biological activities, and it is supposed to induce an antiapoptotic effect *via* STAT3 activation (42, 43). It has been shown that human IL-11R α is overexpressed in several types of cancer, including osteosarcoma (OS) and lung-associated metastases. Immunohistochemistry results from Huang et al. (30) showed that four different OS cell lines overexpress IL-11R α within 20%–60% and 14 of 16 patients were positive for IL-11R α in their OS lung metastasis samples. In contrast, IL-11R α was not expressed in the surrounding normal lung tissue or other essential tissues (30). OS treatment has been stagnant during these years, and finding new treatments is still needed (44).

Because of its orphan disease condition, IL-11R α was proposed as a suitable candidate for CAR-T therapy (45).

A second-generation CAR-T was designed using IL-11 peptide (CGRRAGGSC) as the extracellular domain (46). *In vitro*, IL-11R α -CAR-T cells were cytotoxic to four different OS cell lines compared with control T cells. After *in vitro* injection in OS mouse models, engineered T cells accumulated in lung metastasis nodules that resulted in selective tumor cell lysis and tumor regression, with no visible lung metastases in three of the five mice treated compared with controls (30).

Adnectin-based CAR-T cell

Adnectin is derived from the 10th type III domain of human fibronectin (10Fn3) (47). The 10Fn3 domain interacts with integrins and belongs to the immunoglobulin superfamily. Its structure is close to the antibody variable domain but with better stability and no dependence on disulfide bonds (48). This feature allows the manipulation of this domain to generate mutants with different interactions. Hence, a similar scFv structure, increased stability, and human nature make adnectin an interesting candidate for ligand-based CAR-T therapies (31).

One of the target membrane surface receptors to direct adnectin-CAR-T cells is the epithelial growth factor receptor (EGFR). This receptor has tyrosine kinase activity that governs fundamental cellular processes, including proliferation, cell migration, metabolism, and survival (49). Moreover, it is one of the most suitable candidates targeted in cancer therapies, since it is overexpressed in several tumors such as breast, lung, and head and neck (50).

TABLE 1 List of preclinical studies and current clinical trials using ligand-based CAR-T cells in course.

	References	Ligand	Target	CAR structure	Disease
Preclinical studies	(30)	IL-11	IL11-R α	IL11 - CD28 - CD3 ζ	OS and lung metastases
	(31)	Adnectin	EGFR	Adnectin- CD28 - 4-1BB - CD3 ζ	Lung cancer
	(32)	FLT3L	FLT3	FLT3L - 4-1BB - CD3 ζ	AML
	(33)	GM-CSF	GMR	GM-CSF - CD28 - CD3 ζ	AML, JMML
	(34)	EPHRIN B2	EPHB4	EPHRIN B2 - CD28 - CD3 ζ	RMS
	(35)	Tri-APRIL	BCMA/TACI	Tri-APRIL - 4-1BB - CD3 ζ	MM
	(36)	TPO	MPL R	TPO - CD28 - CD3 ζ	AML
	(37)	IL-10	IL-10R	IL-10 - 4-1BB - CD3 ζ	AML
	(38)	CD27	CD70	CD27- CD3 ζ	Diffuse large B-cell lymphoma, follicular lymphoma, AML
Clinical trials	NCT02208362	IL-13	IL-13R α 2	IL-13(E13Y) - 4-1BB - CD3 ζ	Glioma
	NCT01818323	T1E	ErbB 1-4	T1E - CD28 - CD3 ζ	HNSCC
	NCT03287804	APRIL	BCMA/TACI	APRIL - CD28 - OX40 - CD3 ζ	MM
	NCT04661384	IL-13	IL-13R α 2	IL-13(E13Y) - 4-1BB - CD3 ζ	Leptomeningeal glioblastoma, Ependymoma or medulloblastoma

OS, osteosarcoma; EGFR, epidermal growth factor receptor; FLT3L, FMS-like tyrosine kinase 3 ligand; FLT3, FMS-like tyrosine kinase 3; AML, acute myeloid leukemia; GM-CSF, granulocyte-macrophage colony-stimulating factor; GMR, granulocyte-macrophage colony-stimulating factor receptor; JMML, juvenile myelomonocytic leukemia; EPHB4, ephrin type-B receptor 4; RMS, rhabdomyosarcoma; APRIL, a proliferation-inducing ligand; BCMA, B-cell maturation antigen; TACI, transmembrane activator and calcium-modulator and cyclophilin ligand interactor; TPO, thrombopoietin; MPLR, myeloproliferative leukemia receptor; MM, multiple myeloma; HNSCC, head and neck squamous cell carcinoma. The clinical trials are collected from clinicaltrials.gov.

Han et al. (31) designed CETUX-CAR (scFv derived from cetuximab) and adnectin-CAR-T cells targeting EGFR (both third-generation CAR-T) to compare their activity (31). Ligand-based CAR-T therapy was developed after revising a previous work by Emanuel et al. (51) to generate adnectin clones for this aim. Four adnectin clones were evaluated (E1, E2, E3, E4) with different binding affinities. E3 was considered the most eligible (51). In comparison to CETUX-CAR-T therapy, E3 CAR-T cell displayed relatively lower binding affinity toward EGFR but higher selectivity against EGFR-overexpressing cancer cells. Nevertheless, it has comparable reactivity, cytotoxicity, and hence antitumor response when incubated with lung carcinoma H292 cells (31). These characteristics expect new broad opportunities to selectively target EGFR-positive tumor cells, avoiding classical issues of classic CAR-T therapies, which will be discussed later.

EPHB4-based CAR-T cell

Ephrin type-B receptor 4 (EPHB4), a member of the family of receptor tyrosine kinases (RTKs), is ubiquitously expressed in distinct types of malignancies as rhabdomyosarcoma (RMS). EPHB4 expression is negligible in vital tissues except of a weak expression in normal placenta cells (52, 53). Differences in ligand-dependent or ligand-independent activation of EPHB4 have been reported, being stimulation without ligand binding the one that leads to cell growth and transformation. In RMS and other malignancies, EPHRIN B2 interaction with EPHB4 may induce apoptosis and lack of proliferation (54). Based on the fact that EPHRIN B2 is a unique ephrin ligand that interacts with EPHB4, a second-generation CAR-T cell with an extracellular portion of EPHRIN B2 can be considered for RMS treatment (55).

In vitro robust and sustained killing activity against RMS, OS, and triple-negative breast cancer (TNBC) cells was assessed by Kubo et al. (34), even following multiple tumor rechallenges, indicating no reduction of antitumor effect. Even though the interaction with EPHRIN B2 should induce weak proliferation, *in vitro* results refuse this idea and do not promote proliferation in RMS cells (55). Another considered point was the possible effect off immunomodulatory effect of the P3F fusion gene, which undergoes some RMS variants, on CAR-T activity. Nevertheless, this translocation product did not modulate the EPHB4-CAR-T activity (56).

After substantiating that EPHRIN B2 could bind EPHB4 mouse receptors, the antitumor effect and off-tumor on-target toxicity were *in vivo* verified with RMS tumor xenograft models. The results showed decreased tumor growth rates and prolonged survival in treated animals with EPHB4-CAR-T compared with anti-CD19 CAR-T control without any sign of adverse effects (55). These promising results have led to the generation of novel studies, and future clinical trials are being proposed.

FLT3L CAR-T cell

Acute myeloid leukemia (AML) is still a rare malignancy but represents a third of all diagnosed leukemias. Two ligand-based CAR-T cells have been proposed against AML, FLT3L CAR-T and granulocyte-monocyte colony-stimulating factor receptor (GMR) CAR-T (32, 33). Approximately 30% of AML cases have mutated the FMS-like tyrosine kinase-3 (FLT3), mainly internal tandem duplication (ITD) mutations that lead to constitutive activity of tyrosine kinase domain (TKD) and promote, *via* different signaling pathways, the progression of AML with poor prognosis (57, 58). As scFv-based CAR-T targeting FLT3 has no optimal results, Wang et al. (32) developed a second-generation ligand-based CAR-T cell with the FLT3 ligand (FLT3L) as the recognizing domain (32, 59).

FLT3L CAR-T cell can specifically recognize FLT3-positive cells, and *in vitro* studies have proven their cytotoxic efficacy against 10 different primary AML cell lines, five with FLT3-ITD and five with wild-type (WT) FLT3 expression. Moreover, treated mice showed longer survival, but results also revealed that recognition seemed to be independent of FLT3 levels on cells, relying on the FLT3 genotype (32).

Cytotoxicity efficacy was proven *in vitro* against 10 different primary AML cell lines, five with FLT3-ITD and five with WT FLT3 expression. FLT3L CAR-T cell can specifically recognize FLT3-positive cells and display cytotoxicity. *In vivo* experiments verify this idea, since treated mice showed longer survival. In fact, results revealed that recognition seemed to be independent of FLT3 levels in cells but relied on the FLT3 genotype (32).

FLT3L-FLT3 interaction allows dimerization and phosphorylation of FLT3 and activation of downstream signaling pathways that end up in cell growth and survival (60, 61). Since FLT3L CAR-T allows ligand-dependent activation, it can stimulate this phosphorylation and may promote cell growth in FLT3 WT. Thus, FLT3L WT is less sensitive to CAR-T cytotoxicity. Otherwise, FLT3-ITD is constitutively activated (ligand-independent) developing different phosphorylation profiles that are more sensitive to CAR-T therapy when FLT3 CAR-T interacts. This may allow the CAR-T therapy the ability to distinguish between both types of cells, being more lethal for mutated FLT3. So, distinguishing the receptor by genotype can be a novel strategy with potential benefit in such types of tumors (32).

GMR CAR-T cell

Another different approach for AML treatment is GMR CAR-T cells. The granulocyte-macrophage colony-stimulating factor (GM-CSF) is an immunomodulatory cytokine capable of tuning the phenotype of myeloid cells but also T cells through myeloid

intermediaries (62). Its main target is GM-CSF receptor (GMR), composed of two subunits: α subunit (CD116) that is present in normal and AML and juvenile myelomonocytic leukemia (JMML) myeloid cells and β subunit (CD131) shared with IL-3 and IL-5 receptors. Recent studies revealed that GMR can be found as complexes of two α subunits (low-affinity receptors) or both α and β subunits (high-affinity receptors) (33).

AML expresses both complexes, and since CD116 is overexpressed in more than 60% of AML, mainly in those with poor prognosis, Saito et al. (33) proposed a second-generation ligand-based CAR-T cell targeting GMR (33, 63) after they demonstrated antiproliferative effects of the same construct against JMML (63). Different CAR-Ts were built and evaluated to enhance this effect against AML. Referring to a previous work by López et al. (64), they used GM-CSF as a binding region (33) mutated in residue 21 that plays a key role in the functionality of the cytokine but not affecting the binding (64). After screening analysis of several mutated GM-CSFs, E21K and E21R, both had increased antitumor response. *In vitro* and *in vivo* results revealed E21K mutation as the one with durable *in vitro* cytotoxicity and complete suppression of the progression of CD116+ AML cells *in vivo*, correlating strongly with the CD116 levels in tumor cells. These may appear to conflict with other reported data in which E21K-mutated GM-CSF had a reduced binding capacity to high-affinity receptors but maintained the binding capacity to low-affinity receptors, leading to less AML interaction than scFv-CARs (33, 64). Although the mechanism has not been identified yet, it seems that the reduction of time interaction with receptors would enhance T-cell stimulation (65). Despite all of these important results, off-tumor adverse effects were not tested and this would be necessary to evaluate for further applications (33).

Thrombopoietin-based CAR-T cell

Thrombopoietin (TPO) is a hematopoietic growth factor produced not only by the liver but also in the bone marrow and kidney niches. TPO is defined as a natural ligand to the myeloproliferative leukemia (MPL) receptor, also known as CD110. Overexpression of MPL has been characterized as a negative prognosis factor for AML progression due to the effects of the associated signaling, such as Janus Kinase 2 (JAK2)/STAT5, Phosphoinositide 3-kinase (PI3K)/Protein kinase B (AKT), and proto-oncogene, serine/threonine kinase (Raf1)/Mitogen-activated protein kinase (MAPK) (36).

The TPO/MPL pathway is essential for the survival and self-renewal of leukemia stem cells (LSCs) and hematopoietic stem cells (HSCs) and is therefore involved in the progression of AML. For this reason, Zoine et al. (36) proposed a second-generation ligand-based CAR-T cell using the biologically active region of the TPO protein to target the MPL receptor. The outcomes showed not only a significantly specific cytotoxicity

against MPL+ AML cell lines *in vitro* but also satisfactory results in murine AML xenograft models. Notably, on-target off-tumor toxicities were detected in the bone marrow compartment during the trials. The authors justify that bone marrow toxicity could be advantageous for the model, as most patients with AML receive a bone marrow transplant and treatment with TPO-based CAR-T cells may be helpful to replace the adverse effects of pretransplant conditioning regimens.

IL-10-based CAR-T cell

Among the diverse ways of drawing an antitumor response in AML is that based on the IL-10 receptor (IL-10R). IL-10R is a receptor composed of four members, two alpha (IL-10RA) and two beta (IL-10RB) molecules, being hematopoietic-specific and ubiquitous, respectively. Published data infer that the IL-10/IL-10R pathway, when with aberrant function, is involved in promoting the stemness of AML cells (37). For this reason, it seems reasonable to validate the CAR-T response against IL-10R. To this end, Chen et al. (37) designed a second-generation ligand-based CAR-T cell using IL-10 as a binding motif and assessed the degranulation and cytokine secretion from T cells and killing of the AML-targeted cells in culture. Following good *in vitro* results, they assessed the product in a murine AML xenograft model and obtained prolonged survival in treated models compared with those that did not undergo CAR-T treatment.

CD27 CAR-T cell

CD70 is the membrane-bound ligand of the CD27 receptor, which belongs to the TNF receptor superfamily. This interaction is considered a potential target to address CD70-positive malignancies, such as diffuse large B-cell lymphoma and follicular lymphoma, as well as AML, since CD70 is expressed on most of its leukemic blasts, while its expression is low or absent in normal bone marrow samples (66). Importantly, CD70 expression is transient and restricted to a subset of highly activated T, B, and dendritic cells under physiological conditions, playing a role in T-cell activation. However, it is not essential for the development and maintenance of a functional immune system.

In this context, Sauer et al. (38) developed a first-generation CAR-T cell based on a ligand, CD27z-CAR, which uses the full-length CD27 cDNA as a recognition domain. Additionally, their research incorporated the design of several CAR-T sequences with the CD70-specific scFv to compare reactivity against the target.

All CAR-T cell populations mediated cytotoxicity against CD70-positive tumor cell lines but not CD70-negative cells in *in vitro* assays (38). However, because the efficacy of CAR-T cells is

determined not only by their cytolytic activity but also by their ability to proliferate after the tumor challenge, they were subjected to successive cocultures. The results showed differences in their ability to kill and proliferate during successive cocultures, with CD27z-CAR able to kill tumor cells during five consecutive cocultures in at least two of the four donors in contrast to other CAR-T cell populations, as well as the highest production of T helper 1 (TH1)-type cytokines, such as Interferon (IFN)- γ and TNF- α (38).

Following these results, the same research evaluated the CD27z-CAR *in vivo* effects in CD70-positive AML murine xenograft models. Their results demonstrated an efficient ability to control leukemic growth, leading to complete leukemia remission in all mice by day 21 (38). Furthermore, they could demonstrate a significant expansion of the transduced T cells in the *in vivo* models, thus corroborating the relationship between the administered therapy and the remission of pathology.

Ligand-based CAR-T cell clinical trials

Although anti-CD19 scFv-based CAR-T therapies have clinically succeeded, as several products have already been approved (12, 13), the reality is that limited clinical information is still available for other strategies, as could be for ligand-based CAR-T cells. However, a few phase I/II clinical trials are currently trying to elucidate the safety and bioactivity of different approaches.

IL-13-zetakine CAR-T cell

One of the most hopeful proposals is focused on treating central nervous system (CNS) solid tumors, such as glioblastoma multiforme (GBM) (67–69). GBM is one of the most lethal primary brain tumors, and its outcome remains poor. High-grade glioblastoma does not respond to standard treatments such as surgery or chemotherapy mainly because of tumor heterogeneity (70). Diverse differentiation status has been found in GBM cell populations: stem-like cancer-initiating cells (GSCs), expressing stem cell markers and maintaining certain self-renewal capacity, and differentiated glioblastoma cells (71). It has been proposed that GSCs are responsible for this lack of response because of their natural resistance to conventional treatments (72).

IL-13 receptor $\alpha 2$ (IL13R $\alpha 2$) is demonstrated to be expressed within 50%–80% of GBM cells, independently of differentiation status, but not significantly expressed in normal CNS tissue. IL13R $\alpha 2$ -positive tumors are associated with a

worse prognosis, hypothetically owing to IL-13/IL13R $\alpha 2$ interaction (73–75). IL-13 is an immunomodulatory cytokine that promotes apoptosis and transforming growth factor alpha (TGF- β) secretion when it interacts with IL13R $\alpha 1$ /IL-4R α high-affinity heterodimer. Alternatively, IL-13 has a higher affinity to IL13R $\alpha 2$ but does not induce intracellular signaling (76). Therefore, overexpression of IL13R $\alpha 2$ in GBM may reduce proapoptotic signaling and promote cell survival (75).

Considering these facts, IL13R $\alpha 2$ is a suitable candidate for different treatments as is IL-13-zetakine (77, 78). This product is an adoptive T-cell therapy engineered with a CAR structure whose recognition domain is IL-13 cytokine, which contains the E13Y mutation, for targeting IL13R $\alpha 2$. The importance of this mutation relies on reducing the affinity to IL13R $\alpha 1$ /IL-4R α heterodimer but increasing IL13R $\alpha 2$ binding compared with WT IL-13 (77). The aim is to specifically redirect the cytotoxic activity of T cells to GBM cells that overexpress this TAA compared with normal CNS cells.

During the last few years, a first-generation IL-13 CAR-T was developed and tested, obtaining a sustained cytotoxic response to both cancer-initiating cells and differentiated GBM cells *in vitro*. Also, there was evidence of antitumor activity and limitation of the progression of established IL13R $\alpha 2$ -positive tumors in xenograft mice without clear collateral damage on healthy tissue (77, 78). With these results, Brown et al. (79) conducted a first-in-human pilot clinical trial (NCT00730613) to assess the activity and safety of IL-13-zetakine after intracranial delivery in three patients with recurrent GBM. Indeed, two out of three showed transient antitumor activity in the absence of severe adverse events. Although the survival rate was 11 months, the small cohort denied the capacity to establish the therapy survival benefit (67).

Aware that the CAR-T response needs to be improved, Brown et al. (80) started to tune the IL-13-zetakine structure. Thus, the second-generation CAR-T cell was developed using 4-1BB as the costimulatory domain and CD3 ζ as the intracellular signaling domain (80). Preclinical results showed an enhanced response. As the first-generation IL-13 CAR-T activity was transient, and its persistence was limited, one of the aims was to analyze the antitumor response and cell persistence of the second-generation one. For this reason, a current phase I clinical trial (NCT02208362) (81) studies the activity, adverse effects, and best dose of these CAR-T cells. In fact, one patient has reported a transient complete response after complete CAR-T dose administration with important improvements in the quality of life for up to 7.5 months (68). The trial is still ongoing, but this case appears to be a great hope. Another clinical trial has just started (NCT04661384) to test this CAR-T therapy in patients with leptomeningeal disease from glioblastoma, ependymoma, or medulloblastoma, but the results are not expected to be analyzed until December 2022 (69).

Pan-ErbB CAR-T cell

The ErbB receptor family comprises a synergistic dynamic signaling network composed of four members, EGFR/ErbB-1, ErbB-2/NEU/HER2, ErbB-3/HER3, and ErbB-4/HER4 (49). After ligand-dependent stimulation, diverse homodimer or heterodimer combinations may occur (50). ErbB-2 is demonstrated to be the preferred member for dimer formation, while ErbB-3 pairing is essential, because of its lack of intrinsic tyrosine kinase (TK) activity. Upon dimer activation, tissue development, proliferation, and differentiation are promoted (50).

Several studies have revealed aberrant expression or function of some ErbB receptors, mainly ErbB-2 dimers with ErbB-1 or ErbB-3, as a determinant of the pathogenesis of many malignancies, such as mesothelioma, epithelial ovarian carcinoma (EOC), or head and neck carcinoma [head and neck squamous cell (HNSCC)] (82–85). Consequently, there is a considerable interest in targeting ErbB family members, but problems of selective pressure and tumor resistance have been emerging due to the overexpression of non-targeted receptors (82).

To circumvent this, diverse approaches are currently trying to redirect their mechanism toward two or more ErbB dimers to prevent the signaling network from escaping and continuing tumor progression. This idea includes T1E28z or pan-ErbB CAR-T cell, a second-generation CAR-T therapy that includes T1E as a binding moiety for treating many epithelial malignancies (83).

T1E is a chimeric polypeptide that takes benefit from different ErbB ligand properties: epidermal growth factor (EGF) and TGF- α selectively bind to ErbB-1 with high affinity but weaker or no affinity for ErbB-2/ErbB-3 heterodimers, respectively. Structural analysis of both revealed that EGF is unable to bind ErbB-2/ErbB-3 with high affinity because of the lack of essential amino acids in the N-terminal region, whereas TGF- α cannot bind despite having these crucial residues (86). Thus, a chimera was developed introducing N-terminal linear region of TGF- α into the EGF C-terminal sequence, resulting in high affinity for ErbB-2/ErbB-3 maintaining ErbB-1 specificity (87). ErbB-4 heterodimer binding was also reported. This made T1E a promiscuous ligand ideal for multitargeting ErbB dimers, preventing antigen loss and signaling compensation.

Davies et al. (83) engineered T cells with T1E28z and evaluated its binding capacity, resulting in eight of nine possible ErbB homo and heterodimers, with most affinity detected against cells that coexpressed ErbB-1 and ErbB-2 (83). One of the main challenges of CAR-T therapies is the enrichment and expansion of T cells. For this reason, they also introduced a chimeric cytokine receptor named 4 $\alpha\beta$, in which IL-4 receptor- α ectodomain has been coupled to the shared β chain used by IL-2/15 (88). With IL-4, T cells receive a potent

and selective stimulation, allowing better expansion. Preclinical studies have revealed that T4 immunotherapy (CAR-T combining T1E28 ζ and 4 $\alpha\beta$ chimeric receptors) achieves a relevant antitumor response in HNSCC, EOC, and malignant mesothelioma *in vitro* (83–85).

Considering that T1E polypeptide can efficiently bind to ErbB mouse receptors, *in vivo* efficiency and toxicity were tested in diverse immunocompromised xenograft mice, including all three malignancies mentioned above (89). T cells elicit antitumor activity in the absence of relevant toxicity when delivered intratumorally or intraperitoneally at a moderate dose. Nevertheless, after high-dose intraperitoneal delivery, cytokine release syndrome (CRS) appeared, providing evidence that intratumor administration seems to be the safest route for solid tumors and that CRS dose-dependently appeared (83, 89).

To build on this, van Schalkwyk et al. (90) designed a phase I clinical trial (NCT01818323) to assess the safety of T4 immunotherapy to treat HNSCC that is not suitable for conventional active therapy. Primary results are expected to be published in April 2022. If results are robust, other clinical approaches should be initiated to evaluate CD4+ CAR-T therapy against other malignancies, such as EOC or malignant mesothelioma (91).

AUTO2: APRIL-based CAR-T cell

MM represents 13% of all hematologic cancers, and it is characterized by extreme growth of malignant plasma cells (PCs) in the bone marrow, aberrant production of monoclonal immunoglobulin, and immunosuppression, among others (92, 93). Over the past decade, autologous stem cell transplants, proteasome inhibitors (PIs), and immunomodulatory drugs (IMiDs) have significantly raised survival rates, and moAbs further improved relapsed/refractory multiple myeloma (RRMM) outcomes (93–95). Nonetheless, overall survival is extremely reduced in patients with RRMM after IMiDs or IP treatments. Therefore, there remains a need for new approaches that could lead to durable remissions in MM patients, especially in RRMM (94).

Although the CARTITUDE-1 trial seems to have recently promising results (18), treatment of MM still involves many challenges, focusing on TAA detection. Since CD19 has a reduced expression in malignant cells, some RRMMs appear to be CD19-negative and other well-defined antigens (CD56 or CD38) have expression levels in other tissues, then other antigens need to be validated (95).

BCMA is another suitable candidate for CAR-T therapies because it is absent on hematopoietic stem cells but selectively expressed on PCs, and BCMA is almost present in MM cells. After the first anti-BCMA CAR-T cell trial, remission was reported in four of 12 patients, but high doses were required

for persistent remission due to the low expression of BCMA in MM cells. Moreover, similar to CD19 therapies, tumor escape by downregulation of targeted BCMA was reported (96, 97).

Considering this, Lee et al. (98) attempted overcoming low target density and antigen escape targeting two TNF-receptor superfamily members, BCMA and a transmembrane activator and calcium-modulator and cyclophilin ligand interactor (TACI) (98). Both are coexpressed on the majority of PC and MM cells and may play a similar role in providing PC with survival signaling (35). For this reason, a bispecific third-generation CAR was constructed using a murine truncated version of a proliferation-inducing ligand (APRIL), a natural ligand for both BCMA and TACI with nanomolar affinity (99, 100). The final product, AUTO-2, is retrovirally transduced to produce CAR-T cells expressing APRIL-CAR-T and the RQR8 switch system that acts as a marker but also as a suicide molecule when adverse effects of the therapy occur (101, 102).

The preclinical evaluation demonstrated cytotoxicity at low levels of target antigen, even when the BCMA expression was downregulated or lost. These data were confirmed *in vivo*, where an improved disease control compared with scFv-based CAR was observed (101), but the problem still was the need for considerable T-cell doses to achieve relevant responses with a short follow-up duration. A phase I/II clinical trial (NCT03287804) (102) was initiated to test the safety and efficacy of AUTO2 in RRMM patients. Phase I showed that eight of 11 (81.9%) treated individuals achieved expansion and persistence of CAR-T cells in peripheral blood, while four of 11 (36.4%) had a complete/very good/partial response up to 2 years. However, the average death during the trial was eight of 11 (72, 73), so the duration of response could not be quantified, and thus, phase II was not initiated.

Even though the results of the clinical trial seemed to show a glimmer of hope, APRIL-based CAR-T cells required better optimization. After evaluation of all of these studies, Schmidts et al. (35) generated a second-generation CAR where they changed the extracellular domain of AUTO2 for a tri-APRIL binding moiety (TriPRIL) (35). The study hypothesized that preserving the trimeric form of the natural ligand would increase the binding affinity and efficacy against MM cells. Also, they used human APRIL so it would reduce immunogenicity. Indeed, data revealed that antitumor activity was enhanced *in vitro* against BCMA+ and BCMA- cells and *in vivo* with xenograft models compared with monomeric APRIL-based CAR-T cells (35). Therefore, TriPRIL CAR-T therapy holds promise for treating MM, including the absence of BCMA. Further clinical trials will be required to elucidate its potential clinical benefits.

Beyond ligand-based CAR-T

Although this review focuses mainly on what the literature refers to as ligand-based CAR-T cells, it is necessary to mention

other approaches in which ligands are incorporated as the binding moiety of the CAR structure. In this regard, we found the so-called chimeric autoantibody receptor (CAAR) (103), B-cell receptor antigen for reverse targeting (BAR) (104), and chimeric HLA antibody receptor (CHAR) (Figure 3).

Treatments for autoimmune diseases specifically eliminate self-reactive cells while preserving protective immunity (103). However, this premise is proving difficult to implement, as both autoimmunity and cancer are closely related, requiring optimal management of autoimmune therapies to prevent cancer development due to general immunosuppression (105). For this reason, novel approaches try to avoid the classic issues associated with autoimmunity treatments.

In this sense, CAAR molecules consist of a chimeric immunoreceptor that includes an autoantigen as the extracellular domain. This technology directs the modified T-cell response toward autoreactive memory B cells expressing autoantibodies as their surface immunoglobulins (sIg-BCR), or autoantibody-producing PCs, which are autoantibody-secreting cells (103). This would generate selective therapy against reactive immunity, thus avoiding a general suppression of the abovementioned protective immunity. This strategy has been used by Ellebrecht et al. (103), who have constructed a CAAR T cell using the different forms of the Dsg3 autoantigen target of pathological autoantibodies present in a significant percentage of patients with pemphigus vulgaris (PV). Their results expect potential benefits that these CAARs could bring to the treatment of autoimmune diseases.

BCR signaling has been identified as an important pathway in B-cell lymphomagenesis, and there is increasing evidence that antigenic stimulation of the BCR is a trigger for proliferation. Several autoantigens, such as ARS2 and LRPAP1, have been proposed as stimulatory ligands of the BCR and its pathway in one quarter of diffuse large B-cell lymphomas (DLBCLs) and almost half of the mantle cell lymphomas (MCLs), respectively (104–106).

From the study of these BCR antigens arise structures defined as BAR. BAR-bodies were initially designed with the idea of conjugating toxins to these BCR antigens. One example is the research led by Thurner et al. (107), where it is shown that LRPAP1-based BARs conjugated to *Pseudomonas aeruginosa* exotoxin A toxin are internalized and specifically kill MCL cells with LRPAP1-reactive BCRs by inducing apoptosis.

Further research has led to the construction of an antibody-like structure that incorporates the sequence of these identified BCR antigens, or at least their BCR-binding epitope, replacing the variable fragments of the scFv heavy and light chains, with the aim of transducing T cells and targeting malignant B-clones with unique specificity for these BCRs responsible for tumor expansion (104, 106). Since approaches such as that of Beward et al. (106) that uses the BCR antigen to target MCL cells have exclusive specificity for cells with the specific surface BCR, they do not only represent a strictly tumor-specific approach but can

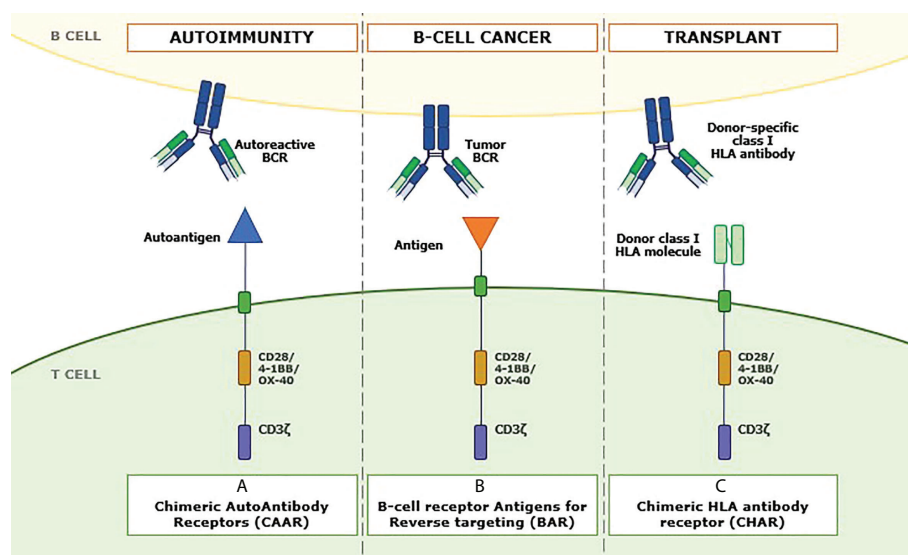


FIGURE 3

Role of ligands in other antibody-mediated diseases. Recently, new approaches have emerged in which different ligands linked to antibody-like structures can be used to address specific pathologies. The sequence of these products shares similar domains to CAR-Ts but changes the extracellular domain. In panel (A), a chimeric autoantibody receptor (CAAR) can be seen in which an autoantigen is incorporated as a recognition domain of the CAAR to redirect it toward autoantibodies on the autoreactive B-cell surface, thus facing autoimmune responses. Panel (B) shows the structure of a B-cell receptor antigen for reverse targeting (BAR). The recognition domain includes an antigen specific to the single B-cell receptor (BCR) clonally specific of each B-cell tumor. Finally, panel (C) represents an example of chimeric HLA antibody receptor (CHAR), where molecules of the class I HLA system replace the conventional recognition domain to direct the transduced T cell toward anti-HLA antibody-producing B cells to cope with posttransplant immune rejection.

also be expected to be more effective but less toxic than the currently available CAR-T cells with specificity for CD19, as they should not affect other cells and should work equally well in the presence of autoantibodies against the antigen in question.

In the same line as CAARs and BARs, T cells that express CHAR with the ability to kill B cells that produce donor-specific class I HLA antibodies are being developed to treat antibody-mediated rejection in the field of solid organ transplantation. One of the main problems in solid organ transplantation is the presence, or *de novo* generation, of donor-specific antibody anti-HLA molecules (anti-HLA-DSA), which is associated with a high risk of antibody-mediated rejection (108). Our thinking has changed from considering rejection as a primarily T cell-mediated process. Insufficient control of the humoral arm of a recipient's immune system by current immunosuppressive regimens is now the pathogenic factor primarily responsible for allograft dysfunction and loss (109). This new CHAR could be a therapeutic approach for personalized desensitization of HLA-sensitized recipients and even for antibody-mediated rejection in solid organ transplantation.

Discussion

CAR-T cell-based therapeutic strategies allow the production of significant numbers of tumor-specific reactive T

cells, resulting in potent responses that can lead to the elimination of tumor cells expressing the target antigen (1). As mentioned above, those approaches are being considered as one of the further progress in the field of antitumor therapies, even including several commercial products available for clinical use (12–16). Specifically, it is the conventional CAR, with the scFv fragment as the recognition domain, that is mostly proposed, since they were the first to appear and to get results. In any case, scFv-based CAR is not exempt from limitations and concerns, such as immunogenicity or toxicity (5, 24). For this reason, ligand-based CAR-T cells are now emerging as a suitable alternative to address them (110). They are presented as an alternative therapy because most of the preliminary and clinical studies conducted to date show similar results in terms of activity and efficacy (110).

It is relevant to highlight the commonalities between the two technologies. The proof of concept involves engineering of autologous T cells, allowing the CAR expression on the cell surface, so that the modified cells can acquire tumor specificity. Since the same intracellular signaling domains are used, upon recognition of the target molecule, the internal signaling necessary to enable T-cell activation and expansion will be triggered (22, 23).

Both approaches share HLA-independent target recognition, which allows for less restriction in the recognition of what they

are meant to act against. The main difference lies in the interaction on which target recognition depends. While scFv-based CAR-T cells rely on mAb–target binding, which is defined as a higher-affinity interaction, ligand-based CAR-Ts use ligand–receptor binding, which is presumably a lower-affinity interaction (28). Using the properties of this modification in the CAR structure, the aim is to mitigate the issues detected after administration of conventional CAR-T therapies.

Immunogenicity

CAR-T cells have the potential to trigger both cellular and humoral immune responses against non-self-components of the CAR structure, but its clinical implication remains poorly investigated and exhibits great variability depending on the CAR-T and type of tumor (24).

Human anti-mouse antibodies (HAMAs) against mouse-derived scFvs have been detected in a subset of patients. Anti-idiotypic antibodies are also reported, directed toward specific regions of scFv binding sequence, since the hypervariable region (the idiotype and the allotype determinants) of the scFv are highly immunogenic. Additionally, antibodies against CAR peptides originated from the fusion of the domains that make up its structure can also be found (24, 25). Regarding the cellular immune response, specific cytotoxic T cells could arise from the processing and cross-presentation of foreign peptides of the CAR structure. Finally, immune response could also be triggered by residual elements from gene transfer viral vectors, which are inevitably immunogenic (24).

Despite the lack of conclusive evidence, it is inferred that these elements may interfere negatively with CAR-T cell activity by either neutralizing their recognition capacity, causing loss of CAR membrane expression, or directly increasing CAR-T cell apoptosis (24, 25). Immunogenicity arising from the non-human origin of scFv could be reversed using human mAbs, but the full ability and a sufficient human mAb library to obtain them are not currently available. Also, humanized scFv can be an option, but problems exist with cell surface stability, dimerization, and aggregation that limit the desired cytotoxic activity (26, 110).

Ligand-based CAR-T cells have been proposed to dodge these adverse effects considering that natural human ligands are used to replace the scFv region, as non-human sequences are eliminated, and the immunogenicity of the product is reduced (both HAMA and cytotoxic T cells). It is worth mentioning that the reduction in immunogenicity will be greater the more original ligand sequence is included (full-length sequence) in the final recombinant molecule (26, 31, 35). Antibodies directed against the region of the fused domains and immunogenicity of

viral vector peptides will still exist, but ligand-based CAR-T cells may be less likely to prompt immune responses (35).

Despite that fact, it requires further investigation to elucidate the possible benefit of using ligand-based CAR-T cells to reduce immunogenicity, as there is a lack of results to prove it.

Tonic CAR signaling and scFv instability

Throughout the design process of scFv molecules, many studies have highlighted problems of oligomerization either as part of a CAR structure or in a soluble form. Oligomerization occurs mainly through a process of domain swapping, where the V_H region of one scFv is incorrectly associated with the V_L region of another scFv (26, 111). This causes the aggregation of CAR structures, which will result in dysfunctions leading to tonic signaling through constitutive activation *via* the signaling described above. Not to mention that these oligomerizations could lead to problems in target recognition by the CAR (111).

CAR-transduced T-cell tonic signaling is widely described in many investigations. In addition to aggregations of scFv, high levels of cell surface CAR expression, the addition of endogenous TCR-associated signaling, and the incorporation of certain intracellular signaling domains into the CAR sequence can trigger constitutive cytokine release, prolonged and excessive expansion, and thus further T-cell exhaustion (26, 111). However, natural ligands are probably more stable and have a lower risk of dimerization and domain swapping if no multimeric ligands appear, and these will require further study. Thus, ligand-based approaches would reduce potential tonic signaling that prevents early exhaustion of CAR-T therapy, thus prolonging its functionality and thus improving the probability of success of the intervention when administered in *in vivo* models.

Affinity-tuning and toxicity management

Another potential advantage of ligand-based CAR-T cells is their capacity to multitarget (110). The native forms of ligands that are proposed for CAR structure often can bind to different receptors, being bispecific or trispecific. Recent publications consider that one of the main drawbacks encountered is the relapsed/refractory state of some malignancies after CAR-T infusion mainly due to downregulation of the specific antigen against which the cytotoxic activity is directed (antigen loss) (21, 31). Given that scFv has a single specificity for a particular peptide, ligand-based CAR-T cells may provide a safeguard against antigen loss, anticipating one of the possible mechanisms of tumor evasion (112). For instance, the APRIL-CAR proposed by Lee et al. (98) has bispecificity for BCMA and

TACI, leading to increased recognition and lysis of MM cells, either BCMA+ or BCMA-, compared to an scFv-based CAR-T cell directed against BCMA that does not prevent the proliferation of BCMA- tumor cells (35, 98).

This potential benefit from ligand-based CAR-T cells must be balanced against the toxicity problems that have already been described in some patients when treated with scFv-based CAR-T cells (5). Specifically, these off-tumor on-target toxicities arise because target molecules can be constitutively expressed in healthy tissues, causing harmful activity by altering normal tissue functionality (3). If a product with bispecificity or trispecificity is infused, the potential number of off-target sites at which it can act increases significantly, thereby increasing the risk of adverse effects (4, 21, 35). Therefore, this promiscuous binding could be also analyzed as a disadvantage of the ligand-based design if other known or unknown binding partners exist in healthy tissues, leading to off-tumor on-target toxicities. For this reason, these potential toxic effects of ligand-based CAR-T cells need to be carefully explored in animal models.

However, this could be countered by considering the sensitivity of the CAR interaction toward the recognized molecule. Normally, the process of production of scFv regions depends on somatic hypermutation mechanisms, in which molecules with the highest affinity for the target are selected (113). Thus, at low concentrations of the target molecule in the tumor, the CAR-T cell is able to reach the activation threshold and trigger the cytotoxic response (31, 114). However, this characteristic of high-affinity CARs makes them poorly able to discriminate between target cells with various levels of antigen expression. Considering that tumors tend to overexpress certain molecules above basal levels present in other tissues (82), this means that the CAR-T cells activate the cytotoxic response not only toward the tumor but also toward other healthy tissues, increasing the risk of off-tumor on-target toxicities. Finally, scFv-CAR-T cells have constitutive basal activation of CAR signaling by their extracellular domain, increasing the off-target effects of the therapies and the earlier exhaustion of the T cell (31).

By using ligands and not antibody chains as the target-binding molecule, a lower-affinity interaction will be achieved (110). Additionally, the ability to modify native ligand sequences also offers some flexibility in CAR binding. An example is the GM-CSF-CAR, where mutations are introduced into the target-binding domain so that the product has less affinity toward its target (33). By reducing the affinity, a high TAA expression level will be needed to activate the T cell, increasing the selectivity of ligand-based CAR-T therapy against tumor cells. However, previous studies have shown that the affinity of a CAR toward its target is inversely proportional to the activation threshold of the T cell, although the mechanism is not yet fully described (114). Thus, by modifying the ligands, we can generate CARs

that are less affine but induce greater cytotoxic activity on the tumor.

Ultimately, if the potential benefits associated with the ability to prevent and/or reduce tumor evasion of the immune response can be balanced during *in vitro* development and testing in *in vivo* models with a thorough analysis of CAR-T interactions with known and undescribed targets, if, in addition, possible modifications of the ligand used to modulate the cytotoxicity of the CAR-T product can be described, and if immunogenicity issues are resolved, we may be talking about a therapeutic alternative that will potentially discriminate tumor from healthy tissue, be tumor-specific, and reduce the risk of adverse effects (31, 110).

Challenges ahead for ligand-based CAR-T cells

Although the use of natural ligand-based CARs presumably has many advantages, these alternative CAR designs have their own limitations. These include the potential for off-tumor toxicity, unwanted target-associated signaling, and possible interference with the physiological interaction between the endogenous ligand and the target.

As has already been mentioned in this review, the possibility of ligand binding to different targets may lead, on the one hand, to a reduction in the ability to evade the antitumor response, at the same time, it may trigger on-target off-tumor toxicities by increasing the range of possible interactions outside the tumor (4, 21). Although this can be contrasted with the modulation of the interaction affinity, making the therapies more selective, this aspect must be widely considered in the testing phases in animal models. It is worth mentioning that toxic effects are also present in conventional CAR-T therapies, and therefore, it is a pending task for all CAR-T cell therapies.

Another aspect to consider is the possible unwanted signaling that may be generated in the target cell because of the interaction with the ligand fused to the CAR. For example, if the ligand plays a role in cell proliferation and survival, their interaction could increase tumor growth. This is a very preliminary approach that requires further study, but a possible alternative would be to introduce modifications in the ligands that prevent signal transduction in the target, as proposed by Saito et al. (33), who introduced mutations in GM-CSF at residue 21, a key to the functionality of the ligand but maintaining the binding capacity.

Finally, possible interference of endogenous ligands on the interaction of the ligand that is used as the CAR binding moiety should also be considered, generating a competition between both for binding to the target (35). This could result in reduced functionality of the CAR-T cell. Although this is presumed to be

a mild effect, it should be considered individually as a reason for the study depending on the type of ligand.

Conclusion

As described in this review, ligand-based CAR-T cells offer several advantages over CARs containing an scFv domain as a binding moiety. Although they should generate greater toxicity problems due to their ability to recognize multiple off-tumor targets, clear advantages are described: 1) they are less likely to provoke an immune response, as the ligands are derived from natural human sequences and therefore fewer murine regions will be present in the CAR structure; 2) somatic hypermutation phenomena are not necessary, thus reducing anti-idiotypic antibodies; 3) ligand-based CARs are often able to bind to multiple targets, thus reducing the potential for tumor escape; 4) the nature of the ligands and their binding to the receptor allow for a certain tuning capacity that reduces their sensitivity and enables therapies with a greater ability to discriminate between tumor tissues, which tend to overexpress the target, and healthy tissues; and 5) less tonic signaling and longer lasting functionality should be detected associated with a reduction in the probability of ligand aggregation.

Ideally, ligand-based CAR-T therapies appear to be proposals that would improve the safety profile of CAR-T cells and increase cell persistence, maintaining similar levels of response to those achieved with scFv-based CAR-T cells in hematological malignancies and translate these to solid tumors. They should therefore be presented as a significant advance in cancer immunotherapy. Nevertheless, there is still a lack of data and much research to be done to truly elucidate their potential benefit and corroborate their safety profile. Therefore, public and private institutions should invest in the development and testing of these products and technologies. However, there is a conflict of interest, as native ligand sequences cannot be patented like scFv; at the basic research level, it would facilitate the production of therapies, but, for the time being, there is a lack of investment to bring them to clinical trials and to be able to analyze the issues mentioned in this review. It is also particularly important for the scientific community to engage with these types of therapies, as more information is still needed. In conclusion, what emerges from this work is that ligands are intended to offer a future alternative for developing new therapies, but more support and effort will be needed to get results.

References

1. June CH, Sadelain M. Chimeric antigen receptor therapy. *N Engl J Med* (2018) 437(1):64–73. doi: 10.1056/NEJMr1706169
2. Sermer D, Brentjens R. CAR T-cell therapy: Full speed ahead. *Hematol Oncol* (2019) 37 Suppl 1(S1):95–100. doi: 10.1002/hon.2591

Data availability statement

The original contributions presented in the study are included in the article/Supplementary Material. Further inquiries can be directed to the corresponding author.

Author contributions

MJ define the main aspects of the review. AR-C, AG, and MM contributed to the conception and design of the review. AR-C organized the database and wrote the first draft of the manuscript. SB-M and AB-I wrote sections of the manuscript. All authors contributed to manuscript revision, read, and approved the submitted version.

Funding

Thanks to Immunology department (Hospital Clínic de Barcelona) and Institute of Biotechnology and Biomedicine (IBB-UAB) for their help during the writing of this article. This work has been partially supported by grants from the Instituto de Salud Carlos III, Spanish Ministry of Health (FIS PI18/00775, PIC18/00012 and complementary grant for CONCORD-023), Fondo Europeo de Desarrollo Regional (FEDER) “una manera de hacer Europa”, “La Caixa” Foundation (CP042702/LCF/PR/GN18/50310007), and Secretaria d'Universitats i Recerca del Departament d'Empresa i Coneixement, Generalitat de Catalunya, project 2020PANDE00079.

Conflict of interest

The authors declare that the research was conducted in the absence of any commercial or financial relationships that could be construed as a potential conflict of interest.

Publisher's note

All claims expressed in this article are solely those of the authors and do not necessarily represent those of their affiliated organizations, or those of the publisher, the editors and the reviewers. Any product that may be evaluated in this article, or claim that may be made by its manufacturer, is not guaranteed or endorsed by the publisher.

3. Neelapu SS, Tummala S, Kebriaei P, Wierda W, Gutierrez C, Locke FL, et al. Chimeric antigen receptor T-cell therapy - assessment and management of toxicities. *Nat Rev Clin Oncol* (2018) 15(1):47–62. doi: 10.1038/nrclinonc.2017.148
4. Abreu TR, Fonseca NA, Gonçalves N, Moreira JN. Current challenges and emerging opportunities of CAR-T cell therapies. *J Control Release* (2020) 319:246–61. doi: 10.1016/j.jconrel.2019.12.047
5. Morgan RA, Yang JC, Kitano M, Dudley ME, Laurencot CM, Rosenberg SA. Case report of a serious adverse event following the administration of T cells transduced with a chimeric antigen receptor recognizing ERBB2. *Mol Ther* (2010) 18(4):843–51. doi: 10.1038/mt.2010.24
6. Atrash S, Bano K, Harrison B, Abdallah AO. CAR-T treatment for hematological malignancies. *J Invest Med* (2020) 68(5):956–64. doi: 10.1136/jim-2020-001290
7. Ying Z, Huang XF, Xiang X, Liu Y, Kang X, Song Y, et al. A safe and potent anti-CD19 CAR T cell therapy. *Nat Med* (2019) 25. 201925(6):947–53. doi: 10.1038/s41591-019-0421-7
8. Grupp SA, Maude SL, Shaw PA, Aplenc R, Barrett DM, Callahan C, et al. Durable remissions in children with Relapsed/Refractory ALL treated with T cells engineered with a CD19-targeted chimeric antigen receptor (CTL019). *Blood* (2015) 126(23):681–1. doi: 10.1182/blood.V126.23.681.681
9. Neelapu SS, Locke FL, Bartlett NL, Lekakis LJ, Miklos DB, Jacobson CA, et al. Axicabtagene ciloleucel CAR T-cell therapy in refractory Large b-cell lymphoma. *N Engl J Med* (2017) 377(26):2531–44. doi: 10.1056/NEJMoa1707447
10. Maude SL, Laetsch TW, Buechner J, Rives S, Boyer M, Bittencourt H, et al. Tisagenlecleucel in children and young adults with b-cell lymphoblastic leukemia. *N Engl J Med* (2018) 378(5):439–48. doi: 10.1056/NEJMoa1709866
11. Catellà M, Caballero-Baños M, Ortiz-Maldonado V, González-Navarro EA, Suñé G, Antofana-Vidóla A, et al. Point-Of-Care CAR T-cell production (ARI-0001) using a closed semi-automatic bioreactor: Experience from an academic phase I clinical trial. *Front Immunol* (2020) 11. doi: 10.3389/fimmu.2020.00482
12. O'Leary MC, Lu X, Huang Y, Lin X, Mahmood I, Przepiorka D, et al. FDA Approval summary: Tisagenlecleucel for treatment of patients with relapsed or refractory b-cell precursor acute lymphoblastic leukemia. *Clin Cancer Res* (2019) 25(4):1142–6. doi: 10.1158/1078-0432.CCR-18-2035
13. Bouchkouj N, Kasamon YL, de CRA, George B, Lin X, Lee S, et al. FDA Approval summary: Axicabtagene ciloleucel for relapsed or refractory Large b-cell lymphoma. *Clin Cancer Res* (2019) 25(6):1702–8. doi: 10.1158/1078-0432.CCR-18-2743
14. BREYANZI (lisocabtagene maraleucel). FDA. Available at: <https://www.fda.gov/vaccines-blood-biologics/cellular-gene-therapy-products/breyanzi-lisocabtagene-maraleucel>.
15. TECARTUS (brexucabtagene autoleucel). FDA. Available at: <https://www.fda.gov/vaccines-blood-biologics/cellular-gene-therapy-products/tecartus-brexucabtagene-autoleucel>.
16. Ortiz-Maldonado V, Rives S, Castellà M, Alonso-Saladrigues A, Benítez-Ribas D, Caballero-Baños M, et al. CART19-BE-01: A multicenter trial of ARI-0001 cell therapy in patients with CD19 + Relapsed/Refractory malignancies. *Mol Ther* (2021) 29(2):636–44. doi: 10.1016/j.ymthe.2020.09.027
17. ABECMA (idecabtagene vicleucel). FDA. Available at: <https://www.fda.gov/vaccines-blood-biologics/abecma-idecabtagene-vicleucel>.
18. Madduri D, Berdeja JG, Usmani SZ, Jakubowiak A, Agha M, Cohen AD, et al. CARTITUDE-1: Phase 1b/2 study of ciltacabtagene autoleucel, a b-cell maturation antigen-directed chimeric antigen receptor T cell therapy, in Relapsed/Refractory multiple myeloma. *Blood* (2020) 136(Supplement 1):22–25. doi: 10.1182/blood-2020-136307
19. Shah NN, Fry TJ. Mechanisms of resistance to CAR T cell therapy. *Nat Rev Clin Oncol* (2019) 16(6):372–85. doi: 10.1038/s41571-019-0184-6
20. Ruella M, Barrett DM, Kenderian SS, Shestova O, Hofmann TJ, Perazzelli J, et al. Dual CD19 and CD123 targeting prevents antigen-loss relapses after CD19-directed immunotherapies. *J Clin Invest* (2016) 126(10):3814–26. doi: 10.1172/JCI87366
21. Petersen CT, Krenziute G. Next generation CAR T cells for the immunotherapy of high-grade glioma. *Front Oncol* (2019) 69. doi: 10.3389/fonc.2019.00069
22. CAR Signaling Networks. Available at: <https://www.cellsignal.com/pathways/car-signaling-networks>.
23. Karlsson H, Svensson E, Gigg C, Jarvius M, Olsson-Strömberg U, Savoldo B, et al. Evaluation of Intracellular Signaling Downstream Chimeric Antigen Receptors. *PLoS One* (2015) 10(12):e0144787. doi: 10.1371/journal.pone.0144787
24. Wagner DL, Fritsche E, Pulsipher MA, Ahmed N, Hamieh M, Hedge M, et al. Immunogenicity of CAR T cells in cancer therapy. *Nat Rev Clin Oncol* (2021) 18(6):379–93. doi: 10.1038/s41571-021-00476-2
25. Potthoff B, McBlane F, Spindeldreher S, Sickert D. A cell-based immunogenicity assay to detect antibodies against chimeric antigen receptor expressed by tisagenlecleucel. *J Immunol Methods* (2020) 476:112692. doi: 10.1016/j.jim.2019.112692
26. Rafiq S, Hackett CS, Brentjens RJ. Engineering strategies to overcome the current roadblocks in CAR T cell therapy. *Nat Rev Clin Oncol* (2020) 17(3):147–67. doi: 10.1038/s41571-019-0297-y
27. Fujiwara K, Tsunai T, Kusabuka H, Ogaki E, Tachibana M, Okada N. Hinge and transmembrane domains of chimeric antigen receptor regulate receptor expression and signaling threshold. *Cells* (2020) 9(5):1182. doi: 10.3390/cells9051182
28. Hanssens H, Meeus F, De Veirman K, Breckpot K, Devoogdt N. The antigen-binding moiety in the driver's seat of CARs. *Med Res Rev* (2021) 42(1):306–42. doi: 10.1002/med.21818
29. Fabian F, Maucher M, Riester Z, Hudecek M. New targets and technologies for CAR-T cells. *Curr Opin Oncol* (2020) 32(5):510–7. doi: 10.1097/CCO.0000000000000653
30. Huang G, Yu L, Cooper LJ, Hollomon M, Huls H, Kleinerman ES. Genetically modified T cells targeting interleukin-11 receptor α -chain kill human osteosarcoma cells and induce the regression of established osteosarcoma lung metastases. *Cancer Res* (2012) 72(1):271–81. doi: 10.1158/0008-5472.CAN-11-2778
31. Han X, Cinay GE, Zhao Y, Guo Y, Xiaoyang Z, Wang P. Adnectin-based design of chimeric antigen receptor for T cell engineering. *Mol Ther* (2017) 25(11):2466–76. doi: 10.1016/j.ymthe.2017.07.009
32. Wang Y, Xu Y, Li S, Liu J, Xing Y, Xing H, et al. Targeting FLT3 in acute myeloid leukemia using ligand-based chimeric antigen receptor-engineered T cells. *J Hematol Oncol* (2018) 11(1): 60. doi: 10.1186/s13045-018-0603-7
33. Saito S, Hasegawa A, Nagai M, Inada Y, Morokawa H, Nakashima I, et al. Mutated GM-CSF-Based CAR T-cells targeting CD116/CD131 complexes exhibit enhanced anti-tumor effects against acute myeloid leukemia. *Blood* (2020) 136(Supplement 1):36–7. doi: 10.1182/blood-2020-134395
34. Kubo H, Yagyu S, Nakamura K, Yamashima K, Tomida A, Kikuchi K, et al. Development of non-viral, ligand-dependent, EPHB4-specific chimeric antigen receptor T cells for treatment of rhabdomyosarcoma. *Mol Ther - Oncolytics* (2021) 20:646–58. doi: 10.1016/j.omto.2021.03.001
35. Schmidts A, Ormhøj M, Choi BD, Taylor AO, Bouffard AA, Scarfò I, et al. Rational design of a trimeric April-based CAR-binding domain enables efficient targeting of multiple myeloma. *Blood Adv* (2019) 3(21):3248–60. doi: 10.1182/bloodadvances.2019000703
36. Zoine JT, Prince C, Story JY, Branella GM, Lytle AM, Fedanov A, et al. Thrombopoietin-based CAR-T cells demonstrate *in vitro* and *in vivo* cytotoxicity to MPL positive acute myelogenous leukemia and hematopoietic stem cells. *Gene Ther* (2021) 29(5), 1–12. doi: 10.1038/s41434-021-00283-5
37. Chen N, Xu Y, Mou J, Rao Q, Xing H, Tian Z, et al. Targeting of IL-10R on acute myeloid leukemia blasts with chimeric antigen receptor-expressing T cells. *Blood Cancer J* (2021) 11(8):144. doi: 10.1038/s41408-021-00536-x
38. Sauer T, Parikh K, Sharma S, Omer B, Sedloev D, Chen Q, et al. CD70-specific CAR T cells have potent activity against acute myeloid leukemia without HSC toxicity. *Blood* (2021) 138(4):318–30. doi: 10.1182/blood.202008221
39. Bagley SJ, O'Rourke DM. Clinical investigation of CAR T cells for solid tumors: Lessons learned and future directions. *Pharmacol Ther* (2020) 205:107419. doi: 10.1016/j.pharmthera.2019.107419
40. Ma S, Li X, Wang X, Cheng L, Li Z, Zhang C, et al. Current progress in CAR-T cell therapy for solid tumors. *Int J Biol Sci* (2019) 15(12):2548–60. doi: 10.7150/ijbs.34213
41. Zhang B-L, Qin D-Y, Mo Z-M, Li Y, Wei W, Wang Y-S, et al. Hurdles of CAR-T cell-based cancer immunotherapy directed against solid tumors. *Sci China Life Sci* (2016) 59(4):340–8.39. doi: 10.1007/s11427-016-5027-4
42. Du X, Williams DA. Interleukin-11: Review of molecular, cell biology, and clinical use. *Blood* (1997) 89(11):3897–908. doi: 10.1182/blood.V89.11.3897
43. Putoczki TL, Ernst M. IL-11 signaling as a therapeutic target for cancer. *Immunotherapy* (2015) 7(4):441–53. doi: 10.2217/imt.15.17
44. Bishop MW, Janeway KA, Gorlick R. Future directions in the treatment of osteosarcoma. *Curr Opin Pediatr* (2016) 28(1):26–33. doi: 10.1097/MOP.0000000000000298
45. Lewis VO, Ozawa MG, Deavers MT, Wang G, Shintani T, Arap W, et al. The interleukin-11 receptor α as a candidate ligand-directed target in osteosarcoma: Consistent data from cell lines, orthotopic models, and human tumor samples. *Cancer Res* (2009) 69(5):1995–9. doi: 10.1158/0008-5472.CAN-08-4845
46. Zurita AJ, Troncoso P, Cardó-Vila M, Logothetis CJ, Pasqualini R, Arap W. Combinatorial screenings in patients: the interleukin-11 receptor alpha as a candidate target in the progression of human prostate cancer. *Cancer Res* (2004) 64(2):435–9. doi: 10.1158/0008-5472.CAN-03-2675
47. Sachdev E, Gong J, Rimel B, Mita M. Adnectin-targeted inhibitors: rationale and results. *Curr Oncol Rep* (2015) 17(8):35. doi: 10.1007/s11912-015-0459-8

48. Simeon R, Chen Z. *In vitro*-engineered non-antibody protein therapeutics. *Protein Cell* (2018) 9(1):3–14. doi: 10.1007/s13238-017-0386-6
49. Wang Z. ErbB receptors and cancer. *Methods Mol Biol* (2017) 1652:3–35. doi: 10.1007/978-1-4939-7219-7_1
50. Olayioye MA, Neve RM, Lane HA, Hynes NE. The ErbB signaling network: receptor heterodimerization in development and cancer. *EMBO J* (2000) 19(13):3159–67. doi: 10.1093/emboj/19.13.3159
51. Emanuel SL, Engle LJ, Chao G, Zhu R-R, Cao C, Lin Z, et al. A fibronectin scaffold approach to bispecific inhibitors of epidermal growth factor receptor and insulin-like growth factor-I receptor. *mAbs* (2011) 3(1):38–48. doi: 10.4161/mabs.3.1.14168
52. Randolph ME, Cleary MM, Bajwa Z, Svalina MN, Young MC, Mansoor A, et al. EphB4/EphrinB2 therapeutics in rhabdomyosarcoma. *PLoS One* (2017) 12(8): e0183161. doi: 10.1371/journal.pone.0183161
53. Berardi AC, Marsilio S, Rofani C, Salvucci O, Altavista P, Perla FM, et al. Up-regulation of EphB and ephrin-b expression in rhabdomyosarcoma. *Anticancer Res* (2008) 28(2 A):763–9.
54. Noren NK, Lu M, Freeman AL, Koolpe M, Pasquale EB. Interplay between EphB4 on tumor cells and vascular ephrin-B2 regulates tumor growth. *Proc Natl Acad Sci USA* (2004) 101(15):5583. doi: 10.1073/pnas.0401381101
55. Kubo H, Yagyu S, Nakamura K, Yamashima K, Tomida A, Kikuchi K, et al. Development of non-viral, ligand-dependent, EPHB4-specific chimeric antigen receptor T cells for treatment of rhabdomyosarcoma. *Mol Ther - Oncolytics* (2021) 20:646–58. doi: 10.1016/j.omto.2021.03.001
56. Kikuchi K, Tsuchiya K, Otabe O, Gotoh T, Tamura S, Katsumi Y, et al. Effects of PAX3-FKHR on malignant phenotypes in alveolar rhabdomyosarcoma. *Biochem Biophys Res Commun* (2008) 365(3):568–74. doi: 10.1016/j.bbrc.2007.11.017
57. Kottaridis PD, Gale RE, Frew ME, Harrison G, Langabeer SE, Belton AA, et al. The presence of a FLT3 internal tandem duplication in patients with acute myeloid leukemia (AML) adds important prognostic information to cytogenetic risk group and response to the first cycle of chemotherapy: analysis of 854 patients from the united kingdom medical research council AML 10 and 12 trials. *Blood* (2001) 98(6):1752–9. doi: 10.1182/blood.V98.6.1752
58. Riccioni R, Diverio D, Riti V, Buffolino S, Mariani G, Boe A, et al. Interleukin (IL)-3/granulocyte macrophage-colony stimulating factor/IL-5 receptor alpha and beta chains are preferentially expressed in acute myeloid leukaemias with mutated FMS-related tyrosine kinase 3 receptor. *Br J Haematol* (2009) 144(3):376–87. doi: 10.1111/j.1365-2141.2008.07491.x
59. Chen L, Mao H, Zhang J, Chu J, Devine S, Caligiuri MA, et al. Targeting FLT3 by chimeric antigen receptor T cells for the treatment of acute myeloid leukemia. *Leukemia* (2017) 31(8):1830. doi: 10.1038/leu.2017.147
60. Kazi JU, Ronnstrand L. FMS-like tyrosine kinase 3/FLT3: From basic science to clinical implications. *Physiol Rev* (2019) 99(3):1433–66. doi: 10.1152/physrev.00029.2018
61. Grafone T, Palmisano M, Nicci C, Storti S. An overview on the role of FLT3-tyrosine kinase receptor in acute myeloid leukemia: biology and treatment. *Oncol Rev* (2012) 6(1):64–74. doi: 10.4081/oncol.2012.e8
62. Bhattacharya P, Thirupathi M, Elshabrawy H, Alharshawy K, Kumar P, Prabhakar BS. GM-CSF: An immune modulatory cytokine that can suppress autoimmunity. *Cytokine* (2015) 75(2):261–71. doi: 10.1016/j.cyt.2015.05.030
63. Nakazawa Y, Matsuda K, Kurata T, Sueki A, Tanaka M, Sakashita K, et al. Anti-proliferative effects of T cells expressing a ligand-based chimeric antigen receptor against CD116 on CD34(+) cells of juvenile myelomonocytic leukemia. *J Hematol Oncol* (2016) 9(1):27. doi: 10.1186/s13045-016-0256-3
64. López AF, Shannon MF, Hercus T, Nicola NA, Cambareri B, Dottore M, et al. Residue 21 of human granulocyte-macrophage colony-stimulating factor is critical for biological activity and for high but not low affinity binding - *EMBO J*. (1992) 11(3):909–16. doi: 10.1002/j.1460-2075.1992.tb05129.x
65. Ghorashian S, Kramer AM, Onuoha S, Wright G, Bartram J, Richardson R, et al. Enhanced CAR T cell expansion and prolonged persistence in pediatric patients with ALL treated with a low-affinity CD19 CAR. *Nat Med* (2019) 25(9):1408–14. doi: 10.1038/s41591-019-0549-5
66. Shaffer DR, Savoldo B, Yi Z, Chow KKH, Kakarla S, Spencer DM, et al. T Cells redirected against CD70 for the immunotherapy of CD70-positive malignancies. *Blood* (2011) 117(16):4304–14. doi: 10.1182/blood-2010-04-278218
67. Brown CE, Badie B, Barish ME, Weng L, Ostberg JR, Chang WC, et al. Bioactivity and safety of IL13Rα2-redirected chimeric antigen receptor CD8+ T cells in patients with recurrent glioblastoma. *Clin Cancer Res* (2015) 21(18):4062–72. doi: 10.1158/1078-0432.CCR-15-0428
68. Brown CE, Alizadeh D, Starr R, Weng L, Wagner JR, Naranjo A, et al. Regression of glioblastoma after chimeric antigen receptor T-cell therapy. *N Engl J Med* (2016) 375(26):2561–9. doi: 10.1056/NEJMoa1610497
69. Feldman LA. Brain tumor-specific immune cells (IL13Rα2-CAR T cells) for the treatment of leptomeningeal glioblastoma, ependymoma, or medulloblastoma. In: *ClinicalTrials.gov* 2022 (City of Hope Medical Center Duarte, California, United States)
70. Shergalis A, Bankhead 3A, Luesakul U, Muangsin N, Neamati N. Current challenges and opportunities in treating glioblastoma. *Pharmacol Rev* (2018) 70(3):412–45. doi: 10.1124/pr.117.014944
71. Gao L, Wang Y, Ma W, Xing B. Glioblastoma cell differentiation trajectory predicts the immunotherapy response and overall survival of patients. *Aging* (2020) 12(18):18297–321. doi: 10.18632/aging.103695
72. Brown CE, Warden CD, Starr R, Deng X, Badie B, Yuan YC, et al. Glioma IL13Rα2 is associated with mesenchymal signature gene expression and poor patient prognosis. *PLoS One* (2013) 8(10):e77769. doi: 10.1371/journal.pone.0077769
73. Debinski W, Gibo DM, Hulet SW, Connor JR, Gillespie GY. Receptor for interleukin 13 is a marker and therapeutic target for human high-grade gliomas. *Clin Cancer Res* (1999) 5(5):985–90.
74. Thaci B, Brown CE, Binello E, Werbaneth K, Sampath P, Sengupta S. Significance of interleukin-13 receptor alpha 2-targeted glioblastoma therapy. *Neuro Oncol* (2014) 16(10):1304–12. doi: 10.1093/neuonc/nou045
75. Hsi LC, Kundu S, Palomo J, Xu B, Ficco R, Vogelbaum MA, et al. Silencing IL-13Rα2 promotes glioblastoma cell death via endogenous signaling. *Mol Cancer Ther* (2011) 10(7):1149–60. doi: 10.1158/1535-7163.MCT-10-1064
76. Hershey GK. IL-13 receptors and signaling pathways: an evolving web. *J Allergy Clin Immunol* (2003) 111(4):677–90. doi: 10.1067/mai.2003.1333
77. Kahlon KS, Brown C, Cooper LJN, Raubitschek A, Forman SJ, Jensen MC. Specific recognition and killing of glioblastoma multiforme by interleukin 13-zetakine redirected cytolytic T cells. *Cancer Res* (2004) 64(24):9160–6. doi: 10.1158/0008-5472.CAN-04-0454
78. Brown CE, Starr R, Aguilar B, Shami AF, Martinez C, D'Apuzzo M, et al. Stem-like tumor-initiating cells isolated from IL13Rα2 expressing gliomas are targeted and killed by IL13-zetakine-redirected T cells. *Clin Cancer Res* (2012) 18(8):2199–209. doi: 10.1158/1078-0432.CCR-11-1669
79. Forman S. Cellular adoptive immunotherapy using genetically modified T-lymphocytes in treating patients with recurrent or refractory high-grade malignant glioma. In: *ClinicalTrials.gov*. (2011) (City of Hope Comprehensive Cancer Center)
80. Brown CE, Aguilar B, Starr R, Yang X, Chang W-C, Weng L, et al. Optimization of IL13Rα2-targeted chimeric antigen receptor T cells for improved anti-tumor efficacy against glioblastoma. *Mol Ther* (2018) 26(1):31. doi: 10.1016/j.ymthe.2017.10.002
81. Brown CE, Alizadeh D, Starr R, Weng L, Wagner JR, Naranjo A, et al. Genetically modified T-cells in treating patients with recurrent or refractory malignant glioma. In: *ClinicalTrials.gov* (2014) (City of Hope Medical Center)
82. Garrett JT, Olivares G, Rinehart C, Granja-Ingram ND, Sánchez V, Chakrabarty A, et al. Transcriptional and posttranslational up-regulation of HER3 (ErbB3) compensates for inhibition of the HER2 tyrosine kinase. *PNAS* (2011) 108(12):5021–6. doi: 10.1073/pnas.1016140108
83. Davies DM, Foster J, van der Stegen S, Parente-Pereria A, Chiapero-Stanke L, Delinasios GJ, et al. Flexible targeting of ErbB dimers that drive tumorigenesis by using genetically engineered T cells. *Mol Med* (2012) 18(1):565–76. doi: 10.2119/molmed.2011.00493
84. Klampatsa A, Achkova DY, Davies DM, Parente-Pereira AC, Woodman N, Rosekilly J, et al. Intracavitary 'T4 immunotherapy' of malignant mesothelioma using pan-ErbB re-targeted CAR T-cells. *Cancer Lett* (2017) 393:52–9. doi: 10.1016/j.canlet.2017.02.015
85. Parente-Pereira AC, Whilding LM, Brewig N, Stegen SJC, Davies DM, Wilkie S, et al. Synergistic chemioimmunotherapy of epithelial ovarian cancer using ErbB-retargeted T cells combined with carboplatin. *J Immunol* (2013) 191(5):2437–45. doi: 10.4049/jimmunol.1301119
86. Wingens M, Walma T, Van Ingen H, Stortelers C, Van Leeuwen JEM, Van Zoelen EJJ, et al. Structural analysis of an epidermal growth factor/transforming growth factor-α chimera with unique ErbB binding specificity. *J Biol Chem* (2003) 278(40):39114–23. doi: 10.1074/jbc.M305603200
87. Stortelers C, Van de Poll MLM, Lenferink AEG, Gadellaa MM, Van Zoelen C, Van Zoelen EJJ. Epidermal growth factor contains both positive and negative determinants for interaction with ErbB-2/ErbB-3 heterodimers. *Biochemistry* (2002) 41(13):4292–301. doi: 10.1021/bi012016n
88. Wilkie S, Burbridge SE, Chiapero-Stanke L, Pereira ACP, Cleary S, van der Stegen SJC, et al. Selective expansion of chimeric antigen receptor-targeted T-cells with potent effector function using interleukin-4. *J Biol Chem* (2010) 285(33):25538–44. doi: 10.1074/jbc.M110.127951
89. Van Der Stegen SJ, Davies DM, Wilkie S, Foster J, Sosabowski JK, Burnet J, et al. Preclinical *in vivo* modeling of cytokine release syndrome induced by ErbB-retargeted human T cells: identifying a window of therapeutic opportunity? *J Immunol* (2013) 191(9):4589–98. doi: 10.4049/jimmunol.1301523

90. Van Schalkwyk MC, Papa SE, Jeannon JP, Urbano TG, Spicer JF, Maher J. Design of a phase I clinical trial to evaluate intratumoral delivery of ErbB-targeted chimeric antigen receptor T-cells in locally advanced or recurrent head and neck cancer. *Hum Gene Ther Clin Dev* (2013) 24(3):134–42. doi: 10.1089/humc.2013.144
91. Papa S, van Schalkwyk M, Maher J. Clinical evaluation of ErbB-targeted CAR T-cells, following intracavity delivery in patients with ErbB-expressing solid tumors. *Methods Mol Biol* (2015) 1317:365–82. doi: 10.1007/978-1-4939-2727-2_21
92. Palumbo A, Anderson K. Multiple myeloma. *N Engl J Med* (2011) 364(11):1046–60. doi: 10.1056/NEJMra1011442
93. Cho SF, Lin L, Xing L, Li Y, Yu T, Andersin KC, et al. BCMA-targeting therapy: Driving a new era of immunotherapy in multiple myeloma. *Cancers (Basel)* (2020) 12(6):1–29. doi: 10.3390/cancers12061473
94. Kazandjian D. Multiple myeloma epidemiology and survival: A unique malignancy. *Semin Oncol* (2016) 43(6):676–81. doi: 10.1053/j.seminoncol.2016.11.004
95. Kumar SK, Rajkumar SV, Dispenzieri A, Lacy MQ, Hayman SR, Buadi FK, et al. Improved survival in multiple myeloma and the impact of novel therapies. *Blood* (2008) 111(5):2516–20. doi: 10.1182/blood-2007-10-116129
96. Ali SA, Shi V, Maric I, Wang M, Stroncek DF, Rose JJ, et al. T Cells expressing an anti-b-cell maturation antigen chimeric antigen receptor cause remissions of multiple myeloma. *Blood* (2016) 128(13):1688–700. doi: 10.1182/blood-2016-04-711903
97. Raje N, Berdeja J, Lin Y, Siegel D, Jagannath S, Deepu M, et al. Anti-BCMA CAR T-cell therapy bb2121 in relapsed or refractory multiple myeloma. *N Engl J Med* (2019) 380(18):1726–37. doi: 10.1056/NEJMoa1817226
98. Lee L, Draper B, Philip B, Chin M, Galas-Filipowicz D, et al. An APRIL-based chimeric antigen receptor for dual targeting of BCMA and TACI in multiple myeloma. *Blood* (2018) 131(7):746–58. doi: 10.1182/blood-2017-05-781351
99. Patel DR, Wallweber HJA, Yin J, Shriver SK, Marsters SA, Gordon NC, et al. Engineering an APRIL-specific B cell maturation antigen *. *J Biol Chem* (2004) 279(16):16727–35. doi: 10.1074/jbc.M312316200
100. Hymowitz SG, Patel DR, Wallweber HJA, Runyon S, Yan M, Yin JP, et al. Structures of APRIL-receptor complexes: Like bcma, taci employs only a single cysteine-rich domain for high affinity ligand binding. *J Biol Chem* (2005) 280(8):7218–27. doi: 10.1074/jbc.M411714200
101. Philip B, Kokalaki E, Mekkaoui L, Thomas S, Straathof K, Flutter B, et al. A highly compact epitope-based marker/suicide gene for easier and safer T-cell therapy. *Blood* (2014) 124(8):1277–87. doi: 10.1182/blood-2014-01-545020
102. Philip B, Kokalaki E, Mekkaoui L, Thomas S, Straathof K, Flutter B, et al. A highly compact epitope-based marker/suicide gene for easier and safer T-cell therapy. *Blood* (2014) 124(8):1277–87. doi: 10.1182/blood-2014-01-545020
103. Ellebrecht CT, Bhoj VG, Nace A, Choi EJ, Mao X, Cho MJ, et al. Reengineering chimeric antigen receptor T cells for targeted therapy of autoimmune disease. *Sci* (2016) 353(6295):179–84. doi: 10.1126/science.aaf6756
104. Bewarder M, Thurner L, Neumann F, Fadl N, Regitz E, Kemele M, et al. BAR-bodies: B-cell receptor antigens as the targeting moiety of antibodies in substitution for the variable region of heavy and light chains. *Blood* (2018) 132(Supplement 1):2940–0. doi: 10.1182/blood-2018-99-115348
105. Yasunaga M. Antibody therapeutics and immunoregulation in cancer and autoimmune disease. *Semin Cancer Biol* (2020) 64:1–12. doi: 10.1016/j.semcancer.2019.06.001
106. Bewarder M, Kiefer M, Will H, Olesch K, Moelle C, Stilgenbauer S, et al. The B-cell receptor autoantigen LRPAP1 can replace variable antibody regions to target mantle cell lymphoma cells. *HemaSphere* (2021) 5(8):E620. doi: 10.1097/HS9.0000000000000620
107. Thurner L, Hartmann S, Fadl N, Kemele M, Bock T, Bewarder M, et al. LRPAP1 is a frequent proliferation-inducing antigen of BCRs of mantle cell lymphomas and can be used for specific therapeutic targeting. *Leuk* (2018) 331.201833(1):148–58. doi: 10.1038/s41375-018-0182-1
108. Lionaki S, Panagiotellis K, Iniotaki A, Boletis JN. Incidence and clinical significance of de novo donor specific antibodies after kidney transplantation. *Clin Dev Immunol* (2013) 2013:849835. doi: 10.1155/2013/849835
109. Loupy A, Hill GS, Jordan SC. The impact of donor-specific anti-HLA antibodies on late kidney allograft failure. *Nat Rev Nephrol* (2012) 8(6):348–57. doi: 10.1038/nrneph.2012.81
110. Murad JM, Graber DJ, Sentman CL. Advances in the use of natural receptor- or ligand-based chimeric antigen receptors (CARs) in hematologic malignancies. *Best Pract Res Clin Haematol* (2018) 31(2):176–83. doi: 10.1016/j.beha.2018.03.003
111. Nieba L, Honegger A, Krebber C, Plückthun A. Disrupting the hydrophobic patches at the antibody variable/constant domain interface: improved *in vivo* folding and physical characterization of an engineered scFv fragment. *Protein Eng Des Sel* (1997) 10(4):435–44. doi: 10.1093/protein/10.4.435
112. Zah E, Lin M-Y, Silva-Benedict A, Jensen MC, Chen YY. T cells expressing CD19/CD20 bispecific chimeric antigen receptors prevent antigen escape by malignant B cells. *Cancer Immunol Res* (2016) 4(6):498–508. doi: 10.1158/2326-6066.CIR-15-0231
113. Ahmad ZA, Yeap SK, Ali AM, Ho WY, Alitheen NBM, Hamid M. scFv antibody: Principles and clinical application. *Clin Dev Immunol* (2012) 2012:980250. doi: 10.1155/2012/980250
114. Chmielewski M, Hombach A, Heuser C, Adams GP, Abken H. T Cell activation by antibody-like immunoreceptors: Increase in affinity of the single-chain fragment domain above threshold does not increase T cell activation against antigen-positive target cells but decreases selectivity. *J Immunol* (2004) 173(12):7647–53. doi: 10.4049/jimmunol.173.12.7647

Glossary

CAR	chimeric antigen receptor
TA	tumor antigen
TAA	tumor-associated antigen
BALL	B-cell acute lymphoblastic leukemia
FDA	Food and Drug Administration
EMA	European Medicines Agency
BCMA	B-cell maturation antigen
AEMPS	Agencia Española del Medicamento y Productos Sanitarios (Spanish drug agency)
scFv	single-chain variable fragment
moAb	monoclonal antibody
OS	osteosarcoma
EGFR	epidermal growth factor receptor
FLT3L	FMS-like tyrosine kinase 3 ligand
FLT3	FMS-like tyrosine kinase 3
AML	acute myeloid leukemia
GM-CSF	granulocyte-monocyte colony-stimulating factor
GMR	granulocyte-monocyte colony-stimulating factor receptor
JMML	juvenile myelomonocytic leukemia
TPO	thrombopoietin
MPLR	myeloproliferative leukemia receptor
EPHB4	ephrin type-B receptor 4
RMS	rhabdomyosarcoma
APRIL	a proliferation-inducing ligand
TACI	transmembrane activator and calcium-modulator and cyclophilin ligand interactor
MM	multiple myeloma
HNSCC	head and neck squamous cell carcinoma
10Fn3	10th type III domain of human fibronectin
TNBC	triple-negative breast cancer
ITD	internal tandem duplication
TKD	tyrosine kinase domain
WT	wild type
CNS	central nervous system
GBM	glioblastoma multiforme
GSC	stem-like cancer-initiating cell
IL13Ra2	interleukin-13 receptor $\alpha 2$
TK	tyrosine kinase
EOC	epithelial ovarian cancer
EGF	epidermal growth factor
TGF- α	transforming growth factor α
CRS	cytokine release syndrome
PC	plasma cell
PI	proteasome inhibitor
IMiD	immunomodulatory drug
RRMM	relapsed/refractory multiple myeloma
TNF	tumor necrosis factor
CAAR	chimeric autoantibody receptor

Continued

BAR	B-cell receptor antigen for reverse targeting
sIg	surface immunoglobulin
BCR	B-cell receptor
PV	pemphigus vulgaris
DLBCL	diffuse large B-cell lymphoma
MCL	mantle cell lymphoma
CHAR	chimeric HLA antibody receptor
DSA	donor-specific antibody
HAMA	human anti-mouse antibody
VH	variable heavy chain
VL	variable light chain

(Continued)



OPEN ACCESS

EDITED AND REVIEWED BY
Catherine Sautes-Fridman,
INSERM U1138 Centre de Recherche
des Cordeliers (CRC), France

*CORRESPONDENCE
Manel Juan
mjjuan@clinic.cat

SPECIALTY SECTION
This article was submitted to
Cancer Immunity
and Immunotherapy,
a section of the journal
Frontiers in Immunology

RECEIVED 23 October 2022
ACCEPTED 09 November 2022
PUBLISHED 21 November 2022

CITATION
Ramírez-Chacón A, Betriu-Méndez S,
Bartoló-Ibars A, González A, Martí M
and Juan M (2022) Corrigendum:
Ligand-based CAR T-cell: Different
strategies to drive T-cells in future
new treatments.
Front. Immunol. 13:1078003.
doi: 10.3389/fimmu.2022.1078003

COPYRIGHT
© 2022 Ramírez-Chacón,
Betriu-Méndez, Bartoló-Ibars, González,
Martí and Juan. This is an open-access
article distributed under the terms of
the [Creative Commons Attribution
License \(CC BY\)](#). The use, distribution
or reproduction in other forums is
permitted, provided the original
author(s) and the copyright owner(s)
are credited and that the original
publication in this journal is cited, in
accordance with accepted academic
practice. No use, distribution or
reproduction is permitted which does
not comply with these terms.

Corrigendum: Ligand-based CAR T-cell: Different strategies to drive T-cells in future new treatments

Alejandro Ramírez-Chacón^{1,2}, Sergi Betriu-Méndez^{3,4},
Ariadna Bartoló-Ibars^{3,4}, Azucena González^{3,4,5}, Mercè Martí^{1,2}
and Manel Juan^{3,4,5*}

¹Immunology Unit, Department of Cellular Biology, Physiology and Immunology, Universitat Autònoma de Barcelona (UAB), Cerdanyola del Vallès, Spain, ²Laboratory of Cellular Immunology, Institute of Biotechnology and Biomedicine (IBB), Cerdanyola del Vallès, Spain, ³Immunology Department, Hospital Clínic de Barcelona, Centre de Diagnòstic Biomèdic (CDB), Barcelona, Spain, ⁴Immunology Department, Institut d'Investigacions Biomèdiques August Pi i Sunyer (IDIBAPS) –Fundació Clínic per a la Recerca Biomèdica (FCRB) Universitat de Barcelona (UB), Barcelona, Spain, ⁵Immunology Department, Hospital Sant Joan de Déu, Barcelona, Spain

KEYWORDS

T cells, chimeric antigen receptor (CAR), ligands, receptor, antigen, CAAR, BAR

A corrigendum on

Ligand-based CAR-T cell: Different strategies to drive T cells in future new treatments

by Ramírez-Chacón A, Betriu-Méndez S, Bartoló-Ibars A, González A, Martí M and Juan M (2022) *Front. Immunol.* 13:932559. doi: 10.3389/fimmu.2022.932559

In the published article, there was an error in the Funding statement. Missing grant supporting this manuscript. The correct Funding statement appears below.

Funding

“Thanks to Immunology department (Hospital Clínic de Barcelona) and Institute of Biotechnology and Biomedicine (IBB-UAB) for their help during the writing of this article. This work has been partially supported by grants from the Instituto de Salud Carlos III, Spanish Ministry of Health (FIS PI18/00775, PIC118/00012 and complementary grant for CONCORD-023), Fondo Europeo de Desarrollo Regional (FEDER) “una manera de hacer Europa”, “La Caixa” Foundation (CP042702/LCF/PR/GN18/50310007), and Secretaria d'Universitats i Recerca del Departament d'Empresa i Coneixement, Generalitat de Catalunya, project 2020PANDE00079.”

The authors apologize for this error and state that this does not change the scientific conclusions of the article in any way. The original article has been updated.

Publisher's note

All claims expressed in this article are solely those of the authors and do not necessarily represent those of their affiliated

organizations, or those of the publisher, the editors and the reviewers. Any product that may be evaluated in this article, or claim that may be made by its manufacturer, is not guaranteed or endorsed by the publisher.



OPEN ACCESS

EDITED BY

Catherine Sautes-Fridman,
INSERM U1138 Centre de Recherche
des Cordeliers (CRC), France

REVIEWED BY

Daniel Carvajal,
Universidad del Desarrollo, Chile
Emanuel Raschi,
University of Bologna, Italy

*CORRESPONDENCE

Zhixia Zhao
zhixia.1002@163.com
Zhuoling An
anzhuoling@163.com

[†]These authors have contributed
equally to this work and share
first authorship

[‡]These authors have contributed
equally to this work and share
the last authorship

SPECIALTY SECTION

This article was submitted to
Cancer Immunity
and Immunotherapy,
a section of the journal
Frontiers in Oncology

RECEIVED 27 May 2022

ACCEPTED 12 August 2022

PUBLISHED 12 September 2022

CITATION

Hu Y, Lu W, Tang B, Zhao Z and An Z
(2022) Urinary incontinence as a
possible signal of neuromuscular
toxicity during immune checkpoint
inhibitor treatment: Case
report and retrospective
pharmacovigilance study.
Front. Oncol. 12:954468.
doi: 10.3389/fonc.2022.954468

COPYRIGHT

© 2022 Hu, Lu, Tang, Zhao and An. This
is an open-access article distributed
under the terms of the [Creative
Commons Attribution License \(CC BY\)](#).
The use, distribution or reproduction
in other forums is permitted, provided
the original author(s) and the
copyright owner(s) are credited and
that the original publication in this
journal is cited, in accordance with
accepted academic practice. No use,
distribution or reproduction is
permitted which does not comply with
these terms.

Urinary incontinence as a possible signal of neuromuscular toxicity during immune checkpoint inhibitor treatment: Case report and retrospective pharmacovigilance study

Yizhang Hu^{1†}, Wenchao Lu^{2†}, Borui Tang²,
Zhixia Zhao^{3*‡} and Zhuoling An^{2*‡}

¹Department of Oncology, Beijing Chao-yang Hospital, Capital Medical University, Beijing, China,

²Department of Pharmacy, Beijing Chaoyang Hospital, Capital Medical University, Beijing, China,

³Department of Pharmacy Clinical Trial Research Center, China-Japan Friendship Hospital,
Beijing, China

Background: Immune checkpoint inhibitors (ICIs) are associated with different immune-related adverse events (irAEs), but there is limited evidence regarding the association between urinary incontinence and ICIs.

Methods: We described the case of a patient experiencing urinary incontinence who later experienced a series of irAEs such as myocarditis, myositis, and neurologic diseases while on ICI treatment in our hospital. In addition, we queried the Food and Drug Administration (FDA) Adverse Event Reporting System (FAERS) from the third quarter of 2010 to the third quarter of 2020 to perform a retrospective study to characterize the clinical features of urinary incontinence associated with ICIs.

Result: In the FAERS study, 59 cases of ICI-related urinary incontinence were retrieved, and approximately 32.2% of the cases were fatal. Combination therapy with nervous system drugs and age >80 years old were the significant risk factors for fatal outcomes. Among these cases of ICI-related urinary incontinence, 40.7% (n = 24) occurred concomitantly with other adverse events, especially, neurological (fifteen cases), cardiovascular (seven cases), musculoskeletal (six cases), and urological disorders (five cases). Five cases had an overlapping syndrome similar to our case report, including one case of myasthenia gravis with myocarditis and another of myasthenic syndrome with polymyositis.

Conclusion: ICI-related urinary incontinence might be a signal of fatal neuromuscular irAEs, especially when it occurs concomitantly with ICI-associated neuromuscular–cardiovascular syndrome. Clinicians should be

aware of the occurrence of urinary incontinence to identify potentially lethal irAEs in the early phase.

KEYWORDS

urinary incontinence, immune-related adverse events, FAERS, neuromuscular adverse events, immune checkpoint inhibitors

Introduction

Immune checkpoint inhibitors (ICIs) have revolutionized cancer therapy and improved clinical outcomes in multiple cancer types (1). To date, approved ICIs include anti-cytotoxic T-lymphocyte-associated antigen 4 (CTLA-4; ipilimumab), anti-programmed cell death-protein-1 (PD-1; pembrolizumab, nivolumab, cemiplimab), and anti-programmed cell death-ligand 1 (PD-L1) therapies (atezolizumab, durvalumab, avelumab) (2). Despite their important clinical benefits, ICIs cause a unique spectrum of side effects termed immune-related adverse events (irAEs). These events can affect many organ systems, and they can be fulminant or even fatal in some cases (3).

During routine surveillance, we identified a patient with unusual urinary incontinence symptoms during immunotherapy treatment. In addition, urinary incontinence did not develop as an isolated adverse effect. A more detailed medical examination revealed that the patient experienced a series of irAEs such as myocarditis, myositis, and neurological diseases. Urinary incontinence is the involuntary leakage of urine (4), and its pathogenic causes include neuromuscular diseases, inflammation, or infection of the bladder or urethral wall and bladder outlet obstruction (5). In addition, the neural control of the lower urinary tract and pelvic floor musculature is essential for urine storage. Therefore, the damage of these areas is one of the leading causes of urinary incontinence (5). ICIs can damage the function of nerves and muscles *via* lymphocyte-rich infiltration, antibody-mediated inflammation, and sterile inflammation (6). No study has demonstrated an association between urinary incontinence and ICI treatment. Conversely, ICI-related neuromuscular adverse events, such as ICI-related myelitis, Guillain-Barré syndrome (GBS), and myasthenia gravis-myositis syndrome, were reported to be linked to urinary incontinence symptoms (7–9). This suggests that urinary incontinence is secondary to irAEs.

To date, there has been limited research investigating the association between ICIs and urinary incontinence. We only identified one similar case report from the published literature (7). Recently, the FDA Adverse Event Reporting System (FAERS) database has been increasingly utilized to quickly detect rare and unexpected adverse events. Therefore, we

reviewed the reported cases of urinary incontinence after ICI treatment and described the concomitant irAEs and characteristics by retrospectively analyzing the FAERS database.

Case report

A 65-year-old woman was diagnosed with clinical stage IIIC (cT3N3M0) pulmonary adenocarcinoma 2 months prior to hospitalization with no actionable somatic mutation and a tumoral cell PD-L1 status of $\geq 50\%$. She had opted to join a clinical trial program that included immunotherapy, anti-vascular endothelial growth factor (VEGF) therapy, and chemotherapy. She received two cycles of treatment consisting of the anti-PD-1 antibody (HLX10 4.5 mg/kg every 3 weeks), anti-VEGF monoclonal antibody (HLX04 bevacizumab biosimilar, 15 mg/kg every 3 weeks), and carboplatin (area under the concentration–time curve = 5 mg/ml/min) plus pemetrexed (500 mg/m²). The initial examination was unremarkable. After the first cycle of treatment, she experienced a liver injury. After oral hepatic protectants (bicyclol, polyene phosphatidylcholine capsules) were used, her symptoms significantly improved.

During the two-cycle treatment, the patient displayed sudden urinary incontinence after her body position changed. The severity of urinary incontinence required the patient to use sanitary napkins to move about in the ward. Subsequently, the patient exhibited mild fatigue. The neurological examination was unremarkable, and no evidence of tenderness to the palpation of major muscle groups, decreased muscle strength, or ptosis were noted. Notable laboratory abnormalities are listed in [Supplementary Table 1](#).

Electrocardiogram (ECG) demonstrated a normal sinus rhythm with a slight decrease in the R wave amplitude. Echocardiography, cardiac magnetic resonance, brain magnetic resonance imaging, abdominal and pelvic computed tomography (CT), and kidney/bladder ultrasound revealed normal findings. Chest CT revealed increased pericardial thickness. Needle electromyography uncovered left external anal sphincter neurogenic impairment ([Supplementary Table 2](#)). In addition, nerve conduction studies revealed peripheral neurogenic impairment, which may have involved

the motor nerves with demyelination (Supplementary Table 3). This finding is consistent with previous clinical observations that the principal manifestation of ICI-related neuropathy is motor nerve demyelination (10). A urodynamic study (UDS) found a reduction in intraurethral pressure. A repetitive nerve stimulation study suggested the abnormality of the neuromuscular junction (Supplementary Table 4). Notably, AChR antibody testing was positive. These results supported a diagnosis of myasthenia gravis or Lambert–Eaton myasthenic syndrome. Additionally, based on her elevated creatine kinase (CK), myocardial enzyme, and cardiac troponin I (cTnI) and the changes of ECG data, she was suspected to have myositis and myocarditis. All of these findings suggested that the patient had developed an overlap of urinary incontinence–myasthenia gravis–neuropathy–myositis–myocarditis-like syndrome.

Then, the patient was administered intravenous methylprednisolone 80 mg/day for 2 days. Her CK and CK-MB isoenzyme (CK-MB) levels were decreased slightly by treatment, but her cTnI levels increased rapidly. Subsequently, the patient received steroid pulse therapy (methylprednisolone 500 mg) and intravenous immune globulin 40 mg/kg/day for 3 days. Her symptom of incontinence improved, and her CK, CK-MB, and cTnI levels were decreased by this treatment (Figure 1). During the process of glucocorticoid tapering (from 80 to 40 mg/day), her myocardial enzyme and cTnI levels rose again (Figure 1), and the patient developed new-onset hoarseness. Mycophenolate mofetil (MMF) 1,000 mg/day was thus prescribed. Following this treatment, the patient's CK-MB and cTnI gradually decreased to normal, and urinary incontinence was relieved. MMF and corticosteroids were discontinued at 11 and 14 weeks following symptom onset, respectively. The radiographic evaluation after two cycles of treatment revealed partial tumor remission. Six months after the last antitumor treatment, retreatment with the

original chemotherapy regimen (carboplatin plus pemetrexed) combined with bevacizumab was performed because of lesion progression. The tumor was effectively controlled again, and urinary incontinence did not recur.

Overall, we suspected that urinary incontinence syndrome was caused by ICI therapy for several reasons. First, there was a temporal association between ICI treatment and the occurrence of urinary incontinence. Second, the patient underwent urinalysis, urine culture, ultrasound, and UDS, and the results did not uncover other potential causes of urinary incontinence. Third, the patient was retreated with the original chemotherapy regimen (carboplatin plus pemetrexed) combined with bevacizumab, and urinary incontinence did not recur.

However, the electrodiagnostic data and clinical manifestations of neuromuscular toxicity were atypical in this case, which could potentially have several explanations. First, we identified the disease in an extremely early stage, and neither the patient's symptoms nor the electrodiagnostic data were typical at this stage. Second, the patient was treated with high-dose steroids and intravenous immunoglobulin in an extremely early stage; therefore, the disease was relieved to a certain extent before electrodiagnostic testing. Finally, the patient had overlapping neuromuscular toxicity, and different diseases interacted with each other, which might have affected the electrodiagnostic data.

Descriptive analysis based on the FDA adverse event reporting system database

Definition and design

We downloaded FAERS data files from the third quarter of 2010 to the third quarter of 2020. We used generic and brand

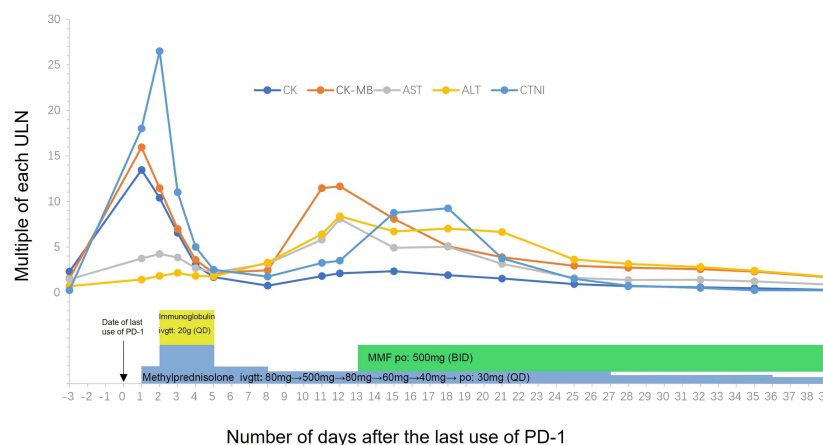


FIGURE 1
Temporal changes of creatinine kinase (CK), cardiac troponin I (cTnI) and myocardial enzyme (AST/ALT/CK-MB). Treatments performed are indicated below the graph. MMF, Mycophenolate Mofetil.

names to identify drugs, including anti-CTLA-4 (ipilimumab), anti-PD-1 (pembrolizumab, nivolumab, cemiplimab), and anti-PD-L1 therapies (atezolizumab, avelumab, durvalumab). We identified cases of urinary incontinence using the preferred term “urinary incontinence” according to the Medical Dictionary for Regulatory Activities (version 23.0). Duplicate reports were excluded from our analysis. In the deduplication process, we extracted the latest (most recent) case version from all available cases based on the case ID, case initial/follow-up code (“I” or “F”), case event date, age, sex, and reporting country (11). We retained the most current case version and removed all others.

To summarize the clinical characteristics of cases of ICI-related urinary incontinence, we analyzed general information, patient characteristics, indications for ICIs, outcomes (serious events defined as death, hospitalization, life-threatening events, or disability), the role of ICIs (primary suspected, secondary suspected, and concomitant), and ICI treatment strategy (monotherapy or combination therapy). Additionally, we analyzed the drugs used concomitantly with ICIs, such as nervous system drugs (including benzodiazepines, antipsychotics, antiepileptics, and antidepressants), α -adrenoceptor antagonists, and diuretics, which have been reported to increase the risk of urinary incontinence (12). We further analyzed the concurrent adverse events (AEs), especially neuromuscular toxicity and cardiotoxicity, which also occurred in our case. Clinical characteristics were described using quantities and proportions for qualitative variables and medians (with the interquartile range) for quantitative variables. We also performed a subgroup analysis to explore the differences in the clinical characteristics of severe and non-severe ICI-associated urinary incontinence. Proportions were compared using Pearson’s chi-square or Fisher’s exact test. Data were analyzed using SPSS (v22.0; IBM Corp, Armonk, NY, USA), and statistical significance was indicated by $p < 0.05$.

Results of the FDA adverse event reporting system analysis

Our analysis of the FAERS database captured 96,814 AEs related to ICI treatment, including 59 cases of urinary incontinence (45, 5, 2, and 7 events associated with anti-PD-1, anti-PD-L1, anti-CTLA-4, and combination therapies, respectively). Table 1 presents the characteristics of patients with ICI-related urinary incontinence. Most cases of ICI-related urinary incontinence occurred in patients with lung cancer and melanoma (35.6% and 23.7%, respectively), and most cases were reported in the Americas (40 [67.8%]). The mean age of the affected patients was 70.0 ± 11.3 years. Meanwhile, patients older than 80 years were more likely to experience fatal outcomes (Table 2, Fisher’s exact test, $p = 0.003$). Urinary incontinence was more common in men than in women (54.2% versus 44.1%). The results of time-to-onset (TTO) analysis for urinary

incontinence associated with ICI are also summarized in Table 1. The median TTO was 16 days (interquartile range = 6–82), suggesting that urinary incontinence most commonly occurred in the early period.

Our study identified patients with urinary incontinence who experienced poor outcomes. Approximately 32.2% of these events resulted in death, 6.8% were life-threatening, and 20.3% led to hospitalization. Most patients with ICI-related urinary incontinence were treated with polypharmacy. In total, 23.7% (14/59) of cases involved the concurrent use of drugs influencing bladder function, and the most common concurrent drugs were nervous system drugs (benzodiazepines, antipsychotics, antidepressants, antiepileptic), followed by α -adrenoceptor antagonists and diuretics. In cases involving concurrent nervous system drug use, the fatality rate was even higher, at 72.7% (8/11). In an analysis of fatal versus non-fatal cases (Table 2), we confirmed that patients who concurrently used nervous system drugs were more likely to have fatal outcomes (Fisher’s exact test, $p = 0.003$).

Considering the possible confounding factors, we also checked the overall anticancer regimen in our case and other risk factors of urinary incontinence recorded in the FAERS database. In total, 16.9% (10/59) of the cases were treated with combination therapy featuring vascular endothelial growth factor receptor (VEGFR) inhibitors and/or chemotherapy. Specifically, 10.2% (6/59) were treated with chemotherapy, 5% (3/59) were treated with VEGFR inhibitors, and only 1.7% (1/59) were treated with both drugs.

Among the cases of ICI-related urinary incontinence, 39.0% ($n = 23$) occurred concurrently with other AEs, especially neurological disorders ($n = 15$ [25.4%]) such as myasthenia gravis (three cases) and myasthenic syndrome (one case). In addition, the most commonly reported concurrent symptoms were neuromuscular systems, including fatigue, muscular weakness, ptosis, hoarseness, and dysphagia, which were found in 86.4% (51/59) of the cases.

Similar to the aforementioned case report, in the FAERS database, we also found five cases of ICI-associated neuromuscular–cardiovascular overlapping syndrome. The neuromuscular AEs mainly included myasthenia gravis, myasthenic syndrome, and myositis. Case 5 was not diagnosed with myasthenia gravis/myasthenic syndrome, but ptosis was the specific symptom. The cardiovascular disorders mainly included myocarditis, cardiac arrhythmias, and pericardial effusion. In addition, the prognosis was poor, and the outcomes included three fatalities and two hospitalizations. Table 3 presents the descriptive characteristics of these reports.

Discussion

In our study, we reported a case of urinary incontinence after ICI treatment in a patient with non-small cell lung cancer who

TABLE 1 The characteristics of patients with immune checkpoint inhibitor (ICI)-related urinary incontinence.

Characteristics	n (%)	Characteristics	n (%)
Total AE (ICIs)	96814	ICI Treatment Strategy	
Total urinary incontinence	59	Monotherapy	
Occurred Region		PD-1 inhibitor	45 (76.3)
Americas	40 (67.8)	Nivolumab	23 (39.0)
Europe	9 (15.2)	Pembrolizumab	22 (37.3)
Asia	4 (6.8)	PD-L1 inhibitor	5 (8.5)
Others	6 (10.2)	Durvalumab	3 (5.1)
Reporting Year		Avelumab	1 (1.7)
2020	13 (22.0)	Atezolizumab	1 (1.7)
2019	8 (13.6)	CTLA-4 inhibitor	
2018	17 (28.8)	Ipilimumab	2 (3.4)
2017	13 (22.0)	Combination Therapy	
2016 and earlier	8 (13.6)	Ipilimumab + nivolumab	7 (11.9)
Reporter Type		Concurrent Drugs	14(23.7)
Healthcare professional	37 (62.7)	Single Concurrent Drugs	8(13.5)
Non-healthcare professional	21 (35.6)	α -Adrenoceptor antagonists	3 (5.1)
Null	1 (1.7)	Nervous system drug	4 (6.7)
Gender		Diuretics	1 (1.7)
Male	32 (54.2)	Multiple Concurrent Drugs	6(10.2)
Female	26 (44.1)	α -Adrenoceptor antagonists +	1 (1.7)
Null	1 (1.7)	Nervous system drug	
Age (n=49)		Multiple nervous system drugs	3 (5.1)
Mean, SD	70.0 \pm 11.30	Diuretics +	2 (3.4)
Range	41-87	Nervous system drug	
Indication for ICI		Concurrent AEs	24 (40.7)
Lung cancer	21 (35.6)	Neurological AEs	15
Melanoma	14 (23.7)	Encephalitis	4 (6.8)
Renal cancer	6 (10.2)	Myasthenia gravis/	
Glioblastoma	3 (5.1)	Myasthenic syndrome	4 (6.8)
Breast cancer	2 (3.4)	Facial paralysis	3 (5.1)
Ovarian cancer	2 (3.4)	Neuropathy	2 (3.4)
Cholangiocarcinoma	2 (3.4)	Encephalopathy	2 (3.4)
Pancreatic carcinoma	1(1.7)	Nervous system disorder	1 (1.7)
Colon cancer	1(1.7)	Cardiovascular AEs	7
Skin cancer	1(1.7)	Myocarditis	2 (3.4)
Acute myeloid leukemia	1(1.7)	Pericardial effusion	2 (3.4)
Transitional cell carcinoma	1(1.7)	Atrial fibrillation	1(1.7)
Prostate cancer	1(1.7)	Cardiac arrest	1 (1.7)
Bladder cancer	1(1.7)	Cardiac disorder	2 (3.4)
Others	2(3.4)	Musculoskeletal AEs	6
Outcomes		Immune-mediated myositis	1 (1.7)
Death	19 (32.2)	Polymyositis	1 (1.7)
Life-Threatening	4 (6.8)	Arthritis	1 (1.7)
Other serious	17 (28.8)	Musculoskeletal disorder	3 (5.1)
Hospitalization	12 (20.3)	Urinary AEs	5 (8.5)
Null	7 (11.9)	Cystitis	1 (1.7)
ICIs Role		Acute kidney injury	1 (1.7)
Primary suspected	48 (81.4)	Renal disorder	3 (5.1)

(Continued)

TABLE 1 Continued

Characteristics	n (%)	Characteristics	n (%)
Secondary suspected	8 (13.6)	Bladder disorder	1 (1.7)
Concomitant	3 (5.1)	Other AEs	13 (22.0)
Suspected Drugs		Time to onset (days)	
Only ICI	41 (69.5)	Median (IQR)	16 (6-82)
ICI plus one other drug	7 (11.9)		
ICI plus two or more other drugs	8 (13.6)		
Only other drugs	3 (5.1)		

also had other irAEs, including myasthenia gravis, neuropathy, myositis, and myocarditis. Then, we reviewed the FAERS database to analyze more cases of ICI-related urinary incontinence, summarized the clinical characteristics, and explored the correlation between urinary incontinence and other ICI-related disorders.

In the published literature, limited research has examined the association between ICIs and urinary incontinence. One study reported a case similar to ours, as it described a patient who developed an overlap syndrome consisting of myasthenia gravis, myositis, and myocarditis after cancer immunotherapy, and the patient also experienced urinary and fecal incontinence. In addition, there were some common characteristics among the cases reported by Ng et al. and our group, such as the early onset of AEs and poor prognoses (7).

Possible mechanisms

The mechanism of ICI-associated urinary incontinence remains unclear. Generally, urinary incontinence is usually caused by neuromuscular disorders that influence urinary storage and voiding. Additionally, some urological diseases such as cystitis can induce urinary incontinence. In our retrospective study of the FAERS database, it was evident that urinary incontinence does not develop as an isolated adverse effect, as it always occurred concomitantly with neuromuscular irAEs.

ICIs can cause nerve and muscle damage through lymphocyte infiltration, antibody-mediated inflammation, and sterile inflammation (13). In addition, irAEs can present as central nervous system (CNS) diseases (such as aseptic meningitis, encephalitis, CNS demyelinating diseases, and transverse myelitis), peripheral nervous system diseases (such as peripheral neuropathy, GBS, myasthenia gravis, and Lambert–Eaton myasthenic syndrome), and myositis (13–15). Several studies reported that ICI-related neuromuscular disorders induced urinary incontinence. For example, sphincter dysfunction occurs in 86%–92% of patients with

ICI-related myelitis, and the related symptoms include urinary incontinence (9). Bladder dysfunction was observed in patients with GBS at rates ranging from 25% to more than 80% (16), and the symptom could present as urinary incontinence (17, 18). Kelly et al. reported that ipilimumab could induce GBS, and their patient presented with dysautonomia that manifested as urinary retention (8). Meanwhile, other neuromuscular irAEs could theoretically cause lower urinary tract dysfunction based on the characteristics of the primary disease. For example, autoimmune encephalitis could present with bladder dysfunction (19, 20). Diabetic peripheral neuropathy may be associated with urinary incontinence, which manifested as urge incontinence (5). In total, 11.7%–72% of patients with multiple sclerosis developed urinary incontinence (21–25). Myasthenia gravis can predispose individuals to a higher risk of urinary incontinence by affecting the tone of the smooth or striated muscle of the distal sphincter (5). The frequency of urinary incontinence was significantly higher in patients with myasthenia gravis than in controls (26, 27). Sandler et al. concluded that voiding dysfunction heralded either a new diagnosis of myasthenia gravis or an exacerbation of the disease process (28). The Lambert–Eaton myasthenic syndrome is characterized by autonomic dysfunction, which is also experienced as voiding dysfunction in some cases (29). Inflammatory myopathies can also affect bladder/urinary function by decreasing pelvic floor function (30).

Moreover, it is well known that in patients with systemic autoimmune diseases (such as systemic lupus erythematosus, Sjögren's syndrome, and rheumatoid arthritis), non-bacterial cystitis can develop and, in turn, contribute to urinary incontinence. In one study, bladder biopsy samples displayed lymphocyte infiltration and increased numbers of mast cells (31). Consistently, there were cases featuring coincident cystitis in our FAERS database analysis. Several studies reported that ICI-related non-bacterial cystitis could also induce bladder dysfunction (32–35). Meanwhile, the analyses of bladder biopsy samples also revealed numerous events of lymphocyte infiltration into the urothelium (32, 35).

TABLE 2 Differences in clinical characteristics of fatal and non-fatal ICI-associated urinary incontinence cases.

		Fatal cases	Non-fatal cases	P value	
Total		19	40		
Gender	Male	9	23	0.465	a
	Female	9	17	0.725	a
	Unknown	1		0.322	b
Age	Median(n=49)	73 (n=18)	67.5 (n=31)		
	<60	4	8	1.000	b
	60–80	7	21	0.260	a
	>80	7	2	0.003	b
Indications	Lung cancer	7	14	0.890	a
	Melanoma	5	9	0.753	b
	Renal cancer	2	4	1.000	b
	Glioblastoma	0	3	0.544	b
	Breast cancer	0	2	1.000	b
	Ovarian cancer	1	1	0.544	b
	Cholangiocarcinoma	1	1	0.544	b
	Pancreatic carcinoma	0	1	1.000	b
	Colon cancer	1	0	0.322	b
	Skin cancer	0	1	1.000	b
	Acute myeloid Leukemia	0	1	1.000	b
	Bladder cancer	1	0	0.322	b
	Transitional cell carcinoma	0	1	1.000	b
	Prostate cancer	1	0	0.322	b
	Others	0	2	1.000	b
ICI drugs	PD-1	14	31	0.753	b
	PD-L1	2	3	0.653	b
	CTLA-4	1	1	0.544	b
	PD-1+CTLA-4	2	5	1.000	b
Concurrent Drugs	Nervous system drug	8	3	0.003	b
	α -Adrenoceptor antagonists	1	3	1.000	b
	Diuretics	2	1	0.240	b
Concurrent AE	Neurological AEs	5	10	1.000	b
	Myasthenia gravis/Myasthenic syndrome	3	1	0.094	b
	Cardiovascular AEs	3	4	0.670	b
	Myocarditis	1	1	0.544	b
	Musculoskeletal AEs	3	3	0.376	b
	Myositis	2	0	0.100	b
	Urinary AEs	2	2	0.588	b
	Other AEs (dermatologic, pulmonary, endocrine, gastrointestinal)	3	10	0.517	b
	Overlapping	5	11	0.924	a

a: Pearson χ^2 test.

b: Fisher's exact test.

Concomitant adverse events

Neuromuscular irAEs were the most frequently reported concomitant AEs with urinary incontinence. Concomitant neurological AEs included encephalitis, encephalopathy, facial paralysis, neuropathy, and myasthenia gravis/myasthenic syndrome. Concomitant musculoskeletal irAEs included two cases of myositis. In addition, concomitant urological irAEs

included one case of cystitis. Myelitis, multiple sclerosis, and GBS are common neurological causes of bladder dysfunction. The related concomitant AEs were not observed in the FAERS database. However, the typical symptoms of these diseases were reported (including paraparesis, paresthesia, muscular weakness, diplopia, seizure, and ataxia). This suggests that many neurological irAEs might be underreported. This might be attributable to their non-specific symptoms, their low

TABLE 3 ICI-related urinary continence concomitant with neuromuscular–cardiovascular syndrome case series in the FDA Adverse Event Reporting System database.

Patient	Age	Gender	Indication	ICIs	Concurrent AEs	Outcome
1	62	F	Non-small cell lung cancer	Nivolumab	Myasthenia gravis, facial paralysis, hepatic enzyme increased	Death
2	73	M	Malignant melanoma	Pembrolizumab	Myasthenia gravis, atrial fibrillation	Hospital
3	54	M	Cholangiocarcinoma	Nivolumab	Myasthenia gravis, myocarditis	Death
4	71	M	Non-small cell lung cancer	Pembrolizumab	Myasthenic syndrome, pericardial effusion, Bradycardia, heart injury, Polymyositis	Death
5	54	M	Cholangiocarcinoma	Nivolumab	Myocarditis, eyelid ptosis	Hospital

incidence, and a lack of recognition of these irAEs among oncologists (36, 37).

(13, 39, 40). Therefore, further investigation into the prognosis and mortality of ICI-related urine incontinence is needed.

Other interferences

We additionally reviewed anticancer regimens reported in the FAERS database. Combined treatment with other anticancer therapies was only reported in limited cases. In our case, the patient was rechallenged with the original chemotherapy regimen combined with VEGFR inhibitors, and urinary incontinence did not recur. We also explore the related literature in PubMed and EMBASE. There is no evidence demonstrating that VEGFR inhibitors can induce urinary incontinence. Regarding chemotherapy, carboplatin/paclitaxel therapy for gynecologic cancers may lead to new-onset or worsening urinary incontinence, most likely related to paclitaxel (38). However, the use of paclitaxel for gynecologic cancers was rare in our findings. Overall, these results suggest that urinary incontinence is mainly relevant to ICIs.

Prognosis and mortality

In this FAERS study, patients with urinary incontinence experienced relatively severe outcomes, especially a high mortality rate. However, urinary incontinence is not inherently dangerous. Therefore, we must realize that death is not necessarily related to the drug/events, but it could possibly be related to the underlying disease. Because of the limitation of the FAERS database, we could not obtain information on the underlying illnesses of patients. By analyzing the concomitant drugs, we found that nervous system drugs were the most common concomitant drugs, which means that patients with urinary incontinence may also have nervous system disease. Notably, patients who used nervous system drugs had a significantly higher risk of fatal outcomes in the analysis (Table 2). Furthermore, ICI-related urine incontinence always occurs concomitantly with neuromuscular irAEs or neuromuscular–cardiovascular overlapping syndrome, both of which have high risks of mortality and are difficult to manage

Management suggestions

The occurrence of urinary incontinence during ICI treatment points toward possible life-threatening neuromuscular AEs, which should be assessed using relevant tests. For example, muscle and myocardial enzyme and cTn levels should be tested. Electrophysiology, neuroimaging, lumbar puncture, and antineuronal/AChR antibody measurements should be used to identify ICI-induced nervous systems toxicity. UDS, urological ultrasound, urinalysis, and urine culture should be performed to identify other urinary system diseases. In addition, ECG should also be performed to identify ICI-induced myocarditis and myositis. The most important thing is to be aware of potentially lethal neuromuscular irAEs based on the presence of urinary incontinence, muscle weakness, fatigue, myalgia, or dyspnea. In addition, proactive and effective treatments are also crucial. Glucocorticoids represent the mainstay of treatment; our case appeared to involve steroid-dependent irAEs. Additional immunosuppressant and intravenous immunoglobulin therapy effectively improved the disease. This was consistent with the disease characteristics of the ICI-associated overlap syndrome in previous studies and the aforementioned similar case (40). These findings remind us that ICI-related urinary incontinence might require intensive monitoring and combination therapy.

Limitations

We acknowledge that our study had limitations. We were unable to calculate the incidence because FAERS lacks denominators, and it does not receive reports for every AE that occurs with a product. Additionally, the lack of test data and clinical elements, such as laboratory data, some radiological findings, and preexisting disease, makes it challenging to fully analyze all of the confounders involved in the occurrence of AEs. Notwithstanding these limitations, information within FAERS

can support the data or information found in clinical research or published studies. In some cases, FAERS data can provide meaningful postmarketing signals of rare AEs not observed in clinical trials.

Conclusion

ICI-related urinary incontinence might represent a signal of neuromuscular irAEs, which are associated with poor prognoses. Among the cases of urinary incontinence featuring concomitant irAEs, it is essential to remain vigilant regarding neuromuscular toxicities, especially myasthenia gravis–myocarditis–myositis syndrome, which has a high fatality rate. In addition, patients who received combination treatment with nervous system drugs or those of age > 80 years might have a higher risk of fatal outcomes. The early detection and engagement of a multidisciplinary team are critical, and high-dose glucocorticoid/immunomodulator therapy should be implemented.

Data availability statement

The datasets presented in this study can be found in online repositories. The names of the repository/repositories and accession number(s) can be found below: <https://www.fda.gov/drugs/questions-and-answers-fdas-adverse-event-reporting-system-faers/fda-adverse-event-reporting-system-faers-latest-quarterly-data-files>.

Ethics statement

Ethical review and approval was not required for the study on human participants in accordance with the local legislation and institutional requirements. The patients/participants provided their written informed consent to participate in this study. Written informed consent was obtained from the

individual(s) for the publication of any potentially identifiable images or data included in this article.

Authors contributions

YH, WL, ZZ, and ZA designed the study and developed the protocol. WL supported programming and prepared the data. YH provided the case report materials. BT did the statistical analysis. YH and WL wrote the first draft of the manuscript. WL, YH, ZZ, and ZA were involved in data review. All authors contributed to the critical revision of the manuscript for important intellectual content and approved the final version of the manuscript.

Conflict of interest

The authors declare that the research was conducted in the absence of any commercial or financial relationships that could be construed as a potential conflict of interest.

Publisher's note

All claims expressed in this article are solely those of the authors and do not necessarily represent those of their affiliated organizations, or those of the publisher, the editors and the reviewers. Any product that may be evaluated in this article, or claim that may be made by its manufacturer, is not guaranteed or endorsed by the publisher.

Supplementary material

The Supplementary Material for this article can be found online at: <https://www.frontiersin.org/articles/10.3389/fonc.2022.954468/full#supplementary-material>

References

1. Postow MA, Sidlow R, Hellmann MD. Immune-related adverse events associated with immune checkpoint blockade. *N Engl J Med* (2018) 378(2):158–68. doi: 10.1056/NEJMra1703481
2. Hargadon KM, Johnson CE, Williams CJ. Immune checkpoint blockade therapy for cancer: An overview of FDA-approved immune checkpoint inhibitors. *Int Immunopharmacol* (2018) 62:29–39. doi: 10.1016/j.intimp.2018.06.001
3. Michot JM, Bigenwald C, Champiat S, Collins M, Carbone F, Postel-Vinay S, et al. Immune-related adverse events with immune checkpoint blockade: A comprehensive review. *Eur J Cancer* (2016) 54:139–48. doi: 10.1016/j.ejca.2015.11.016
4. Hu JS, Pierre EF. Urinary incontinence in women: Evaluation and management. *Am Fam Physician* (2019) 100(6):339–48.
5. Partin AW, AJ W, LR K, Peters CA. *Campbell-Walsh Urology e-book*. Philadelphia: Elsevier Health Sciences (2015).
6. Esfahani K, Elkrief A, Calabrese C, Lapointe R, Hudson M, Routy B, et al. Moving towards personalized treatments of immune-related adverse events. *Nat Rev Clin Oncol* (2020) 17(8):504–15. doi: 10.1038/s41571-020-0352-8
7. Ng AH, Molinero DM, Ngo-Huang AT, Bruera E. Immunotherapy-related skeletal muscle weakness in cancer patients: A case series. *Ann Palliat Med* (2021) 10(2):2359–65. doi: 10.21037/apm-20-454
8. Kelly Wu W, Broman KK, Brownie ER, Kauffmann RM. Ipilimumab-induced Guillain-Barré syndrome presenting as dysautonomia: An unusual presentation of a rare complication of immunotherapy. *J Immunother* (2017) 40(5):196–9. doi: 10.1097/CJI.0000000000000167
9. Picca A, Berzero G, Bihan K, Jachiet V, Januel E, Coustans M, et al. Longitudinally extensive myelitis associated with immune checkpoint inhibitors. *Neurol Neuroimmunol Neuroinflamm* (2021) 8(3):e967. doi: 10.1212/NXI.0000000000000967

10. Chen X, Haggiagi A, Tzatha E, DeAngelis LM, Santomaso B. Electrophysiological findings in immune checkpoint inhibitor-related peripheral neuropathy. *Clin Neurophysiol* (2019) 130(8):1440–5. doi: 10.1016/j.clinph.2019.03.035
11. Banda JM, Evans L, Vanguri RS, Tatonetti NP, Ryan PB, Shah NH. A curated and standardized adverse drug event resource to accelerate drug safety research. *Sci Data* (2016) 3:160026. doi: 10.1038/sdata.2016.26
12. Tsakiris P, Oelke M, Michel MC. Drug-induced urinary incontinence. *Drugs Aging* (2008) 25(7):541–9. doi: 10.2165/00002512-200825070-00001
13. Marini A, Bernardini A, Gigli GL, Valente M, Muñoz-Castrillo S, Honnorat J, et al. Neurologic adverse events of immune checkpoint inhibitors: A systematic review. *Neurology* (2021) 96(16):754–66. doi: 10.1212/WNL.00000000000011795
14. Shi J, Niu J, Shen D, Liu M, Tan Y, Li Y, et al. Clinical diagnosis and treatment recommendations for immune checkpoint inhibitor-related adverse reactions in the nervous system. *Thorac Cancer* (2020) 11(2):481–7. doi: 10.1111/1759-7714.13266
15. Nakatani Y, Tanaka N, Enami T, Minami S, Okazaki T, Komuta K. Lambert-Eaton Myasthenic syndrome caused by nivolumab in a patient with squamous cell lung cancer. *Case Rep Neurol* (2018) 10(3):346–52. doi: 10.1159/000494078
16. Wyndaele JJ, Castro D, Madersbacher H, Kovindha A, Radziszewski P, Ruffion A, et al. Neurologic urinary and faecal incontinence. In: P Abrams, L Cardozo, S Khoury, et al, editors. *Incontinence*. Paris: Health Publications (2005). p. 1059–162.
17. Wheeler JS Jr, Siroky MB, Pavlakis A, Krane RJ. The urodynamic aspects of the Guillain-Barré syndrome. *J Urol* (1984) 131(5):917–9. doi: 10.1016/s0022-5347(17)50709-0
18. Sakakibara R, Hattori T, Kuwabara S, Yamanishi T, Yasuda K. Micturitional disturbance in patients with Guillain-Barré syndrome. *J Neurol Neurosurg Psychiatry* (1997) 63(5):649–53. doi: 10.1136/jnnp.63.5.649
19. Voice J, Ponterio JM, Lakhi N. Psychosis secondary to an incidental teratoma: a “heads-up” for psychiatrists and gynecologists. *Arch Womens Ment Health* (2017) 20(5):703–7. doi: 10.1007/s00737-017-0751-8
20. Sugiyama M, Sakakibara R, Tsunoyama K, Takahashi O, Kishi M, Ogawa E, et al. Cerebellar ataxia and overactive bladder after encephalitis affecting the cerebellum. *Case Rep Neurol* (2009) 1(1):24–8. doi: 10.1159/000226119
21. Litwiller SE, Frohman EM, Zimmern PE. Multiple sclerosis and the urologist. *J Urol* (1999) 161(3):743–57. doi: 10.1016/S0022-5347(01)61760-9
22. Zecca C, Riccitelli GC, Disanto G, Singh A, Digesu GA, Panicari L, et al. Urinary incontinence in multiple sclerosis: prevalence, severity and impact on patients’ quality of life. *Eur J Neurol* (2016) 23(7):1228–34. doi: 10.1111/ene.13010
23. Mauruc E, Guinet-Lacoste A, Falcou L, Manceau P, Verollet D, Le Breton F, et al. Nocturnal urinary disorders and multiple sclerosis: Clinical and urodynamic study of 309 patients. *J Urol* (2017) 197(2):432–7. doi: 10.1016/j.juro.2016.10.112
24. Jacob L, Tanislav C, Kostev K. Multiple sclerosis and incidence of urinary and fecal incontinence in almost 9,000 patients followed up for up to 10 years in Germany. *Neuroepidemiology* (2021) 55(2):92–9. doi: 10.1159/000513234
25. Tudor KI, Bošnjak Pašić M, Nad Škegro S, Bakula M, Nemir J, Mustač F, et al. Lower urinary tract symptoms and depression in patients with multiple sclerosis. *Psychiatr Danub* (2020) 32(Suppl 4):511–9.
26. Tateno F, Sakakibara R, Aiba Y. Lower urinary tract symptoms in myasthenia gravis. *Case Rep Neurol* (2021) 13(2):490–8. doi: 10.1159/000514825
27. Akan O, Polat EC, Çulha MG, Önel SD. The impact of myasthenia gravis on lower urinary tract functions. *Int J Clin Pract* (2021) 75(12):e14873. doi: 10.1111/ijcp.14873
28. Sandler PM, Avillo C, Kaplan SA. Detrusor areflexia in a patient with myasthenia gravis. *Int J Urol* (1998) 5(2):188–90. doi: 10.1111/j.1442-2042.1998.tb00276.x
29. Satoh K, Motomura M, Suzu H, Nakao Y, Fujimoto T, Fukuda T, et al. Neurogenic bladder in Lambert-Eaton myasthenic syndrome and its response to 3,4-diaminopyridine. *J Neurol Sci* (2001) 183(1):1–4. doi: 10.1016/S0022-510X(00)00460-3
30. Heřmanková B, Špiritović M, Oreská S, Štorkánová H, Komarc M, Klein M, et al. Sexual function in patients with idiopathic inflammatory myopathies: A cross-sectional study. *Rheumatol (Oxford)* (2021) 60(11):5060–72. doi: 10.1093/rheumatology/keab397
31. Van De Merwe JP. Interstitial cystitis and systemic autoimmune diseases. *Nat Clin Pract Urol* (2007) 4(9):484–91. doi: 10.1038/ncpuro0874
32. Ueki Y, Matsuki M, Kubo T, Morita R, Hirohashi Y, Sato S, et al. Non-bacterial cystitis with increased expression of programmed death-ligand 1 in the urothelium: An unusual immune-related adverse event during treatment with pembrolizumab for lung adenocarcinoma. *IJU Case Rep* (2020) 3(6):266–9. doi: 10.1002/iju.5.12211
33. Shimatani K, Yoshimoto T, Doi Y, Sonoda T, Yamamoto S, Kanematsu A. Two cases of nonbacterial cystitis associated with nivolumab, the anti-programmed-death-receptor-1 inhibitor. *Urol Case Rep* (2018) 17:97–9. doi: 10.1016/j.eucr.2017.12.006
34. Ozaki K, Takahashi H, Murakami Y, Kiyoku H, Kanayama H. A case of cystitis after administration of nivolumab. *Int Cancer Conf J* (2017) 6(4):164–6. doi: 10.1007/s13691-017-0298-6
35. El Hussein K, Lafoeste H, Mansuet-Lupo A, Arrondeau J, Villeminey C, Bennani S, et al. A case of severe interstitial cystitis associated with pembrolizumab. *Curr Probl Cancer: Case Rep* (2021) 4:100101. doi: 10.1016/j.cpcr.2021.100101
36. Mikami T, Liaw B, Asada M, Niimura T, Zamami Y, Green-LaRoche D, et al. Neuroimmunological adverse events associated with immune checkpoint inhibitor: A retrospective, pharmacovigilance study using FAERS database. *J Neuro Oncol* (2021) 152(1):135–44. doi: 10.1007/s11060-020-03687-2
37. Reynolds KL, Guidon AC. Diagnosis and management of immune checkpoint inhibitor-associated neurologic toxicity: Illustrative case and review of the literature. *Oncologist* (2019) 24(4):435–43. doi: 10.1634/theoncologist.2018-0359
38. Strauchon CJ, Dengler KL, Gruber DD, Katebi Kashi P, Aungst MJ, Trikhacheva A, et al. Urinary symptoms in women receiving carboplatin/paclitaxel for treatment of gynecologic cancers. *Int J Gynecol Cancer* (2020) 30(9):1418–23. doi: 10.1136/ijgc-2020-001529
39. Khan E, Shrestha AK, Elkhooly M, Wilson H, Ebbert M, Srivastava S, et al. CNS and PNS manifestation in immune checkpoint inhibitors: A systematic review. *J Neurol Sci* (2022) 432:120089. doi: 10.1016/j.jns.2021.120089
40. Lipe DN, Galvis-Carvajal E, Rajha E, Wechsler AH, Gaeta S. Immune checkpoint inhibitor-associated myasthenia gravis, myositis, and myocarditis overlap syndrome. *Am J Emerg Med* (2021) 46:51–5. doi: 10.1016/j.ajem.2021.03.005



OPEN ACCESS

EDITED BY

Catherine Sautes-Fridman,
INSERM U1138 Centre de Recherche
des Cordeliers (CRC), France

REVIEWED BY

Bipin N. Savani,
Vanderbilt University, United States
Juliet Barker,
Memorial Sloan Kettering Cancer
Center, United States
Michael Uhlin,
Karolinska Institutet, Sweden

*CORRESPONDENCE

Elizabeth J. Shpall
eshpall@mdanderson.org

SPECIALTY SECTION

This article was submitted to
Cancer Immunity
and Immunotherapy,
a section of the journal
Frontiers in Immunology

RECEIVED 12 August 2022

ACCEPTED 05 September 2022

PUBLISHED 20 September 2022

CITATION

Kumar B, Afshar-Kharghan V,
Mendt M, Sackstein R, Tanner MR,
Popat U, Ramdial J, Daher M,
Jimenez J, Basar R, Melo Garcia L,
Shanley M, Kaplan M, Wan X,
Nandivada V, Reyes Silva F, Woods V,
Gilbert A, Gonzalez-Delgado R,
Acharya S, Lin P, Rafei H, Banerjee PP
and Shpall EJ (2022) Engineered cord
blood megakaryocytes evade killing by
allogeneic T-cells for
refractory thrombocytopenia.
Front. Immunol. 13:1018047.
doi: 10.3389/fimmu.2022.1018047

Engineered cord blood megakaryocytes evade killing by allogeneic T-cells for refractory thrombocytopenia

Bijender Kumar¹, Vahid Afshar-Kharghan², Mayela Mendt¹, Robert Sackstein³, Mark R. Tanner¹, Uday Popat¹, Jeremy Ramdial¹, May Daher¹, Juan Jimenez¹, Rafet Basar¹, Luciana Melo Garcia¹, Mayra Shanley¹, Mecit Kaplan¹, Xinhai Wan¹, Vandana Nandivada¹, Francia Reyes Silva¹, Vernikka Woods¹, April Gilbert¹, Ricardo Gonzalez-Delgado², Sunil Acharya¹, Paul Lin¹, Hind Rafei¹, Pinaki Prosad Banerjee¹ and Elizabeth J. Shpall^{1*}

¹Department of Stem Cell Transplantation and Cellular Therapy, The University of Texas MD Anderson Cancer Center, Houston, TX, United States, ²Section of Benign Hematology, The University of Texas MD Anderson Cancer Center, Houston, TX, United States, ³Department of Translational Medicine, Translational Glycobiology Institute, Herbert Wertheim College of Medicine, Florida International University, Miami, FL, United States

The current global platelet supply is often insufficient to meet all the transfusion needs of patients, in particular for those with alloimmune thrombocytopenia. To address this issue, we have developed a strategy employing a combination of approaches to achieve more efficient production of functional megakaryocytes (MKs) and platelets collected from cord blood (CB)-derived CD34+ hematopoietic cells. This strategy is based on *ex-vivo* expansion and differentiation of MKs in the presence of bone marrow niche-mimicking mesenchymal stem cells (MSCs), together with two other key components: (1) To enhance MK polyploidization, we used the potent pharmacological Rho-associated coiled-coil kinase (ROCK) inhibitor, KD045, resulting in liberation of increased numbers of functional platelets both *in-vitro* and *in-vivo*; (2) To evade HLA class I T-cell-driven killing of these expanded MKs, we employed CRISPR-Cas9-mediated β -2 microglobulin (β 2M) gene knockout (KO). We found that coculturing with MSCs and MK-lineage-specific cytokines significantly increased MK expansion. This was further increased by ROCK inhibition, which induced MK polyploidization and platelet production. Additionally, *ex-vivo* treatment of MKs with KD045 resulted in significantly higher levels of engraftment and donor chimerism in a mouse model of thrombocytopenia. Finally, β 2M KO allowed MKs to evade killing by allogeneic T-cells. Overall, our approaches offer a novel, readily translatable

roadmap for producing adult donor-independent platelet products for a variety of clinical indications.

KEYWORDS

megakaryocyte, rho-associated coiled coil-containing protein kinase, platelet, cord blood, beta2 microglobulin, thrombocytopaenia

Introduction

There is an urgent need for a robust and consistently available platelet supply for thrombocytopenic patients. Platelets have a short shelf-life, and hospitals depend on apheresis procedures with adult donors to continuously replenish the supply. The development of an adult donor-independent, off-the-shelf platelet product would alleviate constraints on the platelet inventory and reduce the demand for donors.

Platelets have been successfully generated from human embryonic stem cell (hESC)- and human induced pluripotent stem cell (hiPSC)-derived megakaryocytes (MKs), the cell-type that produces platelets (1–3). However, various concerns, including the expression of oncogenes in hESCs and hiPSCs (1, 4, 5), the usage of non-human serum and feeder cells during culture (3, 6, 7), as well as low platelet yields from *ex-vivo* generated MKs (8) have prevented widespread clinical use of these techniques. However, progress has been made in generating higher yields of platelet-producing MKs in non-human serum- and feeder-free conditions using various techniques, such as spinning embryoid bodies, bioreactors with turbulent flow and shear forces, and culture on gas-permeable surfaces (9–13). These include a study by Ito et al. (10) that used hiPSCs and bioreactors with vertical reciprocal turbulence, which generated 70–80 platelets per MK. Furthermore, using serum-free conditions, Matsunaga et al. (14) generated upwards of 3.4×10^4 platelets per starting human umbilical cord blood (CB) hematopoietic stem cell (HSC), which indicates the potential of generating clinically useful doses of platelets from CB-HSCs. Various small molecule signaling inhibitors and gene expression modifications have also been used to increase MK maturation and produce more functional platelets (10, 13, 15–18). In this study, we developed a novel method using human CB as a source of platelets. We hypothesized that mesenchymal stem cells (MSCs) and MK-lineage growth factors would provide an *ex-vivo*, surrogate hematopoietic niche (19, 20) for robust expansion and differentiation of CD34+ CB-HSCs into MKs. We previously showed that MSCs induce expansion of CB-HSCs to myeloid cells (21). Here, we assessed whether a modified

MSC-CB co-culture platform could be used to generate and expand MKs for efficient platelet production.

CB-derived MKs have impaired maturation and release fewer platelets than peripheral blood HSC-derived MKs (22, 23). The downregulation of Rho or Rho-associated coiled-coil-containing kinases (ROCK1 and ROCK2) is critical in MK maturation and leads to endomitosis, polyploidization, and proplatelet formation (10, 24–29). We hypothesized that ROCK inhibition would enhance CB-MK maturation in our MSC-CB co-culture platform, thereby optimizing platelet production. Furthermore, alloimmune platelet transfusion refractoriness (PTR) is a life-threatening condition observed in multiply transfused patients and results in bleeding complications and reduced survival (30, 31). The most frequent immune cause of PTR is the presence of alloantibodies against human leukocyte antigen (HLA) class I epitopes, resulting in rejection of transfused platelets unless HLA-I compatible platelets are transfused (31–36). To address this issue, we utilized CRISPR-Cas9-mediated knockout (KO) of the β -2 microglobulin (β 2M) gene to generate HLA-I-deficient CB-HSCs and CB-MKs. We sought to determine whether HLA-I-deficient CB-HSCs could expand *ex-vivo*, differentiate into MKs, evade immune clearance, and generate functional platelets. Overall, this study provides a proof-of-concept for a multifaceted approach to optimize CB-MKs as a consistently available source of off-the-shelf platelets that may be beneficial for alleviating the constraints on the platelet inventory.

Materials and methods

Additional methods regarding CB processing, platelet collection and quantification, MK and platelet analyses, flow cytometry, western blot, T-cell cytotoxicity, bleeding studies, CRISPR, and animal usage are provided in the supplement.

MSC co-culture and MK differentiation

CB samples were collected and CD34+ cells were isolated, as described in the supplement, following written informed consent

under MD Anderson IRB-approved protocols. CD34⁺ cells were seeded over 50% confluent BM- or CB-derived MSC monolayers and grown in serum-free good manufacturing practice (GMP) grade SCGM media (Cell Genix, Portsmouth, NH), supplemented with 1% glutamine, penicillin/streptomycin (Thermo Fisher Scientific, Waltham, MA) and recombinant human thrombopoietin (TPO, 50ng/ml), IL-6 (50ng/ml), stem cell factor (SCF, 50ng/ml), IL-3 (5ng/ml), and FLT3-ligand (FLT3-L, 5ng/ml) at 37°C and 5% CO₂ for the initial 3–4 days. All cytokines were purchased from either Peprotech (East Windsor, NJ) or R&D Systems (Minneapolis, MN). IL-3 and FLT3-L were used for the initial myeloid commitment and were removed after 3 days of culture. Thereafter, the cells were maintained in TPO (50ng/ml), IL-6 (50ng/ml), SCF (25ng/ml), and IL-11 (25ng/ml) until maturation, with media changes every third day. The cells were immunophenotyped at day 10–11 of culture and non-MK-lineage cells were removed using MACS lineage negative selection kits (Miltenyi Biotec, GmbH, Germany). The relatively purified MKs were plated on fresh MSC monolayers and expanded further. ROCK inhibitors (Y27632, 5–10μM, Selleckchem, Houston, TX; KD045, 100nM–10μM, Kadmon Corporation, LLC) were then used for 4–5 days to induce MK polyploidization and maturation in the day 19 CB-MK differentiated product in the absence of MSCs (Supplementary Figure 1A).

CB-MK infusion and chimerism

All animal experiments were performed under MD Anderson Institutional Animal Care and Use Committee-approved protocols. 6-week-old NSG mice were irradiated with 300cGy and infused with CB-MKs at 16–20h post-irradiation. For homing analyses, mice were infused with 5 × 10⁶ KD045-treated or untreated CB-MKs that were labelled with 2μM carboxyfluorescein succinimidyl ester (CFSE, Thermo Fisher). Mice were sacrificed at 16h post-infusion. The BM, liver, blood, and spleen were harvested and analyzed for the percentage of CFSE⁺ human CD42⁺ cells in the non-erythroid (Ter119[−]) fraction of total live cells by flow cytometry. For BM engraftment studies, CB-MKs were infused in sub-lethally (300cGy) irradiated mice and BM cells were harvested from the femur and tibia by crushing and washing with PBS. Single-cell suspensions were stained with hCD41, hCD42, mCD45, and Ter119 antibodies. The percentage engraftment was determined through counting hCD41⁺/hCD42⁺ cells in the Ter119[−] fraction of the live mice BM cells.

CRISPR-Cas9-mediated β 2M KO

CRISPR-Cas9 mediated β2M KO was performed on day 3 of MK differentiation. Following KO confirmation, CD34⁺ cells/MKs were cultured in the standard MK differentiation

conditions mentioned earlier. Details regarding the KO are in the supplement.

Statistics

All statistical analyses were performed using Prism 8 software (GraphPad, San Diego, CA). Two-group comparisons were performed using unpaired *t*-tests unless otherwise noted. Statistically significant *p* values <0.05 are reported as **p*<0.05, ***p*<0.01, ****p*<0.001 and *****p*<0.001. The significance test used and sample sizes (*n*) are reported in each figure legend.

Results

CB CD34⁺ cells undergo robust ex-vivo expansion and differentiation in the MSC co-culture system

We used an *in-vitro* MSC co-culture system with cytokines and pharmacological inhibitors to enrich and differentiate CB-MKs (Figure 1A and Supplementary Figure 1A). Purified CB-HSCs were characterized as the percentage of CD34⁺ lineage-cells, with a positivity of 93.0% (*n*=12 cords) (Figure 1B). We collected an average of 1.33 × 10⁶ CD34⁺ cells per CB unit following positive selection (*n*=15 cords, Figure 1C). CD34⁺ cells were expanded in serum-free media containing human recombinant TPO and a cocktail of cytokines in liquid culture alone or in co-cultures with MSC support, as described in Supplementary Figure 1A. CD34⁺ cells demonstrated a significantly higher fold-expansion when co-cultured with MSCs at day 20, compared to CD34⁺ cells cultured alone (308-fold vs. 114-fold, *p*<0.0001, Figure 1D). The MSC co-cultures supported significantly more CD41a+CD42b⁺ MK expansion and differentiation, compared to the CD34⁺ cells cultured with cytokines alone. The average number of expanded cells was 395.1 × 10⁶ for those expanded with MSCs and 113.8 × 10⁶ for those expanded without MSCs at day 20 (*p*<0.0001, *n*=15 and 5 cords respectively, Figure 1E). The percentage of CD41a+CD42b⁺ CB-MKs expanded with MSCs increased from 31.5% at day 10 to 92.1% (*p*<0.0001, *n*=4 cords) on day 20 (Figure 1F).

We expanded CB-derived CD34⁺ cells for 10–12 days with TPO in collagen-based MegaCult-C MK colony-forming (CFU-Meg) assays and visualized their expression of CD41/CD61 (GPIIb/IIIa receptor complex) (Figure 1G). We found >50 cells in an MK colony that were actively generating platelets, observed by the presence of proplatelet extensions and demarcation membrane systems (Figure 1H) (37). Expanded polyploid MKs on culture day 20 were further verified by the presence of granules and multiple nuclei, as visualized by Giemsa staining (Figure 1I) and transmission electron microscopy (TEM) (Figure 1J and Supplementary Figure 2A). The purity and maturation of the CB-MKs were confirmed by

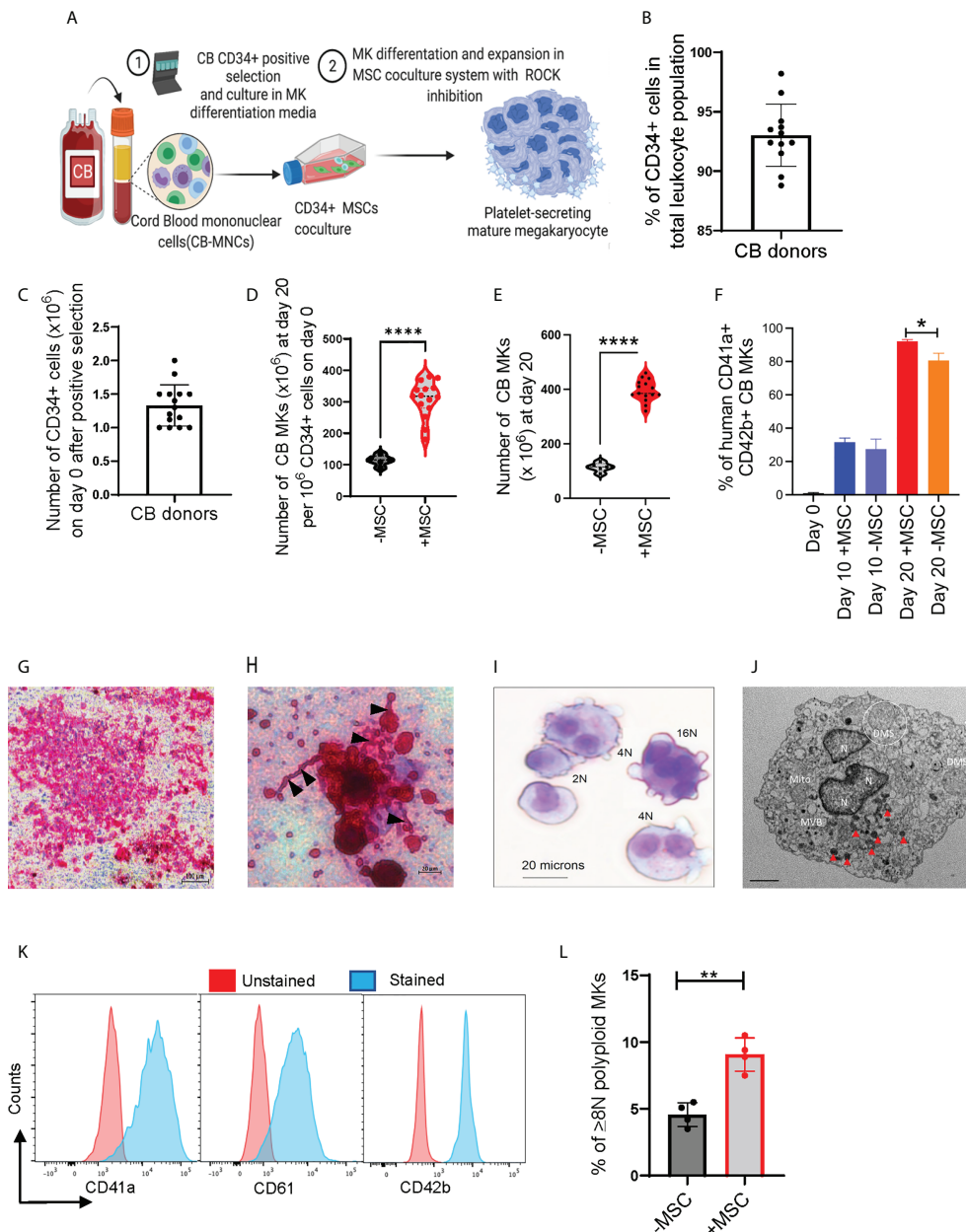


FIGURE 1

MSCs support HSC expansion and MK terminal differentiation from CB CD34⁺ cells. **(A)** Schematic of the experimental workflow of MK differentiation and platelet production from CB-derived CD34⁺ cells in an MSC co-culture system. **(B)** Percentage of CD34⁺ cells after positive selection amongst multiple cord donors ($n=12$, each dot represents a different cord). **(C)** Number of CD34⁺ cells collected per CB unit after positive selection ($n=15$, each dot represents a different cord). **(D, E)** Violin plots comparing fold-change expansion of CD34⁺ cells **(D)** and total MKs generated **(E)** with and without MSC support at day 20 ($n=15$ in MSC co-culture and $n=5$ without MSCs, **** $p < 0.0001$). **(F)** hCD41⁺CD42⁺ expression pattern in CB-MKs cultured with or without MSCs at day 0, 10, and 20 ($n=3-4$ CB). **(G)** Human CFU-MK representative image (5X magnification) exhibiting GPIIb/IIIa receptor complex staining in day 12 differentiated CB-MK colonies (scale bar = 100 μm). **(H)** Proplatelet formation (black triangles) and released platelets in the day 12 CFU-MK image (scale bar = 20 μm). **(I)** Giemsa staining of a day 23 expanded mature CB-MK showing polyploid nuclei. **(J)** Representative transmission electron microscopy (TEM) 5000X magnification image of a CB-MK (Abbreviations: DMS, demarcation membrane system; Mito, mitochondria; MVB, multivesicular bodies; N, nucleus; red arrows, granules; scale bar = 2 μm). **(K)** Representative histograms depicting the expression of hCD41a, hCD42b and hCD61 expression (blue) in day 22 MKs compared to unstained controls (red). **(L)** Ploidy of CB-MKs generated in the presence or absence of MSCs and 10 μM Y27632, quantified by propidium iodide staining ($n=4$ with MSCs and 4 without MSCs, ** $p < 0.01$). All statistical analyses completed with unpaired t-tests. * means $p < 0.05$.

flow cytometry analysis of the MK maturation markers CD41a, CD42b, and CD61 (Figure 1K). Finally, MKs generated in the presence of MSCs and 10 μ M of the ROCK inhibitor Y27632 displayed significantly higher polyploidization ($\geq 8N$ nuclei) than those generated with 10 μ M Y27632 but in the absence of MSCs (9.08% with MSCs vs. 4.58% without MSCs, $p < 0.01$, Figure 1L).

ROCK inhibition increases CB-MK maturation

Downregulation of Rho signaling is a critical step in thrombopoiesis (28). ROCK1/2 are directly downstream of Rho, and ROCK inhibition enhances MK maturation and platelet

shedding (10, 24–26). We therefore sought to determine whether ROCK inhibitors alter CB-MK differentiation and platelet generation. We treated day 17–19 CB-MKs with 5–10 μ M of the ROCK inhibitor Y27632 for 4–5 days in the absence of MSCs and observed an increase in the number of large MKs compared to untreated MKs (19 μ m vs. 10 μ m average cell size, $p=0.02$, $n=3$ cords, Figure 2A). This suggests an acceleration in MK maturation with pharmacological ROCK inhibition. We also used shear stress, which increases platelet release from MKs (10, 38), to increase platelet production in day 23 expanded CB-MKs that were treated with or without Y27632. Slight shear stress induced by 6 hour horizontal shaking generated a higher number of platelets from CB-MKs treated with 10 μ M Y27632, compared to control CB-MKs (2.53×10^{10} vs. 1.37×10^{10} , $p=0.0095$, Figure 2B).

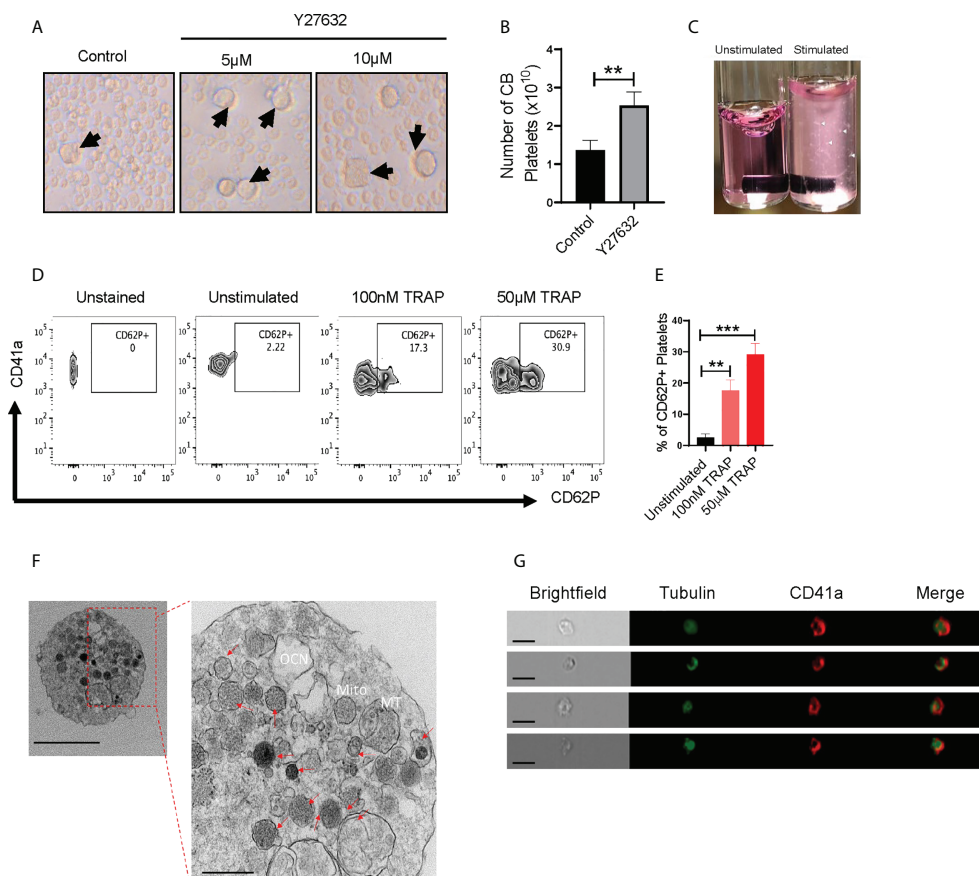


FIGURE 2

CB-MK-derived platelets are functional and exhibit aggregation characteristics. (A) Representative 10X images of differentiating MKs under normal conditions and with 5–10 μ M Y27632, with examples of larger MKs marked by black arrows. (B) Number of secreted platelets from MKs treated with shear stress for 6h and were untreated or pretreated with 10 μ M Y27632 for 96h ($n=3$, $**p<0.01$). (C) Representative image of unstimulated and 5 μ g/ml collagen stimulated platelets in tubes. White triangles indicate aggregating platelets. (D) Flow cytometry contour plots depicting CD62P (P-selectin) expression in unstimulated and TRAP-stimulated platelets. (E) Frequency of CD62P+ platelets after TRAP stimulation or without stimulation ($n=3$, $**p<0.01$ and $***p<0.001$). (F) Transmission electron microscopy (TEM) 10000X (left, scale bar = 2 μ m) and 50000X (right, scale bar = 500nm) resolution images of a CB-MK-derived platelet (Abbreviations: Mito, mitochondria; MT, microtubule; OCN, open canalicular network; red arrows, granules). (G) Imaging flow cytometry of platelets generated from CB-MKs and assessed for the expression of tubulin and CD41a (scale bar = 7 μ m). All statistical analyses completed with unpaired t-tests.

CB-MKs produce functional platelets

Next, we examined if CB-MK-generated platelets are functional, since earlier studies indicated that CB-derived platelets have impaired aggregation and MSCs may reduce platelet activation, as shown by reduced platelet expression of the activation marker CD62P following MSC co-culture (39–41). Following stimulation with collagen, platelets derived from 10 μ M Y27632-treated MKs showed a higher amount of visible aggregation than unstimulated platelets (Figure 2C). We also stimulated CB-MK-derived platelets with thrombin receptor activating peptide (TRAP). We found a significant dose-dependent increase in CD62P expression in stimulated platelets, compared to unstimulated platelets (2.57% for unstimulated platelets vs. 17.63% for those treated with 100nM TRAP, $p=0.0018$; 29.13% for those treated with 50 μ M TRAP, $p=0.0003$, Figures 2D, E). TEM further confirmed the presence of classical surface and intracellular morphology features in CB-derived platelets, including expression of dense, α , and glycogen granules, an open canalicular system, and multiple mitochondria (2–6nm size range, Figure 2F, Supplementary Figures 2B, 3C). Imaging flow cytometry analysis of platelets derived from CB-MKs indicated co-expression of tubulin with CD41a (Figure 2G).

The highly potent KD045 ROCK inhibitor increases MK platelet production *in-vitro*

We compared the impact of Y27632 with that of a newly developed and potent second-generation ROCK inhibitor, KD045, on CB-MK maturation and platelet generation. Day 19 CB-MKs were treated with various doses of Y27632 or KD045 for 96h in the absence of MSCs (Supplementary Figure 1A). KD045-treated CB-MKs exhibited significantly higher polyploidization ($\geq 8N$ nuclei) compared to untreated CB-MKs in a dose-dependent manner (6.55% in the control vs. 11.07% for 100nM KD045, $p<0.0001$; 12.93% for 1 μ M KD045, $p<0.0001$; 15.10% for 5 μ M KD045, $p<0.0001$, Figures 3A, B). KD045-treated CB-MKs also had significantly higher polyploidization than equimolar concentrations of Y27632 (percentage of CB-MKs expressing $\geq 8N$ ploidy was 12.93% for 1 μ M KD045 vs. 7.05% for 1 μ M Y27632, $p<0.0001$; 15.10% for 5 μ M KD045 vs. 9.73% for 5 μ M Y27632, $p=0.0005$, Figure 3B). KD045 treatment also resulted in a higher proportion of large CB-MKs compared to untreated control CB-MKs, suggesting increased terminal maturation (Supplementary Figure 4A).

Furthermore, KD045-treated CB-MKs generated more platelets at day 4 of ROCK inhibitor treatment than untreated CB-MKs. The number of generated platelets from 1 $\times 10^5$ untreated CB-MKs was approximately 3.68 $\times 10^5$ and significantly less than that from 1 $\times 10^5$ CB-MKs treated with

100nM KD045 (7.48 $\times 10^5$, $p<0.0001$), 1 μ M KD045 (8.85 $\times 10^5$, $p<0.0001$), and 5 μ M KD045 (8.74 $\times 10^5$, $p<0.0001$). KD045-treated CB-MKs also produced significantly more platelets than equimolar concentrations of Y27632 (8.85 $\times 10^5$ for 1 μ M KD045 vs. 5.48 $\times 10^5$ for 1 μ M Y27632, $p<0.001$; 8.74 $\times 10^5$ for 5 μ M KD045 vs. 7.18 $\times 10^5$ for 5 μ M Y27632, $p<0.001$, Figure 3C). In an effort to further optimize the platelet yield from the CB-MKs, we subjected day 22 CB-MKs to horizontal shaking for 6 hours prior to platelet collection and quantification. Horizontal shaking resulted in significantly higher platelet yields compared to those of untreated day 22 CB-MKs (1.01 $\times 10^9$ platelets per CB unit in static conditions vs. 4.00 $\times 10^{10}$ with shaking, $p<0.0001$), which was further enhanced in day 22 CB-MKs that were pretreated with KD045 (2.10 $\times 10^9$ platelets per CB unit in static conditions vs. 7.65 $\times 10^{10}$ with shaking, $p<0.0001$, Figure 3D). KD045-treatment also resulted in significantly higher platelet yields following 6h horizontal shaking than equimolar concentrations of Y27632 (3.60 $\times 10^4$ for 1 μ M KD045 vs. 2.16 $\times 10^4$ for 1 μ M Y27632, $p<0.001$; 3.85 $\times 10^4$ for 5 μ M KD045 vs. 2.19 $\times 10^4$ for 5 μ M Y27632, $p<0.001$, Figure 3E). We also found that platelets generated from 100nM KD045-pretreated CB-MKs had significantly higher aggregation following stimulation with collagen compared to those that were unstimulated (Figure 3F). We observed no significant difference in the mean platelet volume of platelets derived from untreated or KD045-pretreated CB-MKs (Supplementary Figure 4B).

We also investigated the effect of ROCK inhibition on the expression of molecules downstream of ROCK in CB-MKs. The relative intracellular expression of pMYPT1(Thr696), which is downstream of ROCK, was significantly reduced after 48h treatment with 100nM and 1 μ M KD045 compared to untreated CB-MKs, as determined by flow cytometry (1.0 for untreated vs. 0.35 for 100nM KD045, $p=0.0006$; and 0.14 for 1 μ M KD045, $p=0.0002$; $n=3$, Figure 3G). Furthermore, 1 μ M Y27632 was less effective at reducing pMYPT1(Thr696) compared to KD045 ($p=0.0019$), consistent with our findings regarding increased platelet production by KD045-treated CB-MKs compared to Y27632-treated CB-MKs. These findings were confirmed by western blot, which showed that KD045 nearly abolished pMYPT1(Thr696) expression (1.0 for untreated vs. 0.20 for 1 μ M KD045, $p<0.0001$; 0.11 for 5 μ M KD045, $p<0.0001$; and 0.08 for 10 μ M KD045, $p<0.0001$, $n=3$ independent experiments, Supplementary Figures 4C, D). KD045 also reduced pLIMK(Thr508) expression at 100nM (1.0 vs. 0.67, $p=0.0068$ in untreated vs. treated cells) and at 1 μ M (1.0 vs. 0.46, $p=0.0012$ in untreated vs. treated cells). Equimolar concentrations of KD045 also more potently reduced pLIMK(Thr508) compared to Y27632 (0.46 for 1 μ M KD045 vs. 0.89 for 1 μ M Y27632, $p=0.002$, Figure 3G). However, the effect of KD045 on pLIMK(Thr508) expression was smaller than its effect on pMYPT1(Thr696). Short durations of KD045 treatment also induced dose-dependent reductions in pMYPT1(Thr696) ($p=0.0013$, $p=0.0004$ and $p=0.0008$ for 100nM, 1 μ M and 5 μ M

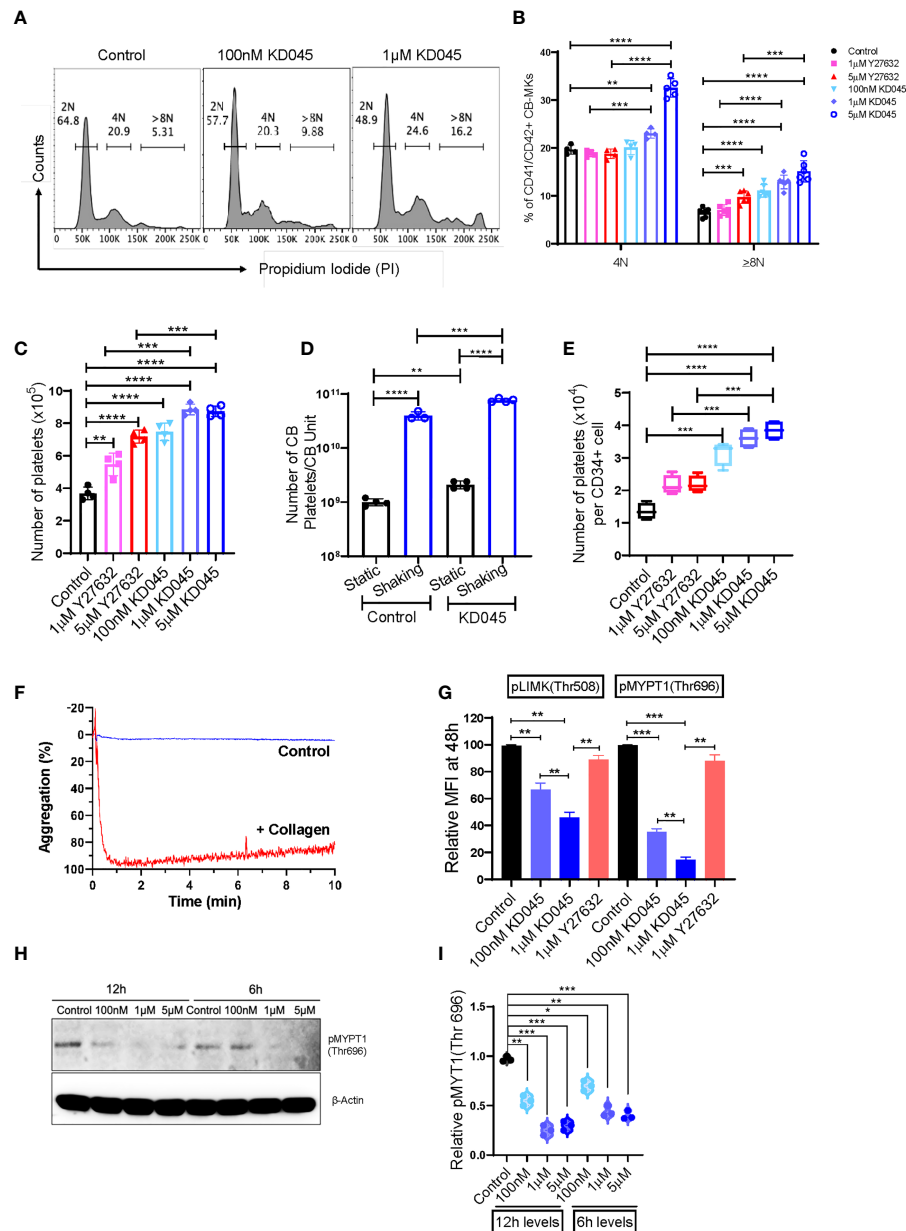


FIGURE 3

KD045 *ex-vivo* treatment enhances CB-MK polyploidization, reduces ROCK signaling, and stimulates MKs to secrete more functional platelets. (A) Histograms showing ploidy analysis by propidium iodide (PI) staining in CD42a+ MKs cultured alone (control) or with 100nM or 1μM KD045 for 96h. (B) Percentages of polyploid levels in MKs that were untreated or treated for 96h with Y27632 or KD045 (n=4-6 different cords in at least 3 independent experiments, **p < 0.01, ***p < 0.001 and ****p < 0.0001). (C) Numbers of secreted platelets from 1x10⁵ CB-MKs that were untreated or treated with Y27632 or KD045 (n=4 different cords in independent experiments, **p < 0.01, ***p < 0.001 and ****p < 0.0001). (D) Number of platelets generated from untreated and KD045-treated day 22 CB-MKs that were subjected to horizontal shaking for 6h prior to platelet quantification. Data are presented as the number of platelets produced per CB unit (n=3-4 per group, **p < 0.01, ***p < 0.001, ****p < 0.0001). (E) Number of platelets generated from untreated, Y27632-, and KD045-treated day 22 CB-MKs that were subjected to horizontal shaking for 6h prior to platelet quantification. Data are presented as the number of platelets generated per seeded CD34+ cell on day 0 (n=4 per group, **p < 0.01, ***p < 0.001, ****p < 0.0001). (F) Aggregation of unstimulated and collagen-stimulated platelets derived from 100nM KD045-treated CB-MKs. (G) Flow cytometry-based pLIMK(Thr508) and pMYPT1(Thr696) intracellular expression, by mean fluorescence intensity (MFI), in untreated, 1μM Y27632, and 100nM-1μM KD045 treated MKs for 48h (n=3, **p < 0.01 and ***p < 0.001 by paired t-tests). (H, I) Western blots and normalized relative pMYPT1(Thr696) levels after 6h and 12h treatment with 100nM, 1μM and 5μM of KD045 in day 22 expanded CB-MKs (n=3 independent experiments, *p < 0.05, **p < 0.01, ***p < 0.001 by paired t-tests). All statistical analyses completed with unpaired t-tests unless otherwise noted.

KD045 respectively at 12h and $p=0.012$, $p=0.0067$ and $p=0.0004$ for 100nM, 1 μ M and 5 μ M KD045, respectively at 6h, $n=3$ independent experiments, **Figures 3H, I**).

We also examined the effect of several cytokines on CB-MK phenotypes. IL-21 reduced the expansion of fully differentiated CB-MKs ($p=0.0082$, **Supplementary Figure 4E**), while IL-11 and IL-1 β increased platelet release by KD045-treated CB-MKs ($p=0.004$, **Supplementary Figure 4F**). Furthermore, KD045 did not alter the expression of CD41/CD42 in CB-MKs ($p=0.14$, **Supplementary Figure 4G**). We also found that fewer platelets generated from CB-MKs expressed CD62P compared to peripheral blood platelets ($p<0.0001$, **Supplementary Figure 4H**). However, CD41/CD42 expression was similar between peripheral blood platelets and CB-MK platelets ($p=0.26$, **Supplementary Figure 4I**).

KD045-pretreated human CB-MKs produce platelets in a murine model of thrombocytopenia

We used a radiation-induced thrombocytopenia model in NSG mice to study the effect of *ex-vivo* ROCK inhibition on donor CB-MKs *in-vivo* (**Supplementary Figure 1C**). Following sublethal exposure of mice to 300cGy radiation, we observed a significant reduction in platelet counts ($1200 \times 10^9/L$ for control vs. $320 \times 10^9/L$ at day 7 post-radiation, **Supplementary Figure 5**). Within 16-20h following sublethal irradiation, KD045-pretreated human CB-MKs were transferred to the mice by intravenous injection. We evaluated human CB-MK (hCD41+CD42+ vs. mCD45) chimerism at 4 weeks post-radiation by flow cytometry and found that the transferred human CB-MKs could be detected in various organs (**Figure 4A**).

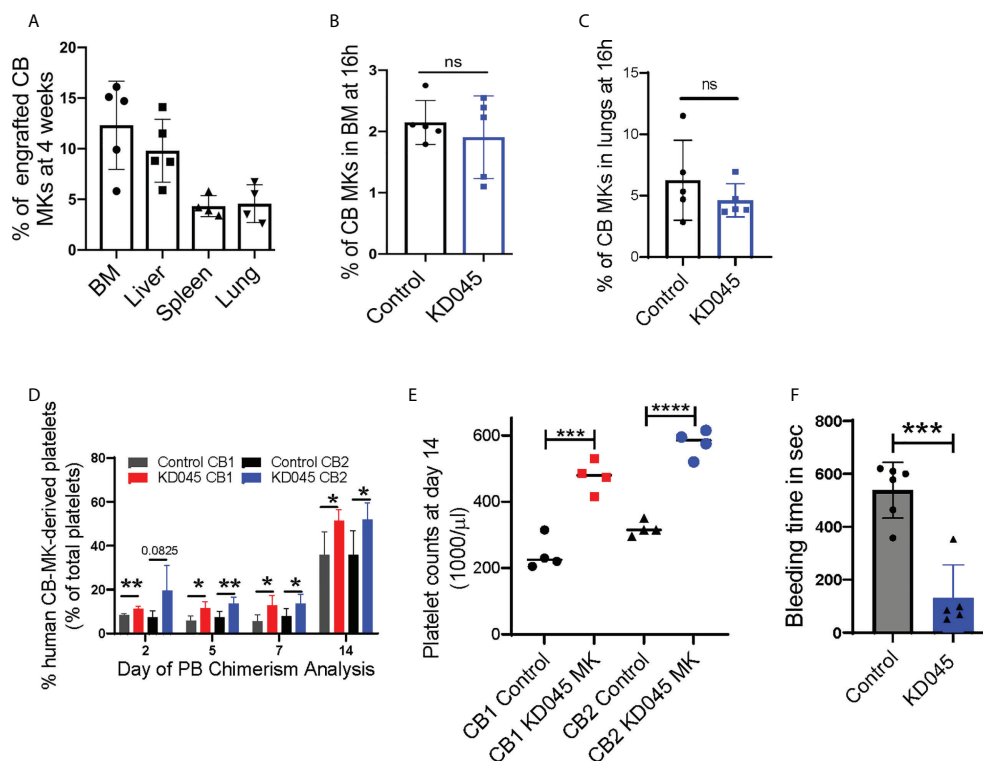


FIGURE 4

ROCK inhibition increases MK platelet production in an *in-vivo* thrombocytopenia model. **(A)** Percentage CB hCD41a+ hCD42+ chimerism in various niches of sub-lethally irradiated NSG mice at 1-month after infusion of 7×10^6 CB-MKs that were pretreated with KD045 ($n=4-5$ mice). **(B, C)** Percentages of untreated or KD045 pretreated CFSE+ CB-MKs (in total Ter119- BM live cells) that homed to mice bone marrow (BM) **(B)** and lungs **(C)** at 16h post 5×10^6 CB-MK transfer ($n=5$ mice per group). **(D)** CB-MK-derived circulating platelet chimerism in mice blood at 2, 5, 7 and 14 days after transfer of 15×10^6 MKs that were either untreated or pretreated with KD045 prior to transfer ($n=4-5$ mice per group from 2 different CB donors, $*p < 0.05$ and $**p < 0.01$). **(E)** Platelet counts in mice blood at 14 days after transfer of 15×10^6 MKs that were either untreated or KD045-pretreated prior to transfer ($n=4$ mice per group, $***p < 0.001$ and $****p < 0.0001$). **(F)** Tail bleeding time in seconds of sub-lethally irradiated NSG mice 14 days after infusion of KD045-pretreated MKs, compared to bleeding time of mice that did not receive MKs ($n=5-6$ mice per group, $***p < 0.001$). All statistical analyses completed with unpaired t-tests. "ns" means not significant.

ROCK inhibition alters cytoskeletal proteins (42), which may hinder CB-MK migration and homing. We therefore determined if KD045-treated CB-MKs have impaired BM homing. NSG mice were irradiated with 300cGy and infused with 5×10^6 untreated or 100nM KD045-pretreated CB-MKs. At 16h post-infusion, human CD41+ CB-MK chimerism in the BM revealed that KD045 treatment did not impact the BM homing potential of CB-MKs (2.2% for control CB-MKs vs. 1.9% for KD045 pretreated CB-MKs, Figure 4B). Similarly, CB-MK homing to the lung was unaltered by KD045 treatment (6.3% for control CB-MKs vs. 4.6% for KD045 pretreated CB-MKs, Figure 4C).

Next, we studied the effect of *ex-vivo* KD045 pretreatment on MKs' platelet generation capacity *in-vivo*. NSG mice were sublethally irradiated and then infused with 15×10^6 KD045-treated or untreated CB-MKs (Supplementary Figure 1D). The percentage of circulating human CD41+ platelets was analyzed ($n=2$ cord donors, Supplementary Figure 4J). We observed a significantly increased percentage of human CD41+ platelets, compared to mouse platelets, in the blood of mice that received KD045-pretreated MKs compared to those that received untreated MKs ($n=4-5$ mice per group from 2 different CB donors, $p=0.03$ for CB1 and $p=0.03$ for CB2 at day 14; Figure 4D). The number of platelets circulating in mice at day 14 that received KD045-pretreated MKs was also significantly higher than in mice that received untreated MKs ($n=4$ mice per group, $p<0.001$ for CB1 and $p<0.0001$ for CB2; Figure 4E). Mice that did not receive CB-MKs had no detectable human CD41+ platelets (data not shown). In this mouse model of thrombocytopenia, mouse MK-derived platelet counts begin to increase approximately 20 days post-irradiation (Supplementary Figure 5). To examine the function of platelets generated from KD045-pretreated CB-MKs, we measured tail vein bleeding time at day 14 post-CB-MK infusion. We found a significant reduction in bleeding time in the recipients of KD045-pretreated CB-MKs (538 seconds for mice that did not receive CB-MKs vs. 130 seconds for mice that received KD045-pretreated CB-MKs, $p=0.0002$, Figure 4F), suggesting that KD045-pretreated CB-MKs and their platelets were functional *in-vivo*.

CRISPR-Cas9 edited HLA-I deficient CB-MKs exhibit normal expansion and undergo reduced cytotoxic T-cell-induced killing

$\beta 2M$ plays an important role in HLA class-I-mediated antigen presentation and recognition. Loss of HLA class-I from a cell surface can help that cell evade the immune system. Therefore, selective removal of $\beta 2M$ from CB-MKs could allow their platelets to escape the removal by the immune system in patients with alloimmune PTR. We

developed CB-CD34+ HLA class-I-deficient CB-MKs ($\beta 2M$ KO, exon 2) (Figure 5A and Supplementary Figure 1B) and evaluated the surface expression of $\beta 2M$. We observed an approximately 90% KO efficiency at day 7 in the differentiating CD34+ cells and early CB-MKs ($n=3$, $p<0.0001$, Figures 5B, C). On day 25 of culture, including 4 days of KD045 treatment, we observed similar numbers of mature CB-MKs in the Cas9 control and HLA-I ($\beta 2M$) KO groups (Figure 5D). The number of platelets released per CB-MK was similar in both groups (Figure 5E), suggesting that $\beta 2M$ ablation does not affect CB-MK proliferation or platelet generation. The levels of CD62P expression were also similar in platelets derived from Cas9 control CB-MKs and $\beta 2M$ KO CB-MKs, indicating similar levels of activation between groups (Figures 5F, G).

Direct co-culture of control or $\beta 2M$ KO mature CB-MKs with cytotoxic T-cells was performed for 4h, followed by assessment of CB-MK apoptosis by measuring annexin V. We found a reduced number of annexin V+ cells in $\beta 2M$ KO CB-MKs (54.80% in the control vs. 6.97% in the $\beta 2M$ KO, $p=0.005$, Figure 5H and Supplementary Figure 6B), suggesting that $\beta 2M$ KO CB-MKs escape cytotoxic T-cell killing. Through chromium release assays, we found that T-cells killed less $\beta 2M$ KO CB-MKs than control CB-MKs at all effector:target ratios tested (81.2% vs. 9.9% at 20:1, $p=0.0005$; 55.1% vs. 4.1% at 10:1, $p=0.004$; 39.0% vs. 1.2% at 5:1, $p=0.008$; and 21.5% vs. 0.3% at 1:1, $p=0.002$; Figure 5I). Our data are consistent with earlier observations showing that $\beta 2M$ KO iPSC-derived MKs are resistant to HLA mismatched-mediated killing (43, 44).

Discussion

With an increasing demand for platelets, the global platelet inventory is continually stressed (45, 46). This is exacerbated by the cumbersome logistics of collecting platelets *via* apheresis and the short shelf-life once the platelets are collected. Novel strategies to produce a consistent and robust supply of platelets are urgently needed. Here, we used several methods, including co-culture with MSCs and ROCK inhibition to promote CB-MKs' maturation and platelet production. In addition, we facilitated immune evasion of MKs by editing their $\beta 2M$ gene expression. Taken together, these modalities may serve as the basis for the development of a new generation of consistently available, off-the-shelf platelets for clinical use in thrombocytopenic patients.

We used CB-derived MKs in this study as CB is a rich source of HSCs and is usually discarded as a waste product but can be readily collected by many world-wide Obstetrical Units and CB banks. These characteristics make CB an ideal source of HSCs from which MKs can be derived. Differentiating MKs requires multiple signals available in the marrow niche (47, 48), including a supportive stromal microenvironment in which MSCs are an integral part (19, 20, 48). We previously developed a co-culture

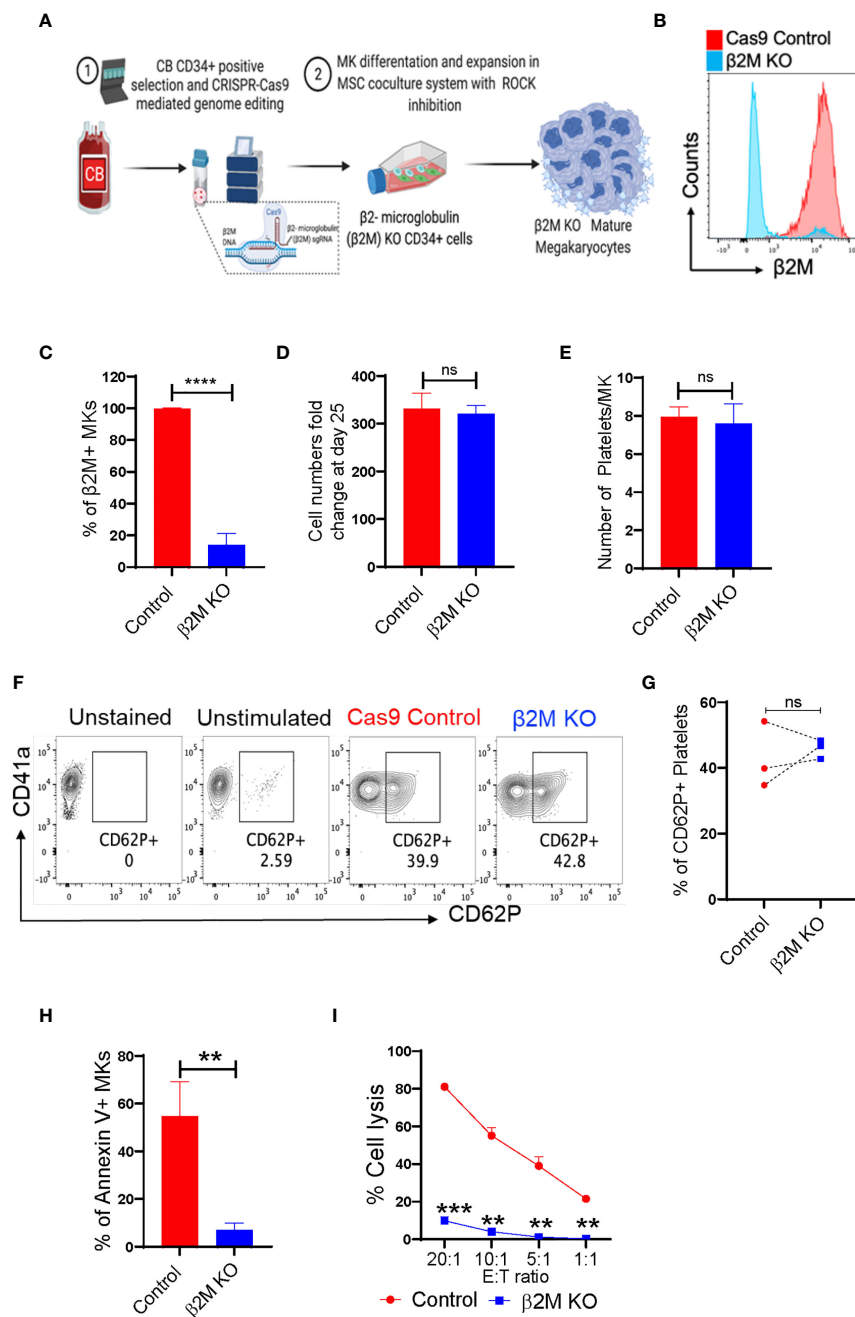


FIGURE 5

CRISPR-Cas9 engineered $\beta 2M$ KO CB-HSCs/MKs have a similar maturation profile and escape allogenic CD8+ T-cell-mediated killing. **(A)** Schematic of the generation of CRISPR-Cas9 edited $\beta 2M$ KO MKs. **(B)** Histogram of $\beta 2M$ expression in Cas9 control and CRISPR-Cas9 $\beta 2M$ KO CD34+ cells at 72h after electroporation. **(C)** $\beta 2M$ expression of the expanding and differentiating day 6 CB-derived CD34+ cells ($n=3$, **** $p < 0.0001$). **(D)** Expansion potential comparison between Cas9 control and $\beta 2M$ crRNA+Cas9 treated CB-derived cells ($n=4$). **(E)** Comparison of the number of platelets secreted per mature MK after 72h culture of day 22, KD045-primed control and $\beta 2M$ KO CB-MKs ($n=3$, $p > 0.15$). **(F)** Flow cytometry contour plots of CD41a and CD62P expression in control and $\beta 2M$ KO CB-MK-derived platelets. **(G)** Percentage of platelets generated from Cas9 control and $\beta 2M$ KO CB-MKs that expressed CD62P ($n=3$). **(H)** Apoptosis analysis of Cas9 control and $\beta 2M$ KO day 20 MKs after MK and pre-activated CD8+ T cell co-culture for 4h, followed by annexin V staining of hCD42+CD3- cells ($n=3$, ** $p < 0.01$). **(I)** Cr51 release assay of day 22 expanded Cas9 control and $\beta 2M$ KO CB-MKs co-cultured with pre-activated CD8+ T cells ($n=2$ cords, ** $p < 0.01$, *** $p < 0.001$). Statistical analyses were performed using unpaired t-tests. "ns" means not significant.

system with human MSCs to expand myeloid cells from CB-HSCs (21). We refined this platform with a cytokine cocktail to expand and differentiate MKs from CB. Our results validate the efficacy of this co-culture approach in that significantly more MKs were derived from a single CB unit expanded in the presence of MSCs compared to those cultured without MSC support.

Cultured CB-MKs also have maturation defects that limit their platelet production (22, 23). ROCK signaling enhances cytokinesis and prevents endomitosis and MK maturation (10, 24–26, 28). Given the availability of highly selective and potent ROCK inhibitors, we used these agents to induce MK maturation. Using a novel ROCK inhibitor, KD045, along with MSC support, we overcame CB-MK maturation defects, allowing their subsequent differentiation into platelet-producing CB-MKs.

We observed that combining KD045 with IL-1 β and IL-11 stimulation further enhanced CB-MK production. Earlier studies have shown that IL-11 enhances megakaryopoiesis and IL-1 β accelerates platelet generation (49–55). Additional cytokines, including CCL5 and MIP, also increase platelet release (56). Contrary to earlier studies identifying megakaryopoiesis and thrombopoiesis-promoting roles of IL-21 (57), we observed significantly reduced numbers of MKs following IL-21 treatment (Supplementary Figure 4E). Although further studies are needed to determine the optimal cytokine milieu for enhancing ROCK inhibition-driven CB-MK maturation, we were able to generate substantial numbers of platelet-producing CB-MKs using our current expansion and ROCK inhibition strategies.

Furthermore, applying shear stress to MKs can increase platelet release (38), and in some experiments (Figures 2B, 3D, E) we used this technique to enhance platelet production *in-vitro*. However, shear stress can damage MKs, which could limit their viability. Thus, in our *in-vivo* studies, we did not apply shear stress to MKs before their transfer to mice. Future studies to determine techniques that allow for the utilization of shear stress to enhance platelet generation without sacrificing MK viability are in progress.

Notably, throughout our *in-vivo* studies, we detected variability in the percentage of CB-MK donor-derived platelets in the peripheral blood of sub-lethally irradiated mice at various time points. This is likely due to inherent differences in the CB cell donors from which the CB-MKs were derived, indicating heterogeneity of MK differentiation potential and platelet production across CB donors. Future studies are in progress to determine the optimal CB donors for MK differentiation. These include examinations of CD34+ cell viability and colony forming unit capability, along with total nucleated cell number and CD34+ cell dose per CB unit. We will compare these characteristics of individual CB units with their capacity to generate CB-MKs and platelets. These findings will enable us to screen CB units to determine which are most suitable for efficient CB-MK production.

Until recently, gene editing of HSC-derived MKs has been challenging and inefficient and as a result, few studies have used CRISPR-Cas9-mediated gene targeting in MKs (58–60). Here, we used CRISPR-Cas9 to knock out (KO) β 2M in CB-CD34+ cells, followed by differentiation to mature MKs that evade allogeneic T-cell killing. We anticipate that β 2M KO for the abrogation of HLA-I antigen expression in MKs/platelets will be a viable technique for patients with PTR due to their immune evasion. However, loss of HLA-I may leave the CB-MKs vulnerable to killing by natural killer (NK) cells, which recognize and kill cells lacking HLA-I antigens. If this arises, we will determine if overexpression of HLA-E in the CB-MKs protects them from NK-mediated killing. HLA-E inhibits NK cells by binding to inhibitory CD94/NKG2A receptors and its upregulation can reduce NK lysis of cells lacking HLA-I antigens (61, 62). We will utilize this characteristic of HLA-E to safeguard CB-MKs if needed.

One of the critical limiting factors in the use of CD34+ cells to generate platelets has been the yield of MKs and platelets that are generated *in-vitro* (8). In our optimized technique with MSC co-culture, we generated approximately 4×10^8 CB-MKs per CB unit, and with KD045 and horizontal shaking we generated approximately 7.65×10^{10} platelets from a CB unit, or 5.8×10^4 platelets per starting CD34+ cell. Yields of MKs and platelets vary widely across previous studies, with upper limits of 2×10^5 MKs and 3.4×10^4 platelets per initial hiPSC or CD34+ HSC placed into culture (63). Our results are in-line with these yields. A unit of transfused platelets typically contains $3\text{--}4 \times 10^{11}$ platelets (64). We are further optimizing the production and processing of CB-MKs in our laboratory to produce the maximal number of platelets from the CB-MKs, but it is possible that even a lower number of CB-MKs can provide optimal hemostasis.

Procedures to scale-up our findings and generate CB-MKs and platelets in a good manufacturing practice (GMP)-compliant manner for clinical use are in progress. We will use CD34+ cells from clinically approved, cryopreserved CB units from our FDA-licensed CB bank. Following positive selection and β 2M KO, CD34+ cells will be cultured in sequential GMP-compliant, closed bioreactors with MSCs and MK lineage-specific cytokines for 18 days, followed by ROCK inhibition without MSCs for 3 days. After collection and quality control product release the cells will be administered to the patient (Supplementary Figure 7). Using this system of CB-MK differentiation, we envision the establishment of a consistent and readily available platelet source that can be given to patients with refractory alloimmune thrombocytopenia. Importantly, our technique will use a closed system, which will reduce potential contamination that can arise with a protocol involving multiple changes in conditions, such as feeder cells, cytokines, and pharmacologic inhibitors. Also, the multistep nature of the process will provide multiple opportunities to increase efficiency with advancing technologies and the use of better reagents once developed.

Overall, we provided a rationale for using multiple modalities to improve CB-MK differentiation and platelet production, including MSC co-culture and the novel ROCK inhibitor KD045 to differentiate CB-MKs and removal of β 2M to improve CB-MK immune evasion. These techniques, applied collectively, provide a readily translatable strategy to provide a universal off-the-shelf platelet source to maintain a reliable supply of platelets for vulnerable thrombocytopenic patients.

Data availability statement

The raw data supporting the conclusions of this article will be made available by the authors, without undue reservation.

Ethics statement

The studies involving human participants were reviewed and approved by Institutional Review Board, The University of Texas MD Anderson Cancer Center. The patients/participants provided their written informed consent to participate in this study. The animal study was reviewed and approved by Institutional Animal Care and Use Committee, The University of Texas MD Anderson Cancer Center.

Author contributions

ES, BK and VA-K conceptualized, designed and directed the study. BK performed experiments, interpreted, and analyzed data. MM and RB assisted in generating the engineered MKs. JJ, XW, VW, AG, RC, RD-G assisted with in-vivo experiments. JJ, MM, FRS, MK, and VN assisted in MK generation and functional experiments. PB assisted with the imaging cytometry experiments. MD, LMG, MS, SA, PL, HR, and PB helped with study planning and discussion. ES, BK, MT, VA-K, RS, UP, and JR reviewed all the data, and wrote and edited the manuscript. ES provided financial and administrative support for the study. All authors contributed to the article and approved the submitted version.

Funding

Funding for this study was provided by National Institutes of Health grants RO1-CA061508-24 and CCSG P30-CA016672 #7690-45.

Acknowledgments

The authors would like to thank Kiersten Maldonado, Vivien Van and other members of animal facility for their help in the animal experiments. The authors also thank Kenneth Dunner Jr. from the high-resolution electron microscopy facility of MD Anderson for TEM imaging. All graphics and schematics were created with BioRender.com.

Conflict of interest

ES, BK, MM, VA, RB have filed for a patent MDA20-0115; UTSC.P1219US.P1 "Production of megakaryocytes and platelets in a co-culture system". ES and RB and the MDACC has an institutional financial conflict of interest with Affimed GmbH and Takeda Pharmaceuticals for the licensing of the technology related to CAR-NK cells. ES participates on Scientific Advisory Board for Bayer, Novartis, Magenta, Adaptimmune, Mesoblast and Axio. According to NIH policies and procedures, the Brigham & Women's Hospital has assigned intellectual property rights regarding cell surface glycan engineering to RS. RS's ownership interests were reviewed and are managed by the Brigham & Women's Hospital and Partners HealthCare in accordance with their conflict of interest policy.

The remaining authors declare that the research was conducted in the absence of any commercial or financial relationships that could be constructed as a potential conflict of interest

Publisher's note

All claims expressed in this article are solely those of the authors and do not necessarily represent those of their affiliated organizations, or those of the publisher, the editors and the reviewers. Any product that may be evaluated in this article, or claim that may be made by its manufacturer, is not guaranteed or endorsed by the publisher.

Supplementary material

The Supplementary Material for this article can be found online at: <https://www.frontiersin.org/articles/10.3389/fimmu.2022.1018047/full#supplementary-material>

References

- Takayama N, Eto K. Pluripotent stem cells reveal the developmental biology of human megakaryocytes and provide a source of platelets for clinical application. *Cell Mol Life Sci* (2012) 69(20):3419–28. doi: 10.1007/s00018-012-0995-4
- Takayama N, Eto K. *In vitro* generation of megakaryocytes and platelets from human embryonic stem cells and induced pluripotent stem cells. *Methods Mol Biol* (2012) 788:205–17. doi: 10.1007/978-1-61779-307-3_15
- Takayama N, Nishikii H, Usui J, Tsukui H, Sawaguchi A, Hiroyama T, et al. Generation of functional platelets from human embryonic stem cells *in vitro* via ES-sacs, VEGF-promoted structures that concentrate hematopoietic progenitors. *Blood* (2008) 111(11):5298–306. doi: 10.1182/blood-2007-10-117622
- Nakamura S, Takayama N, Hirata S, Seo H, Endo H, Ochi K, et al. Expandable megakaryocyte cell lines enable clinically applicable generation of platelets from human induced pluripotent stem cells. *Cell Stem Cell* (2014) 14(4):535–48. doi: 10.1016/j.stem.2014.01.011
- Sone M, Nakamura S, Umeda S, Ginya H, Oshima M, Kanashiro MA, et al. Silencing of p53 and CDKN1A establishes sustainable immortalized megakaryocyte progenitor cells from human iPSCs. *Stem Cell Rep* (2021) 16(12):2861–70. doi: 10.1016/j.stemcr.2021.11.001
- Lu SJ, Li F, Yin H, Feng Q, Kimbrel EA, Hahm E, et al. Platelets generated from human embryonic stem cells are functional *in vitro* and in the microcirculation of living mice. *Cell Res* (2011) 21(3):530–45. doi: 10.1038/cr.2011.8
- Takayama N, Nishimura S, Nakamura S, Shimizu T, Ohnishi R, Endo H, et al. Transient activation of c-MYC expression is critical for efficient platelet generation from human induced pluripotent stem cells. *J Exp Med* (2010) 207(13):2817–30. doi: 10.1084/jem.20100844
- Gollomp K, Lambert MP, Poncz M. Current status of blood ‘pharming’: megakaryocyte transfusions as a source of platelets. *Curr Opin Hematol* (2017) 24(6):565–71. doi: 10.1097/MOH.0000000000000378
- Pick M, Azzola L, Osborne E, Stanley EG, Elefanti AG. Generation of megakaryocytic progenitors from human embryonic stem cells in a feeder- and serum-free medium. *PLoS One* (2013) 8(2):e55530. doi: 10.1371/journal.pone.0055530
- Ito Y, Nakamura S, Sugimoto N, Shigemori T, Kato Y, Ohno M, et al. Turbulence activates platelet biogenesis to enable clinical scale *ex vivo* production. *Cell* (2018) 174(3):636–648.e618. doi: 10.1016/j.cell.2018.06.011
- Yang Y, Liu C, Lei X, Wang H, Su P, Ru Y, et al. Integrated biophysical and biochemical signals augment megakaryopoiesis and thrombopoiesis in a three-dimensional rotary culture system. *Stem Cells Transl Med* (2016) 5(2):175–85. doi: 10.5966/sctm.2015-0080
- Martinez AF, Miller WM. Enabling Large-scale *ex vivo* production of megakaryocytes from CD34(+) cells using gas-permeable surfaces. *Stem Cells Transl Med* (2019) 8(7):658–70. doi: 10.1002/sctm.18-0160
- Sugimoto N, Eto K. Generation and manipulation of human iPSC-derived platelets. *Cell Mol Life Sci* (2021) 78(7):3385–401. doi: 10.1007/s00018-020-03749-8
- Matsunaga T, Tanaka I, Kobune M, Kawano Y, Tanaka M, Kuribayashi K, et al. *Ex vivo* large-scale generation of human platelets from cord blood CD34+ cells. *Stem Cells* (2006) 24(12):2877–87. doi: 10.1634/stemcells.2006-0309
- Jarocho D, Vo KK, Lyde RB, Hayes V, Camire RM, Poncz M. Enhancing functional platelet release *in vivo* from *in vitro*-grown megakaryocytes using small molecule inhibitors. *Blood Adv* (2018) 2(6):597–606. doi: 10.1182/bloodadvances.2017010975
- Bhatlekar S, Basak I, Edelstein LC, Campbell RA, Lindsey CR, Italiano JE Jr., et al. Anti-apoptotic BCL2L2 increases megakaryocyte proplatelet formation in cultures of human cord blood. *Haematologica* (2019) 104(10):2075–83. doi: 10.3324/haematol.2018.204685
- Moroi AJ, Newman PJ. Conditional CRISPR-mediated deletion of Lyn kinase enhances differentiation and function of iPSC-derived megakaryocytes. *J Thromb Haemost* (2022) 20(1):182–95. doi: 10.1111/jth.15546
- Moreau T, Evans AL, Vasquez L, Tijssen MR, Yan Y, Trotter MW, et al. Large-Scale production of megakaryocytes from human pluripotent stem cells by chemically defined forward programming. *Nat Commun* (2016) 7:11208. doi: 10.1038/ncomms11208
- Mendez-Ferrer S, Michurina TV, Ferraro F, Mazloom AR, Macarthur BD, Lira SA, et al. Mesenchymal and hematopoietic stem cells form a unique bone marrow niche. *Nature* (2010) 466(7308):829–34. doi: 10.1038/nature09262
- Kfoury Y, Scadden DT. Mesenchymal cell contributions to the stem cell niche. *Cell Stem Cell* (2015) 16(3):239–53. doi: 10.1016/j.stem.2015.02.019
- de Lima M, McNiece I, Robinson SN, Munsell M, Eapen M, Horowitz M, et al. Cord-blood engraftment with *ex vivo* mesenchymal-cell coculture. *N Engl J Med* (2012) 367(24):2305–15. doi: 10.1056/NEJMoa1207285
- Mattia G, Vulcano F, Milazzo L, Barca A, Macioce G, Giampaolo A, et al. Different ploidy levels of megakaryocytes generated from peripheral or cord blood CD34+ cells are correlated with different levels of platelet release. *Blood* (2002) 99(3):888–97. doi: 10.1182/blood.V99.3.888
- Bornstein R, Garcia-Vela J, Gilsanz F, Auray C, Cales C. Cord blood megakaryocytes do not complete maturation, as indicated by impaired establishment of endomitosis and low expression of G1/S cyclins upon thrombopoietin-induced differentiation. *Br J Haematol* (2001) 114(2):458–65. doi: 10.1046/j.1365-2141.2001.02954.x
- Lordier L, Jalil A, Aurade F, Larbret F, Larghero J, Debili N, et al. Megakaryocyte endomitosis is a failure of late cytokinesis related to defects in the contractile ring and Rho/Rock signaling. *Blood* (2008) 112(8):3164–74. doi: 10.1182/blood-2008-03-144956
- Avanzi MP, Mitchell WB. *Ex vivo* production of platelets from stem cells. *Br J Haematol* (2014) 165(2):237–47. doi: 10.1111/bjh.12764
- Avanzi MP, Goldberg F, Davila J, Langhi D, Chiattone C, Mitchell WB. Rho kinase inhibition drives megakaryocyte polyploidization and proplatelet formation through MYC and NFE2 downregulation. *Br J Haematol* (2014) 164(6):867–76. doi: 10.1111/bjh.12709
- Avanzi MP, Chen A, He W, Mitchell WB. Optimizing megakaryocyte polyploidization by targeting multiple pathways of cytokinesis. *Transfusion* (2012) 52(11):2406–13. doi: 10.1111/j.1537-2995.2012.03711.x
- Chang Y, Aurade F, Larbret F, Zhang Y, Le Couedic JP, Momeux L, et al. Proplatelet formation is regulated by the Rho/ROCK pathway. *Blood* (2007) 109(10):4229–36. doi: 10.1182/blood-2006-04-020024
- Vitrat N, Cohen-Solal K, Pique C, Le Couedic JP, Norol F, Larsen AK, et al. Endomitosis of human megakaryocytes are due to abortive mitosis. *Blood* (1998) 91(10):3711–23. doi: 10.1182/blood.V91.10.3711
- Fasano RM, Mamcarz E, Adams S, Donohue Jerussi T, Sugimoto K, Tian X, et al. Persistence of recipient human leucocyte antigen (HLA) antibodies and production of donor HLA antibodies following reduced intensity allogeneic hematopoietic stem cell transplantation. *Br J Haematol* (2014) 166(3):425–34. doi: 10.1111/bjh.12890
- Stanworth SJ, Navarrete C, Estcourt L, Marsh J. Platelet refractoriness—practical approaches and ongoing dilemmas in patient management. *Br J Haematol* (2015) 171(3):297–305. doi: 10.1111/bjh.13597
- Yankee RA. Importance of histocompatibility in platelet transfusion therapy. *Vox Sang* (1971) 20(5):419–26. doi: 10.1111/j.1423-0410.1971.tb01812.x
- Daly PA, Schiffer CA, Aisner J, Wiernik PH. Platelet transfusion therapy, one-hour posttransfusion increments are valuable in predicting the need for HLA-matched preparations. *JAMA* (1980) 243(5):435–8. doi: 10.1001/jama.1980.03300310023016
- Saito S, Ota S, Seshimo H, Yamazaki Y, Nomura S, Ito T, et al. Platelet transfusion refractoriness caused by a mismatch in HLA-c antigens. *Transfusion* (2002) 42(3):302–8. doi: 10.1046/j.1537-2995.2002.00051.x
- Rebulla P. Refractoriness to platelet transfusion. *Curr Opin Hematol* (2002) 9(6):516–20. doi: 10.1097/00062752-200211000-00009
- Rebulla P. A mini-review on platelet refractoriness. *Haematologica* (2005) 90(2):247–53. doi: 10.3324/ha.2005.90.2
- Nakao K, Angrist AA. Membrane surface specialization of blood platelet and megakaryocyte. *Nature* (1968) 217(5132):960–1. doi: 10.1038/217960a0
- Junt T, Schulze H, Chen Z, Massberg S, Goerge T, Krueger A, et al. Dynamic visualization of thrombopoiesis within bone marrow. *Science* (2007) 317(5845):1767–70. doi: 10.1126/science.1146304
- Netsch P, Elvers-Hornung S, Uhlig S, Klüter H, Huck V, Kirschhöfer F, et al. Human mesenchymal stromal cells inhibit platelet activation and aggregation involving CD73-converted adenosine. *Stem Cell Res Ther* (2018) 9(1):184. doi: 10.1186/s13287-018-0936-8
- Mendelson A, Strat AN, Bao W, Rosston P, Fallon G, Ohn S, et al. Mesenchymal stromal cells lower platelet activation and assist in platelet formation *in vitro*. *JCI Insight* (2019) 4(16):e126982. doi: 10.1172/jci.insight.126982
- Stokhuijzen E, Koornneef JM, Nota B, van den Eshof BL, van Alphen FJ, van den Biggelaar M, et al. Differences between platelets derived from neonatal cord blood and adult peripheral blood assessed by mass spectrometry. *J Proteome Res* (2017) 16(10):3567–75. doi: 10.1021/acs.jproteome.7b00298
- Amano M, Nakayama M, Kaibuchi K. Rho-kinase/ROCK: A key regulator of the cytoskeleton and cell polarity. *Cytoskeleton (Hoboken)* (2010) 67(9):545–54. doi: 10.1002/cm.20472
- Suzuki D, Flahou C, Yoshikawa N, Stirblyte I, Hayashi Y, Sawaguchi A, et al. iPSC-derived platelets depleted of HLA class I are inert to anti-HLA class I and natural killer cell immunity. *Stem Cell Rep* (2020) 14(1):49–59. doi: 10.1016/j.stemcr.2019.11.011

44. Norbnop P, Ingrungruanglert P, Israsena N, Suphapeetiporn K, Shotelersuk V. Generation and characterization of HLA-universal platelets derived from induced pluripotent stem cells. *Sci Rep* (2020) 10(1):8472. doi: 10.1038/s41598-020-65577-x
45. Whitaker B, Rajbhandary S, Kleinman S, Harris A, Kamani N. Trends in united states blood collection and transfusion: results from the 2013 AABB blood collection, utilization, and patient blood management survey. *Transfusion* (2016) 56(9):2173–83. doi: 10.1111/trf.13676
46. Jones JM, Sapiiano MRP, Savinkina AA, Haass KA, Baker ML, Henry RA, et al. Slowing decline in blood collection and transfusion in the united states - 2017. *Transfusion* (2020) 60 (Suppl 2):S1–9. doi: 10.1111/trf.15604
47. Noetzli LJ, French SL, Machlus KR. New insights into the differentiation of megakaryocytes from hematopoietic progenitors. *Arterioscler Thromb Vasc Biol* (2019) 39(7):1288–300. doi: 10.1161/ATVBAHA.119.312129
48. Pinho S, Frenette PS. Hematopoietic stem cell activity and interactions with the niche. *Nat Rev Mol Cell Biol* (2019) 20(5):303–20. doi: 10.1038/s41580-019-0103-9
49. Teramura M, Kobayashi S, Hoshino S, Oshimi K, Mizoguchi H. Interleukin-11 enhances human megakaryocytopoiesis *in vitro*. *Blood* (1992) 79(2):327–31. doi: 10.1182/blood.V79.2.327.327
50. Yang M, Li K, Chui CM, Yuen PM, Chan PK, Chuen CK, et al. Expression of interleukin (IL) 1 type I and type II receptors in megakaryocytic cells and enhancing effects of IL-1beta on megakaryocytopoiesis and NF-E2 expression. *Br J Haematol* (2000) 111(1):371–80. doi: 10.1046/j.1365-2141.2000.02340.x
51. Angchaisuksiri P, Grigus SR, Carlson PL, Krystal GW, Dessypris EN. Secretion of a unique peptide from interleukin-2-stimulated natural killer cells that induces endomitosis in immature human megakaryocytes. *Blood* (2002) 99(1):130–6. doi: 10.1182/blood.V99.1.130
52. Nishimura S, Nagasaki M, Kunishima S, Sawaguchi A, Sakata A, Sakaguchi H, et al. IL-1alpha induces thrombopoiesis through megakaryocyte rupture in response to acute platelet needs. *J Cell Biol* (2015) 209(3):453–66. doi: 10.1083/jcb.201410052
53. Bhatia M, Davenport V, Cairo MS. The role of interleukin-11 to prevent chemotherapy-induced thrombocytopenia in patients with solid tumors, lymphoma, acute myeloid leukemia and bone marrow failure syndromes. *Leuk Lymphoma* (2007) 48(1):9–15. doi: 10.1080/10428190600909115
54. Beaulieu LM, Lin E, Mick E, Koupenova M, Weinberg EO, Kramer CD, et al. Interleukin 1 receptor 1 and interleukin 1beta regulate megakaryocyte maturation, platelet activation, and transcript profile during inflammation in mice and humans. *Arterioscler Thromb Vasc Biol* (2014) 34(3):552–64. doi: 10.1161/ATVBAHA.113.302700
55. Weich NS, Fitzgerald M, Wang A, Calvetti J, Yetz-Aldape J, Neben S, et al. Recombinant human interleukin-11 synergizes with steel factor and interleukin-3 to promote directly the early stages of murine megakaryocyte development *in vitro*. *Blood* (2000) 95(2):503–9. doi: 10.1182/blood.V95.2.503
56. Machlus KR, Johnson KE, Kulenthirarajan R, Forward JA, Tippy MD, Soussou TS, et al. CCL5 derived from platelets increases megakaryocyte proplatelet formation. *Blood* (2016) 127(7):921–6. doi: 10.1182/blood-2015-05-644583
57. Benbarche S, Strassel C, Angenieux C, Mallo L, Freund M, Gachet C, et al. Dual role of IL-21 in megakaryopoiesis and platelet homeostasis. *Haematologica* (2017) 102(4):637–46. doi: 10.3324/haematol.2016.143958
58. Feng Q, Shabrani N, Thon JN, Huo H, Thiel A, Machlus KR, et al. Scalable generation of universal platelets from human induced pluripotent stem cells. *Stem Cell Rep* (2014) 3(5):817–31. doi: 10.1016/j.stemcr.2014.09.010
59. Montenont E, Bhatlekar S, Jacob S, Kosaka Y, Manne BK, Lee O, et al. CRISPR-edited megakaryocytes for rapid screening of platelet gene functions. *Blood Adv* (2021) 5(9):2362–74. doi: 10.1182/bloodadvances.2020004112
60. Zhu F, Feng M, Sinha R, Seita J, Mori Y, Weissman IL. Screening for genes that regulate the differentiation of human megakaryocytic lineage cells. *Proc Natl Acad Sci USA* (2018) 115(40):E9308–16. doi: 10.1073/pnas.1805434115
61. Tomasec P, Braud VM, Rickards C, Powell MB, McSharry BP, Gadola S, et al. Surface expression of HLA-e, an inhibitor of natural killer cells, enhanced by human cytomegalovirus gpUL40. *Science* (2000) 287(5455):1031. doi: 10.1126/science.287.5455.1031
62. Lee N, Llano M, Carretero M, Ishitani A, Navarro F, López-Botet M, et al. HLA-e is a major ligand for the natural killer inhibitory receptor CD94/NKG2A. *Proc Natl Acad Sci USA* (1998) 95(9):5199–204. doi: 10.1073/pnas.95.9.5199
63. Liu H, Liu J, Wang L, Zhu F. *In vitro* generation of megakaryocytes and platelets. *Front Cell Dev Biol* (2021) 9:713434. doi: 10.3389/fcell.2021.713434
64. Kaufman RM, Djulbegovic B, Gernsheimer T, Kleinman S, Tinmouth AT, Capocelli KE, et al. Platelet transfusion: a clinical practice guideline from the AABB. *Ann Intern Med* (2015) 162(3):205–13. doi: 10.7326/M14-1589

COPYRIGHT

© 2022 Kumar, Afshar-Kharghan, Mendt, Sackstein, Tanner, Popat, Ramdial, Daher, Jimenez, Basar, Melo Garcia, Shanley, Kaplan, Wan, Nandivada, Reyes Silva, Woods, Gilbert, Gonzalez-Delgado, Acharya, Lin, Rafei, Banerjee and Shpall. This is an open-access article distributed under the terms of the [Creative Commons Attribution License \(CC BY\)](https://creativecommons.org/licenses/by/4.0/). The use, distribution or reproduction in other forums is permitted, provided the original author(s) and the copyright owner(s) are credited and that the original publication in this journal is cited, in accordance with accepted academic practice. No use, distribution or reproduction is permitted which does not comply with these terms.



OPEN ACCESS

EDITED BY

Catherine Sautes-Fridman,
INSERM U1138 Centre de Recherche
des Cordeliers (CRC), France

REVIEWED BY

Hongji Zhang,
University of Virginia, United States
Firas Hamdan,
University of Maryland, Baltimore,
United States
Kohichi Takada,
Sapporo Medical University, Japan

*CORRESPONDENCE

Di Zhu
zhudi@fudan.edu.cn

SPECIALTY SECTION

This article was submitted to
Cancer Immunity
and Immunotherapy,
a section of the journal
Frontiers in Immunology

RECEIVED 05 June 2022

ACCEPTED 26 September 2022

PUBLISHED 11 October 2022

CITATION

Liu C, Yang M, Zhang D, Chen M
and Zhu D (2022) Clinical cancer
immunotherapy: Current
progress and prospects.
Front. Immunol. 13:961805.
doi: 10.3389/fimmu.2022.961805

COPYRIGHT

© 2022 Liu, Yang, Zhang, Chen and
Zhu. This is an open-access article
distributed under the terms of the
Creative Commons Attribution License
(CC BY). The use, distribution or
reproduction in other forums is
permitted, provided the original author
(s) and the copyright owner(s) are
credited and that the original
publication in this journal is cited, in
accordance with accepted academic
practice. No use, distribution or
reproduction is permitted which does
not comply with these terms.

Clinical cancer immunotherapy: Current progress and prospects

Chenglong Liu ¹, Mengxuan Yang ¹, Daizhou Zhang ²,
Ming Chen ^{3,4} and Di Zhu ^{1,2,5*}

¹Minhang Hospital and Department of Pharmacology, School of Pharmacy, Fudan University, Shanghai, China, ²New Drug Evaluation Center, Shandong Academy of Pharmaceutical Science, Jinan, China, ³Department of Laboratory Medicine, Sixth Affiliated Hospital of Yangzhou University, Yangzhou, China, ⁴Department of Laboratory Medicine, Affiliated Taixing Hospital of Bengbu Medical College, Taizhou, China, ⁵Shanghai Engineering Research Center of ImmunoTherapeutics, Fudan University, Shanghai, China

Immune checkpoint therapy via PD-1 antibodies has shown exciting clinical value and robust therapeutic potential in clinical practice. It can significantly improve progression-free survival and overall survival. Following surgery, radiotherapy, chemotherapy, and targeted therapy, cancer treatment has now entered the age of immunotherapy. Although cancer immunotherapy has shown remarkable efficacy, it also suffers from limitations such as irAEs, cytokine storm, low response rate, etc. In this review, we discuss the basic classification, research progress, and limitations of cancer immunotherapy. Besides, by combining cancer immunotherapy resistance mechanism with analysis of combination therapy, we give our insights into the development of new anticancer immunotherapy strategies.

KEYWORDS

immunotherapy, tumor microenvironment, immune checkpoint inhibitors, CAR-T, cancer vaccines

Introduction

Cancer immune surveillance is an important process by which the immune system can identify and eliminate nascent tumor cells (1). Normally, when tumor cells invade healthy tissue, the immune system can recognize and eliminate them based on tumor-associated antigens (TAAs). However, tumor cells can evade the immune system through a variety of mechanisms called immune escape (2). There are four main mechanisms: 1) decreasing immunogenicity by down-regulating surface antigen expression; 2) up-regulating immune checkpoints on the surface for suppressing T-cell activity; 3) recruiting suppressor immune cells such as myeloid-derived suppressor cells (MDSCs) and regulatory T cells (Treg) as well as cytokines to form a suppressive immune microenvironment; 4) releasing acidic and toxic metabolites that inhibit the activity of immune cells in the tumor microenvironment (3).

Cancer is the second-leading cause of human death after cardiovascular and cerebrovascular diseases, and the number of patients continues to increase. Cancer treatment has progressed from surgical resection, radiation therapy, chemotherapy, and targeted drug therapy to immunotherapy. Cancer immunotherapy reactivates the body's immune system to produce anticancer effects and thus kills and eliminates tumor cells. Immunotherapy is a promising treatment. Different from traditional therapy, immunotherapy uses some cytokines, chemokines, and immune cells to reshape the tumor microenvironment, which can lead to robust effects and prevent recurrence (4, 5). The emergence of immunotherapy has changed the standard and concept of tumor treatment. This article focuses on the latest clinical progress in cancer immunotherapy, including monoclonal antibodies (mAbs), small molecule drugs, adoptive cell therapy, oncolytic viruses, and cancer vaccines (Figure 1). We discuss limitations, immune resistance, and combination strategies in this review and hope to give a promising outlook for the future development of cancer immunotherapy.

Monoclonal antibody therapy

Therapeutic mAbs

mAbs are immunoglobulins (Ig) which commonly include two Fab terminals binding to targets and an Fc terminal binding to

receptors on the surface of immune cells. All mAbs exert their function by direct targeting *via* Fab terminals. Additionally, Fc-Fc receptor (FcR) interaction can modulate their modes of action (MOA) (6, 7). The main Fc-mediated effector functions are classified into complement-dependent cytotoxicity (CDC), antibody-dependent cell-mediated cytotoxicity (ADCC), and antibody-dependent cellular phagocytosis (ADCP). CDC is attributed to the Fc interaction with complement component C1q, followed by the activation of the complement system leading to the downstream immune responses on different immune cells (8, 9). ADCC and ADCP are two mechanisms mediated by the direct interaction of Fc and FcγR. ADCC is mainly attributed to NK cells activated by the interaction of FcγRIIIa with the mAb's Fc part. ADCP is mediated by FcγIIa-activated macrophages, which can phagocytose antibody-bounded tumor cells, leading to the elimination of tumor cells (8, 9). In other MOAs, mAbs are used to bind and block, such as soluble antigens (e.g., α -tumor necrosis factor (TNF- α)) and disease-dependent pathological mediators (e.g., vascular endothelial growth factor (VEGF)). Since rituximab targeting CD20 was first approved for Non-Hodgkin's lymphoma (NHL) in 1997, the US Food and Drug Administration (FDA) has approved a variety of therapeutic monoclonal antibodies, which can target CD19, HER-2, VEGFA, EGFR, and CD52, etc. (Table 1).

Besides non-conjugated mAbs targeting 'naked' antigens, antibody-drug conjugates (ADCs) have shown promising

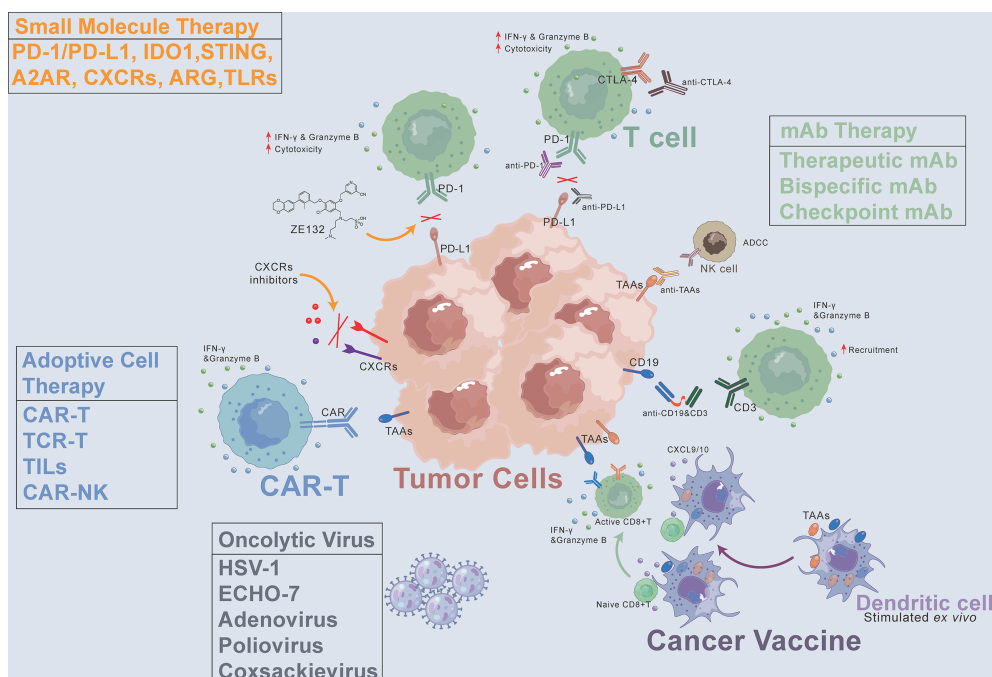


FIGURE 1

Cancer immunotherapy methods, including monoclonal antibodies (mAbs), small molecule drugs, adoptive cell therapy, oncolytic virus, and cancer vaccines. CAR, chimeric antigen receptor. CXCR, C-X-C motif chemokine receptor. TAAs, tumor-associated antigens. ADCC, antibody-dependent cell-mediated cytotoxicity. PD-1, programmed death-1. PD-L1, programmed death-ligand 1. CTLA-4, cytotoxic T-lymphocyte-associated protein 4.

therapeutic effects. ADCs show direct cytotoxicity based on their payloads, which can be ingested through the endocytosis of receptor-bound ADCs. Among the ADCs approved by the FDA, the indications of targets including CD22, CD30, CD33, CD79b, and BCMA are hematological tumors. Besides, HER2, Nectin-4, and Trop-2 are indicated for solid tumors. In terms of target accessibility, solid tumors are more obstructive than

hematological tumors. The microenvironment of solid tumors and other factors make it difficult for mAbs to penetrate. In this regard, the accessibility of hematological tumors is better, which is the key factor why therapeutic mAbs will make breakthroughs in the field of hematological tumors first. But now, ADCs also show promising results for the treatment of solid tumors after the optimization of antibodies, linkers, and payloads. In a phase

TABLE 1 FDA-approved mAbs (Up to March 2022).

Therapeutic mAb

Target	Name	Company	Year of launched	Mechanism of Action
CD20	Rituximab	Roche	1997	CDC, ADCC, ADCP
CD20	Ofatumumab	Novartis	2009	CDC, ADCC, ADCP
CD20	Obinutuzumab	Roche	2013	ADCC, ADCP
CD19	Tafasitamab	MorphoSys & Incyte	2020	CDC, ADCC, ADCP
CD19	Loncastuximab tesirine	ADC Therapeutics	2021	Cytotoxic drug delivery
CD52	Alemtuzumab	Genzyme	2007	CDC, ADCC, ADCP
CD79b	Polatuzumab vedotin	Roche	2019	Cytotoxic drug delivery
CD33	Gemtuzumab ozogamicin	Pfizer	2017	Cytotoxic drug delivery
CD38	Isatuximab	Sanofi	2020	CDC, ADCC, ADCP
CD22	Moxetumomab pasudotox	AstraZeneca	2018	Cytotoxic drug delivery
CD30	Brentuximab vedotin	Seagen	2011	Cytotoxic drug delivery
CCR4	Mogamulizumab	Kyowa Kirin	2018	CDC, ADCC, ADCP
BCMA	Belantamab mafodotin	GSK	2020	Cytotoxic drug delivery
HER-2	Trastuzumab	Roche	1998	CDC, ADCP
HER-2	Ado-Trastuzumab emtansine	Roche	2013	Cytotoxic drug delivery
HER-2	[fam]-trastuzumab deruxtecan	Daiichi-Sankyo & AstraZeneca	2019	Cytotoxic drug delivery
HER-2	Margetuximab	MacroGenics	2020	ADCC, ADCP
EGFR	Cetuximab	Merck	2004	Signal blockade, CDC, ADCC
EGFR	Panitumumab	AMGEN	2006	Signal blockade
EGFR	Necitumumab	Lilly	2015	Signal blockade, ADCC
VEGFA	Bevacizumab	Roche	2004	Signal blockade
VEGFR	Ramucirumab	Lilly	2014	Signal blockade
Nectin-4	Enfortumab vedotin	Astellas	2019	Cytotoxic drug delivery
TROP-2	Sacituzumab govitecan	Gluead	2020	Cytotoxic drug delivery

Bispecific mAb

Target	Name	Company	Year of launched
CD19/CD3	blinatumomab	AMGEN	2014
FIX/FX	emicizumab	Roche	2017
EGFR/METR	amivantamab	J&J	2021

Immune checkpoint mAb

Target	Name	Company	Year of launched
CTLA-4	Ipilimumab	Bristol-Myers Squibb	2011
PD-1	Pembrolizumab	Merck	2014
PD-1	Nivolumab	Bristol-Myers Squibb	2014
PD-1	Cemiplimab	Sanofi/Regeneron	2018
PD-L1	Atezolizumab	Roche	2016
PD-L1	Avelumab	Merck/Pfizer	2017
PD-L1	Durvalumab	AstraZeneca	2017
LAG-3	Relatlimab	Bristol-Myers Squibb	2022 (Orphan Drug)

II clinical trial for HER-2-overexpressing or HER-2-mutated NSCLC (NCT03505710), the results showed that the ORR of Enhertu ([fam]-trastuzumab deruxtecan, an HER-2 ADC) was 61.9% and the median PFS was 14 months. In a phase I clinical trial of triple-negative breast cancer (TNBC), the initial objective response rate (ORR) was 43%, the complete or partial response (CR/PR) was confirmed in 5 patients, and the disease control rate (DCR) was 95% among 21 evaluable patients treated with datopotamab deruxtecan (a Trop-2 ADC).

The structure of mAb determines its MOA. Fc-engineering methods are used to endow therapeutic mAbs with stronger antitumor and immune activation abilities, which are achieved through amino acid mutation and glycosylation modification. Tafasitamab is a therapeutic mAb targeting CD-19 with upregulated MOA activity through Fc-related modifications. S239D and I332E mutations were performed in tafasitamab to enhance ADCC and ADCP. In the RE-MIND study, the ORR of tafasitamab combined with lenalidomide was 67.1%, and the CR was 39.5%, which was much higher than that of the control group treated with lenalidomide singly.

In several patients, the mAb-induced severe or partially life-threatening side effects were caused by a cytokine storm. In some cases caused by anti-CD20 mAb rituximab, it is assumed that the excessive activation of the complement system and the subsequent lysis of the targeted CD20+ cells, as well as the Fc-FcγR interactions with recruited macrophages, lead to a strong cytokine secretion (10, 11). While the side effects of mAbs therapy can be significantly less toxic than that of traditional chemotherapy, mAbs can still pose a significant risk to patients. Using the Fc-engineering strategy to reduce the immunogenicity of mAbs will provide new ideas for future development. Due to the large molecular weight, mAbs can only be administered by injection, which will lead to poor compliance for patients who require long-term treatment. Compared to mAbs, nanobody without Fc terminal has higher tissue permeability and lower production cost, which makes it become the key to succeed in mAbs development. In addition to being used singly, therapeutic antibodies are often combined with chemotherapy drugs and targeted therapy drugs. mAbs therapy will always be an important concept for tumor treatment. Further analyses will contribute to the design of safer therapeutic mAbs with fewer side effects and higher efficacy profiles in the future.

Bispecific mAbs

Bispecific mAbs (bsAbs) can bind multiple targets at the same time and have a better antitumor effect. Compared with ordinary mAbs, bsAbs offer better stability, higher specificity, and fewer side effects. They offer significant effects in clinical treatment. BsAbs are divided into two types: those that target multiple TAAs and those that engage T cells. They can produce multiple stimulations or inhibition effects, or recruit and activate more immune cells to eliminate tumor

cells. Blinatumomab produced by AMGEN is the first FDA-approved bsAb that can specifically target the CD19 of tumor cells and the CD3 of T cells (Table 1). The clinical results of blinatumomab show that the response rate of patients after treatment reaches 72%, and the average life expectancy is more than nine months. Currently, amivantamab (targeting EGFR/METR) has also been approved for the treatment of non-small cell lung cancer (NSCLC) with EGFR exon 20 insertion mutations. Another approved bsAb, emicizumab, is being used to treat hemophilia. In addition to the three bsAbs already on the market, clinical studies of nearly 100 bsAbs are ongoing, which are mainly in the field of tumor therapy (12, 13). Among the bsAbs under clinical research, MEDI5752 developed by AstraZeneca is a monovalent bsAb that can target both PD-1 and CTLA-4. The results of the clinical trial (NCT03530397) have shown that MEDI5752 exhibits promising antitumor activity and durable clinical benefit in the treatment of patients with advanced solid tumors who are not eligible for standard therapy, with an objective response rate (ORR) of 19.8% and a median duration of response (DOR) of 17.5 months (AACR 2022, Abstract#CT016). AFM13 developed by Affirmed can simultaneously bind to CD30 of lymphoma cells and CD16A of natural killer (NK) cells to kill lymphoma cells without costimulatory signals. The results of the clinical trial (NCT03192202) of AFM13 have shown that 53% of patients had a complete response (CR), 37% had a partial response (PR), and progression-free survival (PFS) and overall survival (OS) were 58% and 79%, respectively (AACR 2022, Abstract#CT003).

Although bsAb is a very promising immunotherapy treatment, there are still problems. The manufacturing of bsAbs is time-consuming and costly. There are bsAb-specific byproducts, such as mispaired products, undesired fragments, and higher levels of aggregates. Additional purification strategies are needed to be designed to obtain products of high purity. At the same time, more clinical trials are needed to explore the optimal route of administration and optimal dose to increase the concentration in target tissues and reduce systemic side effects (14). In addition, bsAbs targeting solid tumors are very challenging because of the adverse effects on normal tissues or other complicated factors such as inadequate penetration (12).

Immune Checkpoint mAbs

There are immune checkpoints on the surface of T cells that can regulate the immune system. They play a negative regulatory role to prevent excessive activation of T cells to avoid autoimmune damage. However, tumor cells can use these immune checkpoints to suppress the immune response, thus performing immune escape and allowing tumor cells to escape the clearance of the immune system (15). Immune checkpoint mAbs can restore the relevant functions of T cells by blocking immune checkpoints and releasing the “brake” of the immune system (16). More than ten immune checkpoints have been discovered, and CTLA-4 and PD-1 are the most widely studied (Table 1).

Cytotoxic T lymphocyte-associated antigen-4 (CTLA-4) is a member of the CD28-B7 Ig superfamily. It is expressed on the surface of activated T cells and can act as an immune checkpoint to downregulate immune responses, thereby inhibiting the proliferation and activation of T cells (17, 18). In 2014, the FDA approved ipilimumab, a mAb targeting CTLA-4, for the treatment of melanoma; it significantly improved patient survival (19). Lynch and colleagues improved PFS in patients with NSCLC using ipilimumab in combination with paclitaxel and carboplatin (20). In addition to CTLA-4, programmed death-1 (PD-1) is another immune checkpoint molecule expressed on the surface of T cells. Its ligand (programmed cell death ligand 1 (PD-L1)) is expressed on the surface of various tumor cells (15, 21). mAb targeting the PD-1/PD-L1 pathway can relieve immunosuppression to enhance T cell activity and kill tumor cells. In 2014, the FDA approved pembrolizumab for the treatment of multiple cancers, including NSCLC, melanoma, and bladder cancer (16, 22). In current clinical use, PD-1/PD-L1 mAbs combined with chemotherapy or targeted therapy have achieved remarkable results. A phase III clinical trial of NSCLC (NCT02998528) with nivolumab combined with chemotherapy was promising, and there were event-free survival (EFS) and pathological complete response (pCR) dual-positive outcomes (AACR 2022, Abstract#CT012). AstraZeneca announced the results of a clinical trial (NCT03899610) combining durvalumab and tremelimumab in advanced epithelial ovarian cancer (targets PD-L1 and CTLA-4, respectively): the ORR was 86.7%, and the ratio of TIL, CD8, and CD8/Foxp3 in TME was significantly increased (AACR 2022, Abstract#CT010). Fc-engineering strategies are also performed in immune checkpoint mAbs. Theoretically, since PD-L1 is expressed on tumor cells, retaining ADCC activity of mAbs can simultaneously utilize the killing effect of NK cells to enhance the anti-tumor effect. This provides a new idea for us to use immune checkpoint mAbs to exert new MOAs. Only avelumab, a PD-L1 mAb, is designed with strong ADCC activity currently. Other immune checkpoints expressed on tumor cells can also learn from the design strategy of avelumab, which may greatly improve antitumor activity. For PD-1 mAbs (e.g., Durvalumab), removing FcγR affinity is beneficial to attenuate the ADCC effect, which is beneficial to preclude FcγR1 mediated binding to macrophages/myeloid-derived suppressor cells (MDSCs)-a potential mechanism by which PD-1-bound T cells may be cleared.

More immune checkpoints continue to be discovered, such as TIM-3, LAG-3, and TIGIT. LAG-3 can bind its canonical ligand (MHC-II) to downregulate T cell activity. A phase II/III clinical trial (NCT03470922) demonstrated that the median PFS of the relatlimab plus nivolumab group was 10.12 (6.37 to 15.74), which was over 2-fold compared to the nivolumab group (4.63 (3.38-5.62)). Currently, Opdualag (nivolumab+relatlimab) is the first LAG-3 antibody therapy approved by the FDA and the first innovative cancer immunotherapy approved for a new immune checkpoint in nearly 10 years. LAG-3 antibody is the third immune checkpoint inhibitor approved for marketing after

CTLA4 and PD-1 antibodies (23). In some preclinical studies, anti-TIM-3 therapy can improve anti-tumor efficacy, and combination therapy with anti-PD-1 or anti-PD-L1 can significantly reduce tumor burden and improve anti-tumor immune responses (24). Several antibodies targeting TIM-3 are currently being tested in clinical trials singly or in combination to treat acute myeloid leukemia or solid tumors (NCT04150029, NCT03680508, and NCT03099109). BsAbs targeting two immune checkpoints (PD-1&CTLA-4, PD-1&LAG-3, and PD-1&TIM-3) simultaneously have also been developed. In light of the positive clinical efficacy already noted in combination therapy targeting immune checkpoints, the outcomes of clinical trials with bsABs are promising.

In terms of adverse reactions, immune checkpoint therapy does not cause cytotoxic reactions such as myelosuppression, vomiting, and alopecia, but it can cause immune-related adverse events (irAEs) due to the activation of T cells, which can be reduced by glucocorticoids and disappear after drug discontinuation. Most irAEs are always reversible (25, 26). The overall incidence of irAEs was lower than that of chemotherapy-induced adverse events (27). Most irAEs are grades 1/2, while grades 3/4 irAEs are less frequent (28, 29). Common irAEs include cutaneous toxicity and endocrinological disturbance, while less common but serious irAEs include pulmonary toxicity, renal toxicity, hepatitis, and gastrointestinal disturbance. Rare irAEs include type 1 diabetes, cardiac, neurological, and hematologic-related toxicity (30, 31). Besides, immune checkpoint therapy only has significant effects in some patients. The premise of its effect is that the expression level of immune checkpoints is relatively high in patients. Therefore, it is necessary to carry out genetic screening of patients and apply immune checkpoint therapy to eligible patients.

Small molecule drug immunotherapy

Small molecule targeting PD-1/PD-L1

Immune escape is an important means for tumor cells to escape from being eliminated. Due to the abnormal immune surveillance mediated by immune checkpoints, tumor cells form immune escape and then obtain unlimited proliferation ability, thus leading to tumorigenesis. MAbs therapy suffers from poor tissue penetration, a long half-life, and high production costs. Thus, researchers are trying to develop small molecule inhibitors targeting immune checkpoints. Most inhibitors are currently in the early development stage (Table 2). CA-170 developed by Aurigene and Curis has made the fastest progress and entered phase II clinical trial (CTRI/2017/12/011026) (32). CA-170 targets PD-1/PD-L1 and VISTA pathways, thus leading to the proliferation and activation of T cells to produce

cytokines such as IFN- γ to kill tumor cells (33). CA-170 can effectively inhibit melanoma and colon cancer in rodent models, and CA-170 is superior to mAbs in terms of safety (34–36). In clinical studies, CA-170 has the best effect on NSCLC and Hodgkin lymphoma with a total clinical benefit rate of 70% and 77.8%, respectively (37). AUNP12 was reported by Aurigene and Pierre Fabre in 2014. It is the first polypeptide PD-1/PD-L1 inhibitor and has a structure similar to the extracellular domain of PD-1 (38). The EC₅₀ of peripheral blood mononuclear cells (PBMCs) proliferation rescue experiments reached 0.41 nM (38, 39). The *in vivo* experiments also showed that AUNP-12 can inhibit tumor growth and metastasis. AUNP-12 can inhibit B16F10 and 4T1 tumors in rodent models, and the tumor growth inhibition rate (TGI) of the B16F10 model reached 44% (40). In 2015–2018, BMS successively published a series of patents, and the IC₅₀ of compounds detected by HTRF was generally less than 1 nM (41). In 2021, Liu et al. reported a small molecule inhibitor-ZE132, of which the affinity KD was 19.36 nM. ZE132 can specifically act on PD-L1 and has good antitumor efficacy in a variety of syngeneic mouse models (42).

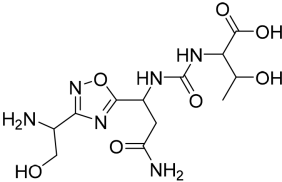
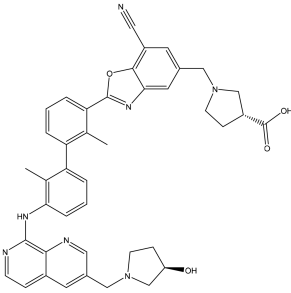
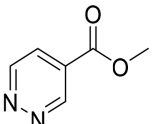
Small molecule inhibitors have lower binding affinity than that of mAbs, and they are prone to off-target effects, which may

even bring unknown off-target toxicity. The interaction between PD-1 to PD-L1 is a protein-protein interaction. The contact interfaces of PD1/PD-L1 are large, highly flat, and hydrophobic, which makes it difficult to design compounds and develop small molecule inhibitors. Nevertheless, small molecule inhibitors have mature R&D pipelines, better tissue permeability, and controllable pharmacokinetic properties, which can help to avoid the defects of mAbs.

IDO1 inhibitors

Indoleamine 2,3-dioxygenase1 (IDO1) is a 45 kDa hemoglobin oxidase and is a key enzyme in the metabolism of the L-tryptophan-kynurenine pathway. IDO1 plays an important regulatory role in the process of immune regulation (43, 44). Functionally, IDO1 plays a key role in carcinogenesis and cancer immune escape by catalyzing the initial step of canine urinary ammonia pathway. IDO1 is overexpressed in tumor cells and antigen-presenting cells (APC). It is conducive to the formation of an immunosuppressive tumor microenvironment and is closely related to the poor prognosis of

TABLE 2 Summary of major marketed and clinically reported small molecule immunotherapy drugs (Up to March 2022).

Target	Name	Structure	Company	Highest Development Phases
PD-L1/VISTA	CA-170		Aurigene, Curis	Phase II (NCT01288911)
		(putative)		
PD-L1	INCB-086550		Incyte	Phase II (NCT04629339)
PD-L1	GS-4224		Gilead	Phase 1b/2 (NCT04049617)
PD-1	MX-10181	undisclosed	Maxinovel	Phase I (NCT04122339)

(Continued)

TABLE 2 Continued

Target	Name	Structure	Company	Highest Development Phases
IDO1	BMS-986205		Bristol-Myers Squibb	Phase III (NCT03661320)
IDO1	INCB-024360		Incyte	Phase III (NCT02752074)
STING	ADU-S100		Aduro, Novartis	Phase II (NCT03937141)
STING	MK-1454		Merck	Phase II (NCT04220866)
A2AR	AZD4635		AstraZeneca	Phase II (NCT04089553)
A2AR	NIR178		Novartis	Phase II (NCT03207867)

(Continued)

TABLE 2 Continued

Target	Name	Structure	Company	Highest Development Phases
CXCR2	AZD5069		AstraZeneca	Phase II (NCT03177187)
CXCR4	Mavoxifafor		X4 Pharmaceuticals	Phase III (NCT03995108)
CCR2/5	BMS-813160		Bristol-Myers Squibb	Phase II (NCT03184870)
TLR7	Imiquimod		3M Pharmaceuticals	Marketed
TLR8	Motolimod		Array Pharma, Celgene	Phase I/II (NCT02431559)
ARG	INCB001158		Calithera Biosciences, Incyte	Phase I/II (NCT02903914)

various cancers (45). Inhibition of IDO1 can activate antitumor immune responses in rodent tumor models (43). A variety of IDO1 inhibitors have entered clinical studies. BMS-986205 and epacadostat have made the fastest progress (Table 2). BMS-986205, developed by BMS, is currently in phase III clinical trial (NCT03661320) in combination with nivolumab, gemcitabine, and

cisplatin in bladder cancer. In addition, there are two phase II clinical trials ongoing for bladder cancer (NCT03519256) and HNSCC (NCT03854032).

Developed by Incyte, epacadostat is one of the most well-studied IDO1 inhibitors. It shows good efficacy in mouse melanoma models and is well-tolerated (46). However, the results of the clinical

trial (NCT02752074) showed that the combination of epacadostat and pembrolizumab in the treatment of melanoma did not meet the main clinical outcomes, and Incyte stopped their phase III trials (47).

The development of IDO1 inhibitors is not going well, and some clinical trials have failed. On one hand, the reason for the failure of ECHO-301 (epacadostat plus pembrolizumab) may be that the pharmacodynamic indicators are not applicable or the drug combination strategy is not matched. On the other hand, the reason may be that the exact regulatory mechanism of IDO1 in physiology and pathology or its impact on the tumor microenvironment are not well understood. The TDO pathway can play a potential compensatory role after epacadostat treatment, causing tumor immunosuppressive effects (48). However, the immune-enhancing function of IDO1 inhibitors has been verified, and IDO1 inhibitors still have the potential for development. In the future, the combination therapy of IDO1 inhibitors with other antitumor drugs should be further explored, which has important implications for the success of clinical development.

Other small molecule drugs

Stimulators of interferon genes (STING) is an immunostimulatory target and an important adaptor protein anchored in the endoplasmic reticulum that senses foreign DNA invasion. Now the STING signaling pathway has become a new target for cancer and autoimmune diseases. Experiments have shown that the activation of STING pathway can induce antitumor effects. A variety of drugs such as ADU-S100 are under clinical studies (Table 2) (49, 50). The clinical application of STING agonists is mainly focused on intratumoral injections, and it is unclear whether systemic administration is safe.

In addition, inhibitors of A2A adenosine receptor (A2AR), chemokine receptors, toll-like receptors (TLRs), arginase 1 (ARG), and other targets are in clinical development and are expected to provide more choices for antitumor drugs (Table 2) (51–54). Many projects have entered phase II/III clinical trials.

Polypeptide inhibitors, which can combine the characteristics of antibodies and small-molecule drugs, are important directions for the development of inhibitors. On one hand, they have similar affinity and specificity as antibodies. On the other hand, they have good tissue penetration and provide tunable pharmacokinetic half-life and renal clearance route to avoid hepatic and gastrointestinal toxicities due to their small molecular weight.

Small molecules are agents with a low molecular weight that are capable of modulation of intracellular targets. And small molecules are promised to improve the therapeutic management of solid tumors due to their easy administration, high bioavailability, and favorable safety profile. Given these characteristics, the development of small molecule-based

strategies in cancer immunotherapy has attracted widespread interest. Although small-molecule drugs targeting the extracellular or intracellular pathways of adaptive immunity or innate immunity have been developed, most of them are in the early stage of clinical trials, and more basic experiments and clinical trials are needed to elucidate their mechanisms, clinical efficacy, and pharmacokinetics. Nevertheless, small-molecule inhibitors may be an effective replacement and supplement for mAbs, and they will remain an important part of tumor immunotherapy in the future.

Adoptive cell therapy

CAR-T

The chimeric antigen receptor (CAR) is a genetically modified and synthesized chimeric antigen receptor. It is a membrane protein composed of different protein domains in series. It is flexible and offers specific antigen recognition. Patient-derived T cells modified by CAR *in vitro* can recognize tumor antigens and exert antitumor effects without MHC restrictions *in vivo* (55).

CAR-T therapy is a revolutionary approach to cancer therapy. CAR-T therapy has made breakthroughs in lymphomas, mainly targeting CD19. In 2017, the FDA approved two CAR-T products targeting CD19 (Kymriah and Yescarta, Table 3) (56, 57). The first generation of CAR contains CD3 ξ , and the second generation adds a costimulatory domain CD28 or 4-1BB based on CD3 ξ . Through March 2022, the FDA has approved five CAR-T products, all of which are second-generation CARs with indications focused on lymphoma (58, 59). The third-generation CAR uses lentivirus as a transfection vector, and the intracellular segment of the CAR can have two or more costimulatory signals. However, some studies have shown that the killing activity of the third-generation CAR-T cells is not significantly improved. This may be because the activation signal generated by one co-stimulatory molecule of ITAM already reaches the threshold of T lymphocyte activation signal. Simply increasing the number of ITAM will not further enhance the activation effect of CAR-T.

New ideas for CAR design are now emerging to improve efficacy. Dual-target CAR-T cells can independently identify target antigens and address the off-target effect. CD19/CD22 CAR-T and CD123/CLL1 CAR-T have shown significant antitumor activity and are currently in clinical studies, some of which have entered phase II/III (Table 3) (60, 61). According to EXUMA Biotech, targeting CD3 T cells by subcutaneous injection of a self-inactivating lentiviral vector encoding a CAR targeting CD19 resulted in the successful generation of corresponding CAR-T cells *in vivo* and showed significant effects in mice (AACR 2022 Abstract #3294/11). This provides a new

TABLE 3 Summary of major marketed and clinically reported adoptive cell therapy (Up to March 2022).

Category	Target	Name	Company	Highest Development Phases
CAR-T	CD19	Kymriah	Novartis	Marketed
CAR-T	CD19	Yescarta	Gluead	Marketed
CAR-T	CD19	Tecartus	Gluead	Marketed
CAR-T	CD19	Breyanzi	BMS	Marketed
CAR-T	BCMA	Abecma	Bluebird Bio & BMS	Marketed
CAR-T	BCMA	bb21217	Bluebird Bio	Phase I (NCT03274219)
CAR-T	CLDN6	BNT211	BioNtech	Phase I/IIa (NCT04503278)
TCR-T	NY-ESO-1	NY-ESO-1 TCR	Adaptimmune Therapeutics	Phase I/II (NCT05296564)
TCR-T	PRAME	MDG1011	MediGene AG	Phase II (NCT03503968)
TILs	–	LN-144	Iovance Biotherapeutics	Phase II (NCT03645928)
TILs	–	LN-145	Iovance Biotherapeutics	Phase II (NCT04614103)
CAR-NK	CD19	FT596	Fate Therapeutics	Phase I (NCT04245722)
CAR-NK	NKG2D	NKX101	Nkarta Therapeutics	Phase I (NCT04623944)
CAR-NK	CD7	anti-CD7 CAR-pNK	PersonGen BioTherapeutics	Phase I/II (NCT02742727)
CAR-NK	CD33	anti-CD33 CAR-NK	PersonGen BioTherapeutics	Phase I/II (NCT02944162)

opportunity to overcome the challenges of production time, scale, and cost of adoptive cell therapies.

For solid tumors, Hegde et al. constructed TanCAR-T that could enhance T cell function and reduce antigen escape by facilitating crosstalk between HER2-ScFv and IL-13R α 2, thus increasing CD28 expression. The data of TanCAR-T showed good efficacy in a mouse glioblastoma model (62). In 2022, Grosskopf et al. published a delivery method for hydrogel that can improve the efficacy of treatment of solid tumors by injection into areas near the tumor (63). BioNtech announced the results of the first human clinical trial (NCT04503278) of BNT211—a new generation of CAR-T therapy targeting solid tumors. The combination of CAR-T targeting CLDN6 and mRNA vaccine CARVac for CLDN6 can effectively enhance the efficacy and provide new ideas for the treatment of solid tumors (AACR 2022, Abstract #CT002). In addition, combination therapy with immune checkpoint inhibitors may also enhance the efficacy of CAR-T for solid tumors (64).

However, there are several limitations to the application of this technology. Firstly, the expression of CAR mediated by retroviral or lentiviral vectors may have an impact on the gene expression of T cells, which may produce unpredictable results. So, a comprehensive safety assessment of CAR-T cells is required before application. Secondly, the proliferation of CAR-T cells can only be achieved after induction and activation. Therefore, whether the large-scale expansion of T cells *in vitro* can maintain immune activity is an important factor. Thirdly, necessary technical processes are required for different patients, which may take high costs and long periods. In addition, immunosuppressive TME and efficiency of delivery to the tumor site are also major barriers to a successful CAR-T therapy. In the future, innovations in CAR design,

transduction methodologies, and allogeneic CAR-T are bound to lead to improved responses and transform the treatment of patients with cancer.

TCR-T

Various new methods have been developed to enhance the antitumor efficacy of immune system, including targeting new antigens, using new engineering or modifying TCR, and creating safety switches for internal suicide genes. By transferring the exogenous TCR gene that specifically recognizes TAAs into T cells, TCR-T can be constructed to improve the affinity to TAAs and exert an MHC-dependent antitumor effect (65). Compared with CAR-T therapy, TCR-T therapy has a better safety profile due to its MHC restriction, which can alleviate adverse reactions such as cytokine storms. The TCR-T category currently in clinical trials is mainly targeting NY-ESO-1. NY-ESO-1 TCR produced by Adaptimmune Therapeutics is currently in phase I/II clinical trials (Table 3).

MART TCR-T, gp100 TCR-T, and TCR-T targeting MAGE-A3 or MAGE-A4 have achieved positive results in clinical trials. However, safe use in the clinic should consider the type of antigen and TCR affinity (66, 67). In a clinical trial of nine patients treated with TCR-T, 56% (5/9) of patients experienced an OR, one of which was a CR. However, three of nine (44%) patients experienced severe neurologic toxicities, including two deaths. The cause of death, in part, may be a cross-reaction of TCR-T with a similar epitope of MAGE-A12 in brain.

While targeting NY-ESO-1, MAGEA3, and other TAAs is an attractive strategy for the application of ACT for the treatment of solid cancers, caution must be taken to ensure a lack of cross-

reactivity with vital normal tissues. In addition, modification of the CDR region of TCR must be performed with caution. Because the modified receptors, similar to those produced after immunization in HLA-transgenic mice, are not negatively selected in the thymus and may be potentially reactive to unrelated normal host proteins. There is a need to develop better screening methods to avoid such toxicity in the future. As more antigen-specific TCRs are identified, more data will become available to better understand how to use TCR-T to treat patients. Immunosuppressive TME also limits the efficacy of TCR-T therapy. Combination therapy targeting TME may be a potential strategy to improve the efficacy of TCR-T immunotherapy.

TILs

Tumor-infiltrating lymphocytes (TILs) are immune cells that exist in tumor tissues and can specifically respond to TAAs. Using TILs is an effective treatment for many cancers. The first clinical pilot study using TILs was reported in 1988 for metastatic melanoma. The result demonstrated partial response in 2 patients and partial regression in 1 patient. Tumor-specific cytolytic activity was observed in 5 patients (68). In another study by Rosenberg et al., three sequential clinical trials about TILs were performed. Objective response rates in the three trials were 49%, 52%, and 72%, respectively. A study showed that 22% of all patients achieved complete tumor regression and 19% of the patients were disease-free for more than three years (69). The OR from patients treated with standard TILs is greater than 50% and many of these patients experiencing durable CRs beyond 5 years (70–72). The effort to extend TIL therapy for the treatment of other solid cancers is ongoing. Galon et al. studied TILs in patients with colorectal cancer by gene expression profiling and *in situ* immunohistochemical staining (73). The results suggested that TILs act as a valuable prognostic tool in the prediction of patient survival, and the results gave convincing information regarding tumor recurrence and survival in patients with early-stage colorectal cancer.

TILs therapy mainly works by isolating TILs from tumor tissues, amplifying them *in vitro* with high doses of IL-2, and then injecting them into patients (68, 74). Iovance's LN-144 therapy has achieved a disease control rate (DCR) of 80% and ORR of 38% for stage IIIc/IV melanoma patients (Table 3). More notably, patients who are not responding to immune checkpoint inhibitors still benefit. Multiple clinical trials of TILs for various types of solid tumors are currently ongoing, thus showing therapeutic potential for malignancies such as melanoma, lung, and colorectal cancers (75). TILs therapy is separate from natural lymphocytes isolated from tumor tissues and it can recognize a variety of different targets with no cytokine storms reported. Thus, TILs therapy is safer than TCR-T and CAR-T therapies and more effective in solid tumors.

However, several issues have emerged that need to be addressed. Firstly, there is an urgent need to identify alternative and predictive biomarkers to better select appropriate patients for TILs treatment to improve response rates and duration. Secondly, TILs are needed to be improved memory and effector characteristics for longer persistence and enhanced antitumor activity. In addition, although TCR-T and CAR-T therapies show very competitive performance, they can only target a single TAA or a limited array of TAAs. By contrast, TILs can recognize a panoply of unknown TAAs, which ultimately demonstrates that TILs therapy has a bright future, especially with approaches that promote TAA release and enhance T-cell persistence. At last, we also need more investigations on combination approaches that can improve long-term efficacies and reduce the cost to a more affordable level.

CAR-NK

NK cells play an important role in innate immunity. CAR-NK is a therapy like CAR-T, which uses CAR to modify NK cells. CAR-NK can be activated by targeting TAAs to release cytotoxic cytokines such as granzyme to kill tumor cells (76). CAR-NK is currently still in preclinical or clinical research, which mainly targets CD19, NKG2D, CD7, or CD33, etc. (Table 3).

In a phase I/IIa clinical trial, 11 patients with non-Hodgkin's lymphoma and chronic lymphocytic leukemia were treated with CD19 CAR-NK. And seven patients experienced CR without serious adverse reactions (77). In 2020, NEJM published a CAR-NK treatment for hematologic tumors using cord blood-derived CAR-NK targeting CD19 that achieved complete remission in seven patients, all without a cytokine storm or neurotoxic response. Moreover, one year after treatment, CAR-NK cells are still present in the patient's body, which is especially important for long-term antitumor therapy (77). NKG2D is an activating receptor of NK cells, which is involved in the recognition of virus-infected cells and the killing of tumor cells. In a phase I clinical trial of NKX101 (allogeneic CAR-NK cells targeting NKG2D), 3 of 5 patients treated with high doses (1.5 billion×3 and 1 billion×3) achieved CR without serious adverse reactions (NCT04623944). At AACR 2022, Senti Bio announced the results of a preclinical study of CAR-NK with a genetic circuit that secretes IL-15 in a controlled manner to improve efficacy in the treatment of solid tumors (AACR 2022 Abstract #584).

Compared with CAR-T, CAR-NK usually produces IFN- γ and GM-CSF, thus it is less likely to produce cytokine storm. CAR-NK is widely available and can be derived from allogeneic delivery without need of HLA matching. However, some factors limit the wide use of CAR-NK. The manufacturing process of CAR-NK can be further simplified and optimized. Current CARs are designed for CAR-T and they are not the best for

application to NK cells. CAR design for optimal NK cell activation and cytotoxicity needs to be improved. Secondly, CAR-NK's unspecific killing function needs to be combined with CAR-derived specific killing. In addition, limited proliferation and inhibition of the tumor microenvironment limit the clinical development of CAR-NK (78).

The lack of *in vivo* durability of infused cells in the absence of cytokine is one of the major drawbacks of CAR-NK therapy. Modified CAR-NK which can secrete IL-2/IL-15 has demonstrated good results in some preclinical research (79). In addition, the induction of a memory-like phenotype of CAR-NKs with a cocktail of cytokines (IL-12, IL-15, and IL-18) resulted in improved responses to B-cell lymphomas *in vitro* and *in vivo* (80, 81). Immunosuppressive TME and efficiency of delivery to tumor site are also major barriers to successful CAR-NK therapy. With more pre- and clinical data in further, CAR-NK therapy may lead to revolutionary advances in tumor immunotherapy. In addition, combined therapy which includes immune checkpoints blockade and targeted therapy may provide a new direction for CAR-NK-based immunotherapy.

Oncolytic virus

Oncolytic viruses (OV) therapy is a new type of antitumor therapy, which can target tumor cells and replicate in cells to kill tumor cells. OV has become the forefront of tumor biotherapy and it is increasingly common. OV can be obtained through natural or genetic engineering, mainly including herpes virus, adenovirus, and pox virus (82). OV exerts its antitumor effects mainly by selectively replicating within tumor cells and eventually leads to tumor cell lysis. The release of TAAs after lysis can activate the immune system to eliminate tumor cells. The release of cytokines by tumor cells infected with OV can eliminate metastatic tumor cells (83, 84). In 2015, AMGEN's T-VEC became the first OV therapy on the market with an indication of melanoma, thus marking the maturity of this technology (Table 4). Researchers are currently using various

techniques to enhance the antitumor effects of OV therapy including replacing some viral genes with oncogenes or integrating TAAs genes into the OV genome to promote the production of specific immune responses (85). In addition, the combination with immune checkpoint therapy has also become an important research direction. The clinical results of CG Oncology's OV therapy CG0070 in combination with Keytruda show 89% CR (AACR 2022 Abstract#CT036) (86).

OV therapy is efficacious and safe, and it is a very promising tool for tumor immunotherapy (87–89). However, its mode of administration is currently limited to intra-tumoral injection, which has limitations in clinical use. Intratumoral administration is expensive and difficult, especially in cases of malignant gliomas. Some of the novel approaches involve the use of nanoparticles, complex viral particle ligands, and immunomodulatory agents to deliver the virus into tumor. Alternatively, delivery of OV *via* nanoparticles using a technologically complex image-guided delivery system has also been considered (90). In the future, OV therapy is expected to make exciting progress by solving the problem of drug delivery and combining with other immunotherapy methods

Cancer vaccines

Preventive cancer vaccines

The immunoprevention of cancer and cancer recurrence has received extensive attention; preventative cancer vaccines have made more progress in preventing cancer than in eliminating established cancer. Nevertheless, preventing tumors obviously impacts survival. Preventive cancer vaccines mainly refer to vaccines against viruses with high carcinogenic relevance. HBV and HPV vaccines are the main representatives. The pathogenesis of HBV-associated hepatocellular carcinoma is well supported by the literature (91, 92). A variety of new HBV vaccines are now on market, such as Hepacare, HEPLISAV-B, and PreHevbrio, which expand the efficiency

TABLE 4 Summary of marketed and clinically reported oncolytic virus (Up to April 2022).

Virus	Name	Company	Highest Development Phases
HSV-1	T-VEC	AMGEN	Marketed (FDA)
ECHO-7	RIGVIR	LATIMA	Marketed (Latvia)
Adenovirus	H101	Sunway	Marketed (NMPA)
HSV-1	DELYTACT	Daiichi-Sankyo	Marketed (MHLW)
Adenovirus	CG0070	CG Oncology	Phase III (NCT04452591)
Adenovirus	Reolysin	Oncolytics Biotech	Phase II (NCT04445844)
Adenovirus	DNX-2401	DNatrix	Phase II (NCT02798406)
Coxsackievirus	Cavatak	Merck	Phase II (NCT04152863)
HSV-1	G207	Treovir	Phase I/II (NCT00028158)
Poliovirus	PVSRIPO	Tocagen	Orphan Drug (Glioma; Glioblastoma)

and scope of protection. HPV vaccines mainly include bivalent (Cervarix), quadrivalent (Gardasil), and nine-valent (Gardasil9), thus focusing on the protection of subtypes 16 and 18 used to prevent cervical cancer, vaginal cancer, and vulvar cancer caused by HPV. Due to the complex pathogenesis of tumors, this method can only be used as an auxiliary preventive method. This type of vaccine can only be used to prevent viral infection—not tumorigenesis.

Therapeutic cancer vaccines

A better understanding of the breadth of TAAs, the development of natural immune response, and new antigen delivery technologies will help to improve vaccine design. Current mature therapeutic vaccines include dendritic cell (DC) vaccine, which has antitumor effects by inducing the patient’s monocytes to become DCs *ex vivo* by TAAs stimulation. The cells are then infused back into the patient to stimulate the activation and expansion of cytotoxic T lymphocytes (CTLs). DC vaccine can offer long-term immune memory and can prevent tumor recurrence. Provenge is the first DC vaccine approved by the FDA for castrate-resistant prostate cancer (Table 5). The DC vaccine Ilixadencel was granted orphan drug status by the FDA in 2021 for the treatment of patients with soft tissue sarcoma. Aivita Biomedical’s DC vaccine AV-GBM-1 clinical trial (NCT03400917) results show a 28% increase in 15-month OS for glioblastoma patients. With the development of sequencing technology and bioinformatics, more and more tumor antigens have been discovered and can be used to distinguish tumor cells from normal cells. A personalized vaccine designed in this way is an important development direction for cancer vaccines in the future (93). Multiple studies are reporting that personalized vaccines have good efficacy in the treatment of melanoma (94, 95). A combination with immune checkpoints is also an important research direction and can show better efficacy than a single vaccine therapy (96). In addition to DC vaccines, therapeutic vaccines include tumor cell vaccines, DNA/mRNA vaccines, and peptide vaccines (97).

DC vaccines suffer from limited cell sources, long preparation periods, and high costs. However, their advantages include low side effects, good tolerance, and long-term immunological memory, which still give them broad market prospects.

The key to the development of the cancer vaccine is the need to identify the appropriate biomarkers and optimize the combination of treatments to improve their effectiveness in patients. The research on vaccines has been advancing in the past few decades, and many different characterized cancer vaccines are now available. However, there are still some problems that must be solved, including suitable tumor antigen and adjuvant components, suitable delivery modes, and effective methods to overcome immune attack. Although neoantigens are the best option for antitumor immunotherapy, the problem of obtaining individualized neoantigens hinders the application of cancer vaccines. This is mainly due to inherent alterations in tumor cells and the formation of an immunosuppressive TIME. Several approaches have been developed to overcome difficulties, including the use of immunostimulatory adjuvants, in combination with ACT and ICB.

Mechanisms in cancer immunotherapy resistance

Cancer immunotherapies, such as immune checkpoint blockade (ICB) and adoptive cell therapies (ACT), are effective for patients with various cancers (98). However, the response rate of cancer immunotherapies is still limited due to the lack of immunogenic antigens and various immune-resistant mechanisms (99). Understanding the immune resistance mechanisms is essential to improve the efficacy of current cancer immunotherapies.

Primary resistance and adaptive resistance

Patients who have primary resistance to cancer immunotherapies do not respond to the initial therapy.

TABLE 5 Research progress of therapeutic cancer vaccines (Up to April 2022).

Name	Company	Highest Development Phases
Provenge	Dendreon	Marketed (FDA)
Cimavax-EGF	Bioven	Marketed (Cuba)
Mutanome	BioNTech	Phase I (NCT04183166)
NEO-PV-01	Neon Therapeutics	Phase I (NCT02897765)
AV-GBM-1	Aivita Biomedical	Phase II (NCT03400917)
TEDOPI	OSE Immunotherapeutics Bristol-Myers Squibb	Orphan Drug (HLA-A2 NSCLC)
Ilixadencel	Immunicum	Orphan Drug (Soft tissue sarcoma)

Adaptive resistance refers to the mechanism by which tumor cells can be recognized by the immune system, but it can adapt to immune attack to protect itself as the tumor progresses. The mechanism of adaptive resistance may include primary resistance, and the mechanism of primary resistance may also be the result of adaptive resistance.

The most fundamental reason why tumor cells cannot be recognized by T cells and thus lead to non-response to immunotherapy is the lack of tumor antigens. In addition, cancer cells may have tumor antigens, but the change in the antigen presentation mechanism can also result in the occurrence of immune resistance (100).

In tumor cell-intrinsic factors, insufficient tumor antigenicity and neoantigens contribute to primary and adaptive resistance. Tumor cells can evade specific immune recognition by T cells by downregulating the expression of TAAs, TSAs, and surface MHC. Tumor cells with relatively weak immunogenicity can escape the surveillance of the immune system and selectively proliferate. After the immune selection process, the immunogenicity of the tumor is getting weaker and weaker. The emergence of neoantigens can inhibit tumor progression, whereas poorly immunogenic tumors lack response to PD-1/PD-L1 blockade. Deletion of neoantigens is responsible for primary resistance to immunotherapy in triple-negative breast cancer (TNBC) (101). LINK-A, a lncRNA that can degrade phospholipase C by ubiquitin ligases, has a negative correlation with cytotoxic T lymphocytes infiltration in TNBC (102). It is currently believed that the higher the tumor mutation burden (TMB), the more neoantigens are produced, and the stronger T cell response are. Clinically, melanoma, renal cell carcinoma, and NSCLC with high TMB have a better response to anti-PD-1 therapy, while pancreatic cancer and prostate cancer with low TMB are less effective (103, 104).

In tumor cell-intrinsic factors, tumor signaling pathways can produce immunosuppressive components, or alter some gene expression to affect the efficacy of ICB. Oncogenic signaling through the MAPK pathway results in the production of VEGF and IL-8, which have inhibitory effects on T cell recruitment and function (105). Activation of AKT signaling through PTEN loss was also correlated with reduced CD8+ T cells in tumors and a poor response to anti-PD-1 in melanoma patients (106). IFN- γ signaling pathway in TIME activates JAK-STAT signaling, which can induce PD-L1 expression (107). Wnt/ β -catenin signaling pathway is closely related to the occurrence and development of various tumors (108). Studies have shown that Wnt/ β -catenin signaling in melanoma cells can prevent antitumor responses by interfering with the recruitment of BATF3-expressing DCs (109, 110).

In tumor-intrinsic factors, immunosuppressive metabolism in TIME can suppress immune response. Various metabolisms in tumor may cause immune resistance. Tumor cells preferentially utilize glycolysis to produce ATPs and molecules necessary for cell division such as nucleic acids, while reducing

mitochondrial activity to decrease the production of reactive oxygen species (ROSs) for survival (Warburg effect) (111). Enhanced glycolysis in melanoma cells is associated with reduced infiltration of CD8+ T cells in tumors and resistance to *in vitro* T cell lysis and *in vivo* pericyte therapy, partially due to increased production of immunosuppressive lactate (112).

In addition, tumor cell-extrinsic mechanisms that lead to primary and adaptive resistance involve components other than tumor cells within TIME. Tregs reduce the expression of MHC-II molecules by secreting the inhibitory cytokine IL-10, which can affect DC maturation and suppress immune responses (113). MDSCs can express CD11b and CD33 to promote blood vessel growth, tumor invasion, and metastasis. CXCR2 can induce MDSCs to infiltrate tumors and mediate immune resistance (114). Tumor-associated macrophages (TAMs) can also affect immunotherapy responses. Several reports have discussed the role of macrophages in mediating therapeutic resistance in cancer (115–117).

Acquired resistance

A hallmark of cancer immunotherapy has been the induction of long-lasting tumor responses. However, patients who once responded to ICB sometimes relapse due to acquired resistance. Schachter et al. showed that 1/4 to 1/3 of patients with metastatic melanoma who received anti-PD-1 or anti-CTLA-4 therapy relapsed after ongoing treatment, even if they were effective against immunotherapy (118). The possible mechanisms of acquired resistance mainly include B2M mutation and loss of HLA heterozygosity, changes in tumor target antigens, and up-regulation of alternative immune checkpoints. There is evidence for each of these mechanisms can lead to acquired resistance to ICB or ACT.

B2M plays an important role in MHC-I antigen-presenting, antigen recognition, and T cell infiltration (119). Mutated B2M gene affects normal folding and transport of MHC-I, resulting in resistance to ICB (120). Sade-Feldman et al. analyzed post-treatment biopsy specimens from 17 metastatic melanoma patients with ICB treated, and they found the percentage of heterozygous deletions and point mutations of B2M was 9.4%, which suggested that B2M loss may be a common mechanism of resistance to targeted CTLA-4 or PD-1 therapy (121). GAO et al. showed that mutations in Janus kinase 1 (JAK1), JAK2, and B2M in tumor samples after immunotherapy may be the mechanisms of acquired resistance to anti-PD-L1 therapy in melanoma patients (122).

Additional evidence of loss of antigen-presenting machinery leading to acquired resistance to cancer immunotherapy is provided by a case of a patient with metastatic colorectal carcinoma who responded to TILs ACT. The TILs recognized mutated KRAS G12D presented by HLA-C*08:02 resulting in an objective antitumor response, followed by an isolated relapse in a

lesion that had lost HLA-C*08:02 in chromosome 6 (123). Therefore, acquired resistance to ICB and ACT could be mediated through genetic mechanisms that altered antigen-presenting machinery and IFN- γ signaling.

Cytotoxicity T cells are specific for cancer cells that express their cognate antigen, but cancer cells may develop acquired resistance through decreased expression or mutations in these antigens. T cells turned on by checkpoint blockade therapy primarily recognize mutational neoantigens (104, 124). Gene deletions, mutations, or epigenetic alterations can lead to a decrease in MHC-presented mutational neoantigens and acquired resistance. One study found that the main cause of resistance to CD19 CAR-T cells for acute lymphoblastic leukemia was the loss of target antigens, which is mainly caused by antigen escape and lineage conversion (125, 126).

After immune checkpoint treatment, due to compensatory effects, the expression of other immune checkpoints is elevated, which in turn causes acquired resistance. TIM-3 is a negative immune checkpoint. It was found that TIM-3 was highly expressed in T-cells from animals that were resistant to anti-PD-1 treatment, which confirmed that the main mechanism of resistance to anti-PD-1 immunotherapy is the selective activation of a new immune checkpoint (23). In addition to TIM-3, other known alternative immune checkpoints are LAG-3, TIGIT, and VISTA, etc. Several clinical trials are currently undergoing to test antibodies against these immune checkpoints, both as monotherapy and combination therapy strategies, to provide additional clinical benefits (127).

Great advances occurred in the field of cancer immunotherapy due to years of mechanism exploration and clinical application development. However, to date, the benefits have been limited to a small number of patients with certain cancer types. In addition, thanks to more successful immunotherapy treatments, we now have a large proportion of patients who initially respond but eventually relapse. The mechanisms of immunotherapy resistance are complicated, and we are likely just observing the tip of the iceberg. To bring clinical benefit to the majority of patients, we need to have a comprehensive understanding of the tumor cell-intrinsic and -extrinsic factors that lead to immunotherapy resistance. These mechanisms can lead to primary, adaptive, and acquired resistance to immunotherapy. Elucidating these mechanisms will provide important clues to overcome resistance to immunotherapy.

Combination strategies for cancer immunotherapy

To enhance the effectiveness of cancer immunotherapy and overcome immunotherapy resistance, combination therapy has become a hot topic of current research (128, 129). Currently, ICB is the most used cancer immunotherapy in clinical combination.

Combination of different ICBs

An example of enhanced efficacy with combination therapy is the use of anti-CTLA-4 and anti-PD-1, which results in higher response rates and improved survival in melanoma patients (130, 131). In the phase III trial in patients with unresectable or metastatic melanoma, the five-year survival rate of the combination group (nivolumab plus ipilimumab) reached 52%, and the five-year survival rate of the nivolumab group and ipilimumab group was 44% and 26% respectively (131, 132).

In addition, blockades of TIM-3, LAG-3, and TIGIT are receiving increasing attention. In the treatment of hepatocellular carcinoma, it was found that blocking both TIM-3 and PD-1 can completely reverse the exhausted state of T cells and has a significant antitumor effect. However, blocking TIM-3 or PD-1 alone only partially restored the function of T cells (133). Both LAG3 and PD-1 can transmit co-inhibitory signals and blocking both LAG3 and PD-1 can play an immune synergistic effect by enhancing CD8⁺ T cell function and clearing Treg (134). TIGIT is mainly expressed on activated T cells and NK cells, which mediates immunosuppressive signal. TIGIT blockade synergizes with anti-PD-1 can enhance CD8⁺ T cell function and promote tumor regression (135).

Combination with chemotherapy and radiotherapy

Previously, it was believed that chemotherapy could lead to immunosuppression by affecting the number or function of lymphocytes. But in-depth studies have found that some chemotherapies can enhance tumor immunogenicity (136). Some studies believe that chemotherapy can enhance the antitumor immune response, among which pembrolizumab combined with chemotherapy has been approved by the FDA. Liposome doxorubicin combined with immunotherapy produces synergistic antitumor effects in mice, and more mice achieve complete tumor remission and prolonged survival (137). High-frequency and low-dose chemotherapy can effectively activate CTLs and inhibit immunosuppressive cells in TIME, which can promote efficacy and solve the problem of immune resistance (138). In an *in-situ* CRC-bearing mouse model with ineffective anti-PD-L1 treatment, the proportion of TILs was significantly increased after combination with oxaliplatin. At the same time, the combination of oxaliplatin and a novel PD-L1 blocker (PD-L1 Trap) significantly prolonged the survival of tumor-bearing mice (139). Chemotherapy combined with anti-PD-1 is used as a first-line treatment for advanced NSCLC, which has significantly more clinical benefits than a single agent (140).

Radiotherapy promotes the release of TAAs, TSAs, or damage associated molecular pattern molecules (DAMPs), which can enhance the immunogenicity of tumor cells and promote the recruitment and infiltration of immune cells. This relationship is the rationale for combination with immunotherapies. In a study of mouse model, radiotherapy combined with anti-PD-1 treatment reversed immune resistance (141). In the treatment of metastatic melanoma, radiotherapy combined with anti-CTLA-4 and anti-PD-1 therapy may become a new idea in combined immunotherapies (142). Pilonis et al. reported that anti-CTLA-4 combined with radiotherapy effectively inhibited the lung metastasis of breast cancer in a mouse model (143). Deselm et al. found that radiotherapy made it more effective for CAR-T cells in a mouse model of pancreatic cancer, and the tumor cells that did not express the CAR target were also killed by CAR-T cells (144).

Combination with targeted therapy

Targeting intracellular signaling pathways with small molecule inhibitors is effective in rapidly reducing tumor volume. However, many of these drugs do not have durable effects, mainly due to the emergence of other compensatory pathways (145, 146). Emerging strategies to enhance immunotherapy response are being developed based on novel insights into T cells and overall immune function. Pembrolizumab combined with BRAF inhibitors shows synergistic antitumor activity and prolongs response time in mice with metastatic melanoma (147).

Tumor angiogenesis has an important relationship with tumor immunity. VEGF is related to the generation and regulation of MDSCs, so anti-angiogenic therapy combined with immunotherapy has a synergistic effect. Preclinical studies have shown that the combination of VEGFR inhibitor Axitinib and anti-CTLA-4 can enhance the antigen-presenting ability of DC to promote T cell proliferation in a mouse melanoma model (148). Data from clinical trials with the combination of ipilimumab and VEGF inhibitor bevacizumab showed that more than 30% of patients in the combination group observed a significant increase in CCR7+ CD8+ T cells, compared to only 6% of patients in the ipilimumab group (149). Studies have shown that sunitinib can reverse tumor-induced immunosuppression by reducing MDSCs (150). Various targeted therapies, such as EGFR, ALK, ROS1, and MEK inhibitors, are being clinically tested in combination with ICBs.

ACT combined with targeted therapy is also an innovative immunotherapeutic approach. Li et al. combine CAIX-specific CAR-T cells and sunitinib, which induces a potent antitumor response in an experimental model of metastatic RCC (151).

Other combination immunotherapies

The functional inhibition of CAR-T by PD-1/PD-L1 has been well established, which also provides the basis for the combination of PD-1/PD-L1 blockade and CAR-T. Existing preclinical studies have shown that CAR-T cells plus PD-1/PD-L1 blockade can effectively enhance the antitumor effect (152, 153).

IDO1 inhibitors have been in active clinical investigation and preliminary results suggest that IDO1 inhibitors produce additive efficacy when combined with cancer immunotherapies despite low activity as a single agent. Results from a phase I/II clinical trial, which combined IDO1 inhibitor epacadostat and Ipilimumab for the treatment of metastatic melanoma, showed an objective response and no tumor progression in some patients (154). In addition, IDO1 inhibitors combined with ICBs are also tested in various clinical trials (NCT03519256, NCT03854032, and NCT03661320). Combinations of type I interferons, TLR inhibitors, or STING agonists have also shown promise in preclinical models (155–157).

T-VEC can selectively replicate within tumors and produce granulocyte-macrophage colony-stimulating factor (GM-CSF), which triggers DC differentiation and enhancement of antigen presentation. This makes OV's susceptible to immunotherapy. OV therapy CG0070 in combination with Keytruda showed 89% CR in a clinical trial (AACR 2022 Abstract#CT036) (86).

Current combined strategies are complex because the potential combination approaches far exceed the available human and technical resources. There is an urgent need for us to test these combinations in appropriate preclinical models and to accelerate clinical translation through novel approaches to clinical trial design.

Discussion

Cancer occurrence and development is a complex process. Various immune-evasion mechanisms can counteract the body's immune response, which becomes more complex as cancer progresses. Cancer immunotherapy can kill and eliminate tumor cells through the immune system, thus becoming another revolutionary treatment after surgical resection, radiotherapy, chemotherapy, and targeted therapy.

Various cancer immunotherapies have shown promising clinical efficacy. However, cancer immunotherapy still faces many problems and challenges. MAbs therapy is a very promising treatment for immunotherapy, which has been repeatedly demonstrated in clinical use. However, due to the immunogenicity, mAbs can cause irAEs, which requires strict monitoring in clinical use. The production process of mAbs is time-consuming and costly, and new purification strategies are needed for higher purity of mAbs. These problems are

determined by the nature of the antibody itself, and we believe these problems will partly be solved with new design strategies and further optimization. The overall immune response rate of patients treated with ICB is not high, and there is a need to find reliable and effective biomarkers for precise and personalized immunotherapy. In combination with chemotherapy, mAbs have generated success against advanced-stage cancers, which previously had poor outcomes. In addition, combinations with different mAbs also showed a strong anti-tumor effect. Combination therapy may provide new opportunities for mAbs to reduce the side effects and improve the therapeutic effect in the future. Conjugation of cytotoxic agents to mAb allows for specific delivery of payloads to tumors, while multispecific antibodies grant novel mechanisms that increase specificity and facilitate delivery to historically intractable compartments. Besides, Fc-engineering mAbs can endow mAbs with stronger antitumor and immune activation ability through the incorporation of amino acid and glycan changes. With an increased understanding of immunobiology and the continued development of molecular biological methods, the possibilities for mAbs therapy are bounded only by the scope of human ingenuity.

Small molecule inhibitors for cancer immunotherapy always occupy an important position, although the sales of mAbs are far ahead. Small molecule inhibitors have mature R&D pipelines and the production process of small molecule inhibitors is more controllable than mAbs, which can help reduce costs. The controllable pharmacokinetic properties can help reduce the impact of side effects, and the good tissue permeability makes small molecule inhibitors useful for solid tumor immunotherapy. Small molecule inhibitors will always be an effective replacement and supplement for mAbs. Currently, a new form of small molecule inhibitor, proteolysis targeting chimeras (PROTAC) is tested in (pre-)clinical, such as IDO1 PROTACs. But many issues need to be addressed especially on whether it is a safe approach or whether there is a saturation in the degradation of proteins that may limit their effectiveness (158, 159).

ACT can be a potent new addition to the toolbox for cancer immunotherapy. However, many TCR-T/CAR-T clinical trials have been hampered by off-target effects and safety concerns (160, 161). While timely intervention is effective in most adverse events, side-effect management of ACT must be held in the whole process of ACT treatment. If tumor antigens are blocked by the self-secretion of tumor cells, they cannot be recognized by the immune system. Rationally designed strategies to identify candidate neoantigens and evaluate their immunogenicity are valuable for boosting the safety and efficacy of ACT. At present, the successful ACT therapy is mainly used in the treatment of hematological tumors. In solid tumors, getting CAR-T cells to infiltrate the tumor is a challenge, which can be compounded by the immunosuppressive TME. ACT combined with small

molecule immunomodulator targeting immunosuppressive TME may be effective for solid tumors.

The major challenge in oncolytic virus therapy is the targeted delivery of the virus into the tumor. In most cases, systemic administration does not work well because of preexisting immunity. Some novel approaches involve the use of nanoparticles, complex viral particle ligands, and immunomodulatory agents to deliver OV into the tumor. Alternatively, delivery of OV via nanoparticles using technologically complex image-guided delivery system has also been considered (90). Immune response after OV infection suppresses the replication of the virus thereby posing a hindrance to the effective functioning of OV therapy. Therefore, increasing anticancer treatments and consequently patient prognosis through contributions from molecular biology, immunology, genomics, and bioinformatics will provide a strong foundation for OV's potential clinical success in the future.

For preventive cancer vaccines, the successes of Gardasil are exciting. The next step is perhaps to look for other important tumorigenic antigens, possibly other viruses, to expand protection for people. In addition, for therapeutic cancer vaccines, an improved antitumor immune response is still in high demand because of the unsatisfactory clinical performance of the vaccine in tumor inhibition and regression. Personalized vaccine design and appropriate combined therapy could represent the best approach to increase the efficacy of cancer vaccines.

Compared with traditional chemoradiotherapy and targeted therapy, immunotherapy has significant advantages. Under the in-depth study of anti-tumor immune response mechanism, great progress has been made in the field of tumor immunotherapy. With the widespread application of immunotherapy, the occurrence of immune resistance has become an unavoidable problem. We are still at a very early stage of understanding the mechanisms of this immune resistance. By understanding mechanisms of immune resistance, we can enable immunotherapy to provide more survival benefits for cancer patients.

Compared with single-drug therapy, combination strategy for immunotherapy has a greater clinical effect. Clinical trials have shown that immunotherapeutic anticancer drugs, which include ICBs, ACT, chemotherapy, targeted therapy, etc., are important components of the combination. A few combination therapies have been approved by the FDA to improve clinical efficacy of cancer immunotherapy. With increasing research in identifying reliable biomarkers in guiding clinical immunology decisions, more convincing and effective combination strategies are expected.

As the development of tumor immunology, bioinformatics, and sequencing technologies, more and more mechanisms in TME will continue to be revealed. This will further the

development of cancer immunotherapy and pave the way for effective cancer treatments in the future.

Author contributions

CL prepared the figures and tables and prepared the manuscript; MY and MC contributed the idea and edited the manuscript; DZ participated in this study and contributed project administration and funding acquisition; DZ contributed the idea, oversaw the process and wrote the manuscript. All authors contributed to the article and approved the submitted version.

Funding

The current study was supported by projects on the Science and Technology Commission of Shanghai (18ZR1403900) (DZ), the National Natural Science Foundation of China (81872895) (DZ), a project on joint translational research in the School of Pharmacy and

Minhang Hospital (RO-MY201712) (DZ), and Jinan Science and Technology Bureau, Innovation team for the development and evaluation of new drugs for oncology immunotherapy (2020GXRC041 to DZ).

Conflict of interest

The authors declare that the research was conducted in the absence of any commercial or financial relationships that could be construed as a potential conflict of interest.

Publisher's note

All claims expressed in this article are solely those of the authors and do not necessarily represent those of their affiliated organizations, or those of the publisher, the editors and the reviewers. Any product that may be evaluated in this article, or claim that may be made by its manufacturer, is not guaranteed or endorsed by the publisher.

References

- Swann JB, Smyth MJ. Immune surveillance of tumors. *J Clin Invest* (2007) 117:1137–46. doi: 10.1172/JCI31405
- Tan AC, Bagley SJ, Wen PY, Lim M, Platten M, Colman H, et al. Systematic review of combinations of targeted or immunotherapy in advanced solid tumors. *J Immunother Cancer* (2021) 9:e002459. doi: 10.1136/jitc-2021-002459
- Chang CH, Qiu J, O'Sullivan D, Buck MD, Noguchi T, Curtis JD, et al. Metabolic competition in the tumor microenvironment is a driver of cancer progression. *Cell* (2015) 162:1229–41. doi: 10.1016/j.cell.2015.08.016
- Sanmamed MF, Chen L. A paradigm shift in cancer immunotherapy: From enhancement to normalization. *Cell* (2018) 175:313–26. doi: 10.1016/j.cell.2018.09.035
- Yang Y. Cancer immunotherapy: harnessing the immune system to battle cancer. *J Clin Invest* (2015) 125:3335–7. doi: 10.1172/JCI83871
- Brandsma AM, Jacobino SR, Meyer S, ten Broeke T, Leusen JH. Fc receptor inside-out signaling and possible impact on antibody therapy. *Immunol Rev* (2015) 268:74–87. doi: 10.1111/immr.12332
- Teige I, Mårtensson L, Frendéus BL. Targeting the antibody checkpoints to enhance cancer immunotherapy-focus on FcγRIIB. *Front Immunol* (2019) 10:481. doi: 10.3389/fimmu.2019.00481
- Strohl WR. Optimization of fc-mediated effector functions of monoclonal antibodies. *Curr Opin Biotechnol* (2009) 20:685–91. doi: 10.1016/j.copbio.2009.10.011
- Brennan FR, Morton LD, Spindeldreher S, Kiessling A, Allenspach R, Hey A, et al. Safety and immunotoxicity assessment of immunomodulatory monoclonal antibodies. *MAbs* (2010) 2:233–55. doi: 10.4161/mabs.2.3.11782
- Kulkarni HS, Kasi PM. Rituximab and cytokine release syndrome. *Case Rep Oncol* (2012) 5:134–41. doi: 10.1159/000337577
- Makino K, Nakata J, Kawachi S, Hayashi T, Nakajima A, Yokoyama M. Treatment strategy for reducing the risk of rituximab-induced cytokine release syndrome in patients with intravascular large b-cell lymphoma: a case report and review of the literature. *J Med Case Rep* (2013) 7:280. doi: 10.1186/1752-1947-7-280
- Labrijn AF, Janmaat ML, Reichert JM, Parren P. Bispecific antibodies: a mechanistic review of the pipeline. *Nat Rev Drug Discovery* (2019) 18:585–608. doi: 10.1038/s41573-019-0028-1
- Krishnamurthy A, Jimeno A. Bispecific antibodies for cancer therapy: A review. *Pharmacol Ther* (2018) 185:122–34. doi: 10.1016/j.pharmthera.2017.12.002
- Elgundi Z, Reslan M, Cruz E, Sifnietis V, Kayser V. The state-of-play and future of antibody therapeutics. *Adv Drug Delivery Rev* (2017) 122:2–19. doi: 10.1016/j.addr.2016.11.004
- Iwai Y, Ishida M, Tanaka Y, Okazaki T, Honjo T, Minato N. Involvement of PD-L1 on tumor cells in the escape from host immune system and tumor immunotherapy by PD-L1 blockade. *Proc Natl Acad Sci U.S.A.* (2002) 99:12293–7. doi: 10.1073/pnas.192461099
- Wei G, Zhang H, Zhao H, Wang J, Wu N, Li L, et al. Emerging immune checkpoints in the tumor microenvironment: Implications for cancer immunotherapy. *Cancer Lett* (2021) 511:68–76. doi: 10.1016/j.canlet.2021.04.021
- Buchbinder EI, Desai A. CTLA-4 and PD-1 pathways: Similarities, differences, and implications of their inhibition. *Am J Clin Oncol* (2016) 39:98–106. doi: 10.1097/COC.0000000000000239
- de Miguel M, Calvo E. Clinical challenges of immune checkpoint inhibitors. *Cancer Cell* (2020) 38:326–33. doi: 10.1016/j.ccell.2020.07.004
- Syn NL, Teng MWL, Mok TSK, Soo RA. De-novo and acquired resistance to immune checkpoint targeting. *Lancet Oncol* (2017) 18:e731–41. doi: 10.1016/S1470-2045(17)30607-1
- Lynch TJ, Bondarenko I, Luft A, Serwatowski P, Barlesi F, Chacko R, et al. Ipilimumab in combination with paclitaxel and carboplatin as first-line treatment in stage IIIB/IV non-small-cell lung cancer: results from a randomized, double-blind, multicenter phase II study. *J Clin Oncol* (2012) 30:2046–54. doi: 10.1016/j.jco.2012.07.009
- Dong H, Strome SE, Salomao DR, Tamura H, Hirano F, Flies DB, et al. Tumor-associated B7-H1 promotes T-cell apoptosis: a potential mechanism of immune evasion. *Nat Med* (2002) 8:793–800. doi: 10.1038/nm730
- Singh S, Hassan D, Aldawsari HM, Molugulu N, Shukla R, Kesharwani P. Immune checkpoint inhibitors: a promising anticancer therapy. *Drug Discovery Today* (2020) 25:223–9. doi: 10.1016/j.drudis.2019.11.003
- Koyama S, Akbay EA, Li YY, Herter-Sprie GS, Buczkowski KA, Richards WG, et al. Adaptive resistance to therapeutic PD-1 blockade is associated with

upregulation of alternative immune checkpoints. *Nat Commun* (2016) 7:10501. doi: 10.1038/ncomms10501

24. Ngiew SF, von Scheidt B, Akiba H, Yagita H, Teng MW, Smyth MJ. Anti-TIM3 antibody promotes T cell IFN- γ -mediated antitumor immunity and suppresses established tumors. *Cancer Res* (2011) 71:3540–51. doi: 10.1158/0008-5472.CAN-11-0096

25. Fadel F, El Karoui K, Knebelmann B. Anti-CTLA4 antibody-induced lupus nephritis. *N Engl J Med* (2009) 361:211–2. doi: 10.1056/NEJMc0904283

26. Boutros C, Tarhini A, Routier E, Lambotte O, Ladurie FL, Carbone F, et al. Safety profiles of anti-CTLA-4 and anti-PD-1 antibodies alone and in combination. *Nat Rev Clin Oncol* (2016) 13:473–86. doi: 10.1038/nrclinonc.2016.58

27. Martins F, Sofiya L, Sykietis GP, Lamine F, Maillard M, Fraga M, et al. Adverse effects of immune-checkpoint inhibitors: epidemiology, management and surveillance. *Nat Rev Clin Oncol* (2019) 16:563–80. doi: 10.1038/s41571-019-0218-0

28. Wang DY, Salem JE, Cohen JV, Chandra S, Menzer C, Ye F, et al. Fatal toxic effects associated with immune checkpoint inhibitors: A systematic review and meta-analysis. *JAMA Oncol* (2018) 4:1721–8. doi: 10.1001/jamaoncol.2018.3923

29. Raschi E, Gatti M, Gelsomino F, Ardizzone A, Poluzzi E, De Ponti F. Lessons to be learnt from real-world studies on immune-related adverse events with checkpoint inhibitors: A clinical perspective from pharmacovigilance. *Target Oncol* (2020) 15:449–66. doi: 10.1007/s11523-020-00738-6

30. Kumar V, Chaudhary N, Garg M, Floudas CS, Soni P, Chandra AB. Current diagnosis and management of immune related adverse events (irAEs) induced by immune checkpoint inhibitor therapy. *Front Pharmacol* (2017) 8:49. doi: 10.3389/fphar.2017.00311

31. Schneider BJ, Naidoo J, Santomaso BD, Lacchetti C, Adkins S, Anadkat M, et al. Management of immune-related adverse events in patients treated with immune checkpoint inhibitor therapy: ASCO guideline update. *J Clin Oncol* (2021) 39:4073–126. doi: 10.1200/jco.21.01440

32. Lin X, Lu X, Luo G, Xiang H. Progress in PD-1/PD-L1 pathway inhibitors: From biomacromolecules to small molecules. *Eur J Med Chem* (2020) 186:111876. doi: 10.1016/j.ejmech.2019.111876

33. Dawkins JB, Wang J, Maniati E, Heward JA, Koniali L, Kocher HM, et al. Reduced expression of histone methyltransferases KMT2C and KMT2D correlates with improved outcome in pancreatic ductal adenocarcinoma. *Cancer Res* (2016) 76:4861–71. doi: 10.1158/0008-5472.CAN-16-0481

34. Carretero-González A, Lora D, Ghanem I, Zugazagoitia J, Castellano D, Sepúlveda JM, et al. Analysis of response rate with ANTI PD1/PD-L1 monoclonal antibodies in advanced solid tumors: a meta-analysis of randomized clinical trials. *Oncotarget* (2018) 9:8706–15. doi: 10.18632/oncotarget.24283

35. Sasikumar PG, Nair R, Muralidharan N, Sudarshan SS. 1,3,4-OXADIAZOLE AND 1,3,4-THIADIAZOLE DERIVATIVES AS IMMUNOMODULATORS. In *Aurigen discovery technologies limited*. (2015) WO2015033301.

36. Sasikumar PG, Nair R, Muralidharan N, Sudarshan SS. 1,2,4-OXADIAZOLE DERIVATIVES AS IMMUNOMODULATORS. In *Aurigen discovery technologies limited*. (2015) WO2015033299.

37. Park JJ, Thi EP, Carpio VH, Bi Y, Cole AG, Dorsey BD, et al. Checkpoint inhibition through small molecule-induced internalization of programmed death-ligand 1. *Nat Commun* (2021) 12:1222. doi: 10.1038/s41467-021-21410-1

38. Sasikumar PGN, Ramachandra M, Vadlamani S, Kumar V, Koteswara R, Satyam L, et al. Immunosuppression modulating compounds. In *Aurigen discovery technologies limited*. (2011) US2011318373.

39. Sasikumar PG, Ramachandra RK, Adurthi S, Dhudashya AA, Vadlamani S, Vemula K, et al. A rationally designed peptide antagonist of the PD-1 signaling pathway as an immunomodulatory agent for cancer therapy. *Mol. Cancer Ther* (2019) 18:1081–91. doi: 10.1158/1535-7163.MCT-18-0737

40. Sasikumar PG, Satyam LK, Shrimali RK, Subbarao K, Ramachandra R, Vadlamani S, et al. Abstract 2850: Demonstration of anti-tumor efficacy in multiple preclinical cancer models using a novel peptide inhibitor (Aurigen-012) of the PD1 signaling pathway. *Cancer Res* (2012) 72:2850–0. doi: 10.1158/1538-7445.AM2012-2850

41. Yeung K-S, Grant-Young KA, Zhu J, Saulnier MG, Frennesson DB, Langley DR, et al. Biaryl compounds useful as immunomodulators. In *Bristol-Myers Squibb company*. (2018) WO201804963.

42. Liu C, Zhou F, Yan Z, Shen L, Zhang X, He F, et al. Discovery of a novel, potent and selective small-molecule inhibitor of PD-1/PD-L1 interaction with robust *in vivo* anti-tumour efficacy. *Br J Pharmacol* (2021) 178:2651–70. doi: 10.1111/bph.15457

43. Le Naour J, Galluzzi L, Zitvogel L, Kroemer G, Vacchelli E. Trial watch: IDO inhibitors in cancer therapy. *Oncoimmunology* (2020) 9:1777625. doi: 10.1080/2162402X.2020.1777625

44. Cheong JE, Sun L. Targeting the IDO1/TDO2-KYN-AhR pathway for cancer immunotherapy - challenges and opportunities. *Trends Pharmacol Sci* (2018) 39:307–25. doi: 10.1016/j.tips.2017.11.007

45. Uytendhove C, Pilotte L, Théate I, Stroobant V, Colau D, Parmentier N, et al. Evidence for a tumoral immune resistance mechanism based on tryptophan degradation by indoleamine 2,3-dioxygenase. *Nat Med* (2003) 9:1269–74. doi: 10.1038/nm934

46. Yue EW, Sparks R, Polam P, Modi D, Douthy B, Wayland B, et al. INCB24360 (Epacadostat), a highly potent and selective indoleamine-2,3-dioxygenase 1 (IDO1) inhibitor for immuno-oncology. *ACS Med Chem Lett* (2017) 8:486–91. doi: 10.1021/acsmchemlett.6b00391

47. Companies scaling back IDO1 inhibitor trials. *Cancer Discovery* (2018) 8:OF5. doi: 10.1158/2159-8290.CD-ND2018-007

48. Prendergast GC, Malachowski WJ, Mondal A, Scherle P, Muller AJ. Indoleamine 2,3-dioxygenase and its therapeutic inhibition in cancer. *Int Rev Cell Mol Biol* (2018) 336:175–203. doi: 10.1016/bs.ircmb.2017.07.004

49. Fu J, Kanne DB, Leong M, Glickman LH, McWhirter SM, Lemmens E, et al. STING agonist formulated cancer vaccines can cure established tumors resistant to PD-1 blockade. *Sci Transl Med* (2015) 7:283ra252. doi: 10.1126/scitranslmed.aaa4306

50. Liu Y, Lu X, Qin N, Qiao Y, Xing S, Liu W, et al. STING, a promising target for small molecular immune modulator: A review. *Eur J Med Chem* (2021) 211:113113. doi: 10.1016/j.ejmech.2020.113113

51. Lim EA, Bendell JC, Falchook GS, Bauer TM, Drake CG, Choe JH, et al. Phase 1a/b, open-label, multicenter study of AZD4635 (an adenosine 2A receptor antagonist) as monotherapy or combined with durvalumab, in patients with solid tumors. *Clin Cancer Res* (2022) 31:CCR-22-0612. doi: 10.1158/1078-0432.CCR-22-0612

52. Chiappori AA, Creelan B, Tanvetyanon T, Gray JE, Haura EB, Thapa R, et al. Phase I study of taminadenant (PBF509/NIR178), an adenosine 2A receptor antagonist, with or without spartalizumab (PDR001), in patients with advanced non-small cell lung cancer. *Clin Cancer Res* (2022) 28:2313–20. doi: 10.1158/1078-0432.CCR-21-2742

53. Jia HX, He YL. Efficacy and safety of imiquimod 5% cream for basal cell carcinoma: a meta-analysis of randomized controlled trial. *J Dermatolog Treat* (2020) 31:831–8. doi: 10.1080/09546634.2019.1638883

54. Choueiri TK, Atkins MB, Rose TL, Alter RS, Ju Y, Niland K, et al. A phase 1b trial of the CXCR4 inhibitor mavoxixafor and nivolumab in advanced renal cell carcinoma patients with no prior response to nivolumab monotherapy. *Invest New Drugs* (2021) 39:1019–27. doi: 10.1007/s10637-020-01058-2

55. Huang X, Yang Y. Driving an improved CAR for cancer immunotherapy. *J Clin Invest* (2016) 126:2795–8. doi: 10.1172/JCI88959

56. Bach PB, Giral SA, Saltz LB. FDA Approval of tisagenlecleucel: Promise and complexities of a \$475 000 cancer drug. *Jama* (2017) 318:1861–2. doi: 10.1001/jama.2017.15218

57. FDA Approves second CAR T-cell therapy. *Cancer Discovery* (2018) 8:5–6. doi: 10.1158/2159-8290.CD-NB2017-155

58. Abreu TR, Fonseca NA, Gonçalves N, Moreira JN. Current challenges and emerging opportunities of CAR-T cell therapies. *J Control Release* (2020) 319:246–61. doi: 10.1016/j.jconrel.2019.12.047

59. Tang J, Hubbard-Lucey VM, Pearce L, O'Donnell-Tormey J, Shalabi A. The global landscape of cancer cell therapy. *Nat Rev Drug Discovery* (2018) 17:465–6. doi: 10.1038/nrd.2018.74

60. Dai H, Wu Z, Jia H, Tong C, Guo Y, Ti D, et al. Bispecific CAR-T cells targeting both CD19 and CD22 for therapy of adults with relapsed or refractory B cell acute lymphoblastic leukemia. *J Hematol Oncol* (2020) 13:30. doi: 10.1186/s13045-020-00856-8

61. Zhao J, Song Y, Liu D. Clinical trials of dual-target CAR T cells, donor-derived CAR T cells, and universal CAR T cells for acute lymphoid leukemia. *J Hematol Oncol* (2019) 12:17. doi: 10.1186/s13045-019-0705-x

62. Hegde M, Mukherjee M, Grada Z, Pignata A, Landi D, Navai SA, et al. Tandem CAR T cells targeting HER2 and IL13R α 2 mitigate tumor antigen escape. *J Clin Invest* (2016) 126:3036–52. doi: 10.1172/JCI83416

63. Grosskopf AK, Labanieh L, Klysz DD, Roth GA, Xu P, Adebowale O, et al. Delivery of CAR-T cells in a transient injectable stimulatory hydrogel niche improves treatment of solid tumors. *Sci Adv* (2022) 8:eabn8264. doi: 10.1126/sciadv.abn8264

64. Gargett T, Yu W, Dotti G, Yvon ES, Christo SN, Hayball JD, et al. GD2-specific CAR T cells undergo potent activation and deletion following antigen encounter but can be protected from activation-induced cell death by PD-1 blockade. *Mol Ther* (2016) 24:1135–49. doi: 10.1038/mt.2016.63

65. Ping Y, Liu C, Zhang Y. T-Cell receptor-engineered T cells for cancer treatment: current status and future directions. *Protein Cell* (2018) 9:254–66. doi: 10.1007/s13238-016-0367-1

66. June CH, O'Connor RS, Kawalekar OU, Ghassemi S, Milone MC. CAR T cell immunotherapy for human cancer. *Science* (2018) 359:1361–5. doi: 10.1126/science.aar6711
67. Shafer P, Kelly LM, Hoyos V. Cancer therapy with TCR-engineered T cells: Current strategies. *Challenges Prospects Front Immunol* (2022) 13:835762. doi: 10.3389/fimmu.2022.835762
68. Rosenberg SA, Packard BS, Aebersold PM, Solomon D, Topalian SL, Toy ST, et al. Use of tumor-infiltrating lymphocytes and interleukin-2 in the immunotherapy of patients with metastatic melanoma. a preliminary report. *N Engl J Med* (1988) 319:1676–80. doi: 10.1056/NEJM19881223192527
69. Rosenberg SA, Yang JC, Sherry RM, Kammula US, Hughes MS, Phan GQ, et al. Durable complete responses in heavily pretreated patients with metastatic melanoma using T-cell transfer immunotherapy. *Clin Cancer Res* (2011) 17:4550–7. doi: 10.1158/1078-0432.Ccr-11-0116
70. Dudley ME, Wunderlich JR, Yang JC, Sherry RM, Topalian SL, Restifo NP, et al. Adoptive cell transfer therapy following non-myeloablative but lymphodepleting chemotherapy for the treatment of patients with refractory metastatic melanoma. *J Clin Oncol* (2005) 23:2346–57. doi: 10.1200/JCO.2005.00.240
71. Pilon-Thomas S, Kuhn L, Ellwanger S, Janssen W, Royster E, Marzban S, et al. Efficacy of adoptive cell transfer of tumor-infiltrating lymphocytes after lymphopenia induction for metastatic melanoma. *J Immunother* (2012) 35:615–20. doi: 10.1097/CJI.0b013e31826e8f5f
72. Goff SL, Smith FO, Klapper JA, Sherry R, Wunderlich JR, Steinberg SM, et al. Tumor infiltrating lymphocyte therapy for metastatic melanoma: analysis of tumors resected for TIL. *J Immunother* (2010) 33:840–7. doi: 10.1097/CJI.0b013e3181f05b91
73. Galon J, Costes A, Sanchez-Cabo F, Kirilovsky A, Mlecnik B, Lagorce-Pagès C, et al. Type, density, and location of immune cells within human colorectal tumors predict clinical outcome. *Science* (2006) 313:1960–4. doi: 10.1126/science.1129139
74. Sanmamed MF, Nie X, Desai SS, Villaroel-Espindola F, Badri T, Zhao D, et al. A burned-out CD8(+) T-cell subset expands in the tumor microenvironment and curbs cancer immunotherapy. *Cancer Discovery* (2021) 11:1700–15. doi: 10.1158/2159-8290.CD-20-0962
75. Hall M, Liu H, Malafa M, Centeno B, Hodul PJ, Pimiento J, et al. Expansion of tumor-infiltrating lymphocytes (TIL) from human pancreatic tumors. *J Immunother Cancer* (2016) 4:61. doi: 10.1186/s40425-016-0164-7
76. Wang W, Jiang J, Wu C. CAR-NK for tumor immunotherapy: Clinical transformation and future prospects. *Cancer Lett* (2020) 472:175–80. doi: 10.1016/j.canlet.2019.11.033
77. Liu E, Marin D, Banerjee P, Macapinlac HA, Thompson P, Basar R, et al. Use of CAR-transduced natural killer cells in CD19-positive lymphoid tumors. *N Engl J Med* (2020) 382:545–53. doi: 10.1056/NEJMoa1910607
78. Hu Y, Tian Z, Zhang C. Natural killer cell-based immunotherapy for cancer: Advances and prospects. *Engineering* (2019) 5:106–14. doi: 10.1016/j.eng.2018.11.015
79. Liu M, Meng Y, Zhang L, Han Z, Feng X. High-efficient generation of natural killer cells from peripheral blood with preferable cell vitality and enhanced cytotoxicity by combination of IL-2, IL-15 and IL-18. *Biochem Biophys Res Commun* (2021) 534:149–56. doi: 10.1016/j.bbrc.2020.12.012
80. Romee R, Rosario M, Berrien-Elliott MM, Wagner JA, Jewell BA, Schappe T, et al. Cytokine-induced memory-like natural killer cells exhibit enhanced responses against myeloid leukemia. *Sci Transl Med* (2016) 8:357ra123. doi: 10.1126/scitranslmed.aaf2341
81. Ni J, Miller M, Stojanovic A, Garbi N, Cerwenka A. Sustained effector function of IL-12/15/18-pretreated NK cells against established tumors. *J Exp Med* (2012) 209:2351–65. doi: 10.1084/jem.20120944
82. Bommarreddy PK, Shettigar M, Kaufman HL. Integrating oncolytic viruses in combination cancer immunotherapy. *Nat Rev Immunol* (2018) 18:498–513. doi: 10.1038/s41577-018-0014-6
83. Raja J, Ludwig JM, Gettinger SN, Schalper KA, Kim HS. Oncolytic virus immunotherapy: future prospects for oncology. *J Immunother Cancer* (2018) 6:140. doi: 10.1186/s40425-018-0458-z
84. Hemminki O, Dos Santos JM, Hemminki A. Oncolytic viruses for cancer immunotherapy. *J Hematol Oncol* (2020) 13:84. doi: 10.1186/s13045-020-00922-1
85. Kaufman HL, Kohlhaup FJ, Zloza A. Oncolytic viruses: a new class of immunotherapy drugs. *Nat Rev Drug Discovery* (2015) 14:642–62. doi: 10.1038/nrd4663
86. Rosewell Shaw A, Suzuki M. Oncolytic viruses partner With T-cell therapy for solid tumor treatment. *Front Immunol* (2018) 9:2103. doi: 10.3389/fimmu.2018.02103
87. Ylösmäki E, Cerullo V. Design and application of oncolytic viruses for cancer immunotherapy. *Curr Opin Biotechnol* (2020) 65:25–36. doi: 10.1016/j.copbio.2019.11.016
88. Macedo N, Miller DM, Haq R, Kaufman HL. Clinical landscape of oncolytic virus research in 2020. *J Immunother Cancer* (2020) 8:e001486. doi: 10.1136/jitc-2020-001486
89. Watanabe N, McKenna MK, Rosewell Shaw A, Suzuki M. Clinical CAR-T cell and oncolytic virotherapy for cancer treatment. *Mol Ther* (2021) 29(2):505–20. doi: 10.1016/j.jymthe.2020.10.023
90. Roy DG, Bell JC. Cell carriers for oncolytic viruses: current challenges and future directions. *Oncolytic Virother* (2013) 2:47–56. doi: 10.2147/OV.S36623
91. Gao Q, Zhu H, Dong L, Shi W, Chen R, Song Z, et al. Integrated proteomic characterization of HBV-related hepatocellular carcinoma. *Cell* (2019) 179:1240. doi: 10.1016/j.cell.2019.10.038
92. Ren L, Zeng M, Tang Z, Li M, Wang X, Xu Y, et al. The antiresection activity of the X protein encoded by hepatitis virus b. *Hepatology* (2019) 69:2546–61. doi: 10.1002/hep.30571
93. Chen F, Zou Z, Du J, Su S, Shao J, Meng F, et al. Neoantigen identification strategies enable personalized immunotherapy in refractory solid tumors. *J Clin Invest* (2019) 129:2056–70. doi: 10.1172/JCI99538
94. Ott PA, Hu Z, Keskin DB, Shukla SA, Sun J, Bozym DJ, et al. An immunogenic personal neoantigen vaccine for patients with melanoma. *Nature* (2017) 547:217–21. doi: 10.1038/nature22991
95. Sahin U, Derhovanessian E, Miller M, Kloke BP, Simon P, Löwer M, et al. Personalized RNA mutanome vaccines mobilize poly-specific therapeutic immunity against cancer. *Nature* (2017) 547:222–6. doi: 10.1038/nature23003
96. Herrera ZM, Ramos TC. Pilot study of a novel combination of two therapeutic vaccines in advanced non-small-cell lung cancer patients. *Cancer Immunol Immunother* (2014) 63:737–47. doi: 10.1007/s00262-014-1552-9
97. Saxena M, van der Burg SH, Melief CJM, Bhardwaj N. Therapeutic cancer vaccines. *Nat Rev Cancer* (2021) 21:360–78. doi: 10.1038/s41568-021-00346-0
98. Couzin-Frankel J. Breakthrough of the year 2013. *Cancer immunotherapy Sci* (2013) 342:1432–3. doi: 10.1126/science.342.6165.1432
99. Yaguchi T, Kawakami Y. Cancer-induced heterogeneous immunosuppressive tumor microenvironments and their personalized modulation. *Int Immunol* (2016) 28:393–9. doi: 10.1093/intimm/dxw030
100. Liu D, Jenkins RW, Sullivan RJ. Mechanisms of resistance to immune checkpoint blockade. *Am J Clin Dermatol* (2019) 20:41–54. doi: 10.1007/s40257-018-0389-y
101. Jia H, Truica CI, Wang B, Wang Y, Ren X, Harvey HA, et al. Immunotherapy for triple-negative breast cancer: Existing challenges and exciting prospects. *Drug Resist Update* (2017) 32:1–15. doi: 10.1016/j.drug.2017.07.002
102. Hu Q, Ye Y, Chan LC, Li Y, Liang K, Lin A, et al. Oncogenic lncRNA downregulates cancer cell antigen presentation and intrinsic tumor suppression. *Nat Immunol* (2019) 20:835–51. doi: 10.1038/s41590-019-0400-7
103. Rizvi NA, Hellmann MD, Snyder A, Kvistborg P, Makarov V, Havel JJ, et al. Cancer immunology. mutational landscape determines sensitivity to PD-1 blockade in non-small cell lung cancer. *Science* (2015) 348:124–8. doi: 10.1126/science.aaa1348
104. Schumacher TN, Schreiber RD. Neoantigens in cancer immunotherapy. *Science* (2015) 348:69–74. doi: 10.1126/science.aaa4971
105. Liu C, Peng W, Xu C, Lou Y, Zhang M, Wargo JA, et al. BRAF inhibition increases tumor infiltration by T cells and enhances the antitumor activity of adoptive immunotherapy in mice. *Clin Cancer Res* (2013) 19:393–403. doi: 10.1158/1078-0432.CCR-12-1626
106. Peng W, Chen JQ, Liu C, Malu S, Creasy C, Tetzlaff MT, et al. Loss of PTEN promotes resistance to T cell-mediated immunotherapy. *Cancer Discovery* (2016) 6:202–16. doi: 10.1158/2159-8290.Cd-15-0283
107. Zhang X, Zeng Y, Qu Q, Zhu J, Liu Z, Ning W, et al. PD-L1 induced by IFN- γ from tumor-associated macrophages via the JAK/STAT3 and PI3K/AKT signaling pathways promoted progression of lung cancer. *Int J Clin Oncol* (2017) 22:1026–33. doi: 10.1007/s10147-017-1161-7
108. Steinhart Z, Pavlovic Z, Chandrasekhar M, Hart T, Wang X, Zhang X, et al. Genome-wide CRISPR screens reveal a wnt-FZD5 signaling circuit as a druggable vulnerability of RNF43-mutant pancreatic tumors. *Nat Med* (2017) 23:60–8. doi: 10.1038/nm.4219
109. Spranger S, Dai D, Horton B, Gajewski TF. Tumor-residing Batf3 dendritic cells are required for effector T cell trafficking and adoptive T cell therapy. *Cancer Cell* (2017) 31:711–723.e714. doi: 10.1016/j.ccell.2017.04.003
110. Spranger S, Bao R, Gajewski TF. Melanoma-intrinsic β -catenin signalling prevents anti-tumour immunity. *Nature* (2015) 523:231–5. doi: 10.1038/nature14404

111. Satoh K, Yachida S, Sugimoto M, Oshima M, Nakagawa T, Akamoto S, et al. Global metabolic reprogramming of colorectal cancer occurs at adenoma stage and is induced by MYC. *Proc Natl Acad Sci U.S.A.* (2017) 114:E7697–e7706. doi: 10.1073/pnas.1710366114
112. Cascone T, McKenzie JA, Mboufung RM, Punt S, Wang Z, Xu C, et al. Increased tumor glycolysis characterizes immune resistance to adoptive T cell therapy. *Cell Metab* (2018) 27:977–987.e974. doi: 10.1016/j.cmet.2018.02.024
113. Commeren DL, Van Soest PL, Karimi K, Löwenberg B, Cornelissen JJ, Braakman E. Paradoxical effects of interleukin-10 on the maturation of murine myeloid dendritic cells. *Immunology* (2003) 110:188–96. doi: 10.1046/j.1365-2567.2003.01730.x
114. Highfill SL, Cui Y, Giles AJ, Smith JP, Zhang H, Morse E, et al. Disruption of CXCR2-mediated MDSC tumor trafficking enhances anti-PD1 efficacy. *Sci Transl Med* (2014) 6:237ra267. doi: 10.1126/scitranslmed.3007974
115. Mantovani A, Marchesi F, Malesci A, Laghi L, Allavena P. Tumour-associated macrophages as treatment targets in oncology. *Nat Rev Clin Oncol* (2017) 14:399–416. doi: 10.1038/nrclinonc.2016.217
116. Kuang DM, Zhao Q, Peng C, Xu J, Zhang JP, Wu C, et al. Activated monocytes in peritumoral stroma of hepatocellular carcinoma foster immune privilege and disease progression through PD-L1. *J Exp Med* (2009) 206:1327–37. doi: 10.1084/jem.20082173
117. Kryczek I, Zou L, Rodriguez P, Zhu G, Wei S, Mottram P, et al. B7-H4 expression identifies a novel suppressive macrophage population in human ovarian carcinoma. *J Exp Med* (2006) 203:871–81. doi: 10.1084/jem.20050930
118. Schachter J, Ribas A, Long GV, Arance A, Grob JJ, Mortier L, et al. Pembrolizumab versus ipilimumab for advanced melanoma: final overall survival results of a multicentre, randomised, open-label phase 3 study (KEYNOTE-006). *Lancet* (2017) 390:1853–62. doi: 10.1016/S0140-6736(17)31601-X
119. Yaguchi T, Kobayashi A, Inozume T, Morii K, Nagumo H, Nishio H, et al. Human PBMC-transferred murine MHC class I/II-deficient NOG mice enable long-term evaluation of human immune responses. *Cell Mol Immunol* (2018) 15:953–62. doi: 10.1038/cmi.2017.106
120. Zaretsky JM, Garcia-Diaz A, Shin DS, Escuin-Ordinas H, Hugo W, Hu-Lieskovan S, et al. Mutations associated with acquired resistance to PD-1 blockade in melanoma. *N Engl J Med* (2016) 375:819–29. doi: 10.1056/NEJMoa1604958
121. Sade-Feldman M, Jiao YJ, Chen JH, Rooney MS, Barzily-Rokni M, Eliane JP, et al. Resistance to checkpoint blockade therapy through inactivation of antigen presentation. *Nat Commun* (2017) 8:1136. doi: 10.1038/s41467-017-01062-w
122. Gao J, Shi LZ, Zhao H, Chen J, Xiong L, He Q, et al. Loss of IFN- γ pathway genes in tumor cells as a mechanism of resistance to anti-CTLA-4 therapy. *Cell* (2016) 167:397–404.e399. doi: 10.1016/j.cell.2016.08.069
123. Tran E, Robbins PF, Lu YC, Prickett TD, Gartner JJ, Jia L, et al. T-Cell transfer therapy targeting mutant KRAS in cancer. *N Engl J Med* (2016) 375:2255–62. doi: 10.1056/NEJMoa1609279
124. van Rooij N, van Buuren MM, Philips D, Velds A, Toebes M, Heemskerk B, et al. Tumor exome analysis reveals neoantigen-specific T-cell reactivity in an ipilimumab-responsive melanoma. *J Clin Oncol* (2013) 31:e439–442. doi: 10.1200/JCO.2012.47.7521
125. Explaining resistance to CAR T cells. *Cancer Discovery* (2018) 8:784–5. doi: 10.1158/2159-8290.CD-NB2018-065
126. Majzner RG, Heitzeneder S, Mackall CL. Harnessing the immunotherapy revolution for the treatment of childhood cancers. *Cancer Cell* (2017) 31:476–85. doi: 10.1016/j.ccell.2017.03.002
127. Anderson AC, Joller N, Kuchroo VK. Lag-3, Tim-3, and TIGIT: Co-inhibitory receptors with specialized functions in immune regulation. *Immunity* (2016) 44:989–1004. doi: 10.1016/j.immuni.2016.05.001
128. Ninomiya S, Narala N, Huye L, Yagyu S, Savoldo B, Dotti G, et al. Tumor indoleamine 2,3-dioxygenase (IDO) inhibits CD19-CAR T cells and is downregulated by lymphodepleting drugs. *Blood* (2015) 125:3905–16. doi: 10.1182/blood-2015-01-621474
129. Moon EK, Wang LC, Dolfi DV, Wilson CB, Ranganathan R, Sun J, et al. Multifactorial T-cell hypofunction that is reversible can limit the efficacy of chimeric antigen receptor-transduced human T cells in solid tumors. *Clin Cancer Res* (2014) 20:4262–73. doi: 10.1158/1078-0432.CCR-13-2627
130. Postow MA, Chesney J, Pavlick AC, Robert C, Grossmann K, McDermott D, et al. Nivolumab and ipilimumab versus ipilimumab in untreated melanoma. *N Engl J Med* (2015) 372:2006–17. doi: 10.1056/NEJMoa1414428
131. Larkin J, Hodi FS, Wolchok JD. Combined nivolumab and ipilimumab or monotherapy in untreated melanoma. *N Engl J Med* (2015) 373:1270–1. doi: 10.1056/NEJMoa1509660
132. Larkin J, Chiarion-Sileni V, Gonzalez R, Grob JJ, Rutkowski P, Lao CD, et al. Five-year survival with combined nivolumab and ipilimumab in advanced melanoma. *N Engl J Med* (2019) 381:1535–46. doi: 10.1056/NEJMoa1509660
133. Liu F, Zeng G, Zhou S, He X, Sun N, Zhu X, et al. Blocking Tim-3 or/and PD-1 reverses dysfunction of tumor-infiltrating lymphocytes in HBV-related hepatocellular carcinoma. *Bull Cancer* (2018) 105:493–501. doi: 10.1016/j.bulcan.2018.01.018
134. Huang RY, Eppolito C, Lele S, Shrikant P, Matsuzaki J, Odunsi K. LAG3 and PD1 co-inhibitory molecules collaborate to limit CD8+ T cell signaling and dampen antitumor immunity in a murine ovarian cancer model. *Oncotarget* (2015) 6:27359–77. doi: 10.18632/oncotarget.4751
135. Johnston RJ, Comps-Agrar L, Hackney J, Yu X, Huseni M, Yang Y, et al. The immunoreceptor TIGIT regulates antitumor and antiviral CD8(+) T cell effector function. *Cancer Cell* (2014) 26:923–37. doi: 10.1016/j.ccell.2014.10.018
136. Pauken KE, Wherry EJ. Overcoming T cell exhaustion in infection and cancer. *Trends Immunol* (2015) 36:265–76. doi: 10.1016/j.it.2015.02.008
137. Rios-Doria J, Durham N, Wetzel L, Rothstein R, Chesebrough J, Holowickjy N, et al. Doxil synergizes with cancer immunotherapies to enhance antitumor responses in syngeneic mouse models. *Neoplasia* (2015) 17:661–70. doi: 10.1016/j.neo.2015.08.004
138. Banissi C, Ghiringhelli F, Chen L, Carpentier AF. Treg depletion with a low-dose metronomic temozolomide regimen in a rat glioma model. *Cancer Immunother* (2009) 58:1627–34. doi: 10.1007/s00262-009-0671-1
139. Song W, Shen L, Wang Y, Liu Q, Goodwin TJ, Li J, et al. Synergistic and low adverse effect cancer immunotherapy by immunogenic chemotherapy and locally expressed PD-L1 trap. *Nat Commun* (2018) 9:2237. doi: 10.1038/s41467-018-04605-x
140. Langer CJ, Gadgil SM, Borghaei H, Papadimitrakopoulou VA, Patnaik A, Powell SF, et al. Carboplatin and pemetrexed with or without pembrolizumab for advanced, non-squamous non-small-cell lung cancer: a randomised, phase 2 cohort of the open-label KEYNOTE-021 study. *Lancet Oncol* (2016) 17:1497–508. doi: 10.1016/S1470-2045(16)30498-3
141. Deng L, Liang H, Burnette B, Beckett M, Darga T, Weichselbaum RR, et al. Irradiation and anti-PD-L1 treatment synergistically promote antitumor immunity in mice. *J Clin Invest* (2014) 124:687–95. doi: 10.1172/JCI67313
142. Twyman-Saint Victor C, Rech AJ, Maity A, Rengan R, Pauken KE, Stelekati E, et al. Radiation and dual checkpoint blockade activate non-redundant immune mechanisms in cancer. *Nature* (2015) 520:373–7. doi: 10.1038/nature14292
143. Pilonis KA, Aryankalayil J, Babb JS, Demaria S. Invariant natural killer T cells regulate anti-tumor immunity by controlling the population of dendritic cells in tumor and draining lymph nodes. *J Immunother Cancer* (2014) 2:37. doi: 10.1186/s40425-014-0037-x
144. DeSelm C, Palomba ML, Yahalom J, Hamieh M, Eyquem J, Rajasekhar VK, et al. Low-dose radiation conditioning enables CAR T cells to mitigate antigen escape. *Mol Ther* (2018) 26:2542–52. doi: 10.1016/j.ymthe.2018.09.008
145. Flaherty KT, Infante JR, Daud A, Gonzalez R, Keeford RF, Sosman J, et al. Combined BRAF and MEK inhibition in melanoma with BRAF V600 mutations. *N Engl J Med* (2012) 367:1694–703. doi: 10.1056/NEJMoa1210093
146. Lynch TJ, Bell DW, Sordella R, Gurubhagavatula S, Okimoto RA, Brannigan BW, et al. Activating mutations in the epidermal growth factor receptor underlying responsiveness of non-small-cell lung cancer to gefitinib. *N Engl J Med* (2004) 350:2129–39. doi: 10.1056/NEJMoa040938
147. Cooper ZA, Juneja VR, Sage PT, Frederick DT, Piris A, Mitra D, et al. Response to BRAF inhibition in melanoma is enhanced when combined with immune checkpoint blockade. *Cancer Immunol Res* (2014) 2:643–54. doi: 10.1158/2326-6066.CIR-13-0215
148. Du Four S, Maenhout SK, Niclou SP, Thielemans K, Neyns B, Aerts JL. Combined VEGFR and CTLA-4 blockade increases the antigen-presenting function of intratumoral DCs and reduces the suppressive capacity of intratumoral MDSCs. *Am J Cancer Res* (2016) 6:2514–31.
149. Wu X, Li J, Connolly EM, Liao X, Ouyang J, Giobbie-Hurder A, et al. Combined anti-VEGF and anti-CTLA-4 therapy elicits humoral immunity to galectin-1 which is associated with favorable clinical outcomes. *Cancer Immunol Res* (2017) 5:446–54. doi: 10.1158/2326-6066.CIR-16-0385
150. Li W, Zhan M, Quan YY, Wang H, Hua SN, Li Y, et al. Modulating the tumor immune microenvironment with sunitinib malate supports the rationale for combined treatment with immunotherapy. *Int Immunopharmacol* (2020) 81:106227. doi: 10.1016/j.intimp.2020.106227
151. Li H, Ding J, Lu M, Liu H, Miao Y, Li L, et al. CAIX-specific CAR-T cells and sunitinib show synergistic effects against metastatic renal cancer models. *J Immunother* (2020) 43:16–28. doi: 10.1097/CJI.0000000000000301
152. Suarez ER, Chang de K, Sun J, Sui J, Freeman GJ, Signoretti S, et al. Chimeric antigen receptor T cells secreting anti-PD-L1 antibodies more effectively regress renal cell carcinoma in a humanized mouse model. *Oncotarget* (2016) 7:34341–55. doi: 10.18632/oncotarget.9114
153. John LB, Devaud C, Duong CP, Yong CS, Beavis PA, Haynes NM, et al. Anti-PD-1 antibody therapy potentially enhances the eradication of established

tumors by gene-modified T cells. *Clin Cancer Res* (2013) 19:5636–46. doi: 10.1158/1078-0432.CCR-13-0458

154. Nanda VGY, Peng W, Hwu P, Davies MA, Ciliberto G, Fattore L, et al. Melanoma and immunotherapy bridge 2015 : Naples, Italy. 1-5 December 2015. *J Transl Med* (2016) 14:65. doi: 10.1186/s12967-016-0791-2

155. Takeda Y, Kataoka K, Yamagishi J, Ogawa S, Seya T, Matsumoto M. A TLR3-specific adjuvant relieves innate resistance to PD-L1 blockade without cytokine toxicity in tumor vaccine immunotherapy. *Cell Rep* (2017) 19:1874–87. doi: 10.1016/j.celrep.2017.05.015

156. Ager CR, Reilley MJ, Nicholas C, Bartkowiak T, Jaiswal AR, Curran MA. Intratumoral STING activation with T-cell checkpoint modulation generates systemic antitumor immunity. *Cancer Immunol Res* (2017) 5:676–84. doi: 10.1158/2326-6066.CIR-17-0049

157. Liang Y, Tang H, Guo J, Qiu X, Yang Z, Ren Z, et al. Targeting IFN α to tumor by anti-PD-L1 creates feedforward antitumor responses to overcome

checkpoint blockade resistance. *Nat Commun* (2018) 9:4586. doi: 10.1038/s41467-018-06890-y

158. Hu B, Zhou Y, Sun D, Yang Y, Liu Y, Li X, et al. PROTACs: New method to degrade transcription regulating proteins. *Eur J Med Chem* (2020) 207:112698. doi: 10.1016/j.ejmech.2020.112698

159. Hu M, Zhou W, Wang Y, Yao D, Ye T, Yao Y, et al. Discovery of the first potent proteolysis targeting chimera (PROTAC) degrader of indoleamine 2,3-dioxygenase 1. *Acta Pharm Sin B* (2020) 10:1943–53. doi: 10.1016/j.apsb.2020.02.010

160. Morgan RA, Chinnasamy N, Abate-Daga D, Gros A, Robbins PF, Zheng Z, et al. Cancer regression and neurological toxicity following anti-MAGE-A3 TCR gene therapy. *J Immunother* (2013) 36:133–51. doi: 10.1097/CJI.0b013e3182829747

161. van den Berg JH, Gomez-Eerland R, van de Wiel B, Hulshoff L, van den Broek D, Bins A, et al. Case report of a fatal serious adverse event upon administration of T cells transduced with a MART-1-specific T-cell receptor. *Mol Ther* (2015) 23:1541–50. doi: 10.1038/mt.2015.60



OPEN ACCESS

EDITED BY

Catherine Sautes-Fridman,
INSERM U1138 Centre de Recherche
des Cordeliers (CRC), France

REVIEWED BY

Elba Mónica Vermeulen,
Instituto de Biología y Medicina
Experimental, Argentina
Raghothama Chaerkady,
AstraZeneca (United States),
United States

*CORRESPONDENCE

Paula A. Bousquet
a.p.bousquet@kjemi.uio.no
Ernesto Moreno
emoreno@udmedellin.edu.co
Ute Krengel
ute.krengel@kjemi.uio.no

SPECIALTY SECTION

This article was submitted to
Cancer Immunity
and Immunotherapy,
a section of the journal
Frontiers in Immunology

RECEIVED 15 July 2022

ACCEPTED 20 October 2022

PUBLISHED 09 November 2022

CITATION

Bousquet PA, Manna D, Sandvik JA,
Arntzen MØ, Moreno E, Sandvig K and
Krengel U (2022) SILAC-based
quantitative proteomics and
microscopy analysis of cancer cells
treated with the *N*-glycolyl GM3-
specific anti-tumor antibody 14F7.
Front. Immunol. 13:994790.
doi: 10.3389/fimmu.2022.994790

COPYRIGHT

© 2022 Bousquet, Manna, Sandvik,
Arntzen, Moreno, Sandvig and Krengel.
This is an open-access article
distributed under the terms of the
[Creative Commons Attribution License](#)
(CC BY). The use, distribution or
reproduction in other forums is
permitted, provided the original
author(s) and the copyright owner(s)
are credited and that the original
publication in this journal is cited, in
accordance with accepted academic
practice. No use, distribution or
reproduction is permitted which does
not comply with these terms.

SILAC-based quantitative proteomics and microscopy analysis of cancer cells treated with the *N*-glycolyl GM3-specific anti-tumor antibody 14F7

Paula A. Bousquet^{1*}, Dipankar Manna¹, Joe A. Sandvik²,
Magnus Ø. Arntzen³, Ernesto Moreno^{4*}, Kirsten Sandvig^{3,5,6}
and Ute Krengel^{1*}

¹Department of Chemistry, University of Oslo, Oslo, Norway, ²Department of Physics, University of Oslo, Oslo, Norway, ³Department of Biosciences, University of Oslo, Oslo, Norway, ⁴Facultad de Ciencias Básicas, Universidad de Medellín, Medellín, Colombia, ⁵Department of Molecular Cell Biology, Institute for Cancer Research, The Norwegian Radium Hospital, Oslo, Norway, ⁶Centre for Cancer Cell Reprogramming, Faculty of Medicine, University of Oslo, Oslo, Norway

Cancer immunotherapy represents a promising approach to specifically target and treat cancer. The most common mechanisms by which monoclonal antibodies kill cells include antibody-dependent cell-mediated cytotoxicity, complement-dependent cytotoxicity and apoptosis, but also other mechanisms have been described. 14F7 is an antibody raised against the tumor-associated antigen NeuGc GM3, which was previously reported to kill cancer cells without inducing apoptotic pathways. The antibody was reported to induce giant membrane lesions in tumor cells, with apparent changes in the cytoskeleton. Here, we investigated the effect of humanized 14F7 on HeLa cells using stable isotope labeling with amino acids in cell culture (SILAC) in combination with LC-MS and live cell imaging. 14F7 did not kill the HeLa cells, however, it caused altered protein expression (MS data are available via ProteomeXchange with identifier PXD024320). Several cytoskeletal and nucleic-acid binding proteins were found to be strongly down-regulated in response to antibody treatment, suggesting how 14F7 may induce membrane lesions in cells that contain higher amounts of NeuGc GM3. The altered expression profile identified in this study thus contributes to an improved understanding of the unusual killing mechanism of 14F7.

KEYWORDS

cytoskeleton, NeuGc GM3/Neu5Gc GM3, 14F7, SILAC, transcription factors, immunotherapy, ganglioside, glycosphingolipid

Introduction

The past few decades have seen much progress in the field of cancer immunotherapy (1–3). Many monoclonal antibodies are in advanced clinical development, and several are already licensed for clinical use (4, 5). Most clinically interesting antibodies bind to immune or cancer cells, triggering cell death. Antibodies can kill cells by different mechanisms, the most common being antibody-dependent cell-mediated cytotoxicity (ADCC), complement-dependent cytotoxicity (CDC) and induction of apoptosis (6, 7). Less frequent types of killing mechanisms include Fc-independent induction of cytotoxicity (without inducing morphological changes; often observed in cell death linked to apoptosis) and non-apoptotic mechanisms, where membrane lesions are formed upon treatment with mAbs (8–14).

14F7 is a clinically promising monoclonal antibody raised against the ganglioside NeuGc GM3, which represents an attractive target for cancer immunotherapy since this glycolipid is absent from healthy adult human tissues (15), but present in several malignancies (16–26). 14F7 is an IgG1 antibody with high affinity for its antigen (in the low nanomolar range) (19, 27–29). This interaction has been characterized structurally (complex with the carbohydrate part of the glycolipid) (30, 31) and by mutation analysis (32). In mouse models, 14F7 showed strong anti-tumor effects (20, 33). In order to prevent a possible human anti-mouse antibody response, and thereby increase its potential for immunotherapy, the original murine 14F7 mAb was humanized (14F7hT) (34). The cytotoxic properties of 14F7 were retained in the humanized variant, and no difference compared to the murine antibody was observed, however, 14F7hT also gained the ability to induce cell death by ADCC (35). While recent studies have found that anti-ganglioside antibodies of different IgG subclasses are commonly found in pathological processes (36), high-affinity anti-carbohydrate antibodies are rare (37).

The mechanism by which 14F7 activates signaling leading to cell death remains poorly understood. Carr et al. showed that

14F7-induced cell death in murine cancer cells (P3X63-Ag8.653) was caused by a complement-independent mechanism (20). A similar finding was reported by Casadesús et al., who observed complement-independent cell killing for 14F7 and a 14F7 variant that recognizes both NeuGc and NeuAc GM3 (38). Roque-Navarro et al. found in another murine tumor cell line (L1210) that 14F7 induced cell swelling and giant membrane lesions, but not the typical phenomena of apoptosis (DNA fragmentation, caspase activation or Fas mediation), suggesting a novel oncosis-like cell death mechanism (39–41). Several other antibodies with pore-formation mechanisms have been described in the literature (8, 12, 42, 43). Both Roque-Navarro et al. and Dorvignit et al. found indications of cytoskeletal involvement in 14F7-mediated cell death, but the details of this mechanism remain unexplored and there are currently no indications as to which cytoskeletal proteins may be involved (39, 44).

We have recently solved the crystal structure of the complex between 14F7 (a single-chain version) and the NeuGc GM3 trisaccharide (31) and investigated how 14F7 recognizes NeuGc GM3 in a membrane-like environment (29). Here we seek to understand the effects that 14F7 induces in the cell, to gain a deeper understanding of the novel oncosis-like cell death mechanism induced by 14F7. To reveal differences in the expression profile between treated and untreated cells, we used stable isotope labeling with amino acids in cell culture (SILAC) in combination with LC-MS. Building on previous work (45, 46), we chose to work with HeLa cells. SILAC is a mass spectrometry (MS)-based quantitative method relying on the incorporation of 'light' and 'heavy' forms of amino acids (such as lysine and arginine) into proteins (Figure 1). It enables easy and comprehensive peptide identification by providing a defined number of labels per peptide (47). We identified twelve HeLa proteins that exhibited strongly altered expression after treatment with 14F7hT. Five of these proteins are related to the cytoskeleton and all of them were found to be downregulated in this investigation. No macroscopic changes were observed in the

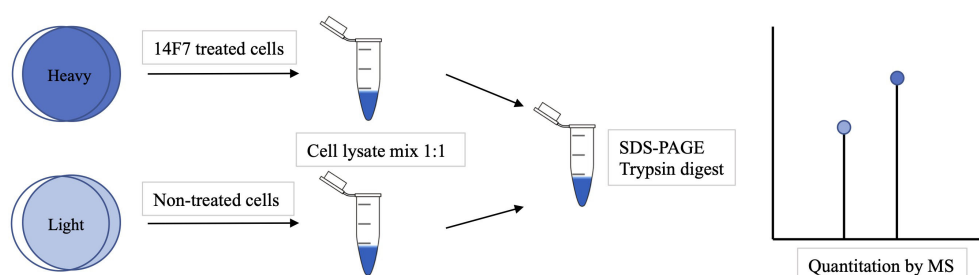


FIGURE 1

Overview of a SILAC experiment. First the cells were grown in 'light' or 'heavy' media. The 'heavy' cells were incubated with 14F7hT for 3 h before the cells were lysed and mixed. The proteins were separated by SDS-PAGE, trypsin-digested and identified by LC-MS analysis. The ratio of 'heavy' versus 'light' amino acids indicates which proteins were up- or down-regulated.

cells, however, this is likely due to the limited amount of NeuGc GM3 in the HeLa cell line.

Materials and methods

Cell culture

HeLa (ATCC: CCL-2) cells were incubated in Dulbecco's Modified Eagle Medium (DMEM) supplemented with 10% (v/v) fetal bovine serum (FBS) to increase the amount of NeuGc GM3 as well as with 2 ml L-glutamine, 50 U/ml penicillin and 50 mg/ml streptomycin. The cells were kept at 5% CO₂, 37°C between experiments and split when the confluence was approaching 80–90%. HeLa cells were seeded in 6, 24 or 96-well plates 24–72 h prior to experiments and incubated at 37°C in a 5% CO₂ incubator. Experiments were performed using an unspecific secondary antibody as control.

Incorporation of labeled amino acids and 14F7hT treatment of HeLa cells

For SILAC experiments, HeLa cells were cultured for at least five cell doublings in media either containing ¹³C- and ¹⁵N-labeled L-arginine (89990-Fisher) and ¹³C-labeled L-lysine (89988-Fisher) or media containing unlabeled L-arginine (89989-Fisher) and L-lysine (89987-Fisher) amino acids. The cells were treated with 14F7hT (25 µg/ml) for 3 h in 37°C, which was kindly provided by the Center of Molecular Immunology (CIM), Havana, Cuba.

NanoLC-LTQ orbitrap mass spectrometry

HeLa cell lysates from each labeling, heavy and light, were mixed 1:1 and subjected to sodium dodecyl sulfate–polyacrylamide gel electrophoresis (SDS–PAGE). Each Coomassie G-250 stained SDS–PAGE gel lane was cut into 12 slices, destained at 37°C for 30 min, followed by reduction at 60°C for 10 min and alkylation for 1 h in the dark. The samples, were in-gel digested at 37°C for 4 h using 0.1 µg of trypsin in 25 µl of 50 mM ammonium bicarbonate, pH 7.8. After micropurification using µ-C18 ZipTips (Millipore, Oslo, Norway), the peptides were dried in a SpeedVac and dissolved in 10 µl 1% formic acid, 5% acetonitrile in water. Half of the volume was injected into an Ultimate 3000 nanoLC system (Dionex, Sunnyvale CA, USA) connected to a linear quadrupole ion trap-orbitrap (LTQ-Orbitrap XL) mass spectrometer (ThermoScientific, Bremen, Germany) equipped with a nanoelectrospray ion source. For liquid chromatography

separation, an Acclaim PepMap 100 column (C18, 3 µm beads, 100 Å, 75 µm inner diameter) (Dionex, Sunnyvale CA, USA) capillary of 50 cm bed length was used. The flow rate was 0.3 µl/min, with a solvent gradient of 7% B to 35% B in 110 minutes. Solvent A was aqueous 0.1% formic acid, and solvent B aqueous 90% acetonitrile in 0.1% formic acid. The mass spectrometer was operated in the data-dependent mode to automatically switch between Orbitrap-MS and LTQ-MS/MS acquisition. Survey full scan MS spectra (from m/z 300 to 2,000) were acquired in the Orbitrap with the resolution R = 60,000 at m/z 400. The method used allowed the sequential isolation of up to the seven most intense ions for fragmentation on the linear ion trap using collision-induced dissociation (CID) at a target value of 10,000 charges. Target ions already selected for MS/MS were dynamically excluded for 60 sec. The lock mass option was enabled in MS mode for internal recalibration during the analysis. Other instrument parameters were set as previously described (48).

Protein identification and quantification

Protein identification and quantification were performed with MaxQuant (49) (v.1.2.2.5) utilizing the Andromeda search engine (50). The tolerance level for matching the database was 6 ppm for MS1 and 20 ppm for MS/MS. Trypsin was used as digestion enzyme, and two missed cleavages were allowed. Carbamidomethylation of cysteines was used as fixed modification, whereas variable modifications included protein N-terminal acetylation, oxidation of methionines, deamination of asparagines and glutamines, and formation of pyro-glutamic acid at N-terminal glutamines. For estimation of the false discovery rate (FDR), which is the rate of falsely discovered proteins in our dataset, we included the reversed sequences into the database search. All hits to the reversed database could thus be regarded as false hits. By restricting the number of matches to this database to only 1% of total matches, we thus proceeded with an FDR of 1% to ensure reliable protein identification. For quantification, at least two quantification events were required per protein, and we further required the proteins to be quantified in at least 2 of 3 biological replicates. Normalized protein ratios H/L were reported by MaxQuant and used as is for analysis. A Student's t-test was used to assess ratio significances.

Bioinformatics analysis

Functional annotation was performed using DAVID Bioinformatics Resources version 6.7 (51, 52) available at <http://david.abcc.ncifcrf.gov/>, using whole genome (*Homo sapiens*) as background), and Panther (<http://www.pantherdb.org>).

Measurement of cellular protein synthesis

HeLa cells were washed with leucine-free 4-(2-hydroxyethyl)-1-piperazineethanesulfonic acid (HEPES)-buffered medium and incubated with increasing concentrations of 14F7hT for 3 h or 18 h at 37°C. Cells were then incubated with leucine-free HEPES-buffered medium complemented with 2 $\mu\text{Ci/ml}$ [^3H] leucine (PerkinElmer) at 37°C for 20 min before proteins were precipitated with 5% (w/v) trichloroacetic acid (TCA) and washed once with the same solution (48). Finally, the proteins were dissolved in 0.1 M KOH and radioactively labeled leucine incorporation was quantified by β -counting with Tri-Carb 2100TR[®] Liquid Analyzer (Packard Bioscience). Three independent experiments were performed with biological duplicates.

Measurement of cellular ATP level

Quantitation of the cellular ATP level was performed following the prescribed protocol by the commercially available CellTiter[®]-Glo 3D Cell Viability Assay kit (Promega). Briefly, HeLa cells (1×10^4 cells/well, 96-well plate) were washed with 200 μl /well leucine-free HEPES medium. Thereafter, 50 μl fresh leucine-free medium was added to each well. 14F7hT was added to corresponding plates at increasing concentrations (25 ng/ml to 25 $\mu\text{g/ml}$). The plate was then incubated for 20 h at 37°C. After incubation, 50 μl CellTiter[®]-Glo was added to each well, followed by an incubation of 10 min in the dark at room temperature. The signal was measured using Syngene Chemi-Genious. Three independent experiments were performed with biological duplicates.

Structural interference microscopy and live cell imaging

HeLa cells were cultured as described before and seeded on coverslips. The cells were washed in PBS and then fixed in a 4% (w/v) paraformaldehyde solution at room temperature (Alfa Aesar) for 15 min and permeabilized in 0.1% Triton X-100 in PBS for 2 min. The cells were incubated with the relevant primary antibodies diluted in blocking solution (10% PBS in FCS) for 1 h at room temperature or at 4°C overnight. The cells were again washed in PBS and incubated with blocking solution for 5 min. They were then incubated with secondary antibodies for 1 h. After the final washing step, the coverslips were mounted on ProLong Gold (Molecular Probes) supplemented with the nuclear staining reagent 4',6-diamidino-2-phenylindole (DAPI) overnight at 37°C. Detailed analysis of single cells was either performed by confocal microscopy (Zeiss LSM 780) and analyzed with IMAGEJ software or super-resolution 3D SIM imaging performed on a DeltaVision OMX V4 system (Applied

Precision) equipped with an Olympus 60X numerical aperture (NA) 1.42 object, cooled sCMOS camera and 405, 488 and 642 nm diode lasers, Z-stacks covering the whole cell were recorded with a Z-spacing of 125 nm. A total of 15 raw images (five phases, three rotations) per plane were collected and reconstructed by using SOFTWORX software (Applied Precision).

For live cell imaging, cells were seeded in 50 mm MatTek glass bottom dishes. Images were captured under controlled CO₂ conditions at 37°C with a DeltaVision microscope (Applied Precision), equipped with a live cell Elite TruLight Illumination System and cooled Photometrics CoolSNAP HQ2 charge-coupled device (CCD) camera. Optical sections were acquired by using a 60X objective (Olympus, Plan Fluor, NA 1.42) and images were deconvolved by using SOFTWORX software (Applied Precision).

Results and discussion

Using a quantitative proteomics approach and bioinformatics analysis, we compared the expression profile of 14F7hT-treated HeLa cells with control cells. To increase the amount of NeuGc GM3, we supplemented the media with 10% FBS. An overview of the experimental strategy for SILAC is depicted in [Figure 1](#). HeLa cells were maintained in SILAC medium (containing 'light' or 'heavy' forms of the amino acids lysine and arginine). The cells grown in the 'heavy' medium were treated with the anti-tumor antibody 14F7hT, while the cells grown in the 'light' medium served as control in the experiment. Cell lysates from each labeling were mixed 1:1 and fractionized by SDS-PAGE. After in-gel digestion, protein identification and quantification, bioinformatics analysis was performed.

SILAC and bioinformatic data analyses

The proteomes of 'heavy' and 'light' HeLa cells, treated with 14F7hT and untreated, respectively, were compared by LC-MS. In total, 3685 proteins were identified. Two thirds of these proteins were quantified in at least two replicates and used for further analysis ([Table S1](#)). Following stringent criteria ($p < 0.05$, at least two peptides per protein in two of three replicates and a minimum fold-change of 2), four proteins were found to be significantly down-regulated ([Table 1](#); note that in [Figure 2](#), two of the "significant" hits had only few peptides). In addition, we identified one protein that was up-regulated 2.7-fold and seven proteins that were clearly down-regulated; however, with p -values > 0.05 (or where p -values could not be obtained). Among these, one protein only marginally missed the target p -value (cystatin A, $p = 0.051$; 4-fold down-regulated), and two additional proteins had higher p -values, but at least two

TABLE 1 Strongly regulated proteins.

Protein	Protein ID (Gene name)	H/L ratio	Function	Identified peptides	p- value ^a
Down-regulated proteins					
Dystrophin	P11532 (DMD)	0.02	cytoskeletal protein	4	0.018
Glucosamine/Glutamine-fructose-6-phosphate transaminase 2	O94808 (GFPT2)	0.07	controls the flux of glucose into the hexosamine pathway	5	0.035
CLIP-associating protein 2	B4DM73 (CLASP2)	0.07	cytoskeletal protein	7	n.a.
POTE ankyrin domain family, putative beta-actin-like protein 3	Q9BYX7 (POTEI)	0.13	ATP-binding cytoskeletal protein	6	n.a.
Brix domain containing 1/ribosome production factor 2 homolog	Q9H7B2 (RPF2)	0.20	associated with the nucleolus in an RNA- dependent manner	5	n.a.
Drug-sensitive protein 1/Gastric associated differentially-expressed protein YA61P	Q9NZ23 (YA61)	0.22	oxidoreductase activity	4	0.026
Kinesin-like protein KIF 14	Q15058 (KIF14)	0.23	cytoskeletal protein	5	0.490
Histidyl t-RNA synthetase, mitochondrial	P49590 (HARS2)	0.24	translation	7	n.a.
Cystatin A	P01040 (CSTA)	0.25	cytoskeletal protein	2	0.051
DERP12	Q8TE01 (DERP12)	0.26	oxidoreductase activity, acting on a sulfur group of donors	9	0.022
F-actin-uncapping leucine-rich repeat protein LRRC16A	Q5VZK9 (LRRC16A)	0.33	cytoskeletal protein	2	0.162
Up-regulated proteins					
Metastasis associated protein	Q13330 (MTA1)	2.70	identified in a screen for genes expressed in metastatic cells	2	n.a.

^ap-values were based on Student's t-test. Listed are proteins significantly regulated ($p < 0.05$ and >2 -fold change, corresponding to normalized H/L ratio) upon 14F7hT mAb binding to HeLa cells. In addition, the list includes three proteins with higher p-values and five proteins, for which no valid t-test could be carried out (but which all had at least two peptides per protein in two of three replicates). The function was assigned using DAVID (51, 52).

n.a. (= not available, since there were not sufficient values for a valid t-test).

peptides in three replicates (kinesin-like protein KIF14, $p = 0.490$, H/L = 0.23; and F-actin-uncapping protein LRRC16A, $p = 0.162$, H/L = 0.33). For all of these proteins, p-values were <0.001 if calculated based on z-statistics instead. Adding these proteins to the number of strongly regulated proteins yields eleven down- and one up-regulated protein (Table 1). A volcano plot of all data points with valid p-value is shown in Figure 2. In addition, we screened the data for large differentials that may have been missed due to p-values >0.1 or less peptides identified in the replicates. The proteomics data have been deposited to the ProteomeXchange Consortium via the PRIDE partner repository, where they are freely accessible with the dataset identifier PXD024320 (53).

The bioinformatic tools DAVID (51, 52) and PANTHER (<http://www.pantherdb.org>) were used to categorize the regulated proteins (Figure 3).

19 transcription factors were identified as interacting partners of the 12 strongly regulated proteins listed in Table 1. These interactions were generated by DAVID protein-protein interaction analysis and are listed in Table 2. Three of the transcription factors interacting with the regulated proteins belong to the so-called homeobox genes. These genes express proteins that are spatially and temporally regulated during

embryonic development (MEIS1B, HOXA3, TGIF). Several transcription factors (MEF2, GR, HSF2, EVI1, GATA and STAT) are also involved in cell development and growth. IRF and STAT are associated with interferon regulation and cell survival. Another transcription factor (JunB, ID: P17275) was directly down-regulated, by 1.4-fold, with 43 identified peptides (although slightly missing our criteria concerning p-value, with $p = 0.062$). This transcription factor is involved in regulating gene activity following primary growth factor response.

Proteins affecting the cytoskeleton

There are three major types of filaments in the cellular cytoskeleton, namely actin- and intermediate-filaments and microtubules, which all assemble from small building blocks. DAVID functional annotation analysis revealed five significantly down-regulated proteins belonging to the cluster of cytoskeletal proteins (Table 1). These proteins include cystatin A, CLIP-associating protein 2, leucine-rich repeat-containing protein 16A, Kinesin-like protein KIF 14 and dystrophin. Of additional interest is a member of the POTE ankyrin domain family, a pseudogene belonging to the actin family.

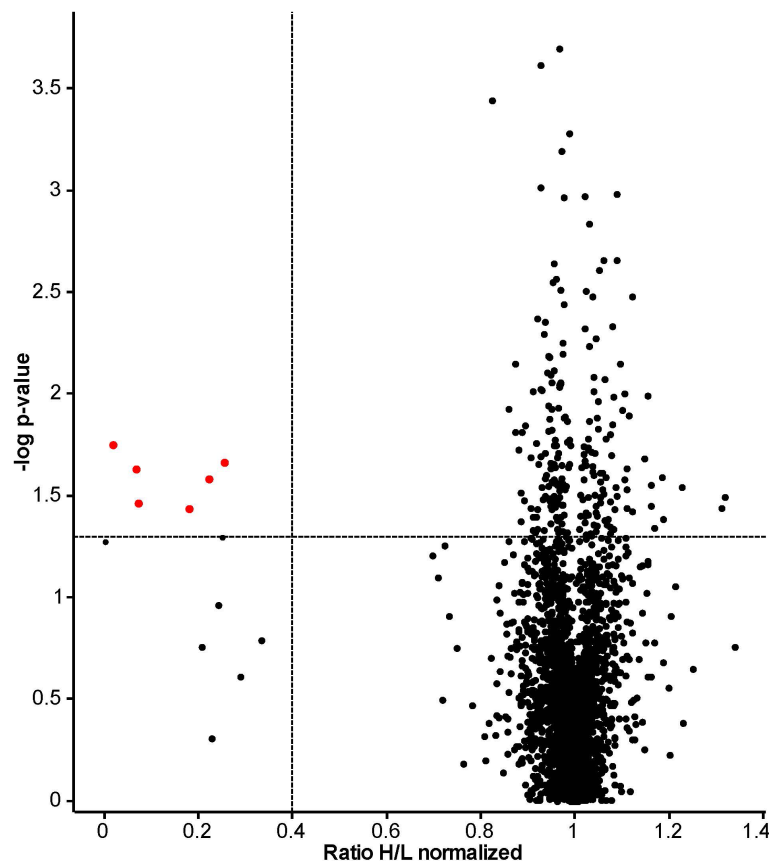


FIGURE 2

Volcano plot based on results obtained from 14F7hT-treated HeLa cells. This plot combines statistical significance, p-value (y-axis) with fold change (x-axis), to allow a quick visual overview over the interesting data. Points corresponding to the proteins with >2.5-fold altered expression levels and $p < 0.05$ are colored in red. The dotted lines represent the cut-off values ($p < 0.05 = 1.3$ at y-axis and 0.4, corresponding to 2.5-fold down-regulation, at x-axis). The discrepancy to Table 1 results from the exclusion of proteins that did not fulfill our strict peptide criteria in the table, and exclusion of proteins without valid p-value from the plot. Excluded from Table 1 were also two proteins identified as significant based on the p-value (labeled red in this plot): a glycosyltransferase ($p = 0.024$, H/L = 0.07, Protein ID: B7ZB85) and dermcidin, a secreted peptide with antimicrobial activity ($p = 0.037$, H/L = 0.18, Protein ID: P81605).

Dystrophin (50-fold down-regulated). A cytoskeletal protein present in a variety of tissues. It is involved in many biological processes and is associated with several disorders, in particular muscular and cardiac diseases (54–56). Surprisingly, this protein was almost completely absent in response to 14F7 treatment. Dystrophin has been connected to cell death, although the relationship is controversial. For example, the processes occurring in dystrophin-deficient muscle cells are linked to a pathological increase in intracellular Ca^{2+} concentration, which causes an increase in the volume of sarcoplasmic reticulum lumen (57–60). However, how the absence of dystrophin leads to increased cytosolic calcium levels is poorly understood, although damage to the membrane and defective calcium channels have been suggested as possible explanations (61–63). The cellular swelling observed in 14F7hT-treated cells may be partially explained by the down-regulation of dystrophin, if the same

regulation occurs during 14F7hT-mediated cell death. Membrane damage is linked to the swelling phenotype of antibody-treated cells, and could be an explanation for an increased Ca^{2+} level. Ca^{2+} is stored and released by several organelles, in particular the acidic lysosomes (64), providing a link to the observed down-regulation of cystatin, sensitizing cells for lysosomal cell death.

CLIP-associating protein 2 (14-fold down-regulated). Regulation of the dynamic behavior of microtubules occurs through microtubule-associated proteins. Proteins that associate with the tips of microtubules are called +TIPs since they are ‘plus-end’ tracking proteins (65). The mechanisms used by +TIPs are not fully elucidated, but one of the significantly down-regulated proteins in response to 14F7hT mAb treatment, the cytoplasmic linker associated protein 2 (CLIP-associated protein 2, CLASP2) is a +TIP contributing to generate cellular

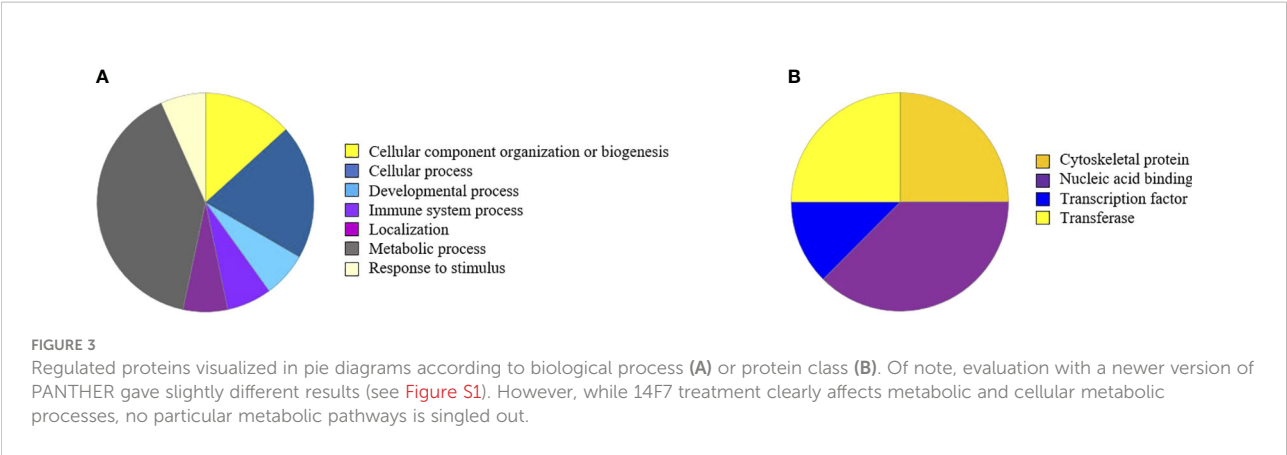


TABLE 2 Transcription factors interacting with the regulated proteins.

Transcription factor	Proteins interacting with transcription factor	Fold enrichment	p-value
TGIF	P01040, P11532, O94808, P49590, Q5VZK9, Q15058, B4DM73, Q13330	2.56	0.003
CDPCR1	P01040, P11532, P49590, Q5VZK9, Q15058, B4DM73, Q13330	2.45	0.015
MRF2	P01040, P11532, Q9H7B2, P49590, Q5VZK9, Q15058, B4DM73	1.83	0.066
HNF3B	P11532, Q9H7B2, O94808, P49590, Q5VZK9, B4DM73	1.98	0.092
GR	P11532, Q9H7B2, O94808, P49590, Q5VZK9, Q15058, B4DM73, Q13330	2.05	0.014
HSF2	P11532, Q9H7B2, O94808, P49590, Q5VZK9, B4DM73, Q13330	2.27	0.023
EVI1	P01040, P11532, Q9H7B2, O94808, P49590, Q5VZK9, Q15058, B4DM73, Q13330	1.41	0.062
GATA	P01040, P11532, O94808, P49590, Q5VZK9, Q15058, Q13330	2.11	0.033
IRF1	P11532, Q9H7B2, O94808, P49590, Q15058	2.73	0.059
STAT	P11532, O94808, P49590, Q5VZK9, Q15058, B4DM73	2.33	0.048
OCT	P11532, Q9H7B2, O94808, P49590, Q5VZ09, B4DM73, Q13330	2.04	0.039
LMO2COM	P01040, P11532, O94808, P49590, Q5VZK9, Q15058, B4DM73, Q13330	1.80	0.032
FOXJ2	P11532, Q9H7B2, O94808, P49590, Q5VZK9, Q15058, B4DM73, Q13330	1.59	0.068
MEIS1BHOXA9	P01040, P11532, Q9H7B2, P49590, Q5VZK9, Q15058, B4DM73	1.86	0.062
MEF2	P01040, P11532, Q9H7B2, O94808, P49590, Q5VZK9, Q15058, B4DM73, Q13330	1.58	0.026
SRY	P11532, P49590, Q5VZK9, Q15058, B4DM73, Q13330	1.94	0.098
HOXA3	P11532, P49590, Q5VZK9, Q15058, B4DM73, Q13330	1.95	0.097
FREAC2	P01040, P11532, O94808, P49590, Q5VZK9, Q15058, B4DM73	1.92	0.052
GATA1	P01040, P11532, Q9H7B2, O94808, P49590, Q5VZK9, Q15058, B4DM73, Q13330	1.43	0.057

asymmetry. A study using yeast two-hybrid analysis identified CLASP1 and CLASP2 as interaction partners to CLIPs (cytoplasmic linker proteins) (66). Interestingly, several proteins of this family (CLASP1, Cap-Gly domain of CLIP2 and CLIP1) were identified in the present work, but not considered significantly regulated according to our strict criteria.

In cells, the minus end of microtubules is localized deep in the microtubule-organizing center (MTOC), and microtubule bundles will grow out from the center. This will prevent dynamic instability at the minus end, but alternating between growth, pause and shrinkage will occur at the plus

ends. When the microtubules grow towards the cell membrane, +TIPs, such as CLIP-associated protein 1, will ensure continuous growth until the microtubules reach the end, where shrinking can occur. This alteration from growth to shrinkage is termed ‘catastrophe’ (67–69). +TIPs thus function as anti-catastrophe factors, meaning that they prevent premature microtubules.

In studies using RNAi or antibodies targeting CLIP-associated protein 2, the formation of leading-edge-orientated microtubules was inhibited (66, 70). CLIP-associated protein was almost absent in the cells after 3 h of 14F7hT treatment. This

can contribute to an inability of the microtubules to continuously grow, thus leading to morphological changes.

POTE ankyrin domain family, putative beta-actin-like protein 3 (8-fold down-regulated). Post-translational modifications of this pseudogene belonging to the actin family, such as oxidation and methylation, have (by similarity) been suggested to regulate polymerization of actin filament and actin-myosin processes like cleavage furrow ingression during cytokinesis, respectively. For the latter process, demethylation by a protein named alkylation repair homolog 5 (ALKBH) is required. This protein was identified, but not considered significantly regulated according to our criteria (fold change 0.88). Down-regulation of the POTE ankyrin protein caused by 14F7hT treatment could destabilize the processes of microtubule polymerization and cleavage furrow ingression.

Kinesin-like protein KIF14 (4-fold down-regulated). KIF14 is a motor protein playing an essential role in cytokinesis that has been associated with poor prognosis in breast cancer. It is localized in the nucleus during interphase (71) and associates with developing spindle poles and microtubules in mitotic cells, to then accumulate at the central spindle and midbody in the later stages of mitosis (72). The latter process is dependent on the presence of protein regulator of cytokinesis 1 (PRC1) and citron rho-interacting kinase (CIT). The expression levels of these proteins were altered, but not significantly. Carleton et al. showed that silencing of KIF14 generated a variety of mitotic phenotypes in HeLa cells, possibly linked to the efficacy of siRNA silencing (72). Using time-lapse microscopy, less efficacious silencing was shown to cause induction of distinct phenotypes, all resulting in acute apoptosis. However, a strong KIF14 silencing induced cytokinesis failure, resulting in multinucleated cells. This correlation between silencing efficacy and phenotypic outcome suggests that KIF14 alteration may disrupt different stages of the cell cycle, explaining the multitude of phenotypes reported (73–75). As KIF14 expression decreased significantly when cells were treated with 14F7hT, this may cause a phenotype change associated with cell fatality.

Cystatin A (4-fold down-regulated). Cystatin A (Stefin A) has been detected in higher levels in invasive tumors, where tumors positive for cystatin A were larger and exhibited an increased mitotic activity, suggesting a growth advantage for the cells (76). This protein was shown to be a potent inhibitor of exogenous proteases (77) and suggested to protect cytosolic and cytoskeleton proteins from degradation. High levels of cystatin A may be relevant for regulation of apoptosis by inhibiting cathepsin B, when initiated by the lysosomal cell death pathway. Cells lacking the closely related cystatin B (Stefin B) exhibit a higher sensitivity to lysosomal induced cell death (78). The significant down-regulation of cystatin A in 14F7hT-treated cells may sensitize the cells for lysosomal cell death as well as induce increased degradation of cytoskeletal proteins.

F-actin-uncapping protein LRRC16A (3-fold down-regulated). This *leucine-rich repeat* protein is also associated with actin polymerization. It was not clustered as cytoskeletal protein by DAVID, however, it decreases the affinity of capping proteins for actin ends by binding to the capping proteins (CAPZA2) with high affinity, thus inhibiting capping activity. Polymerization of actin filaments occurs *via* elongation at the end. By capping the ends, actin elongation terminates (79). Down-regulation of leucine-rich repeat-containing protein 16A, as observed in this study, may enhance the affinity for capping proteins to actin ends, hence leading to a termination of actin elongation.

Another cytoskeletal protein of potential interest is desmoplakin, a protein with a function in cell-to-cell adhesion. This protein was found to be down-regulated 1.4-fold ($p = 0.080$, 43 peptides; ID: P15924). Desmoplakin is involved in the organization of cadherin-plakoglobin complexes and in the anchoring of intermediate filaments to cell structures called desmosomes. In contrast, clathrin was slightly up-regulated (1.28-fold, $p = \text{n.a.}$, 19 peptides; ID: P53675), which may suggest that 14F7 is taken up into cells by clathrin-dependent mechanisms.

Other proteins up- or down-regulated

The only protein found to be significantly up-regulated (although not accessible to t-test statistics) was the metastasis-associated protein MTA1 (fold change 2.7; Table 1). MTAs belong to chromatin modifying proteins, functioning as integral parts of nucleosome remodeling and histone deacetylation (NuRD) complexes. MTA1 has been correlated with metastatic potential of carcinomas, but details of the process are poorly understood. However, it is known that MTA1 interacts with histone deacetylase 1 and 2 (HDAC1/2) (80), estrogen receptor alpha (81), CDK-activating kinase assembly factor MAT1 (MNAT1) (82) and tumor protein p53 (TP53) (83). Many cellular pathways are associated with MTA1, including cell fate programs. A possible explanation for MTA1 up-regulation upon antibody treatment is that it alters deacetylation of crucial target genes. Regarding the cell death mechanism, we noticed the down-regulation of TPX2 (fold change 0.82, $p = 0.199$, ID: Q96RR5; Table S1), which is involved in the assembly of microtubules during apoptosis, however, the effect was small, and contrary to what would be expected if cell death occurred by apoptosis. In contrast, a programmed cell-death protein (ID: Q9BRP1) was found to be almost 15-fold up-regulated, although with very weak criteria ($p = \text{n.a.}$, 2 different peptides, but only one in two samples).

Two proteins with oxidoreductase activity, the drug-sensitive protein and the dermal papilla derived protein 12 (DERP12), were found to be down-regulated (fold change 0.22/0.26, $p = 0.026/0.022$) when HeLa cells were subjected to

14F7hT treatment (Table 1), whereas glutathione peroxidase was up-regulated 1.64-fold ($p = \text{n.a.}$, ID: Q8TED1). Further studies will be required to suggest an explanation for the up- and down-regulated oxidoreductase activity.

Interestingly, one protein associated with carbohydrate biosynthesis, glucosamine/glutamine-fructose-6-phosphate aminotransferase 2, was found to be significantly down-regulated in our study (fold-change 0.07, *i.e.*, 14-fold, $p = 0.035$; Table 1), and an additional enzyme, glycosyltransferase-like protein, was found to be similarly down-regulated, although with less stringent criteria regarding the peptides (fold change 0.07, p -values = 0.024, ID: B7ZB85; Table S1). This is interesting since the target of 14F7, the NeuGc GM3 ganglioside, is a glycosphingolipid not normally present in human healthy cells, but found in the plasma membrane of several malignant cells (16–18). The synthesis of these gangliosides involves glycosyltransferases, which catalyze the attachment of carbohydrate residues to the hydrophobic ceramide part of the ganglioside. Decreased expression of these enzymes may be linked to down-regulation of the antibody target and/or associated with cellular metabolic processes. In contrast, we noticed that the catalytic subunit of dolichyl-oligosaccharyl transferase was slightly up-regulated, with good statistics (1.3-fold, $p = 0.032$, ID: P46977; Table S1).

Three other proteins that were found to be upregulated, by 4-, 5- and 18-fold, respectively, were a tyrosine phosphatase (ID: Q05209), an outer dense fiber protein (ID: Q5BJF6) and Hermansky-Pudlak syndrome protein, which is involved in the biogenesis of early melanosomes (ID: Q969F9) (84), however, all with rather poor statistics.

In this study, HeLa cells were analyzed, showing alteration in *e.g.* glycosylation, biosynthetic and primary metabolic processes, but other cell lines may have dissimilar glycolytic and lipid metabolic levels, affecting survival differently.

14F7hT neither inhibits protein synthesis nor changes cellular ATP level

To investigate the toxic effect of 14F7hT more directly, we assessed protein synthesis of 14F7hT-treated cells. Measuring protein synthesis is a very sensitive method to study cell leakage. A 3h-treatment of HeLa cells with increasing concentrations of 14F7hT (25 ng/ml to 25 $\mu\text{g/ml}$) did not show any changes of cellular protein synthesis. In the four 14F7hT-treated samples, the total protein content remained unchanged compared to untreated cells (Figure 4). Even after 18 h, no changes were observed, indicating that 14F7hT treatment did not affect protein synthesis in the HeLa cells.

We also investigated whether 14F7hT treatment would affect the cellular ATP level, since ATP depletion can lead to necrosis (85). To that end, we incubated HeLa cells with increasing concentrations of 14F7hT (25 ng/ml to 25 $\mu\text{g/ml}$) and subsequently measured the ATP level in the cells. The results showed no changes in the cellular ATP level 20 h after 14F7hT treatment (Figure 5), indicating that 14F7hT did not induce ATP leakage.

14F7hT does not disrupt the actin cytoskeleton or the microtubule network

Actin filaments and microtubules are important structural components of the cells, and interference with these components is associated with morphological changes or membrane disruptions. To evaluate the changes in cytoskeleton upon 14F7hT-treatment, we incubated HeLa cells with 14F7hT mAb, varying both 14F7 concentration and incubation times. The cells were stained for actin and tubulin to visualize the cytoskeleton with fluorescence microscopy (Figures 6A, B). For

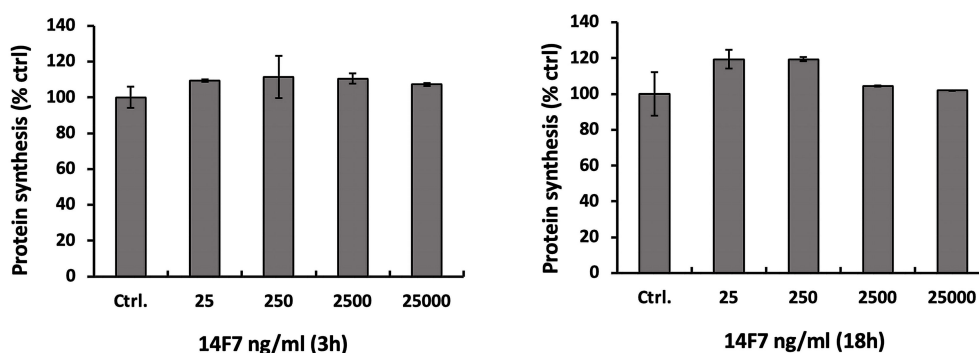


FIGURE 4

14F7hT treatment does not inhibit protein synthesis in HeLa cells. HeLa cells were incubated with varying concentrations (25 ng/ml to 25 $\mu\text{g/ml}$) of 14F7hT in serum-free medium for 3 h (left) or 18 h (right) at 37°C ($n = 3$). The level of protein synthesis was measured as described in the Methods section.

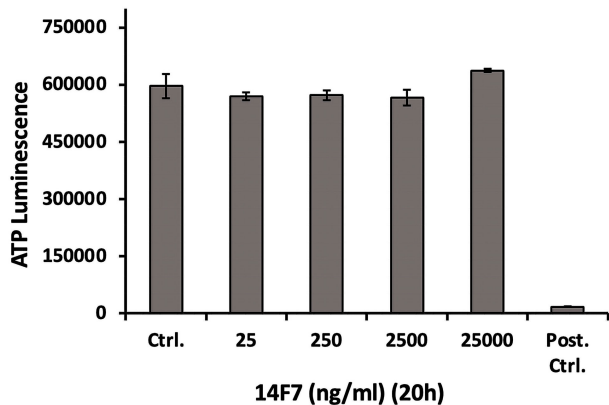


FIGURE 5
14F7hT mAb treatment does not affect the cellular ATP level. HeLa cells were treated with increasing concentrations (25 ng/ml to 25 µg/ml) of 14F7hT in leucine-free medium for 20 h at 37 °C (n = 3). The positive control contained a mixture of 10 mM NaN₃ and 50 mM 2-deoxy glucose, and showed a strong decrease in cellular ATP, as expected.

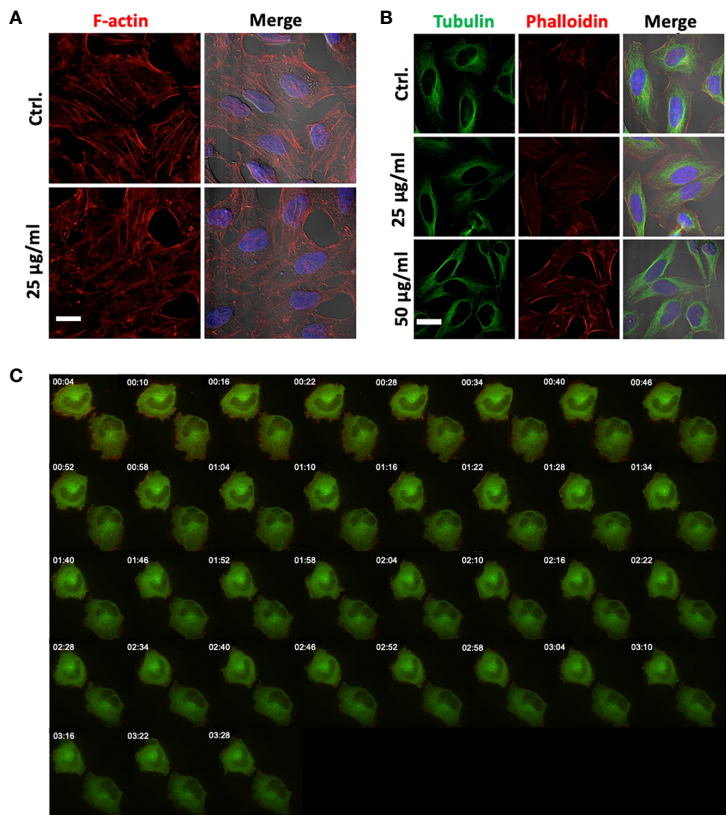


FIGURE 6
14F7hT mAb treatment does not lead to disruption of actin filaments or the tubulin network. HeLa cells were treated with either 25 µg/ml (**A**, **B**) or 50 µg/ml (**B**) 14F7hT and incubated for 6 h (**A**) or 15 h (**B**), and thereafter stained for actin and tubulin, and analyzed by SIM microscopy (scale bar 7 µm). Fluorescence live cell imaging was performed to analyze the effects on actin (red) and tubulin (green) filament dynamics after treatment with 2 µg/ml 14F7hT over a period of 3.5 h (**C**). 14F7hT treatment does not induce disruption or fragmentation of actin (**A**) or tubulin (**B**) filaments, nor does it have obvious effects on the dynamics of actin or tubulin filaments (**C**). Representative pictures of three independent experiments are shown with >50 (**A**, **B**) and 10–20 visualized cells (**C**), respectively.

the analysis of filament dynamics, HeLa cells were transfected with RFP-actin and GFP-tubulin, to visualize the filaments by live cell microscopy after addition of 14F7hT (Figure 6). To our surprise, 14F7hT-treated cells did not display any morphological changes compared to non-treated cells. The HeLa cells contained an intact actin cytoskeleton and microtubule network with no obvious disruptions or fragmentations of these structural components even at the highest concentration (25 µg/ml) of 14F7hT and after long incubation times. Thus, the data clearly showed that the changes in expression profile revealed by SILAC are not manifested on the macroscopic level. The results obtained for the cells transfected with recombinant RFP-actin and GFP-tubulin, however, should be interpreted with caution since the expression levels of these proteins were artificially set with the transfection.

Conclusion

Cancer immunotherapy is a growing research field. Several monoclonal antibodies are already applied in cancer therapy, and additional molecules are in the pipeline. These antibodies kill the malignant cells by different mechanisms, most commonly by ‘classical’ cell killing mechanisms, such as ADCC or CDC, but other mechanisms have also been suggested. 14F7hT has been reported to cause giant lesions in tumor cells and kill these cells by a non-apoptotic oncosis-like mechanism (39). Using a proteomics-based approach, we revealed 12 proteins that exhibited strongly altered expression upon 14F7hT binding to the target cells. Five of these are cytoskeletal proteins, affecting *e.g.* actin filament-based and microtubule-based processes. The HeLa cells studied in this work were not killed upon application of 14F7hT. Their NeuGc GM3 content is probably too low. Nevertheless, we suspect that the observed changes may represent early stages of cellular transformations that could be difficult to observe when the membrane lesions have formed and cells are dying. For example, we observed a slight down-regulation of TPX2 (1.2-fold), a protein involved in the assembly of microtubules during apoptosis, and 15-fold up-regulation of a programmed cell-death protein, although with poor statistics. A picture emerges that 14F7 treatment down-regulates proteins of the cytoskeleton and cell-cell-adhesion, and ultimately induces cell death. While further studies are required to verify the involvement of the identified proteins and the processes they inhibit or trigger, this work already considerably advances our current understanding of the 14F7 cell death mechanism, and identifies candidates for future therapies. An important question that remains unanswered is how this event of 14F7 binding to NeuGc GM3 on the cell membrane can connect with cell pathways that affect the expression of proteins related with the cytoskeleton.

Data availability statement

Data are available *via* ProteomeXchange with identifier PXD024320.

Author contributions

PB and UK conceived the study. PB carried out all SILAC-related experiments. MA processed the proteomics data. DM performed the microscopy studies, and analyzed protein inhibition and ATP levels, supervised by KS. UK served as main supervisor of PB and DM and coordinated the work. EM contributed to the discussion and manuscript revision. The first complete draft of the manuscript was written by PB and DM and revised in close collaboration with UK, with contributions from all authors. All authors contributed to the article and approved the submitted version.

Funding

Work at UiO was funded by the University of Oslo (including the PhD position of PB). The PhD position of DM was funded by Norwegian loan funds. Work by EM at UdeMedellin was supported by Minciencias, Mineducación, Mincit and Icetex, through the Program NanoBioCáncer, grant no. FP44842-211-2018. Work in the lab of KS was supported by the Norwegian Cancer Society, grant no. 208239-2019.

Acknowledgments

We wish to thank Sascha Pust for his strong support of the cell biology and microscopy experiments and co-supervision of DM, Nina F. J. Edin for advice regarding the SILAC experiments, Christian Köhler for assistance with data deposition into PRIDE, and Bernd Thiede for general support of the proteomics study. SP and BT also helped us to improve the manuscript. We further thank Erik O. Pettersen (Physics Department, University of Oslo) for access to his laboratory and support, and the Center of Molecular Immunology (CIM), Havana for providing us with 14F7hT mAb. The HeLa cell line was derived from Henrietta Lacks in 1951, who made significant contributions to biomedical research. We would like to thank her and her family members for this.

Conflict of interest

EM was involved in developing 14F7 in the period 2000-2015 at the Center for Molecular Immunology in Havana, Cuba.

The remaining authors declare that the research was conducted in the absence of any commercial or financial relationships that could be construed as a potential conflict of interest.

Publisher's note

All claims expressed in this article are solely those of the authors and do not necessarily represent those of their affiliated organizations, or those of the publisher, the editors and the

reviewers. Any product that may be evaluated in this article, or claim that may be made by its manufacturer, is not guaranteed or endorsed by the publisher.

Supplementary material

The Supplementary Material for this article can be found online at: <https://www.frontiersin.org/articles/10.3389/fimmu.2022.994790/full#supplementary-material>

References

- Kruger S, Ilmer M, Kobold S, Cadilha BL, Endres S, Ormanns S, et al. Advances in cancer immunotherapy 2019 - latest trends. *J Exp Clin Cancer Res* (2019) 38:268. doi: 10.1186/s13046-019-1266-0
- Diken M, Ravoori S, Brodsky AN. Translating science into survival: Report on the fourth international cancer immunotherapy conference. *Cancer Immunol Res* (2019) 7:2–5. doi: 10.1158/2326-6066.CIR-18-0866
- Waldman AD, Fritz JM, Lenardo MJ. A guide to cancer immunotherapy: from T cell basic science to clinical practice. *Nat Rev Immunol* (2020) 20:651–68. doi: 10.1038/s41577-020-0306-5
- Kimiz-Gebologlu I, Gulce-Iz S, Biray-Avci C. Monoclonal antibodies in cancer immunotherapy. *Mol Biol Rep* (2018) 45:2935–40. doi: 10.1007/s11033-018-4427-
- Kaplon H, Chenoweth A, Crescioli S, Reichert JM. Antibodies to watch in 2022. *mAbs* (2022) 14:1. doi: 10.1080/19420862.2021.2014296
- Chan AC, Carter PJ. Therapeutic antibodies for autoimmunity and inflammation. *Nat Rev Immunol* (2010) 10:301–16. doi: 10.1038/nri2761
- Liu X, Pop LM, Vitetta ES. Engineering therapeutic monoclonal antibodies. *Immunol Rev* (2008) 222:9–27. doi: 10.1111/j.1600-065X.2008.00601.x
- Hellström I, Garrigues HJ, Garrigues U, Hellström KE. Highly tumor-reactive, internalizing, mouse monoclonal antibodies to le(y)-related cell surface antigens. *Cancer Res* (1990) 50:2183–90.
- Garrigues J, Garrigues U, Hellström I, Hellström KE. Le^y specific antibody with potent anti-tumor activity is internalized and degraded in lysosomes. *Am J Pathol* (1993) 142:607–22.
- Matsouka S, Asano Y, Sano K, Kishimoto H, Yamashita I, Yorifuji H, et al. A novel type of cell death of lymphocytes induced by a monoclonal antibody without participation of complement. *J Exp Med* (1995) 181:2007–15. doi: 10.1084/jem.181.6.2007
- Bhat NM, Bieber MM, Stevenson FK, Teng NNH. Rapid cytotoxicity of human b lymphocytes induced by VH4-34 (VH4.21) gene-encoded monoclonal antibodies. *Clin Exp Immunol* (1996) 105:183–90. doi: 10.1046/j.1365-2249.1996.d01-733.x
- Zhang C, Xu Y, Gu J, Schlossman SF. A cell surface receptor defined by a mAb mediates a unique type of cell death similar to oncosis. *Proc Natl Acad Sci U.S.A.* (1998) 95:6290–5. doi: 10.1073/pnas.95.11.6290
- Ma F, Zhang C, Prasad KVS, Freeman GJ, Schlossman SF. Molecular cloning of porimin, a novel cell surface receptor mediating oncotic cell death. *Proc Natl Acad Sci U.S.A.* (2001) 98:9778–83. doi: 10.1073/pnas.171322898
- Fernández-Marrero Y, López-Requena A. Lonely killers: effector cell- and complement-independent non-proapoptotic cytotoxic antibodies inducing membrane lesions. *mAbs* (2011) 3:528–34. doi: 10.4161/mabs.3.6.17770
- Malykh YN, Schauer R, Shaw L. N-glycolylneuraminic acid in human tumours. *Biochimie* (2001) 83:623–34. doi: 10.1016/s0300-9084(01)01303-7
- Müthing J, Steuer H, Peter-Katalinić J, Marx U, Bethke U, Neumann U, et al. Expression of gangliosides G_{M3} (NeuAc) and G_{M3} (NeuGc) in myelomas and hybridomas of mouse, rat, and human origin. *J Biochem* (1994) 116:64–73. doi: 10.1093/oxfordjournals.jbchem.a124504
- Vázquez AM, Alfonso M, Lanne B, Karlsson K-A, Carr A, Barroso O, et al. Generation of a murine monoclonal antibody specific for N-glycolylneuraminic acid-containing gangliosides that also recognizes sulfated glycolipids. *Hybridoma* (1995) 14:551–6. doi: 10.1089/hyb.1995.14.551
- Marquina G, Waki H, Fernandez LE, Kon K, Carr A, Valiente O, et al. Gangliosides expressed in human breast cancer. *Cancer Res* (1996) 56:5165–71.
- Carr A, Mullet A, Mazorra Z, Vázquez AM, Alfonso M, Mesa C, et al. A mouse IgG₁ monoclonal antibody specific for N-glycolyl GM3 ganglioside recognized breast and melanoma tumors. *Hybridoma* (2000) 19:241–7. doi: 10.1089/02724570050109639
- Carr A, Mesa C, del Carmen Arango M, Vázquez AM, Fernández LE. *In vivo* and *in vitro* anti-tumor effect of 14F7 monoclonal antibody. *Hybrid Hybridomics* (2002) 21:463–8. doi: 10.1089/153685902321043990
- van Cruysen H, Ruiz MG, van der Valk P, de Gruijl TD, Giaccone G. Tissue micro array analysis of ganglioside n-glycolyl GM3 expression and signal transducer and activator of transcription (STAT)-3 activation in relation to dendritic cell infiltration and microvessel density in non-small cell lung cancer. *BMC Cancer* (2009) 9:180. doi: 10.1186/1471-2407-9-180
- Scursoni AM, Galluzzo L, Camarero S, Lopez J, Lubieniecki F, Sampor C, et al. Detection of n-glycolyl GM3 ganglioside in neuroectodermal tumors by immunohistochemistry: an attractive vaccine target for aggressive pediatric cancer. *Clin Dev Immunol* (2011) 2011:245181. doi: 10.1155/2011/245181
- Blanco R, Rengifo E, CE R, Cedeño M, Frómata M, Carr A. Immunohistochemical reactivity of the 14F7 monoclonal antibody raised against n-glycolyl GM3 ganglioside in some benign and malignant skin neoplasms. *ISRN Dermatol* (2011) 2011:848909. doi: 10.5402/2011/848909
- Blanco R, Rengifo E, Cedeño M, CE R, DF A, Carr A. Immunoreactivity of the 14F7 mAb raised against n-glycolyl GM3 ganglioside in epithelial malignant tumors from digestive system. *ISRN Gastroenterol* (2011) 2011:645641. doi: 10.5402/2011/645641
- Torbidoni AV, Scursoni A, Camarero S, Segatori V, Gabri M, Alonso D, et al. Immunoreactivity of the 14F7 mAb raised against N-glycolyl GM3 ganglioside in retinoblastoma tumours. *Acta Ophthalmol* (2015) 93:e294–300. doi: 10.1111/aos.12578
- Pilco-Janeta D, de la Cruz Puebla M, Soriano J, Osorio M, Caballero I, Pérez AC, et al. Aberrant expression of n-glycolyl GM3 ganglioside is associated with the aggressive biological behavior of human sarcomas. *BMC Cancer* (2019) 19:556. doi: 10.1186/s12885-019-5743-9
- Rojas G, Talavera A, Munoz Y, Rengifo E, Kregel U, Ångström J, et al. Light chain shuffling results in successful phage display of antibody fragments to N-glycolyl GM3 ganglioside. *J Immunol Meth* (2004) 293:71. doi: 10.1016/j.jim.2004.07.002
- Bjerregaard-Andersen K, Johannesen H, Abdel-Rahman N, Heggelund JE, Hoås HM, Abraha F, et al. Crystal structure of an l chain optimised 14F7 anti-ganglioside fv suggests a unique tumour-specificity through an unusual h-chain CDR3 architecture. *Sci Rep* (2018) 8:10836. doi: 10.1038/s41598-018-28918-5
- Bjerregaard-Andersen K, Johannesen H, Abraha F, Šakanović A, Groß D, Coskun Ü, et al. Insight into glycosphingolipid crypticity: Crystal structure of the anti-tumor antibody 14F7 and recognition of NeuGc GM3 ganglioside. *bioRxiv* (2020) 2020.9.18.294777. doi: 10.1101/2020.09.18.294777
- Kregel U, Olsson L-L, Martínez C, Talavera A, Rojas G, Mier E, et al. Structure and molecular interactions of a unique anti-tumor antibody specific for N-glycolyl GM3. *J Biol Chem* (2004) 279:5597. doi: 10.1074/jbc.M311693200
- Bjerregaard-Andersen K, Abraha F, Johannesen H, Oscarson S, Moreno E, Kregel U. Key role of a structural water molecule for the specificity of 14F7 – an antitumor antibody targeting the NeuGc GM3 ganglioside. *Glycobiology* (2021) 31:1500. doi: 10.1093/glycob/cwab076

32. Rojas G, Pupo A, Gómez S, Krengel U, Moreno E. Engineering the binding site of an antibody against *N*-glycolyl GM3: from functional mapping to novel anti-ganglioside specificities. *ACS Chem Biol* (2013) 8:376. doi: 10.1021/cb3003754
33. Piperno G, López-Requena A, Predonzani A, Dorvignit D, Labrada M, Zentilin L, et al. Recombinant AAV-mediated *in vivo* long-term expression and antitumor activity of an anti-ganglioside GM3(Neu5Gc) antibody. *Gene Ther* (2015) 22:960–7. doi: 10.1038/gt.2015.71
34. Fernández-Marrero Y, Roque-Navarro L, Hernández T, Dorvignit D, Molina-Pérez M, González A, et al. A cytotoxic humanized anti-ganglioside antibody produced in a murine cell line defective of *N*-glycosylated-glycoconjugates. *Immunobiology* (2011) 216:1239–47. doi: 10.1016/j.imbio.2011.07.004
35. Dorvignit D, García-Martínez L, Rossin A, Sosa K, Viera J, Hernández T, et al. Antitumor and cytotoxic properties of a humanized antibody specific for the GM3(Neu5Gc) ganglioside. *Immunobiology* (2015) 220:1343–50. doi: 10.1016/j.imbio.2015.07.008
36. Cutillo G, Saariho A-H, Meri S. Physiology of gangliosides and the role of antiganglioside antibodies in human diseases. *Cell Mol Immunol* (2020) 17:313–22. doi: 10.1038/s41423-020-0388-9
37. Haji-Ghassemi O, Blackler RJ, Young NM, Evans SV. Antibody recognition of carbohydrate epitopes. *Glycobiology* (2015) 25:920–52. doi: 10.1093/glycob/cwv037
38. Casadesús AV, Fernández-Marrero Y, Clavell M, JA Gómez, Hernández T, Moreno E, et al. A shift from *N*-glycolyl- to *N*-acetyl-sialic acid in the GM3 ganglioside impairs tumor development in mouse lymphocytic leukemia cells. *Glycoconjugate J* (2013) 30:687–99. doi: 10.1007/s10719-013-9473-y
39. Roque-Navarro L, Chakrabandhu K, de León J, Rodríguez S, Toledo C, Carr A, et al. Anti-ganglioside antibody-induced tumor cell death by loss of membrane integrity. *Mol Cancer Ther* (2008) 7:2033–41. doi: 10.1158/1535-7163
40. Kroemer G, Galluzzi L, Vandenabeele P, Abrams J, Alnemri ES, Baehrecke EH, et al. Classification of cell death: recommendations of the nomenclature committee on cell death 2009. *Cell Death Differ* (2009) 16:3–11. doi: 10.1038/cdd.2008.150
41. D'Arcy MS. Cell death: a review of the major forms of apoptosis, necrosis and autophagy. *Cell Biol Int* (2019) 43:582–92. doi: 10.1002/cbin.11137
42. Tan HL, Fong WJ, Lee EH, Yap M, Choo A. mAb 84, a cytotoxic antibody that kills undifferentiated human embryonic stem cells *via* oncosis. *Stem Cells* (2009) 27:1792–801. doi: 10.1002/stem.109
43. Horwacik I, Rokita H. Targeting of tumor-associated gangliosides with antibodies affects signaling pathways and leads to cell death including apoptosis. *Apoptosis* (2015) 20:679–88. doi: 10.1007/s10495-015-1103-7
44. Dorvignit D, Boligan KF, Relova-Hernández E, Clavell M, López A, Labrada M, et al. Antitumor effects of the GM3(Neu5Gc) ganglioside-specific humanized antibody 14F7hT against *Cmah*-transfected cancer cells. *Sci Rep* (2019) 9:1–12. doi: 10.1038/s41598-019-46148-1
45. Bousquet PA, Sandvik JA, Arntzen MØ, Jeppesen Edin NF, Christoffersen S, Krengel U, et al. Hypoxia strongly affects mitochondrial ribosomal proteins and translocases, as shown by quantitative proteomics of HeLa cells. *Int J Proteomics* (2015) 2015:678527. doi: 10.1155/2015/678527
46. Bousquet PA, Sandvik JA, Jeppesen Edin NF, Krengel U. Hypothesis: Hypoxia induces *de novo* synthesis of NeuGc gangliosides in humans through CMAH domain substitute. *Biochem Biophys Res Commun* (2018) 495:1562–6. doi: 10.1016/j.bbrc.2017.11.183
47. Ong S-E, Blagoev B, Kratchmarova I, Kristensen DB, Steen H, Pandey A, et al. Stable isotope labeling by amino acids in cell culture, SILAC, as a simple and accurate approach to expression proteomics. *Mol Cell Proteomics* (2002) 1:376–86. doi: 10.1074/mcp.m200025-mcp200
48. Koehler CJ, Strozynski M, Kozielski F, Treumann A, Thiede B. Isobaric peptide termini labeling for MS/MS-based quantitative proteomics. *J Proteome Res* (2009) 8:4333–41. doi: 10.1021/pr900425n
49. Cox J, Mann M. MaxQuant enables high peptide identification rates, individualized p.p.b.-range mass accuracies and proteome-wide protein quantification. *Nat Biotechnol* (2008) 26:1367–72. doi: 10.1038/nbt.1511
50. Cox J, Neuhauser N, Michalski A, Scheltema RA, Olsen JV, Mann M. Andromeda: a peptide search engine integrated into the MaxQuant environment. *J Proteome Res* (2011) 10:1794–805. doi: 10.1021/pr101065j
51. Huang DW, Sherman BT, Lempicki RA. Bioinformatics enrichment tools: paths toward the comprehensive functional analysis of large gene lists. *Nucleic Acids Res* (2009) 37:1–13. doi: 10.1093/nar/gkn923
52. Huang DW, Sherman BT, Lempicki RA. Systematic and integrative analysis of large gene lists using DAVID bioinformatics resources. *Nat Protoc* (2009) 4:44–57. doi: 10.1038/nprot.2008.211
53. Perez-Riverol Y, Csordas A, Bai J, Bernal-Llinares M, Hewapathirana S, Kundu DJ, et al. The PRIDE database and related tools and resources in 2019: improving support for quantification data. *Nucleic Acids Res* (2019) 47:D442–50. doi: 10.1093/nar/gky1106
54. Eraslan S, Kayserili H, Apak MY, Kirdar B. Identification of point mutations in Turkish DMD/BMD families using multiplex-single stranded conformation analysis (SSCA). *Eur J Hum Genet* (1999) 7:765–70. doi: 10.1038/sj.ejhg.5200370
55. Feng J, Yan J, Buzin CH, Sommer SS, Towbin JA. Comprehensive mutation scanning of the dystrophin gene in patients with nonsyndromic X-linked dilated cardiomyopathy. *J Am Coll Cardiol* (2002) 40:1120–4. doi: 10.1016/s0735-1097(02)02126-5
56. Prior TW, Papp AC, Snyder PJ, Burghes AHM, Bartolo C, Sedra MS, et al. A missense mutation in the dystrophin gene in a duchenne muscular dystrophy patient. *Nat Genet* (1993) 4:357–60. doi: 10.1038/ng0893-357
57. Bakker AJ, Head I, Williams DA, Stephenson DG. Ca^{2+} levels in myotubes grown from the skeletal muscle of dystrophic (*mdx*) and normal mice. *J Physiol* (1993) 460:1–13. doi: 10.1113/jphysiol.1993.sp019455
58. Bulfield G, Siller WG, Wight PAL, Moore KJ. X Chromosome-linked muscular dystrophy (*mdx*) in the mouse. *Proc Natl Acad Sci U.S.A.* (1984) 81:1189–92. doi: 10.1073/pnas.81.4.1189
59. Cullen MJ, Jaros E. Ultrastructure of the skeletal muscle in the X chromosome-linked dystrophic (*mdx*) mouse. comparison with duchenne muscular dystrophy. *Acta Neuropathol* (1988) 77:69–81. doi: 10.1007/BF00688245
60. Turner PR, Fong P, Denetclaw WF, Steinhardt RA. Increased calcium influx in dystrophic muscle. *J Cell Biol* (1991) 115:1701–12. doi: 10.1083/jcb.115.6.1701
61. Carpenter S, Karpati G. Duchenne muscular dystrophy: plasma membrane loss initiates muscle cell necrosis unless it is repaired. *Brain* (1979) 102:147–61. doi: 10.1093/brain/102.1.147
62. Franco A, Lansman JB. Calcium entry through stretch-inactivated ion channels in *mdx* myotubes. *Nature* (1990) 344:670–3. doi: 10.1038/344670a0
63. Mokri B, Engel AG. Duchenne dystrophy: electron microscopic findings pointing to a basic or early abnormality in the plasma membrane of the muscle fiber. *Neurology* (1975) 25:1111–20. doi: 10.1212/wnl.25.12.1111
64. Morgan AJ, Platt FM, Lloyd-Evans E, Galione A. Molecular mechanisms of endolysosomal Ca^{2+} signalling in health and disease. *Biochem J* (2011) 439:349–74. doi: 10.1042/BJ20110949
65. Schuyler SC, Pellman D. Microtubule "plus-end-tracking proteins": The end is just the beginning. *Cell* (2001) 105:421–4. doi: 10.1016/s0092-8674(01)00364-6
66. Akhmanova A, Hoogenraad CC, Drabek K, Stepanova T, Dortal B, Verkerk T, et al. Clasps are CLIP-115 and -170 associating proteins involved in the regional regulation of microtubule dynamics in motile fibroblasts. *Cell* (2001) 104:923–35. doi: 10.1016/S0092-8674(01)00288-4
67. Bornens M. Centrosome composition and microtubule anchoring mechanisms. *Curr Opin Cell Biol* (2002) 14:25–34. doi: 10.1016/s0955-0674(01)00290-3
68. Desai A, Mitchison TJ. Microtubule polymerization dynamics. *Annu Rev Cell Dev Biol* (1997) 13:83–117. doi: 10.1146/annurev.cellbio.13.1.83
69. Galjart N. CLIPs and CLASPs and cellular dynamics. *Nat Rev Mol Cell Biol* (2005) 6:487–98. doi: 10.1038/nrm1664
70. Mimori-Kiyosue Y, Grigoriev I, Lansbergen G, Sasaki H, Matsui C, Severin F, et al. CLASP1 and CLASP2 bind to EB1 and regulate microtubule plus-end dynamics at the cell cortex. *J Cell Biol* (2005) 168:141–53. doi: 10.1083/jcb.200405094
71. Gruneberg U, Neef R, Li X, Chan EHY, Chalamalasetty RB, Nigg EA, et al. KIF14 and citron kinase act together to promote efficient cytokinesis. *J Cell Biol* (2006) 172:363–72. doi: 10.1083/jcb.200511061
72. Carleton M, Mao M, Biery M, Warren P, Kim S, Buser C, et al. RNA Interference-mediated silencing of mitotic kinesin KIF14 disrupts cell cycle progression and induces cytokinesis failure. *Mol Cell Biol* (2006) 26:3853–63. doi: 10.1128/MCB.26.10.3853-3863.2006
73. Molina I, Baars S, Brill JA, Hales KG, Fuller MT. Ripol p. a chromatin-associated kinesin-related protein required for normal mitotic chromosome segregation in *Drosophila*. *J Cell Biol* (1997) 139:1361–71. doi: 10.1083/jcb.139.6.1361
74. Nigg EA. Mitotic kinases as regulators of cell division and its checkpoints. *Nat Rev Mol Cell Biol* (2001) 2:21–32. doi: 10.1038/35048096
75. Zhu C, Zhao J, Bibikova M, Leverson JD, Bossy-Wetzel E, Fan J-B, et al. Functional analysis of human microtubule-based motor proteins, the kinesins and dyneins, in mitosis/cytokinesis using RNA interference. *Mol Biol Cell* (2005) 16:3187–99. doi: 10.1091/mbc.e05-02-0167
76. Kuopio T, Kankaanranta A, Jalava P, Kronqvist P, Kotkansalo T, Weber E, et al. Cysteine proteinase inhibitor cystatin a in breast cancer. *Cancer Res* (1998) 58:432–6.
77. Blaydon DC, Nitoiu D, Eckl K-M, Cabral RM, Bland P, Hausser I, et al. Mutations in *CSTA*, encoding cystatin a, underlie exfoliative ichthyosis and reveal a

role for this protease inhibitor in cell-cell adhesion. *Am J Hum Genet* (2011) 89:564–71. doi: 10.1016/j.ajhg.2011.09.001

78. Butinar M, Prebanda MT, Rajković J, Jerić B, Stoka V, Peters C, et al. Stefin b deficiency reduces tumor growth *via* sensitization of tumor cells to oxidative stress in a breast cancer model. *Oncogene* (2014) 33:3392–400. doi: 10.1038/ncr.2013.314

79. Yang C, Pring M, Wear MA, Huang M, Cooper JA, Svitkina TM, et al. Mammalian CARMIL inhibits actin filament capping by capping protein. *Dev Cell* (2005) 9:209–21. doi: 10.1016/j.devcel.2005.06.008

80. Yao Y-L, Yang W-M. The metastasis-associated proteins 1 and 2 form distinct protein complexes with histone deacetylase activity. *J Biol Chem* (2003) 278:42560–8. doi: 10.1074/jbc.M302955200

81. Mazumdar A, Wang R-A, Mishra SK, Adam L, Bagheri-Yarmand R, Mandal M, et al. Transcriptional repression of oestrogen receptor by metastasis-associated protein 1 corepressor. *Nat Cell Biol* (2001) 3:30–7. doi: 10.1038/35050532

82. Talukder AH, Mishra SK, Mandal M, Balasenthil S, Mehta S, Sahin AA, et al. MTA1 interacts with MAT1, a cyclin-dependent kinase-activating kinase complex ring finger factor, and regulates estrogen receptor transactivation functions. *J Biol Chem* (2003) 278:11676–85. doi: 10.1074/jbc.M209570200

83. Lee M-H, Na H, Na T-Y, Shin Y-K, Seong J-K, Lee M-O. Epigenetic control of metastasis-associated protein 1 gene expression by hepatitis b virus X protein during hepatocarcinogenesis. *Oncogenesis* (2012) 1:e25. doi: 10.1038/oncsis.2012.26

84. Oh J, Liu Z-X, Feng GH, Raposo G, Spritz RA. The hermannsky-pudlak syndrome (HPS) protein is part of a high molecular weight complex involved in biogenesis of early melanosomes. *Hum Mol Genet* (2000) 9:375–85. doi: 10.1093/hmg/9.3.375

85. Eguchi Y, Shimizu S, Tsujimoto Y. Intracellular ATP levels determine cell death fate by apoptosis or necrosis. *Cancer Res* (1997) 57:1835–40.



OPEN ACCESS

EDITED BY

Catherine Sautes-Fridman,
INSERM U1138 Centre de Recherche
des Cordeliers (CRC), France

REVIEWED BY

Norihiro Watanabe,
Baylor College of Medicine,
United States
Elisabetta Xue,
San Raffaele Hospital (IRCCS), Italy
Pouya Safarzadeh Kozani,
Guilan University of Medical Sciences,
Iran
Pooria Safarzadeh Kozani,
Tarbiat Modares University, Iran

*CORRESPONDENCE

Fang Zhou
zhoufang1@medmail.com.cn

SPECIALTY SECTION

This article was submitted to
Cancer Immunity
and Immunotherapy,
a section of the journal
Frontiers in Immunology

RECEIVED 08 September 2022

ACCEPTED 31 October 2022

PUBLISHED 17 November 2022

CITATION

Deng L, Xiaolin Y, Wu Q, Song X, Li W,
Hou Y, Liu Y, Wang J, Tian J, Zuo X
and Zhou F (2022) Multiple CAR-T cell
therapy for acute B-cell lymphoblastic
leukemia after hematopoietic stem
cell transplantation: A case report.
Front. Immunol. 13:1039929.
doi: 10.3389/fimmu.2022.1039929

COPYRIGHT

© 2022 Deng, Xiaolin, Wu, Song, Li,
Hou, Liu, Wang, Tian, Zuo and Zhou.
This is an open-access article
distributed under the terms of the
[Creative Commons Attribution License
\(CC BY\)](https://creativecommons.org/licenses/by/4.0/). The use, distribution or
reproduction in other forums is
permitted, provided the original
author(s) and the copyright owner(s)
are credited and that the original
publication in this journal is cited, in
accordance with accepted academic
practice. No use, distribution or
reproduction is permitted which does
not comply with these terms.

Multiple CAR-T cell therapy for acute B-cell lymphoblastic leukemia after hematopoietic stem cell transplantation: A case report

Lei Deng¹, Yu Xiaolin¹, Qian Wu¹, Xiaochen Song¹, Wenjun Li¹,
Yixi Hou¹, Yue Liu¹, Jing Wang¹, Jun Tian², Xiaona Zuo³
and Fang Zhou^{1*}

¹Hematology Department, The 960th Hospital of The People's Liberation Army (PLA) Joint Logistics Support Force, Jinan, China, ²Nuclear Medicine Department, The 960th Hospital of the People's Liberation Army (PLA) Joint Logistics Support Force, Jinan, China, ³Department of Pathology, Beijing Boren Hospital, Beijing, China

B-cell acute lymphoblastic leukemia (B-ALL) is the most common childhood malignancy. The cure rate has reached 90% after conventional chemotherapy and hematopoietic stem cell transplantation (HSCT), but the prognosis of patients with relapsed and refractory (R/R) leukemia is still poor after conventional treatment. Since FDA approved CD19 CAR-T cell (Kymriah) for the treatment of R/R B-ALL, increasing studies have been conducted on CAR-T cells for R/R ALL. Herein, we report the treatment of a patient with ALL who relapsed after allogeneic HSCT, had a complete remission (CR) to murine scFv CD19 CAR-T but relapsed 15 months later. Partial response was achieved after humanized CD19 CAR-T treatment, and the patient finally achieved disease-free survival after sequential CD22 CAR-T treatment. By comparing the treatment results of different CAR-T cells in the same patient, this case suggests that multiple CAR-T therapies are effective and safe in intramedullary and extramedullary recurrence in the same patient, and the expansion of CAR-T cells and the release of inflammatory cytokines are positively correlated with their efficacy. However, further clinical studies with large sample sizes are still needed for further clarification.

KEYWORDS

B-ALL, extramedullary recurrence, hematopoietic (stem) cell transplantation (HCST), cytosine, CAR (chimeric antigen receptor) T cells

Introduction

B-cell acute lymphoblastic leukemia (ALL) is the most common childhood malignancy and is usually treated with chemotherapy and allogeneic hematopoietic stem cell transplantation (1). The cure rate has reached 90%, but the prognosis of patients with relapsed and refractory (R/R) leukemia after conventional treatment is very poor (2, 3). Patients with recurrence after allogeneic hematopoietic stem cell transplantation (allo-HSCT) are usually treated with donor lymphocyte infusions (DLI) (4, 5). DLI can induce complete remission (CR); however, many patients do not achieve sustained CR (6, 7).

Drugs such as monoclonal antibodies (anti-CD20), anti-CD19 bi-specific T cell binding agents, and anti-CD22 antibody-drug conjugates have shown unexpected results both in the prophase and R/R settings and continue to change the treatment paradigm for ALL (8–10). In one phase 3 trial (11), inotuzumab ozogamicin, an anti-CD22 antibody conjugated to caricomycin, showed significantly higher response rates and better progression-free survival (PFS) than standard intensive chemotherapy in adults with R/R B-ALL. In addition, more patients became minimal residual disease (MRD)-negative and required allo-HSCT. In another randomized phase 3 trial involving adults with Ph-negative R/R B-cell precursor ALL (12), treatment with blinatumomab, a bi-specific monoclonal antibody construct that enables CD3-positive T cells to recognize and eliminate CD19-positive ALL blasts, resulted in significantly longer overall survival (OS) than standard chemotherapy. The blinatumomab group also had a 29% lower risk of death than the chemotherapy group.

Since the first CD19 chimeric antigen receptor T (CAR-T) cell (Kymriah) was approved by the FDA for R/R acute lymphoblastic leukemia, several CD19 CAR-T cells have been approved by the FDA, including Yescarta, Tecartus, and Breyanzi (13). Kymriah and other CD19 CAR-Ts have also shown high CR rates (70%–93%) in r/r B-ALL patients (14–19). However, some patients did not respond, and some relapsed within one year (43–55%) (15–19). However, one study showed that CD22 CAR-T cell therapy had a 74% response rate in 21 patients with R/R B-ALL (20). CD22 CAR-T cell therapy has a good response rate, even in patients who failed to respond to CD19 CAR-T therapy or those who have relapsed. Herein, we report the treatment of a patient who relapsed after allo-HSCT, relapsed after murine scFv CD19 CAR-T therapy, had a partial response after humanized CD19 CAR-T therapy and finally achieved disease-free survival after sequential CD22 CAR-T therapy.

Case

On November 5, 2016, a five-year-old male patient was admitted to the hematology department of a local hospital due to a neck mass. Physical examination showed scattered ecchymosis

on the skin, the lymph nodes were swollen in the neck, axilla, and groin, and a mass of approximately 10 cm × 8 cm × 2 cm was detected on the right side of the neck with poor mobility, no tenderness, no congestion in the pharynx, grade 2 tonsil enlargement, and no abnormalities in the cardiopulmonary region, abdomen, or nervous system. Results of a routine blood examination revealed a white blood cell (WBC) count of $16.66 \times 10^9/L$, hemoglobin (HB) 114 g/L, and platelet (PLT) count of $172 \times 10^9/L$. Bone marrow cytology showed that hyperplasia was active, the proportion of granulocytes was low, the proportion of lymphocytes, mainly primitive naive lymphocytes, had increased (83.5%), and the proportion of peripheral blood blast cells was 59%. Immunophenotyping showed that abnormal cells accounted for 84.66% of nuclear cells and expressed CD34, human leukocyte antigen DR(HLA-DR), CD123, CD10, CD19, cCD79a, terminal deoxynucleotidyl transferase (TdT), CD38, and CD22. Cytosolic immunoglobulin M (CIgM), secretory immunoglobulin M (sIgM), CD117, CD20, CD7, CD33, CD15, CD13, CD11b, CD64, CD36, CD4, CD14, CD56, myeloperoxidase (MPO), cytoplasmic CD3 (cCD3), and membrane CD3 (mCD3) were not expressed. All 43 fusion genes were negative. The results of the karyotype analysis were as follows: 58-60, XY, + 4, + 5, + 6, + 7, + 14, + 17, + 18, and + 22 [CP5]. A diagnosis of acute lymphoblastic leukemia was made. The course of treatment for this patient is shown in Figure 1A.

On November 10, 2016, the VDLD (Vincristine, Daunorubicin, L-asparaginase, and Dexamethasone) chemotherapy regimen was administered. On day 15, bone marrow cell morphology showed a severe reduction of bone marrow hyperplasia and a naive lymphocyte proportion of 12%. On day 33, marrow cell morphology revealed an MRD of 4.61%. The MRD was negative after two courses of CAM (Cyclophosphamide, Cytarabine, and Azathioprine) regimen consolidation. Two rounds of chemotherapy with the HR-1 (Dexamethasone, Vincristine, High dose methotrexate, Cyclophosphamide, Cytarabine, and L-asparaginase), HR-2 (Dexamethasone, Vindesine, High dose methotrexate, Ifosfamide, Vincristine, and L-asparaginase), and HR-3 (Dexamethasone, High dose cytarabine, Etoposide, and L-asparaginase) protocols began in February 2017, and the VDLD+CAM×2 regimen began on August 27, 2017. On November 8, 2017, the MTX+6-MP/CA/VD (Methotrexate, Azathioprine, Cyclophosphamide, Cytarabine, Vincristine, and Dexamethasone) regimen was administered, during which time the bone marrow MRD was 0.18%. The second cycle of MTX+6-MP/CA/VD chemotherapy was initiated in December 2017 and the third cycle of MTX+6-MP/CA/VD chemotherapy was initiated in March 2018. Subsequently, the MTX+6-MP/CA/VD regimen was used for maintenance treatment. During the period, multiple lumbar punctures were performed and chemotherapeutic drugs were injected to prevent central nervous system leukemia, and cerebrospinal fluid examination showed no abnormalities.

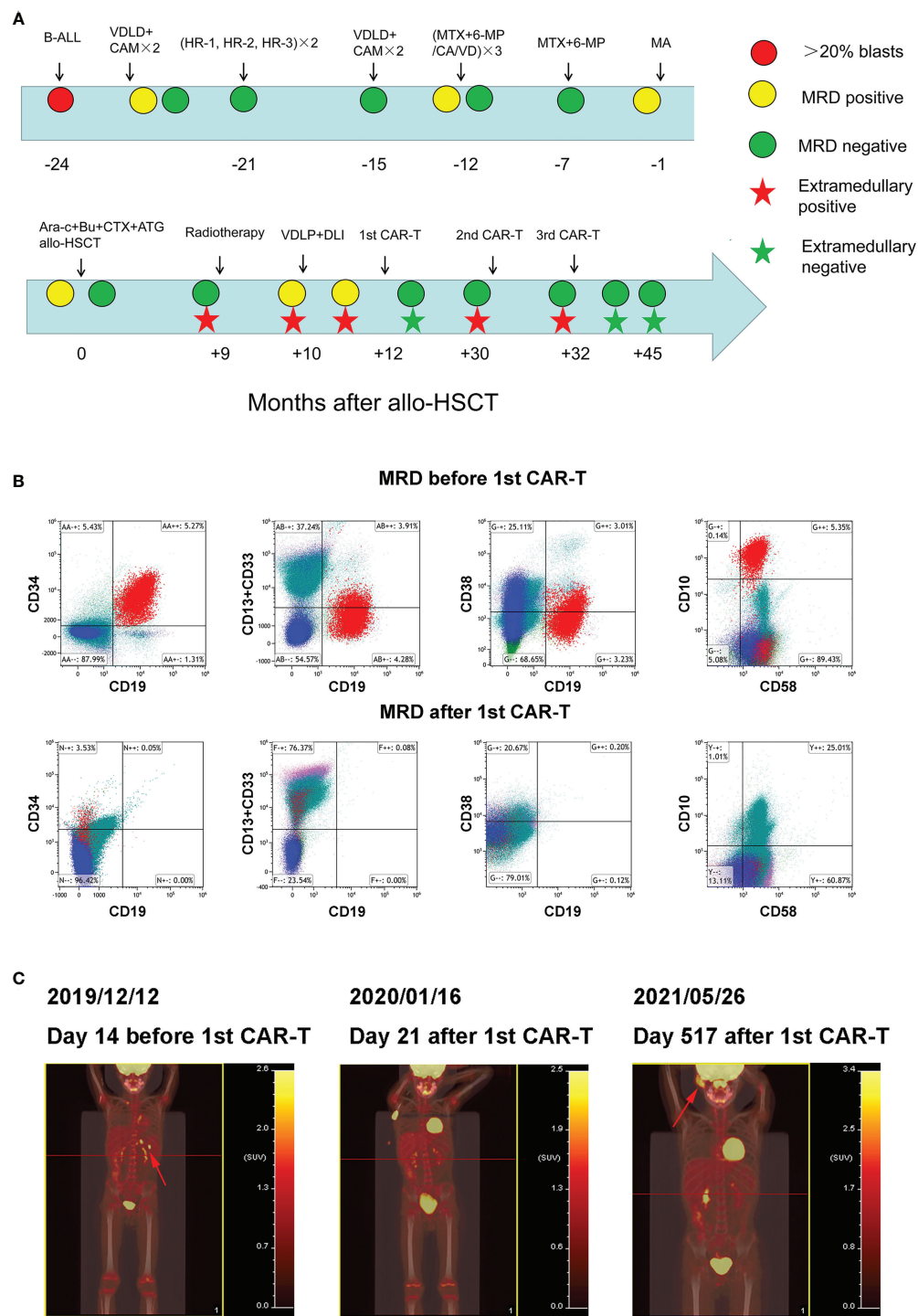


FIGURE 1

Clinical treatment process and the response of the patient (A) Clinical treatment process and response of the patient. (B) Bone marrow MRD before and after 1st CAR-T treatment. (C) Whole body PET/CT before and after 1st CAR-T treatment.

On September 27, 2018, the patient visited our hospital for further diagnosis and treatment, and a physical examination revealed no abnormalities. Results of a routine blood examination were: WBC count, $2.77 \times 10^9/L$; HB 89 g/L; and

PLT $353 \times 10^9/L$. We also noted bone marrow cytological remission, MRD of 1.1%, and CD9, CD10, CD19, CD20, CD34, CD38, and CD58. Chromosome analysis results were 46, XY [20]. MA (Methotrexate and Cytarabine) chemotherapy

was subsequently administered. On November 5, 2018, bone marrow cytology revealed that the MRD was 2.01%. On November 21, 2018, the pretreatment regimen of BUCY + ARA-C + ATG (Busulfan, Cyclophosphamide, Cytarabine, and Antithymocyte globulin) was started. Allo-HSCT (MNC $11.8 \times 10^8/\text{kg}$, CD34+ cells $9.84 \times 10^6/\text{kg}$) was performed on November 28 and 29, and the donor was the father of the patient with 5/10 HLA matches. Multiple bone marrow test results after transplantation were negative for MRD.

In September 2019 (the ninth month after transplantation), the patient experienced left scrotal swelling and pain; the bone marrow morphology was relieved, MRD was negative, and donor chimerism was 98.89%. A biopsy of the mass (left bolus biopsy tissue) showed that it was consistent with B-cell lymphoblastic leukemia or lymphoma. Immunohistochemistry results were: CD10 (+), the TdT (+), MPO (+), CD43 (+), CD79a (+), aired box gene 5+ (Pax-5 +), leucocyte common antigen (LCA) (focal +), CD20 + (part), P53 (approximately + 25%), CD3 (in +), CD2 (in +), CD21 (-), the Placental alkaline phosphatase (PLAP) (-), Mum - 1 (-), Bcl-6 (-), CD30 (-), CD5 (-), and Ki-67 (approximately 50% +). *In situ* hybridization results: Epstein-Barr virus-encoded small RNA (EBER) (-). Three-dimensional conformal radiotherapy (200 cGy/time \times 13 times) was administered to the left testis and the left scrotum was significantly reduced. Bone marrow morphology on October 26 revealed: 1.55% naive lymphocytes, 0.78% MRD, and 99.78% donor chimerism. VDLT chemotherapy was then administered. On the 14th day of chemotherapy, bone marrow morphology showed low proliferation, and the percentage of proto-jvenile cells was 5%. Donor lymphocyte infusion (MNC $1.29 \times 10^8/\text{kg}$) was performed. Bone marrow morphology 12 days after infusion (on December 2) revealed hyperplasia was active, and that the proportion of primary and juvenile lymphocytes was 3.5%. MRD was 5.35%, and this population of cells expressed CD10, CD19, CD34, and CD58 (Figure 1B). The donor chimerism rate was 93.47%. PET/CT revealed: multiple lymph nodes with increased FDG metabolism in the left side of the abdominal aorta, posterior to the pancreas, and splenic hilum, considering leukemia infiltration; and after radiotherapy, the left testicle was enlarged compared to the contralateral testicle, and FDG metabolism was not significantly increased (Figure 1C).

On December 16, 2019, peripheral blood mononuclear cells were collected from the patient and murine scFv CAR-T cells were cultured at Shanghai YaKe Biotechnology Ltd. After pretreatment with the FC (Fludarabine, cyclophosphamide) regimen, CAR-T cells were infused on December 26. On day seven after infusion, the patient showed increased heart rate, elevated transaminase levels, and elevated inflammatory factors, and the CRS was assessed as grade 1 (Table 1). The CRS classification scheme is based on the report of Lee DW et al. (21). On January 14, 2020, the bone marrow morphology was relieved, and immunoreactivity was negative. PET/CT revealed

that: the left para-abdominal aorta, posterior pancreas, and splenic hilar lymph nodes were slightly smaller than the anterior ones, the FDG metabolism was not significantly increased, and FDG metabolism did not increase after radiotherapy for left testicular infiltration (Figure 1C). These results suggested that the patient was in CR, which persisted for 15 months after discharge.

On April 11, 2021, the patient developed a facial mass on the right side that gradually increased in size. On May 6, an ultrasound examination revealed a 44 mm \times 8 mm mass with a poorly defined border and an irregular shape. A biopsy under B-ultrasound guidance was performed on May 13. Pathological findings of the biopsy tissue of the right facial mass showed a lymphoproliferative lesion, consistent with B-lymphoblastic leukemia/lymphoma (Figure 2A). Immunohistochemical staining results were: CD79a+, CD43+, TdT+, CD20 scattered+, PAX-5 scattered+, P53 approximately 25% weak+, CD5-, CD23-, CD3-, CD2-, CD7-, MPO-, and Ki-67 (approximately 60%+). *In situ* hybridization results: FBER. On May 22, examinations showed bone marrow morphologic remission and negative MRD, with complete donor-type chimerism. PET/CT revealed: newly found space-occupying lesions with increased FDG metabolism in the subcutaneous soft tissue of the right face; and newly observed increased FDG metabolism in the nasopharynx and slightly increased bilateral small cervical lymph nodes (Figure 1C). On June 8, peripheral blood mononuclear cells were collected from the donor (the patient's father), and humanized CD19 CAR-T cells were cultured. After pretreatment with the FC regimen, CAR-T cells were injected on June 17. On the fifth day after infusion, the patient developed a low fever (37.5°C) without other discomfort symptoms. CRS was rated grade 1. Facial MRI on days 13 and 42 after infusion revealed that the mass was smaller than before infusion (Figure 2B).

On July 30, 2021, the patient was pretreated with the FC protocol, and on August 3, humanized CD22 CAR-T cells cultured from the peripheral blood mononuclear cells of the donor (the patient's father) were transfused back. On the first day after the infusion, the patient developed a fever with the highest temperature of 38.6°C. Subsequently, the patient continued to have repeated high fevers, with the highest temperature of 39°C, and a cough accompanied by chest tightness and breathlessness. Chest CT showed a pulmonary infection, which improved after antipyretic symptomatic treatment and anti-infective treatment. Drugs used included ibuprofen, meropenem, voriconazole, and caspofungin. No steroid hormones were used. CRS was graded as grade 2. As shown in Figure 3, CAR-T cell expansion and cytokine elevation were the most dramatic after the third CAR-T cell infusion (Supplementary Figure 1). After the third CAR-T cell infusion, the tumor was significantly reduced in size, with no activity in the lesion 191 and 297 days (February 10, 2022, and May 27, 2022) after the third CAR-T cell infusion (Figure 2B).

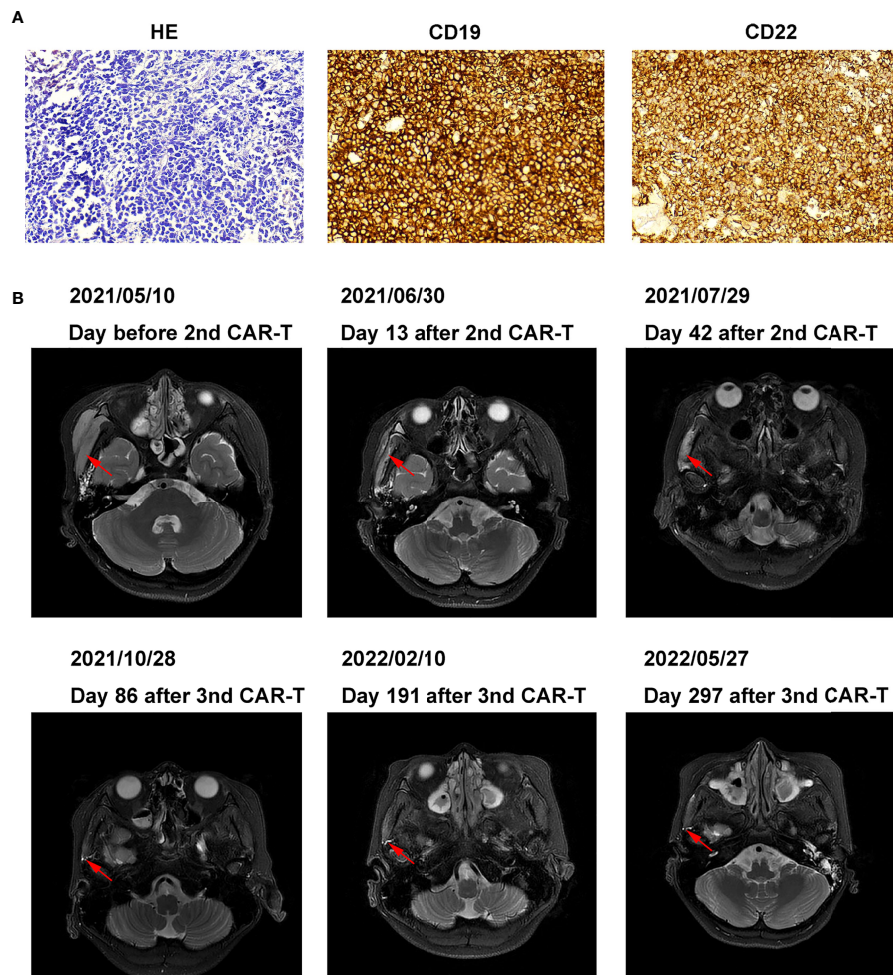


FIGURE 2
Pathology, histochemistry, and MRI images of right facial mass (A) Pathology and histochemistry of right facial mass. (B) MRI images of the right facial mass before and after 2nd, the 3rd CAR-T cell treatment.

Discuss

In this patient with acute lymphoblastic leukemia, the first extramedullary (testicular) recurrence occurred more than nine months after allogeneic transplantation. After radiotherapy, the extramedullary lesions disappeared, but the bone marrow MRD was positive. The MRD increased after chemotherapy and donor lymphocyte infusion. After the first CAR-T cell treatment, the MRD was negative. Extramedullary (facial) recurrence occurred after 15 months, which improved after two CAR-T cell treatments, following which the patient continued to live disease-free.

Occasionally ($\leq 2\%$), testicular recurrence occurs in acute lymphoblastic leukemia (22). Ding et al. (23) showed that testicular recurrence might directly evolve from leukemia

clones that survive chemotherapy. It is also likely to have relapsed independently from the bone marrow. Radiotherapy is a good choice for patients with isolated testicular recurrences (24). Besides, CAR-T therapy for testicular recurrence has been started in several studies. In the study of Chen X et al. (25), all 7 patients had CR. One patient had bone marrow recurrence 6 months after CAR-T treatment, and 6 patients were still in remission during the follow-up period (median 14 months). Only 5 patients developed grade 1 CRS, and the remaining two patients did not develop CRS. Rubinstein JD et al. (26) and Yu J et al. (27) each reported 1 case of ALL with testicular recurrence and remission after CAR-T treatment.

Based on flow cytometric assessment of CD19 expression in B-ALL, relapse after CD19 CAR-T cell treatment can be divided

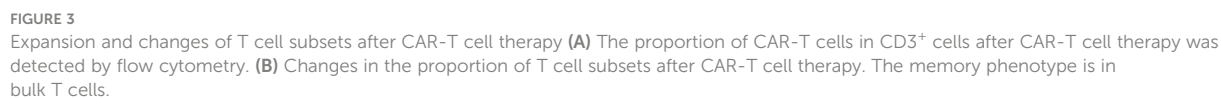


TABLE 1 Characterization of the three infusions of CAR-T cells.

	1st CAR-T	2nd CAR-T	3rd CAR-T
Vector	lentivirus	lentivirus	lentivirus
scfv	Murine	Humanized	Humanized
CAR structure	Anti-CD19(FMC63)scFV-CD8a-4-1BB-CD3 ζ	Anti-CD19 scFV-CD8a-4-1BB-CD3 ζ	Anti-CD22 scFV-CD8a-4-1BB-CD3 ζ
Derived	Autologous	Allogenic	Allogenic
Total cells dose	1.85 $\times 10^8$	2.4 $\times 10^8$	2.81 $\times 10^8$
CAR-T ratio	79%	69.53%	56.4%
Weight (kg)	28	31	31
CAR-T cells (/kg)	5.2 $\times 10^6$	5.3 $\times 10^6$	5.17 $\times 10^6$
Blasts% pre-CAR-T cell infusion	EM+ and 5.35% in BM	EM+ and MRD-	EM+ and MRD-
ECOG score pre-CAR-T cell infusion	1	1	1
Expression of CD19/CD22 Before treatment	CD19+CD22+	CD19+CD22+	CD19+CD22+
Maximum of CAR-T cells/CD3+ cells	0.19%	3.3%	17.4%
Precondition	FC	FC	FC
Response	CR	Mass decrease	CR
CRS	1	1	2

CAR, chimeric antigen receptor; scFv, single-chain fragment variable; ECOG, Eastern Cooperative Oncology Group; EM, extramedullary; BM, bone marrow; MRD, minimal residual disease; FC, fludarabine cyclophosphamide; CR, complete remission; CRS, cytokine release syndrome.

into two groups: CD19-negative relapse and CD19-positive relapse (28, 29). When the patient relapsed after the first CD19 CAR-T cell treatment, immunohistochemistry showed strong CD19 positivity (Figure 2A), and the patient was classified as a CD19-positive relapse. Positive relapse is usually due to low potency or CAR-T cell loss. Several factors limit CAR-T cell power and efficacy, including limited long-term persistence, immunosuppressive tumor microenvironment, and intrinsic dysfunction associated with T cell exhaustion (30–33).

In some cases of treatment failure, secondary infusions of CD19 CAR-T cells were not reproducibly successful if the CD19 expression in leukemic cells remained high, possibly partly due to immune-mediated clearance of murine scFv CAR-T cells (34–36). Previous studies have shown that humanized CAR-T remains effective in patients who relapsed after murine scFv CAR-T cells treatment (37, 38). Therefore, we treated the patient with a second humanized CD19 CAR-T, resulting in a reduction of the patient's lesions. In this patient, the expression rate of CD19 was still very high at the time of recurrence (Figure 2A). Among patients with CD19-positive ALL who relapsed after murine scFv CD19 CAR-T treatment, the humanized CD19 CAR-T CR rate (50%–64%) was still lower than in patients who had not received CAR-T therapy (37, 38). We believe that it may be caused by the resistance of tumor cells to CD19 CAR-T, and the mechanism needs to be further studied. In contrast, approximately 80% of patients with ALL after CD19 CAR-T cell therapy had CR after CD22 CAR-T

cell therapy, which was not different from patients who did not receive CD19 CAR-T cell therapy (20, 39). Although we did not detect the mean fluorescence intensity (MFI) of CD19 and CD22, CD19 and CD22 in Figure 2A were analyzed by Image-Pro Plus software through the method of Liu X et al. (40). The mean density of CD19 (0.32 ± 0.01) was higher than that of CD22 (0.21 ± 0.00), indicating that the expression intensity of CD19 was still very high. The success of CD22 CAR-T may be due to the resistance of tumor cells to CD19 CAR-T at this time, but not to CD22 CAR-T.

The third CAR-T cell therapy yielded surprising results, with the patient's lesions continuing to shrink with no significant activity. We also found a positive correlation between CAR-T cell expansion and the efficacy of the second and third CAR-T therapy in the same patient. The inflammatory cytokines IFN γ , IL-2R, TNF α , and IL-6 also showed a positive correlation with CAR-T efficacy (Supplementary Figure 1). Treg cells inhibit excessive immune responses by expressing CTLA4 and secreting IL-10 and TGF β (41), reflected in changes to Treg and IL-6 levels along with changes in inflammatory cytokines.

Relapse is observed in 30–60% of patients with acute lymphoblastic leukemia after CD19 CAR-T cell therapy, mostly within one year (16, 19, 28, 42, 43). Data from both murine studies and integration site analysis after adoptive T cell transfer in humans suggest that long-term persisting T cells are predominantly derived from stem cell-like memory T cells

(TSCM) and central memory T cell (TCM) compartments of the infused product (44). In this patient, effective memory T Cell (TEM) increased after three CAR-T cell treatments and only began to decrease six days after the second CAR-T cell treatment. TCM increased significantly after the first and third treatments (17.1% and 14.4%, respectively) and increased to 4% after the second treatment (Figure 2B). Our data suggest that this is also likely to be true after CAR-T cell therapy.

In some studies, CAR-T therapies result in antigen escape/loss, and the rate of CD19-negative recurrence in ALL patients is 7%–25% (14–16, 34, 45, 46), while more patients have CD19-positive recurrence. To combat immune escape, studies continue to combine CAR T cells with radiation (47), checkpoint suppression (48), vaccines (49), or other immune agonists (50, 51). Another approach is to simultaneously target more than one antigen on cancer cells, such as CD19, CD20, and CD22 (20, 52–54). We believe that even if patient antigen escapes/loss, other antigens can still be searched, and more studies are still in progress. Summers et al. (55) showed no benefit of a second allogeneic HSCT after CAR-T treatment for patients with recurrence after HSCT. Moreover, the outcome of the second HSCT is usually worse in B-ALL patients (56–58). This patient is currently in sustained remission 14 months after the third CAR-T treatment, and we will continue to follow him closely.

By comparing the results of different CAR-T cells in the same patient, this case suggests that multiple CAR-T therapies is effective and safe in both intramedullary and extramedullary recurrence in the same patient and that CAR-T cell expansion and inflammatory cytokine release are positively associated with its efficacy. Further clinical studies with large sample sizes are needed for further clarification.

Data availability statement

The original contributions presented in the study are included in the article/Supplementary Material. Further inquiries can be directed to the corresponding author.

References

1. Hunger SP, Mullighan CG. Acute lymphoblastic leukemia in children. *N Engl J Med* (2015) 373(16):1541–52. doi: 10.1056/NEJMra1400972
2. Sun W, Malvar J, Spoto R, Verma A, Wilkes JJ, Dennis R, et al. Outcome of children with multiply relapsed b-cell acute lymphoblastic leukemia: a therapeutic advance in childhood leukemia & lymphoma study. *Leukemia* (2018) 32(11):2316–25. doi: 10.1038/s41375-018-0094-0
3. Sellar RS, Rowntree C, Vora AJ, Furness CL, Goulden N, Mitchell C, et al. Relapse in teenage and young adult patients treated on a paediatric minimal residual disease stratified ALL treatment protocol is associated with a poor

Ethics statement

The studies involving human participants were reviewed and approved by The Ethical Committee of the 960th Hospital of the People's Liberation Army. Written informed consent to participate in this study was provided by the participants' legal guardian/next of kin.

Author contributions

LD and FZ contributed to data collection, data analyses, wrote the draft of the paper and had final responsibility to submit for publication. QW, XY, QW, XS, WL, and YH contributed to clinical protocol. All authors contributed to the article and approved the submitted version.

Conflict of interest

The authors declare that the research was conducted in the absence of any commercial or financial relationships that could be construed as a potential conflict of interest.

Publisher's note

All claims expressed in this article are solely those of the authors and do not necessarily represent those of their affiliated organizations, or those of the publisher, the editors and the reviewers. Any product that may be evaluated in this article, or claim that may be made by its manufacturer, is not guaranteed or endorsed by the publisher.

Supplementary material

The Supplementary Material for this article can be found online at: <https://www.frontiersin.org/articles/10.3389/fimmu.2022.1039929/full#supplementary-material>

outcome: results from UKALL2003. *Br J Haematol* (2018) 181(4):515–22. doi: 10.1111/bjh.15208

4. Bacher U, Klyuchnikov E, Le-Rademacher J, Carreras J, Armand P, Bishop MR, et al. Conditioning regimens for allotransplants for diffuse large b-cell lymphoma: myeloablative or reduced intensity? *Blood* (2012) 120(20):4256–62. doi: 10.1182/blood-2012-06-436725

5. Pavletic SZ, Kumar S, Mohty M, de Lima M, Foran JM, Pasquini M, et al. NCI first international workshop on the biology, prevention, and treatment of relapse after allogeneic hematopoietic stem cell transplantation: report from the committee

on the epidemiology and natural history of relapse following allogeneic cell transplantation. *Biol Blood Marrow Transplant* (2010) 16(7):871–90. doi: 10.1016/j.bbmt.2010.04.004

6. Porter DL, Alyea EP, Antin JH, DeLima M, Estey E, Falkenburg JH, et al. NCI first international workshop on the biology, prevention, and treatment of relapse after allogeneic hematopoietic stem cell transplantation: report from the committee on treatment of relapse after allogeneic hematopoietic stem cell transplantation. *Biol Blood Marrow Transplant* (2010) 16(11):1467–503. doi: 10.1016/j.bbmt.2010.08.001

7. Roddie C, Peggs KS. Donor lymphocyte infusion following allogeneic hematopoietic stem cell transplantation. *Expert Opin Biol Ther* (2011) 11(4):473–87. doi: 10.1517/14712598.2011.554811

8. Avivi I, Stroopinsky D, Katz T. Anti-CD20 monoclonal antibodies: beyond b-cells. *Blood Rev* (2013) 27(5):217–23. doi: 10.1016/j.blre.2013.07.002

9. Li Z, Wang M, Yao X, Li H, Li S, Liu L, et al. Development of novel anti-CD19 antibody-drug conjugates for b-cell lymphoma treatment. *Int Immunopharmacol* (2018) 62:299–308. doi: 10.1016/j.intimp.2018.06.034

10. Lejeune M, Köse MC, Duray E, Einsele H, Beguin Y, Caers J. Bispecific, T-Cell-Recruiting antibodies in b-cell malignancies. *Front Immunol* (2020) 11:762. doi: 10.3389/fimmu.2020.00762

11. Kantarjian HM, DeAngelo DJ, Stelljes M, Martinelli G, Liedtke M, Stock W, et al. Inotuzumab ozogamicin versus standard therapy for acute lymphoblastic leukemia. *N Engl J Med* (2016) 375(8):740–53. doi: 10.1056/NEJMoa1509277

12. Kantarjian H, Stein A, Gökbuğut N, Fielding AK, Schuh AC, Ribera JM, et al. Blinatumomab versus chemotherapy for advanced acute lymphoblastic leukemia. *N Engl J Med* (2017) 376(9):836–47. doi: 10.1056/NEJMoa1609783

13. Watanabe N, Mo F, McKenna MK. Impact of manufacturing procedures on CAR T cell functionality. *Front Immunol* (2022) 13:876339. doi: 10.3389/fimmu.2022.876339

14. Maude SL, Laetsch TW, Buechner J, Rives S, Boyer M, Bittencourt H, et al. Tisagenlecleucel in children and young adults with b-cell lymphoblastic leukemia. *N Engl J Med* (2018) 378(5):439–48. doi: 10.1056/NEJMoa1709866

15. Maude SL, Teachey DT, Rheingold SR, Shaw PA, Aplenc R, Barrett DM, et al. Sustained remissions with CD19-specific chimeric antigen receptor (CAR)-modified T cells in children with relapsed/refractory ALL. *J Clin Oncol* (2016) 34: Suppl 15:3011–1. doi: 10.1200/JCO.2016.34.15

16. Maude SL, Frey N, Shaw PA, Aplenc R, Barrett DM, Bunin NJ, et al. Chimeric antigen receptor T cells for sustained remissions in leukemia. *N Engl J Med* (2014) 371(16):1507–17. doi: 10.1056/NEJMoa1407222

17. Lee DW, Stetler-Stevenson M, Yuan CM, Fry TJ, Shah NN, Delbrook C, et al. Safety and response of incorporating CD19 chimeric antigen receptor T cell therapy in typical salvage regimens for children and young adults with acute lymphoblastic leukemia. *Blood* (2015) 126:684. doi: 10.1182/blood.V126.23.684.684

18. Kenderian SS, Porter DL, Gill S. Chimeric antigen receptor T cells and hematopoietic cell transplantation: How not to put the CART before the horse. *Biol Blood Marrow Transplant* (2017) 23(2):235–46. doi: 10.1016/j.bbmt.2016.09.002

19. Lee DW, Kochenderfer JN, Stetler-Stevenson M, Cui YK, Delbrook C, Feldman SA, et al. T Cells expressing CD19 chimeric antigen receptors for acute lymphoblastic leukaemia in children and young adults: a phase 1 dose-escalation trial. *Lancet* (2015) 385(9967):517–28. doi: 10.1016/S0140-6736(14)61403-3

20. Fry TJ, Shah NN, Orentas RJ, Stetler-Stevenson M, Yuan CM, Ramakrishna S, et al. CD22-targeted CAR T cells induce remission in b-ALL that is naive or resistant to CD19-targeted CAR immunotherapy. *Nat Med* (2018) 24(1):20–8. doi: 10.1038/nm.4441

21. Lee DW, Gardner R, Porter DL, Louis CU, Ahmed N, Jensen M, et al. Current concepts in the diagnosis and management of cytokine release syndrome. *Blood* (2014) 124(2):188–95. doi: 10.1182/blood-2014-05-552729

22. Nguyen HTK, Terao MA, Green DM, Pui CH, Inaba H. Testicular involvement of acute lymphoblastic leukemia in children and adolescents: Diagnosis, biology, and management. *Cancer* (2021) 127(17):3067–81. doi: 10.1002/cncr.33609

23. Ding LW, Sun QY, Mayakonda A, Tan KT, Chien W, Lin DC, et al. Mutational profiling of acute lymphoblastic leukemia with testicular relapse. *J Hematol Oncol* (2017) 10(1):65. doi: 10.1186/s13045-017-0434-y

24. Hijiya N, Liu W, Sandlund JT, Jeha S, Razzouk BI, Ribeiro RC, et al. Overt testicular disease at diagnosis of childhood acute lymphoblastic leukemia: lack of therapeutic role of local irradiation. *Leukemia* (2005) 19(8):1399–403. doi: 10.1038/sj.leu.2403843

25. Chen X, Wang Y, Ruan M, Li J, Zhong M, Li Z, et al. Treatment of testicular relapse of b-cell acute lymphoblastic leukemia with CD19-specific chimeric antigen receptor T cells. *Clin Lymphoma Myeloma Leuk*. (2020) 20(6):366–70. doi: 10.1016/j.clml.2019.10.016

26. Rubinstein JD, Krupski C, Nelson AS, O'Brien MM, Davies SM, Phillips CL. Chimeric antigen receptor T cell therapy in patients with multiply relapsed or

refractory extramedullary leukemia. *Biol Blood Marrow Transplant* (2020) 26(11): e280–5. doi: 10.1016/j.bbmt.2020.07.036

27. Yu J, Hu Y, Pu C, Liang Z, Cui Q, Zhang H, et al. Successful chimeric Ag receptor modified T cell therapy for isolated testicular relapse after hematopoietic cell transplantation in an acute lymphoblastic leukemia patient. *Bone Marrow Transplant* (2017) 52(7):1065–7. doi: 10.1038/bmt.2017.64

28. Gardner R, Wu D, Cherian S, Fang M, Hanafi LA, Finney O, et al. Acquisition of a CD19-negative myeloid phenotype allows immune escape of MLL- rearranged b-ALL from CD19 CAR-t-cell therapy. *Blood* (2016) 127:2406–10. doi: 10.1182/blood-2015-08-665547

29. Park JH, Riviere I, Wang X, Bernal YB, Yoo S, Purdon T, et al. CD19-targeted 19–28z CAR-modified autologous T cells induce high rates of complete remission and durable responses in adult patients with relapsed, refractory b-cell ALL. *Blood* (2014) 124:382. doi: 10.1182/blood.V124.21.382.382

30. Fraietta JA, Lacey SF, Orlando EJ, Pruteanu-Malinici I, Gohil M, Lundh S, et al. Determinants of response and resistance to CD19 chimeric antigen receptor (CAR) T cell therapy of chronic lymphocytic leukemia. *Nat Med* (2018) 24:563–71. doi: 10.1038/s41591-018-0010-1

31. Long AH, Highfill SL, Cui Y, Smith JP, Walker AJ, Ramakrishna S, et al. Reduction of MDSCs with all-trans retinoic acid improves CAR therapy efficacy for sarcomas. *Cancer Immunol Res* (2016) 4:869–80. doi: 10.1158/2326-6066.CIR-15-0230

32. Lynn RC, Weber EW, Sotillo E, Gennert D, Xu P, Good Z, et al. C-jun overexpression in CAR T cells induces exhaustion resistance. *Nature* (2019) 576:293–300. doi: 10.1038/s41586-019-1805-z

33. Long AH, Haso WM, Shern JF, Wanhainen KM, Murgai M, Ingaramo M, et al. 4-1BB costimulation ameliorates T cell exhaustion induced by tonic signaling of chimeric antigen receptors. *Nat Med* (2015) 21(6):581–90. doi: 10.1038/nm.3838

34. Turtle CJ, Hanafi LA, Berger C, Gooley TA, Cherian S, Hudecek M, et al. CD19 CAR-T cells of defined CD4+:CD8+ composition in adult b cell ALL patients. *J Clin Invest* (2016) 126(6):2123–38. doi: 10.1172/JCI85309

35. Jain MD, Davila ML. Concise review: Emerging principles from the clinical application of chimeric antigen receptor T cell therapies for b cell malignancies. *Stem Cells* (2018) 36(1):36–44. doi: 10.1002/stem.2715

36. Cao J, Wang G, Cheng H, Wei C, Qi K, Sang W, et al. Potent anti-leukemia activities of humanized CD19-targeted chimeric antigen receptor T (CAR-T) cells in patients with relapsed/refractory acute lymphoblastic leukemia. *Am J Hematol* (2018) 93(7):851–8. doi: 10.1002/ajh.25108

37. Myers RM, Li Y, Barz Leahy A, Barrett DM, Barrett DM, Teachey DT, Callahan C, et al. Humanized CD19-targeted chimeric antigen receptor (CAR) T cells in CAR-naïve and CAR-exposed children and young adults with relapsed or refractory acute lymphoblastic leukemia. *J Clin Oncol* (2021) 39(27):3044–55. doi: 10.1200/JCO.20.03458

38. Maude SL, Barrett DM, Rheingold SR, Aplenc R, Teachey DT, Callahan C, et al. Efficacy of humanized CD19-targeted chimeric antigen receptor (CAR)-modified T cells in children and young adults with relapsed/refractory acute lymphoblastic leukemia. *Blood* (2016) 128:217–1217. doi: 10.1182/blood.V128.22.217.217

39. Shah NN, Highfill SL, Shalabi H, Yates B, Jin J, Wolters PL, et al. CD4/CD8 T-cell selection affects chimeric antigen receptor (CAR) T-cell potency and toxicity: Updated results from a phase I anti-CD22 CAR T-cell trial. *J Clin Oncol* (2020) 38(17):1938–50. doi: 10.1200/JCO.19.03279

40. Liu X, Ren X, Zhou L, Liu K, Deng L, Qing Q, et al. Tollip orchestrates macrophage polarization to alleviate intestinal mucosal inflammation. *J Crohns Colitis* (2022) 16(7):1151–67. doi: 10.1093/ecco-jcc/jjac019

41. Yu L, Yang F, Zhang F, Guo D, Li L, Wang X, et al. CD69 enhances immunosuppressive function of regulatory T-cells and attenuates colitis by prompting IL-10 production. *Cell Death Dis* (2018) 9(9):905. doi: 10.1038/s41419-018-0927-9

42. Brentjens RJ, Davila ML, Riviere I, Park J, Wang X, Cowell LG, et al. CD19-targeted T cells rapidly induce molecular remissions in adults with chemotherapy-refractory acute lymphoblastic leukemia. *Sci Transl Med* (2013) 5(177):177ra38. doi: 10.1126/scitranslmed.3005930

43. Brentjens RJ, Riviere I, Park JH, Davila ML, Wang X, Stefanski J, et al. Safety and persistence of adoptively transferred autologous CD19-targeted T cells in patients with relapsed or chemotherapy refractory b-cell leukemias. *Blood* (2011) 118(18):4817–28. doi: 10.1182/blood-2011-04-348540

44. Rivat C, Izotova N, Richardson R, Pellin D, Hough R, Wynn R, et al. Clonal dynamics of early responder and long-term surviving CAR-T cells in humans. *Blood* (2019) 134(Supplement_1):52. doi: 10.1182/blood-2019-125916

45. Rabilloud T, Potier D, Pankaew S, Nozais M, Loosveld M, Payet-Bornet D, et al. Single-cell profiling identifies pre-existing CD19-negative subclones in a b-ALL patient with CD19-negative relapse after CAR-T therapy. *Nat Commun* (2021) 12(1):865. doi: 10.1038/s41467-021-21168-6

46. Lee DW, Stetler-Stevenson M, Yuan CM, Shah NN, Delbrook C, Yates B, et al. Long-term outcomes following CD19 CAR T cell therapy for b-ALL are

superior in patients receiving a fludarabine/cyclophosphamide preparative regimen and post-CAR hematopoietic stem cell transplantation. *Blood* (2016) 128:218–8. doi: 10.1182/blood.V128.22.218.218

47. Weiss T, Weller M, Guckenberger M, Sentman CL, Roth P. NKG2D-based CAR T cells and radiotherapy exert synergistic efficacy in glioblastoma. *Cancer Res* (2018) 78:1031–43. doi: 10.1158/0008-5472.CAN-17-1788

48. Li S, Siriwon N, Zhang X, Yang S, Jin T, He F, et al. Enhanced cancer immunotherapy by chimeric antigen receptor-modified T cells engineered to secrete checkpoint inhibitors. *Clin Cancer Res* (2017) 23:6982–92. doi: 10.1158/1078-0432.CCR-17-0867

49. Tanaka M, Tashiro H, Omer B, Lapteva N, Ando J, Ngo M, et al. Vaccination targeting native receptors to enhance the function and proliferation of chimeric antigen receptor (CAR)-modified T cells. *Clin Cancer Res* (2017) 23:3499–509. doi: 10.1158/1078-0432.CCR-16-2138

50. Majzner RG, Heitzeneder S, Mackall CL. Harnessing the immunotherapy revolution for the treatment of childhood cancers. *Cancer Cell* (2017) 31:476–85. doi: 10.1016/j.ccell.2017.03.002

51. Khalil DN, Smith EL, Brentjens RJ, Wolchok JD. The future of cancer treatment: immunomodulation, CARs and combination immunotherapy. *Nat Rev Clin Oncol* (2016) 13:273–90. doi: 10.1038/nrclinonc.2016.25

52. Zah E, Lin MY, Silva-Benedict A, Jensen MC, Chen YY. T Cells expressing CD19/CD20 bispecific chimeric antigen receptors prevent antigen escape by malignant b cells. *Cancer Immunol Res* (2016) 4:498–508. doi: 10.1158/2326-6066.CIR-15-0231

53. Schneider D, Xiong Y, Wu D, Nlle V, Schmitz S, Haso W, et al. A tandem CD19/CD20 CAR lentiviral vector drives on-target and off-target antigen

modulation in leukemia cell lines. *J Immunother Cancer* (2017) 5:42. doi: 10.1186/s40425-017-0246-1

54. Fousek K, Watanabe J, George A, An X, Samaha H, Navai SA, et al. Targeting primary pre-b cell acute lymphoblastic leukemia and CD19-negative relapses using trivalent CAR T cells. *Blood* (2017) 130:4614–4. doi: 10.1182/blood.V130.Suppl_1.4614.4614

55. Summers C, Wu QV, Annesley C, Bleakley M, Dahlberg A, Narayanaswamy P, et al. Hematopoietic cell transplantation after CD19 chimeric antigen receptor T cell-induced acute lymphoblastic lymphoma remission confers a leukemia-free survival advantage. *Transplant Cell Ther* (2022) 28(1):21–9. doi: 10.1016/j.jtct.2021.10.003

56. Lund TC, Ahn KW, Tecca HR, Hilgers MV, Abdel-Azim H, Abraham A, et al. Outcomes after second hematopoietic cell transplantation in children and young adults with relapsed acute leukemia. *Biol Blood Marrow Transplant* (2019) 25:301–6. doi: 10.1016/j.bbmt.2018.09.016

57. Yaniv I, Krauss AC, Beohou E, Dalissier A, Corbacioglu S, Zecca M, et al. Second hematopoietic stem cell transplantation for post-transplantation relapsed acute leukemia in children: A retrospective EBMT-PDWP study. *Biol Blood Marrow Transplant* (2018) 24(8):1629–42. doi: 10.1016/j.bbmt.2018.03.002

58. Kharfan-Dabaja MA, Labopin M, Bazarbachi A, Ciceri F, Finke J, Bruno B, et al. Comparing outcomes of a second allogeneic hematopoietic cell transplant using HLA-matched unrelated versus T-cell replete haploidentical donors in relapsed acute lymphoblastic leukemia: a study of the acute leukemia working party of EBMT. *Bone Marrow Transplant* (2021) 56(9):2194–202. doi: 10.1038/s41409-021-01317-7



OPEN ACCESS

EDITED BY

Catherine Sautes-Fridman,
INSERM U1138 Centre de Recherche
des Cordeliers (CRC), France

REVIEWED BY

Yuri Matteo Falzone,
San Raffaele Scientific Institute
(IRCCS), Italy
Nilo Riva,
San Raffaele Hospital (IRCCS), Italy

*CORRESPONDENCE

Guanqiao You
youguanqiao@163.com
Wei Li
liwei71@126.com

SPECIALTY SECTION

This article was submitted to
Cancer Immunity
and Immunotherapy,
a section of the journal
Frontiers in Oncology

RECEIVED 25 July 2022

ACCEPTED 02 November 2022

PUBLISHED 21 November 2022

CITATION

Liu H, Dong Z, Zhang M, Pang R, Xu J,
He P, Mei W, Zhang S, You G and Li W
(2022) Case report: Complex
paraneoplastic syndromes in thymoma
with nephrotic syndrome, cutaneous
amyloidosis, myasthenia gravis, and
Morvan's syndrome.
Front. Oncol. 12:1002808.
doi: 10.3389/fonc.2022.1002808

COPYRIGHT

© 2022 Liu, Dong, Zhang, Pang, Xu, He,
Mei, Zhang, You and Li. This is an open-
access article distributed under the
terms of the [Creative Commons
Attribution License \(CC BY\)](https://creativecommons.org/licenses/by/4.0/). The use,
distribution or reproduction in other
forums is permitted, provided the
original author(s) and the copyright
owner(s) are credited and that the
original publication in this journal is
cited, in accordance with accepted
academic practice. No use,
distribution or reproduction is
permitted which does not comply with
these terms.

Case report: Complex paraneoplastic syndromes in thymoma with nephrotic syndrome, cutaneous amyloidosis, myasthenia gravis, and Morvan's syndrome

Huiqin Liu¹, Zeqin Dong¹, Milan Zhang¹, Rui Pang¹, Jiajia Xu¹,
Pan He², Wenli Mei³, Shuai Zhang⁴,
Guanqiao You^{2*} and Wei Li^{1*}

¹Department of Neurology, Henan Provincial People's Hospital, Zhengzhou, China, ²Department of Nephrology, Henan Provincial People's Hospital, Zhengzhou, China, ³Department of Electromyography, Henan Provincial People's Hospital, Zhengzhou, China, ⁴Department of Dermatology, Henan Provincial People's Hospital, Zhengzhou, China

Background: Apart from myasthenia gravis (MG), thymoma is associated with a wide spectrum of autoimmune paraneoplastic syndromes (PNSs). Here, we report on a rare case presenting with four different PNSs, namely, MG, membranous nephropathy, cutaneous amyloidosis, and Morvan's syndrome associated with thymoma.

Case presentation: A middle-aged man was frequently hospitalized because of nephrotic syndrome (stage I membranous nephropathy), cutaneous amyloidosis, and MG with acetylcholine receptor (AChR) antibody and titin antibody positivity. Chest CT showed a thymic mass in the left anterior mediastinum, and he received intravenous immunoglobulin (IVIG), methylprednisolone pulse therapy, thoracoscopic thymoma resection, and radiotherapy. Postoperative pathological examination revealed a type B2 thymoma. During the perioperative stage, his electrocardiogram (ECG) showed myocardial infarction-like ECG changes; however, his levels of cardiac enzymes and troponin were normal, and he had no symptoms of precordial discomfort. Six months after thymectomy, his nephrotic syndrome and MG symptoms were relieved; however, he presented with typical manifestations of Morvan's syndrome, including neuromyotonia, severe insomnia, abnormal ECG activity, and antibodies against leucine-rich glioma-inactivated 1 (LGI1) and γ -amino-butyric acid-B receptor (GABABR). His symptoms did not improve after repeated IVIG and steroid therapies. Finally, he received low-dose rituximab, and his symptoms gradually resolved.

Conclusion: This case serves to remind us that apart from MG, thymoma is also associated with other autoimmune PNSs such as membranous nephropathy, cutaneous amyloidosis, and Morvan's syndrome. Autoimmune PNSs can present concurrently with or after surgical or medical therapy for thymoma. For Morvan's syndrome post-thymectomy with LGI1 antibody positivity, B-cell depletion therapy such as intravenous rituximab is an effective treatment.

KEYWORDS

thymoma, myasthenia gravis, membranous nephropathy, cutaneous amyloidosis, morvan's syndrome, paraneoplastic syndromes, leucine-rich glioma inactivated 1

Introduction

Apart from myasthenia gravis (MG), thymoma is also associated with a wide spectrum of autoimmune paraneoplastic syndromes (PNSs), including systemic lupus erythematosus, autoimmune cytopenia, neuromyotonia, Morvan's syndrome, limbic encephalitis, polymyositis, Good's syndrome, autoimmune thyroid diseases, autoimmune hepatitis, and cutaneous autoimmune disorders (1–6). The clinical manifestations of PNSs associated with thymomas pose a challenge to clinicians because of the need to decipher the association between the presenting symptoms and the underlying mass. Here, we report a rare case of four different PNSs associated with thymoma: nephrotic syndrome (stage I membranous nephropathy), cutaneous amyloidosis, MG with acetylcholine receptor (AChR) and titin antibodies, and Morvan's syndrome post-thymectomy with antibodies against leucine-rich glioma-inactivated 1 (LGI1) and γ -amino-butyric acid-B receptor (GABABR). The symptoms of nephrotic syndrome, cutaneous amyloidosis, and MG gradually improved after receiving intravenous immunoglobulin (IVIG), steroids, thoracoscopic thymoma resection, and radiotherapy. The symptoms of Morvan's syndrome post-thymectomy did not improve after receiving IVIG and oral steroids but were relieved after receiving intravenous rituximab therapy.

Case presentation

A 49-year-old male patient was admitted to the Department of Nephrology of Henan Provincial People's Hospital on 23

March 2020. He presented with symptoms of edema of both lower limbs for 2 months and eyelid edema for 15 days. Physical examination showed pitting edema of both legs, edema of double eyelids, and extensive pigmentation of the skin of the whole body. The patient subsequently underwent a series of examinations. The results showed that his level of 24-h urinary protein was 21.72 g/L, level of serum albumin was 9.5 g/L, serum total cholesterol was 9.07 mmol/L, creatinine was 125 μ mol/L, and titer of antinuclear antibody (ANA) was 1:1,000, and he was also positive for anti-histone antibody (AHA). His electrocardiogram (ECG) at that time was normal. This patient underwent kidney biopsy, and the biopsy revealed that there was mild thickening of the glomerular basement membrane, normal mesangial cellularity, and no interstitial fibrosis or tubular atrophy. Immunofluorescence staining showed granular deposits along the capillary walls for IgG, C3, kappa, and lambda light chains, and electron microscopy showed subepithelial electron-dense deposits. Based on the above observations, the patient was diagnosed with stage I membranous nephropathy (Figure 1). This patient also underwent skin biopsy, where pathology showed cutaneous amyloidosis (Figure 1). He received methylprednisolone at an initial dosage of 40 mg per day and intravenous cyclophosphamide at a total dose of 2 g, with steroids tapered down gradually. In addition, he received treatment such as intravenous albumin supplementation and diuresis.

Four months after the above examinations, the patient was rehospitalized in our hospital for follow-up on 10 August 2020. The edema of his legs and eyelids had disappeared, the concentration of 24-h urinary protein decreased to 0.77 g/L, and the serum creatinine level had returned to normal. Thus, the steroid dosage was tapered to 20 mg/day. However, the patient complained of weakness in his neck and both hands, as well as chest distress, shortness of breath, inability to lie flat, and dysphagia. These symptoms were indicative of the fatigue phenomenon. Subsequent neostigmine test results were positive, while repetitive nerve stimulation showed 51.4% and 31% decremental compound muscle action potential responses at low- and high-stimulation frequencies, respectively. The

Abbreviations: MG, myasthenia gravis; PNSs, paraneoplastic syndromes; AChR, acetylcholine receptor; LGI1, leucine-rich glioma-inactivated 1; GABABR, γ -amino-butyric acid-B receptor; ANA, antinuclear antibody; AHA, anti-histone antibody; ECG, electrocardiogram; CT, computed tomography; EMG, electromyography; ANCA, anti-neutrophil cytoplasmic antibody; CASPR2, contactin-associated protein 2; AMPA, alpha-amino-3-hydroxy-5-methyl-4-iso-oxazepropionic acid; aNMT, acquired neuromyotonia.

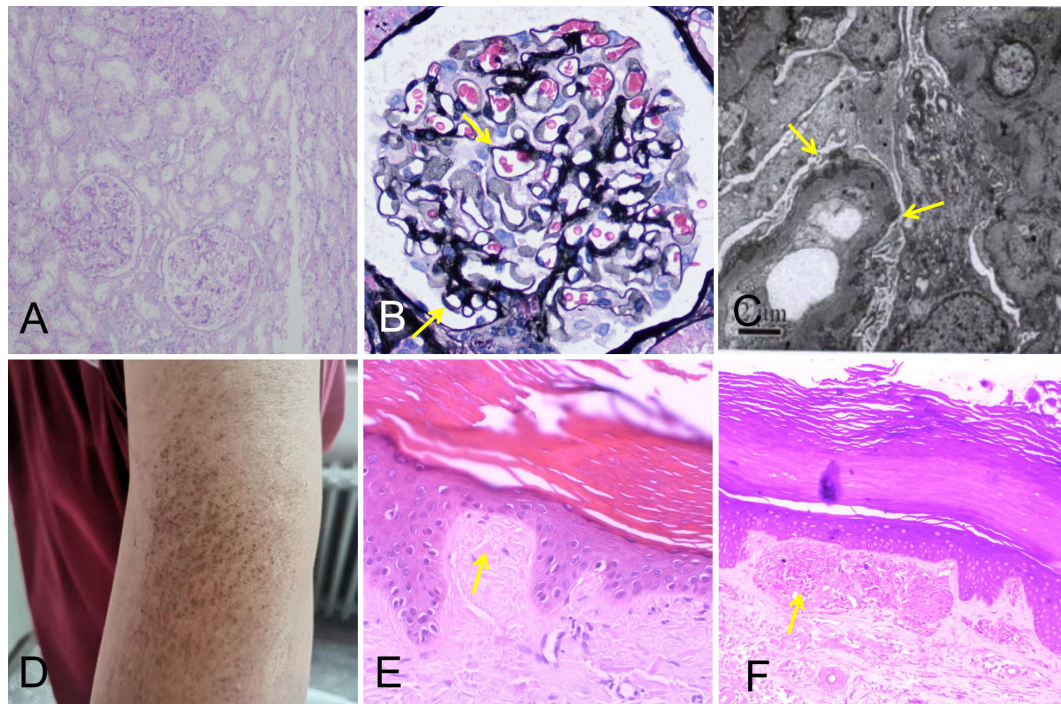


FIGURE 1

Kidney biopsy findings showing stage I membranous nephropathy (A–C). (A) Normal mesangial cellularity (periodic acid–Schiff; original magnification, x100). (B) Slight global glomerular basement membrane thickening (yellow arrows; Jones methenamine silver; original magnification, x400). (C) Subepithelial electron-dense deposits, partially in the glomerular basement membrane (yellow arrows; original magnification, x4,000). (D) Skin lesions on the patient's left upper arm. (E, F) Skin biopsy findings showing cutaneous amyloidosis. (E) The skin specimen stained by hematoxylin–eosin revealed parakeratosis with focal hyperkeratosis, widened dermal papilla, and an amorphous red-stained mass substance (yellow arrow; x400). (F) The skin specimen stained by crystal violet was positive (yellow arrow; x400).

patient underwent chest computed tomography (CT), which revealed a thymic mass in the left anterior mediastinum (Figure 2). Antibodies associated with MG in his serum were tested and demonstrated the following: the level of AChR antibody was higher than 320 nmol/L, and his titin antibody was also strongly positive.

The patient was diagnosed with thymoma-associated MG based on the observations above and received treatments such as IVIG at a dose of 0.4 g/kg/day * 5 days, methylprednisolone pulse therapy, and pyridostigmine administration. His muscle weakness then gradually improved. Subsequently, the patient underwent thoracoscopic thymoma resection using the subxiphoid approach under general anesthesia. The size of the thymus tissue examined was 5 × 3 × 1.5 cm, and its pathological diagnosis was type B2 thymoma. After surgery, the patient was transferred to the intensive care unit for respiratory support, anti-infection treatment, and immunomodulatory treatment. During this period, his ECG showed acute anterior, lateral, and high lateral myocardial infarctions (Figure 2); however, the myocardial enzyme profile and troponin levels were normal, and he had no symptoms of precordial discomfort.

After a period of recovery, he was transferred to the oncology department for radiotherapy. The patient was discharged on 28 November 2020. At that time, his symptoms of MG were relieved, the level of AChR antibody decreased to 19.6 nmol/L, and he was able to take care of himself.

In the following 6 months, the patient received oral prednisone and pyridostigmine bromide with regular follow-up. On 15 April 2021, the patient was readmitted for follow-up. His nephrotic syndrome and MG symptoms were relieved with 10 mg of oral prednisone per day. However, he complained of diffuse muscle twitching within the last week, as well as limb pain, blurred vision, and poor sleep. He could only sleep for 1–2 h every night. Physical examination revealed extensive myokymia in the limbs and trunk involving spontaneous, continuous, undulated muscle movements, similar to a bag of worms under the skin (Video 1). Needle electromyography (EMG) showed duplet, triplet, and multiplet bursts of spontaneous motor unit discharges in the tested muscles of the limbs at rest, and after discharges were observed in the F wave, suggesting peripheral nerve hyperexcitability syndrome (Figure 2). His ECG showed abnormal Q waves in the inferior

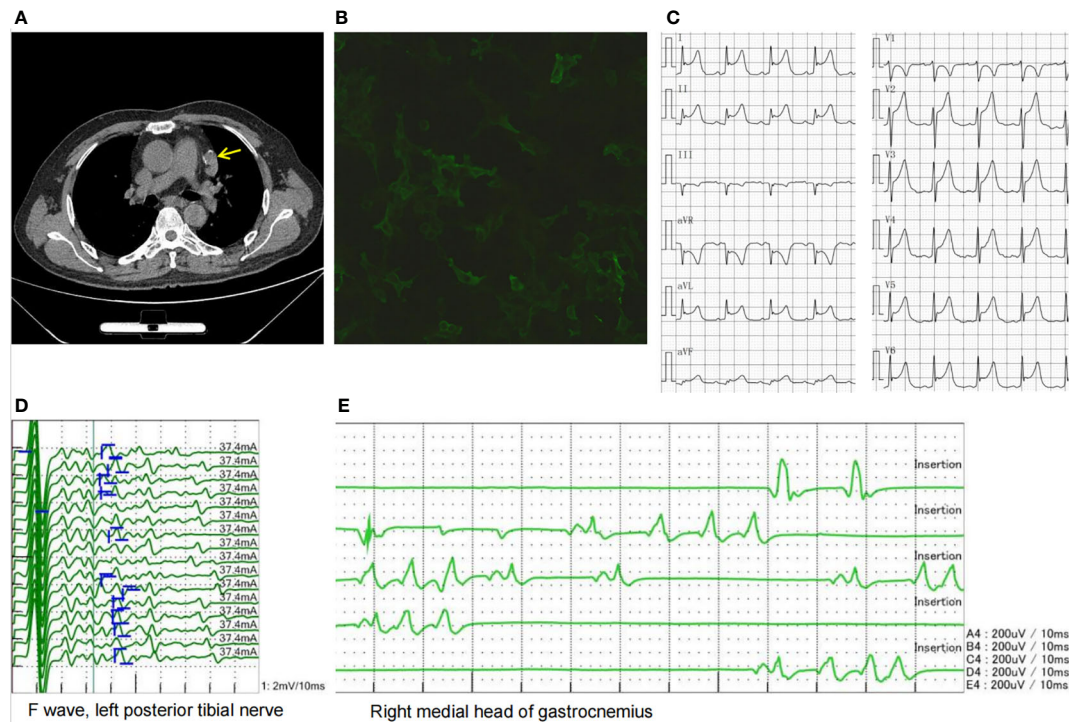


FIGURE 2

(A) Chest CT showing a thymic mass in the left anterior mediastinum (yellow arrow). (B) LGI1 antibody cell-based assay showing a 1:32 positive ratio. (C) ECG showing acute anterior, lateral, and high lateral myocardial infarction-like ECG changes. (D) Afterdischarges were observed in the F wave. (E) Needle EMG showing duplet, triplet, and multiplet bursts of spontaneous motor unit discharges in the tested muscles of the limbs at rest suggestive of myokymia. CT, computed tomography; LGI1, leucine-rich glioma-inactivated 1; ECG, electrocardiogram; EMG, electromyography.

wall leads and an ST-segment elevation of 1–1.5 mm. Blood tests showed that apart from ANA and AHA, anti-neutrophil cytoplasmic antibody (ANCA) was also positive. The patient's serum was also tested for antibodies to cell-surface antigens, including N-methyl-D-aspartate receptor, LGI1, contactin-associated protein 2 (CASPR2), GABABR, and alpha-amino-3-hydroxy-5-methyl-4-iso-xazolepropionic acid (AMPA) receptors (EUROIMMUN, Germany), and the results showed that antibodies against LGI1 and GABABR were both positive, with titers of 1:32 (Figure 2) and 1:10, respectively. The patient was diagnosed with Morvan's syndrome and treated with IVIG at a dose of 0.4 g/kg/day for 5 days and oral steroids; however, his symptoms of myokymia and insomnia did not improve 1 month later. Considering that the patient's immune test indicated that he was in an immunosuppressive state at the time, he was treated with low-dose rituximab (7, 8) at a dose of 100 mg/week for 4 weeks. During the follow-up 1 month later, the muscle twitching, limb pain, and insomnia symptoms were significantly improved. Subsequently, the patient received 100 mg of rituximab intravenously every 6 months, and his symptoms have not recurred for 1 year. The timeline of the diagnosis and treatment is shown in Figure 3.

Discussion

Thymomas are epithelial tumors arising from the thymus and are the most commonly found tumors in the anterior mediastinum. Approximately 40%–50% of thymomas present with PNSs (5, 9). It has been noted that 25%–40% of patients with thymoma present with MG, and more than 15% of patients diagnosed with thymoma present with a PNS other than MG (2, 4, 10, 11). PNSs can be antibody- or non-antibody-mediated, leading to both organ-specific and systemic effects (2, 4, 11). Approximately one-third of patients with PNSs have two or more conditions (9). PNSs can also present before, concurrently with, or after surgical or medical therapy for thymomas (5, 11). Here, we present a rare case of a middle-aged male patient who was successively diagnosed with multiple thymoma-associated PNSs, including membranous nephropathy, cutaneous amyloidosis, MG, and Morvan's syndrome, as well as with multiple positive serum antibodies (ANA, AHA, ANCA, AChR, titin, LGI1, and GABABR).

This patient was diagnosed with membranous nephropathy at the first visit due to nephrotic syndrome, and his symptoms were completely relieved after receiving steroids,

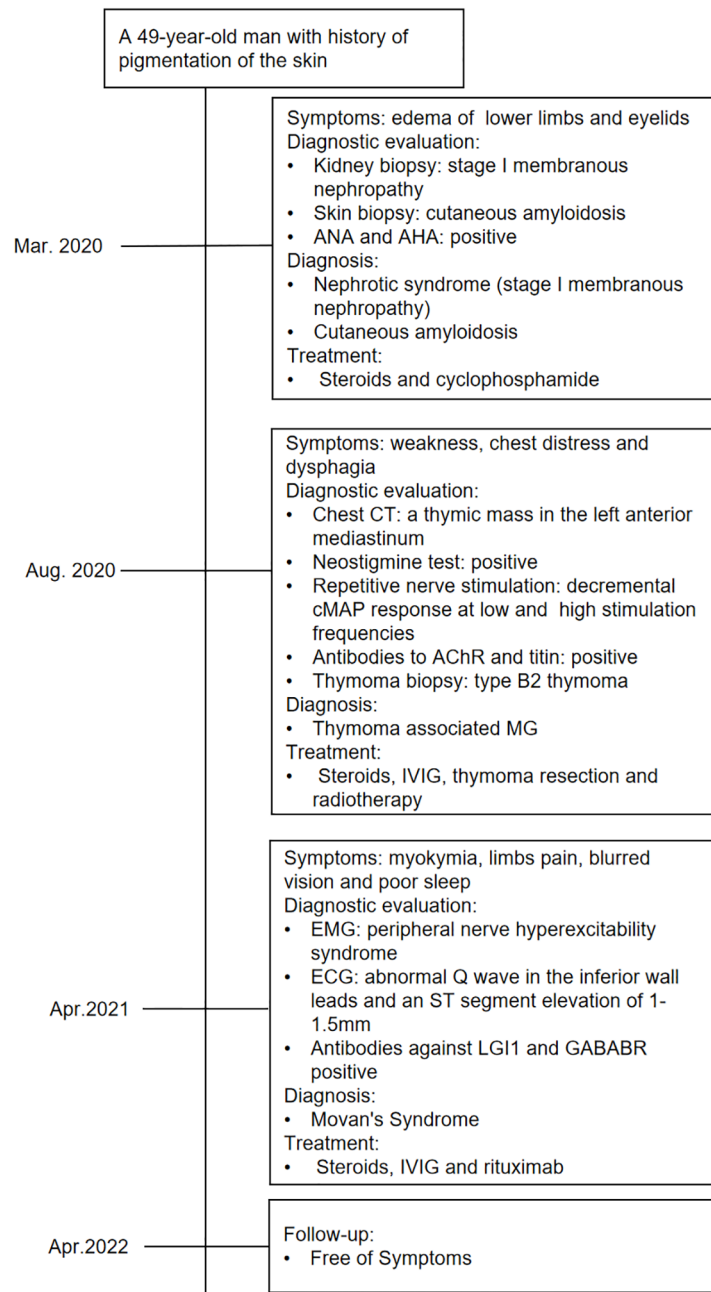


FIGURE 3

Timeline of the diagnosis, treatment, and outcome. CT, computed tomography; cMAP, compound muscle action potential responses.

cyclophosphamide, and thymectomy. Thymoma-associated nephropathy is very rare, with only 10% of nephrologists in France encountering patients with thymoma-associated renal disease (12). In thymoma-associated nephropathy, the most common pathology is minimal change glomerulopathy, followed by membranous nephropathy, focal segmental glomerulosclerosis, and others (12). Membranous nephropathy is usually associated with active thymoma, either newly

diagnosed or recurrent. Tumor treatment (thymectomy, radiotherapy, or chemotherapy) frequently induces remission of nephrotic syndrome in membranous nephropathy (12). The good outcome in this patient confirmed this view. Immunological tests were disturbed in many cases of thymoma-associated nephropathy, and it was reported that ANA was positive in 13/18 (72%) of such cases (12). Our patient also showed many autoantibodies, such as ANA, AHA, and ANCA.

Cutaneous disorders associated with thymomas are widely heterogeneous and include pemphigus, lichen planus, vitiligo, alopecia areata, lupus erythematosus, and graft-versus-host-like disease (5, 13). However, our case is the first report of cutaneous amyloidosis associated with thymoma. As previously reported, the effect of thymectomy seems to be variable but can, in some cases, induce the regression of paraneoplastic cutaneous disorders (14, 15). In view of this, the patient's skin manifestations improved after complete thymoma resection.

MG is the most common PNS associated with thymoma, with 10%–15% of MG patients presenting with thymoma and 25%–40% of patients with thymoma developing MG (2, 4, 10). Nearly all patients with thymoma-associated MG have detectable AChR antibodies (1, 10, 16). The AChR antibody concentration in our patient was very high, reaching 320 nmol/L. To date, no correlation has been observed between AChR antibody concentration and disease severity. The value of repeated AChR antibody testing in patients with this disorder has been debated; however, changes in antibody concentrations may predict disease severity in patients administered immunosuppressive drugs and can therefore support therapeutic decisions (16). After our patient underwent thymoma resection and immunotherapy, the concentration of AChR antibody decreased to 19.6 nmol/L, supporting the view that longitudinal observation of AChR antibody concentrations is needed for the long-term treatment of MG patients. In addition, the titer of the titin antibody in this patient was very high. The presence of titin antibody is suggested to be a strong indication of thymoma and is associated with more severe MG (17).

Acquired neuromyotonia (aNMT) is a disorder characterized by peripheral nerve hyperexcitability that results in continuous muscle activity. Clinical presentations include myokymia, fasciculations, and cramps (3, 18), and EMG shows spontaneous motor unit discharges as doublet, triplet, or multiplet bursts (myokymic discharges) or longer bursts with high intraburst frequencies (neuromyotonic discharges) (18). The clinical symptoms and EMG findings of this patient were typical manifestations of neuromyotonia. In 20% of cases, aNMT is associated with signs of central nervous system involvement, such as mood changes, hallucinations, and insomnia, together with autonomic dysfunction, collectively known as Morvan's syndrome (19). Aside from neuromyotonia, the patient's symptoms of severe insomnia, blurred vision, and myocardial infarction-like ECG changes support the diagnosis of Morvan's syndrome.

Morvan's syndrome is a rare disease associated with thymoma. In a study of 29 patients with Morvan's syndrome, thymoma was found in 37% of the patients (19). aNMT is associated with antibodies to the Kv1 voltage-gated potassium channel complex. These antibodies do not target Kv1 channels

directly; rather, they target two associated proteins, LGI1 and CASPR2 (6, 20, 21). In this patient, antibodies against LGI1 and GABABR were both positive, while antibodies against CASPR2 were negative. The LGI1 antibody was pathogenic in this patient, as it has been reported to alter Kv1.1 and AMPA receptors and modify synaptic excitability, plasticity, and memory (22). In addition, the role of the GABABR antibody in this patient's disease is not clear, and it may only be a concomitant antibody.

The ECG of the patient showed serious abnormalities similar to those of myocardial infarction. A similar phenomenon has been reported in previous literature: severe bradycardia and even sudden death due to myocardial ischemia with normal coronary arteries occurred in patients with LGI1 antibody-associated encephalitis (21, 23). This emphasizes that in patients with Morvan's syndrome associated with LGI1 antibody, cardiac complications are potentially life-threatening and require clinical vigilance. The patient received IVIG therapy after he was diagnosed with Morvan's syndrome; however, his symptoms did not improve. The reason why IVIG did not work might be that most subclasses of LGI1 antibodies belong to IgG4, which is inadequate for activating a cellular- or complement-mediated immune response (24). The patient recovered after receiving B-cell depletion therapy. His good response to rituximab is consistent with previous research that reported the effectiveness of rituximab treatment in patients with LGI1 encephalitis (25).

We questioned why multiple coexisting autoimmune syndromes occur in patients with thymoma. Notably, the thymus is a key site for the establishment of immune tolerance. This process involves the maturation and selection of T cells during their migration through the thymic cortex and medulla. Thus, defective negative selection with the export of autoreactive CD4⁺ T cells together with a reduced level of regulatory T cells may appear to be the key features associated with the occurrence of PNS in thymoma patients (4, 26).

Conclusion

Overall, we present a rare case of a middle-aged male patient who was successively diagnosed with multiple thymoma-associated PNSs, including membranous nephropathy, cutaneous amyloidosis, MG, and Morvan's syndrome, and who presented with multiple positive serum antibodies (ANA, AHA, ANCA, AChR, titin, LGI1, and GABABR). This case serves to remind us that, apart from MG, thymoma may also be associated with other autoimmune PNSs. Thymectomy, related tumor therapy, and immunotherapy are important for the management of PNSs. For Morvan's syndrome post-thymectomy with LGI1 antibody positivity, B-cell depletion therapy such as intravenous rituximab is an effective treatment.

Data availability statement

The original contributions presented in this study are included in the article/[Supplementary Material](#). Further inquiries can be directed to the corresponding authors.

Ethics statement

Written informed consent was obtained from the individual(s) for the publication of any potentially identifiable images or data included in this article.

Author contributions

WL contributed to the conception and design of the study. HL, ZD, RP, and JX collected and organized the clinical data. PH and GY collected and analyzed the kidney biopsy data. WM collected and analyzed the EMG data. SZ collected and analyzed the skin biopsy data. HL and GY drafted the manuscript. All authors contributed to the article and approved the submitted version.

Funding

This work was supported by a grant to HL from the Science and Technology Development Program of Henan Province (No. 212102310833).

References

1. Evoli A, Minicuci GM, Vitaliani R, Battaglia A, Della Marca G, Lauriola L, et al. Paraneoplastic diseases associated with thymoma. *J Neurol* (2007) 254(6):756–62. doi: 10.1007/s00415-006-0429-z
2. Tormoehlen LM, Pascuzzi RM. Thymoma, myasthenia gravis, and other paraneoplastic syndromes. *Hematol Oncol Clin North Am* (2008) 22(3):509–26. doi: 10.1016/j.hoc.2008.03.004
3. Fleisher J, Richie M, Price R, Scherer S, Dalmau J, Lancaster E. Acquired neuromyotonia heralding recurrent thymoma in myasthenia gravis. *JAMA Neurol* (2013) 70(10):1311–4. doi: 10.1001/jamaneurol.2013.2863
4. Evoli A, Lancaster E. Paraneoplastic disorders in thymoma patients. *J Thorac Oncol* (2014) 9(9 Suppl 2):S143–7. doi: 10.1097/JTO.0000000000000300
5. Bernard C, Frih H, Pasquet F, Kerever S, Jamilloux Y, Tronc F, et al. Thymoma associated with autoimmune diseases: 85 cases and literature review. *Autoimmun Rev* (2016) 15(1):82–92. doi: 10.1016/j.autrev.2015.09.005
6. Gastaldi M, De Rosa A, Maestri M, Zardini E, Scaranzin S, Guida M, et al. Acquired neuromyotonia in thymoma-associated myasthenia gravis: a clinical and serological study. *Eur J Neurol* (2019) 26(7):992–9. doi: 10.1111/ene.13922
7. Meng X, Zeng Z, Wang Y, Guo S, Wang C, Wang B, et al. Efficacy and safety of low-dose rituximab in anti-MuSK myasthenia gravis patients: A retrospective study. *Neuropsychiatr Dis Treat* (2022) 18:953–64. doi: 10.2147/NDT.S358851
8. Wang BJ, Wang CJ, Zeng ZL, Yang Y, Guo SG. Lower dosages of rituximab used successfully in the treatment of anti-NMDA receptor encephalitis without tumour. *J Neurol Sci* (2017) 377:127–32. doi: 10.1016/j.jns.2017.04.007
9. Morgenthaler TI, Brown LR, Colby TV, Harper CM Jr, Coles DT. Thymoma. *Mayo Clin Proc* (1993) 68(11):1110–23. doi: 10.1016/s0025-6196(12)60907-0
10. Álvarez-Velasco R, Gutiérrez-Gutiérrez G, Trujillo JC, Martínez E, Segovia S, Arribas-Velasco M, et al. Clinical characteristics and outcomes of thymoma-associated myasthenia gravis. *Eur J Neurol* (2021) 28(6):2083–91. doi: 10.1111/ene.14820
11. Zhao J, Bhatnagar V, Ding L, Atay SM, David EA, McFadden PM, et al. A systematic review of paraneoplastic syndromes associated with thymoma: Treatment modalities, recurrence, and outcomes in resected cases. *J Thorac Cardiovasc Surg* (2020) 160(1):306–14.e14. doi: 10.1016/j.jtcvs.2019.11.052
12. Karras A, de Montpreville V, Fakhouri F, Grünfeld JP, Lesavre PGroupe d'Etudes des Néphropathies Associées aux Thymomes. Renal and thymic pathology in thymoma-associated nephropathy: report of 21 cases and review of the literature. *Nephrol Dial Transplant* (2005) 20(6):1075–82. doi: 10.1093/ndt/gfh615
13. Nagano T, Kotani Y, Kobayashi K, Tomita N, Nakata K, Sakashita A, et al. Chemotherapy improves thymoma-associated graft-versus-host-disease-like erythroderma. *BMJ Case Rep* (2011) 2011:bcr0320113936. doi: 10.1136/bcr.03.2011.3936

Acknowledgments

The authors thank their patient for his participation and the EUROIMMUN Weiwei Medical Laboratory for the anti-neuronal antibody tests.

Conflict of interest

The authors declare that the research was conducted in the absence of any commercial or financial relationships that could be construed as a potential conflict of interest.

Publisher's note

All claims expressed in this article are solely those of the authors and do not necessarily represent those of their affiliated organizations, or those of the publisher, the editors and the reviewers. Any product that may be evaluated in this article, or claim that may be made by its manufacturer, is not guaranteed or endorsed by the publisher.

Supplementary material

The Supplementary Material for this article can be found online at: <https://www.frontiersin.org/articles/10.3389/fonc.2022.1002808/full#supplementary-material>

SUPPLEMENTARY VIDEO 1

The video shows extensive myokymia in the patient's lower limbs.

14. Barbetakis N, Samanidis G, Paliouras D, Chnaris A. eComment: Paraneoplastic skin diseases in thymoma patients. *Interact Cardiovasc Thorac Surg* (2009) 9(2):346. doi: 10.1510/icvts.2009.207308A
15. Yoshida M, Miyoshi T, Sakiyama S, Kondo K, Tangoku A. Pemphigus with thymoma improved by thymectomy: report of a case. *Surg Today* (2013) 43(7):806–8. doi: 10.1007/s00595-012-0272-z
16. Gilhus NE, Verschuuren JJ. Myasthenia gravis: subgroup classification and therapeutic strategies. *Lancet Neurol* (2015) 14(10):1023–36. doi: 10.1016/S1474-4422(15)00145-3
17. Zisimopoulou P, Brenner T, Trakas N, Tzartos SJ. Serological diagnostics in myasthenia gravis based on novel assays and recently identified antigens. *Autoimmun Rev* (2013) 12(9):924–30. doi: 10.1016/j.autrev.2013.03.002
18. Gutmann L, Gutmann L. Myokymia and neuromyotonia 2004. *J Neurol* (2004) 251(2):138–42. doi: 10.1007/s00415-004-0331-5
19. Irani SR, Pettingill P, Kleopa KA, Schiza N, Waters P, Mazia C, et al. Morvan syndrome: clinical and serological observations in 29 cases. *Ann Neurol* (2012) 72(2):241–55. doi: 10.1002/ana.23577
20. Irani SR, Alexander S, Waters P, Kleopa KA, Pettingill P, Zuliani L, et al. Antibodies to Kv1 potassium channel-complex proteins leucine-rich, glioma inactivated 1 protein and contactin-associated protein-2 in limbic encephalitis, morvan's syndrome and acquired neuromyotonia. *Brain* (2010) 133(9):2734–48. doi: 10.1093/brain/awq213
21. Binks SNM, Klein CJ, Waters P, Pitttock SJ, Irani SR. LGI1, CASPR2 and related antibodies: a molecular evolution of the phenotypes. *J Neurol Neurosurg Psychiatry* (2018) 89(5):526–34. doi: 10.1136/jnnp-2017-315720
22. Petit-Pedrol M, Sell J, Planagumà J, Mannara F, Radosevic M, Haselmann H, et al. LGI1 antibodies alter Kv1.1 and AMPA receptors changing synaptic excitability, plasticity and memory. *Brain* (2018) 141(11):3144–59. doi: 10.1093/brain/awy253
23. Rizzi R, Fisicaro F, Zangrandi A, Ghidoni E, Baiardi S, Ragazzi M, et al. Sudden cardiac death in a patient with LGI1 antibody-associated encephalitis. *Seizure* (2019) 65:148–50. doi: 10.1016/j.seizure.2019.01.013
24. Huijbers MG, Querol LA, Niks EH, Plomp JJ, van der Maarel SM, Graus F, et al. The expanding field of IgG4-mediated neurological autoimmune disorders. *Eur J Neurol* (2015) 22(8):1151–61. doi: 10.1111/ene.12758
25. Thaler FS, Zimmermann L, Kammermeier S, Strippel C, Ringelstein M, Kraft A, et al. Rituximab treatment and long-term outcome of patients with autoimmune encephalitis: Real-world evidence from the GENERATE registry. *Neurol Neuroimmunol Neuroinflamm* (2021) 8(6):e1088. doi: 10.1212/NXI.0000000000001088
26. Marx A, Pfister F, Schalke B, Saruhan-Direskeneli G, Melms A, Ströbel P. The different roles of the thymus in the pathogenesis of the various myasthenia gravis subtypes. *Autoimmun Rev* (2013) 12(9):875–84. doi: 10.1016/j.autrev.2013.03.007



OPEN ACCESS

EDITED BY

Catherine Sautes-Fridman,
U1138 Centre de Recherche des
Cordeiers (CRC) (INSERM), France

REVIEWED BY

Vijay Bhoj,
University of Pennsylvania,
United States
Sarwish Rafiq,
School of Medicine, Emory University,
United States
Stephen Gottschalk,
St. Jude Children's Research Hospital,
United States

*CORRESPONDENCE

Winfried F. Pickl
winfried.pickl@meduniwien.ac.at

[†]These authors have contributed
equally to this work

SPECIALTY SECTION

This article was submitted to
Cancer Immunity
and Immunotherapy,
a section of the journal
Frontiers in Immunology

RECEIVED 27 July 2022

ACCEPTED 28 November 2022

PUBLISHED 09 January 2023

CITATION

Worel N,
Grabmeier-Pfistershammer K,
Kratzer B, Schlager M, Tanzmann A,
Rottal A, Körmöcz U, Porpacz E,
Staber PB, Skrabs C, Herkner H,
Gudipati V, Huppa JB, Salzer B,
Lehner M, Sachsenhuber N, Friedberg E,
Wohlfarth P, Hopfinger G, Rabitsch W,
Simonitsch-Klupp I, Jäger U and
Pickl WF (2023) The frequency of
differentiated CD3⁺CD27⁻CD28⁻ T
cells predicts response to CART
cell therapy in diffuse large
B-cell lymphoma.
Front. Immunol. 13:1004703.
doi: 10.3389/fimmu.2022.1004703

The frequency of differentiated CD3⁺CD27⁻CD28⁻ T cells predicts response to CART cell therapy in diffuse large B-cell lymphoma

Nina Worel^{1†}, Katharina Grabmeier-Pfistershammer^{2†},
Bernhard Kratzer^{2†}, Martina Schlager³, Andreas Tanzmann¹,
Arno Rottal², Ulrike Körmöcz², Edit Porpacz³,
Philipp B. Staber³, Cathrin Skrabs³, Harald Herkner⁴,
Venugopal Gudipati⁵, Johannes B. Huppa⁵, Benjamin Salzer⁶,
Manfred Lehner⁶, Nora Sachsenhuber³, Eleonora Friedberg³,
Philipp Wohlfarth⁷, Georg Hopfinger⁷, Werner Rabitsch⁷,
Ingrid Simonitsch-Klupp⁸, Ulrich Jäger³ and Winfried F. Pickl^{2*}

¹Department of Blood Group Serology and Transfusion Medicine, Medical University of Vienna, Vienna, Austria, ²Institute of Immunology, Center for Pathophysiology, Infectiology and Immunology, Medical University of Vienna, Vienna, Austria, ³Department of Medicine I, Division of Hematology and Hemostaseology, Medical University of Vienna, Vienna, Austria, ⁴Department of Emergency Medicine, Medical University of Vienna, Vienna, Austria, ⁵Institute for Hygiene and Applied Immunology, Center for Pathophysiology, Infectiology and Immunology, Medical University of Vienna, Vienna, Austria, ⁶Christian Doppler Laboratory for Next Generation CAR T Cells, St. Anna Children's Cancer Research Institute, Vienna, Austria, ⁷Department of Medicine I, Division of Blood and Bone Marrow Transplantation, Medical University of Vienna, Vienna, Austria, ⁸Department of Pathology, Medical University of Vienna, Vienna, Austria

Background: Chimeric antigen receptor T (CART) cell therapy targeting the B cell specific differentiation antigen CD19 has shown clinical efficacy in a subset of relapsed/refractory (r/r) diffuse large B cell lymphoma (DLBCL) patients. Despite this heterogeneous response, blood pre-infusion biomarkers predicting responsiveness to CART cell therapy are currently understudied.

Methods: Blood cell and serum markers, along with clinical data of DLBCL patients who were scheduled for CART cell therapy were evaluated to search for biomarkers predicting CART cell responsiveness.

Findings: Compared to healthy controls (n=24), DLBCL patients (n=33) showed significant lymphopenia, due to low CD3⁺CD4⁺ T helper and CD3⁺CD56⁺ NK cell counts, while cytotoxic CD3⁺CD8⁺ T cell counts were similar. Although lymphopenic, DLBCL patients had significantly more activated HLA-DR⁺ (P=0.005) blood T cells and a higher frequency of differentiated CD3⁺CD27⁻CD28⁻ (28.7 ± 19.0% versus 6.6 ± 5.8%; P<0.001) T cells. Twenty-six patients were infused with CART cells (median 81 days after leukapheresis) and were analyzed for the overall response (OR) 3 months later. Univariate and multivariate regression

analyses showed that low levels of differentiated CD3⁺CD27⁺CD28⁺ T cells (23.3 ± 19.3% versus 35.1 ± 18.0%) were independently associated with OR. This association was even more pronounced when patients were stratified for complete remission (CR versus non-CR: 13.7 ± 11.7% versus 37.7 ± 17.4%, $P=0.001$). A cut-off value of ≤ 18% of CD3⁺CD27⁺CD28⁺ T cells predicted CR at 12 months with high accuracy ($P<0.001$). *In vitro*, CD3⁺CD8⁺CD27⁺CD28⁺ compared to CD3⁺CD8⁺CD27⁺CD28⁺ CART cells displayed similar CD19⁺ target cell-specific cytotoxicity, but were hypoproliferative and produced less cytotoxic cytokines (IFN- γ and TNF- α). CD3⁺CD8⁺ T cells outperformed CD3⁺CD4⁺ T cells 3- to 6-fold in terms of their ability to kill CD19⁺ target cells.

Interpretation: Low frequency of differentiated CD3⁺CD27⁺CD28⁺ T cells at leukapheresis represents a novel pre-infusion blood biomarker predicting a favorable response to CART cell treatment in r/r DLBCL patients.

KEYWORDS

diffuse large B cell lymphoma, chimeric antigen receptor T cells therapy, CD27, CD28, biomarker

Introduction

Diffuse large B cell lymphoma (DLBCL) represents the most frequent form of non-Hodgkin's lymphoma (NHL). Five-year survival rates range from 55% to 64% (1, 2); however, patients who experience early relapse, or who are refractory to initial immunochemotherapy have a poor prognosis (3). In fact, salvage therapy for patients with refractory NHL has been associated with frequent therapy failures (>70%) and poor long-term outcome with an overall survival of only 6 months (3). Even consolidation therapy with subsequent autologous stem cell transplantation leads to only 50% long-term survival (4, 5).

Chimeric antigen receptor T (CART) cells represent a novel treatment option for patients with refractory/relapsing (r/r) DLBCL (6, 7). CART cell therapy takes advantage of autologous peripheral blood (PB) T cells, which are genetically modified *ex vivo* to express a chimeric antigen receptor (CAR) designed to target the CD19 antigen on the surface of the malignant B cell clone (8). Despite initial promising results with tisagenlecleucel (formerly CTL019) (7, 9), axicabtagene ciloleucel (formerly KTE-C19) (10) and lisocabtagene maraleucel (formerly JCAR017) (11), leading to overall response (OR) and complete remission (CR) rates of 83% to 52% and 58% to 40% (7, 11, 12), respectively, clearly not all patients benefit from CART cell therapy in the long-term (7). In fact, response rates decline to approximately 32% after one year (7). However, the identification of patients most likely to benefit from CART cell therapy is difficult to achieve by solely using clinical and basic laboratory criteria. Therefore, a reliable predictor of response to CART cell therapy at the time of

enrollment, e.g., by a simple blood test, is an unmet need for optimal patient selection (13).

Currently, the best predictors of responsiveness to CART cell therapy are low lactate dehydrogenase (LDH) levels after lymphodepletion before CART cell infusion, a low tumor volume and a low Eastern Cooperative Oncology Group (ECOG) performance status (7, 14–16). Owing to the mode of action of CART cells, the immune system most likely plays a major role in its effectiveness. However, all three markers (LDH, tumor volume, ECOG) are not directly related to the immune system, and thus can, at best, represent surrogate markers for future tumor-immune surveillance by the gene modified autologous CART cells. More recently, other factors strongly linked to the immune system and possibly impacting on the response to CART cell therapy have been suggested. These factors include, but are not restricted to: i) defective T cell function (poor initial “pre-CAR” T cell quality or decreasing “post-CAR” T cell function) (17); ii) microenvironmental suppression (check point inhibition and suppressive cytokines) (18); and iii) antigen escape (target antigen modulation (19) or myeloid lineage switch) (20). In addition, increased frequencies of CD27⁺CD45RO⁺CD8⁺ T cells at the time of leukapheresis have been implicated to correlate with sustained remission in patients with chronic lymphocytic leukemia treated with CD19 CART cells (21), in multiple myeloma patients treated with B cell maturation antigen (BCMA)-specific CART cells (22), and recently in patients with DLBCL (23). It has been suggested that CD27⁺CD45RO⁺CD8⁺ T cells belong to the group of antigen-experienced CD3⁺CD8⁺ T lymphocytes that have long-lasting memory capabilities and improved ability to expand *in vitro* and

in vivo (21, 22, 24). While of interest, the respective marker combination does not define a single cellular phenotype since CD45RO negativity may identify both naïve CD8⁺ T cells as well as antigen-experienced “stem cell memory” cells (23). Moreover, focusing the analyses exclusively on CD8⁺ T cells has the problem of potentially underestimating the cytotoxic potency of CD4⁺ T cells turned into CART cells during the manufacturing process. However, it has been clearly shown in adoptive T cell transfer studies in preclinical melanoma models that more differentiated CD8⁺ effector T cells are less effective for *in vivo* tumor treatment and that the renewal capacity of CD8⁺ T cells as determined by their telomer length plays an important role in that respect (25). In line with these studies, adoptive T cell transfer studies with autologous CD8⁺CD27⁺ T cells led to durable responses in heavily pretreated patients with metastatic melanoma (26). Apart from phenotypic data, a recent study suggested that germline mutations in UNC13D and compound heterozygous forms of CXCR1 may represent additional resistance factors to CART therapy (17). Whether and how they correlate with the cell surface phenotype of CD3⁺ T cells remains to be shown in the future. Furthermore, it should also be noted that for many patients, it is not possible to generate a suitable CART cell product due to prolonged lymphopenia and the associated inability to isolate a sufficient number of functional T cells (27).

Lymphopenia, as well as poor T cell quality and function, may reflect the intensity of previous immuno-chemotherapies, but may also result from hyperactivation of T cells, a process well-known to lead to their subsequent hypoproliferation and reduced life expectancy. Hyperactivated HLA-DR⁺ T cells have been shown to down-modulate cell surface expression of the co-stimulatory molecules CD27 and CD28 (28–31), which are otherwise decisively involved in the regulation of T cell activation (32, 33), the formation and maintenance of antigen-experienced T cells (34) and tumor immune surveillance (35). However, increased frequencies of HLA-DR⁺ T cells may also be the result of homeostatic proliferation (36). The expression levels of CD27 and CD28 as well as those of the high molecular weight form of CD45, i.e., CD45RA, and the chemokine receptor CCR7 allow, in principle, the determination of the position of a given T cell within the linear T cell differentiation model proposed by Romero et al. (37). In that model, CD3⁺CD27⁺CD28⁺ T cells are mainly composed of T effector memory cells re-expressing CD45RA (TEMRA) cells and to a lower degree also contain effector memory type 3 (EM3) cells. While CCR7 is a robust marker for distinguishing between central and effector memory T cells, CD45RA is somewhat problematic because it is expressed on both naïve and terminally differentiated TEMRA cells and is overexpressed in 1 of 20 Caucasian individuals due to the C77G mutation (38), making it much more difficult to distinguish between *bona fide* CD45RA⁺ and CD45RA⁺ cell

subsets. Therefore, we here analyzed leukocyte subset distribution, T cell activation, and focused on CD27 and CD28 expression of bulk CD3⁺ T cells in the blood and corresponding leukapheresis products of adult r/r DLBCL patients and correlated the results with 3 months OR to CART cell therapy.

Patients and methods

Patients and clinical trial conduct

Between January 2016 and January 2022, 33 patients diagnosed with r/r DLBCL and scheduled for treatment with CART cells at our institution were enrolled into this study to investigate the composition of leukocyte subpopulations, their activation and differentiation status, together with serum markers in peripheral blood (PB) and leukapheresis samples. Patients gave their written informed consent in accordance with the Declaration of Helsinki. Patients received CART cells in clinical trials with tisagenlecleucel (n=15; Ethics Committee (EC) No.: 1422/2015, 1607/2018), YTB323 [n=2; EC No.: 2055/2019 (39)], or in routine applications of tisagenlecleucel (n=6) or axicabtagene ciloleucel (n=3). Analysis of data was approved by the EC of the Medical University of Vienna (EC No.: 1290/2020). Patient characteristics are presented in Table 1 and S1. Of the 33 enrolled patients, 26 already received CART cells, more than 3 months previously, at the time of data cut-off of this study. Seven patients were excluded from the study because they died before CART cell infusion (n=5), or received another treatment (n=2). The patients included into this study were heavily pretreated, showing failure to respond to two or more treatment lines, thus representing the subpopulation of patients with relapsed DLBCL eligible for CART therapy. The healthy control subjects (n=24) were age- (median 60 years; range 33–77 years) and sex- (10 women; 41.7%) matched and similar to the patients of Caucasian ethnicity.

Flow cytometric analyzes

Immunophenotyping of PB and the leukapheresis products was performed with fresh samples according to standard procedures (40) using directly conjugated monoclonal antibodies (Supplemental Table S2). To keep numbers of flow cytometric parameters low, the CD27 and CD28 expression status was analyzed on bulk CD45⁺CD3⁺ T cells. Acquisition was performed on flow cytometers (FACS Calibur and LSR Fortessa, Becton Dickinson, San Jose, CA; Navios or Cytoflex, Beckman Coulter, Krefeld, Germany) supported by the Cellquest, Diva and Kaluza software, respectively. Acquired data were analyzed with Flow Jo software (BD).

TABLE 1 Demographics, pathological features and clinical performance of patients.

	All DLBCL patients enrolled in study	Patients who received CART cell treatment (n=26; 78.8%)					
		3 mos responders (CR+PR) 15 (45.5)	3 mos non- responders 11 (33.3)	P- value	3 mos CR 11 (33.3)	3 mos non-CR 15 (45.5)	P- value
No. of DLBCL patients (%)	33 (100)						
Demographics, disease type and clinical presentation							
Demographics							
Age in years, median (range)	61.8 (32.9-77.2)	67.5 (36.1-77.2)	48.9 (32.9-66.5)	0.003*	65.6 (36.1-77.2)	53.8 (32.9-74.9)	0.07
Gender, female (%)	14 (42.4)	8 (53.3)	4 (36.4)	0.45	5 (45.5)	6 (46.7)	1.00
Disease Form							
Bulky (total)	11 (35.5)	3 (14)	5 (11)	0.39	1 (10)	7 (46.7)	0.09
Pathological features							
Double/triple Hit (total)	21 (27)	9 (10)	9 (11)	1	6 (6)	12(15)	0.53
Molecular biological features							
MYC rearrangement positive by FISH (total)	16 (28)	5 (12)	8 (11)	0.21	4 (9)	9 (14)	0.68
BCL-2 rearrangement positive by FISH (total)	22 (27)	10 (11)	8 (11)	0.59	8 (8)	10 (14)	0.28
BCL-6 rearrangement positive by FISH (total)	16 (22)	6 (8)	8 (10)	1.00	5 (6)	9 (12)	1.00
Cell of origin GCB (total)	15 (30)	5 (13)	8 (11)	0.12	3 (9)	10 (15)	0.21
Double-hit score 2 (accord. Green et al.)	19 (30)	6 (13)	10 (11)	0.03	3 (9)	13 (15)	0.02
Clinical performance at relapse							
IPI (international prognostic index), median (range)	2 (0-4)	2 (0-4)	2 (0-2)	0.89**	1.5 (0-2)	2 (0-4)	0.09**
IPI (age adjusted), median (range)	2 (0-3)	1 (0-3)	2 (0-2)	1.00**	1 (0-2)	2 (0-3)	0.07**
Ann-Arbor staging, median (range)	3 (1-4)	3 (1-4)	2 (1-4)	0.42**	2 (1-4)	3 (1-4)	0.46**
ECOG performance status: 0 (1)	25 (8)	12 (3)	8 (2)	1.00	8 (3)	12 (2)	0.62
Pretreatment							
No. prior treatment lines pre leukapheresis, median (range)	3 (1-11)	3 (1-11)	3 (1-6)	0.85	3 (1-11)	3 (1-6)	0.87
<4 treatment lines (total)	25 (23)	13 (15)	8 (11)	0.62	9 (12)	12 (15)	1.00
Laboratory parameters							
At leukapheresis							
LDH (<245 U/L), mean ± SD	325.9 ± 180.3	236.1 ± 114.0	366.1 ± 162.5	0.02*	246.4 ± 132.2	323.9 ± 155.9	0.19*
CRP (<0.5 mg/L), mean ± SD	2.6 ± 4.2	0.8 ± 0.8	3.2 ± 5.0	0.07*	0.7 ± 0.9	2.6 ± 4.3	0.16*
Fibrinogen (200-400 mg/dL), mean ± SD	476.7 ± 155.2	424.5 ± 114.5	465.2 ± 11.7	0.39*	405.4 ± 99.6	467.1 ± 120.3	0.19*
B2M (0.8-2.2 mg/L), mean ± SD	2.8 ± 0.9	2.8 ± 1.1	2.8 ± 0.7	0.85*	2.8 ± 1.2	2.8 ± 0.7	0.96*
At CART infusion							
LDH (<245 U/L), mean ± SD	354.7 ± 394.6	234.9 ± 92.9	518.2 ± 560.0	0.06*	232.3 ± 103.4	444.5 ± 490.9	0.17*
B2M (0.8-2.2 mg/L), mean ± SD	3.0 ± 1.0	2.6 ± 0.8	3.6 ± 1.1	0.02*	2.4 ± 0.6	3.5 ± 1.1	0.01*

Table shows demographics, pathological features and clinical performance of all patients, and patients stratified according to response at 3 months (CR plus PR) versus non-response. Hypothesis testing using normally distributed data has been performed with the Student's t-test, while for categorized data such as demographic data like sex, cytogenetic marker positivity, the Fisher's Exact test was used. Non-normally ordinally distributed data were tested by the Mann-Whitney U test. *) P-values calculated with Student's t-test **) Mann-Whitney U-Test, all other P-values calculated with Fisher's exact test; CR, complete remission; PR, partial remission; Hb, Hemoglobin; Plt, platelets; LDH, lactate dehydrogenase; CRP, C-reactive protein; B2M, beta-2-microglobulin; GCB, germinal center B cell; ECOG, Eastern cooperative oncology group score; IPI, international performance index; mos, months.

Generation of CART cells for *in vitro* studies

Buffy coats from anonymous healthy donor's blood were purchased from the Austrian Red Cross, Vienna. CD3⁺ primary human T cells were isolated using the RosetteSep Human T cell Enrichment Cocktail (STEMCELL Technologies, Vancouver Canada) and immediately cryopreserved in RPMI-1640 GlutaMAX medium (Thermo Fisher Scientific, Waltham, MA) supplemented with 20% FCS and 10% DMSO (both from Merck, Darmstadt, Germany). Primary human T cells were thawed in RPMI-1640 GlutaMAX medium, supplemented with 10% FCS, 1% penicillin-streptomycin (Thermo Fisher Scientific) and 200 IU mL⁻¹ recombinant human IL-2 (Peprotech, Waltham, MA) and activated with Dynabeads Human T-Activator CD3/CD28 beads (Thermo Fisher Scientific) at a 1:1 ratio according to the manufacturer's instructions. Twenty-four hours after stimulation, T cells were transduced in cell culture plates, which were coated with RetroNectin (Takara, Shiga, Japan), according to the manufacturer's instructions. Thawed lentiviral supernatant was added to the T cells at a final dilution of 1:2, yielding a cell concentration of 0.5 x 10⁶ cells mL⁻¹. Forty-eight hours after transduction, selection of CART cells was initiated by treatment with 1 µg mL⁻¹ puromycin (Merck, Germany) for two days. Transduced T cells were cultivated in AIM V medium (Thermo Fisher Scientific) supplemented with 2% Octaplas (Octapharma, Vienna, Austria), 1% L-glutamine, 2.5% HEPES (both from Thermo Fisher Scientific) and 200 IU mL⁻¹ recombinant human IL-2 for 14 days and then frozen in liquid nitrogen in IMDM medium containing 20% FB and 10% DMSO until further use.

Construction of lentiviral vector

VSV-G pseudotyped lentivirus was generated by co-transfection of Lenti-X 293T cells (Takara) with a puromycin-selectable pCDH expression vector (System Biosciences, USA) encoding the second-generation anti-CD19-CAR (FMC63.4-1BB.ζ) and viral packaging plasmids pMD2.G and psPAX2 (Addgene plasmids #12259 and #12260, respectively; kind gifts from Didier Trono) using the PureFection Transfection Reagent (System Biosciences, Palo Alto, CA) according to the manufacturer's instructions. Viral supernatants were collected on day 2 and 3 after transfection and were concentrated 100-fold using the Lenti-X Concentrator (Takara) according to the manufacturer's instructions. Viral suspensions were frozen at -80°C until further use.

Functional *in vitro* assays with CART cells

For *in vitro* experiments, CART cells were gently thawed and cultured in AIMV medium (Thermo Fisher Scientific, USA)

supplemented with 2% Octaplas (Octapharma), 1% L-glutamine, 2.5% HEPES (both from Thermo Fisher Scientific, USA) and 50 IU mL⁻¹ recombinant human IL-2 (Peprotech). One day after thawing, CART cells were expanded by adding five times the number of irradiated (120 Gray) TM-LCL cells, a human B lymphocyte cell line immortalized by Epstein-Barr virus infection (41), which have been optimized as feeder cells for CD19 CART cell expansion (42). Expansion of CD19 CART cells after removal of CD3CD28-beads with CD19⁺LCL cells has been used in the past and represents an accepted procedure for CART cell expansion and propagation (43). After three days, cells were further expanded every two to three days by adding fresh medium in a 1:2 ratio. Ten days after expansion, CART cells were FACS sorted with the antibodies listed in Table S2 to obtain CD3⁺CD8⁺CD27⁺CD28⁺, CD3⁺CD8⁺CD27⁻CD28⁻ T, CD3⁺CD4⁺CD27⁺CD28⁺ and CD3⁺CD4⁺CD27⁻CD28⁻ cell populations on a Sony SH800 Sorter (Sony Biotechnology, San Jose, CA) and cultured in the presence of IL-2 in medium as described above. Five to seven days later, cells were used for *in vitro* assays. For proliferation assays, 1 x 10⁵ CART cells were incubated with the indicated amounts of irradiated (120 Gray) CD19⁺ TM-LCL cells (ranging from 2 x 10⁵ to 1 x 10⁴ cells) in triplicates in 96-well round-bottom tissue culture plates (Sarstedt, Nümbrecht, Germany) in a total volume of 200 µl for 48 h. Cells were pulsed with [methyl-³H]-thymidine (1 µCi per well) for 18 hours and thymidine up-take was analyzed as previously described (44). For analysis of T cell activation and cytokine production, 1 x 10⁵ CART cells were incubated with the indicated amounts of CD19⁺ TM-LCL cells (ranging from 2 x 10⁵ to 1 x 10⁴ cells) in triplicates in 96-well round-bottom plates in a total volume of 200 µl for 72 hours. Subsequently, cell suspensions were transferred to 1.5 ml microcentrifuge tubes, centrifuged at 600 g for 5 minutes, supernatants were collected and subjected to cytokine analyses with a cytometric bead array (Luminex, Austin, TX) as described previously (45). Cells were stained as described (44), acquired on a Cytoflex flow cytometer (Beckmann Coulter) and data analyzed with the Flow Jo software package (Becton Dickinson).

For cytotoxicity assays, 1 x 10⁶ CD19⁺ TM-LCL or CD19⁻ K562 cells were resuspended in 50 µl of culture medium each and labelled with 50 µl of Na⁵¹CrO₄ (Perkin Elmer, Boston, MA) at 37°C for 1 hour. After four subsequent washes, 5 x 10³ TM-LCL and K562 cells were seeded into individual wells of 96-well round-bottom tissue-culture plates and incubated with the indicated amounts of sorted CART cells in duplicates/triplicates. Medium or 2% triton-X100 was added to target cells to determine spontaneous and maximum release, respectively. Subsequently, plates were centrifuged at 100 g for 5 minutes and incubated at 37°C for 5 hours. Supernatants were then collected with the Skatron system (Molecular Devices, Biberach an der Riss, Germany) and radioactivity was determined on a Cobra II gamma-counter (Packard, Meriden, CT). The percentage of specific release was determined as

follows [CART cell induced release (cpm) – spontaneous release (cpm)]/[maximum release (cpm) – spontaneous release (cpm)] \times 100.

Statistics

The study was designed as a cohort study. Response to CART cell treatment was defined as complete response (CR) or partial remission (PR) at three months after CART cell infusion. No response was defined as stable disease (SD) or progressive disease (PD) after receiving CART cells. We present categorized data as absolute counts and relative frequencies, continuous data as mean and standard deviation, or median and range. Where applicable, we log-transformed variables to yield approximate normal distributions. To test the H_0 of no association of T cell subsets with the outcome to CART cell therapy, the Fisher's exact test and the independent sample t-test was used. To quantify the association between the outcome overall response at 3 months and the percentage of CD3⁺CD27⁺CD28⁺ T cells, we used exact logistic regression, owing to the limited sample size. We also assessed other predefined variables and added these variables as co-variables into the main model separately. Generally, a two-sided P-value <0.05 was considered statistically significant.

Data Sharing

Please contact Dr. Nina Worel for sharing of data at nina.worel@meduniwien.ac.at.

Results

Enrollment and clinical characterization of r/r DLBCL patients

Our study aimed to identify robust pre-infusion biomarkers in the blood and leukapheresis samples of r/r DLBCL patients, as possible predictors to the subsequent response to CART cell therapy. Accordingly, between January 2016 and January 2022, 33 patients with r/r DLBCL were enrolled into this cohort study (Figure S1). Patients consisted of 19 males and 14 females, with a median age of 61.8 years (range, 32.9 to 77.2 years, Table 1) and a median disease duration at leukapheresis of 18.0 months (range, 3.7–266.4 months) (Table S1). Median time from PB assessment at the time of leukapheresis to CART cell infusion was 3.3 months (range, 1.2 to 14.1 months). These patients had a median follow-up time of 15.5 months (range, 6.1 to 57.1 months). OR at 3 months was observed in 15 patients (57.7%), with 11 patients achieving a CR (42.3%).

Cellular parameters of r/r DLBCL patients at leukapheresis

First, we assessed PB leukocyte subpopulations at the time of leukapheresis (Table 2 and Figure 1). Remarkably, r/r DLBCL patients had significant lymphopenia compared to healthy controls (HC) ($1009 \pm 927 \times 10^6/L$ versus $1785 \pm 478 \times 10^6/L$; $P < 0.001$), due to reduced CD3⁺CD4⁺ T helper ($297 \pm 236 \times 10^6/L$ versus $735 \pm 229 \times 10^6/L$; $P < 0.001$) and CD3⁺CD56⁺ NK cell numbers ($164 \pm 218 \times 10^6/L$ versus $313 \pm 176 \times 10^6/L$; $P = 0.009$). CD3⁺CD8⁺ T cell, NKT cell, neutrophil and overall leukocyte numbers were similar to HC (Table 2 and Figure S2). The CD3⁺CD4⁺ lymphopenia led to a significantly lower CD4/CD8-ratio (0.9 ± 0.6 versus 2.1 ± 1.1 , $P < 0.001$) in DLBCL patients. Moreover, patients' T cells had clear signs of activation, as determined by HLA-DR co-expression ($315 \pm 322 \times 10^6/L$ versus $113 \pm 116 \times 10^6/L$; $P = 0.005$). Notably, chronic activation of T cells may lead to cell differentiation and replicative senescence, which is frequently accompanied by downregulation of the co-stimulatory molecules CD27 and CD28 (30, 31), the acquisition of memory (CD45RO/RA) and the loss of lymphnode homing (CCR7) markers (37). Indeed, when we examined the overall study population of r/r DLBCL patients in that regard, we found significantly higher percentages of differentiated CD3⁺CD27⁺CD28⁺ ($28.7 \pm 19.0\%$ versus $6.6 \pm 5.8\%$; $P < 0.001$), CD3⁺CD27⁺ ($38.6 \pm 19.2\%$ versus $19.6 \pm 11.9\%$; $P < 0.001$) and CD3⁺CD28⁺ ($41.7 \pm 19.6\%$ versus $15.5 \pm 8.5\%$; $P < 0.001$) PB T cells when compared to age-matched HC (Table 3; Figures 2A and S3). CD3⁺CD27⁺CD28⁺ consisted exclusively of highly differentiated CCR7⁺ CD45RA^{+/+} T effector memory (EM)/T effector memory RA cells (TEMRA) (Figure S4). Not unexpectedly, almost complete B cell aplasia was seen in most DLBCL patients ($P < 0.001$).

Low frequency of differentiated CD3⁺CD27⁺CD28⁺ PB T cells in r/r DLBCL patients at leukapheresis correlates with OR

Stratification of patients into CART cell responders at 3 months after CART infusion (CR and PR) versus non-responders (SD and PD) revealed that the T cells of the latter group were in particular more activated, as indicated by HLA-DR co-expression ($215 \pm 205 \times 10^6/L$ versus $465 \pm 397 \times 10^6/L$; $P < 0.08$) (Table 2). Accordingly, a higher frequency of differentiated CD3⁺CD27⁺CD28⁺ PB T cells was also associated with non-responsiveness, while a lower frequency of differentiated CD3⁺CD27⁺CD28⁺ PB T cells was a salient feature of patients with OR ($35.1 \pm 18.1\%$ versus $23.3 \pm 19.3\%$; $P = 0.14$) (Table 3 and Figure 2). This was due to a trend towards lower frequencies of CD3⁺CD27⁺ PB T cells ($33.5 \pm 17.7\%$ versus

TABLE 2 Differences in lymphocyte populations between r/r DLBCL patients and healthy controls.

N (%)	DLBCL patients enrolled in study [§] 31 (94.0)	Healthy controls 24 (100.0)	P-value [§]	CART cell recipients analyzed (n=24; 72.7%)		
				3 mos CART responders (CR+PR) 13 (39.4) [§]	3 mos CART non-responders 11 (33.3)	P-value [§]
Leukocytes	5803 ± 2579*	6475 ± 1792*	0.28	4977 ± 1938*	6209 ± 2810*	0.22
Neutrophils	4183 ± 2321	4207 ± 1530	0.97	3445 ± 1454	4177 ± 2406	0.37
Monocytes	613 ± 324	483 ± 179	0.08	561 ± 211	720 ± 446	0.26
Lymphocytes	1009 ± 927	1785 ± 478	<0.001	972 ± 743	1315 ± 1258	0.42
CD3 ⁺ T cells	791 ± 722	1232 ± 337	0.008	777 ± 658	1020 ± 904	0.45
CD3 ⁺ CD4 ⁺ T cells	297 ± 236	735 ± 229	<0.001	322 ± 223	345 ± 292	0.83
CD3 ⁺ CD8 ⁺ T cells	462 ± 453	406 ± 163	0.57	452 ± 456	594 ± 528	0.49
CD4/CD8-Ratio	0.9 ± 0.6	2.1 ± 1.1	<0.001	1.1 ± 0.6	0.8 ± 0.5	0.19
CD19 ⁺ B cells	12 ± 37	155 ± 53	<0.001	14 ± 31	18 ± 54	0.81
CD3 ⁺ CD56 ⁺ NK cells	164 ± 218	313 ± 176	0.009	144 ± 86	230 ± 351	0.40
CD3 ⁺ HLA-DR ⁺ T cells	315 ± 322	113 ± 116	0.005	215 ± 205	465 ± 397	0.08
CD3 ⁺ CD56 ⁺ NKT cells (%)	12.4 ± 9.4	11.2 ± 9.1	0.65	11.8 ± 10.6	14.0 ± 9.8	0.63

Shown are leukocyte and lymphocyte counts of DLBCL patients enrolled into the study compared to age and sex matched healthy control individuals. Patients were stratified according to response at 3 months (CR plus PR) versus patients with no-response. [§] Statistical differences between collectives were determined by Student's t-test. [§] The peripheral blood of two patients belonging to the CR group could not be analyzed. *) Data show absolute counts $\times 10^6$ cells/L as mean \pm standard deviation of the respective populations, except for CD3⁺CD56⁺ NKT cells, for which relative numbers of lymphocytes are given; CART, chimeric antigen receptor T cells; CR, complete remission; PR, partial remission; mos, months.

43.5 \pm 21.2%; P=0.22) and CD3⁺CD28⁻ PB T cells (36.4 \pm 20.6 versus 49.2 \pm 15.9; P=0.11) (Table 3 and Figure 2A). We found a tendency of low numbers of CD3⁺CD27⁻CD28⁻ T cells being associated with month 3 OR (odds-ratio 0.97; 95% confidence interval 0.92-1.01; P=0.14; Figure S5A). This association remained virtually unchanged after pairwise adjustment for clinical (international prognostic index, double/triple hit mutation, cell of origin, gender, age at leukapheresis, NOS mutations) and PB parameters (LDH levels at CART cell infusion, frequency of CD3⁺CD27⁻CD28⁻ T cells).

Low frequency of differentiated CD3⁺CD27⁻CD28⁻ PB T cells at leukapheresis identifies patients with a high likelihood for CR

Next, we compared the CD27 and CD28 expression status on PB T cells of 9 of 11 CR patients to 15 patients presenting with non-CR (PR, SD and PD). From two CR patients no PB was available. Notably, a low frequency of CD3⁺CD27⁻CD28⁻ T cells at the time of leukapheresis (13.7 \pm 11.7% versus 37.7 \pm 17.4%) was significantly associated with CR at month 3 (P=0.001) (Figure 2B and Table 3). Inclusion of CD3⁺CD27⁻CD28⁻ values of the two patients with missing PB data but available

values of the leukapheresis products (i.e., 16.5% and 37.4% of CD3⁺CD27⁻CD28⁻, respectively) changed the strength of the statistical comparison between CR and non-CR only very slightly (p-values 0.002 versus 0.001, respectively). For ease of comparison, the type of CAR used is given in Figure 2. Patients with low or high numbers of CD3⁺CD27⁻CD28⁻ T cells were equally distributed in the subgroups treated with different CAR products suggesting that the type of CAR used did not appear to affect CR rates.

Similar to the above analyses obtained with CART cell responders versus non-responders, pairwise adjustment for clinical and PB parameters did not significantly change this association (Figure S5B). Both CD3⁺CD27⁻ (25.1 \pm 12.0% versus 45.9 \pm 19.4%; P=0.008) and CD3⁺CD28⁻ T cells (27.2 \pm 15.3 versus 51.3 \pm 15.8; P=0.001) contributed to this association (Table 3; Figures 2C and S3). Of note, the residual CD27 expression on the CD27⁺ T cells within the CD3⁺CD28⁻ subset was found to be reduced compared to the one within the CD3⁺CD27⁺CD28⁺ subset. This indicated that the CD3⁺CD28⁻ subgroup had already begun to downregulate also CD27 expression (data not shown). Therefore, determining the double-negative CD27⁻CD28⁻ status of CD3⁺ T cells appeared to be the most robust strategy for enumerating differentiated T cells and also resulted in a moderately better statistical discrimination between CR and non-CR groups (P=0.001

versus $P=0.006$) when compared to the $CD3^+CD27^+CD28^+$ subset. To exclude a sampling bias due to the lack of PB samples from the two CR patients, in addition we compared the leukapheresis products of the CR patients with those of the non-CR patients, for whom the full dataset of 11 and 15 patients was available, in terms of their $CD3^+CD27^-CD28^-$ T cell counts (Table 3). Very similar to PB, we found that low frequencies of $CD3^+CD27^-CD28^-$ T cells ($15.2 \pm 12.6\%$ versus $35.8 \pm 17.2\%$) were significantly associated with CR at month 3 ($P=0.003$) also in the leukapheresis product. Receiver operator characteristics (ROC) curve was used to determine the cut-off above which non-CR could be expected. Numbers of $CD3^+CD27^-CD28^-$ T cells greater 18% or 35% predicted non-CR with 78% or 100% specificity, (Figure 2D). Moreover, the cut-off value of $\leq 18\%$ $CD3^+CD27^-CD28^-$ T cells predicted the duration of response over the subsequent 12-month follow-up period with high accuracy ($p<0.001$) (Figure 2E).

$CD3^+CD8^+CD27^-CD28^-$ are inferior to $CD3^+CD8^+CD27^+CD28^+$ CART cells in terms of proliferation and cytotoxic cytokine production, but not regarding target-cell cytotoxicity

CD19 CART cells kill malignant and normal CD19⁺ B cells without MHC restriction. $CD3^+CD8^+$ CD19 CART cells have been reported to be able to perform serial killings with higher efficiency and speed than $CD3^+CD4^+$ CD19 CART cells (46). Our above finding that patients with lower numbers of $CD3^+CD27^-CD28^-$ T cells at leukapheresis have a much better chance of achieving CR, when undergoing CD19-directed CART cell therapy, prompted us to test whether $CD3^+CD8^+CD27^+CD28^+$ are, in fact, functionally superior to $CD3^+CD8^+CD27^-CD28^-$ CD19 CART cells. Accordingly, we analyzed their cytotoxic, proliferative and cytokine-producing capabilities. Remarkably,

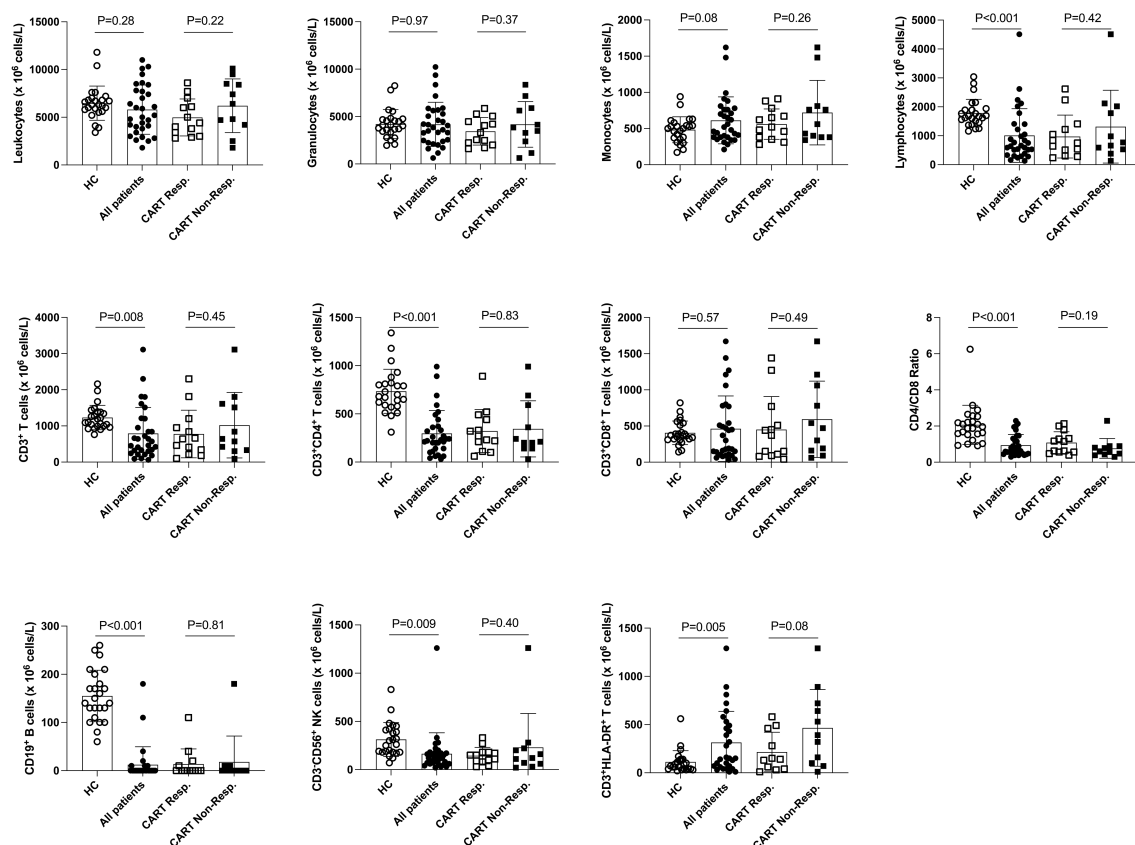


FIGURE 1

Distribution of leukocyte populations in the PB of healthy control subjects, total *r/r* DLBCL patients and CART cell recipients. Here, the distribution of PB cell populations of 24 healthy control subjects (HC) and 31 of 33* *r/r* DLBCL patients is shown. Data of 13 of 15* CART cell responders (except 11 for $CD3^+HLA-DR^+$ T cells) and 11 CART non-responders 3 months after CART therapy are shown separately. P-values (unpaired t-test) are indicated. *) PB of two patients belonging to the CART responders was not available for analyses at this stage.

TABLE 3 PB and leukapheresis material of r/r DLBCL patients scheduled for CART cell therapy contain significantly more CD3⁺ T cells with a differentiated CD27⁺CD28⁺ phenotype when compared to healthy control individuals.

	CD3 ⁺ CD27 ⁺ CD28 ⁺	CD3 ⁺ CD27 ⁺	CD3 ⁺ CD28 ⁺	CD3 ⁺ CD27 ⁺ CD28 ⁺	CD3 ⁺ CD27 ⁺ CD28 ⁺	CD3 ⁺ CD27 ⁺ CD28 ⁺
Peripheral blood						
All r/r DLBCL patients PB (n=31; 94.0%) [§]	48.7 ± 18.4*	38.6 ± 19.2	41.7 ± 19.6	13.0 ± 8.5	9.9 ± 7.3	28.7 ± 19.0
Healthy controls (n=24; 100%)	71.5 ± 12.3	19.6 ± 11.9	15.5 ± 8.5	8.9 ± 5.1	13.0 ± 7.8	6.6 ± 5.8
P-value [§]	<0.001	<0.001	<0.001	0.042	0.05	<0.001
CART responders (CR+PR) at 3 months (n=13; 39.4%) [§]	53.4 ± 18.6	33.5 ± 17.7	36.4 ± 20.6	13.1 ± 10.7	10.3 ± 6.0	23.3 ± 19.3
CART non-responders at 3 months (n=11; 33.3%)	43.2 ± 17.4	43.5 ± 21.2	49.2 ± 15.9	14.1 ± 7.7	8.4 ± 5.5	35.1 ± 18.1
P-values	0.18	0.22	0.11	0.79	0.43	0.14
CR at 3 months (n=9; 27.3%) [§]	61.5 ± 14.3	25.1 ± 12.0	27.2 ± 15.3	13.5 ± 12.0	11.3 ± 6.8	13.7 ± 11.7
Non-CR at 3 months (n=15; 45.5%)	41.0 ± 16.6	45.9 ± 19.4	51.3 ± 15.8	13.6 ± 7.7	8.3 ± 4.8	37.7 ± 17.4
P-values	0.006	0.008	0.001	0.97	0.21	0.001
Leukapheresis material						
CART Responders (CR+PR) at 3 months (n=15; 45.5%)	54.8 ± 15.4	32.3 ± 15.1	34.6 ± 17.4	12.9 ± 10.4	10.6 ± 6.1	21.7 ± 16.6
CART non-responders at 3 months (n=11; 33.3%)	42.7 ± 19.3	43.5 ± 21.6	48.3 ± 17.8	13.8 ± 7.4	9.1 ± 5.7	34.5 ± 18.8
P-values	0.09	0.13	0.06	0.80	0.51	0.08
CR at 3 months (n=11; 33.3%)	60.1 ± 13.5	26.3 ± 11.9	28.7 ± 15.2	13.5 ± 11.5	11.2 ± 6.9	15.2 ± 12.6
Non-CR at 3 months (n=15; 45.5%)	42.0 ± 17.1	44.9 ± 19.1	49.0 ± 16.2	13.1 ± 7.2	9.1 ± 5.1	35.8 ± 17.2
P-values	0.008	0.009	0.004	0.91	0.38	0.003

Shown are relative numbers of CD3⁺ T cells subsets in PB and the leukapheresis material differentially expressing CD27 and CD28. All enrolled and analyzed patients are compared to healthy control individuals. Alternatively patients have been stratified into CART responders (CR plus PR) versus non-responders. Another comparison examines patients with CR versus patients with non-CR. [§] The PB of two patients belonging to the CR group could not be analyzed. *) data show relative amounts of CD3⁺ T cells; [§] P-values were calculated with Student's t-test. CART, chimeric antigen receptor T cells; CR, complete remission; PB, peripheral blood; PR, partial remission; PD, progressive disease; SD, stable disease.

CD3⁺CD8⁺CD27⁺CD28⁺ and CD3⁺CD8⁺CD27⁺CD28⁺ CD19 CART cells (expressing the CD19-specific CART cell receptor on 91.6 ± 0.1% and 91.4 ± 0.1% of CD8⁺ T cells, respectively, **Figure S7**) killed CD19⁺ B cells (TM-LCL) with nearly identical efficacies over the entire range of effector to target (E:T) ratios tested, while no such killing of CD19⁺ K562 cells was observed with either of the two CD3⁺CD8⁺ CD19 CART cell subsets (**Figure 3A**). Notably, also CD3⁺CD4⁺ CART cells (expressing the CD19-specific CART cell receptor on 95.3 ± 0.8% of CD27⁺CD28⁺ and 94.9 ± 2.2% of CD27⁺CD28⁺ CD4⁺ T cells, respectively, **Figure S8**) killed the CD19⁺ B cells (TM-LCL), however, with at least 3- to 6-fold lower efficacy when compared to their CD3⁺CD8⁺ counterparts (**Figure 3A**). Notably, CD4⁺CD27⁺CD28⁺ outperformed CD4⁺CD27⁺CD28⁺ T cells in the killing of CD19⁺ target cells by a factor of 2. However, both CD3⁺CD8⁺CD27⁺CD28⁺ and CD3⁺CD4⁺CD27⁺CD28⁺ CART cells proliferated significantly more efficiently than CD3⁺CD8⁺CD27⁺CD28⁺ and CD3⁺CD4⁺CD27⁺CD28⁺ CART cells, respectively, when co-incubated with CD19⁺ TM-LCL cells at all E:T-ratios tested, with differences ranging between 1.5 ± 0.4 and 2.7 ± 1.7-fold for CD3⁺CD8⁺ and 1.0 ± 0.1 and 1.9 ± 1.1-fold for CD3⁺CD4⁺ T cells (**Figure 3B**). Moreover, CD3⁺CD8⁺CD27⁺CD28⁺ CART cells secreted higher levels of the Th1 cytokines IL-2, IFN-γ

and TNF-α, while CD3⁺CD8⁺CD27⁺CD28⁺ CART cells seemed to overproduce the Th2 cytokine IL-13 (**Figure 3C**). The situation was similar for CD3⁺CD4⁺ CART cells, with the sole exception that CD3⁺CD4⁺CD27⁺CD28⁺ as compared to CD3⁺CD4⁺CD27⁺CD28⁺ CART cells produced higher levels of IFN-γ. Notably, the elevated IL-2 secretion levels of CD3⁺CD8⁺CD27⁺CD28⁺ CART cells were paralleled by their increased high-affinity IL-2R (CD25) expression when compared to CD3⁺CD8⁺CD27⁺CD28⁺ CART cells (**Figure 3D**). The limited functional capabilities (i.e., proliferation, IL-2 and TNF-α production both subsets; IFN-γ production for CD8⁺ T cells) of CD27⁺CD28⁺ T cells can be explained by their belonging to the TEMRA and EM3 subsets of memory cells (CCR7⁺CD45RA⁺), which are known to have limited renewal capacity (**Figure S4**) (37).

Discussion

In this cohort study, we aimed to identify a simple and robust pre-infusion blood biomarker to predict the future response to CART cell treatment in r/r DLBCL patients. Compared to HC, r/r DLBCL patients presented with significantly more activated HLA-

DR-expressing PB T cells, indicating cellular activation and/or homeostatic proliferation (36), as well as pathologically increased, frequencies of CD3⁺CD27⁺CD28⁺ T cells. According to the linear T cell differentiation model proposed by Romero *et al.* and substantiated by our own analyses (Figure S4), T cells with this phenotype belong to the CCR7⁺CD45RA⁺ terminally differentiated T effector memory RA (TEMRA) and effector memory type 3 (EM3) cells, respectively (37). We stratified patients according to OR (CR and PR) versus non-response (SD and PD), or CR versus non-CR (PR, SD and PD) 3 months after CART cell treatment, respectively. This revealed that the pathologically high levels of CD3⁺CD27⁺CD28⁺ T cells were associated with non-CR (37.7 ± 17.4%), while patients with CR presented with low, almost physiological, levels of CD3⁺CD27⁺CD28⁺ T cells compared to HC (13.7 ± 11.7% versus 6.6 ± 5.8%). A numeric predictor of CR

was determined by plotting a ROC curve, which showed that a cut-off value of ≤18% CD3⁺CD27⁺CD28⁺ T cells (Figure 2B) predicted CR with high accuracy even 12 months after CART cell transfusion (Figure 2E). This is the first study identifying low numbers of CD3⁺CD27⁺CD28⁺ T cells as a valuable pre-infusion blood biomarker for long-term response to CART cell treatment in r/r DLBCL. Our clinical data corroborate previous *in vitro* findings indicating that both CD27 and CD28 are functionally important co-stimulatory molecules on T cells, which are critically involved in cellular activation programs (32, 47). Moreover, we have demonstrated herein that CD3⁺CD8⁺CD27⁺CD28⁺ CART cells have comparable CD19⁺ target cell killing activity when compared to CD3⁺CD8⁺CD27⁺CD28⁺ CART cells, however, they are clearly inferior regarding CD19⁺ target cell-dependent proliferation and cytotoxic cytokine production, such as IFN-γ

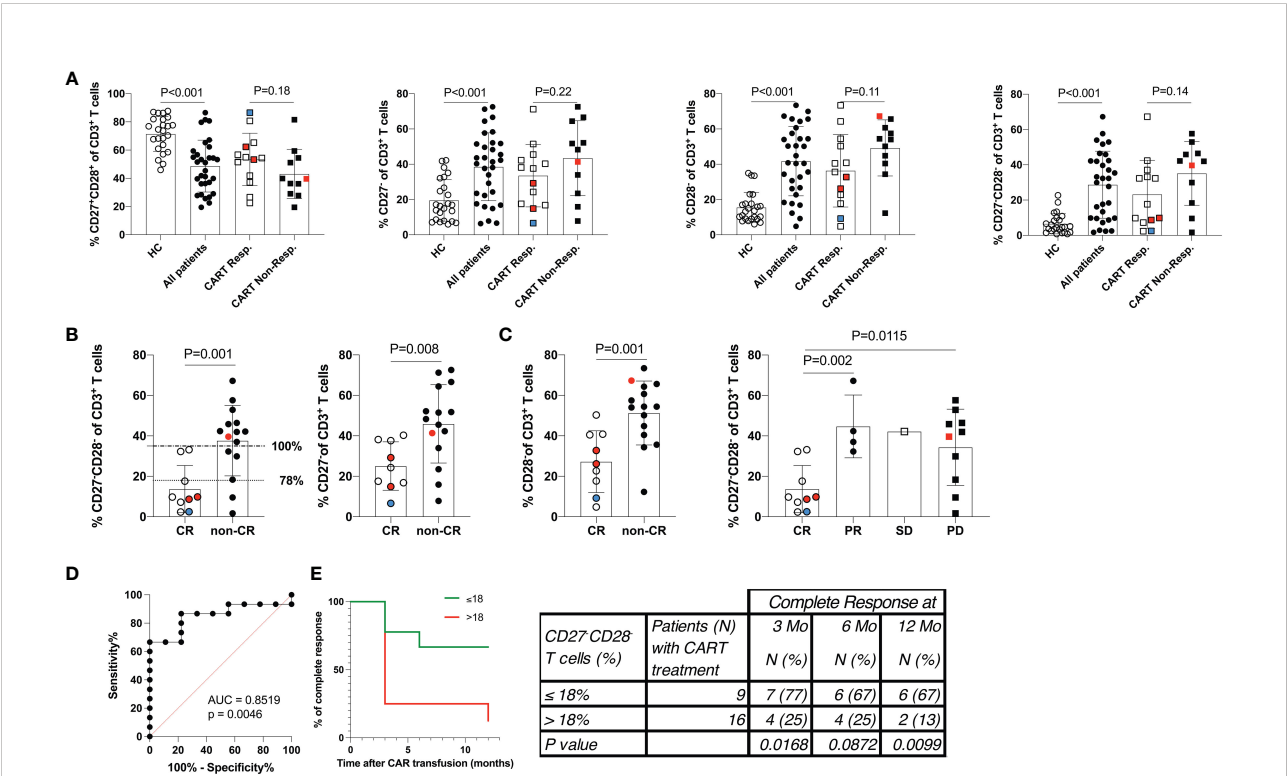


FIGURE 2 Low frequency of differentiated CD3⁺CD27⁺CD28⁺ T cells predicts a favorable response to CART cell therapy. **(A)** The distribution of PB CD3⁺ T cell populations stratified by the CD27 and CD28 expression status is given. Data show 24 healthy control subjects (HC), 31 of 33* r/r DLBCL patients scheduled for CART cell therapy, and more detailed data for 13 of 15* CART cell responders and all non-responders (n=11). **(B)** Shows the distribution of PB CD3⁺ T cell populations stratified by the CD27 and CD28 expression status in patients who were further separated into 9 of 11* complete responders and compared to 15 non-complete responders. Horizontal lines at 18% of CD3⁺CD27⁺CD28⁺ T cells indicate the 78% (dotted line) and at 35% of CD3⁺CD27⁺CD28⁺ T cells indicate 100% (dashed-and-dotted line) specificity levels (at sensitivity levels of 87% and 67%, respectively) of numbers of CD3⁺CD27⁺CD28⁺ T cell numbers to predict CR **(C)** Shown are the numbers of CD3⁺CD27⁺CD28⁺ T cells of patients who achieved complete remission (CR), partial remission (PR), stable disease (SD) or progressive disease (PD). P-values (unpaired Student's t-test) are indicated. Cell frequencies were determined in 31 of 33* patients. Patients were treated with tisagenlecleumab (white/black symbols), axicabtagene ciloleumab (red symbols) or YT323 (blue symbols). * PB of two patients belonging to the CART responders was not available for analyses at this stage. **(D)** ROC (receiver operator characteristics) curve indicating the performance of numbers CD3⁺CD27⁺CD28⁺ T cells for classifying CR. **(E)** Duration of complete remission (CR) after CART cell therapy. Shown are the percent of patients presenting with CR over the observational period of 12 months (Mo) with staging at 0, 3, 6 and 12 months. Patients were stratified according to those with >18% or ≤18% of CD3⁺CD27⁺CD28⁺ T cells at the time of leukapheresis. Table shows the number (N) of patients within each group at each time point (percent of group in parenthesis). P values were calculated with Fisher's exact test.

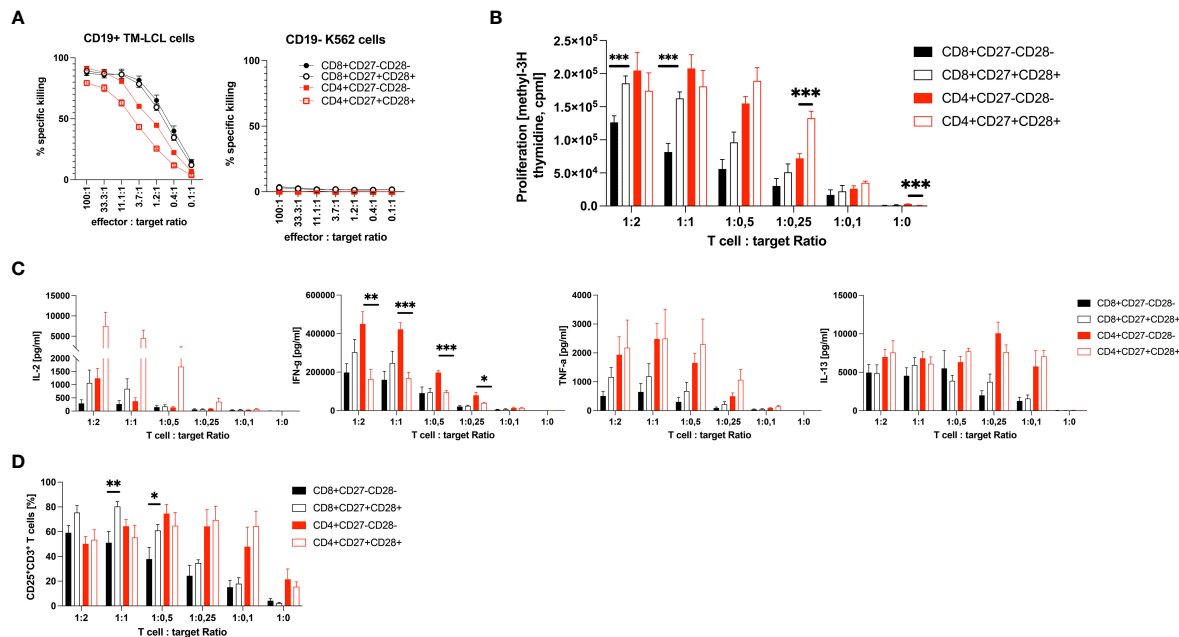


FIGURE 3

Functional comparison of CD3⁺CD8⁺ and CD3⁺CD4⁺ CD27⁺CD28⁺ to CD3⁺CD8⁺ and CD3⁺CD4⁺ CD27⁻CD28⁻ CD19 CART cells *in vitro*. Shown is (A) the cytotoxic potential as percent specific killing in 5-hour ⁵¹Cr-release assays, (B) the proliferation as count per minutes (cpm) (C) the cytokine production in pg/ml and (D) the percent expression of the high-affinity IL-2R (CD25) on CD27⁻CD28⁻ CD3⁺CD8⁺ and CD3⁺CD4⁺ T cells in comparison to CD27⁺CD28⁺ CD3⁺CD8⁺ and CD3⁺CD4⁺ T cells upon co-culture with CD19⁺ TM-LCL cells. The cytotoxic potential of CD27⁻CD28⁻ and CD27⁺CD28⁺ T cells in (A) is also shown against CD19⁺ K562 cells. X-axes show the effector to target ratios with either a constant amount of 5 × 10³ target cells (A), or a constant amount of effector cells of 1 × 10⁵ (B–D). Data are shown as means plus SEM (whiskers). Numbers of CD19 CAR positive T cells were 91.5 ± 0.1% and 96.0 ± 0.3%, respectively. Data show the summary of three (A, D) or four (B, C) independent experiments with three different donors in biological triplicates for CD8⁺ T cells, except one donor in duplicates for Cytotoxicity tests, and two independent experiments with two different donors in biological triplicates for CD4⁺ T cells. *P < 0.05, **P < 0.01, ***P < 0.001 as determined by unpaired Student's t-test.

and TNF-α (48, 49). Interferon-γ is well-known to contribute to the CART cells' cytotoxicity by targeting and destroying the tumor stroma (48), while TNF-α has been shown to sensitize tumor cells themselves for getting killed by CD8⁺ T cells (49). In addition, the elevated CD25 (high-affinity IL-2R) expression levels, along with their increased IL-2 secretion, speaks for a better overall fitness of CD3⁺CD8⁺CD27⁺CD28⁺ compared to CD3⁺CD8⁺CD27⁻CD28⁻ CART cells.

We show here that CD3⁺CD4⁺ T cells can also be turned into CART killer cells, however, they have a 3- to 6-fold lower killing efficacy when compared to CD3⁺CD8⁺ T cells. Similar to CD8⁺CD27⁺CD28⁺ T cells, CD4⁺CD27⁺CD28⁺ T cells proliferated better and produced more IL-2 and TNF-α when compared to CD4⁺CD27⁻CD28⁻ T cells. However, it is noteworthy that CD4⁺CD27⁻CD28⁻ T cells produced significantly more IFN-γ than CD4⁺CD27⁺CD28⁺ T cells, which may explain their moderately superior killing activity compared with CD4⁺CD27⁺CD28⁺ T cells.

Accordingly, our findings also provide an explanation as to why the lack of CD27 and/or CD28 on T cells has been described

to be associated with impaired immuno-surveillance capabilities of non-CART cells, previously (35). While the engagement of CD28 with an agonistic CD28 monoclonal antibody was, in fact “too potent *in vivo*” and induced a highly problematic cytokine storm in six participants of a first-in-human phase I clinical trial in a previous study (50), engagement of CD27 by varilumab (CDX-1127), a novel, agonistic, fully human CD27 monoclonal antibody, revealed durable antigen-specific antitumor efficacy (51), by increasing effector T cell numbers with an activated phenotype which was at the expense of naïve and Treg cell numbers in pre-clinical and human phase I and II immunotherapy trials (52). Moreover, conditioning treatment with CD27 mAb in a preclinical model enhanced the expansion and anti-tumor activity of adoptively transferred T cells (53) and by activating T cells recruits and stimulates myeloid cells for enhanced killing of CD27 mAb-opsonized tumors (54). In some CD27 mAb-treated melanoma patients, increased numbers of T cells that recognize melanoma-related antigens were revealed (52). Thus, the expression and active engagement on T cells of CD27 by mAbs has the potential to positively affect adaptive

immunotherapy against cancer (55), suggesting conversely that the pathological increase of T cells which lack CD27 expression could be a gradually increasing disadvantage.

Until recently, the best predictors for response to CART cell treatment in r/r DLBCL have been factors not related to immune system function, such as low tumor volume, number of extranodal sites, low serum LDH levels immediately prior to CART cell infusion and a low ECOG performance status (7, 14–16). However, tumor volume/burden lacks specificity because it is a predictor of therapeutic success for the treatment of a large collection of different disease entities and therapies (56). The same holds true for serum LDH levels, which are an established marker of tumor burden, metabolic activity and thus aggressiveness of NHL. Very similar to tumor volume, the serum LDH level has been established as a prognostic factor for the disease course and treatment success of NHL since the 1970s and therefore is also included in the IPI score. Accordingly, while we found elevated serum LDH levels in the overall r/r DLBCL study group (325.9 ± 180.3 U/L), they were lower in OR (236.1 ± 114.0 versus 366.1 ± 162.5 ; $P=0.08$) and CR (246.4 ± 132.2 versus 323.9 ± 155.9 ; $P=0.19$) patients as compared to non-OR and non-CR patients, respectively, especially when determined at leukapheresis (Table 1), although, without reaching statistical significance.

More recently, the search for new biomarkers has turned to studying the nature of the tumor microenvironment, with the intention to identify the mechanistic basis of putative inhibitory factors, followed by the development of strategies for their inhibition/neutralization with, e.g., checkpoint inhibitors (57). These experimental approaches will help us to understand how to pave the way for the facilitated tumor invasion by the infused CART cells and to ultimately steer and support the activation and cytotoxicity of the latter. However, access to the site of tumor cell accumulation in DLBCL for diagnostic purposes, i.e., the bone marrow and/or lymph nodes, demands utterly invasive and thus burdensome procedures (e.g., bone marrow and/or lymph node biopsies). In contrast, the herein described assessment of the levels of peripheral blood CD3⁺CD27⁺CD28⁺ T cells is easy to perform and standardize, also in sequential series of biological samples and thus suitable for daily clinical laboratory routine. In addition, numbers of CD3⁺CD27⁺CD28⁺ T cells can reliably be determined in the leukapheresis product, as well with similar accuracy to peripheral blood (Figure S6 and Table S3).

Which mechanism(s) could be responsible for the down-regulation of CD27 and CD28 on the surface of CD3⁺ T cells in the PB of CART cell non-responders?

The fact that almost 90% of patients expressed elevated levels of HLA-DR⁺ T cells in their circulation (Table 2), indicates a possible hyperactivation of the immune system (58), which may be a reflection of the lengthy disease course (35.9 ± 53.8 months) and the associated microbial pressure on the lymphodepleted patients and/or the number of prior therapy lines given (median 3, range 1–11) to our patients. In this study, we found no

correlation between the total number of different treatment lines and the number of CD3⁺CD27⁺CD28⁺ T cells in the PB at the time of leukapheresis. However, we found a weak correlation between the number of R-CHOP cycles administered and the number of CD3⁺CD27⁺CD28⁺ T cells ($r=0.3931$, $P=0.0287$).

Alternatively, the increased number of HLA-DR⁺ T cells could also be a sign of homeostatic proliferation due to treatment-induced lymphopenia. In this regard, it is important to note that homeostatically proliferating CD8⁺ T cells have been shown to neo-express HLA-DR, but always in conjunction with telomerase activity (36).

One mechanism explaining the loss of CD27 on activated T cells is that these cells tend to upregulate CD70, which is the ligand for CD27 (59). In turn, CD70 up-regulation and interaction with its ligand CD27, either on the same or on adjacent cells, may then lead to reactive downregulation of the latter (60). Similarly, CD28 modulation is known to be the result of cellular activation and replicative senescence (31, 61). Notably, the molecular mechanism(s) leading to CD70 upregulation on T cells during chronic systemic inflammation, such as in lupus erythematosus, are governed by epigenetic changes in T cells, such as histone modifications at the TNFSF7 (CD70) promoter (62) with subsequent downregulation of CD27 on terminally differentiated T effector memory RA cells (TEMRA) (63). CD28^{null} cells were also found to exhibit significant changes in their whole-genome methylation pattern (64) and to receive less signaling through the ERK and JNK pathways, reducing the expression of the DNA methyltransferases Dnmt1 and Dnmt3a, which in turn contributes to the epigenetic downregulation of CD28 expression (65). Taken together, both CD27 and CD28 modulation seem to be governed by several factors, including ligand- and epigenetic/promoter-driven downregulation, all supported by chronic hyperactivation of the immune system.

The fact that low lymphocyte counts are frequently detected in DLBCL patients at initial presentation (66) and that lymphocytopenia after first-line therapy is a predictor of relapse (67) is well known. Therefore, it was not entirely surprising that our patient population suffered from significant lymphopenia. Several reasons can be suggested for the intrinsic activation-induced lymphocyte depletion, such as i) canonical tumor antigen-specific activation by lymphoma cells, ii) cytokine-dependent bystander activation caused by DLBCL-secreted and T cell tropic cytokines like IL-2 and IL-6 (68), or iii) reactivation of latent viruses such as CMV or EBV, which have been shown to be associated with the increased appearance of CD3⁺CD27⁺CD28⁺ PB T cells previously (28). While the first two explanations are the matter of intense research, the latter can be excluded since no CMV and EBV reactivation was observed in our patients.

Previous studies suggested that an increased frequency of CD27⁺CD45RO⁺CD8⁺ T cells at the time of leukapheresis may

correlate with sustained remission in patients with chronic lymphocytic leukemia treated with CD19 CART cells (21), in multiple myeloma patients treated with B cell maturation antigen (BCMA)-specific CART cells (22), and very recently in patients with DLBCL (23). The authors suggested that CD27⁺CD45RO⁻CD8⁺ T cells belong to the group of antigen-experienced CD3⁺CD8⁺ T lymphocytes that have long-lasting memory capabilities and improved ability to expand *in vitro* and *in vivo* (21, 22, 24). However, this T cell subset, which according to our algorithm belongs to T cells with a CD3⁺CD27⁺CD28⁻ phenotype (29), was not found to be associated with OR and/or CR in our study (Table 3). We considered it important to focus on a combination of T lymphocyte surface markers with proven importance during the T cell activation process, i.e., well-established co-stimulatory molecules, such as CD27 and CD28, rather than the combination of one such marker (CD27) with a purely phenotypic marker, such as CD45RO negativity, which may, in fact, identify more than one T cell phenotype, e.g., naïve T cells and antigen-experienced “stem cell memory” cells (23). Romero *et al.*, showed in healthy individuals that the majority of CD3⁺CD8⁺CD27⁻CD28⁻ T cells is composed of CCR7⁻CD45RA⁺ terminally differentiated T effector memory RA cells (TEMRA), while they clearly also contain a smaller 10–20% fraction of CD27⁻CD28⁻ T cells which belongs to the effector memory (EM) subset. The latter subset is commonly referred to as EM3 cells (37). Indeed, in CART patients at leukapheresis and healthy controls, it turned out that CD3⁺CD8⁺CD27⁻CD28⁻ T cells are also highly enriched for CD45RA⁺CCR7⁻ TEMRA cells (72.3±18.8% in healthy donors vs. 59.2±19.2% in lymphoma patients), the rest of the cells presented with a CD45RA⁻CCR7⁻ EM phenotype, which is compatible with their relationship to EM3 cells (Figure S4). Within the CD3⁺CD4⁺ T cell subset, the picture was different. Herein, CD27⁻CD28⁻ T cells are mainly composed of CCR7⁻CD45RA⁻ EM cells belonging to the EM3 phenotype, while the number of TEMRA is usually low to non-existent among CD3⁺CD4⁺ T cells in healthy individuals (Figure S4). Thus, when gating on CD3⁺CD27⁻CD28⁻ T cells one reads out the “sum of TEMRA and EM3 T cells” of both CD8⁺ and CD4⁺ T cells, with CD8⁺ T cells mainly contributing to the CD27⁻CD28⁻ phenotype (65.4 ± 23.3% for healthy controls and 59.1 ± 23.8% for patients). A similar picture is seen in typical DLBCL patients (Figure S4).

Furthermore, analyzes of activation marker expression on T cells used for *in vitro* experiments confirmed that HLA-DR was clearly expressed on all cell types with a tendency for up-regulation on CD27⁻CD28⁻ T cells as compared to CD27⁺CD28⁺ T cells on CD4 and CD8 T subsets. Moreover, CD69 was upregulated on both CD4⁺ and CD8⁺ CD27⁻CD28⁻ T cells as compared to their CD27⁺CD28⁺ counterparts (Table S4). The picture was different for CD25 expression, which was downregulated on CD4⁺CD27⁻CD28⁻ T cells as compared to CD4⁺CD27⁺CD28⁺ T cells. However, no clear sign for the

upregulation of exhaustion markers (LAG-3, TIM-3 and PD-1) was evident on *in vitro* tested CART cells (Table S4), except TIM-3 on CD8⁺ T cells.

Comparable albeit slightly different changes were found on cells of patients undergoing leukapheresis. Here, HLA-DR was generally more up-regulated on CD27⁻CD28⁻ T cells when compared to CD27⁺CD28⁺ T cells in patients. CD69 was found to be upregulated more on CD8⁺CD27⁻CD28⁻ T cells as compared to CD8⁺CD27⁺CD28⁺ T cells, while no significant expression of CD69 was found on CD4⁺ T cells (Figure S9). CD25 expression was lower in all patients on the CD27⁻CD28⁻ when compared to the CD27⁺CD28⁺ subset. Notably, PD-1 was clearly upregulated on CD4⁺CD27⁻CD28⁻ as compared to CD4⁺CD27⁺CD28⁺ T cells which was in clear contrast to the CD8⁺ subset, in which PD-1 expression was higher on the CD27⁺CD28⁺ T cells when compared to CD27⁻CD28⁻ T cells (Figure S9). The latter findings points to a remarkable and potentially functionally relevant dissociation of the expression of co-stimulatory and exhaustion marker molecules in DLBCL patients.

The significant association of low numbers of CD3⁺CD27⁻CD28⁻ T cells in PB at the time of leukapheresis with CR at 3 months with the cut-off of ≤ 18% CD3⁺CD27⁻CD28⁻ T cells to predict CR at 12 months after CART cell treatment seems to be a promising new predictive biomarker. Although our study shows that patients with high numbers of CD3⁺CD27⁻CD28⁻ T cells may not respond as well to CART cell therapy as patients with low numbers of CD3⁺CD27⁻CD28⁻ T cells, we are far from claiming that this circumstance is irreversible. For example, it may well turn out that administration of checkpoint inhibitors at the time of CART cell administration, e.g., against PD-1, could improve the inferior outcome of this group of patients. Of note in that respect, two of our patients with high numbers of differentiated T cells responded to CART cells when pretreated with pembrolizumab (69). Moreover, recent studies have shown that the use of the Bruton's tyrosine kinase inhibitor ibrutinib (70), or the phosphoinositide-3 kinase inhibitor idelalisib (71, 72) can improve CART cell production in patients with chronic lymphocytic leukemia. Similar effects may be realized in r/r DLBCL in the future.

The better *in vivo* performance of CART cell products containing a low baseline amount of CD3⁺CD27⁻CD28⁻ T cells may also have adverse effects. Patients receiving such T cells may suffer from more treatment-related toxicities after CART cell transfusion because the CART cells may exhibit greater CD19 target cell-dependent proliferation and cytotoxic factor (IFN-γ, TNF-α) production *in vivo* and thus a likely higher killing rate. However, no significant associations were found between the number of CD3⁺CD27⁻CD28⁻ T cells in the leukapheresis product and the occurrence of i) cytokine release syndrome (CRS, $r=0.1$ and $P=0.072$), ii) clinical requirements for tocilizumab therapy ($r=0.14$ and $P=0.51$), or iii) long-term

cytopenias ($r=0.16$ and $P=0.57$) (Spearman's r -tests) in the present study.

Several important limitations of this trial should be considered. During the planning and recruitment phase of this trial no validated flow cytometric assay was available to monitor CART cell expansion *in vivo* and respective binding reagents for reliable monitoring had only become available very recently (73). Therefore, the relationship between the $CD3^+CD27^-CD28^-$ T cell status determined at leukapheresis and the kinetics of CART cell expansion *in vivo* could not be monitored.

In addition, our study is limited by a small sample size of only 33 patients with 26 patients who received CART cells at least three-month before response assessment. Therefore, larger multi-center studies are certainly needed to confirm our findings in the future. Due to the limited sample size, we were not able to test our biomarker in an independent validation cohort.

It has to be noted that the ethical permission did not include to test CART cells from patients in *in vitro* studies.

Therefore, in the CD19 CART cell *in vitro* studies shown here, T cells of healthy donors were transduced with a CD19-CAR. For that purpose, PBMC from healthy donors were processed for CART cell production using a protocol comparable to that used for the processing of the leukapheresis products from patients, without prior sorting into $CD4^+$ and $CD8^+$ T cells subsets before transduction and expansion. Accordingly, CD3CD28-bead stimulated PBMC were transduced with the CD19 CAR and further expanded for 14 days. Upon cryopreservation and recultivation, CART cells were further expanded by incubation with irradiated (120 Gy) $CD19^+$ TM-LCL cells for 10 days followed by FACS-sorting for CD27 and CD28 expression. TM-LCL cells, while being non-proliferative, are still able to provide the CD19 antigen necessary for antigen-dependent proliferation of CD19 CART cells. They have been successfully used in the past for CD19 CART cell expansion (42). In fact, upon co-culturing with irradiated TM-LCL cells, the authors of this report routinely observed a 18-20-fold expansion of CD19 CART cells within 10 days. Expanded and sorted CART cells were then rested for 7 days followed by determination of their CD27 and CD28 expression status, their antigen-dependent cytotoxicity, proliferative capacity and factor production capabilities. While we did not observe a significant difference in the killing capacity between $CD27^+CD28^+$ and $CD27^-CD28^-$ CART cells, we consider the differences in the proliferative capacity of $CD3^+CD27^+CD28^+$ CD19 CART cells versus $CD3^+CD27^-CD28^-$ CD19 CART cells worth reporting, especially since previous studies had already shown that the ability to proliferate and expand well is associated with the expression of T cell clusters harboring upregulated proliferation-associated genes (74). Our study now shows that a similar stratification of T cells can be achieved by virtue of separating T cells according to their surface-expression status of the co-stimulatory molecules CD27 and CD28. It is in line with the

linear differentiation model of T cells which has shown previously that $CD3^+CD27^-CD28^-$ T cells consist of TEMRA and EM3 cells, both belong to the terminally differentiated T effector memory cells with undetectable TREC numbers and short telomers (37). Elevated numbers of this phenotype are not found in healthy individuals (Figure 2A), but are a salient feature of individuals with considerable immunological dysregulation (chronic inflammation), such as the one found in r/r DLBCL patients.

In summary, our study has identified that a low number of $CD3^+CD27^-CD28^-$ T cells is a new biomarker associated with better treatment response to CART cell therapy. This novel insight has the potential to contribute to an improved selection of patients with a high chance of CR after CART cell treatment and/or to form the rational basis for co-medications, such as ibrutinib, at the time of leukapheresis or administration of checkpoint-inhibitors at the time of CART transfusion. Such findings may thus provide the basis for further increasing the success rates of this innovative and potentially curative therapy.

Data availability statement

The raw data supporting the conclusions of this article will be made available by the authors. Requests to access the datasets should be directed to Dr. Nina Worel at nina.worel@meduniwien.ac.at.

Ethics statement

The studies involving human participants were reviewed and approved by Ethics Committee of the Medical University of Vienna, EC No.:1422/2015, 1607/2018, 2055/2019, 1290/2020. The patients/participants provided their written informed consent to participate in this study.

Author contributions

UJ, NW, and WP designed research; NW, KG-P, BK, MS, AT, AR, UK, EP, PS, CS, HH, VG, JH, BS, ML, NS, EF, PW, WR, and IS-K performed research and analyzed data; UJ, GH, PW, NW, and WP supervised experiments and clinical study; WP, NW, KG-P, and UJ wrote the paper. All authors contributed to the article and approved the submitted version.

Funding

UJ, VG and JH were supported by the Innovative Medicines Initiative (IMI) T2EVOLVE. This project has received funding

from the Innovative Medicines Initiative 2 Joint Undertaking under grant agreement No 945393. This Joint Undertaking receives support from the European Union's Horizon 2020 research and innovation program and EFPIA. The funders had no role in study design, data collection and analysis, decision to publish, or preparation of the manuscript.

Acknowledgments

We want to thank Beate Pribitzer, Karin Feldmann, Martina Muck, Martina Preslmayr, Verena Raggl and Marie-Christin Rösseisen for their laboratory support, the team of nurses for taking excellent care of patients and patient's samples, and the physicians who referred the patients for further treatment with CART cells. The authors are indebted to Dr. Mairi McGrath for expert proofreading.

Conflict of interest

With regards to the authors' disclosure of potential conflicts of interest we would like to indicate that WP receives honoraria from Novartis, Astra Zeneca and Roche. UJ reports honoraria and advisory roles for Novartis, BMS/

Celgene, Gilead, Miltenyi. NW, PW, and GH report honoraria from Novartis, BMS/Celgene and Gilead. WR reports honoraria from BMS/Celgene. JH reports honoraria from Novartis.

The remaining authors declare that the research was conducted in the absence of any commercial or financial relationships that could be construed as a potential conflict of interest.

Publisher's note

All claims expressed in this article are solely those of the authors and do not necessarily represent those of their affiliated organizations, or those of the publisher, the editors and the reviewers. Any product that may be evaluated in this article, or claim that may be made by its manufacturer, is not guaranteed or endorsed by the publisher.

Supplementary material

The Supplementary Material for this article can be found online at: <https://www.frontiersin.org/articles/10.3389/fimmu.2022.1004703/full#supplementary-material>

References

- Howlader N, Noone AM, Krapcho M, Miller D, Brest A, Yu M, et al. *SEER cancer statistics review*. Bethesda, MD: National Cancer Institute (2020).
- Sant M, Minicozzi P, Mounier M, Anderson LA, Brenner H, Holleczer B, et al. Survival for haematological malignancies in Europe between 1997 and 2008 by region and age: Results of EURO-CARE-5, a population-based study. *Lancet Oncol* (2014) 15:931–42. doi: 10.1016/S1470-2045(14)70282-7
- Crump M, Neelapu SS, Farooq U, Van Den Neste E, Kuruvilla J, Westin J, et al. Outcomes in refractory diffuse large b-cell lymphoma: Results from the international SCHOLAR-1 study. *Blood* (2017) 130:1800–8. doi: 10.1182/blood-2017-03-769620
- Hamadani M, Hari PN, Zhang Y, Carreras J, Akpek G, Aljurj MD, et al. Early failure of frontline rituximab-containing chemo-immunotherapy in diffuse large b cell lymphoma does not predict futility of autologous hematopoietic cell transplantation. *Biol Blood Marrow Transplant* (2014) 20:1729–36. doi: 10.1016/j.bbmt.2014.06.036
- Gisselbrecht C, Schmitz N, Mounier N, Singh Gill D, Linch DC, Trneny M, et al. Rituximab maintenance therapy after autologous stem-cell transplantation in patients with relapsed CD20(+) diffuse large b-cell lymphoma: Final analysis of the collaborative trial in relapsed aggressive lymphoma. *J Clin Oncol* (2012) 30:4462–9. doi: 10.1200/JCO.2012.41.9416
- June CH, Sadelain M. Chimeric antigen receptor therapy. *N Engl J Med* (2018) 379:64–73. doi: 10.1056/NEJMra1706169
- Schuster SJ, Bishop MR, Tam CS, Waller EK, Borchmann P, McGuirk JP, et al. Tisagenlecleucel in adult relapsed or refractory diffuse large b-cell lymphoma. *N Engl J Med* (2019) 380:45–56. doi: 10.1056/NEJMoa1804980
- Hopfinger G, Jager U, Worel N. CAR-T cell therapy in diffuse large b cell lymphoma: Hype and hope. *Hemasphere* (2019) 3:e185. doi: 10.1097/HS9.0000000000000185
- Awasthi R, Pacaud L, Waldron E, Tam CS, Jager U, Borchmann P, et al. Tisagenlecleucel cellular kinetics, dose, and immunogenicity in relation to clinical factors in relapsed/refractory DLBCL. *Blood Adv* (2020) 4:560–72. doi: 10.1182/bloodadvances.2019000525
- Neelapu SS, Locke FL, Bartlett NL, Lekakis LJ, Miklos DB, Jacobson CA, et al. Axicabtagene ciloleucel CAR T-cell therapy in refractory large b-cell lymphoma. *N Engl J Med* (2017) 377:2531–44. doi: 10.1056/NEJMoa1707447
- Abramson JS, Palomba ML, Gordon LI, Lunning MA, Wang M, Arnason J, et al. Lisocabtagene maraleucel for patients with relapsed or refractory large b-cell lymphomas (TRANSCEND NHL 001): A multicentre seamless design study. *Lancet* (2020) 396:839–52. doi: 10.1016/S0140-6736(20)31366-0
- Locke FL, Ghobadi A, Jacobson CA, Miklos DB, Lekakis LJ, Oluwole OO, et al. Long-term safety and activity of axicabtagene ciloleucel in refractory large b-cell lymphoma (ZUMA-1): A single-arm, multicentre, phase 1-2 trial. *Lancet Oncol* (2019) 20:31–42. doi: 10.1016/S1470-2045(18)30864-7
- Mirzaei HR, Mirzaei H, Namdar A, Rahmati M, Till BG, Hadjati J. Predictive and therapeutic biomarkers in chimeric antigen receptor T-cell therapy: A clinical perspective. *J Cell Physiol* (2019) 234:5827–41. doi: 10.1002/jcp.27519
- Nastoupil LJ, Jain MD, Feng L, Spiegel JY, Ghobadi A, Lin Y, et al. Standard-of-Care axicabtagene ciloleucel for relapsed or refractory large b-cell lymphoma: Results from the US lymphoma CAR T consortium. *J Clin Oncol* (2020) 38:3119–28. doi: 10.1200/JCO.19.02104
- Vercellino L, Di Blasi R, Kanoun S, Tessoulin B, Rossi C, D'Aveni-Piney M, et al. Predictive factors of early progression after CAR T-cell therapy in relapsed/refractory diffuse large b-cell lymphoma. *Blood Adv* (2020) 4:5607–15. doi: 10.1182/bloodadvances.2020003001
- Westin JR, Tam CS, Borchmann P, Jaeger U, McGuirk JP. Correlative analyses of patient and clinical characteristics associated with efficacy in tisagenlecleucel-treated relapsed/refractory diffuse large b-cell lymphoma patients in the Juliet trial. *Blood* (2019) 134:4103. doi: 10.1182/blood-2019-129107
- Wang X, Riviere I. Clinical manufacturing of CAR T cells: Foundation of a promising therapy. *Mol Ther Oncolytics* (2016) 3:16015. doi: 10.1038/mt.2016.15

18. Rodriguez-Garcia A, Palazon A, Noguera-Ortega E, Powell DJ Jr., Guedan S. CAR-T cells hit the tumor microenvironment: Strategies to overcome tumor escape. *Front Immunol* (2020) 11:1109. doi: 10.3389/fimmu.2020.01109
19. Orlando EJ, Han X, Tribouley C, Wood PA, Leary RJ, Riester M, et al. Genetic mechanisms of target antigen loss in CAR19 therapy of acute lymphoblastic leukemia. *Nat Med* (2018) 24:1504–6. doi: 10.1038/s41591-018-0146-z
20. Perna F, Sadelain M. Myeloid leukemia switch as immune escape from CD19 chimeric antigen receptor (CAR) therapy *Transl Cancer Res* (2016) 5:S221–S225. doi: 10.21037/tcr.2016.08.15
21. Fraietta JA, Lacey SF, Orlando EJ, Pruteanu-Malinici I, Gohil M, Lundh S, et al. Determinants of response and resistance to CD19 chimeric antigen receptor (CAR) T cell therapy of chronic lymphocytic leukemia. *Nat Med* (2018) 24:563–71. doi: 10.1038/s41591-018-0010-1
22. Cohen AD, Garfall AL, Stadtmauer EA, Melenhorst JJ, Lacey SF, Lancaster E, et al. B cell maturation antigen-specific CAR T cells are clinically active in multiple myeloma. *J Clin Invest* (2019) 129:2210–21. doi: 10.1172/JCI126397
23. Cuffel A, Allain V, Faivre L, Di Blasi R, Morin F, Vercellino L, et al. Real-world characteristics of T-cell apheresis and clinical response to tisagenlecleucel in b-cell lymphoma. *Blood Adv* (2022) 6:4657–60. doi: 10.1182/bloodadvances.2022007057
24. Garfall AL, Dancy EK, Cohen AD, Hwang WT, Fraietta JA, Davis MM, et al. T-Cell phenotypes associated with effective CAR T-cell therapy in postinduction vs relapsed multiple myeloma. *Blood Adv* (2019) 3:2812–5. doi: 10.1182/bloodadvances.2019000600
25. Gattinoni L, Klebanoff CA, Palmer DC, Wrzesinski C, Kerstann K, Yu Z, et al. Acquisition of full effector function *in vitro* paradoxically impairs the *in vivo* antitumor efficacy of adoptively transferred CD8+ T cells. *J Clin Invest* (2005) 115:1616–26. doi: 10.1172/JCI24480
26. Rosenberg SA, Yang JC, Sherry RM, Kammula US, Hughes MS, Phan GQ, et al. Durable complete responses in heavily pretreated patients with metastatic melanoma using T-cell transfer immunotherapy. *Clin Cancer Res* (2011) 17:4550–7. doi: 10.1158/1078-0432.CCR-11-0116
27. Allen ES, Stroncek DF, Ren J, Eder AF, West KA, Fry TJ, et al. Autologous lymphapheresis for the production of chimeric antigen receptor T cells. *Transfusion* (2017) 57:1133–41. doi: 10.1111/trf.14003
28. Appay V, Dunbar PR, Callan M, Klennerman P, Gillespie GM, Papagno L, et al. Memory CD8+ T cells vary in differentiation phenotype in different persistent virus infections. *Nat Med* (2002) 8:379–85. doi: 10.1038/nm0402-379
29. Appay V, van Lier RA, Sallusto F, Roederer M. Phenotype and function of human T lymphocyte subsets: Consensus and issues. *Cytometry A* (2008) 73:975–83. doi: 10.1002/cyto.a.20643
30. van Baarle D, Tsegaye A, Miedema F, Akbar A. Significance of senescence for virus-specific memory T cell responses: Rapid ageing during chronic stimulation of the immune system. *Immunol Lett* (2005) 97:19–29. doi: 10.1016/j.imlet.2004.10.003
31. Effros RB. Loss of CD28 expression on T lymphocytes: A marker of replicative senescence. *Dev Comp Immunol* (1997) 21:471–8. doi: 10.1016/S0145-305X(97)00027-X
32. Hintzen RQ, Lens SM, Lammers K, Kuiper H, Beckmann MP, van Lier RA. Engagement of CD27 with its ligand CD70 provides a second signal for T cell activation. *J Immunol* (1995) 154:2612–23.
33. Lenschow DJ, Walunas TL, Bluestone JA. CD28/B7 system of T cell costimulation. *Annu Rev Immunol* (1996) 14:233–58. doi: 10.1146/annurev.immunol.14.1.233
34. Hendriks J, Gravestien LA, Tesselaar K, van Lier RA, Schumacher TN, Borst J. CD27 is required for generation and long-term maintenance of T cell immunity. *Nat Immunol* (2000) 1:433–40. doi: 10.1038/80877
35. Kamphorst AO, Wieland A, Nasti T, Yang S, Zhang R, Barber DL, et al. Rescue of exhausted CD8 T cells by PD-1-targeted therapies is CD28-dependent. *Science* (2017) 355:1423–7. doi: 10.1126/science.aaf0683
36. Speiser DE, Migliccio M, Pittet MJ, Valmori D, Lienard D, Lejeune F, et al. Human CD8(+) T cells expressing HLA-DR and CD28 show telomerase activity and are distinct from cytolytic effector T cells. *Eur J Immunol* (2001) 31:459–66. doi: 10.1002/1521-4141(200102)31:2<459::AID-IMMU459>3.0.CO;2-Y
37. Romero P, Zippelius A, Kurth I, Pittet MJ, Touvrey C, Iancu EM, et al. Four functionally distinct populations of human effector-memory CD8+ T lymphocytes. *J Immunol* (2007) 178:4112–9. doi: 10.4049/jimmunol.178.7.4112
38. Tchilian EZ, Wallace DL, Imami N, Liao HX, Burton C, Gotch F, et al. The exon a (C77G) mutation is a common cause of abnormal CD45 splicing in humans. *J Immunol* (2001) 166:6144–8. doi: 10.4049/jimmunol.166.10.6144
39. Flinn IW, Jaeger U, Shah NN, Blaise D, Briones J, Shune L, et al. A first-in-Human study of YTB323, a novel, autologous CD19-directed CAR-T cell therapy manufactured using the novel T-charge TM platform, for the treatment of patients (Pts) with Relapsed/Refractory (r/r) diffuse Large b-cell lymphoma (DLBCL). *Blood* (2021) 138:740. doi: 10.1182/blood-2021-146268
40. Cossarizza A, Chang HD, Radbruch A, Acs A, Adam D, Adam-Klages S, et al. Guidelines for the use of flow cytometry and cell sorting in immunological studies (second edition). *Eur J Immunol* (2019) 49:1457–973. doi: 10.1002/eji.201970107
41. Pelloquin F, Lamelin JP, Lenoir GM. Human b lymphocytes immortalization by Epstein-Barr virus in the presence of cyclosporin a. *In Vitro Cell Dev Biol* (1986) 22:689–94. doi: 10.1007/BF02621085
42. Terakura S, Yamamoto TN, Gardner RA, Turtle CJ, Jensen MC, Riddell SR. Generation of CD19-chimeric antigen receptor modified CD8+ T cells derived from virus-specific central memory T cells. *Blood* (2012) 119:72–82. doi: 10.1182/blood-2011-07-366419
43. Turtle CJ, Hanafi LA, Berger C, Gooley TA, Cherian S, Hudecek M, et al. CD19 CAR-T cells of defined CD4+:CD8+ composition in adult b cell ALL patients. *J Clin Invest* (2016) 126:2123–38. doi: 10.1172/JCI85309
44. Kratzert B, Trapin D, Gattinger P, Oberhofer T, Sehgal ANA, Waidhofer-Sollner P, et al. Lack of induction of RBD-specific neutralizing antibodies despite repeated heterologous SARS-CoV-2 vaccination leading to seroconversion and establishment of T cell-specific memory in a patient in remission of multiple myeloma. *Vaccines (Basel)* (2022) 10:374. doi: 10.3390/vaccines10030374
45. Harrison N, Grabmeier-Pfistershammer K, Graf A, Trapin D, Tauber P, Aberle JH, et al. Tick-borne encephalitis specific lymphocyte response after allogeneic hematopoietic stem cell transplantation predicts humoral immunity after vaccination. *Vaccines (Basel)* (2021) 9:908. doi: 10.3390/vaccines9080908
46. Liadi I, Singh H, Romain G, Rey-Villamizar N, Merouane A, Adolacion JR, et al. Individual motile CD4(+) T cells can participate in efficient multikilling through conjugation to multiple tumor cells. *Cancer Immunol Res* (2015) 3:473–82. doi: 10.1158/2326-6066.CIR-14-0195
47. June CH, Ledbetter JA, Linsley PS, Thompson CB. Role of the CD28 receptor in T-cell activation. *Immunol Today* (1990) 11:211–6. doi: 10.1016/0167-5699(90)90085-N
48. Textor A, Listopad JJ, Wuhrmann LL, Perez C, Kruschinski A, Chmielewski M, et al. Efficacy of CAR T-cell therapy in large tumors relies upon stromal targeting by IFN γ . *Cancer Res* (2014) 74:6796–805. doi: 10.1158/0008-5472.CAN-14-0079
49. Kearney CJ, Vervoort SJ, Hogg SJ, Ramsbottom KM, Freeman AJ, Lalaoui N, et al. Tumor immune evasion arises through loss of TNF sensitivity. *Sci Immunol* (2018) 3:ear3451. doi: 10.1126/sciimmunol.aar3451
50. Suntharalingam G, Perry MR, Ward S, Brett SJ, Castello-Cortes A, Brunner MD, et al. Cytokine storm in a phase 1 trial of the anti-CD28 monoclonal antibody TGN1412. *N Engl J Med* (2006) 355:1018–28. doi: 10.1056/NEJMoa063842
51. He LZ, Prostak N, Thomas LJ, Vitale L, Weidlick J, Crocker A, et al. Agonist anti-human CD27 monoclonal antibody induces T cell activation and tumor immunity in human CD27-transgenic mice. *J Immunol* (2013) 191:4174–83. doi: 10.4049/jimmunol.1300409
52. Burris HA, Infante JR, Ansell SM, Nemunaitis JJ, Weiss GR, Villalobos VM, et al. Safety and activity of varlilumab, a novel and first-in-Class agonist anti-CD27 antibody, in patients with advanced solid tumors. *J Clin Oncol* (2017) 35:2028–36. doi: 10.1200/JCO.2016.70.1508
53. Wasiuk A, Weidlick J, Sisson C, Widger J, Crocker A, Vitale L, et al. Conditioning treatment with CD27 ab enhances expansion and antitumor activity of adoptively transferred T cells in mice. *Cancer Immunol Immunother* (2022) 71:97–109. doi: 10.1007/s00262-021-02958-9
54. Turaj AH, Hussain K, Cox KL, Rose-Zerilli MJ, Testa J, Dahal LN, et al. Antibody tumor targeting is enhanced by CD27 agonists through myeloid recruitment. *Cancer Cell* (2017) 32:777–91.e776. doi: 10.1016/j.ccell.2017.11.001
55. Bullock TN. Stimulating CD27 to quantitatively and qualitatively shape adaptive immunity to cancer. *Curr Opin Immunol* (2017) 45:82–8. doi: 10.1016/j.coi.2017.02.001
56. Eisenhauer EA, Therasse P, Bogaerts J, Schwartz LH, Sargent D, Ford R, et al. New response evaluation criteria in solid tumours: Revised RECIST guideline (version 1.1). *Eur J Cancer* (2009) 45:228–47. doi: 10.1016/j.ejca.2008.10.026
57. Chen DS, Mellman I. Oncology meets immunology: The cancer-immunity cycle. *Immunity* (2013) 39:1–10. doi: 10.1016/j.immuni.2013.07.012
58. Ko HS, Fu SM, Winchester RJ, Yu DT, Kunkel HG. Ia determinants on stimulated human T lymphocytes. occurrence on mitogen- and antigen-activated T cells. *J Exp Med* (1979) 150:246–55. doi: 10.1084/jem.150.2.246
59. Hintzen RQ, Lens SM, Koopman G, Pals ST, Spits H, van Lier RA. CD70 represents the human ligand for CD27. *Int Immunol* (1994) 6:477–80. doi: 10.1093/intimm/6.3.477
60. Arens R, Tesselaar K, Baars PA, van Schijndel GM, Hendriks J, Pals ST, et al. Constitutive CD27/CD70 interaction induces expansion of effector-type T cells and

results in IFN γ -mediated B cell depletion. *Immunity* (2001) 15:801–12. doi: 10.1016/S1074-7613(01)00236-9

61. Vallejo AN, Brandes JC, Weyand CM, Goronzy JJ. Modulation of CD28 expression: Distinct regulatory pathways during activation and replicative senescence. *J Immunol* (1999) 162:6572–9.

62. Zhou Y, Qiu X, Luo Y, Yuan J, Li Y, Zhong Q, et al. Histone modifications and methyl-CpG-binding domain protein levels at the TNFSF7 (CD70) promoter in SLE CD4⁺ T cells. *Lupus* (2011) 20:1365–71. doi: 10.1177/0961203311413412

63. Fritsch RD, Shen X, Sims GP, Hathcock KS, Hodes RJ, Lipsky PE. Stepwise differentiation of CD4 memory T cells defined by expression of CCR7 and CD27. *J Immunol* (2005) 175:6489–97. doi: 10.4049/jimmunol.175.10.6489

64. Suarez-Alvarez B, Rodriguez RM, Schlagen K, Raneros AB, Marquez-Kisinosky L, Fernandez AF, et al. Phenotypic characteristics of aged CD4⁺ CD28(null) T lymphocytes are determined by changes in the whole-genome DNA methylation pattern. *Aging Cell* (2017) 16:293–303. doi: 10.1111/acer.12552

65. Chen Y, Gorelik GJ, Strickland FM, Richardson BC. Decreased ERK and JNK signaling contribute to gene overexpression in "senescent" CD4⁺CD28[−] T cells through epigenetic mechanisms. *J Leukoc Biol* (2010) 87:137–45. doi: 10.1189/jlb.0809562

66. Talaulikar D, Choudhury A, Shadbolt B, Brown M. Lymphocytopenia as a prognostic marker for diffuse large B cell lymphomas. *Leuk Lymphoma* (2008) 49:959–64. doi: 10.1080/10428190801959026

67. Aoki T, Nishiyama T, Imahashi N, Kitamura K. Lymphopenia following the completion of first-line therapy predicts early relapse in patients with diffuse large B cell lymphoma. *Ann Hematol* (2012) 91:375–82. doi: 10.1007/s00277-011-1305-1

68. Gupta M, Han JJ, Stenson M, Maurer M, Wellik L, Hu G, et al. Elevated serum IL-10 levels in diffuse large B-cell lymphoma: A mechanism of aberrant JAK2 activation. *Blood* (2012) 119:2844–53. doi: 10.1182/blood-2011-10-388538

69. Jaeger U, Worel N, McGuirk JP, Riedell PA, Fleury I, Du Y, et al. Safety and efficacy of tisagenlecleucel plus pembrolizumab in patients with r/r DLBCL: Results from the phase Ib PORTIA study. *Blood Adv* (2022). doi: 10.1182/bloodadvances.2022007779

70. Fan F, Yoo HJ, Stock S, Wang L, Liu Y, Schubert ML, et al. Ibrutinib for improved chimeric antigen receptor T-cell production for chronic lymphocytic leukemia patients. *Int J Cancer* (2021) 148:419–28. doi: 10.1002/ijc.33212

71. Stock S, Ubelhart R, Schubert ML, Fan F, He B, Hoffmann JM, et al. Idelalisib for optimized CD19-specific chimeric antigen receptor T cells in chronic lymphocytic leukemia patients. *Int J Cancer* (2019) 145:1312–24. doi: 10.1002/ijc.32201

72. Funk CR, Wang S, Chen KZ, Waller A, Sharma A, Edgar CL, et al. PI3Kdelta/gamma inhibition promotes human CART cell epigenetic and metabolic reprogramming to enhance antitumor cytotoxicity. *Blood* (2022) 139:523–37. doi: 10.1182/blood.2021011597

73. Laurent E, Sieber A, Salzer B, Wachernig A, Seigner J, Lehner M, et al. Directed evolution of stabilized monomeric CD19 for monovalent CAR interaction studies and monitoring of CAR-T cell patients. *ACS Synth Biol* (2021) 10:1184–98. doi: 10.1021/acssynbio.1c00010

74. Sheih A, Voillet V, Hanafi LA, DeBerg HA, Yajima M, Hawkins R, et al. Clonal kinetics and single-cell transcriptional profiling of CAR-T cells in patients undergoing CD19 CAR-T immunotherapy. *Nat Commun* (2020) 11:219. doi: 10.1038/s41467-019-13880-1

COPYRIGHT

© 2023 Worel, Grabmeier-Pfistershammer, Kratzer, Schlager, Tanzmann, Rottal, Körmöczy, Porpaczy, Staber, Skrabs, Herkner, Gudipati, Huppa, Salzer, Lehner, Sachsenhuber, Friedberg, Wohlfarth, Hopfinger, Rabitsch, Simonitsch-Klupp, Jäger and Pickl. This is an open-access article distributed under the terms of the [Creative Commons Attribution License \(CC BY\)](https://creativecommons.org/licenses/by/4.0/). The use, distribution or reproduction in other forums is permitted, provided the original author(s) and the copyright owner(s) are credited and that the original publication in this journal is cited, in accordance with accepted academic practice. No use, distribution or reproduction is permitted which does not comply with these terms.



OPEN ACCESS

EDITED BY

Catherine Sautes-Fridman,
U1138 Centre de Recherche des
Cordeliers (CRC)(INSERM), France

REVIEWED BY

Limin Xia,
Huazhong University of Science and
Technology, China
Matias I. Hepp,
Universidad Católica de la Santísima
Concepción, Chile

*CORRESPONDENCE

Jie Ding
✉ dingjiexy@126.com

[†]These authors have contributed
equally to this work and share
first authorship

SPECIALTY SECTION

This article was submitted to
Cancer Immunity
and Immunotherapy,
a section of the journal
Frontiers in Immunology

RECEIVED 16 November 2022

ACCEPTED 23 December 2022

PUBLISHED 11 January 2023

CITATION

Zhang Y, Chen J, Liu H, Mi R, Huang R,
Li X, Fan F, Xie X and Ding J (2023)
The role of histone methylase and
demethylase in antitumor immunity:
A new direction for immunotherapy.
Front. Immunol. 13:1099892.
doi: 10.3389/fimmu.2022.1099892

COPYRIGHT

© 2023 Zhang, Chen, Liu, Mi, Huang, Li,
Fan, Xie and Ding. This is an open-
access article distributed under the
terms of the [Creative Commons
Attribution License \(CC BY\)](#). The use,
distribution or reproduction in other
forums is permitted, provided the
original author(s) and the copyright
owner(s) are credited and that the
original publication in this journal is
cited, in accordance with accepted
academic practice. No use,
distribution or reproduction is
permitted which does not comply
with these terms.

The role of histone methylase and demethylase in antitumor immunity: A new direction for immunotherapy

Yuanling Zhang^{1,2†}, Junhao Chen^{3†}, Hang Liu⁴, Rui Mi⁵,
Rui Huang², Xian Li⁶, Fei Fan⁷, Xueqing Xie¹ and Jie Ding^{2*}

¹School of Medicine, Guizhou University, Guiyang, China, ²Department of Gastrointestinal Surgery, Guizhou Provincial People's Hospital, Guiyang, China, ³Graduate School of Zunyi Medical University, Zunyi, China, ⁴Department of Medical Cosmetology, Guizhou Provincial People's Hospital, Guiyang, China, ⁵Department of General Surgery, Zhijin County People's Hospital, Bijie, China, ⁶Orthopedics Department, Dongguan Songshan Lake Tungwah Hospital, DongGuan, China, ⁷Department of Thyroid and Breast Surgery, Affiliated Hospital of Panzhihua University, Panzhihua, China

Epigenetic modifications may alter the proliferation and differentiation of normal cells, leading to malignant transformation. They can also affect normal stimulation, activation, and abnormal function of immune cells in the tissue microenvironment. Histone methylation, coordinated by histone methylase and histone demethylase to stabilize transcription levels in the promoter area, is one of the most common types of epigenetic alteration, which gained increasing interest. It can modify gene transcription through chromatin structure and affect cell fate, at the transcriptome or protein level. According to recent research, histone methylation modification can regulate tumor and immune cells affecting anti-tumor immune response. Consequently, it is critical to have a thorough grasp of the role of methylation function in cancer treatment. In this review, we discussed recent data on the mechanisms of histone methylation on factors associated with immune resistance of tumor cells and regulation of immune cell function.

KEYWORDS

histone methylation, epigenetic modification, tumor, antitumor immunity, immunotherapy

Introduction

Over the past decade, immunotherapy, such as immune checkpoint and CAR T cell therapy, has become a promising strategy for treating cancer (1, 2). Cancer treatment is achieved by increasing the number and effectiveness of immune cells, which can recognize tumor cells, collaborating with tumor surface suppressors and soluble factors in the tumor microenvironment to prevent the tumor invasion and metastasis, thus

maintaining the immune microenvironment homeostasis of the body, and improving immune response (3–5). However, due to the tumor heterogeneity and primary or acquired treatment resistance, only 10% to 30% of patients can benefit from immunotherapy (6–8). Therefore, identifying the source of low immune reactivity, effectively regulating immune cell and tumor cell therapeutic targets, and improving immunogenicity are of utmost importance.

The oncogenic transformation caused by the accumulation of related oncogene and tumor suppressor gene mutations accompanied by alteration of histone methylation modification has been observed in various human cancers, further emphasizing the importance of histone methylation modification in medical oncology research (9, 10). Many studies have suggested that aberrant methylation of histones can reduce the expression of tumor-associated antigens, hinder antigen presentation, and affect the exercise of anti-tumor immunity by anti-tumor effector T cells, specialized antigen-presenting cells (APCs), and other cells (11, 12). Moreover, it can alter the number and differentiation process of non-specialized APC infiltration, such as myeloid-derived suppressor cells (MDSCs), regulatory T cells (Tregs), and tumor-associated macrophages (TAMs), assisting tumor cell immune escape (13). Given the impact of histone methylation modification on the immune system and tumor cells, it is worth exploring whether targeting these enzymes may alter the tumor immune microenvironment and improve the efficacy of immunotherapy. Our findings showed that enzymes involved in histone methylation regulate tumor immunity, providing innovative strategies for formulating more perfect immunotherapy strategies. In this review, we discussed the effect and mechanism of aberrant histone methylation in the tumor immune microenvironment on immune cells and tumor cells.

Classification and biological functions of histone methyltransferases (HMTs)

The amino terminus of histones can be modified to create a class of “histone codes” that increase the amount of information in the genetic code of genes, resulting in different cell fate and pathological development in the same cases (14). Lysine and arginine residues of certain histones are catalyzed by a family of conserved proteins known as the histone methyltransferases (HMTs), consisting of two species based on their structure and modification sites, i.e., histone lysine methyltransferase (KMT) and protein arginine methyltransferase (PRMT), both of which use N-terminal residues as modification sites, such as H3K4, H3K9, H3K27, H3K36, H3K79, and H4K20 (15). Most KMT contain a conserved catalytic domain, called the SET domain. Accordingly, the KMT family can be divided into SET domain-

containing enzymes, including EZH2, G9a, SETD2, SUV39H1, and SET domain-free DOT1-like proteins (16). PRMT is a group of enzymes that use S-adenosine methionine (SAM) as a methyl donor. The PRMT family has nine members (PRMT1-9) that generate a single methyl group, which is added to the target protein to create a monomethylarginine (MMA) tag (17). Based on the catalyzed methylation reaction type, the PRMT family is divided into three isoforms, a class of highly conserved genetic products (18).

HMTs have a major role in the epigenetic regulation of gene expression, especially in the regulation of genes related to tumor invasion and metastasis. HMTs catalyze the lysine and arginine residues of particular histones, which are involved in a variety of biological activities, including packaging of chromosome structures, affecting transcription factor recruitment and binding, initiation and extension factors and target DNA binding, RNA processing, editing, and other processes. They also regulate genome mutations, ultimately leading to cancer (10). These methyltransferases have been demonstrated to have an important role in tumor maturation, carcinogenesis, and maintenance of stem cell components. HMTs act in a closely controlled manner to direct the necessary cellular processes under normal cell physiological settings. However, these enzymes may dysregulate and modify the epigenetic landscape and proteome to drive cell growth and survival in malignant circumstances (18, 19).

Histone lysine methyltransferase (KMT) and tumor immunity

KMT abnormalities in the complex tumor microenvironment cause expression mutations of key immune regulators in tumor cells and effector genes in immune cells, which may lead to antigen presentation suppression, loss of immune tolerance, blocked anti-tumor immunity, and negative effects on immunotherapy. In the following paragraphs, we discuss the regulatory mechanisms of numerous popular histone lysine methylases in tumors and their effect on immune cells, further emphasizing the crucial necessity of inhibiting histone lysine methylases for immunotherapy (Table 1) (Figure 1).

EZH2

The Zeste homology 2 (EZH2) is responsible for modifying the lysine methylation of histone 3 (H3K27me3) to silence the gene (61). Previous studies have shown that EZH2 participates in malignant biological phenotypes such as the cell cycle, proliferation, invasion and metastasis actin, which is an important target for solid tumors and hematological tumors (62, 63). Moreover, several potential molecular mechanisms have revealed that EZH2 enrichment shapes the immunosuppressive tumor microenvironment. In tumor cells, EZH2 mutations down-

TABLE 1 Related functions of lysine methylase and tumor immunity.

Protein	Tumor type	Regulate cell	Target	Mechanistic	References
EZH2	Diffuse large B-cell lymphoma	Tumor cell	MHC-I/ MHC-II	Inhibition of both MHC-I and MHC-II expression	(20)
	Pan cancer	Tumor cell	MHC-I	Down-regulate MHC-I expression	(21)
	Prostate cancer	Tumor cell	STING	Blocking the activation of RNA-STING-IRG stress response	(22)
	Hepatocellular carcinoma	Tumor cell	IRF1	Suppress PD-L1 expression by upregulating the promoter H3K27me3 levels of CD274 and IRF1	(23)
	Breast cancer	Macrophage	miR-29b/ miR-30d	Promoting LOXL4 expression through repressing the expression of miR-29b and miR-30d to regulating macrophage activation	(24)
	Glioblastoma multiforme	Macrophage	iNOS/ TGFβ2	Inhibition of EZH2 activates iNOS and increases TGFβ2 levels to enhance phagocytic activity and survival of microglia	(25)
	Ovarian cancer/Colon cancer	CD8 ⁺ T cell	CXCL9, CXCL10	Affects T cell migration <i>via</i> controlling the expression of CXCL9 and CXCL10	(26, 27)
	Pan cancer	T cell	ARID1A	Combines with ARID1A to restore CXCL9 and CXCL10 expression and promote T cell infiltration	(28)
	Colorectal	Treg cell	N/A	Control H3K27me3 levels to block antitumor T cell responses	(29)
	cancer Ovarian cancer	T cell	Numb, Fbxw7	Activate Notch pathway and stimulate T cell polyfunctional cytokine expression	(30)
	N/A	CAR T cell	N/A	Remodeling the epigenome associated with CAR T cell exhaustion	(31)
G9a	Melanoma/Colon cancer	Tumor cell	N/A	Inhibit the IFN-induced expression of the CXCL9 and CXCL10	(32, 33)
	Oophoroma	Tumor cell	N/A	Involved in inhibiting the expression of multiple chemokines	(34)
	Melanoma	Tumor cell	LC3B II	Increase H3K9 enrichment in the LC3B II promoter region and decrease immune blocker reactivity	(35)
	Colon Carcinoma	Tumor cell	Fas	Restrict the transcriptional initiation of Fas and limit the release signal of Fas-FasL	(36)
	Hepatocellular carcinoma	Tumor cell	SLC7A2	Downregulation of SLC7A2 induces MDSO chemotaxis <i>via</i> CXCL1	(37)
SETDB1	Melanoma/Lung cancer	Tumor cell	TE	Derepresses TEs to generate MHC-I peptides and triggers T-cell responses	(38)
	Pan cancer	Tumor cell	PD-L1	Inhibit PD-L1 expression and reduce T cell infiltration	(39, 40)
	Pan cancer	Tumor cell	TE	Disruption of TEs prompts cells to maintain cancerous state	(41, 42)
SUV39H1	Cervical carcinoma	Tumor cell	DNMT1	H3K9me2 interacts with the DNMT1 promoter region to affect downstream SMAD3 expression	(43)
	N/A	T cell	N/A	Expression of the silent memory genes	(44)
	N/A	T cell	SMAD3	Interacts with Smad3 and enhances the IL-2 promoter repressor activity	(45)
SETD2	Pan-cancer	N/A	N/A	Participate in the efficacy of immunotherapy	(46)
	Lung adenocarcinoma	N/A	N/A	Enrichment of the mutations involved in PD-L1	(47)
	Renal cell carcinoma	Tumor cell	FBW7	Increase PD-L1 expression by targeting the FBW7/NFAT1 axis	(48)
KMT2A	Pancreatic cancer	Tumor cell	CD274	Directly binds to the CD274 promoter to catalyze H3K4me3 to activate PD-L1 transcription in tumor cells	(49)
	Hepatocellular carcinoma/ Non-small cell lung cancer	N/A	N/A	Mutations are associated with PD-L1	(50, 51)
	Pan-cancer	N/A	N/A	Participate in immune regulation	(52–57)

(Continued)

TABLE 1 Continued

Protein	Tumor type	Regulate cell	Target	Mechanistic	References
DOT1L	N/A	T cell	TCR	Controll CD8 T cell differentiation by ensuring normal T cell receptor density and signaling	(58, 59)
	Colorectal cancer	Treg cell	N/A	Altering the T cell subsets	(60)

regulate the expression of tumor antigens, thereby evading specific immune recognition by T cells. Major histocompatibility complex-I (MHC-I) acts as a potent marker for T cells to monitor tumors sensitively, and EZH2 suppresses its normal expression. Treatment with EPZ-6438 or EPZ-011989, EZH2 inhibitor, significantly depleted H3K27me3 and increased the expression of surface MHC-I protein (20, 21). In addition, studies have shown that the overexpression of EZH2 can inhibit programmed cell death protein 1 (PD-L1) in prostate cancer and hepatocellular carcinoma by enhancing the H3K27me3 level of the interferon regulatory factor 1(IRF1) transcription factor (22,

23). The use of EZH2 inhibitors (EPZ) activates the STING stress response to promote INF- γ -induced PD-L1 expression. Furthermore, EZH2 inhibitor combined with PD-1 treatment did not produce resistance or toxicity and had significant therapeutic effects (22).
EZH2 can also drive tumor cells to release certain mediators to affect the transport and activity of immune cells. LOXL4 is an important chemical inducer of macrophages. It was reported that EZH2 regulates macrophage activation through the miR-29b/miR-30d-LOXL4 axis and enhances tumor-associated macrophage (TAM) infiltration in breast cancer (24). In

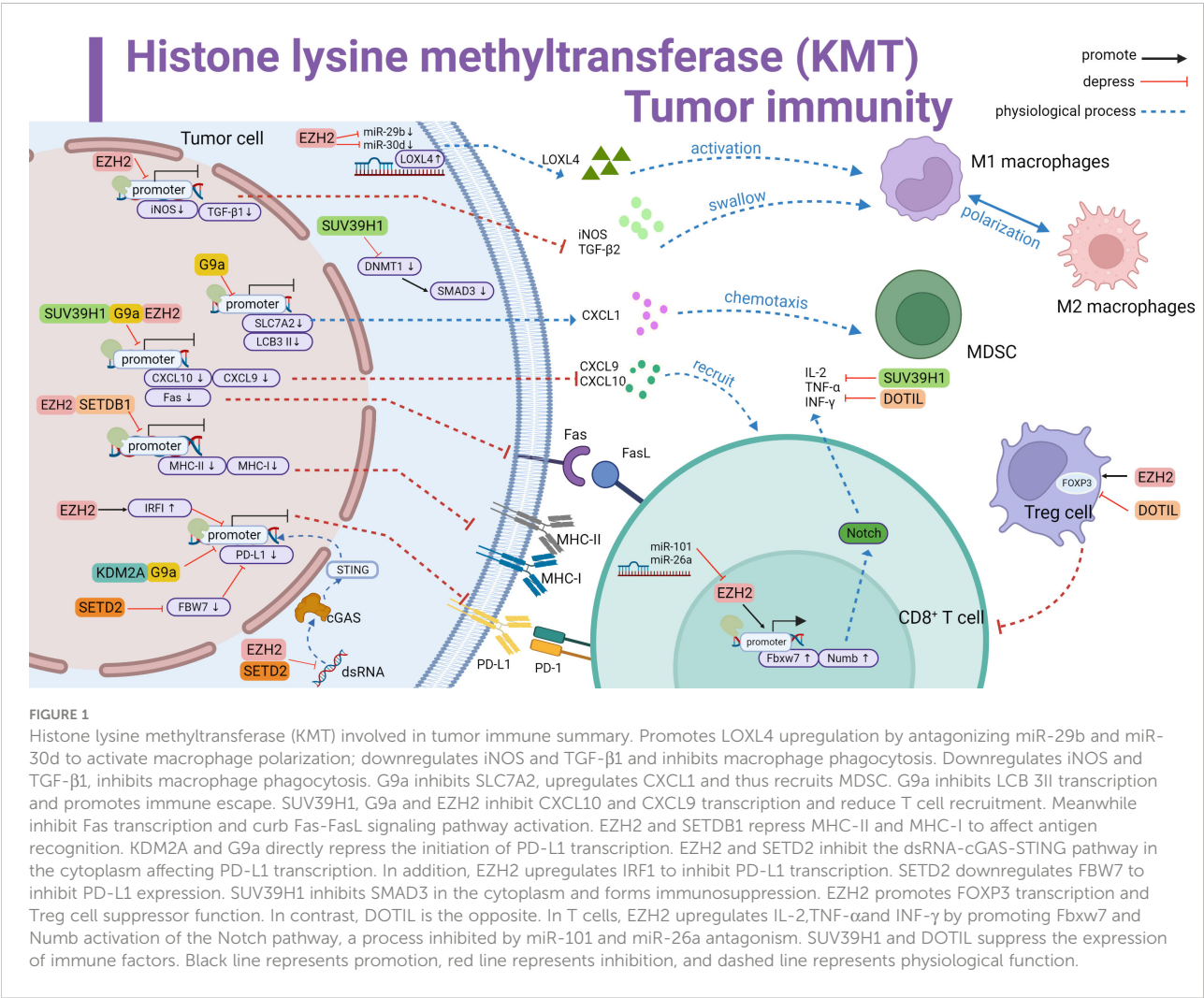


FIGURE 1
Histone lysine methyltransferase (KMT) involved in tumor immune summary. Promotes LOXL4 upregulation by antagonizing miR-29b and miR-30d to activate macrophage polarization; downregulates iNOS and TGF- β 1 and inhibits macrophage phagocytosis. Downregulates iNOS and TGF- β 1, inhibits macrophage phagocytosis. G9a inhibits SLC7A2, upregulates CXCL1 and thus recruits MDSC. G9a inhibits LCB 3II transcription and promotes immune escape. SUV39H1, G9a and EZH2 inhibit CXCL10 and CXCL9 transcription and reduce T cell recruitment. Meanwhile inhibit Fas transcription and curb Fas-FasL signaling pathway activation. EZH2 and SETDB1 repress MHC-II and MHC-I to affect antigen recognition. KDM2A and G9a directly repress the initiation of PD-L1 transcription. EZH2 and SETD2 inhibit the dsRNA-cGAS-STING pathway in the cytoplasm affecting PD-L1 transcription. In addition, EZH2 upregulates IRF1 to inhibit PD-L1 transcription. SETD2 downregulates FBW7 to inhibit PD-L1 expression. SUV39H1 inhibits SMAD3 in the cytoplasm and forms immunosuppression. EZH2 promotes FOXP3 transcription and Treg cell suppressor function. In contrast, DOTIL is the opposite. In T cells, EZH2 upregulates IL-2,TNF- α and INF- γ by promoting Fbxw7 and Numb activation of the Notch pathway, a process inhibited by miR-101 and miR-26a antagonism. SUV39H1 and DOTIL suppress the expression of immune factors. Black line represents promotion, red line represents inhibition, and dashed line represents physiological function.

glioblastoma multiforme (GBM), iNOS and TGF- β 2 can impair engulfing and viability of macrophages (25). The number of infiltrating cells and the lethality of T cells represent the improved anticancer immunity of the body. Genome-wide studies showed that EZH2 levels are negatively correlated with CD8⁺ T cells, mainly inhibiting the production of tumor TH1-type chemokines CXCL9 and CXCL10 and thus reducing the recruitment of T cells (22, 26, 27), while the binding of carboxyl structure of ARID1A to EZH2 can reverse this step (28). Animal experiments have shown that the synergistic treatment of ovarian cancer with GSK126 (EZH2 inhibitor) and DNMT inhibitor improves the therapeutic efficacy of anti-PD-L1 therapy and overt T-cell therapy (27). In addition, the use of CPI-1205 (EZH2 inhibitor) in a mouse colorectal cancer tumor (MC38) model had a synergistic effect on the immunotherapeutic modality (29). Meanwhile, the activity of EZH2 in Treg cells maintains the stability of FOXP3 protein, increases the number of tumor-infiltrating FOXP3⁺ Tregs, alters the homeostatic balance with tumor effector T cells in the microenvironment and impairs the anti-tumor immune response (29). In contrast, EZH2 in CD8⁺ T cell can activate the Notch pathway, promote the release of cytokines in T cells, and maintain its good antineoplastic activity (30). Moreover, EZH2 is also involved in genome remodeling related to T-cell failure and promotes functional recovery (31). However, the tumor microenvironment can limit the conversion of oxidative phosphorylation to aerobic glycolysis by maintaining high expression of microRNA101 and microRNA26a, and limit the expression of EZH2 in T cells by controlling glucose metabolism. This hinders the normal expression of multifunctional cytokines (30). In overview, EZH2 has an important regulatory role on immune microenvironment components. Several clinical trials are currently recruiting to test the CPI-1205 or tazemetostat (an EZH2-targeted agent) in combination with Pembrolizumab in solid tumors (NCT03854474 and NCT03337698).

G9a

G9a (Euchromatic histone-lysine N-methyltransferase 2, EHMT2) is frequently upregulated in different types of cancer (64). G9a overexpression enhances H3K9me2 deposition, silencing and inhibiting tumor suppressor genes, and promoting tumor proliferation and migration through the Wnt pathway and epithelial-to-mesenchymal transformation (EMT), which can be a useful target for anticancer therapy (65). Notably, the special effects of G9a and the tumor microenvironment (TME) may explain the poor immunogenicity in specific cancers. For example, G9a is inversely associated with CD8⁺ T cell infiltration in melanoma and colon cancer. Moreover, it can inhibit the activation of Th1 cytokines/chemokines (32, 33). Further investigation revealed that G9a induces chromatin variability in chemokine-related genes, involved in homing of intratumoral effector lymphocytes and natural killer cells (34). In clinical

cases, immunohistochemistry showed high intensity of G9a staining in 12 melanoma patients who did not respond to anti-PD-1 or anti-CTLA-4 treatment. Mouse melanoma resistance models treated with UNC0642 (a G9a inhibitor) in combination with anti-PD-1 therapy significantly reduced H3K9 levels in the LC3B II promoter region activating cellular autophagic responses and increasing PD-L1 levels, enhancing the blockade response to PD-1 immune checkpoint inhibitors (35).

G9a can also influence the methylation levels of multiple activated molecules of immune-related pathways. A previous study showed that G9a enhances H3K9me3 enrichment in the Fas promoter, restricts Fas-fasL release signals, and inhibits the tumor immune surveillance of host T cells (36). Moreover, in hepatocellular carcinoma (HCC), G9a silences SLC7A2 expression to induce CXCL1, promoting the recruitment of bone marrow-derived suppressor cells (MDSC) to the microenvironment (37). Given the above regulatory mechanisms, inhibition of G9a can remodel active tumor antigens and substantially modulate the tumor immune microenvironment. The combination of G9a inhibitors and immunotherapy strategies may be able to convert some “cold” immune tumors into “hot” tumors to achieve good immunotherapeutic results.

SETDB1

The Forked histone lysine methyltransferase 1 (SETDB1) containing the SET domain is responsible for the di- and trimethylation of the H3K9 residues. It is abnormally amplified and overexpressed in tumors (66). Yet, the underlying mechanisms of SETD2 gene mutations or loss of function leading to the corresponding dysfunction of tumor tissue proteins remain largely unexplored. Animal experiments showed that accumulation of SETDB1 mutations downregulates MHC-I-associated antigen presentation, thus preventing CD8⁺ T from correctly recognizing tumor cells and affecting sensitivity to PD-1/CTLA-4 treatment (38). On the other hand, SETDB1 in tumor cells forms a complex with TRIM28 or acts together with KDM5B that interferes with PD-L1 expression by blocking double-stranded RNA (dsRNA) production through the endogenous retroviral (ERV) pathway (39, 40). The loss of the SETDB1 gene also triggers type I interferon-induced PD-L1 expression through the cyclic GMP-AMP synthase (cGAS)-stimulator of interferon genes (STING) pathway and enhances anti-PD-L1 immune checkpoint blockade for antitumor effects (39–42). cGAS-STING pathway, an important pathway regulating host innate immunity, has been successively validated in various tumor models where SETD2 is an important epigenetic regulator. Thus, SETD2 is an attractive target for promoting immunotherapeutic responses.

SUV39H1

The variant suppressor 39 homolog 1 (SUV39H1), also known as KMT1A, is responsible for the introduction of the

dimethylation and trimethylation of histone 3 lysine 9 (H3K9me3) (67). It mainly disrupts some important gene regulatory elements in tumor cells and reduces the sensitivity to immune response. In cervical cancer, SMAD3 is a key mediator of activation of multiple immune signaling pathways. SUV39H1 negatively regulates DNMT1 and reduces the direct binding of DNMT1 to the promoter region of the SMAD3 gene, thus inhibiting the activation of signaling by multiple downstream immune signaling pathways (43). In colon cancer, SUV39H1 negatively regulates Fas transcription and impairs the sensitivity of tumor cells to CTL Fas L-mediated cytotoxicity (35). More importantly, SUV39H1 has a non-negligible role in the dysfunction of tumor-infiltrating cells (CTL). It deprives effector T cells of their long-term memory reprogramming capacity (44) and induces SMAD2/3 inhibition of T cells to produce IL-2-mediated immune modulation (45). In conclusion, the inhibition of tumor cell gene expression by SUV39H1 under pathological conditions and its central role in suppressing the killing and memory functions of effector T cells provide new evidence in support of its effectiveness.

SETD2

SETD2 is the only human gene responsible for the trimethylation of histone H3 lysine 36 (H3K36me3) that interacts with RNA polymerase II (68, 69). Although there is clear evidence that SETD2 is abnormally expressed in various tumors, its causal relationship with tumorigenesis is still unclear. In the analysis of clinical sample, mutations in SETD2 led to the enrichment of tumor cell surface mutation-specific neoantigens, such as mutational load (TMB) microsatellite instability-high (dMMR/MSI-H). In addition, these patients with SETD2 mutated cancer were accompanied by transcriptional upregulation of genes associated with immune activity (46). Another clinical analysis of lung adenocarcinoma found many SETD2 gene mutations and significantly higher IFN- γ expression in the PD-L1 high-expression group (47). Furthermore, an experimental study in renal cell carcinoma found that SETD2 acts as a transcription factor regulating E3 ubiquitin ligase FBW7 target gene expression, causing altered PD-L1 expression levels and promoting CD4⁺ and CD8⁺ T cell infiltration and enhancing the anti-tumor effects of PD-1 antibodies (48). Based on the above studies, mutations in SETD2 are significantly correlated with tumor immune-specific genes and can drive tumor immunophenotypic alterations. However, extensive experimental studies are still needed to identify specific regulatory mechanisms of SETD2 on immune-related factors, which could provide new insights into the heterogeneous immune treatment of individual tumor patients.

KMT2 family

The histone-lysine N-methyltransferase 2 (KMT2) family of proteins is one of the most common mutations in human

genome and confers the key functions of chromatin modifiability and DNA accessibility by modifying lysine 4 (H3K4) in the H3 tail of histone H3 (70). The current anti-tumor effects involving the KMT2 family are mainly focused on investigating immune checkpoints. In pancreatic cancer, inhibition of MLL1(KMT2A) activity or silencing expression reduces H3K4me3 levels in the CD274 promoter region and downregulates PD-L1 expression. Moreover, a KMT2A inhibitor combined with anti-PD-L1 or anti-PD-1 antibodies can effectively restrain the growth of a mouse model of pancreatic tumor in a Fas L- and CTL-dependent manner (49). Also, KMT2D is the main mutated gene in PD-L1-positive patients with hepatocellular carcinoma, whose large accumulation may lead to the ineffective response of PD-1 reagents (50). Frequent mutations in KMT2D have also been observed in non-small-cell carcinomas, along with mutations in TP53 (51). The response to immune checkpoint inhibitor (ICI) therapy is mainly influenced by intracellular tumor factors (e.g., tumor mutational load and microsatellite instability) and the tumor microenvironment. In an analysis of the immune assessment of ICI-treated patients through the Biocredit database, KMT2D was identified to have a critical role in a variety of tumor such as bladder cancer (52), esophageal cancer (53), gastric adenocarcinoma (54), lymphoma (56), and head and neck cancer (57, 71). These findings confirm that the KMT2 family is one of the drivers of immune escape. Alterations in its family-related genes may serve as predictive biomarkers for immunotherapy and help us to understand the prognostic effect of immune checkpoint therapy.

DOT1L

DOT1L (telomere silencing interference; also known as KMT4), which mainly catalyzes the methylation of H3K79, leads to gene mutations and impairs the interaction between Sir2 and Sir3 in the telomeric region (71). Inhibition of its catalytic activity has been widely used in cancer therapy. Recent studies have suggested that DOT1L is a central player in CD8⁺ T cell physiology, ensuring the activation of normal T cell receptor signaling and related signaling pathways that control CD8⁺ T cell differentiation. In the CD4-CRE transgenic mouse model, deletion of the DOT1L gene inhibited CD8⁺ T cells apoptosis, as well as TNF and INF- γ expression. Furthermore, inhibition of DOT1L increased the threshold for TCR activation in T cells (58). Another study suggested that the loss of DOT1L directly impairs TCR/CD3 expression, resulting in an impaired immune response (59). Furthermore, DOT1L controls the subset differentiation of Foxp3⁺ regulatory T cells during carcinogenesis, reducing local inflammatory production in the microenvironment (60). The above results suggest that DOT1L is an important epigenetic target for regulating allogeneic T-cell responses, affecting the amount of immune cell infiltration, the direction of cell differentiation, and the secretion of immunomodulatory factors.

Protein arginine methyltransferase (PRMT) and tumor immunity

As a common post-translational modification, PRMT can catalyze the transfer of methyl groups from S-adenosine methionine (AdoMet) to the guanidine nitrogen atom of arginine. It can also affect the methylation status of the cancer genome, leading to activation or inhibitory recruitment of transcriptional mechanisms that are dysregulated in most tumors (72). In recent years, the development of PRMT-targeted drugs has been widely used in cancer therapy. Considering that PRMT1, PRMT4, and PRMT5 have the highest expression in cancer, their immunosuppressive effect have been well investigated (Table 2) (Figure 2).

PRMT1

Protein arginine methyltransferase 1 (PRMT1) is the main type I PRMT. Many experimental studies have shown that PRMT1 is overexpression or has an shear state in many cancer types (90). Using a genome-wide CRISPR immune screening system to screen for tumor-intrinsic factors that modulate tumor cell sensitivity to T cell-mediated killing, Hou J et al. identified PRMT1 as an intrinsic factor affecting T cell transport and lethality. The possible mechanism is the altered RNA levels of the cytokines/chemokines (73). In some tumor types, PRMT1 is an important regulator of the immune checkpoint pathway. In human hepatocellular carcinoma (HCC), PRMT1 expression is positively correlated with both PD-L1 and PD-L2 immune checkpoint expression (74). Similarly, PT1001B (PRMT1 inhibitor) enhances antitumor immunity by

TABLE 2 Related functions of arginine methylase and tumor immunity.

Protein	Tumor type	Regulate cell	Target	Mechanistic	References
PRMT1	N/A	CD8 ⁺ T cell	N/A	Affects the anti-tumor activity of T cells	(73)
	Hepatocellular carcinoma	Tumor cell/Macrophage	PD-L1,PD-L2	Regulates PD-L1 and PD-L2 expression	(74)
	Pancreatic ductal adenocarcinoma	Tumor cell	PD-L1	Promoting the expression of PD-L1	(75)
	Hepatocellular carcinoma	Macrophage	IL-6,IL-10	Control both IL-6 and IL-10 expression and the downstream activation of STAT3, affecting the polarization levels	(76)
PRMT4	Pan-cancer	N/A	N/A	Participate in the regulation of immune response and infiltration	(77)
	Ovarian cancer	Tumor cell	XBP1	Form a complex with XBP1s to regulate their target gene expression, thus determining the ER stress response by controlling the IRE1 α /XBP1s pathway	(78)
	Triple-negative breast cancer	Tumor cell	BAF155	Induction of BAF155 methylation and repression of interferon α/γ pathway genes	(79)
	Non-small cell lung cancer	Tumor cell	cirCHMGB2	As a cirCHMGB2 downstream gene, inhibiting the type 1 interferon response	(80)
	Carcinoma of colon	Tumor cell	N/A	Inhibition to achieve better immune infiltration	(81)
	Pan-cancer	Tumor cell/CD8 ⁺ T cell	N/A	Shape the immunosuppressive environment	(82)
PRMT5	Melanoma	Tumor cell	NLR5	Inhibition of the transcription of NLR5, modulating the genes implicated in MHC I antigen presentation	(83)
	Hepatocellular carcinoma	Tumor cell	CIITA, CD74	Increasing the enrichment of H3R8me2 and H4R3me2 at the CIITA and CD74 promoters, regulates MHC II expression	(84)
	Lung cancer	Tumor cell	CD247	Increases H3R4me2 deposition at the CD274 promoter site and represses gene expression	(85)
	Cervical carcinoma	Tumor cell	STAT1	The expression of both STAT1 and PD-L1 is driven by the IFN/JAK/STAT1 pathway	(86)
	N/A	CD8 ⁺ T cell	Blimp1	Klrg1 CD8 + Tcell differentiation was inhibited by deposition at the H4R3me2s and H3R8me2s sites of Blimp	(87)
	N/A	CD8 ⁺ T cell	AKT	Impact on the metabolic reprogramming of cells through the AKT/mTOR signaling pathway	(88)
	N/A	Treg cell	FOXP3	Increase signaling to FOXP3 dimethylation to promote Treg function and migration capacity	(89)

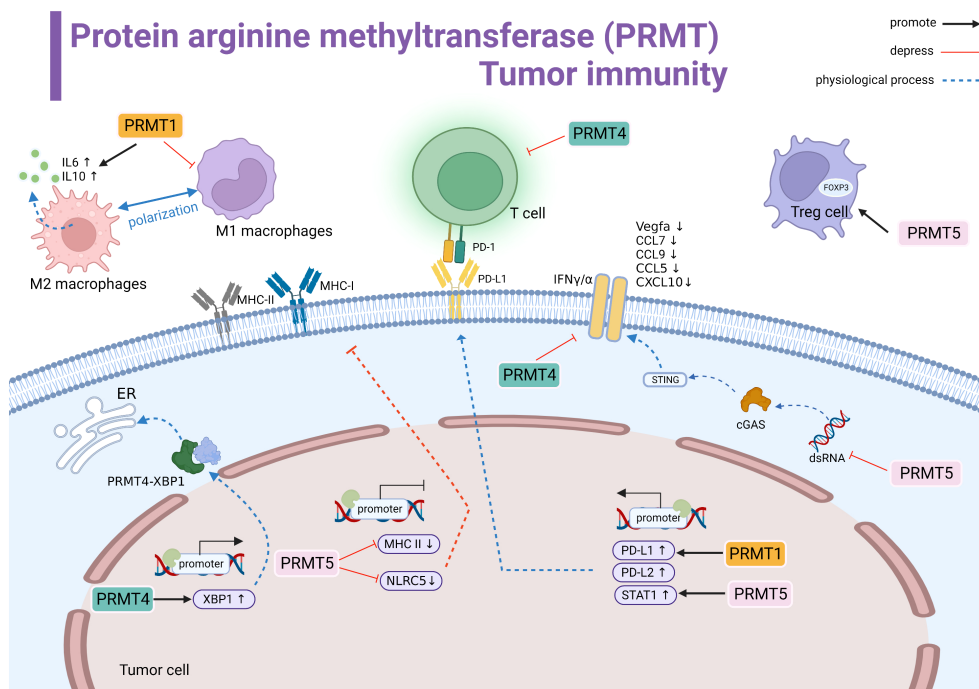


FIGURE 2

Protein arginine methyltransferase (PRMT) involved in tumor immune summary. PRMT1 regulates M2 macrophage polarization and promotes the transcription of IL-6 and IL-10. PRMT1 promotes the transcriptional level of PD-L1. PRMT4 negatively regulates T cells. PRMT4 promotes the transcription of XBP1 and forms the PRMT4-XBP1 complex to activate the endoplasmic reticulum stress pathway. PRMT5 inhibits the transcription of MHC-I and MHC-II and suppresses antigen recognition. PRMT5 promotes STAT1 expression to promote PD-L1 expression levels. In the cytoplasm, PRMT5 inhibits the dsRNA-cGAS-STING pathway, downregulates the interferon pathway, and downstream genes Vegfa, CCL7, CCL9, CCL5, and CXCL10 expression are suppressed. PRMT4 inhibits IFN γ / α . PRMT5 promotes the immunosuppressive function of Foxp3 regulatory T cells. Black line indicates promotion, red line indicates suppression, and dashed line indicates physiological function.

inhibiting PD-L1 expression on tumor cells, upregulating tumor-infiltrating CD8⁺ T lymphocytes. When the anti-PD-L1 monoclonal antibody was combined with PT1001B, the proportion of tumor-infiltrating effector cells was significantly increased in mice, and resistance to anti-PD-L1 treatment was well reversed (75). In addition, PRMT1 can protect the tumor cells, which can induce macrophages to assist in immune escape. Inhibition of PRMT1 in mice led to the inhibition of IL6 signaling and downstream STAT3 activation and decreased the number of tumor cells and M2 type macrophages (76). Taken together, these studies suggested that effective inhibition of PRMT1 can control T cell-mediated tumor killing and can effectively remodel the tumor immune microenvironment.

PRMT4

Protein arginine methyltransferase 4 (PRMT4), also known as coactivator-associated arginine methyltransferase 1 (CARM1), has a carcinogenic role in human cancer and is closely involved in the process of tumor growth and immune tolerance (91). CARM1 is overexpressed in different tumors and negatively associated with CD8⁺ T cells. It can also be used as a potent biomarker for pan-cancer prediction (77). In ovarian cancer, CARM1 acts as a transcriptional activator to promote XBP1 target gene expression.

CARM1 and interacts with XBP1 to modulate the ER stress response in the IRE1 α /XBP1 pathway, triggering an immunosuppressive environment (78). Furthermore, CARM1 mainly targets BAF155 in triple-negative breast cancer by inhibiting the interferon pathway to inhibit the host immune response (79). Similarly, CARM1 is positively regulated by circHMGB2, which inhibits type I interferon responses and downstream genes. EZM2302 (a CARM1 inhibitor) and anti-PD-1 antibody significantly inhibited the immunosuppressive environment *in vivo* shaped by tumor growth in mice and reduced the efficacy of anti-PD-1 monotherapy in non-small cell lung cancer (80). In a mouse colon cancer model, inhibitors targeting CARM1 were effective in arresting solid tumor progression and enhancing immune infiltration (81). In addition, the inactivation of the CARM1 gene in T cells can increase the number of specific memory-like T cell populations in the microenvironment, allowing the body to maintain a continuous and effective immune attack against tumors. EZM2302 (CARM1) enhances the checkpoint blockade sensitivity of CTLA-4 mAb in a synergistic manner (82). Overall, the inhibition of the activity against CARM1 suppresses tumor progression, promotes T-cell infiltration and sustained immune memory, and may be an effective for immunotherapy of drug-resistant tumors.

PRMT5

PRMT5 is the major type II arginine methyltransferase, active in a variety of cellular activities, that achieve tumor-promoting effects through methylation-mediated transcription repression, including inhibition of normal expression of the tumor surface antigen proteins in different tumor types (92). For example, in melanoma, PRMT5 activity inhibits NLRC5 transcription and changes the regulation of the expression of genes involved in the presentation of the major histocompatibility complex class I (MHC I) antigen. Meanwhile, PRMT5 interfere with the dsRNA-cGAS-STING pathway to affect type I interferon responses, promoting immune escape (83). In addition, inhibition of PRMT5 promotes the expression of MHC II (84). Treatment with GSK3326595 (PRMT5 inhibitor) plus anti-PD-1 antibody enhanced the anti-tumor response in the mouse organism (83, 84). Thus, targeting PRMT5 may synergize with immune checkpoint therapy to improve therapeutic efficacy. PD-L1 is a key molecule highly expressed in tumor cells that interacts with immune cells to constitute an immunosuppressive environment. In lung cancer, GSK591 drug inhibits PRMT5-induced PD-L1 expression, which then trigger immune resistance (85). Thus, the combination with PD-1 treatment and inhibition and elimination of PRMT5 may promote synergistic inhibition. In contrast, in cervical cancer, PRMT5 promotes cancer progression by increasing the expression of histone H3R2 symmetric dimethylation (H3R2me2s), which is enriched in the promoter region of STAT1 to enhance transcription and drive up-regulation of PD-L1 expression (86).

Furthermore, PRMT5 also acts directly on the host immune cells to maintain cellular physiology and homeostasis, especially on the effector CD8⁺ T cells. PRMT5 can affect the deposition of H4R3me2s and H3R8me2s at the Blimp1 locus and force the differentiation of transient effector CD8⁺ T cells, resulting in a substantial loss of CD8⁺ T cell numbers and function (87). Inhibition of PRMT5 is a “double-edged sword”, its inhibition causes reduced AKT/mTOR signaling, which impairs glycolysis and increases fatty acid utilization after human CD8⁺ T cells’ stimulation leading to metabolic reprogramming (88). In addition, PRMT5 can interact with the FOXP3 transcription factor in Tregs to maintain the functional stabilization of Treg cells (89). In conclusion, given the selective role of PRMT5 in the tumor microenvironment, more attention should be paid to the mechanism of side effects in immune cells, and combined immunotherapy may maximize the efficacy.

Classification and biological functions of histone demethylases(HDMs)

With the progress of science and technology, almost all histone lysine methylation sites have been found to be reversible. To date, two classes of histone demethylases have been identified, mainly the lysine-specific demethylase-1 (LSD1)

family and the jumonji (JmjC) domain-containing family (93). LSD1, which was identified first acts only on monomethylated and dimethylated lysines (94). The JmjC family is another class of JmjC domain-containing Fe (II). Ketoglutarate-dependent enzymes are divided into different species according to the sequence homology of the JmjC domain and the overall structure of the related motifs. Thus far, those active against H3K4, H3K9, H3K27, H3K36, and H4K20 have been identified (95). Their special structure allows them to function together with many other biological macromolecules (96).

Histone demethylases do not change the DNA sequence, and dynamically regulate in specific chromatin regions. They are important regulators of the physiological functions of embryonic development, gene regulation, cell reprogramming and other physiological functions, and they maintain genome integrity and epigenetic stability (97). Their role in cancer is particularly important, and it is closely related to the pathogenesis of the disease, including the demethylation of the oncogenes/tumor suppressor genes for mastering the cell fate, the enrichment of transcription factors, gene copy number alterations, and increased mutations. Targeting partial demethylases opens up an emerging field for anticancer therapy. In this process, some enzymes also have a prominent role in regulating the immune microenvironment (Table 3) (Figure 3).

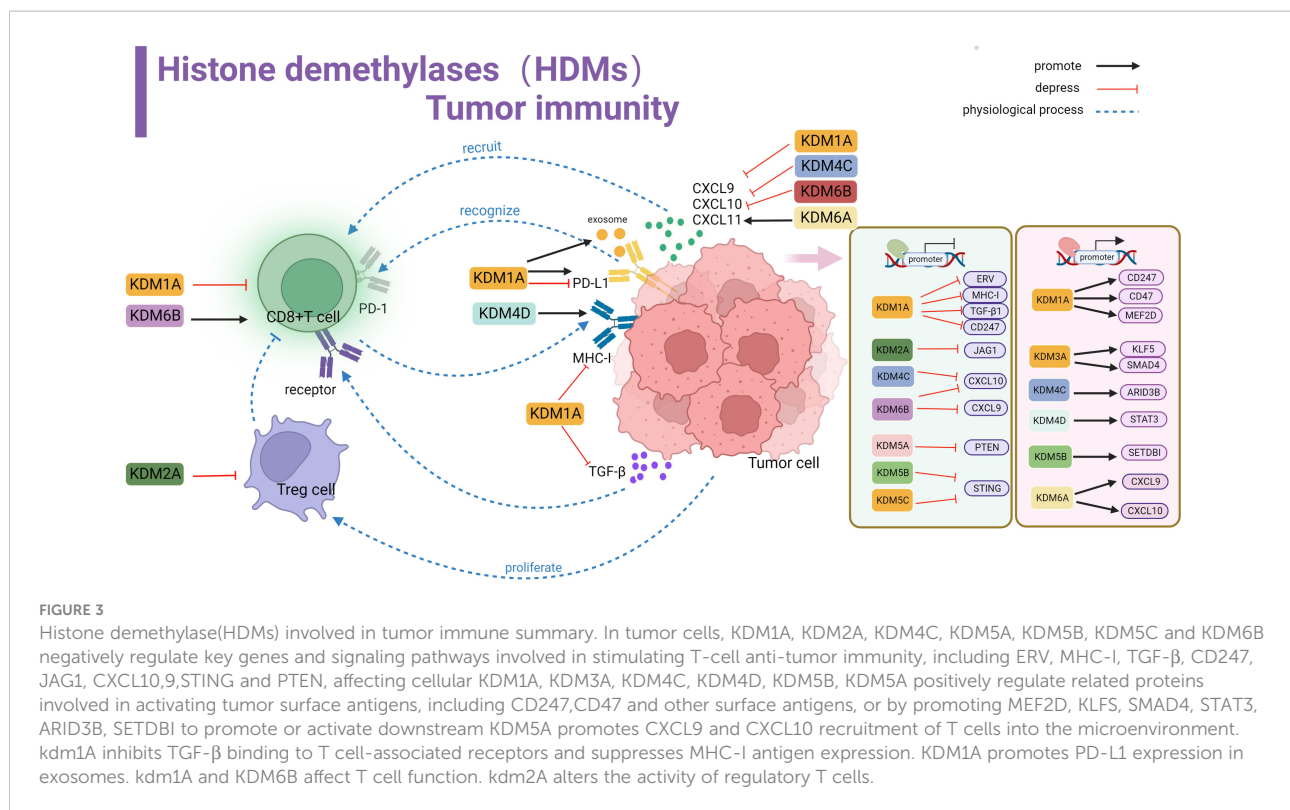
LSD1 and tumor immunity

Lysine-specific demethylase 1 (LSD1), also known as KDM1A, acts as an H3K4/9me eraser that binds to CoREST or nucleosome remodeling to repress gene transcription (131). LSD1 is highly expressed in most solid tumors, altering tumor immunogenicity and immune response by inhibiting or activating different signaling pathways. Shi et al. first discovered that inhibiting LSD1 can enhance endogenous transcription (EVR) expression, activate dsRNA stress and type I interferon activation, and improve the immunotherapy response of poorly immunogenic tumors (98). More importantly, LSD1 is inversely associated with CD8⁺ T cells in various tumors. In tumor cells, LSD1 largely affects the normal expression of MHC-I protein antigen by inhibiting the MHC-I encoding genes H2-D1 and H2-K2, which leads to the possibility that CD8⁺ T cells do not effectively recognize MHC-I prompting immune escape. The above mechanism has been observed in melanoma, breast cancer, and small-cell lung cancer (98–100).

Conclusions regarding the regulation of PD-L1 expression are inconsistent. In cervical cancer, LSD1 seems to be positively correlated with PD-L1 levels, in which H3K4me2 demethylation directly promoted the increase in PD-L1 expression (101). On the other hand, the demethylation of MEF2D in HCC indirectly promotes the PD-L1 expression, and this process is competitively inhibited by has-miR-329-3p (102). Moreover, in gastric cancer, LSD1 increases the level of PD-L1 found in exosomes and is transported to T-cell expression to inhibit tumor immunity (103). In contrast, LSD1 significantly

TABLE 3 Related functions of lysine demethylase and tumor immunity.

Protein	Tumor type	Regulate cell	Target	Mechanistic	References
KDM1A	Pan-cancer	Tumor cell	ERV	Suppressing ERV expression and curbing activation, such as dsRNA stress and type I interferon	(98)
	Melanoma/Breast cancer/Small-cell lung cancer	Tumor cell	MHC-I	Inhibition of MHC-I gene expression and reduced antigen presentation	(98–100)
	Cervical cancer	Tumor cell	CD274, CD47	Mediated demethylation of H3K4 in the CD274/CD47 promoter region	(101)
	Hepatocarcinoma	Tumor cell	MEF2D	Promote PD-L1 expression by MEF2D demethylation	(102)
	Gastric cancer	Tumor cell	PD-L1	Altering PD-L1 expression in exosomes did not affect membrane PD-L1 levels	(103)
	Squamous cell carcinoma of the head and neck	Tumor cell	PD-L1	Inhibition of PD-L1 expression	(104)
	Breast cancer	Tumor cell	TGF- β 1	Binding to the TGF-1 promoter region, which upregulates its expression	(105)
	Pan-cancer	CD8 ⁺ T cell	TCF1	The LSD1/CoREST complex physically interacts with TCF1 and antagonizes its transcriptional activity	(106)
	Melanoma/Breast cancer	CD8 ⁺ T cell	EOMES	Affect the posttranslational level status of the EOMES	(107)
KDM2A	Glioma	Tumor cell	JAG1	Promotes JAG1 demethylation and mediates the proliferation and activity of regulatory T cells	(108)
KDM3A	Pancreatic cancer	Tumor cell	KLF5, SMAD4	In coordination with KLF5, SMAD4 regulates transcription in tumor cells to inhibit anti-tumor immunity	(109)
KDM4A	Squamous cell carcinoma of the head and neck	Tumor cell	N/A	Inhibition of immune-related signaling pathways	(110)
KDM4B	Carcinoma of endometrium	N/A	N/A	Associated with immune cell infiltration and immune checkpoint molecular expression	(111)
	Colon cancer	Tumor cell	HOXC4	PD-L1 expression was induced by the H3K27me3/HOXC4 axis	(112)
KDM4C	Lung cancer	Tumor cell	CXCL10	Promoting the accumulation of H3K36me3 in the CXCL10 promoter region to repress the transcription level of genes affects T cell recruitment	(113)
	Colorectal cancer	Tumor cell	ARID3B	Recruited by ARID3B to activate downstream Notch and PD-L1 expression	(114)
KDM4D	Colorectal cancer	Tumor cell	IFNGR1	Co-activating SP-1 promotes IFNGR1 expression, thereby enhancing STAT3-IRF1 signaling and promoting PD-L1 expression	(115)
KDM5A	Melanoma/Colon cancer	Tumor cell	PTEN	Inhibition of PTEN expression and induction of PI3K-AKT-S6K signaling pathway to increase the PD-L1 abundance in the tumor cells	(116)
KDM5B	Melanoma	Tumor cell	SETDB1	Recruiting the H3K9 methyltransferase SETDB1 to exert antitumor effects	(40)
KDM5B/C	Breast cancer	Tumor cell	STING	Binds to the STING promoter to directly suppress transcription, causing disruption of the cGAS/STING pathway signaling	(120)
KDM6A	Hepatocarcinoma	N/A	N/A	Correlation with the immune infiltration	(123)
	Bladder cancer	N/A	N/A	Negative correlation with immune-related pathways	(124–126)
	Medulloblastoma	Tumor cell	CXCL9, CXCL10	Activates Th-1 type chemokine expression, and enhances T cell recruitment	(127)
KDM6B	Colon cancer	Tumor cell	CXCL9, CXCL10	Inhibition of the expression of both CXCL9 and CXCL10	(26)
	N/A	CD8 ⁺ T cell	GZMB, FasL	Promote the expression of GZMB and FasL effector genes through demethylation	(128)
	N/A	CD8 ⁺ T cell	N/A	Promote cytotoxicity-related gene expression	(129)
	Pan-cancer	N/A	N/A	Associated with TMB, MSI and immune cell infiltration	(130)



suppresses the PD-L1 expression level in HNSCC (104). The surprising finding is that using the LSD1 inhibitor alone, despite its effective tumor suppression, the resulting exogenous TGF-1 binding to the CD8⁺ T cell surface receptors inhibits the cytotoxic effects (105), which may be one of the reasons why the clinical effects of LSD1 inhibitors are suboptimal. Alternatively, LSD1 performs an epigenetic program within CD8⁺ T cells. On the one hand, it inhibits the transcription of the progenitor phenotype gene TCF1, disrupting the progenitor cell population (106). On the other hand, eomesodermin (EOMES), a transcription factor associated with the regulation of T cell failure, promotes T cell dysfunction (107). These make T cell depletion fast and unsustainable recovery, resulting in poor persistence of PD-1 blocking therapy. Current experimental data suggest that treatment with LSD1 inhibitors (ORY-1001, SP2509 or GSK2879552) in combination with PD-1/PD-L1 monoclonal antibodies enhances *in vivo* immunogenicity and has a long-term response (101, 104, 106).

JmjC family and tumor immunity

KDM2

KDM2 is mainly responsible for the demethylation of the H3 lysine 36(H3K36) residues, and its family members include KDM2A and KDM2B (132). In glioma, LncRNA HOXA-AS2 promotes KDM2A expression by binding to miR-302a, thus recruiting H3K4me3 to demethylate JAG1 and promoting the proliferation and immune tolerance of regulatory T cells (108).

In addition, KDM2A may promote immune body suppression Fumarate as an important metabolite may antagonize inhibitory histones and promote immune regulation (133, 134). In conclusion, KDM2 serves as a considerable therapeutic target.

KDM3

KDM3 is mainly composed of KDM3A, KDM3B, and KDM3C, which can specifically catalyze the demethylation of histone H3K9me1/2 (135). Using CRISPR screening in a mouse model of pancreatic cancer, KDM3A was found to be an epigenetic modulator of the response to immunotherapy. KDM3A mainly affects the KLF5 and SMAD4 transcription factor activity, regulates the epidermal growth factor receptor (EGFR) expression, and affects the T cell infiltration and the infiltration of dendritic cell DC (109). This suggests that KDM3A is closely related to the composition of the immune microenvironment. Therefore, eliminating KDM3A could help overcome immunotherapy resistance and enhance sensitivity to therapeutic effects, thereby creating a microenvironment for T-cell inflammation.

KDM4

The KDM4 protein family is composed of (KDM4A-C) and KDM4D, and several studies have found them to be overexpressed in cancer and to have the ability to malignant tumor growth (136). Notably, while maintaining tumor growth, they simultaneously suppress the activity of some pathways to interfere with normal

immunosuppression. In HNSCC, the knockdown of KDM4A led to the activation of both types I IFN interferon signaling and DNA replication stress signal cGAS-STING, along with the significant upregulation of CXCL9, CXCL10, and CXCL11, and significantly increases the effect of the combined PD-1 blocking treatment (110). KDM4B is also recommended as a clinical prognostic marker and is closely associated with immune cell infiltration and immune checkpoint molecular expression (111). In colon cancer cell culture, KDM4B elevates HOXC4 expression by driving H3K27me3 demethylation to induce the expression of PD-L1, and exogenous miR-15a was able to prevent tumor escape events from occurring (112). Moreover, KDM4C is negatively associated with CD8⁺ T cells in lung cancer; transcription sequencing found that KDM4C mainly downregulates the transcript level of CXCL10 and inhibits T cell recruitment to tumors and killing (113). KDM4C is also involved in the regulation of PD-L1 expression, and the main mechanism is the transcriptional activation of the Notch gene and PD-L1 through ARID3B recruitment to regulate chromatin structure, whereas KDM4D promotes PD-L1 expression through the SP-1/STAT3/IRF1 signaling pathway, assisting the immune escape of in colorectal cancer (114, 115).

KDM5

The KDM5 protein family, including KDM5A-C and KDM5D, is responsible for removing histone H3 lysine 4 dimethylation and trimethylation (H3K4me2 and H3K4me3) (116). It is an attractive target in cancer therapy. Several prospective raw letter analyses have shown that KDM5 is closely associated with regulating immune infiltration and expressing immune-related molecules, and is considered a prospective candidate for epigenetic anti-tumor therapy (117–119). In clinical treatment, some patients have low tumor cell PD-L1 abundance, so they cannot respond well to ICB. One study showed that increased KDM5A gene expression or protein abundance, promoting PD-L1 upregulation to accommodate the PD-1 treatment response, is a valuable clinical response tag (137). In melanoma, high expression of KDM5B can recruit the H3K9 methyltransferase SETDB1 to interact in the suppression of endogenous retrotransposable elements and block subsequent RNA and DNA sensing pathways as well as type I interferon responses, resulting in the inability of the organism to respond positively to tumor rejection and immune responses (40). A similar mechanism has been found in breast cancer. The STING promoter is directly transcriptionally repressed by KDM5B and KDM5C, disrupting the cGAS/STING pathway signaling and failing to activate a robust interferon response (120). Using KDM5 inhibitors reversed the normal transmission of this signaling pathway. It has also been suggested that combining of immunotherapy and KDM5 inhibitors could maximize the anti-tumor immune response, thus representing a potential therapeutic modality of interest.

KDM6

The KDM6 subfamily consists of three distinct members, i.e., KDM6A (also called UTX), KDM6B (also called JMJD3), and KDM6C (also called UTY), capable of removing di- and trimethylated H3K27, thereby activating or repressing target gene transcription (121). Its function is highly dependent on the specific of the cell type pathological environment (122). The molecular basis of KDM6 in tumors is still in its infancy, and only a few studies have addressed this issue. Yet, several studies have shown a high correlation between its mutations and tumor immunity. A functional screen for lysine demethylase in HCC showed that KDM6A is closely associated with immune infiltration (123). In bladder cancer and its subtypes, KDM6A is a more frequently mutated gene, that negatively regulates the signaling pathways of the immune system and suppresses tumor immunity (124–126). In medulloblastoma, KDM6A activates the expression of Th1-type chemokines and promotes cell migration (127). Moreover, KDM6B inhibits CXCL9 and CXCL10 expression in colon cancer and exerts an anti-tumor immune effects (26). In contrast, the effect of KDM6B is positively regulated for CD8⁺ T cells. KDM6B can promote the differentiation of mature CD8⁺ T cells by demethylating the expression of GZMB and FasL (128). Inhibition of KDM6B resulted in reduced toxicity-related genes in CD8⁺ T cells (129). Little experimental support exists for the specific mechanism of KDM6B in tumor progression and immune cell infiltration. However, available pan-cancer analyses suggest that KDM6B expression is associated with TMB, MSI and immune cell infiltration, and influences the response to immunotherapy and clinical outcome (130).

Conclusions and outlook

In the past decade, human cancer prevention and treatment have entered a new era with the emergence of immunotherapy. In the process of gradually understanding the potential mechanism of tumor cell occurrence and development, to the mechanism of killing malignant cells and avoiding the effect of the immune system, researchers have also developed corresponding therapeutic drugs for clinical practice, including immune checkpoint inhibitors, epigenetic targeted drugs, etc. Nevertheless, the low response rate and immune resistance in practical clinical applications led to identification of so-called “cold tumor”.

The concentrated research on histone methylation modifying enzymes in epigenetics advances our new understanding of “cold tumors” in human cancer, and builds the bridge between tumor cells and immune cells, promoting a deeper understanding of the complexity and diversity of the tumor immune microenvironment. Current studies on the involvement of histone methylase and demethylase in anti-tumor immunity

mainly includes (1): regulation of tumor immunogenic antigen expression; (2) their influence on the activation of immune-related pathways; (3) regulation of expression of chemokines/cytokines and induced immune-related factors; (4) regulation of immune cells, including immune cell activation, immune cell depletion and functional remodeling, and immune memory. The above regulatory mechanisms provide a more comprehensive picture of the facilitative/suppressive immune microenvironment shaped by aberrant histone methylation modifications at the transcriptional and translational levels. Furthermore, the contribution of histone methylation modifications for tumor immune escape mechanism, immunotherapy tolerance mechanism, and immune stress has brought new perspectives and approaches for solving the “cold tumor” dilemma.

The above studies are still in their infancy but provide a solid theoretical basis for future preclinical and clinical development of combination therapies using epigenetic modulators and immunotherapeutic agents and show great potential. This will be a new therapeutic paradigm targeting improved and enhanced immune efficacy. We expect that based on the rapid development of immunogenomics, immunoproteomics, and immunobioinformatics, the complex structures in the tumor immune microenvironment will be revealed more comprehensively in the future. Together with the development of research on immune features in preclinical tumor models, this will greatly improve our understanding of the role of histone methylation in the immune microenvironment, facilitating clinical translation and the construction of precise therapeutic systems. Therefore, the development of this field is an important breakthrough to improve the efficacy of immunotherapy for the benefit of more patients. Based on the current research, we still need further studies to explore the role of histone methylation mutations in the regulation of immune resistance in different types of tumors. Meanwhile, the combination of single cell sequencing and spatial transcriptome sequencing will fully reveal the importance of histone methyl esterases in the tumor microenvironment, providing finer evidence to support the mechanism of epigenetic involvement in immune regulation. In addition, experimental models of combining multiple histone

methylation modulators with immunotherapeutic agents will be developed, and rational and less toxic optimization protocols will be sought to advance clinical practice.

In conclusion, understanding the regulatory mechanisms of histone methylation modifying enzymes will improve immunotherapy.

Author contributions

YZ and JC collected relevant literature, prepared data, and drafted the manuscript. HL and RM participated in the design of this review. RH, FF and XX participated in the summary and drawing of tables and pictures. XL and JD made strict revisions to the manuscript. All authors read and approve the final draft.

Funding

This work was supported in part by the National Natural Science Foundation of China (81360366,81302169); Guizhou Science and Technology Plan Project (Foundation (2019) 1198, Foundation Foundation [2020] 1Z064).

Conflict of interest

The authors declare that the research was conducted in the absence of any commercial or financial relationships that could be construed as a potential conflict of interest.

Publisher's note

All claims expressed in this article are solely those of the authors and do not necessarily represent those of their affiliated organizations, or those of the publisher, the editors and the reviewers. Any product that may be evaluated in this article, or claim that may be made by its manufacturer, is not guaranteed or endorsed by the publisher.

References

- Li B, Chan HL, Chen P. Immune checkpoint inhibitors: Basics and challenges. *Curr Med Chem* (2019) 26(17):3009–25. doi: 10.2174/0929867324666170804143706
- Abreu TR, Fonseca NA, Gonçalves N, Moreira JN. Current challenges and emerging opportunities of CAR-T cell therapies. *J Control Release*. (2020) 319:246–61. doi: 10.1038/s41423-020-0488-6
- Yarchoan M, Johnson BA3rd, Lutz ER, Laheru DA, Jaffee EM. Targeting neoantigens to augment antitumor immunity. *Nat Rev Cancer*. (2017) 17(9):569. doi: 10.1038/nrc.2017.74
- Haanen JB, Robert C. Immune checkpoint inhibitors. *Prog Tumor Res* (2015) 42:55–66. doi: 10.1159/000437178
- Pansy K, Uhl B, Krstic J, Szmyra M, Fechter K, Santiso A, et al. Immune regulatory processes of the tumor microenvironment under malignant conditions. *Int J Mol Sci* (2021) 22(24):13311. doi: 10.3390/ijms222413311
- Fiala O, Šorejs O, Šustr J, Fínek J. Side effects and efficacy of immunotherapy. nežádoucí účinky a efekt imunoterapie. *Klin Onkol*. (2020) 33(1):8–10. doi: 10.14735/amko20208
- van den Bulk J, Verdegaal EM, de Miranda NF. Cancer immunotherapy: broadening the scope of targetable tumours. *Open Biol* (2018) 8(6):180037. doi: 10.1098/rsob.180037
- Schoenfeld AJ, Hellmann MD. Acquired resistance to immune checkpoint inhibitors. *Cancer Cell* (2020) 37(4):443–55. doi: 10.1016/j.ccell.2020.03.017

9. Filipp FV. Crosstalk between epigenetics and metabolism-yin and yang of histone demethylases and methyltransferases in cancer. *Brief Funct Genomics* (2017) 16(6):320–5. doi: 10.1093/bfgp/elix001
10. Tian X, Zhang S, Liu HM, Zhang YB, Blair CA, Mercola D, et al. Histone lysine-specific methyltransferases and demethylases in carcinogenesis: New targets for cancer therapy and prevention. *Curr Cancer Drug Targets*. (2013) 13(5):558–79. doi: 10.2174/1568009611313050007
11. Tost J, Gay S, Firestein G. Epigenetics of the immune system and alterations in inflammation and autoimmunity. *Epigenomics*. (2017) 9(4):371–3. doi: 10.2217/epi-2017-0026
12. Li B, Severson E, Pignon JC, Zhao H, Li T, Novak J, et al. Comprehensive analyses of tumor immunity: Implications for cancer immunotherapy. *Genome Biol* (2016) 17(1):174. doi: 10.1186/s13059-016-1028-7
13. Li J, Byrne KT, Yan F, Yamazoe T, Chen Z, Baslan T, et al. Tumor cell-intrinsic factors underlie heterogeneity of immune cell infiltration and response to immunotherapy. *Immunity*. (2018) 49(1):178–193.e7. doi: 10.1016/j.immuni.2018.06.006
14. Jenuwein T, Allis CD. Translating the histone code. *Science*. (2001) 293(5532):1074–80. doi: 10.1126/science.1063127
15. Peterson CL, Laniel MA. Histones and histone modifications. *Curr Biol* (2004) 14(14):R546–51. doi: 10.1016/j.cub.2004.07.007
16. Schneider R, Bannister AJ, Kouzarides T. Unsafe SETs: Histone lysine methyltransferases and cancer. *Trends Biochem Sci* (2002) 27(8):396–402. doi: 10.1016/s0968-0004(02)02141-2
17. Yang Y, Bedford MT. Protein arginine methyltransferases and cancer. *Nat Rev Cancer*. (2013) 13(1):37–50. doi: 10.1038/nrc3409
18. Moore KE, Gozani O. An unexpected journey: Lysine methylation across the proteome. *Biochim Biophys Acta* (2014) 1839(12):1395–403. doi: 10.1016/j.bbagr.2014.02.008
19. Shen C, Vakoc CR. Gain-of-function mutation of chromatin regulators as a tumorigenic mechanism and an opportunity for therapeutic intervention. *Curr Opin Oncol* (2015) 27(1):57–63. doi: 10.1097/CCO.0000000000000151
20. Ennishi D, Takata K, Béguelin W, Duns G, Mottok A, Farinha P, et al. Molecular and genetic characterization of MHC deficiency identifies EZH2 as therapeutic target for enhancing immune recognition. *Cancer Discovery* (2019) 9(4):546–63. doi: 10.1158/2159-8290.CD-18-1090
21. Burr ML, Sparbier CE, Chan KL, Chan YC, Kersbergen A, Lam EYN, et al. An evolutionarily conserved function of polycomb silences the MHC class I antigen presentation pathway and enables immune evasion in cancer. *Cancer Cell* (2019) 36(4):385–401.e8. doi: 10.1016/j.ccell.2019.08.008
22. Morel KL, Sheahan AV, Burkhart DL, Baca SC, Boufaied N, Liu Y, et al. EZH2 inhibition activates a dsRNA-STING-interferon stress axis that potentiates response to PD-1 checkpoint blockade in prostate cancer. *Nat Cancer*. (2021) 2(4):444–56. doi: 10.1038/s43018-021-00185-w
23. Xiao G, Jin LL, Liu CQ, Wang YC, Meng YM, Zhou ZG, et al. EZH2 negatively regulates PD-L1 expression in hepatocellular carcinoma. *J Immunother Cancer*. (2019) 7(1):300. doi: 10.1186/s40425-019-0784-9
24. Yin H, Wang Y, Wu Y, Zhang X, Zhang X, Liu J, et al. EZH2-mediated epigenetic silencing of miR-29/miR-30 targets LOXL4 and contributes to tumorigenesis, metastasis, and immune microenvironment remodeling in breast cancer. *Theranostics*. (2020) 10(19):8494–512. doi: 10.7150/tno.44849
25. Yin Y, Qiu S, Li X, Huang B, Xu Y, Peng Y. EZH2 suppression in glioblastoma shifts microglia toward M1 phenotype in tumor microenvironment. *J Neuroinflammation*. (2017) 14(1):220. doi: 10.1186/s12974-017-0993-4
26. Nagarsheth N, Peng D, Kryczek I, Wu K, Li W, Zhao E, et al. PRC2 epigenetically silences Th1-type chemokines to suppress effector T-cell trafficking in colon cancer. *Cancer Res* (2016) 76(2):275–82. doi: 10.1158/0008-5472.CAN-15-1938
27. Peng D, Kryczek I, Nagarsheth N, Zhao L, Wei S, Wang W, et al. Epigenetic silencing of Th1-type chemokines shapes tumour immunity and immunotherapy. *Nature*. (2015) 527(7577):249–53. doi: 10.1038/nature15520
28. Li J, Wang W, Zhang Y, Cieślak M, Guo J, Tan M, et al. Epigenetic driver mutations in ARID1A shape cancer immune phenotype and immunotherapy. *J Clin Invest*. (2020) 130(5):2712–26. doi: 10.1016/j.jcelrep.2018.05.050
29. Wang D, Quiros J, Mahuron K, Pai CC, Ranzani V, Young A, et al. Targeting EZH2 reprograms intratumoral regulatory T cells to enhance cancer immunity. *Cell Rep* (2018) 23(11):3262–74. doi: 10.1016/j.celrep.2018.05.050
30. Zhao E, Maj T, Kryczek I, Li W, Wu K, Zhao L, et al. Cancer mediates effector T cell dysfunction by targeting microRNAs and EZH2 via glycolysis restriction. *Nat Immunol* (2016) 17(1):95–103. doi: 10.1038/ni.3313
31. Weber EW, Parker KR, Sotillo E, Lynn RC, Anbunathan H, Lattin J, et al. Transient rest restores functionality in exhausted CAR-T cells through epigenetic remodeling. *Science*. (2021) 372(6537):eaba1786. doi: 10.1126/science.aba1786
32. Kato S, Weng QY, Insko ML, Chen KY, Muralidhar S, Pozniak J, et al. Gain-of-Function genetic alterations of G9a drive oncogenesis. *Cancer Discovery* (2020) 10(7):980–97. doi: 10.1158/2159-8290.CD-19-0532
33. Seier JA, Reinhardt J, Saraf K, Ng SS, Layer JP, Corvino D, et al. Druggable epigenetic suppression of interferon-induced chemokine expression linked to MYCN amplification in neuroblastoma. *J Immunother Cancer*. (2021) 9(5):e001335. doi: 10.1136/jitc-2020-001335
34. Spiliopoulou P, Spear S, Mirza H, Garner I, McGarry L, Grundland-Freile F, et al. Dual G9a/EZH2 inhibition stimulates antitumor immune response in ovarian high-grade serous carcinoma. *Mol Cancer Ther* (2022) 21(4):522–34. doi: 10.1158/1078-0432.CCR-20-3463
35. Kelly GM, Al-Ejeh F, McCuaig R, Casciello F, Ahmad Kamal N, Ferguson B, et al. G9a inhibition enhances checkpoint inhibitor blockade response in melanoma. *Clin Cancer Res* (2021) 27(9):2624–35. doi: 10.1158/1078-0432.CCR-20-3463
36. Paschall AV, Yang D, Lu C, Choi JH, Li X, Liu F, et al. H3K9 trimethylation silences fas expression to confer colon carcinoma immune escape and 5-fluorouracil chemoresistance. *J Immunol* (2015) 195(4):1868–82. doi: 10.4049/jimmunol.1402243
37. Xia S, Wu J, Zhou W, Zhang M, Zhao K, Liu J, et al. SLC7A2 deficiency promotes hepatocellular carcinoma progression by enhancing recruitment of myeloid-derived suppressors cells. *Cell Death Dis* (2021) 12(6):570. doi: 10.1038/s41419-021-03853-y
38. Griffin GK, Wu J, Iracheta-Vellve A, Patti JC, Hsu J, Davis T, et al. Epigenetic silencing by SETDB1 suppresses tumour intrinsic immunogenicity. *Nature*. (2021) 595(7866):309–14. doi: 10.1038/s41586-021-03520-4
39. Lin J, Guo D, Liu H, Zhou W, Wang C, Müller I, et al. The SETDB1-TRIM28 complex suppresses antitumor immunity. *Cancer Immunol Res* (2021) 9(12):1413–24. doi: 10.1158/2326-6066.CIR-21-0754
40. Zhang SM, Cai WL, Liu X, Thakral D, Luo J, Chan LH, et al. KDM5B promotes immune evasion by recruiting SETDB1 to silence retroelements. *Nature*. (2021) 598(7882):682–7. doi: 10.1038/s41586-021-03994-2
41. Guo E, Xiao R, Wu Y, Lu F, Liu C, Yang B, et al. WEE1 inhibition induces anti-tumor immunity by activating ERV and the dsRNA pathway. *J Exp Med* (2022) 219(1):e20210789. doi: 10.1084/jem.20210789
42. Cuellar TL, Herzner AM, Zhang X, Goyal Y, Watanabe C, Friedman BA, et al. Silencing of retrotransposons by SETDB1 inhibits the interferon response in acute myeloid leukemia. *J Cell Biol* (2017) 216(11):3535–49. doi: 10.1083/jcb.201612160
43. Zhang L, Tian S, Zhao M, Yang T, Quan S, Song L, et al. SUV39H1-mediated DNMT1 is involved in the epigenetic regulation of Smad3 in cervical cancer. *Anticancer Agents Med Chem* (2021) 21(6):756–65. doi: 10.2174/187520620666200721110016
44. Pace L, Goudot C, Zueva E, Gueguen P, Burgdorf N, Waterfall JJ, et al. The epigenetic control of stemness in CD8+ T cell fate commitment. *Science*. (2018) 359(6372):177–86. doi: 10.1126/science.aah6499
45. Wakabayashi Y, Tamiya T, Takada I, Fukaya T, Sugiyama Y, Inoue N, et al. Histone 3 lysine 9 (H3K9) methyltransferase recruitment to the interleukin-2 (IL-2) promoter is a mechanism of suppression of IL-2 transcription by the transforming growth factor- β -Smad pathway. *J Biol Chem* (2011) 286(41):35456–65. doi: 10.1074/jbc.M111.236794
46. Lu M, Zhao B, Liu M, Wu L, Li Y, Zhai Y, et al. Pan-cancer analysis of SETD2 mutation and its association with the efficacy of immunotherapy. *NPJ Precis Oncol* (2021) 5(1):51. doi: 10.1038/s41698-021-00193-0
47. Li K, Liu J, Wu L, Xiao Y, Li J, Du H, et al. Genomic correlates of programmed cell death ligand 1 (PD-L1) expression in Chinese lung adenocarcinoma patients. *Cancer Cell Int* (2022) 22(1):138. doi: 10.1186/s12935-022-02488-z
48. Liu W, Ren D, Xiong W, Jin X, Zhu L. A novel FBW7/NFAT1 axis regulates cancer immunity in sunitinib-resistant renal cancer by inducing PD-L1 expression. *J Exp Clin Cancer Res* (2022) 41(1):38. doi: 10.1186/s13046-022-02253-0
49. Lu C, Paschall AV, Shi H, Savage N, Waller JL, Sabbatini ME, et al. The MLL1-H3K4me3 axis-mediated PD-L1 expression and pancreatic cancer immune evasion. *J Natl Cancer Inst* (2017) 109(6):djw283. doi: 10.1093/jnci/djw283
50. Xu H, Liang XL, Liu XG, Chen NP. The landscape of PD-L1 expression and somatic mutations in hepatocellular carcinoma. *J Gastrointest Oncol* (2021) 12(3):1132–40. doi: 10.21037/jgo-21-251
51. Shi Y, Lei Y, Liu L, Zhang S, Wang W, Zhao J, et al. Integration of comprehensive genomic profiling, tumor mutational burden, and PD-L1 expression to identify novel biomarkers of immunotherapy in non-small cell lung cancer. *Cancer Med* (2021) 10(7):2216–31. doi: 10.1002/cam4.3649
52. Lv J, Zhu Y, Ji A, Zhang Q, Liao G. Mining TCGA database for tumor mutation burden and their clinical significance in bladder cancer. *Biosci Rep* (2020) 40(4):BSR20194337. doi: 10.1042/BSR20194337

53. Ji Q, Cai Y, Shrestha SM, Shen D, Zhao W, Shi R. Construction and validation of an immune-related gene prognostic index for esophageal squamous cell carcinoma. *BioMed Res Int* (2021) 2021:7430315. doi: 10.1155/2021/7430315
54. Salem ME, Puccini A, Xiu J, Raghavan D, Lenz HJ, Korn WM, et al. Comparative molecular analyses of esophageal squamous cell carcinoma, esophageal adenocarcinoma, and gastric adenocarcinoma. *Oncologist*. (2018) 23 (11):1319–27. doi: 10.1634/theoncologist.2018-0143
55. Isshiki Y, Melnick A. Epigenetic mechanisms of therapy resistance in diffuse Large B cell lymphoma (DLBCL). *Curr Cancer Drug Targets*. (2021) 21(4):274–82. doi: 10.2174/1568009620666210106122750
56. Farah CS. Molecular landscape of head and neck cancer and implications for therapy. *Ann Transl Med* (2021) 9(10):915. doi: 10.21037/atm-20-6264
57. Oreskovic E, Wheeler EC, Mengwasser KE, Fujimura E, Martin TD, Tothova Z, et al. Genetic analysis of cancer drivers reveals cohesin and CTCF as suppressors of PD-L1. *Proc Natl Acad Sci U S A*. (2022) 119(7):e2120540119. doi: 10.1073/pnas.2120540119
58. Kwesi-Maliepaard EM, Aslam MA, Alemdehy MF, van den Brand T, McLean C, Vlaming H, et al. The histone methyltransferase DOT1L prevents antigen-independent differentiation and safeguards epigenetic identity of CD8+ T cells. *Proc Natl Acad Sci U S A*. (2020) 117(34):20706–16. doi: 10.1073/pnas.1920372117
59. Kagoya Y, Nakatsugawa M, Saso K, Guo T, Anczurowski M, Wang CH, et al. DOT1L inhibition attenuates graft-versus-host disease by allogeneic T cells in adoptive immunotherapy models. *Nat Commun* (2018) 9(1):1915. doi: 10.1038/s41467-018-04262-0
60. Sun D, Wang W, Guo F, Pitter MR, Du W, Wei S, et al. DOT1L affects colorectal carcinogenesis via altering T cell subsets and oncogenic pathway. *Oncoimmunology*. (2022) 11(1):2052640. doi: 10.1080/2162402X.2022.2052640
61. Sellers WR, Loda M. The EZH2 polycomb transcriptional repressor—a marker or mover of metastatic prostate cancer? *Cancer Cell* (2002) 2(5):349–50. doi: 10.1016/s1535-6108(02)00187-3
62. Kim KH, Roberts CW. Targeting EZH2 in cancer. *Nat Med* (2016) 22 (2):128–34. doi: 10.1038/nm.4036
63. Booth CAG, Barkas N, Neo WH, Boukarabila H, Soilleux EJ, Giotopoulos G, et al. Ezh2 and Runx1 mutations collaborate to initiate lympho-myeloid leukemia in early thymic progenitors. *Cancer Cell* (2018) 33(2):274–291.e8. doi: 10.1016/j.ccell.2018.01.006
64. Cao H, Li L, Yang D, Zeng L, Yewei X, Yu B, et al. Recent progress in histone methyltransferase (G9a) inhibitors as anticancer agents. *Eur J Med Chem* (2019) 179:537–46. doi: 10.1016/j.ejmech.2019.06.072
65. Jan S, Dar MI, Wani R, Sandey J, Mushtaq I, Lateef S, et al. Targeting EHMT2/G9a for cancer therapy: Progress and perspective. *Eur J Pharmacol* (2021) 893:173827. doi: 10.1016/j.ejphar.2020.173827
66. Karanth AV, Maniswami RR, Prashanth S, Govindaraj H, Padmavathy R, Jegatheesan SK, et al. Emerging role of SETDB1 as a therapeutic target. *Expert Opin Ther Targets*. (2017) 21(3):319–31. doi: 10.1080/14728222.2017.1279604
67. Weirich S, Khella MS, Jeltsch A. Structure, activity and function of the Suv39h1 and Suv39h2 protein lysine methyltransferases. *Life (Basel)*. (2021) 11 (7):703. doi: 10.3390/life11070703
68. Li W. *Histone methyltransferase SETD2 in lymphoid malignancy*. Gallamini M, Juweid M, eds. Lymphoma. Brisbane (AU): Exon Publications. (2021).
69. Yuan H, Han Y, Wang X, Li N, Liu Q, Yin Y, et al. SETD2 restricts prostate cancer metastasis by integrating EZH2 and AMPK signaling pathways. *Cancer Cell* (2020) 38(3):350–365.e7. doi: 10.1016/j.ccell.2020.05.022
70. Rao RC, Dou Y. Hijacked in cancer: the KMT2 (MLL) family of methyltransferases. *Nat Rev Cancer*. (2015) 15(6):334–46. doi: 10.1038/nrc3929
71. Bernt KM, Zhu N, Sinha AU, Vempati S, Faber J, Krivtsov AV, et al. MLL-rearranged leukemia is dependent on aberrant H3K79 methylation by DOT1L. *Cancer Cell* (2011) 20(1):66–78. doi: 10.1016/j.ccr.2011.06.010
72. Cha B, Jho EH. Protein arginine methyltransferases (PRMTs) as therapeutic targets. *Expert Opin Ther Targets*. (2012) 16(7):651–64. doi: 10.1517/14728222.2012.688030
73. Hou J, Wang Y, Shi L, Chen Y, Xu C, Saeedi A, et al. Integrating genome-wide CRISPR immune screen with multi-omic clinical data reveals distinct classes of tumor intrinsic immune regulators. *J Immunother Cancer*. (2021) 9(2):e001819. doi: 10.1136/jitc-2020-001819
74. Schonfeld M, Zhao J, Komatz A, Weinman SA, Tikhonovich I. The polymorphism rs975484 in the protein arginine methyltransferase 1 gene modulates expression of immune checkpoint genes in hepatocellular carcinoma. *J Biol Chem* (2020) 295(20):7126–37. doi: 10.1074/jbc.RA120.013401
75. Zheng NN, Zhou M, Sun F, Huai MX, Zhang Y, Qu CY, et al. Combining protein arginine methyltransferase inhibitor and anti-programmed death-ligand-1 inhibits pancreatic cancer progression. *World J Gastroenterol* (2020) 26(26):3737–49. doi: 10.3748/wjg.v26.i26.3737
76. Zhao J, O'Neil M, Vittal A, Weinman SA, Tikhonovich I. PRMT1-dependent macrophage IL-6 production is required for alcohol-induced HCC progression. *Gene Expr*. (2019) 19(2):137–50. doi: 10.3727/105221618X15372014086197
77. Liu K, Ma J, Ao J, Mu L, Wang Y, Qian Y, et al. The oncogenic role and immune infiltration for CARM1 identified by pancancer analysis. *J Oncol* (2021) 2021:2986444. doi: 10.1155/2021/2986444
78. Lin J, Liu H, Fukumoto T, Zundell J, Yan Q, Tang CA, et al. Targeting the IRE1α/XBP1s pathway suppresses CARM1-expressing ovarian cancer. *Nat Commun* (2021) 12(1):5321. doi: 10.1038/s41467-021-25684-3
79. Kim EJ, Liu P, Zhang S, Donahue K, Wang Y, Schehr JL, et al. BAF155 methylation drives metastasis by hijacking super-enhancers and subverting anti-tumor immunity. *Nucleic Acids Res* (2021) 49(21):12211–33. doi: 10.1093/nar/gkab1122
80. Zhang LX, Gao J, Long X, Zhang PF, Yang X, Zhu SQ, et al. The circular RNA circHMGB2 drives immunosuppression and anti-PD-1 resistance in lung adenocarcinomas and squamous cell carcinomas via the miR-181a-5p/CARM1 axis. *Mol Cancer*. (2022) 21(1):110. doi: 10.1186/s12943-022-01586-w
81. Zhang Z, Guo Z, Xu X, Cao D, Yang H, Li Y, et al. Structure-based discovery of potent CARM1 inhibitors for solid tumor and cancer immunology therapy. *J Med Chem* (2021) 64(22):16650–74. doi: 10.1021/acs.jmedchem.1c01308
82. Kumar S, Zeng Z, Bagati A, Tay RE, Sanz LA, Hartono SR, et al. CARM1 inhibition enables immunotherapy of resistant tumors by dual action on tumor cells and T cells. *Cancer Discovery* (2021) 11(8):2050–71. doi: 10.1158/2159-8290.CD-20-1144
83. Kim H, Kim H, Feng Y, Li Y, Tamiya H, Tocci S, et al. PRMT5 control of cGAS/STING and NLRG5 pathways defines melanoma response to antitumor immunity. *Sci Transl Med* (2020) 12(551):eaaz5683. doi: 10.1126/scitranslmed.aaz5683
84. Luo Y, Gao Y, Liu W, Yang Y, Jiang J, Wang Y, et al. Myelocytomatosis-protein arginine n-methyltransferase 5 axis defines the tumorigenesis and immune response in hepatocellular carcinoma. *Hepatology*. (2021) 74(4):1932–51. doi: 10.1002/hep.31864
85. Hu R, Zhou B, Chen Z, Chen S, Chen N, Shen L, et al. PRMT5 inhibition promotes PD-L1 expression and immuno-resistance in lung cancer. *Front Immunol* (2022) 12:722188. doi: 10.3389/fimmu.2021.722188
86. Jiang Y, Yuan Y, Chen M, Li S, Bai J, Zhang Y, et al. PRMT5 disruption drives antitumor immunity in cervical cancer by reprogramming T cell-mediated response and regulating PD-L1 expression. *Theranostics*. (2021) 11(18):9162–76. doi: 10.7150/tno.59605
87. Zheng Y, Chen Z, Zhou B, Chen S, Han L, Chen N, et al. PRMT5 deficiency enforces the transcriptional and epigenetic programs of Klrj1+CD8+ terminal effector T cells and promotes cancer development. *J Immunol* (2022) 208(2):501–13. doi: 10.4049/jimmunol.2100523
88. Strobl CD, Schaffer S, Haug T, Völkl S, Peter K, Singer K, et al. Selective PRMT5 inhibitors suppress human CD8+ T cells by upregulation of p53 and impairment of the AKT pathway similar to the tumor metabolite MTA. *Mol Cancer Ther* (2020) 19(2):409–19. doi: 10.1158/1535-7163.MCT-19-0189
89. Nagai Y, Ji MQ, Zhu F, Xiao Y, Tanaka Y, Kambayashi T, et al. PRMT5 associates with the FOXP3 homomer and when disabled enhances targeted p185erbB2/neu tumor immunotherapy. *Front Immunol* (2019) 10:174. doi: 10.3389/fimmu.2019.00174
90. Tang J, Frankel A, Cook RJ, Kim S, Paik WK, Williams KR, et al. PRMT1 is the predominant type I protein arginine methyltransferase in mammalian cells. *J Biol Chem* (2000) 275(11):7723–30. doi: 10.1074/jbc.275.11.7723
91. Chen D, Ma H, Hong H, Koh SS, Huang SM, Schurter BT, et al. Regulation of transcription by a protein methyltransferase. *Science*. (1999) 284(5423):2174–7. doi: 10.1126/science.284.5423.2174
92. Stopa N, Krebs JE, Shechter D. The PRMT5 arginine methyltransferase: Many roles in development, cancer and beyond. *Cell Mol Life Sci* (2015) 72 (11):2041–59. doi: 10.1007/s00018-015-1847-9
93. Pedersen MT, Helin K. Histone demethylases in development and disease. *Trends Cell Biol* (2010) 20(11):662–71. doi: 10.1016/j.tcb.2010.08.011
94. Shi Y, Lan F, Matson C, Mulligan P, Whetstone JR, Cole PA, et al. Histone demethylation mediated by the nuclear amine oxidase homolog LSD1. *Cell*. (2004) 119(7):941–53. doi: 10.1016/j.cell.2004.12.012
95. Tsukada Y, Fang J, Erdjument-Bromage H, Warren ME, Borchers CH, Tempst P, et al. Histone demethylation by a family of JmjC domain-containing proteins. *Nature*. (2006) 439(7078):811–6. doi: 10.1038/nature04433
96. Arifuzzaman S, Khatun MR, Khatun R. Emerging of lysine demethylases (KDMs): From pathophysiological insights to novel therapeutic opportunities. *BioMed Pharmacother*. (2020) 129:110392. doi: 10.1016/j.biopha.2020.110392
97. Yang J, Hu Y, Zhang B, Liang X, Li X. The JMJD family histone demethylases in crosstalk between inflammation and cancer. *Front Immunol* (2022) 13:881396. doi: 10.3389/fimmu.2022.881396

98. Sheng W, LaFleur MW, Nguyen TH, Chen S, Chakravarthy A, Conway JR, et al. LSD1 ablation stimulates anti-tumor immunity and enables checkpoint blockade. *Cell*. (2018) 174(3):549–563.e19. doi: 10.1016/j.cell.2018.05.052
99. Zhou Z, van der Jeught K, Fang Y, Yu T, Li Y, Ao Z, et al. An organoid-based screen for epigenetic inhibitors that stimulate antigen presentation and potentiate T-cell-mediated cytotoxicity. *Nat BioMed Eng*. (2021) 5(11):1320–35. doi: 10.1038/s41551-021-00805-x
100. Nguyen EM, Taniguchi H, Chan JM, Zhan YA, Chen X, Qiu J, et al. Targeting lysine-specific demethylase 1 rescues major histocompatibility complex class I antigen presentation and overcomes programmed death-ligand 1 blockade resistance in SCLC. *J Thorac Oncol* (2022) 17(8):1014–31. doi: 10.1016/j.jtho.2022.05.014
101. Xu S, Wang X, Yang Y, Li Y, Wu S. LSD1 silencing contributes to enhanced efficacy of anti-CD47/PD-L1 immunotherapy in cervical cancer. *Cell Death Dis* (2021) 12(4):282. doi: 10.1038/s41419-021-03556-4
102. Wang Y, Cao K. KDM1A promotes immunosuppression in hepatocellular carcinoma by regulating PD-L1 through demethylating MEF2D. *J Immunol Res* (2021) 2021:9965099. doi: 10.1155/2021/9965099
103. Shen DD, Pang JR, Bi YP, Zhao LF, Li YR, Zhao LJ, et al. LSD1 deletion decreases exosomal PD-L1 and restores T-cell response in gastric cancer. *Mol Cancer*. (2022) 21(1):75. doi: 10.1186/s12943-022-01557-1
104. Han Y, Xu S, Ye W, Wang Y, Zhang X, Deng J, et al. Targeting LSD1 suppresses stem cell-like properties and sensitizes head and neck squamous cell carcinoma to PD-1 blockade. *Cell Death Dis* (2021) 12(11):993. doi: 10.1038/s41419-021-04297-0
105. Sheng W, Liu Y, Chakraborty D, Debo B, Shi Y. Simultaneous inhibition of LSD1 and TGF β enables eradication of poorly immunogenic tumors with anti-PD-1 treatment. *Cancer Discovery* (2021) 11(8):1970–81. doi: 10.1158/2159-8290.CD-20-0017
106. Liu Y, Debo B, Li M, Shi Z, Sheng W, Shi Y. LSD1 inhibition sustains T cell invigoration with a durable response to PD-1 blockade. *Nat Commun* (2021) 12(1):6831. doi: 10.1038/s41467-021-21719-7
107. Tu WJ, McCuaig RD, Tan AHY, Hardy K, Seddiki N, Ali S, et al. Targeting nuclear LSD1 to reprogram cancer cells and reinvigorate exhausted T cells via a novel LSD1-EOMES switch. *Front Immunol* (2020) 11:1228. doi: 10.3389/fimmu.2020.01228
108. Zhong C, Tao B, Li X, Xiang W, Peng L, Peng T, et al. HOXA-AS2 contributes to regulatory T cell proliferation and immune tolerance in glioma through the miR-302a/KDM2A/JAG1 axis. *Cell Death Dis* (2022) 13(2):160. doi: 10.1038/s41419-021-04471-4
109. Li J, Yuan S, Norgard RJ, Yan F, Sun YH, Kim IK, et al. Epigenetic and transcriptional control of the epidermal growth factor receptor regulates the tumor immune microenvironment in pancreatic cancer. *Cancer Discovery* (2021) 11(3):736–53. doi: 10.1158/2159-8290.CD-20-0519
110. Zhang W, Liu W, Jia L, Chen D, Chang I, Lake M, et al. Targeting KDM4A epigenetically activates tumor-cell-intrinsic immunity by inducing DNA replication stress. *Mol Cell* (2021) 81(10):2148–2165.e9. doi: 10.1016/j.molcel.2021.02.038
111. Zhang M, Liu Y, Hou S, Wang Y, Wang C, Yin Y, et al. KDM4B, a potential prognostic biomarker revealed by large-scale public databases and clinical samples in uterine corpus endometrial carcinoma. *Mol Omics*. (2022) 18(6):506–19. doi: 10.1039/d1mo00287b
112. Liu L, Yu T, Jin Y, Mai W, Zhou J, Zhao C. MicroRNA-15a carried by mesenchymal stem cell-derived extracellular vesicles inhibits the immune evasion of colorectal cancer cells by regulating the KDM4B/HOXC4/PD-L1 axis. *Front Cell Dev Biol* (2021) 9:629893. doi: 10.3389/fcell.2021.629893
113. Jie X, Chen Y, Zhao Y, Yang X, Xu Y, Wang J, et al. Targeting KDM4C enhances CD8+ T cell mediated antitumor immunity by activating chemokine CXCL10 transcription in lung cancer. *J Immunother Cancer*. (2022) 10(2):e003716. doi: 10.1136/jitc-2021-003716
114. Liao TT, Lin CC, Jiang JK, Yang SH, Teng HW, Yang MH. Harnessing stemness and PD-L1 expression by AT-rich interaction domain-containing protein 3B in colorectal cancer. *Theranostics*. (2020) 10(14):6095–112. doi: 10.7150/thno.44147
115. Chen Q, Zhuang S, Hong Y, Yang L, Guo P, Mo P, et al. Demethylase JMJD2D induces PD-L1 expression to promote colorectal cancer immune escape by enhancing IFNGR1-STAT3-IRF1 signaling. *Oncogene*. (2022) 41(10):1421–33. doi: 10.1038/s41388-021-02173-x
116. Rasmussen PB, Staller P. The KDM5 family of histone demethylases as targets in oncology drug discovery. *Epigenomics*. (2014) 6(3):277–86. doi: 10.2217/epi.14.14
117. Hao F. Systemic profiling of KDM5 subfamily signature in non-Small-Cell lung cancer. *Int J Gen Med* (2021) 14:7259–75. doi: 10.2147/IJGM.S329733
118. Duan Y, Du Y, Gu Z, Zheng X, Wang C. Expression, prognostic value, and functional mechanism of the KDM5 family in pancreatic cancer. *Front Cell Dev Biol* (2022) 10:887385. doi: 10.3389/fcell.2022.887385
119. Chen XJ, Ren AQ, Zheng L, Zheng ED. Predictive value of KDM5C alterations for immune checkpoint inhibitors treatment outcomes in patients with cancer. *Front Immunol* (2021) 12:664847. doi: 10.3389/fimmu.2021.664847
120. Wu L, Cao J, Cai WL, Lang SM, Horton JR, Jansen DJ, et al. KDM5 histone demethylases repress immune response via suppression of STING. *PLoS Biol* (2018) 16(8):e2006134. doi: 10.1371/journal.pbio.2006134
121. Chen S, Shi Y. A new horizon for epigenetic medicine? *Cell Res* (2013) 23(3):326–8. doi: 10.1038/cr.2012.136
122. Hua C, Chen J, Li S, Zhou J, Fu J, Sun W, et al. KDM6 demethylases and their roles in human cancers. *Front Oncol* (2021) 11:779918. doi: 10.3389/fonc.2021.779918
123. Qu LH, Fang Q, Yin T, Yi HM, Mei GB, Hong ZZ, et al. Comprehensive analyses of prognostic biomarkers and immune infiltrates among histone lysine demethylases (KDMs) in hepatocellular carcinoma. *Cancer Immunol Immunother*. (2022) 71(10):2449–67. doi: 10.1186/s12885-021-08372-9
124. Chen X, Lin X, Pang G, Deng J, Xie Q, Zhang Z. Significance of KDM6A mutation in bladder cancer immune escape. *BMC Cancer* (2021) 21(1):635. doi: 10.1186/s12885-021-08372-9
125. Kardos J, Chai S, Mose LE, Selitsky SR, Krishnan B, Saito R, et al. Claudin-low bladder tumors are immune infiltrated and actively immune suppressed. *JCI Insight* (2016) 1(3):e85902. doi: 10.1172/jci.insight.85902
126. Zhu G, Pei L, Li Y, Gou X. EP300 mutation is associated with tumor mutation burden and promotes antitumor immunity in bladder cancer patients. *Aging (Albany NY)*. (2020) 12(3):2132–41. doi: 10.18632/aging.102728
127. Yi J, Shi X, Xuan Z, Wu J. Histone demethylase UTX/KDM6A enhances tumor immune cell recruitment, promotes differentiation and suppresses medulloblastoma. *Cancer Lett* (2021) 499:188–200. doi: 10.1016/j.canlet.2020.11.031
128. Zhang H, Hu Y, Liu D, Liu Z, Xie N, Liu S, et al. The histone demethylase Kdm6b regulates the maturation and cytotoxicity of TCR $\alpha\beta$ +CD8 $\alpha\alpha$ + intestinal intraepithelial lymphocytes. *Cell Death Differ* (2022) 29(7):1349–63. doi: 10.1038/s41418-021-00921-w
129. Xu T, Schutte A, Jimenez L, Gonçalves ANA, Keller A, Pipkin ME, et al. Kdm6b regulates the generation of effector CD8+ T cells by inducing chromatin accessibility in effector-associated genes. *J Immunol* (2021) 206(9):2170–83. doi: 10.4049/jimmunol.2001459
130. Ding JT, Yu XT, He JH, Chen DZ, Guo F. A pan-cancer analysis revealing the dual roles of lysine (K)-specific demethylase 6B in tumorigenesis and immunity. *Front Genet* (2022) 13:912003. doi: 10.3389/fgene.2022.912003
131. Hino S, Kohroggi K, Nakao M. Histone demethylase LSD1 controls the phenotypic plasticity of cancer cells. *Cancer Sci* (2016) 107(9):1187–92. doi: 10.1111/cas.13004
132. Liu L, Liu J, Lin Q. Histone demethylase KDM2A: Biological functions and clinical values (Review). *Exp Ther Med* (2021) 22(1):723. doi: 10.3892/etm.2021.10155
133. Xiao M, Yang H, Xu W, Ma S, Lin H, Zhu H, et al. Inhibition of α -KG-dependent histone and DNA demethylases by fumarate and succinate that are accumulated in mutations of FH and SDH tumor suppressors. *Genes Dev* (2012) 26(12):1326–38. doi: 10.1101/gad.191056.112
134. Kornberg MD, Bhargava P, Kim PM, Putluri V, Snowman AM, Putluri N, et al. Dimethyl fumarate targets GAPDH and aerobic glycolysis to modulate immunity. *Science*. (2018) 360(6387):449–53. doi: 10.1126/science.aan466
135. Sui Y, Gu R, Janknecht R. Crucial functions of the JMJD1/KDM3 epigenetic regulators in cancer. *Mol Cancer Res* (2021) 19(1):3–13. doi: 10.1158/1541-7786.MCR-20-0404
136. Berry WL, Janknecht R. KDM4/JMJD2 histone demethylases: epigenetic regulators in cancer cells. *Cancer Res* (2013) 73(10):2936–42. doi: 10.1158/0008-5472.CAN-12-4300
137. Wang L, Gao Y, Zhang G, Li D, Wang Z, Zhang J, et al. Enhancing KDM5A and TLR activity improves the response to immune checkpoint blockade. *Sci Transl Med* (2020) 12(560):eaax2282. doi: 10.1126/scitranslmed.aax2282



OPEN ACCESS

EDITED BY

Catherine Sautes-Fridman,
INSERM U1138 Centre de Recherche
des Cordeliers (CRC), France

REVIEWED BY

Steven F Gameiro,
McMaster University, Canada
Tasduq H. Wani,
University of Oxford, United Kingdom

*CORRESPONDENCE

Pei Du
✉ 13711079681@163.com

SPECIALTY SECTION

This article was submitted to
Cancer Immunity
and Immunotherapy,
a section of the journal
Frontiers in Immunology

RECEIVED 09 October 2022

ACCEPTED 22 December 2022

PUBLISHED 11 January 2023

CITATION

Du P, Li G, Wu L and Huang M (2023)
Perspectives of ERCC1 in early-stage
and advanced cervical cancer: From
experiments to clinical applications.
Front. Immunol. 13:1065379.
doi: 10.3389/fimmu.2022.1065379

COPYRIGHT

© 2023 Du, Li, Wu and Huang. This is
an open-access article distributed under
the terms of the [Creative Commons
Attribution License \(CC BY\)](#). The use,
distribution or reproduction in other
forums is permitted, provided the
original author(s) and the copyright
owner(s) are credited and that the
original publication in this journal is
cited, in accordance with accepted
academic practice. No use,
distribution or reproduction is
permitted which does not comply with
these terms.

Perspectives of ERCC1 in early-stage and advanced cervical cancer: From experiments to clinical applications

Pei Du*, Guangqing Li, Lu Wu and Minger Huang

Department of Gynaecology and Obstetrics, Guangzhou Panyu Central Hospital, Guangzhou, Guangdong, China

Cervical cancer is a public health problem of extensive clinical importance. Excision repair cross-complementation group 1 (ERCC1) was found to be a promising biomarker of cervical cancer over the years. At present, there is no relevant review article that summarizes such evidence. In this review, nineteen eligible studies were included for evaluation and data extraction. Based on the data from clinical and experimental studies, ERCC1 plays a key role in the progression of carcinoma of the uterine cervix and the therapeutic response of chemoradiotherapy. The majority of the included studies (13/19, 68%) suggested that ERCC1 played a pro-oncogenic role in both early-stage and advanced cervical cancer. High expression of ERCC1 was found to be associated with the poor survival rates of the patients. ERCC1 polymorphism analyses demonstrated that ERCC1 might be a useful tool for predicting the risk of cervical cancer and the treatment-related toxicities. Experimental studies indicated that the biological effects exerted by ERCC1 in cervical cancer might be mediated by its associated genes and affected signaling pathways (i.e., XPF, TUBB3, and *TO*). To move towards clinical applications by targeting ERCC1 in cervical cancer, more clinical, *in-vitro*, and *in-vivo* investigations are still warranted in the future.

KEYWORDS

ercc1, cervical cancer, cisplatin, survival, mechanism

Introduction

Despite an upward trend in the HPV vaccination rates, cervical cancer remains the fourth most common female cancer worldwide (1, 2). Cervical cancer accounts for 527,600 new cases, representing 5% of all new cancer cases, and around 265,700 deaths annually worldwide (3). Patients with cervical cancer tend to metastasize early, resulting in a poor prognosis and a low 5-year survival rate of 30-60% (4). The major cause of it is infection with High-risk Human Papillomavirus and its diagnosis requires

histopathological evaluation. Radical hysterectomy remains the first-choice therapy for patients at an early stage. A growing number of young patients have been diagnosed with this disease in recent years (5). As a result, some patients wish to preserve their fertility. In the late 1980s, the radical vaginal trachelectomy with bilateral pelvic lymphadenectomy was proposed as one of the standard approaches for fertility-sparing treatment (6). As for locally advanced cervical cancer, platinum-based concurrent chemoradiotherapy remain the gold-standard of treatment (7). It is problematic to treat locally advanced cervical cancers at stage IIb of the Federation of Gynecology and Obstetrics (FIGO). It invades the parametrium and lymph node, and is usually considered inoperable. Several studies demonstrated that neoadjuvant chemotherapy (NAC) reduced the tumor volume and increased tumor resectability, which achieved satisfactory outcomes in locally advanced cervical cancer (8, 9). As known, resistance to chemotherapy is the main obstacle to locally advanced cervical cancer treatment (10). Therefore, it is urgent to identify the biomarkers to predict chemotherapy or NAC response in locally advanced cervical cancer.

Excision repair cross-complementation group 1 (ERCC1) (the DNA repair gene) is a gene associated with platinum sensitivity and has been proposed as a novel biomarker of cervical cancer over the years (11, 12). ERCC1 gene is located on 19q13.2-q13.3, and encodes a 297 amino acid protein (13, 14). The C-terminal domain of ERCC1 interacts with xeroderma pigmentosum group F (XPF), which forms a heterodimeric protein complex. The complex is considered to be the main component of the nucleotide excision repair (NER) pathway (15). There are several major pathways for repairing DNA damage in human cells, one of which is NER (16). It can remove great varieties of helix-distorting DNA lesions, including UV-induced pyrimidine dimers, bulky chemical adducts, and photoproducts (17). The NER complex stabilizes the unwound DNA intermediate by recruiting xeroderma pigmentosum group A and replication protein A (18). Cisplatin is an alkylating compound that exerts its cytotoxic action by interfering with DNA replication by forming strong intrastructural cross-links, which activates cell apoptosis (19). Therefore, ERCC1 overexpression may have an adverse impact on cisplatin-induced cell death. Conversely, the inhibition of ERCC1 may sensitize cancer cells to cisplatin. In a study reported by Kassem et al. (20) on 80 colorectal cancer patients who received first-line oxaliplatin-based chemotherapy, patients with low ERCC1 expression had longer overall survival than those with high ERCC1 expression ($P=0.011$). Similarly, Torii et al. (21) also demonstrated that the expression level of ERCC1 was significantly increased by cisplatin treatment. They also found an association between ERCC1 expression and chemotherapeutic sensitivity of cervical adenocarcinoma cells. Additionally, a case-control study showed that low expression of ERCC1 was closely related to a significantly increased risk for cervical cancer (22). Though ERCC1 can be used not only as a

prognostic biomarker but also to identify patients who will benefit from chemotherapy, the evidence has been debatable (23). In this present study, we summarize all published clinical and experimental data on ERCC1 applications in cervical cancer.

ERCC1 in cervical cancer

Roles of ERCC1 in cervical cancer among the current relevant studies

A systematic search was conducted in four databases, including MEDLINE, EMBASE (OVID), Cochrane Library, and PsychINFO to screen related studies prior to August 1, 2022. We included only studies that were reported in English. For identifying eligible studies in PubMed databases, the following search strategy was employed: ((excision repair cross-complementation group1) OR (ERCC1)) AND ((Cervical Neoplasm, Uterine) OR (Cervical Neoplasms, Uterine)) OR (Neoplasm, Uterine Cervical)) OR (Neoplasms, Uterine Cervical)) OR (Uterine Cervical Neoplasm)) OR (Neoplasms, Cervical)) OR (Cervical Neoplasms)) OR (Cervical Neoplasm)) OR (Neoplasm, Cervical)) OR (Neoplasms, Cervix)) OR (Cervix Neoplasms)) OR (Cervix Neoplasm)) OR (Neoplasm, Cervix)) OR (Cancer of the Uterine Cervix)) OR (Cancer of the Cervix)) OR (Cervical Cancer)) OR (Uterine Cervical Cancer)) OR (Cancer, Uterine Cervical)) OR (Cancers, Uterine Cervical)) OR (Cervical Cancer, Uterine)) OR (Cervical Cancers, Uterine)) OR (Uterine Cervical Cancers)) OR (Cancer of Cervix)) OR (Cervix Cancer))). The publication's reference lists were manually checked to detect additional studies. On the basis of a data collection form, the following information was extracted, including the first authors' names of the included studies, study publication year, the study type, median/mean age, stage of cervix cancer, treatment for cervix cancer, assessment for ERCC1 examination, the number of moderate/high/positive ERCC1 patients and low/negative ERCC1 patients, and the clinical implications or significances of ERCC1 in cervix cancer.

As shown in Tables 1–3, there were nineteen relevant studies (11, 12, 21–37) that were finally included for further evaluation. Among these eligible studies, thirteen studies were clinical trials reporting the ERCC1 expression and cervix cancer, three studies (33–35) were clinical studies reporting the ERCC1 polymorphism and cervix cancer, and three experimental studies (21, 36, 37) reporting the molecular roles of ERCC1 in cervix cancer. Study publication years ranged from 2000 to 2021 for the included studies. All the clinical studies were retrospective design. The median/mean age of the cervix cancer patients ranged from 43–58 years. The stage of cervix cancer patients included I to IVB, metastatic stage, recurrent stage, advanced stage, and locally advanced stage. The treatment methods for cervix cancer included radiation (i.e., EBRT),

TABLE 1 Clinical findings of ERCC1 in cervical cancer.

Study	Study type	Median/mean Age, Years	Stage	Treatment regimen	ERCC1 expression assessment	Moderate/high/positive ERCC1 patients (n)	Low/negative ERCC1 patients (n)	Clinical significances
Doll et al. (24)	Retrospectiv	NA	Locally advanced	Radiation	Fluorescent IHC	NA	NA	Patients with low ERCC1 expression had significantly worse OS (17.9% vs. 50.1%, $P = 0.046$) and worse DFS (21.4% vs. 47.4%, $P = 0.083$) than those with higher expression levels.
Hasegawa et al. (25)	Retrospectiv	46	FIGO Stage I to II	Radical hysterectomy	IHC	7	29	Patients with high ERCC1 expression had significantly worse DFS than those with low ERCC1 expression ($P = 0.005$). Similar trends were also observed in those patients received cisplatin-based chemotherapy or chemoradiotherapy with cisplatin ($P = 0.002$).
Liang et al. (26)	Retrospectiv	54	Locally Advanced	Concurrent chemoradiotherapy	IHC	16	34	The 5-year disease-specific survival rates of the ERCC1-positive and ERCC1-negative groups were 43.8% vs. 76.5% ($P = 0.011$). The 5-year OS rates for the ERCC1-positive and ERCC1-negative groups were 50.0% vs. 85.3% ($P = 0.008$).
Park et al. (Park et al. (27))	Retrospectiv	50	Stage II B	Neoadjuvant chemotherapy (etoposide and cisplatin)	IHC	34	9	Response to chemotherapy was detected in all patients with negative ERCC1 expression. ERCC1 negativity was an independent predictor for responsiveness to neoadjuvant chemotherapy ($P = 0.021$). Low ERCC1 expression was a significant prognostic factor of DFS in multivariate analysis ($P = 0.046$).
Bai et al. (Bai et al. (28))	Retrospectiv	53	Locally Advanced	Chemoradiotherapy (cisplatin)	RT-PCR	29	31	Patients with low ERCC1 mRNA expression had a significantly higher rate of complete response (86.21%) than those with high level of ERCC1 (19.36%, $P < 0.001$).
Doll et al. (Doll et al. (29))	Retrospectiv	NA	Locally Advanced	Chemoradiation	Immunofluorescent	NA	NA	Tumoral ERCC1 status (nuclear to cytoplasmic ratio) was correlated to OS ($HR = 3.13$, 95%CI: 1.27-7.71, $P = 0.013$) and PFS ($HR = 2.33$, 95%CI: 1.05-5.18, $P = 0.038$).
Bajpai et al. (22)	Retrospectiv	43	NA	Chemoradiotherapy (cisplatin)	RT-PCR, Western blot	11	39	ERCC1 expressions were statistically lower in cervical cancer tissues than that in the normal cervix tissues ($P = 0.025$)
Muallem et al. (23)	Retrospective	44	advanced	EBRT and Cisplatin	IHC	72	40	The 2-year OS in the low, intermediate, and high ERCC1 group was 68.6%, 71.7%, and 90.7%, respectively. The 2-year PFS in the low, intermediate, and high ERCC1 group was 49.7%, 33.5%, and 72.7%, respectively.
KATO et al. (11)	Retrospectiv	46	Stage I B1-IV B	Nedaplatin	IHC	26	19	There were no significant differences in ERCC1 expression between the low and high sensitivity to nedaplatin groups ($P = 0.079$).
Zwenger et al. (30)	Prospective	43.5	advanced	Cisplatin	IHC	35	53	Poor DFS ($P = 0.021$) and OS ($P = 0.005$) were observed in cisplatin chemoradiotherapy patents with high ERCC1 expression.

(Continued)

TABLE 1 Continued

Study	Study type	Median/mean Age, Years	Stage	Treatment regimen	ERCC1 expression assessment	Moderate/high/positive ERCC1 patients (n)	Low/negative ERCC1 patients (n)	Clinical significances
Karageorgopoulou et al. (12)	Retrospective	58	metastatic/recurrent	Cisplatin and ifosfamide	IHC	32	11	Higher ERCC1 expression had shorter PFS and OS than those with low ERCC1 expression (mPFS: 5.1 vs 10.2 months, $P = 0.027$; mOS: 10.5 vs. 21.4 months, $P = 0.006$).
Ryu et al. (31)	Retrospective	51	IVB/metastatic/recurrent	Cisplatin	IHC	13	19	The median OS of ERCC1-high patients was 320 days and that of ERCC1-low patients was 617 days (HR=2.322, 95%CI: 1.051–5.129; $P=0.037$). The median PFS was significantly poorer in ERCC1-high than in ERCC1-low patients (135 vs 242 days; HR=2.428, 95%CI: 1.145–5.148; $P=0.032$).
Jeong et al. (32)	Retrospective	46	I B1 to II B	Chemoradioresistance	IHC	60	71	High ERCC1 expression suggested significantly unfavorable DFS (76.8% vs. 88.6%, $P=0.022$).

ERCC1, excision repair cross-complementation group1; IHC, immunohistochemistry; OS, overall survival; PD, progressive disease; HR, hazard ratio; PFS, progression free survival; DFS, disease-free survival; RT-PCR, real-time polymerase chain reaction.

radical hysterectomy, neoadjuvant chemotherapy, chemoradiotherapy, and concurrent chemoradiotherapy. The common-used chemotherapeutic drugs among the included studies included etoposide, cisplatin, ifosfamide, fluorouracil (FU), cyclophosphamide (CTX), cyclophosphamide (CTP), etc. The assessments for evaluating the expression of ERCC1 mainly included immunohistochemistry (IHC), real-time polymerase chain reaction (RT-PCR), immunofluorescence, and fluorescence. The number of moderate/high/positive ERCC1 patients among the eligible clinical studies ranged from 7 to 72, while the number of low/negative ERCC1 patients in these studies ranged from 9 to 71.

In the three clinical studies reporting the ERCC1 polymorphism, the sample size ranged from 260 to 433. The results of polymorphism examination derived from the peripheral blood and white blood cell. The methods for polymorphism detection in these studies included PCR restriction fragment length polymorphism assay, SNPware 12plex assay, and allelic discrimination RT-PCR. The reported ERCC1 polymorphisms among the three studies were C19007T, 118C>T, and rs3212986.

There were three experimental studies that investigated the aberrant expression of ERCC1 in cervix cancer. The research models among these studies were all *in-vitro* designed, which included a variety of cervical carcinoma lines, i.e., HT137, HT155, HT172, HT180, HT212, CASKI, and C33A cells. These cancer cells were treated with cisplatin resistance, 5-FU, and radiotherapy. A summary of the nineteen studies included in this study can be found in Tables 1–3.

Pro-oncogenic effects of ERCC1 in FIGO stage I to Stage III uterine cervix cancer

Currently, there is evidence that ERCC1 contributes to resistance to platinum-based chemotherapy or chemoradiotherapy coupled with platinum agents in multiple malignancies (38). For example, the relationship between ERCC1 expression and clinical characteristics and outcomes in patients with uterine cervical cancer has been detected in a number of studies. Such an association was not only observed in the early stage but also the advanced stage of uterine cervix cancer. According to the published data, high expression of ERCC1 might be correlated with poor prognosis in cervix cancer. Hasegawa et al. (25) reported that patients with FIGO stage I to II uterine cervix cancer with high ERCC1 expression had significantly worse DFS than those with low ERCC1 expression ($P = 0.005$). In addition, worse DFS was also observed in those patients who had a high level of ERCC1 under cisplatin-based chemotherapy/chemoradiotherapy ($P=0.002$). The log-rank test indicated that high ERCC1 expression might be an independent prognostic factor in patients receiving cisplatin treatment ($P<0.05$). This finding

TABLE 2 ERCC1 polymorphism in cervical cancer.

Study/Reference	Sample size	Examination sample/tissue and method	ERCC1 polymorphism	Main findings
HAN et al. (33)	Invasive cervical cancer: 229; non-cancer controls: 204	Peripheral blood; PCR restriction fragment length polymorphism assay	C19007T	The allelic frequencies of cancer patients were not significantly different from that of controls ($P = 0.925$); The C/C genotype had no increased risk for cervical cancer susceptibility compared with the TT genotype ($P = 0.932$). There was no significant relationship between the ERCC1 C19007T polymorphism and cervical cancer invasiveness (all $P < 0.05$).
Zhang et al. (34)	Cervical cancer: 154; non-cancer controls: 177	Peripheral blood; SNPware 12plex assay	118C>T	ERCC1 118C>T was associated with high risk of cervical squamous cell carcinomas under additive genetic model and the dominant genetic model (all $P < 0.05$)
Soares et al. (35)	260 patents with cervical cancer who underwent cisplatin treatment	White blood cell; Allelic discrimination RT-PCR	rs3212986	An association between ERCC1 rs3212986 and the onset of late gastrointestinal toxicity underwent cisplatin treatment ($P=0.038$); Patients carrying AA homozygous genotype have an increased risk of developing late gastrointestinal toxicity as compared to patents with the C allele (OR = 3.727, 95%CI: 1.199-11.588, $P= 0.017$).
ERCC1, excision repair cross-complementation group1; OR, odds ratio; CI, confidence interval; RT-PCR, real-time polymerase chain reaction.				

was consistent with Park et al.'s study (27) which investigated the roles of ERCC1 in patients with Stage II B cervix cancer under neoadjuvant chemotherapy (etoposide and cisplatin). It was found that chemotherapy was responsive in all patients with negative ERCC1 expression. ERCC1 negativity was an independent predictor for responsiveness to neoadjuvant chemotherapy ($P=0.021$). This study also reported that low ERCC1 expression was a significant prognostic factor of DFS in multivariate analysis ($P=0.046$). In a more recent study (32) developed by Jeong et al., the authors investigated the prognostic significance of ERCC1 in early-stage (FIGO I B1 to II B) cervical cancer with chemoradioresistance. They observed that high ERCC1 expression was associated with significantly

unfavorable DFS than those with low ERCC1 expression (76.8% vs. 88.6%, $P=0.022$). The above three clinical studies demonstrated that ERCC1 might play a pro-cancer role in early-stage uterine cervix cancer, especially in patients with cisplatin chemotherapy.

Pro-oncogenic Effects of ERCC1 in advanced uterine cervix cancer

In addition to the early stage of uterine cervix cancer, ERCC1 expression was also found to be associated with the prognosis of advanced cervix adenocarcinoma. An early study conducted by

TABLE 3 Molecular mechanisms underlying the effects of ERCC1 in cervical cancer.

Study/Reference	Treatments for cervical cancer	Experimental model	Main findings
Britten et al. (36)	Cisplatin resistance	Cervical carcinoma lines (HT137, HT155, HT172, HT180 and HT212)	There was a significant correlation between ERCC1 mRNA expression and cisplatin resistance in all cervical carcinoma lines (all $P < 0.05$), but such an association was not significant in ERCC1 protein expression (all $P > 0.05$). It might be possible to identify cervical tumors likely to be resistant to cisplatin by examining pre-treatment ERCC1 mRNA levels.
Torii et al. (21)	Cisplatin and 5-FU	Uterine cervical adenocarcinoma cells (HCA-1 and TCO-2)	There was an association between ERCC1 expression and sensitivity to cisplatin in cervical adenocarcinoma cells. A cisplatin-resistant cell line HCA-1R showed a dramatically higher level of ERCC1 mRNA expression than the native cells. Co-administration of cisplatin and 5-FU showed the synergistic or additive effects <i>via</i> inhibiting of ERCC1 expression.
Almeida et al. (37)	Radiotherapy	CASKI and C33A cells	Absent or weak modulations of ERCC1 was detected after exposure to 1.8 Gy of radiotherapy in cell lines, which might be associated with the inhibition of the regulatory axis p53-EGFR-ERCC1. Increased expressions of ERCC1 (5/10 patients; $P=0.0294$) was found in malignant tissues after radiotherapy with the same radiation dose. This study showed that upregulation of ERCC1 may be part of a radioresistance mechanism in cervical cancer.
ERCC1, excision repair cross-complementation group1; EGFR, epidermal growth factor receptor.			

Bai et al. (28) demonstrated that advanced cervical squamous cell carcinoma patients with low ERCC1 mRNA expression had a significantly higher rate of complete response to cisplatin-based concurrent chemoradiotherapy (86.21%) than those with a high level of ERCC1 (19.36%, $P < 0.001$). Further analysis indicated that low ERCC1 mRNA level was an independent predictive factor for a complete response to chemoradiotherapy ($P < 0.001$). The authors also found that the sensitivity for detecting a complete response was 81.48% with a specificity of 96.97%. Liang et al. (26) investigated the clinical outcome in patients administrated with cisplatin-based concurrent chemoradiotherapy for locally advanced cervical cancer. They found that the 5-year DFS rates of the ERCC1-positive and ERCC1-negative groups were 43.8% vs. 76.5% ($P = 0.011$) and the 5-year OS rates for the ERCC1-positive and ERCC1-negative groups were 50.0% vs. 85.3% ($P = 0.008$). Zwenger et al. (30) demonstrated that poor DFS ($P=0.021$) and OS ($P=0.005$) were observed in patients with advanced cervical cancer who received cisplatin chemoradiotherapy with high ERCC1 expression when compared to those with low ERCC1 levels.

In addition to the above evidence, A correlation was also found between ERCC1 expression and survival in patients with metastatic or recurrent uterine cervix carcinoma treated with cisplatin and ifosfamide. Karageorgopoulou et al. (12) demonstrated that higher ERCC1 expression had shorter PFS and OS than those with low ERCC1 expression (median PFS: 5.1 vs 10.2 months, $P = 0.027$; median OS: 10.5 vs. 21.4 months, $P = 0.006$). Similarly, a study done in Korea showed the median OS of ERCC1-high patients was 320 days and that of ERCC1-low patients was 617 days (HR=2.322, 95%CI: 1.051–5.129; $P=0.037$) (31). Also, the median PFS was significantly poorer in ERCC1-high than in ERCC1-low patients (135 vs 242 days; HR=2.428, 95%CI: 1.145–5.148; $P=0.032$) (31). These preliminary studies indicated the prognosis and survival of patients with metastatic and recurrent uterine cervix cancer is poor when high ERCC1 expression is confirmed.

The Kaplan-Meier OS, PFS, and DFS curves stratified by ERCC1 status that reported in the included studies were displayed in Figures 1, 2.

ERCC1 serves as a tumor suppressor in advanced uterine cervix cancer

Inconsistencies from the above studies, Bajpai et al. (22) indicated that the level of ERCC1 was statistically lower in cervical cancer tissues than that in the normal cervix tissues ($P=0.025$) in patients under chemoradiotherapy (cisplatin combined with radiotherapy). Doll et al. (24) reported that uterine cervix cancer patients with low ERCC1 expression had significantly worse OS (17.9% vs. 50.1%, $P = 0.046$) and worse DFS (21.4% vs. 47.4%, $P = 0.083$) than those with higher expression levels. Also, in a subsequent study developed by

Doll et al. (29), they observed that tumoral ERCC1 status (nuclear to cytoplasmic ratio) was dramatically associated with the OS of the patients with cervical cancer (HR=3.13, 95%CI: 1.27-7.71, $P=0.013$) as well as correlated with the PFS (HR=2.33, 95%CI: 1.05-5.18, $P=0.038$). Based on the results from Doll et al., patients with cervical cancer who expressed high levels of ERCC1 were thought to have a better survival.

Consistent with Doll et al.'s findings, Muallem et al. (23) also indicated that the high level of ERCC1 was associated with poor prognosis for patients with malignant cervical carcinoma and this tendency was presented as a “dose-response”. It was reported that the 2-year OS of advanced cervical cancer patients in the low, intermediate, and high ERCC1 group was 68.6%, 71.7%, and 90.7%, respectively (23). However, such trend in PFS was not always the same as the tendency of OS. It was reported that the 2-year PFS in the low, intermediate, and high ERCC1 group was 49.7%, 33.5%, and 72.7%, respectively (23). Overall, these results showed that patients with advanced cervical cancer who have a low level of ERCC1 have a worse OS and PFS.

Of note, some studies have also shown that ERCC1 expression does not have a clinical significance in patients with cervical cancer. For example, a previous trial conducted in Japan had recruited 45 patients with Stage I B1-IV B carcinoma of the cervix and found that there were no significant differences in ERCC1 expression between the low and high sensitivity to nedaplatin groups ($P=0.079$) (11). As a result of this study, it was suggested that ERCC1 was not an essential component of the cervical cancer process.

ERCC1 polymorphism and the risk of cervical cancer in women

Genetic mutagenesis can be caused by DNA alterations under environmental or endogenous carcinogens, leading to carcinogenesis (39). Single nucleotide polymorphisms (SNPs) are proposed to be one of the important biomarkers in the prognosis and therapeutic response of oncologic patients (40). In this comprehensive review, there were three studies (Table 2) reporting the association between ERCC1 polymorphisms and the risk of cervical cancer. Zhang et al. (34) analyzed the ERCC1 polymorphisms in peripheral blood from 154 cervical cancer patients and 177 non-cancer controls. The results showed that ERCC1 118C>T was associated with a high risk of cervical squamous cell carcinomas under the additive genetic model and the dominant genetic model (all $P < 0.05$). Platinum agents and ionizing radiation can induce hematological toxicities, genitourinary toxicity, and gastrointestinal toxicity (41). In a more recent study, Soares et al. (35) demonstrated that there was an association between ERCC1 rs3212986 and the onset of late gastrointestinal toxicity underwent cisplatin treatment ($P=0.038$). Patients carrying AA homozygous genotype had an increased risk of developing late gastrointestinal toxicity as

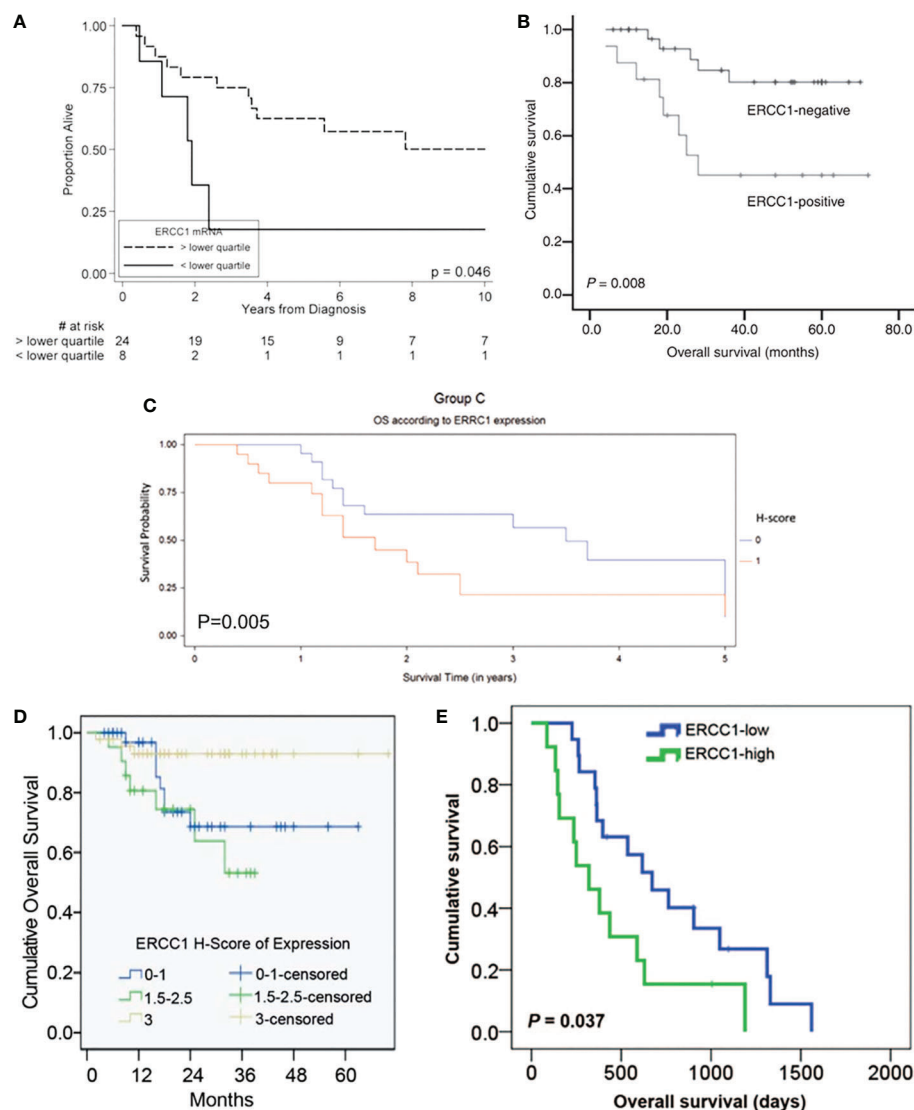


FIGURE 1

Kaplan-Meier overall survival curve stratified by ERCC1 status that reported in five included studies with the corresponding citation. (A) derived from the study of (24), namely A = (24); B = (29); C = (30); D = (23); E = (31).

compared to patients with the C allele (OR = 3.727, 95%CI: 1.199-11.588, $P = 0.017$). The underlying mechanisms might be correlated to the altered DNA repair capacity induced by ERCC1 rs3212986 polymorphism. However, some researchers in Korea did not find a positive association between ERCC1 polymorphisms and cervical cancer by evaluating the peripheral blood through the PCR restriction fragment length polymorphism assay in 229 invasive cervical cancer patients and 204 non-cancer controls (33). The allelic frequencies of ERCC1 in cervical cancer patients were not significantly different from those of the controls in this study ($P = 0.925$). The C/C genotype had no increased risk for cervical cancer susceptibility compared with the TT genotype ($P = 0.932$) (33). The authors concluded

that there was no significant relationship between the ERCC1 C19007T polymorphism and cervical cancer invasiveness in Korean women (all $P < 0.05$) (33).

Based on the above 3 included studies, 67% (2/3) of them suggested there was a positive relationship lying in ERCC1 polymorphism and the development and therapeutic response of cervical cancer. Since the genetic polymorphisms often vary between ethnic groups, the clinical outcomes of ERCC1 polymorphism might be not significant. Even though, detection of ERCC1 polymorphism might be a useful method for implementing strategies when choosing a proper treatment for a patient so as to reduce the toxicities or improve the treatment response rates in cervical cancer women.

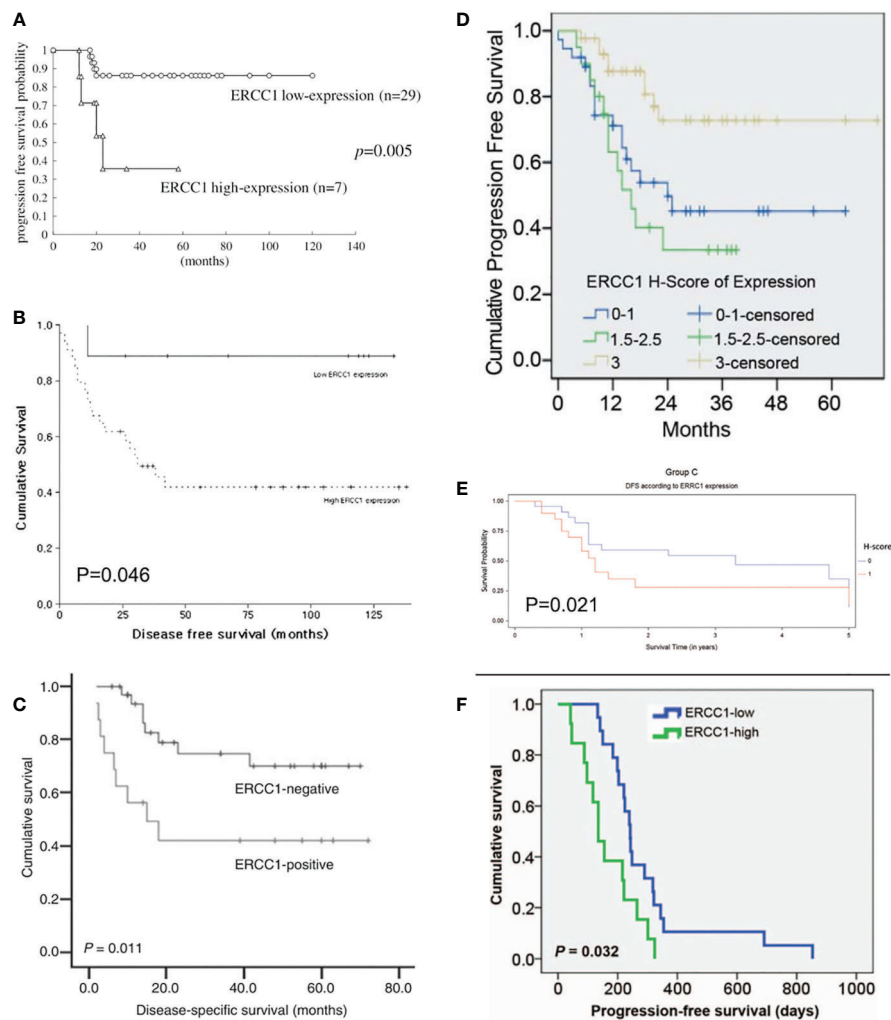


FIGURE 2

Kaplan-Meier disease-free and progression-free survival curve stratified by ERCC1 status that reported in six included studies with the corresponding citation. (A) derived from the study of (25), namely A = (25); B = (26); C = (29); D = (23); E = (30); F = (31).

Roles of ERCC1 in cervical cancer reported in experimental studies

Three *in-vitro* studies (Table 3) reported the molecular mechanisms of ERCC1 in cervical cancer that were available in the literatures. Cisplatin is one of the valuable adjuvants to radiotherapy for treating cervical cancer (42). However, patients are at risk for developing drug-resistant cervical cancer due to the progression of the disease. Britten et al. (36) developed several cervical carcinoma cell lines (e.g. HT137, HT155, HT172, HT180, and HT212) of cisplatin resistance. The authors found that there was a significant correlation between ERCC1 mRNA expression and cisplatin resistance in all cervical carcinoma lines (all $P < 0.05$), but such an association was not significant in ERCC1 protein expression (all $P > 0.05$) (36). According to this study, it might be possible to identify

cervical tumors likely to be resistant to cisplatin by examining pre-treatment ERCC1 mRNA levels.

It was suggested that combined chemotherapy had additive or synergistic effects on various specific malignancies, which could significantly prolong the survival of the sufferers (43). Torii et al. (21) examined the expression of ERCC1 in uterine cervical adenocarcinoma cells treated with cisplatin and 5-FU. The results turned out that a positive association between ERCC1 expression and sensitivity to cisplatin in cervical adenocarcinoma cells (HCA-1 and TCO-2). Cancer cells treated with cisplatin resulted in a significant elevation of ERCC1 expression, while a cisplatin-resistant cell line HCA-1R presented with a dramatically higher level of ERCC1 mRNA expression than the native cells. Interestingly, co-administration of cisplatin and 5-FU remarkably reduced the expression of ERCC1 in both HCA-1 and HCA-1R cells. Thus, co-

administration of cisplatin and 5-FU showed synergistic or additive effects *via* inhibiting of ERCC1 expression, indicating a clinical advantage of combining these two drugs for suppressing ERCC1 in cervical adenocarcinoma cells. From the point of view of ERCC1 suppression, such combination therapy with cisplatin and 5-FU might be a promising treatment regimen for cervical adenocarcinoma.

Cisplatin-based chemotherapy and radiotherapy are the common-used combined treatments for locally advanced cancer diseases, while radiotherapy alone is considered to be applied for patients with early disease (44). Almeida et al. (37) conducted a clinical and experimental study. Immunohistochemical analysis on the tissues of the patients showed that increased expressions of ERCC1 (5/10 patients; $P=0.0294$) were found in malignant tissues after radiotherapy. An elevated expression of ERCC1 was found in half of the patients after treatment with 1.8 Gy. *In-vitro* experiments suggested that absent or weak modulations of ERCC1 were detected after exposure to 1.8 Gy of radiotherapy in cervical cell lines. The authors also supposed that the mechanisms might be correlated with the inhibition of the regulatory axis p53-EGFR-ERCC1 in tumor cells exposed to radiation *in vivo* (37). This study showed that the upregulation of ERCC1 might be part of a radio-resistance mechanism in cervical cancer.

Other molecular mechanisms underlying ERCC1 expression and cervical cancer

ERCC1 is one of the DNA repair genes (45). Its enzyme involves the nucleotide excision repair pathway that recognizes and eliminates cisplatin-associated DNA adducts (13, 46). One proposed mechanism for ERCC1 in cancer development might be due to the aberrant expression of ERCC1 causing the dysfunction of DNA-repair capacity, leading to the accumulation of genetic damage, which might induce the emergence of an aggressive tumor phenotype (47). ERCC1 status represents both the cellular intrinsic DNA damage repair ability and the extent of accumulated intratumoral DNA damage, which may be associated with the progression of the cancers (48). Besides, abnormal ERCC1 expression resulted in genetic instability and thus affected the therapeutic response under cisplatin to radiotherapy. Human gliomas seem to be resistant to cisplatin because of hypermethylation of the promoter of the ERCC1 gene (49).

Affected genes and signaling pathways might contribute to the effects of ERCC1 in cervical cancer. The 3' side incision by ERCC4 requires ERCC1, which is located on chromosome 19. The ERCC1-ERCC4 complex was found to play roles in interstrand cross-link repair induced by the recombination repair mechanisms (22). ERCC1 is an endonuclease, serving as a heterodimer with xeroderma protein F (XPF). ERCC1/XPF complexes play roles in the incision that cleaves the damaged nucleotide strand at the 5'

end of the lesion (50). ERCC1 exerts effects on the response to a range of DNA-damaging chemotherapeutic agents. It was reported that ERCC1 might act together with class III β -tubulin (TUBB3), which was jointly involved in the development of locally advanced cervical squamous cell carcinoma (30).

The potential molecular mechanisms underlying the roles of ERCC1 in cervical cancer were shown in Figure 3.

Potential roles of targeting of ERCC1 in cervical cancer

As aforementioned, mounting clinical studies have confirmed the outstanding prognostic effects of ERCC1 in cervical cancer, thus the development of immunotherapy by targeting ERCC1 (i.e., ERCC1 inhibitor) may have important implications for modulating the antitumor immune responses in patients with advanced cervical cancer. There is a tight relationship between chemotherapy resistance and immunosuppression (51). In this review, ERCC1 expression was found to be correlated to chemotherapy-resistance (i.e., cisplatin and 5-FU) in cervical carcinoma, chemotherapy combined with ERCC1 inhibitor may dramatically reduce the immunosuppression and thus reinstate the immune function.

ERCC1 inhibitor may be not only applied for the combination with chemo/radiotherapy, but also the

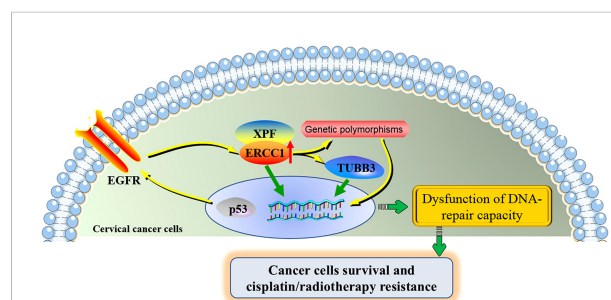


FIGURE 3

The potential molecular mechanisms underlying the roles of ERCC1 in cervical cancer. ERCC1 involves in the development and cisplatin/radiotherapy resistance in cervical cancer through the interaction with several specific genes and genetic polymorphisms. ERCC1 and XPF form a heterodimeric protein complex that cleaves the damaged nucleotide strand at the 5' end of the lesion. ERCC1 acts together with TUBB3, contributing to the poor prognosis of cervical cancer. The activation of the regulatory axis p53-EGFR-ERCC1 may be part of a radio-resistance mechanism in cervical cancer. ERCC1 genetic polymorphisms partially contribute to the progression of cervical cancer and the toxicities under cisplatin treatment. Aberrant expression of ERCC1 and its associated genes and affected signaling pathways were jointly involved in the dysfunction of DNA-repair capacity of cervical cancer cells, increasing the proliferation of cervical cancer cells and allowing the resistance of cisplatin/radiotherapy. ERCC1, excision repair cross-complementation group 1; XPF, xeroderma pigmentosum group F; TUBB3, class III β -tubulin; EGFR, epidermal growth factor receptor.

immunotherapy with check point inhibitors (i.e., anti-PD1 and anti-CTLA4). Combination of anti-PD-1 plus anti-CTLA-4 immunotherapy shows greater response rates than anti-PD-1 or anti-CTLA-4 antibody alone in multiple malignancies (52, 53). Due to a different anti-tumor mechanism of antitumor agents in a specific cancer type, a combination of drugs is recommended. For example, the combination of anti-PD-1 inhibitor and bevacizumab (an anti-vascular endothelial growth factor (VEGF) antibody, namely VEGF inhibitor) was found to have better outcomes in patients compared to sorafenib (54). Poly(ADP-ribose) polymerase inhibitor (PARPi) exerts therapeutic effect on various types of cancers. Trapping of PARP on the DNA by a small molecule PARPi generates DNA-PARP complexes. The capability of DNA repair is subsequently suppressed, resulting in replication fork collapse and catastrophic DNA double strand breaks which are selectively lethal to the cancer cell (55). It was reported that targeting PARP-1 with metronomic therapy might enhance anti-PD-1 immunotherapy in colon cancer (56). Similarly, since ERCC1 serving as a key DNA repair gene, ERCC1 inhibitor may be also applied for combining immunotherapy with check point inhibitors, which may help to enhance antitumor efficacy. Thus, ERCC1 inhibitor combined with either traditional regimens (i.e., chemotherapy or radiotherapy) or lately immunotherapies (i.e., anti-PD1, anti-CTLA4, or both) may obtain promising antitumor efficacy on cervical cancer.

Directions for future research

Cervical cancer is a public health problem of extensive clinical importance (57). Based on the above evidence from both clinical and experimental studies, ERCC1 is one of the essential and important factors in the progression of carcinoma of the uterine cervix and the therapeutic response of chemoradiotherapy. However, there are several points worth noting when interpreting the results. First, in this review, the relationship between ERCC1 expression and the status of cisplatin-based treatments in early and advanced cervical cancer has been extensively studied. However, the association between ERCC1 expression and chemosensitivity to other common chemotherapeutic medicines has not been fully investigated. Second, ERCC1 polymorphisms might also play roles in predicting the risk of cervical cancer and the toxicities that underwent cisplatin treatment, but whether these polymorphisms function in patients' survival has not been elucidated. Third, the exact and in-depth molecular mechanisms underlying the effects of ERCC1 expression and the development of cervical cancer are not clear due to limited studies and need to be further elucidated. Therefore, more clinical, *in-vitro*, and *in-vivo* investigations are still warranted for future studies. Fourth, the importance of the development of

immunotherapy trials by targeting ERCC1, i.e., ERCC1 inhibitor, should be addressed in the future.

Conclusion

The present review highlights the crucial roles of ERCC1 expression in cervical cancer. The majority of the included studies suggested that the ERCC1 served as a pro-oncogenic factor in both early-stage and advanced cervix cancer due to high expression of ERCC1 has been found to be associated with poor survival of the patients. ERCC1 polymorphism detection might be a useful tool for predicting the risk of cervical cancer and the toxicities that underwent cisplatin treatment. Experimental studies suggested that the biological effects exerted by ERCC1 in cervical cancer might be mediated by its associated genes and affected signaling pathways. To move toward clinical applications by targeting ERCC1 in cervical cancer, more investigations are still warranted in the future.

Author contributions

PD and GL contributed to the design of the study. LW and MH conducted the systematical search and extracted the clinical and experimental data. PD and GL wrote the manuscript. LW and MH supervised the manuscript. All authors contributed to the article and approved the submitted version.

Funding

This work was supported by the grants from the Science and Technology Planning Project of Guangzhou (No. 201904010401) and the Science and Technology Project of Panyu District, Guangzhou (No. 2020-Z04-006).

Conflict of interest

The authors declare that the research was conducted in the absence of any commercial or financial relationships that could be construed as a potential conflict of interest.

Publisher's note

All claims expressed in this article are solely those of the authors and do not necessarily represent those of their affiliated organizations, or those of the publisher, the editors and the reviewers. Any product that may be evaluated in this article, or claim that may be made by its manufacturer, is not guaranteed or endorsed by the publisher.

References

- Cohen PA, Jhingran A, Oaknin A, Denny L. Cervical cancer. *Lancet* (2019) 393:169–82. doi: 10.1016/S0140-6736(18)32470-X
- Bray F, Ferlay J, Soerjomataram I, Siegel RL, Torre LA, Jemal A. Global cancer statistics 2018: GLOBOCAN estimates of incidence and mortality worldwide for 36 cancers in 185 countries. *CA Cancer J Clin* (2018) 68:394–424. doi: 10.3322/caac.21492
- Ono S, Nozaki A, Matsuda K, Takakuwa E, Sakamoto N, Watari H. *In vivo* optical cellular diagnosis for uterine cervical or vaginal intraepithelial neoplasia using flexible gastrointestinal endoscopy - a prospective pilot study. *BMC Cancer* (2020) 20:955. doi: 10.1186/s12885-020-07460-6
- Wu X, Peng L, Zhang Y, Chen S, Lei Q, Li G, et al. Identification of key genes and pathways in cervical cancer by bioinformatics analysis. *Int J Med Sci* (2019) 16:800–12. doi: 10.7150/ijms.34172
- Yin L, Lu S, Zhu J, Zhang W, Ke G. Ovarian transposition before radiotherapy in cervical cancer patients: functional outcome and the adequate dose constraint. *Radiat Oncol* (2019) 14:100. doi: 10.1186/s13014-019-1312-2
- Lakhman Y, Akin O, Park KJ, Sarasohn DM, Zheng J, Goldman DA, et al. Stage IB1 cervical cancer: Role of preoperative MR imaging in selection of patients for fertility-sparing radical trachelectomy. *Radiology* (2013) 269:149–58. doi: 10.1148/radiol.13121746
- Ouyang Y, Wang Y, Chen K, Cao X, Zeng Y. Clinical outcome of extended-field irradiation vs. pelvic irradiation using intensity-modulated radiotherapy for cervical cancer. *Oncol Lett* (2017) 14:7069–76. doi: 10.3892/ol.2017.7077
- Lissoni AA, Colombo N, Pellegrino A, Parma G, Zola P, Katsaros D, et al. A phase II, randomized trial of neo-adjuvant chemotherapy comparing a three-drug combination of paclitaxel, ifosfamide, and cisplatin (TIP) versus paclitaxel and cisplatin (TP) followed by radical surgery in patients with locally advanced squamous cell cervical carcinoma: The snap-02 Italian collaborative study. *Ann Oncol* (2009) 20:660–5. doi: 10.1093/annonc/mdn690
- Sardi JE, Giaroli A, Sananes C, Ferreira M, Soderini A, Bermudez A, et al. Long-term follow-up of the first randomized trial using neoadjuvant chemotherapy in stage IB squamous carcinoma of the cervix: The final results. *Gynecol Oncol* (1997) 67:61–9. doi: 10.1006/gyno.1997.4812
- Sherer MV, Kotha NV, Williamson C, Mayadev J. Advances in immunotherapy for cervical cancer: Recent developments and future directions. *Int J Gynecol Cancer* (2022) 32:281–7. doi: 10.1136/ijgc-2021-002492
- Kato R, Hasegawa K, Torii Y, Udagawa Y, Fukasawa I. Factors affecting platinum sensitivity in cervical cancer. *Oncol Lett* (2015) 10:3591–8. doi: 10.3892/ol.2015.3755
- Karageorgopoulou S, Kostakis ID, Gazouli M, Markaki S, Papadimitriou M, Bournakis E, et al. Prognostic and predictive factors in patients with metastatic or recurrent cervical cancer treated with platinum-based chemotherapy. *BMC Cancer* (2017) 17:451. doi: 10.1186/s12885-017-3435-x
- Koutsoukos K, Andrikopoulou A, Dedes N, Zagouri F, Bamias A, Dimopoulos MA. Clinical perspectives of ERCC1 in bladder cancer. *Int J Mol Sci* (2020) 26(12):1839–44. doi: 10.3390/ijms21228829
- Hamilton G, Rath B. Pharmacogenetics of platinum-based chemotherapy in non-small cell lung cancer: Predictive validity of polymorphisms of ERCC1. *Expert Opin Drug Metab Toxicol* (2018) 14:17–24. doi: 10.1080/17425255.2018.1416095
- Hu H, Jing J, Lu X, Yuan Y, Xing C. XPF expression and its relationship with the risk and prognosis of colorectal cancer. *Cancer Cell Int* (2021) 21:12. doi: 10.1186/s12935-020-01710-0
- Zhang X, Yin M, Hu J. Nucleotide excision repair: A versatile and smart toolkit. *Acta Biochim Biophys Sin (Shanghai)* (2022) 54:807–19. doi: 10.3724/abbs.2022054
- Kraemer KH, Patronas NJ, Schiffmann R, Brooks BP, Tamura D, DiGiovanna JJ. Xeroderma pigmentosum, trichothiodystrophy and cockayne syndrome: A complex genotype-phenotype relationship. *Neuroscience* (2007) 145:1388–96. doi: 10.1016/j.neuroscience.2006.12.020
- Jiang G, Zou Y, Wu X. Replication-mediated disassociation of replication protein a-XPA complex upon DNA damage: Implications for RPA handing off. *Cell Biol Int* (2012) 36:713–20. doi: 10.1042/CBI20110633
- Lee TH, Park D, Kim YJ, Lee I, Kim S, Oh CT, et al. Lactobacillus salivarius BP121 prevents cisplatin-induced acute kidney injury by inhibition of uremic toxins such as indoxyl sulfate and p-cresol sulfate via alleviating dysbiosis. *Int J Mol Med* (2020) 45:1130–40. doi: 10.3892/ijmm.2020.4495
- Kassem AB, Salem SE, Abdelrahim ME, Said AS, Salahuddin A, Hussein MM, et al. ERCC1 and ERCC2 as predictive biomarkers to oxaliplatin-based chemotherapy in colorectal cancer patients from Egypt. *Exp Mol Pathol* (2017) 102:78–85. doi: 10.1016/j.yexmp.2017.01.006
- Torii Y, Kato R, Minami Y, Hasegawa K, Fujii T, Udagawa Y. ERCC1 expression and chemosensitivity in uterine cervical adenocarcinoma cells. *Anticancer Res* (2014) 34:107–15.
- Bajpai D, Banerjee A, Pathak S, Jain SK, Singh N. Decreased expression of DNA repair genes (XRCC1, ERCC1, ERCC2, and ERCC4) in squamous intraepithelial lesion and invasive squamous cell carcinoma of the cervix. *Mol Cell Biochem* (2013) 377:45–53. doi: 10.1007/s11010-013-1569-y
- Muallem MZ, Marnitz S, Richter R, Kohler C, Sehoul J, Arsenic R. ERCC1 expression as a predictive marker of cervical cancer treated with cisplatin-based chemoradiation. *Anticancer Res* (2014) 34:401–6.
- Doll CM, Prystajek M, Eliasziw M, Klimowicz AC, Petrillo SK, Craighead PS, et al. Low ERCC1 mRNA and protein expression are associated with worse survival in cervical cancer patients treated with radiation alone. *Radiother Oncol* (2010) 97:352–9. doi: 10.1016/j.radonc.2010.08.019
- Hasegawa K, Kato R, Torii Y, Ichikawa R, Oe S, Udagawa Y. The relationship between ERCC1 expression and clinical outcome in patients with FIGO stage I to stage II uterine cervical adenocarcinoma. *Int J Gynecol Cancer* (2011) 21:1479–85. doi: 10.1097/IGC.0b013e31822265e7
- Liang ZL, Song EK, Ko YB, Lee NR, Yhim HY, Noh HT, et al. Excision repair cross-complementation group 1 expression predicts response and survival in locally advanced cervical carcinoma patients treated with concurrent chemoradiotherapy. *Histopathology* (2011) 59:564–7. doi: 10.1111/j.1365-2559.2011.03943.x
- Park JS, Jeon EK, Chun SH, Won HS, Lee A, Hur SY, et al. ERCC1 (excision repair cross-complementation group 1) expression as a predictor for response of neoadjuvant chemotherapy for FIGO stage 2B uterine cervix cancer. *Gynecol Oncol* (2011) 120:275–9. doi: 10.1016/j.ygyno.2010.10.034
- Bai ZL, Wang YY, Zhe H, He JL, Hai P. ERCC1 mRNA levels can predict the response to cisplatin-based concurrent chemoradiotherapy of locally advanced cervical squamous cell carcinoma. *Radiat Oncol* (2012) 7:221. doi: 10.1186/1748-717X-7-221
- Doll CM, Aquino-Parsons C, Pintilie M, Klimowicz AC, Petrillo SK, Milosevic M, et al. The significance of tumoral ERCC1 status in patients with locally advanced cervical cancer treated with chemoradiation therapy: A multicenter clinicopathologic analysis. *Int J Radiat Oncol Biol Phys* (2013) 85:721–7. doi: 10.1016/j.ijrobp.2012.06.021
- Zwenger AO, Grosman G, Iturbe J, Leone J, Vallejo CT, Leone JP, et al. Expression of ERCC1 and TUBB3 in locally advanced cervical squamous cell cancer and its correlation with different therapeutic regimens. *Int J Biol Markers* (2015) 30:e301–14. doi: 10.5301/ijbm.5000161
- Ryu H, Song IC, Choi YS, Yun HJ, Jo DY, Kim JM, et al. ERCC1 expression status predicts the response and survival of patients with metastatic or recurrent cervical cancer treated via platinum-based chemotherapy. *Med (Baltimore)* (2017) 96:e9402. doi: 10.1097/MD.00000000000009402
- Jeong SY, Chung JY, Byeon SJ, Kim CJ, Lee YY, Kim TJ, et al. Validation of potential protein markers predicting chemoradioresistance in early cervical cancer by immunohistochemistry. *Front Oncol* (2021) 11:665595. doi: 10.3389/fonc.2021.665595
- Han SS, Kim JW, Lee SH, Kim DH, Park NH, Song YS, et al. ERCC1 C19007T polymorphism and the risk and invasiveness of cervical cancer in Korean women. *Asia Pac J Clin Oncol* (2012) 8:e63–7. doi: 10.1111/j.1743-7563.2011.01495.x
- Zhang L, Ruan Z, Hong Q, Gong X, Hu Z, Huang Y, et al. Single nucleotide polymorphisms in DNA repair genes and risk of cervical cancer: A case-control study. *Oncol Lett* (2012) 3:351–62. doi: 10.3892/ol.2011.463
- Soares S, Nogueira A, Coelho A, Assis J, Pereira D, Bravo I, et al. Relationship between clinical toxicities and ERCC1 rs3212986 and XRCC3 rs861539 polymorphisms in cervical cancer patients. *Int J Biol Markers* (2018) 33:116–23. doi: 10.5301/ijbm.5000279
- Britten RA, Liu D, Tessier A, Hutchison MJ, Murray D. ERCC1 expression as a molecular marker of cisplatin resistance in human cervical tumor cells. *Int J Cancer* (2000) 89:453–7. doi: 10.1002/1097-0215(20000920)89:5<453::AID-IJC9>3.0.CO;2-E
- de Almeida VH, de Melo AC, Meira DD, Pires AC, Nogueira-Rodrigues A, Pimenta-Inada HK, et al. Radiotherapy modulates expression of EGFR, ERCC1 and p53 in cervical cancer. *Braz J Med Biol Res* (2017) 51:e6822. doi: 10.1590/1414-431X20176822
- Bamias A, Koutsoukos K, Gavalas N, Zakopoulou R, Tzannis K, Dedes N, et al. ERCC1 19007 polymorphism in Greek patients with advanced urothelial cancer treated with platinum-based chemotherapy: Effect of the changing treatment paradigm: A cohort study by the Hellenic GU cancer group. *Curr Oncol* (2021) 28:4474–84. doi: 10.3390/curroncol28060380

39. Mertz TM, Collins CD, Dennis M, Coxon M, Roberts SA. APOBEC-induced mutagenesis in cancer. *Annu Rev Genet* (2022) 30(56):229–52. doi: 10.1146/annurev-genet-072920-035840
40. Adolf IC, Almars A, Dharsee N, Mselle T, Akan G, Nguma IJ, et al. HLA-G and single nucleotide polymorphism (SNP) associations with cancer in African populations: Implications in personal medicine. *Genes Dis* (2022) 9:1220–33. doi: 10.1016/j.gendis.2021.06.004
41. Marnitz S, Martus P, Kohler C, Stromberger C, Asse E, Mallmann P, et al. Role of surgical versus clinical staging in chemoradiated FIGO stage IIB-IVA cervical cancer patients-acute toxicity and treatment quality of the uterus-11 multicenter phase III intergroup trial of the German radiation oncology group and the gynecologic cancer group. *Int J Radiat Oncol Biol Phys* (2016) 94:243–53. doi: 10.1016/j.ijrobp.2015.10.027
42. Bacorro W, Baldivia K, Yu KK, Mariano J, Gonzalez G, Sy OT. Outcomes with definitive radiotherapy among patients with locally advanced cervical cancer with relative or absolute contraindications to cisplatin: A systematic review and meta-analysis. *Gynecol Oncol* (2022) 166:614–30. doi: 10.1016/j.ygyno.2022.06.018
43. Gennigens C, Jerusalem G, Lapaille L, De Cuypere M, Streel S, Kridelka F, et al. Recurrent or primary metastatic cervical cancer: current and future treatments. *ESMO Open* (2022) 7:100579. doi: 10.1016/j.esmoop.2022.100579
44. Miriyala R, Mahantshetty U, Maheshwari A, Gupta S. Neoadjuvant chemotherapy followed by surgery in cervical cancer: Past, present and future. *Int J Gynecol Cancer* (2022) 32:260–5. doi: 10.1136/ijgc-2021-002531
45. Faridounnia M, Folkers GE, Boelens R. Function and interactions of ERCC1-XPF in DNA damage response. *Molecules* (2018) 5(23):3205. doi: 10.3390/molecules23123205
46. Sancar A. Mechanisms of DNA excision repair. *Science* (1994) 266:1954–6. doi: 10.1126/science.7801120
47. Simon GR, Sharma S, Cantor A, Smith P, Bepler G. ERCC1 expression is a predictor of survival in resected patients with non-small cell lung cancer. *CHEST* (2005) 127:978–83. doi: 10.1378/chest.127.3.978
48. Simon GR, Ismail-Khan R, Bepler G. Nuclear excision repair-based personalized therapy for non-small cell lung cancer: From hypothesis to reality. *Int J Biochem Cell Biol* (2007) 39:1318–28. doi: 10.1016/j.biocel.2007.05.006
49. Chen HY, Shao CJ, Chen FR, Kwan AL, Chen ZP. Role of ERCC1 promoter hypermethylation in drug resistance to cisplatin in human gliomas. *Int J Cancer* (2010) 126:1944–54. doi: 10.1002/ijc.24772
50. de Laat WL, Appeldoorn E, Jaspers NG, Hoeijmakers JH. DNA Structural elements required for ERCC1-XPF endonuclease activity. *J Biol Chem* (1998) 273:7835–42. doi: 10.1074/jbc.273.14.7835
51. Zhu M, Zhang P, Yu S, Tang C, Wang Y, Shen Z, et al. Targeting ZFP64/GAL-1 axis promotes therapeutic effect of nab-paclitaxel and reverses immunosuppressive microenvironment in gastric cancer. *J Exp Clin Cancer Res* (2022) 41(1):14. doi: 10.1186/s13046-021-02224-x
52. Olson DJ, Eroglu Z, Brockstein B, Poklepovic AS, Bajaj M, Babu S, et al. Pembrolizumab plus ipilimumab following anti-PD-1/L1 failure in melanoma. *J Clin Oncol* (2021) 39(24):2647–55. doi: 10.1200/JCO.21.00079
53. van Dijk N, Gil-Jimenez A, Silina K, Hendricksen K, Smit LA, de Feijter JM, et al. Preoperative ipilimumab plus nivolumab in locoregionally advanced urothelial cancer: the NABUCCO trial. *Nat Med* (2020) 26(12):1839–44. doi: 10.1038/s41591-020-1085-z
54. Marzi L, Mega A, Gitto S, Pelizzaro F, Seeber A, Spizzo G. Impact and novel perspective of immune checkpoint inhibitors in patients with early and intermediate stage HCC. *Cancers (Basel)* (2022) 14(14):3332. doi: 10.3390/cancers14143332
55. Fennell DA, Porter C, Lester J, Danson S, Blackhall F, Nicolson M, et al. Olaparib maintenance versus placebo monotherapy in patients with advanced non small cell lung cancer (PIN): A multicentre, randomised, controlled, phase 2 trial. *EClinicalMed* (2022) 52:101595. doi: 10.1016/j.eclinm.2022.101595
56. Ghonim MA, Ibba SV, Tarhuni AF, Errami Y, Luu HH, Dean MJ, et al. Targeting PARP-1 with metronomic therapy modulates MDSC suppressive function and enhances anti-PD-1 immunotherapy in colon cancer. *J Immunother Cancer* (2021) 9(1):e001643. doi: 10.1136/jitc-2020-001643
57. Chakrabarti M, Nordin A, Khodabocus J. Debulking hysterectomy followed by chemoradiotherapy versus chemoradiotherapy for FIGO stage, (2019) IB3/II cervical cancer. *Cochrane Database Syst Rev* (2022) 9:CD012246. doi: 10.1002/14651858.CD012246.pub2



OPEN ACCESS

EDITED BY
Gaurisankar Sa,
Bose Institute, India

REVIEWED BY
Chih-Lung Wu,
National Tsing Hua University, Taiwan
Caterina Mancarella,
Istituto Ortopedico Rizzoli (IRCCS), Italy

*CORRESPONDENCE
Tao Xie
✉ xietao899@163.com
Xiaobiao Zhang
✉ xiaobiao_zhang@163.com

[†]These authors have contributed equally to this work

SPECIALTY SECTION
This article was submitted to
Cancer Immunity
and Immunotherapy,
a section of the journal
Frontiers in Immunology

RECEIVED 16 October 2022
ACCEPTED 11 January 2023
PUBLISHED 25 January 2023

CITATION
Chen P, Xu J, Cui Z, Wu S, Xie T and
Zhang X (2023) Multi-omics analysis of N6-
methyladenosine reader IGF2BP3 as a
promising biomarker in pan-cancer.
Front. Immunol. 14:1071675.
doi: 10.3389/fimmu.2023.1071675

COPYRIGHT
© 2023 Chen, Xu, Cui, Wu, Xie and Zhang.
This is an open-access article distributed
under the terms of the [Creative Commons
Attribution License \(CC BY\)](#). The use,
distribution or reproduction in other
forums is permitted, provided the original
author(s) and the copyright owner(s) are
credited and that the original publication in
this journal is cited, in accordance with
accepted academic practice. No use,
distribution or reproduction is permitted
which does not comply with these terms.

Multi-omics analysis of N6-methyladenosine reader IGF2BP3 as a promising biomarker in pan-cancer

Pin Chen^{1†}, Jing Xu^{2†}, Zihan Cui^{3,4†}, Silin Wu¹, Tao Xie^{1,5*}
and Xiaobiao Zhang^{1,5,6*}

¹Department of Neurosurgery, Zhongshan Hospital, Fudan University, Shanghai, China,

²Department of Endocrinology and Metabolism, Zhongshan Hospital, Fudan University, Shanghai, China,

³Department of Thoracic Surgery, The First Affiliated Hospital of Soochow University, Medical College of Soochow University, Suzhou, China, ⁴Institute of Thoracic Surgery, The First Affiliated Hospital of Soochow University, Suzhou, China, ⁵Cancer Center, Shanghai Zhongshan Hospital, Fudan University, Shanghai, China, ⁶Digital Medical Research Center, Fudan University, Shanghai, China

Background: Insulin-like growth factor 2 mRNA-binding protein 3 (IGF2BP3) has been reported to exhibit an oncogenic effect as an RNA-binding protein (RBP) by promoting tumor cell proliferation, migration and invasion in several tumor types. However, a pan-cancer analysis of IGF2BP3 is not currently available, and the exact roles of IGF2BP3 in prognosis and immunology in cancer patients remain enigmatic. The main aim of this study was to provide visualization of the systemic prognostic landscape of IGF2BP3 in pan-cancer and to uncover the potential relationship between IGF2BP3 expression in the tumor microenvironment and immune infiltration profile.

Methods: Raw data on IGF2BP3 expression were obtained from GTEx, CCLE, TCGA, and HPA data portals. We have investigated the expression patterns, diagnostic and prognostic significance, mutation landscapes, functional analysis, and functional states of IGF2BP3 utilizing multiple databases, including HPA, TISIDB, cBioPortal, GeneMANIA, GESA, and CancerSEA. Moreover, the relationship of IGF2BP3 expression with immune infiltrates, TMB, MSI and immune-related genes was evaluated in pan-cancer. IGF2BP3 with drug sensitivity analysis was performed from the CellMiner database. Furthermore, the expression of IGF2BP3 in different grades of glioma was detected by immunohistochemical staining and western blot.

Results: We found that IGF2BP3 was ubiquitously highly expressed in pan-cancer and significantly correlated with diagnosis, prognosis, TMB, MSI, and drug sensitivity in various types of cancer. Besides, IGF2BP3 was involved in many cancer pathways and varied in different immune and molecular subtypes of cancers. Additionally, IGF2BP3 is critically associated with genetic markers of immunomodulators in various cancers. Finally, we validated that IGF2BP3 protein expression was significantly higher in glioma than in normal tissue, especially in GBM.

Conclusions: IGF2BP3 may be a potential molecular biomarker for diagnosis and prognosis in pan-cancer, especially for glioma. It could become a novel therapeutic target for various cancers.

KEYWORDS

insulin-like growth factor 2 mRNA-binding protein 3 (IGF2BP3), pan-cancer analysis, genetic alteration, prognosis, the Cancer Genome Atlas (TCGA), immune infiltration

Introduction

The N⁶ adenosine methylation (m6A) is methylated at the N6 site of adenosine and thought to be a dynamic modification of mRNA in mammalian cells (1–3). Distinct from DNA methylation and histone modification is playing a role at the transcriptional level, the m6A modification functions at a post-transcriptional level. Specifically, the m6A modifications achieve the control of the target gene expression through the coordination of 3 classes of regulators, including m6A methyltransferases ('writers'), m6A modified binding proteins ('readers'), and m6A demethylase ('erasers') (4). In mammals, the m6A 'writer' complex mainly contains methyltransferase-like protein 3 (METTL3), methyltransferase-like 14 (METTL14), Wilms-tumour associated protein (WTAP), which catalyzes the m6A modification of adenosine on RNA. Conversely, the m6A erasers mainly consists of fat mass, obesity-associated protein (FTO) and AlkB homolog 5 (ALKBH5) demethylases, which are responsible for removing the m6A marks selectively. Therefore, the m6A modification process is highly dynamic and reversible. The m6A 'readers' proteins (such as YTH, IGF2BP, and HNRNP families) are preferentially bind to the m6A-modified mRNA (also called the RNA Binding Proteins, RBPs) and regulate RNA metabolism by serving as readers. Among various readers, the Insulin-like growth factor 2 mRNA-binding proteins (IGF2BPs) including IGF2BP1/2/3 was first identified in 2018. As an essential m6A reader, the stability of target mRNA can be enhanced by modification of m6A (5, 6).

IGF2BP3, a member belonging to the conserved IGF2BP family is highly expressed during both embryogenesis and carcinogenesis and lowly expressed in tissues of healthy adults (7, 8). IGF2BP3 has demonstrated to the malignant transformation of tumor. It includes proliferation, invasion, migration, and drug resistance (9–15). Besides its role as a newly reported m6A reader, IGF2BP3 has also been well-proven to function in cancer metabolism, immunity, angiogenesis, stemness, and differentiation (16–21). Specifically, previous evidence has indicated that IGF2BP3 plays a crucial role in human cancer development, such as breast cancer (10, 22), mesothelioma (11), colon cancer (15, 19), lung cancer (18), melanoma (13), nasopharyngeal carcinoma (NPC) (14), and hepatocellular carcinoma (HCC) (20). Nevertheless, there is still a lack of comprehensive and systematic studies assessing the impact of IGF2BP3 on multiple cancer types.

Recently, pan-cancer analysis of tumorigenesis and progression has become a research focus. Therefore, it is of importance to further investigate the oncogene profile using a pan-cancer strategy. However, there are still no relevant articles on IGF2BP3 and pan-cancer. Here, we performed comprehensive research on the roles of

IGF2BP3 in human pan-cancer. Our findings showed that IGF2BP3 expression was significantly higher in most tumors than in adjacent paired normal tissues. Besides, both the diagnostic utility and predictive value of IGF2BP3 in the pan-cancer TCGA cohorts were evaluated. IGF2BP3 genetic alternations were identified using the cBioPortal database. Additionally, we investigated the potential relationship between IGF2BP3 mRNA expression level and clinicopathologic characteristics, tumor mutation burden (TMB), microsatellite instability (MSI), and infiltrating immune cells in pan-cancer. Drug sensitivity analysis of IGF2BP3 was also performed *via* the CellMiner database.

We concluded that IGF2BP3 could serve as a candidate prognostic factor across diverse tumor types. IGF2BP3 exerted its function *via* the regulation of TMB, MSI, tumor immune microenvironment (TME), and drug sensitivity. This study highlights the manifold roles of IGF2BP3 in pan-cancer, which is promising as a prospective biomarker and potential target for cancer therapy.

Materials and methods

Data collection and software availability

IGF2BP3 gene expression data and clinical profiles of tumors and their corresponding normal samples were acquired from The Cancer Genome Atlas (TCGA) database (<https://portal.gdc.cancer.gov/>) and gene type-tissue expression (GTEx) using UCSC Xena (<https://xena.ucsc.edu/>) (23). Multidimensional analysis of IGF2BP3 expression in different cancer cell lines using the Cancer Cell Line Encyclopedia (CCLE) database (<https://portals.broadinstitute.org/>) (24). The expression level of IGF2BP3 across human cancer tissues and normal tissues (such as liver, lung, and stomach), as well as the corresponding 24 tumor cell lines (such as liver, thyroid, and lung) was systematically analyzed. The RNA-seq data in TPM format were converted into log2 format for expression comparison between samples (ns, $p \geq 0.05$; * $p < 0.05$; ** $p < 0.01$; *** $p < 0.001$; **** $p < 0.0001$).

Protein level analysis

The Human Protein Atlas (HPA) (<http://www.proteinatlas.org/>) is a milestone protein research database that contains protein expression in both tumor and normal tissues and is used to probe

the protein levels of IGF2BP3. IHC Images of IGF2BP3 protein expression in normal and tumor tissues were downloaded from HPA, including brain, lung, pancreas, colon, cervix, nasopharynx and ovary. The antibody for IHC used was HPA076951.

IGF2BP3 expression in immune and molecular subtypes of cancers

The correlations between IGF2BP3 expression and immune or molecular subtypes were explored through the TISIDB database (25), an integrated database with a diversity of data types to evaluate tumor-immune system interactions. The association between IGF2BP3 expression and immunomodulators in pan-cancer was also explored based on the TISIDB database.

Specimen collection

Twenty-two glioma samples were provided by the Department of Neurosurgery, Zhongshan Hospital of Fudan University (Shanghai, China). The three normal tissues surrounding the tumor were normal brain tissues obtained by cortical resection during resection of deep brain glioma. All patients did not receive preoperative chemotherapy or radiotherapy. Tissue samples were extracted and immediately frozen in liquid nitrogen or formalin-fixed. All human samples were used only for research purposes. This study was approved by the Ethics Committee of Zhongshan Hospital, Fudan University.

Diagnostic value analysis

The subject operating characteristic (ROC) curve was established to assess the diagnostic performance of IGF2BP3 in pan-cancer. The area under the curve was taken to be in the range of 0.5 to 1, with higher values indicating a better diagnostic effect. An AUC value of 0.5–0.7 suggests poor diagnostic efficacy, 0.7–0.9 represents moderate accuracy, and above 0.9 indicates high diagnostic accuracy.

Survival prognosis analysis

Kaplan–Meier (KM) curve analysis were applied to estimate the association between IGF2BP3 expression and inter-tumor prognosis (OS, DSS, PFI). Next, we explored the relationship between IGF2BP3 expression and prognostic values (OS, DSS and PFI) in different clinical GBMLGG subgroups. The survival package was used for statistical analysis, and the “survminer” package for data visualization.

Association of IGF2BP3 expression with different clinical features of glioma

The IGF2BP3 gene expression levels in glioma patients with different clinicopathological features are shown by box plots and tables. Gene expression (RNAseq) and corresponding clinical information were extracted from the TCGA database, transformed into transcripts per

million reads (TPM) format, and analyzed by log2-transformation. The Wilcoxon rank sum test was applied to compute the data of two groups, and $p < 0.05$ was considered to a statistically significant difference (ns, $p \geq 0.05$; * $p < 0.05$; ** $p < 0.01$; *** $p < 0.001$).

Univariate and multivariate Cox regression analyses in glioma

Survival information of overall survival (OS), disease-specific survival (DSS), and progression-free interval (PFI) was downloaded from TCGA database to display the relationship between IGF2BP3 expression and patient outcomes. The median expression of IGF2BP3 within each tumor type was used as a cut-off value to distinguish low- and high-expression subgroups. The univariate survival analysis was performed to analyze the hazard ratio (HR) and 95% confidence intervals (95% C.I.). A hazard ratio (HR) < 1 suggests that IGF2BP3 is a beneficial prognostic factor, while $HR > 1$ indicates that IGF2BP3 is a risk factor for survival. Univariate and multifactorial Cox regression analyses of IGF2BP3 and clinical features were undertaken to ascertain their prognostic value in OS, DSS and PFI in GBMLGG. A survival kit was utilized for survival analysis.

Genetic alteration analysis

The cBioCancer for Cancer Genomics (cBioPortal) (www.cbioportal.org) was utilized to investigate genomic alteration analysis of specific genes (26, 27). In this study, we applied the “Cancer Types Summary” and below “Cancer Type” button for visualizing genomic alterations of IGF2BP3 among cancers from TCGA database. The frequency of IGF2BP3 copy number alterations and mutations in all TCGA tumors was examined, and the results are shown as plotted bar plots.

Tumor mutation burden, microsatellite instability

Tumor mutational burden (TMB) and microsatellite instability (MSI) have been characterized as the key biological markers of TME (28–31). Spearman’s correlation coefficient was employed to analyze the relationship between IGF2BP3 expression and TMB and MSI.

Tumor microenvironment

Estimation of stromal and immune cell components in malignant tumor tissues by differences in expression data (ESTIMATE) is a method for calculating stromal or immune scores, represented by the abundance of the immune and stromal components, respectively (32). The higher the score, the greater the proportion of the corresponding component in the TME. The ESTIMATE score is the sum of the stroma score and the immune score, suggesting the combined proportion of both in the TME. IGF2BP3 expression levels and ImmuneScore and StromalScore were acquired for each tumor by “estimate” R package and Spearman correlation analysis. Immune cell

infiltration correlation analysis was performed *via* the TIMER2 database (<http://timer.cistrome.org>) (33).

Single-cell functional analysis

The functional status of IGF2BP3 in various cancers was studied using CancerSEA (<http://biocc.hrbmu.edu.cn/CancerSEA/>) (34), a database that can be used to assess the integrated functional status of diverse tumor cells at the single-cell level. In this study, we explored the average correlation of IGF2BP3 with functional status in 18 cancers, including angiogenesis, proliferation, apoptosis, cell cycle, DNA damage, DNA repair, inflammation, hypoxia, epithelial-mesenchymal transition (EMT), invasion, metastasis, differentiation, quiescence, and stemness. The threshold of IGF2BP3 associated with each tumor functional status was established as a threshold value of $|r| > 0.3$ and a discrimination significance ($p < 0.05$).

Protein–protein interaction network and enrichment analysis

GeneMANIA (<http://www.genemania.org>) is an interactive and flexible online tool for building and visualizing protein-protein interaction (PPI) networks using bioinformatics methods such as physical interaction, co-expression, co-localization, gene enrichment analysis, gene interaction and site prediction, including generating reasonable hypotheses about gene function prediction and detecting Genes that share similar functions (35, 36). In this study, GeneMANIA was employed for PPI analysis of IGF2BP3. Gene set enrichment analysis (GSEA) was used to detect the IGF2BP3 affected pathway in tumors. The entire biological process is assessed on the basis of the Kyoto Encyclopedia of Genes and Genomes (KEGG) and HALLMARK pathways.

Drug sensitivity of IGF2BP3 in pan-cancer

NCI-60 compound activity data and RNA-seq expression profiles from the CellMiner™ were downloaded to analyze the drug sensitivity of IGF2BP3 in pan-cancer (<https://discover.nci.nih.gov/cellminer/home.do>) (37). Drugs approved by FDA or clinical trials were selected for analysis.

Immunohistochemistry

Tissues were formalin-fixed and paraffin-embedded and sectioned to 4 mm layer thickness regularly. Tissue sections were processed and stained with the following antibodies: IGF2BP3 (1:300, 14642-1-AP, Proteintech).

Western blot analysis

Total protein was isolated from tissues and quantified with the BCA protein quantification kit (Beyotime, #P001). Equal amounts of

proteins separated by 10% SDS-PAGE, transferred to polyvinylidene fluoride membranes (0.45 μ M PVDF, Millipore, USA), then the membranes were blocked with skimmed milk for 1 hour and incubated with primary antibody IGF2BP3 (1:1000, 14642-1-AP, Proteintech) overnight at 4°C. The corresponding HRP-conjugated secondary antibody (#A0208, 1:2000, Beyotime Biotechnology, Shanghai, China) used, and the bands visualized by ECL Western blotting substrate (Thermo Fisher Scientific, USA). The intensity of protein expression was detected *via* ImageJ software.

Results

Expression and mutant aspects of IGF2BP3 in pan-cancer

The study flowchart is illustrated in **Supplementary Figure 1**. First, we assessed IGF2BP3 mRNA levels in normal human tissues, using the GTEx dataset. As shown in **Figure 1A**, the IGF2BP3 level varied across multiple types of tissue was remarkably high in bone marrow (BM). BM is known to be a highly differentiating tissue, and higher expression levels are not entirely unexpected. In addition, we examined the expression levels of IGF2BP3 across various tumor types. In different cancer cell lines from the CCLE database, not only were IGF2BP3 expression levels significantly and generally elevated but smaller ranges were shown compared to the range of expression in normal human tissues (**Figure 1B**).

Further comparison between the tumors and adjacent normal tissues displayed that the expression level of IGF2BP3 was upregulated in most types of human cancers. Directly, considering TCGA data alone, the gene expression difference achieved considerable significance in 20 of 26 TCGA cancer types, with the exception of glioma (GBMLGG), brain lower grade glioma (LGG), prostate adenocarcinoma (PRAD), rectum adenocarcinoma (READ), pancreatic adenocarcinoma (PAAD) and pheochromocytoma and paraganglioma (PCPG). Moreover, only in thyroid carcinoma (THCA) IGF2BP3 had an increased expression in corresponding normal tissues instead of tumor samples, which was the opposite of the condition in other cancer types (**Figure 1C**).

To further compare IGF2BP3 expression between the tumor and normal tissues, we combined data from TCGA and GTEx. Results from combined databases revealed that IGF2BP3 was over-expressed significantly in 31 out of 34 cancer types (exceptions were READ, TGCT, and PCPG). Mainly, IGF2BP3 was highly expressed in diverse tumor types, such as GBMLGG, glioblastoma multiforme (GBM), LGG, lung adenocarcinoma (LUAD), lung squamous cell carcinoma (LUSC), PAAD, head and neck squamous cell carcinoma (HNSC), uterine corpus endometrial carcinoma (UCEC), colon adenocarcinoma (COAD), and esophageal carcinoma (ESCA). However, reversed results with significance were observed in PRAD and THCA (**Figure 1D**).

Next, we verified the expression of IGF2BP3 between cancer tissues and adjacent normal tissues at protein level using the HPA database. Compared to weak IHC positive staining in normal brain, lung, pancreas, colon, cervix, nasopharynx, and ovary tissues, much stronger staining of IGF2BP3 was examined in GBMLGG, LUAD, LUSC, PAAD, COAD, cervical squamous cell carcinoma and

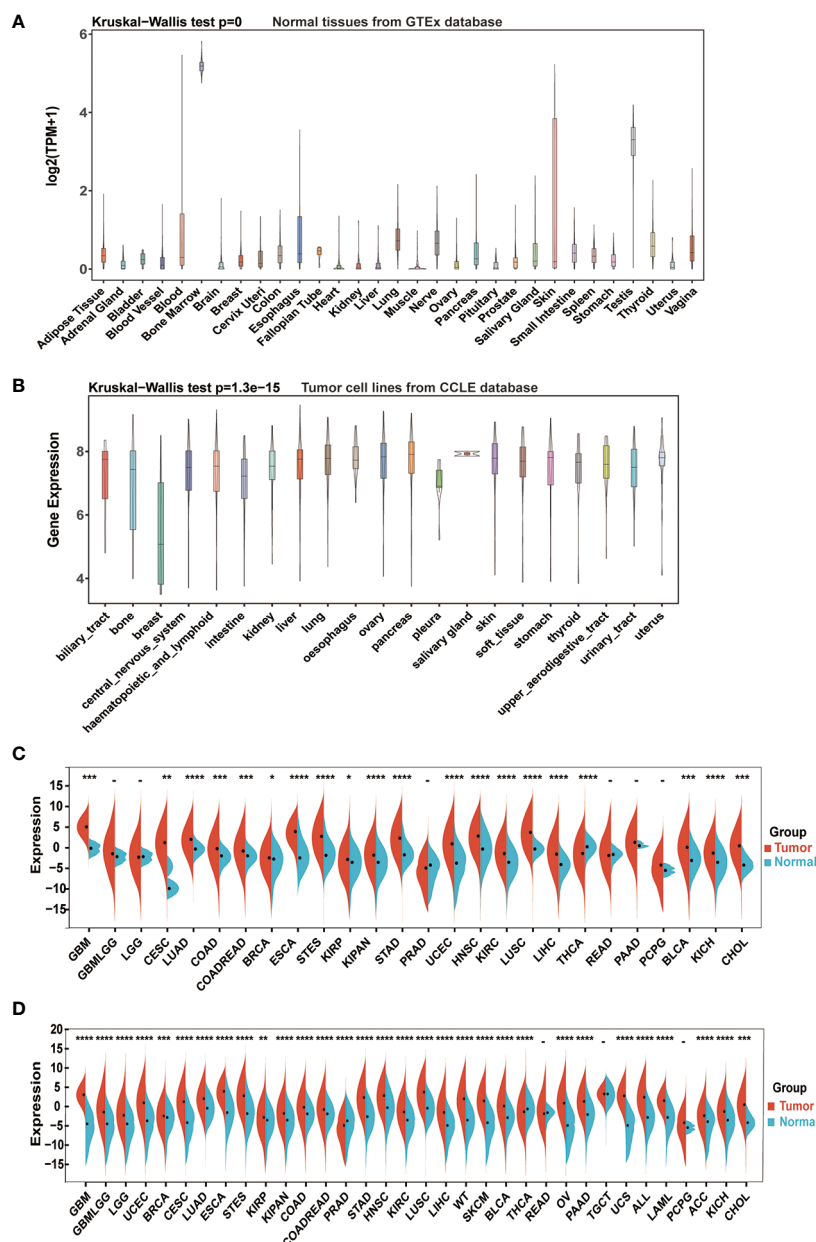


FIGURE 1

IGF2BP3 mRNA expression levels in pan-cancer. (A) IGF2BP3 expression levels in normal tissues from GTEx database. (B) IGF2BP3 expression levels in tumor cell lines from CCLE database. (C) IGF2BP3 expression levels in tumor tissues from TCGA database. (D) IGF2BP3 expression difference between tumor tissues from TCGA database and normal tissues from the GTEx database; ns, no significance; * $p < 0.05$, ** $p < 0.01$, *** $p < 0.001$, and **** $p < 0.0001$.

endocervical adenocarcinoma (CESC), HNSC, and ovarian serous cystadenocarcinoma (OV) tissues in terms of protein level (Figures 2A–H). The results from the two databases (TCGA and HPA) were broadly consistent.

Further, we assessed the associations between IGF2BP3 and different clinical characteristics in pan-cancer. For GBMLGG, IGF2BP3 expression was significantly correlated with World Health Organization (WHO) grade, histological type, IDH status, 1p/19q codeletion, primary therapy outcome, and age of GBMLGG (Supplementary Table 1). Specifically, the expression level of IGF2BP3 increased significantly with increasing WHO grade gliomas (Figure 3A). Moreover, IGF2BP3 showed higher levels in patients with GBM in comparison with other histological types of glioma (Figure 3B).

Next, we subdivided the TCGA patients according to different IDH mutations and 1p/19q codeletion status and found that high IGF2BP3 expression positively correlated with IDH status (wildtype), and 1p/19q non-codeletion (Figures 3C, D). Additionally, IGF2BP3 was expressed higher in patients with age >60 (Figure 3E), and primary therapy outcome (PD) (Figure 3F), respectively.

Mutation analysis of IGF2BP3

It is well recognized that DNA methylation and genetic alterations are tightly linked to the occurrence and development of tumors. Herein, we initially analyzed the IGF2BP3 alteration status across

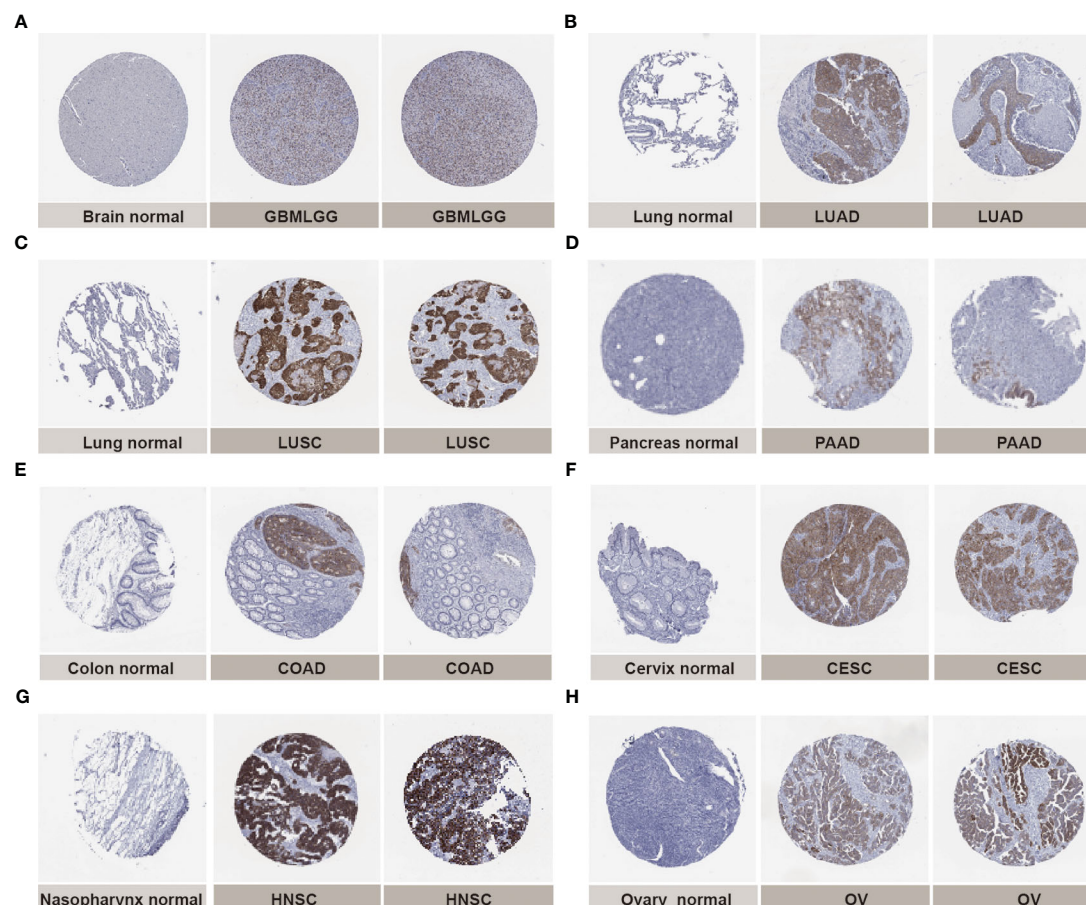


FIGURE 2

Representative immunohistochemical staining (IHC) in multiple normal (left) and tumor (right) tissues. The protein expression of IGF2BP3 in (A) glioma, GBMLGG; (B) lung adenocarcinoma, LUAD; (C) lung squamous cell carcinoma, LUSC; (D) pancreatic adenocarcinoma, PAAD; (E) colon adenocarcinoma, COAD; (F) cervical squamous cell carcinoma and endocervical adenocarcinoma, CESC; (G) head and neck squamous cell carcinoma, HNSC; (H) ovarian serous cystadenocarcinoma, OV.

multiple cancer types using cBioPortal database ([Supplementary Figure 2](#)). Among all cancers tested, the IGF2BP3 gene was amplified in multiple types of cancer, with the highest alteration frequency (>6%) in uterine carcinosarcoma (UCS). Notably, the type of mutation was the primary type in the UCEC, skin cutaneous melanoma (SKCM), stomach adenocarcinoma (STAD), and COAD, which show an alteration frequency of ~4% ([Supplementary Figure 2A](#)). The types, sites and case numbers of the IGF2BP3 gene mutation were further displayed above the bars ([Supplementary Figure 2C](#)). Overall, as shown in [Supplementary Figure 2B](#), amplification was the main type of alteration, while the most frequent putative copy-number alterations of IGF2BP3 were amplification, gain function, and diploid. Finally, in the present study, the gene alteration of DNAH11, GPNMB, TP53, KLHL7, NUP42, MALSU1, ABCB5, STK31, TRA2A, and HDAC9 was more common in the altered group than in the unaltered group across the cBioPortal database ([Supplementary Figure 2D](#)). As dysregulated IGF2BP3 was implicated in the process of RNA regulation and transcription in cancer, we further investigated whether IGF2BP3

was associated with the mutation of cancer-related genes. Here, we took LGG as an example to illustrate the correlation between the IGF2BP3 expression level and mutation frequencies. As shown in [Supplementary Figure 2E](#), in LGG, the top five frequently mutated genes remained as IDH1 (82.6%), CIC (20.6%), TTN (12.8%), MUC16 (7.4%), and EGFR (7.2%). Moreover, the previously mentioned mutated genes with significance defined by $FDR < 0.05$. These results indicate that the IGF2BP3 is tightly correlated with cancer-related gene mutation status.

Diagnostic value of IGF2BP3 in pan-cancer

As shown in [Figures 4A–H](#), IGF2BP3 has an exact accuracy ($AUC > 0.7$) in predicting 24 cancer types, and even exceeded 0.9 in 8 cancers including LAML ($AUC = 1.0$), GBM ($AUC = 0.998$), UCS ($AUC = 0.983$), LUSC ($AUC = 0.939$), STAD ($AUC = 0.936$), OV ($AUC = 0.927$), CHOL ($AUC = 0.926$), and ESCA ($AUC = 0.920$) ([Supplemental Table 2](#)), which had high diagnostic value.

Cancer: GBMLGG

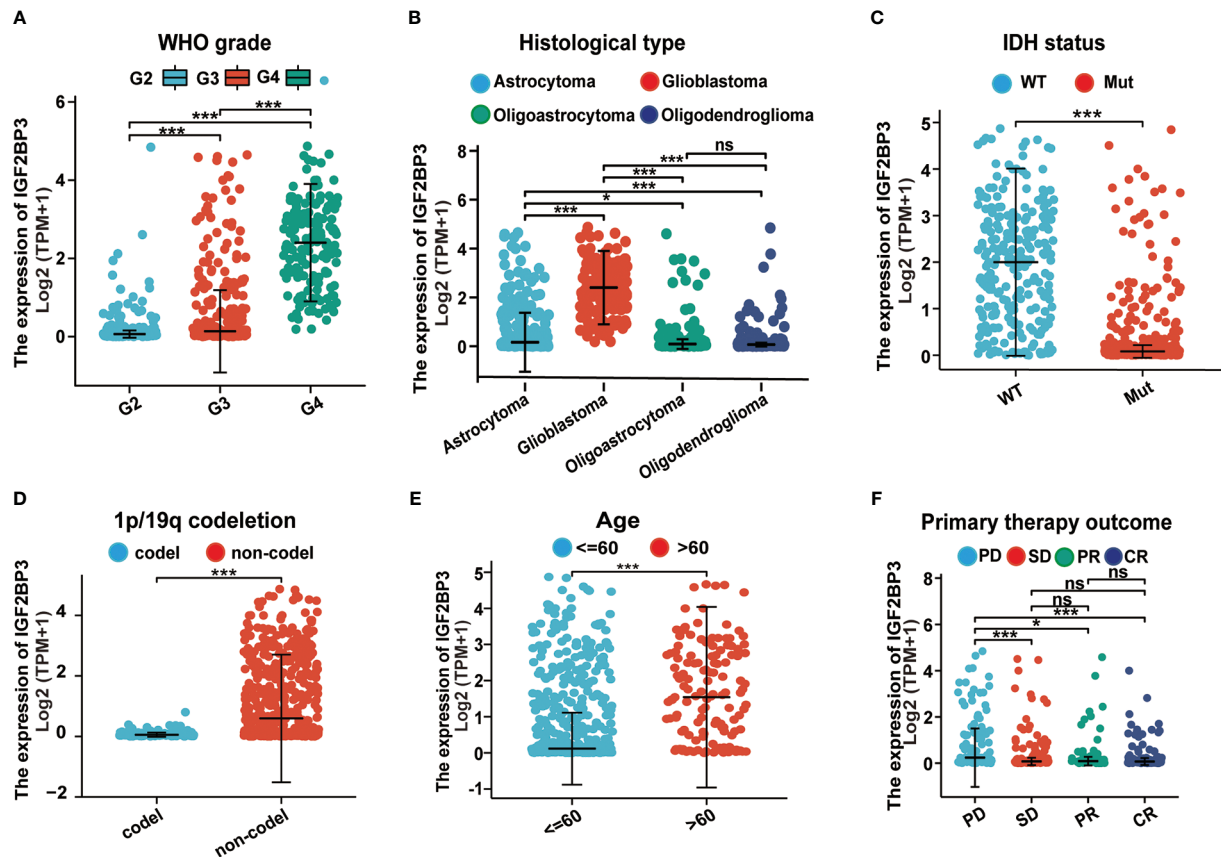


FIGURE 3

Associations between IGF2BP3 expression and different clinical characteristics in GBMLGG. (A) WHO grade; (B) Histological type; (C) IDH status; (D) p/19q codeletion; (E) Age; (F) Primary therapy outcome. ns, $p \geq 0.05$; * $p < 0.05$; *** $p < 0.001$.

Prognostic value of IGF2BP3 across cancers

Further, each cancer's survival analysis was performed to investigate the association between IGF2BP3 expression level and prognosis, concentrating on OS, DSS, and PFI. The forest plot of the univariate Cox model suggested that IGF2BP3 was a significant risk factor for OS in GBMLGG ($p < 0.001$), LGG ($p < 0.001$), KIPAN ($p < 0.001$), KIRP ($p < 0.001$), KIRC ($p < 0.001$), PAAD ($p < 0.001$), LUAD ($p < 0.001$), LAML ($p = 0.0011$), MESO ($p = 0.0014$), ACC ($p = 0.0028$), UVM ($p = 0.02$), STES ($p = 0.03$), LIHC ($p = 0.03$), and BLCA ($p = 0.03$) patients (Figure 5A). Next, the Kaplan-Meier analysis of OS indicated that patients with high expression of IGF2BP3 was significantly correlated with poor prognosis in patients with GBMLGG ($p < 0.001$), LGG ($p < 0.001$), KIRP ($p < 0.001$), KIRC ($p < 0.001$), MESO ($p < 0.001$), LAML ($p = 0.004$), LUAD ($p = 0.008$), SARC ($p = 0.008$), UVM ($p = 0.008$), BLCA ($p = 0.015$), UCEC ($p = 0.018$), PAAD ($p = 0.024$), and LIHC ($p = 0.044$) (Figures 5B–N).

Moreover, as presented in Supplementary Figure 3A, we performed Cox regression analysis of DSS and identified that IGF2BP3 was an independent risk factor in patients with GBMLGG ($p < 0.001$), LGG ($p < 0.001$), KIPAN ($p < 0.001$), KIRP ($p < 0.001$), KIRC ($p < 0.001$), PAAD ($p < 0.001$), MESO

($p < 0.001$), LUAD ($p = 0.0013$), ACC ($p = 0.0017$), UVM ($p = 0.0079$), STES ($p = 0.0084$), SKCM-P ($p = 0.03$), and KICH ($p = 0.04$). Notably, the resulting Kaplan-Meier survival analysis indicated that patients with higher IGF2BP3 expression tended to exhibit a significantly shorter DSS as compared to those with lower IGF2BP3 expression, respectively, in GBMLGG ($p < 0.001$), LGG ($p < 0.001$), KIRP ($p < 0.001$), KIRC ($p < 0.001$), MESO ($p < 0.001$), UVM ($p = 0.008$), SARC ($p = 0.009$), PAAD ($p = 0.01$), UCEC ($p = 0.018$), and LUAD ($p = 0.023$) (Supplementary Figures 3B–K).

Also, univariate Cox regression analysis of PFI analyses was performed, and the results showed that IGF2BP3 was a risk factor in patients with high-risk factor in GBMLGG ($p < 0.001$), LGG ($p < 0.001$), KIPAN ($p < 0.001$), KIRC ($p < 0.001$), KIRP ($p < 0.001$), PAAD ($p < 0.001$), UVM ($p < 0.001$), LUAD ($p = 0.0043$), LIHC ($p = 0.005$), ACC ($p = 0.0061$), SKCM-P ($p = 0.0064$), and MESO ($p = 0.02$) (Supplementary Figure 4A). Furthermore, KM plotter analysis revealed that patients with higher IGF2BP3 expression had poorer PFI than those with lower IGF2BP3 expression in GBMLGG ($p < 0.001$), LGG ($p < 0.001$), KIRP ($p < 0.001$), KIRC ($p < 0.001$), MESO ($p < 0.001$), UVM ($p = 0.005$), LIHC ($p = 0.006$), and UCEC ($p = 0.014$), as seen in Supplementary Figures 4B–I.

We further examined the associations of IGF2BP3 with prognosis (OS, DSS and PFI) in different clinical glioma subgroups. The results

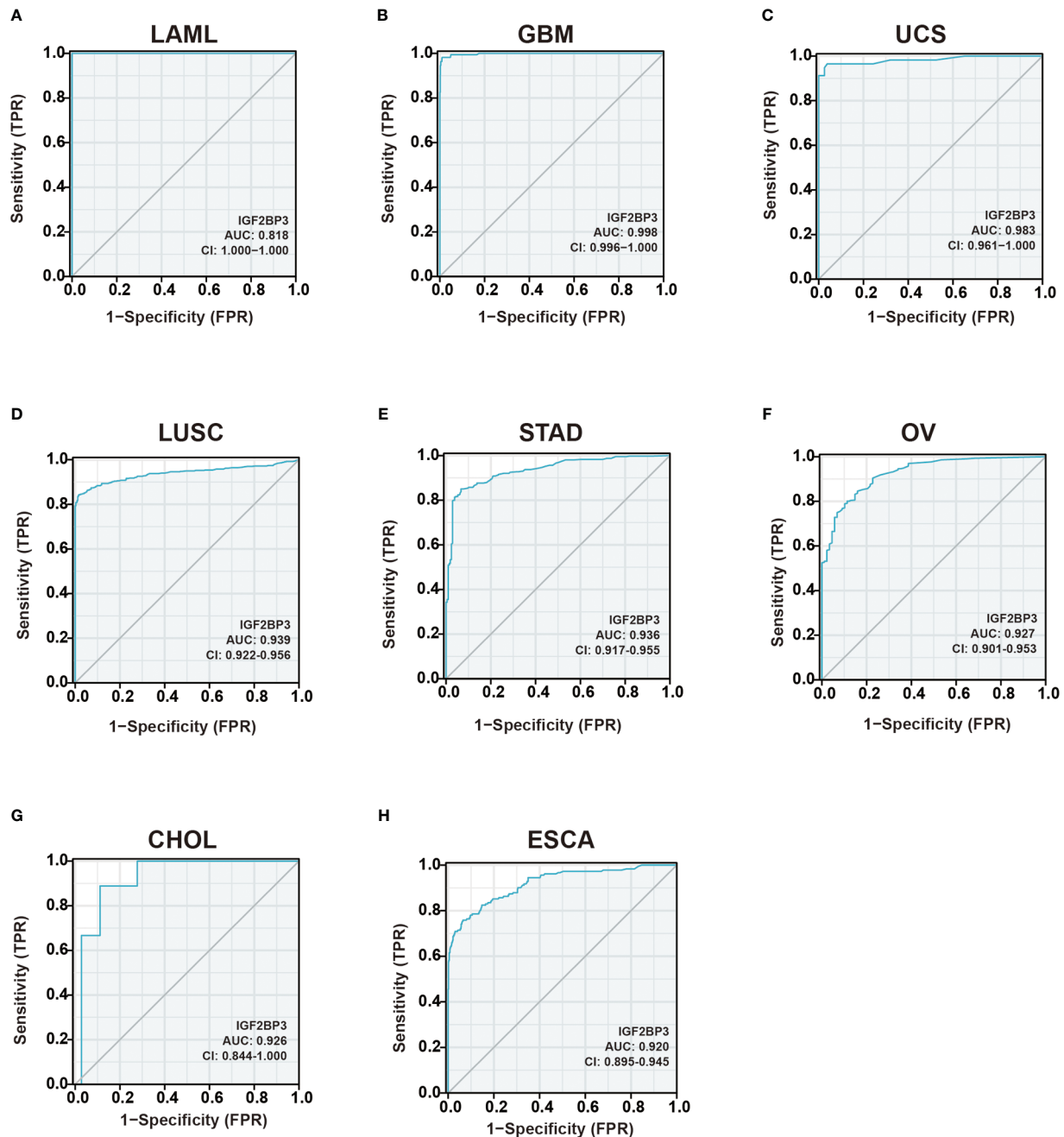


FIGURE 4
Receiver operating characteristic (ROC) curve for IGF2BP3 expression in pan-cancer. (A) LAML; (B) GBM; (C) UCS; (D) LUSC; (E) STAD; (F) OV; (G) CHOL; (H) ESCA.

of the subgroup analysis demonstrated that high expression of IGF2BP3 was associated with worse OS in most clinical subgroups, including a subgroup of WHO grade: G3 (Figure 6A), 1p/19q codeletion: non-codeletion (Figure 6B), a subgroup of IDH status: WT (Figure 6C), a subgroup of IDH status: Mut (Figure 6D), a subgroup of Primary therapy outcome: PD (Figure 6E), a subgroup of Primary therapy outcome: SD (Figure 6F), a subgroup of Gender: Female (Figure 6G), a subgroup of Gender: Male (Figure 6H), a subgroup of Race: Black or African American (Figure 6I), subgroup of Race: White (Figure 6J), a subgroup of Age: ≤ 60 (Figure 6K), a subgroup of Age: > 60 (Figure 6L), a subgroup of Histological type: Astrocytoma (Figure 6M), and Histological type: Oligoastrocytoma (Figure 6N).

For DSS, the higher expression of IGF2BP3 had a worse DSS in a subgroup of WHO grade: G3, a subgroup of IDH status: WT, a subgroup of IDH status: Mut, a subgroup of 1p/19q codeletion: non-codeletion, a subgroup of Primary therapy outcome: PD, a subgroup of Primary therapy outcome: SD, a subgroup of Gender: Female, a subgroup of Gender: Male, a subgroup of Race: Black or African American, a subgroup of Race: White, a subgroup of Age: ≤ 60 , a subgroup of Age: > 60 , a subgroup of Histological type: Astrocytoma, and Histological type: Oligoastrocytoma (Supplementary Figures 5A–M).

For PFI, the higher expression of IGF2BP3 had a worse PFI in a subgroup of WHO grade: G3, a subgroup of IDH status: WT, a

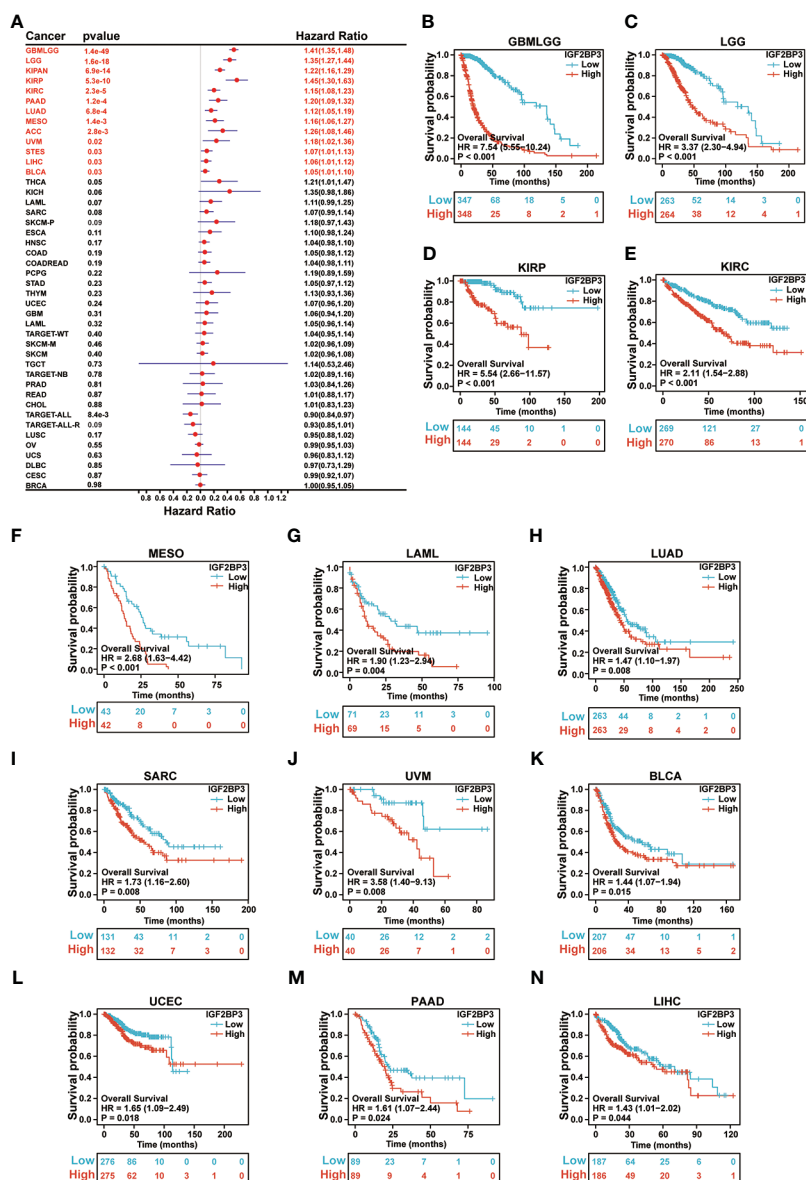


FIGURE 5

Relationship of IGF2BP3 expression with patient Overall Survival (OS). (A) Forest map shows the univariate Cox regression analysis results for IGF2BP3 in TCGA pan-cancer samples. (B–N) Kaplan–Meier analysis of the association between IGF2BP3 expression and OS.

subgroup of IDH status: Mut, a subgroup of 1p/19q codeletion: non-codeletion, a subgroup of Primary therapy outcome: PD, a subgroup of Gender: Female, a subgroup of Gender: Male, a subgroup of Race: Black or African American, a subgroup of Race: White, a subgroup of Age: ≤60, a subgroup of Age: >60, and a subgroup of Histological type: Astrocytoma (Supplementary Figures 6A–L).

Univariate and multivariate Cox regression analyses in GBMLGG patients

Uni- and multivariate Cox regression analyses of IGF2BP3 and clinical characteristics, were performed in TCGA-GBMLGG cohort. In univariate and multivariate Cox regression analyses, age, WHO grade, IDH status, 1p/19q codeletion, primary therapy outcome, histological

type, and IGF2BP3 were significantly associated with the OS (Table 1). In contrast, primary therapy outcome, age, and IGF2BP3 were significantly correlated with DSS (Supplementary Table 3), and primary therapy outcome, IDH status, age, and IGF2BP3 were correlated significantly with PFI (Supplementary Table 4).

IGF2BP3 expression in different immune and molecular subtypes of cancers

Correlation of IGF2BP3 differential expression with molecular subtypes in pan-cancer was investigated by the TISIDB database. We found that IGF2BP3 was expressed differently in different immune subtypes (C1: wound healing, C2: IFN-gamma dominant, C3: inflammatory, C4: lymphocyte depleted, C5: immunologically quiet, C6: TGF-β dominant) of 29 cancer types. These include, for example,

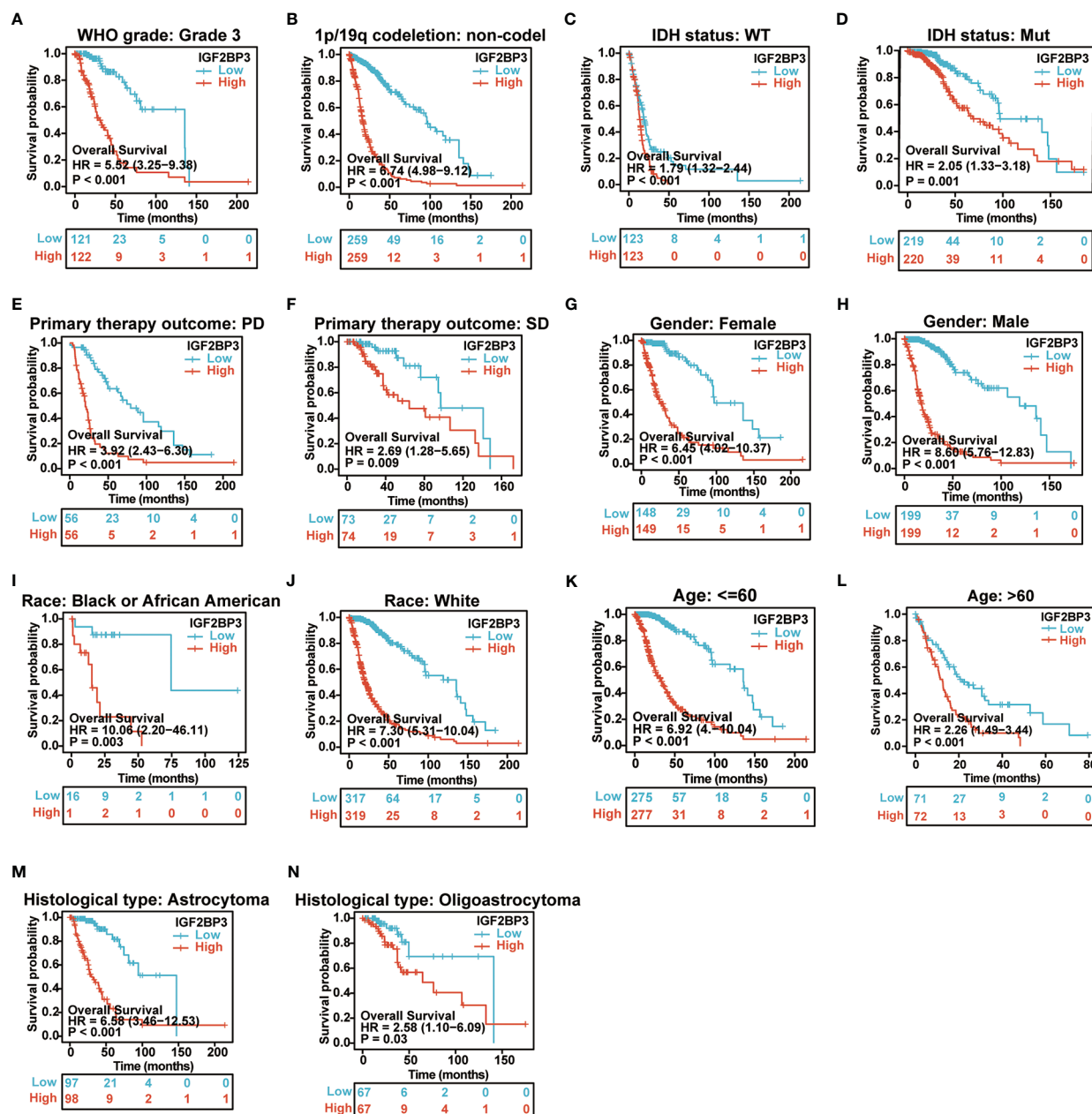


FIGURE 6

Associations between IGF2BP3 expression and the OS in different clinical subgroups of GBMLGG. (A) WHO grade (G3); (B) 1p/19q codeletion (non-codelet); (C) IDH status (WT); (D) IDH status (Mut); (E) Primary therapy outcome (PD); (F) Primary therapy outcome (SD); (G) Gender (Female); (H) Gender (Male); (I) Race (Black or African American) (J) Race (White); (K) Age ≤ 60; (L) Age > 60; (M) Histological type (Astrocytoma); (N) Histological type (Oligoastrocytoma).

TABLE 1 Univariate and multivariate Cox regression analyses of clinical characteristics associated with OS of glioma.

Characteristics	Total (N)	Univariate analysis		Multivariate analysis	
		Hazard ratio (95% CI)	P value	Hazard ratio (95% CI)	P value
WHO grade	634				
G2	223	Reference			
G3	243	2.999 (2.007–4.480)	<0.001	2.258 (1.452–3.511)	<0.001
G4	168	18.615 (12.460–27.812)	<0.001	11.151 (3.459–35.948)	<0.001

(Continued)

TABLE 1 Continued

Characteristics	Total (N)	Univariate analysis		Multivariate analysis	
		Hazard ratio (95% CI)	P value	Hazard ratio (95% CI)	P value
Age	674				
<=60	541	Reference			
>60	133	4.500 (3.409-5.940)	<0.001	3.929 (2.282-6.764)	<0.001
IDH status	664				
WT	232	Reference			
Mut	432	0.110 (0.083-0.146)	<0.001	0.506 (0.276-0.930)	0.028
1p/19q codeletion	688				
Codel	170	Reference			
non-codel	518	4.428 (2.885-6.799)	<0.001	2.050 (1.224-3.435)	0.006
Primary therapy outcome	461				
PD	112	Reference			
SD	147	0.440 (0.294-0.658)	<0.001	0.425 (0.266-0.680)	<0.001
PR	64	0.170 (0.074-0.391)	<0.001	0.209 (0.075-0.586)	0.003
CR	138	0.133 (0.064-0.278)	<0.001	0.143 (0.068-0.302)	<0.001
Histological type	674				
Astrocytoma	192	Reference			
Glioblastoma	155	6.602 (4.739-9.197)	<0.001		
Oligoastrocytoma	132	0.604 (0.374-0.975)	0.039	1.117 (0.633-1.970)	0.703
Oligodendroglioma	195	0.543 (0.363-0.813)	0.003	0.504 (0.273-0.933)	0.029
IGF2BP3 (High vs. Low)	695	1.776 (1.650-1.910)	<0.001	1.539 (1.264-1.875)	<0.001

CESC (Figure 7A), LUAD (Figure 7B), LUSC (Figure 7C), LGG (Figure 7D), COAD (Figure 7E), STAD (Figure 7F), BLCA (Figure 7G), OV (Figure 7H), and BRCA (Figure 7I). In addition, we observed that IGF2BP3 expression was strongly associated with immune stimulators and immune inhibitors (Supplementary Figure 7) among nearly all malignancies, represented by UVM, GBMLGG, LGG, LUAD, and KIRC.

Meanwhile, we observed that IGF2BP3 expression was significantly correlated with molecular subtypes of 16 cancer types, such as LGG (Figure 8A), GBM (Figure 8B), LUSC (Figure 8C), HNSC (Figure 8D), ACC (Figure 8E), BRCA (Figure 8F), UCEC (Figure 8G), COAD (Figure 8H), and KIRP (Figure 8I). Further, for LGG and GBM, IGF2BP3 was identified to express the highest in the molecular subtype of G-CIMP-low (Figures 8A, B). For LUSC and HNSC, IGF2BP3 was identified to express the highest in the molecular subtype of classical (Figures 8C, D). For ACC, IGF2BP3 expression was identified to be the highest in CIMP-intermediate molecular subtype (Figure 8E). For COAD, IGF2BP3 was expressed the highest in the molecular subtype of HM-SNV (Figure 8H). For STAD, IGF2BP3 was the most highly expressed in the molecular subtype of CIN (Figure 8E). For BRCA, IGF2BP3 showed the highest expression in the molecular subtype of basal (Figure 8F). For UCEC, IGF2BP3 expression was identified to be the highest in the molecular subtype of CN_HIGH (Figure 8G). For KIRP, IGF2BP3 was expressed the highest in the molecular subtype of C2c-CIMP (Figure 8I).

Immune aspects of IGF2BP3 in the tumor microenvironment

We further investigated the relationship between IGF2BP3 expression and immune cell infiltration in pan-cancer levels using immune cell infiltration data extracted from various databases. First, based on the TIMER (Tumor Immune Estimation Resource) database (<https://cistrome.shinyapps.io/timer/>), we measured six subpopulations of immune cells in TCGA data set including B cells, CD4+ T cells, CD8 + T cells, Neutrophils, Macrophages and Dendritic cells. Generally, as shown in Figure 9A, the IGF2BP3 expression had a significantly positive relationship with the infiltration of multiple immune cells, including T cells CD4, T cells CD8, Neutrophil, Macrophages and dendritic cells (DC) in a variety of cancer types. Significantly, some particular cancer types such as LGG, PRAD, and KIRC had a high infiltration level of all three types of immune cells (Figure 9B).

Moreover, a co-expression analysis was performed among 33 tumors to investigate the relationships between IGF2BP3 expression and immune-related genes. In accordance with the results (Figures 10A–E), there was a strong correlation between IGF2BP3 and most immune-related genes in specific cancer types such as GBMLGG, LGG, LUAD, PAAD, BRCA, and PRAD. Specifically, chemokines such as CXCL9, CXCL10, and CXCL11 and chemokine receptors such as CXCR5, CCR4, CCR8, and CCR1 were positively correlated with IGF2BP3 expression in various cancer types. MHC

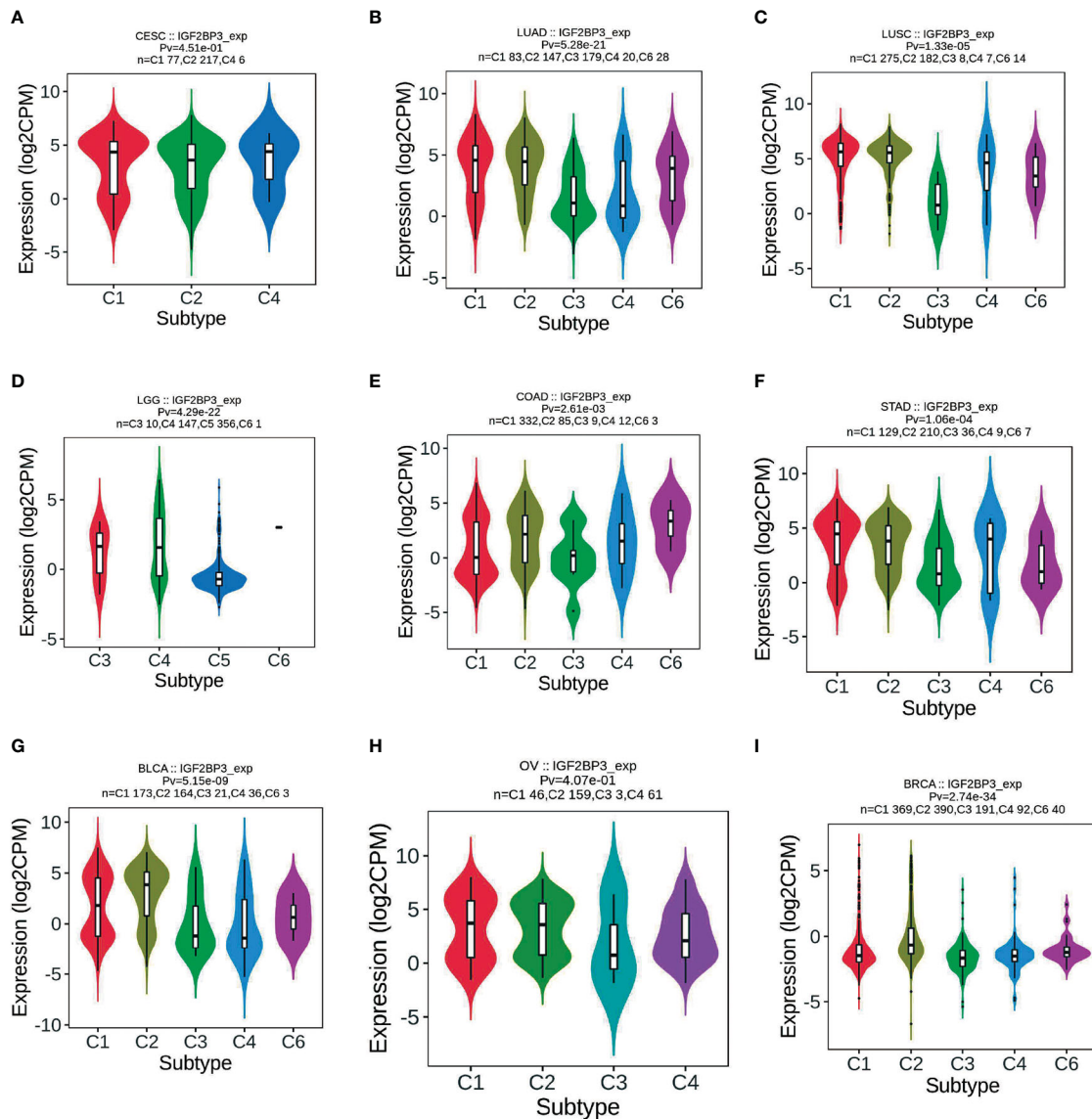


FIGURE 7

Correlations between IGF2BP3 expression and immune subtypes across TCGA tumors. (A) CESC; (B) LUAD; (C) LUSC; (D) LGG; (E) COAD; (F) STAD; (G) BLCA; (H) OV; (I) BRCA.

genes co-expressed with IGF2BP3 in almost all tumor types, particularly in UVM, PAAD, GBMLGG, LGG, KIRC, KIPAN, KIRP, COAD, BLCA, BRCA, PRAD, and LIHC. Moreover, immunostimulatory factors and immunosuppressive factors were also tightly correlated with IGF2BP3 expression in TCGA pan-cancer. Overall, these results show that the expression of IGF2BP3 is closely linked to the biological function of various cytokines and immune-relevant genes.

As it is well known, TMB and MSI in the tumor microenvironment are the most important biomarkers for predicting the therapeutic efficacy of tumor immunotherapy in various tumor types. Outcomes from several studies indicated that tumors with high TMB/MSI status considered to manifest better responses to immunotherapy than those with low TMB/MSI. Thus, we evaluated the correlation between the IGF2BP3 gene expression and TMB and MSI in pan-cancer. As can be seen in [Supplementary Figure 8A](#), a significant correlation ($P < 0.05$) existed between IGF2BP3 expression and TMB in 14 categories of

cancer. Specifically, IGF2BP3 expression was positively correlated with TMB in LGG, LUAD, LUSC, PRAD, BLCA, PAAD, SARC, BRCA, COAD, SKCM, KIRC, HNSC, and ACC while negatively correlated with TMB only in THCA. Further, we found that the expression of IGF2BP3 was positively related to the MSI in 6 cancers, including LUSC, BLCA, TGCT, ESCA, SARC, and COAD, but had a negative correlation with MSI in SKCM, THCA, HNSC, and DLBC ([Supplementary Figure 8B](#)).

Functional states of IGF2BP3 in scRNA-Seq datasets

To evaluate the functional state of IGF2BP3 in various cancer types at the single-cell level, we analyzed the correlation of IGF2BP3 with multiple functional states of cancer cells *via* the CancerSEA. This cancer's single-cell state atlas revealed a positive correlation of

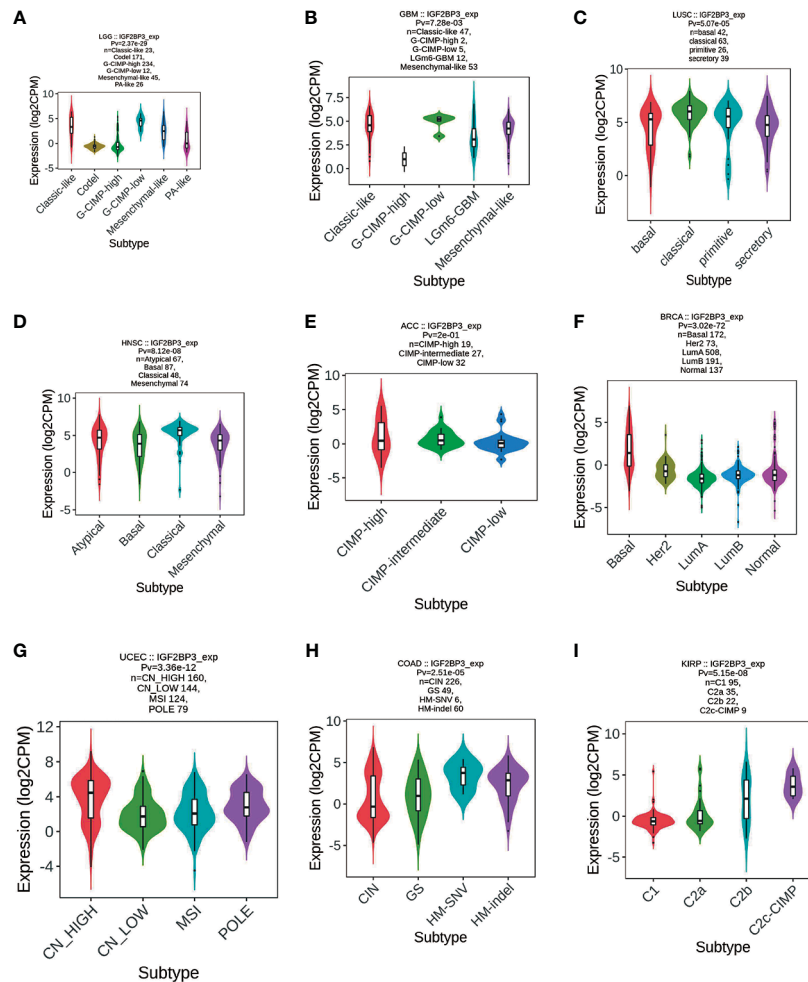


FIGURE 8
Correlations between IGF2BP3 expression and molecular subtypes across TCGA tumors. (A) LGG; (B) GBM; (C) LUSC; (D) HNSC; (E) ACC; (F) BRCA; (G) UCEC; (H) COAD; (I) KIRP.

IGF2BP3 with angiogenesis, differentiation, inflammation, metastasis, and quiescence. Negative correlations were observed between IGF2BP3 expression and apoptosis, cell cycle, DNA damage, and DNA repair (Supplementary Figure 9A). We then explored the correlation between IGF2BP3 and the functional state in specific cancers. The results found that IGF2BP3 positively correlated with cell cycle and DNA damage in GBM; with metastasis in Astrocytoma; with metastasis, angiogenesis, quiescence, and differentiation in LUAD; with stemness and DNA damage in NSCLC; with angiogenesis, differentiation, and inflammation in RB; with invasion in AML. Conversely, the IGF2BP3 was negatively correlated with cell cycle and DNA damage in Glioma, apoptosis in NSCLC, DNA repair, cell cycle, and DNA damage in RB, angiogenesis in AML, DNA repair, DNA damage, apoptosis, and differentiation in UM (Supplementary Figures 9B–I).

PPI network of IGF2BP3 in cancers and enrichment analysis

Next, functional network was constructed through GeneMANIA database to explore the potential interactome with IGF2BP3 protein as hub, and the result is shown in Figure 11. As evident in the figure,

IGF2BP3 had strong physical interactions with IGF2BP1, which are both conserved IGF2BPs predominantly expressed during embryonic development but comparatively lower or silenced in adulthood (5). Moreover, high expression level of IGF2BP1 and IGF2BP3 has been detected in many human cancers, including glioma and lung adenocarcinoma. They have been correlated with invasiveness, aggressiveness and a poorer prognosis (38, 39). This analysis demonstrates good agreement with the predictions from the co-expression.

Furthermore, there was a significantly predictable link between IGF2BP3, LAPTM4A, and DHX57. GSEA was then conducted to determine the functional enrichment of high and low IGF2BP3 expression. The KEGG and HALLMARK analyses showed that IGF2BP3 was significantly linked to many immune-related signaling pathways (Figure 12).

Drug sensitivity analysis of IGF2BP3

Enhancing drug sensitivity is crucial for preventing the drug resistance of cancer cells. We further investigated the potential correlation analysis between drug sensitivity and IGF2BP3 expression

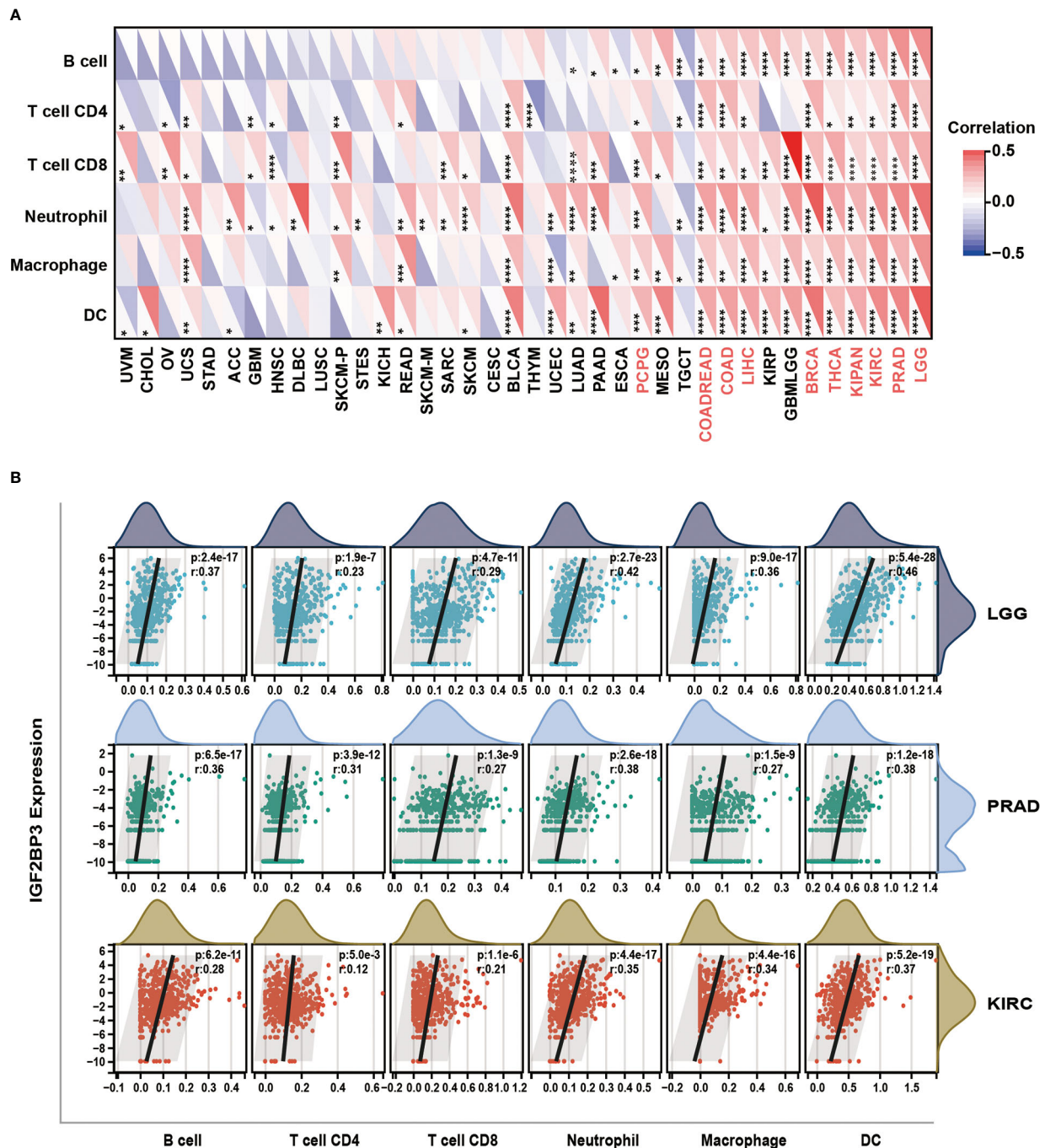


FIGURE 9

Relationship of IGF2BP3 expression with Immune cell infiltration analysis. (A) The relationship between IGF2BP3 expression levels and the levels of infiltration of six immune-related cells based on TIMER database. (B) Analysis of immune-associated cells infiltration with IGF2BP3 expression in pan-cancer. $p \geq 0.05$; * $p < 0.05$; ** $p < 0.01$; *** $p < 0.001$.

level accessed from the CellMiner database. Specifically, our results exhibited that IGF2BP3 had a significant and positive correlation with the clinical drug sensitivity of ARRY-704, RO-4987655, Trametinib, TAK-733, Mirdametininib, Cobimetininib, RO-5126766, Ulixertininib, ARRY-162, Selumetinib, *etc* ($p < 0.01$) (Figures 13A–J), while significant but negative associations with GDC-0810, AZD-9496, BAY-876, VT-464, and Acetalax sensitivity ($p < 0.05$) (Figures 13K–

O). The data indicated that IGF2BP3 might be associated with chemoresistance of specific chemotherapeutic agents, such as Trametinib, Cobimetininib, ARRY-162 and Selumetinib, which were commonly used MEK inhibitors approved by the FDA for cancer therapy. These results established that IGF2BP3 was tightly linked to diverse drug sensitivity in different cancer cell lines and might serve as a promising therapeutic target for cancer immunotherapies.

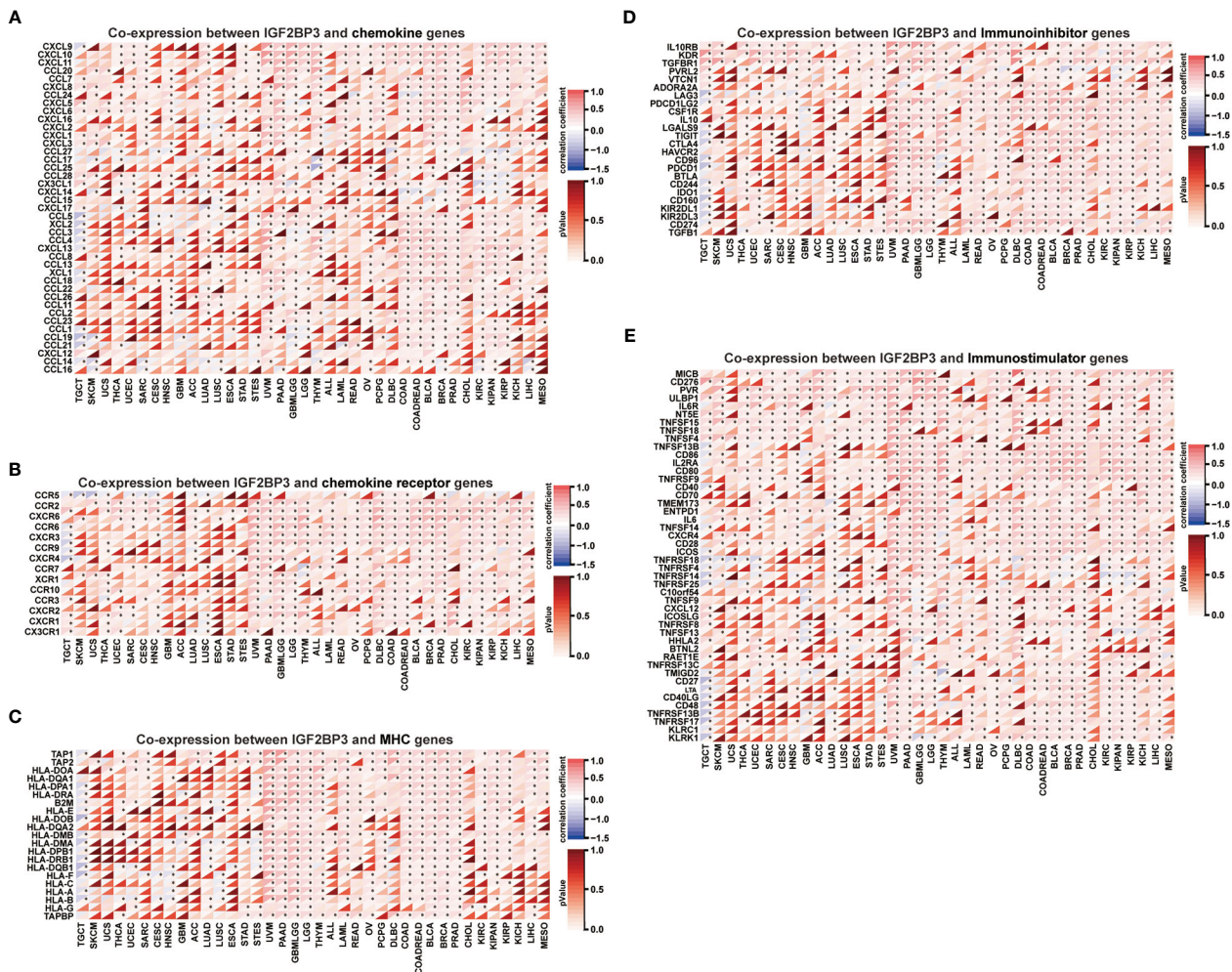


FIGURE 10

Co-expression of IGF2BP3 and immune-related genes in pan-cancer. Heatmaps indicating the co-expression of IGF2BP3 with immune-relevant genes in pan-cancer, including chemokine genes (A), chemokine-receptor genes (B), MHC molecules (C), immunoinhibitors (D), and immunostimulators (E). *p-value < 0.05, **p-value < 0.01, ***p-value < 0.001, and ****p-value < 0.0001.

Validation of IGF2BP3 expression in glioma

To further verify the pathophysiological roles of IGF2BP3, we applied experimental validation to determine its clinicopathological characteristics. We first evaluated the protein levels of IGF2BP3 in a series of clinical specimens, including nine glioma tissues (three specimens each from WHO grade 2,3,4 groups) and three peritumoral normal tissue using immunohistochemistry. The results showed that IGF2BP3 protein expression was significantly higher in glioma compared to normal tissue, especially in GBM (Figure 14A). Western blot analysis further verified the expression of IGF2BP3 protein in glioma. We confirmed a similar expression trend at the protein level (Figure 14B), suggesting that IGF2BP3 may be a potential molecular biomarker for the diagnosis and prognosis of glioma, especially GBM, which is expected to be a new therapeutic target for glioma.

Discussion

IGF2BP3, also known as IMP3, a newly identified “reader” of m6A belonging to a highly conserved IGF2BP family (IGF2BP1/2/3)

has been recognized to play an irreplaceable role in m6A modifications, mRNA stabilization, cell proliferation, and migration during the early stages of embryogenesis (40). Structurally, IGF2BP3 contains two N-terminal RNA recognition motifs (RRMs) and four C-terminal KH domains, which are critical for RNA-binding (5). As a m6A reader, IGF2BP3 was first reported in 1997 due to its high expression in pancreatic carcinoma (41). Subsequently, accumulative evidence has implied that the IGF2BP3 is post-transcriptionally active and plays a tumor-promoting role in various cancer types such as lung cancer (42), hepatocellular carcinoma (43), melanoma (44), and colorectal cancer (45), mainly by promoting tumor growth, invasion, metastasis, survival, and chemo-resistance (7–9).

In recent years, evidence has also suggested that IGF2BP3 might be a predictor of metastasis and clinical prognosis in different malignancies (46–50). For instance, IGF2BP3 could be a useful marker in predicting invasion in papillary biliary tumors (47). Moreover, both mRNA and protein levels of IGF2BP3 were remarkably up-regulated in cutaneous squamous cell carcinoma and IGF2BP3 was also identified as a novel therapeutic target for squamous cell carcinoma (48). Also, significant associations were

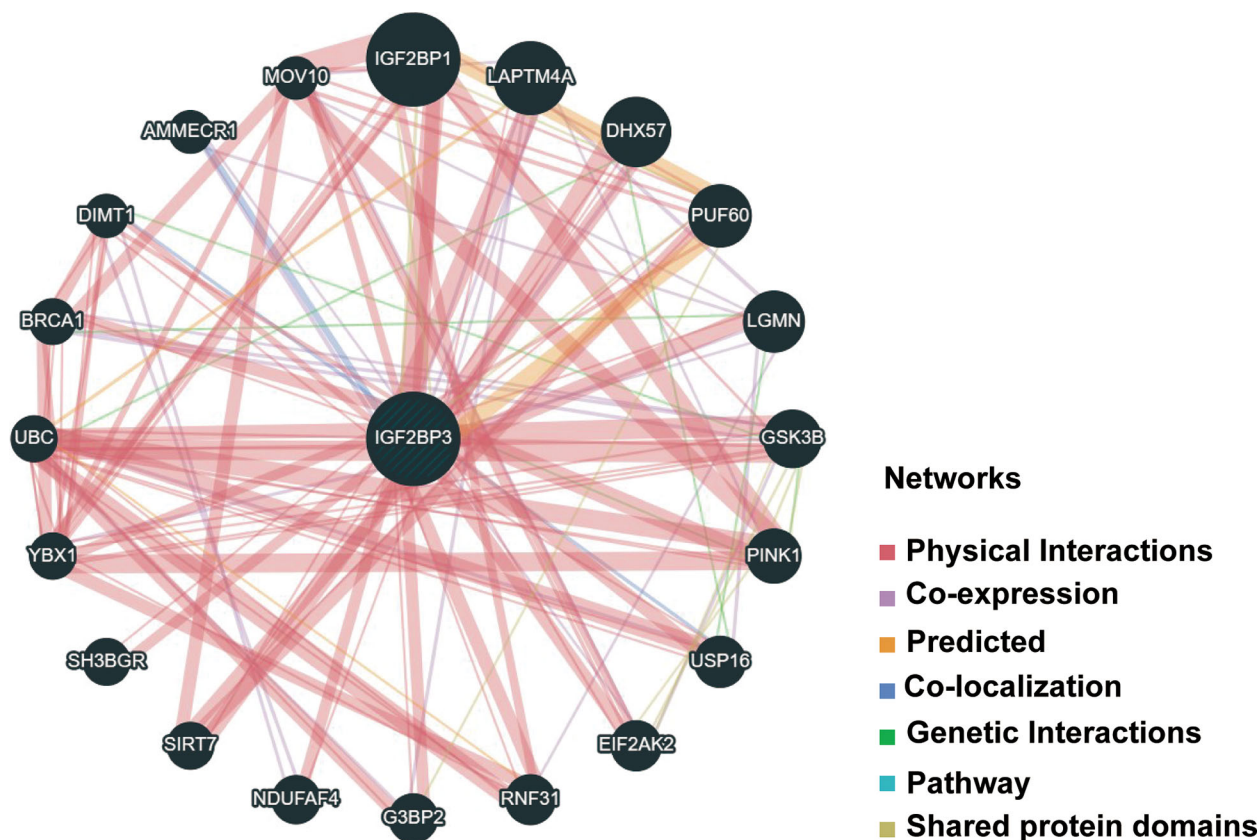


FIGURE 11

PPI network for IGF2BP3 was constructed via GeneMANIA. Different colors of the network edge indicate the bioinformatics methods applied: physical interaction, coexpression, predicted, colocalization, pathway, genetic interaction, and shared protein domains. PPI, protein–protein interaction.

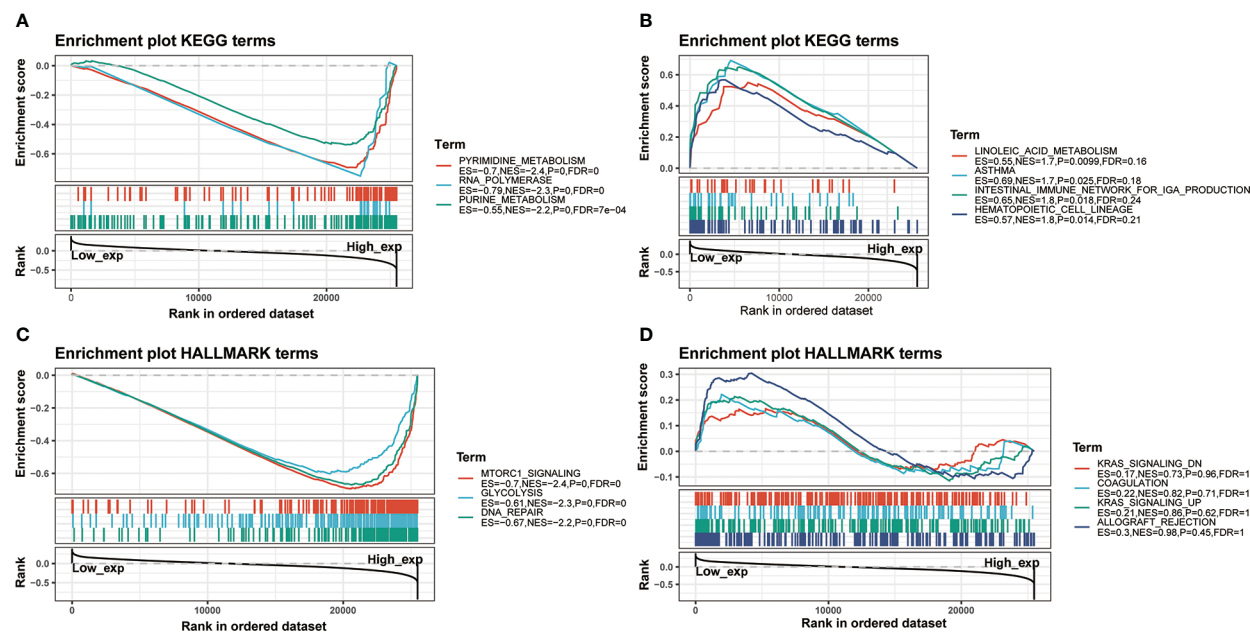


FIGURE 12

GSEA for samples with high IGF2BP3 expression and low expression. (A) The enriched gene sets in KEGG collection by the high IGF2BP3 expression sample. (B) The enriched gene sets in KEGG by samples with low IGF2BP3 expression. (C) Enriched gene sets in HALLMARK collection, the immunologic gene sets, by samples of high IGF2BP3 expression. (D) Enriched gene sets in HALLMARK by the low IGF2BP3 expression. Each line represented one particular gene set with unique color, and up-regulated genes located in the left approaching the origin of the coordinates, by contrast the down-regulated lay on the right of x-axis. Only gene sets with NOM $p < 0.05$ and FDR $q < 0.25$ were considered statistically significant. And only the leading-edge genes were displayed.

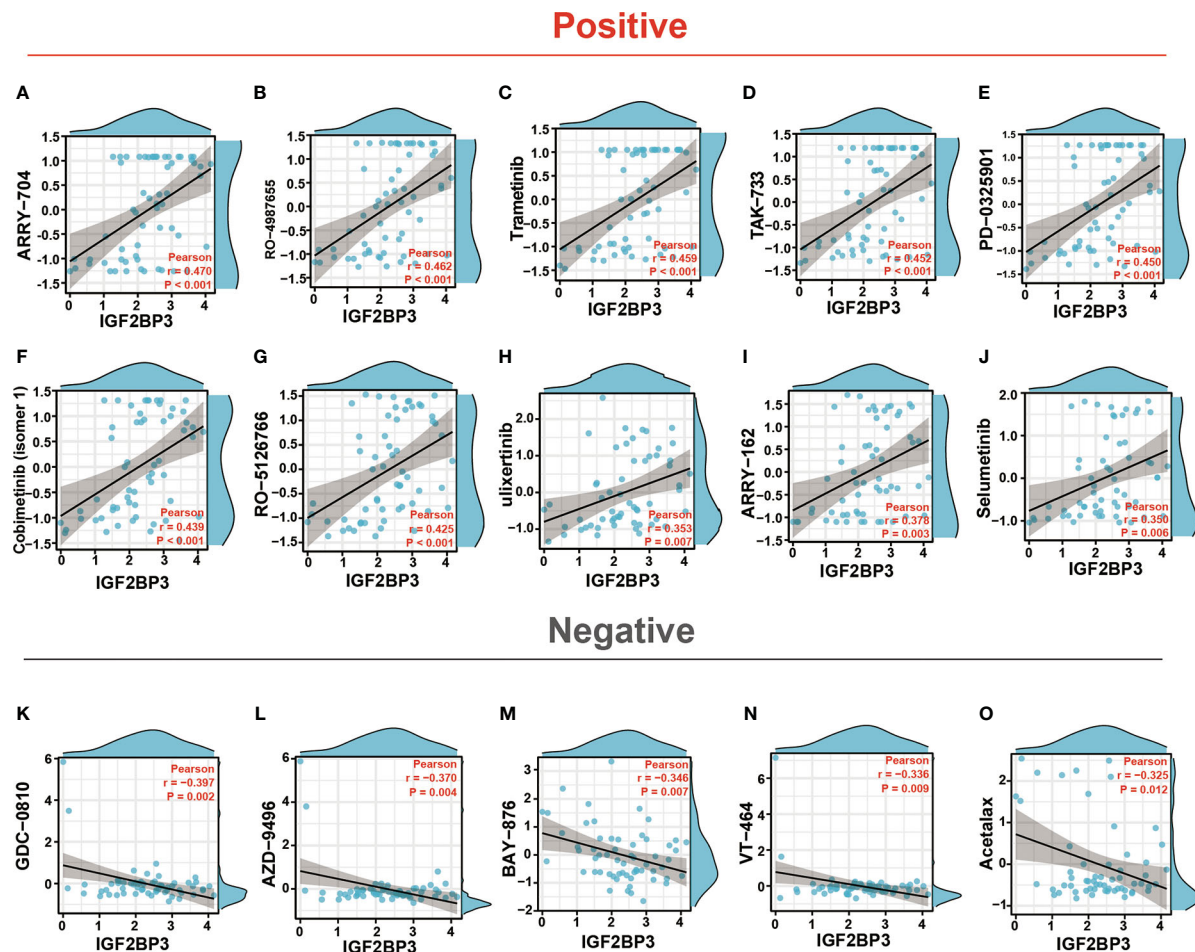


FIGURE 13

Drug sensitivity analysis of IGF2BP3. The expression of IGF2BP3 was associated with the sensitivity of ARRY-704 (A), RO-4987655 (B), Trametinib (C), TAK-733 (D), PD-0325901 (E), Cobimetinib (isomer1) (F), RO-5126766 (G), Ulixertinib (H), ARRY-162 (I), Selumetinib (J), GDC-0810 (K), AZD-9496 (L), BAY-876 (M), VT-464 (N), and Acetalax sensitivity (O).

found in colorectal cancer between IGF2BP3 positivity, poorer differentiation, and increased mortality, thus serving as a promising diagnostic biomarker for colorectal cancer in which higher expression indicates poorer prognosis (49). Further, a recent study revealed that m6A methylation regulators, IGF2BP2 and IGF2BP3, in particular, play essential roles in the malignant progression of glioma (50). However, upon reviewing the literature, there is no existing study comprehensively evaluating the significance of IGF2BP3 in pan-cancer on the whole scale. Of note, the pan-cancer analysis, which is of significant importance for understanding differences and similarities among different tumor types, can provide novel insights into cancer prevention and targeted therapy across cancer types. In recent years, there is increasing recognition of the value of a comprehensive pan-cancer analysis, which could potentially describe the essential roles of some driver mutations or genes in developing specific cancer types (51, 52).

In the present study, firstly, we used multiple databases to evaluate the expression level of IGF2BP3 across pan-cancer. The results showed that IGF2BP3 gene mRNA was highly expressed in most cancer types than in the normal samples, namely, GBM, GBMLGG, LGG, UCEC, CESC, LUAD, COAD, COADREAD, BRCA, ESCA, KIRP, KIPAN, STAD, HNSC, KIRC, LUSC, LIHC, SKCM, OV,

PAAD, UCS, LAML, BLCA, ACC, KICH and CHOL, whereas low expression was detected in PRAD and THCA, which was consistent with previous studies in prostate and thyroid cancer (Figure 1) (53–55). IHC analysis from the HPA was in accordance with the IGF2BP3 mRNA level discrepancy and confirmed these results (Figure 2). It is also noteworthy that either prostate or thyroid cancer has been thought to be a malignant disease-carrying a relatively favorable prognosis that can be diagnosed earlier (56). Additionally, according to prior studies, the oncofetal protein IGF2BP3 has been reported as a predominant cancer-specific marker differentiating benign from malignant lesions of pancreas and uterine cervix (57, 58), highly indicating that increased IGF2BP3 expression was associated with unfavorable prognosis among tumor tissues. These results demonstrated that IGF2BP3 could indeed promote cancer development and progression.

In addition, IGF2BP3 expression levels are tightly correlated with the immune subtypes of nine cancers, including CESC, LUAD, LUSC, LGG, COAD, STAD, BLCA, OV, and BRCA. Meanwhile, IGF2BP3 was significantly associated with diverse molecular subtypes in nine cancer types. For instance, IGF2BP3 was most highly expressed in the G-CIMP-low molecular isoforms in LGG and GBM, in the molecular subtype of classical in both LUSC and HNSC, and the molecular

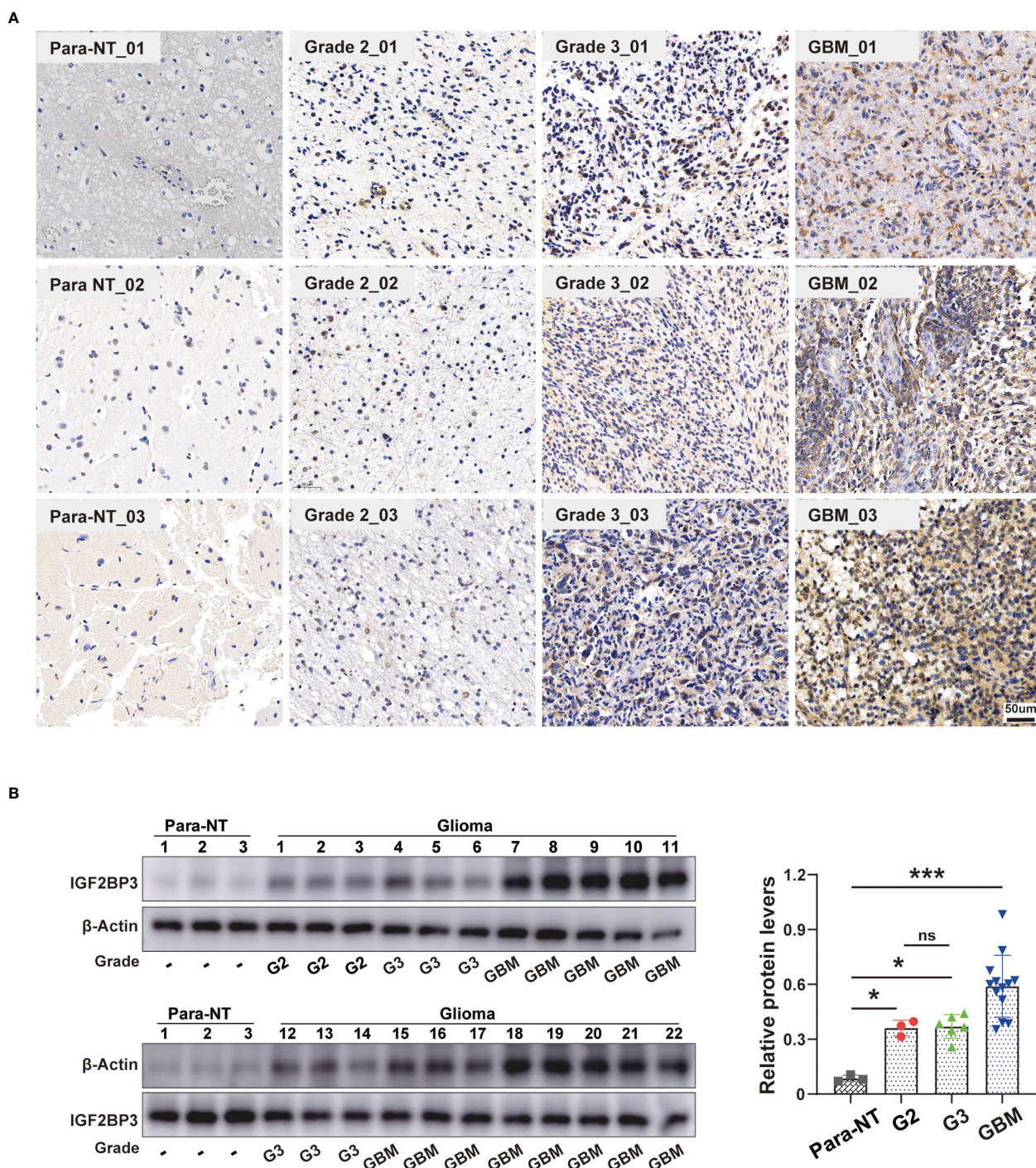


FIGURE 14

Validation of IGF2BP3 Expression in Glioma. (A) Representative immunohistochemical staining of IGF2BP3 expression in clinical glioma tissue and normal peritumor tissues. Scale bar=50 µm. (B) Western blot analysis of IGF2BP3 protein level in human glioma patient samples (grade 2 (n = 3), grade 3 (n = 6), grade GBM (n = 13)) and normal peritumor brain tissues (n = 3). β-actin was used as a loading control. All data are shown as the mean ± SD (at least three independent experiments). ns, no significance, *P < 0.05, ***P < 0.001.

subtype of basal in BRCA. It is important to mention that IGF2BP3 is tightly associated with both immune and molecular subtypes in four types of cancers, including LGG, LUSC, BRCA, and COAD (Figures 7, 8).

Furthermore, we wondered whether IGF2BP3 played a critical role in cancer diagnosis and prognosis. ROC curve and Survival curve

in pan-cancer plotted by Kaplan-Meier estimate revealed that IGF2BP3 had a certain accuracy (AUC>0.7) in predicting 24 cancer types, especially had a strong predictive power (AUC>0.9) in predicting LAML, GBM, UCS, LUSC, STAD, OV, CHOL, and ESCA. Moreover, IGF2BP3 was closely related to the OS, DSS, and PFI in GBMLGG, LGG, KIRP, KIRC, MESO, UVM, UCEC, and

PAAD. Thus, IGF2BP3 might represent significant value as diagnostic and prognostic biomarkers in the individualized precision cancer therapy (Figure 4).

Considering the important role of IGF2BP3 in gliomas, we further analyzed the role of IGF2BP3 in GBMLGG and identified significant correlations between IGF2BP3 expression levels and age, histological type and histological grade. Subsequently, we discovered that high expression of IGF2BP3 could cause a poorer OS, DSS, or PFI among a variety of clinical subgroups of GBMLGG. Since then, we confirmed WHO grade, age, IDH status, primary therapy outcome, gender, race, and IGF2BP3 expression level as independent indicators for the risk of OS, DSS, and PFI of GBMLGG through both univariate and multivariate Cox regression analyses (Figure 6; Supplementary Figures 5, 6).

IGF2BP3 may also have the potential as a therapeutic target for cancer treatment. Unlike chemotherapy, Immune checkpoint inhibitors help restore anti-tumor immune response, which has been shown to have a durable anti-tumor benefit in multiple cancers such as renal, melanoma, and lung cancers (59–61). Recently, increasing studies have reported that both TMB and MSI could be predictive biomarkers for identifying patients benefiting from immune checkpoint blockade therapies among multiple cancers (62–64), suggesting their potential response to immunotherapy. Moreover, the existing theory proved that an elevated TMB represented genomic instability associated with enhanced response to tumor immunotherapy (65, 66). In the present study, aberrant IGF2BP3 expression was found to be correlated with TMB in 14 cancer types, and MSI in 10 cancer types. The above correlation proved that IGF2BP3 was closely associated with the TME and might function as a promising biomarker for cancer immunotherapy in specific types of cancer. However, further experimental research is to prove its function (Supplementary Figure 8).

Another principal finding of this study was the primary role of IGF2BP3 in cancer immunity. Recently, it has been well documented that the immune status of the tumor is closely associated with both critical components and tumor-infiltrating immune cell concentrations in TME (32, 67). ESTIMATE algorithm has been shown to be a favorable predictor of the levels of both tumor purity and immune infiltration in a variety of malignancies (32), including pancreatic cancer (68), colon cancer (69), and lung adenocarcinoma (70). Herein, using the TCGA database, we discovered that IGF2BP3 was significantly positively associated with the immune component of TME in 11 cancers, including BLCA, BRCA, COAD, KIRC, KIRP, LAML, LGG, PCPG, PRAD, READ, and UVM, negatively associated with the stromal component of TME in 4 cancers, including ACC, GBM, LUSC and UCEC (Figure 9).

Following that, we found that IGF2BP3 expression was significantly positively correlated with the degree of B cell, neutrophil, CD8+, DC, and macrophage infiltration in LGG, PRAD, KIRC, THCA, BRCA, and GBMLGG. These cells are known to widely involved in both innate and adaptive immune responses (71, 72). Then, a close positive association between IGF2BP3 expression and several immune scores was detected in pan-cancer analysis. Thus, IGF2BP3 may represent a promising biomarker related to tumor immune cell infiltration, and it provides a possible regimen of immune-related therapies for many cancers.

Finally, in our current study of IGF2BP3 biological function, it was shown that IGF2BP3 presented significant participation in

biological processes related to immune response and facilitated tumor development in various cancers (Figure 12). A recent study uncovered better responses in patients with higher IGF2BP3 expression in anti-PD-1/PD-L1 therapy (22). Also, in the current study, IGF2BP3 was found to significantly correlate with classic immune checkpoint in human cancers, which remained one of the most successful immunotherapy strategies for multiple cancers. The results above implied the role of IGF2BP3 as a target in immunotherapy.

CellMiner is a website that provides genomics and pharmacology tools to identify drug patterns and transcripts in the NCI-60 cell line. Specifically, the CellMiner database contains 360 microRNAs, 22,379 genes, and 20,503 compounds incorporating 102 FDA-approved drugs (37). In our study, by searching the CellMiner database, we first explored the correlation between IGF2BP3 expression and anticancer drug sensitivity in detail. Results revealed that IGF2BP3 had a significantly positive association with most anticancer drugs, such as ARRY-704, RO-4987655, Trametinib, TAK-733, Cobimetinib, Mirdametinib, RO-5126766, AZD-0364, Ulixertinib, and Selumetinib (Figure 13). Remarkably, the drugs mentioned here were all confirmed to be within the spectrum of inhibitors against the components (mainly MEK and ERK) of MAPK signaling pathway, which remains a key driver of tumor growth in human cancers (73). This finding also partly agreed with the previous work by Ramaswamy Suvasini et al. (74), while the latter established IGF2BP3 as a pivotal oncogenic factor expressed solely in the GBMs. Therefore, we deduced that IGF2BP3 might promote tumorigenesis by inhibiting positive regulators of the Raf/MEK/ERK pathway.

Although we have explored the pan-cancer role of IGF2BP3 from the perspective of bioinformatics in depth, we must acknowledge some limitations in the present study. To begin with, despite the conclusion that aberrant IGF2BP3 expression was associated with immune cell infiltration and prognosis of human cancers, we cannot definitively ascertain whether IGF2BP3 may exert functional effects on patient survival *via* an immune response. Therefore, the involvement of IGF2BP3 during immune regulation is still unclear and needs further investigation. Second, there is no clinical trial to evaluate the use of IGF2BP3-related therapeutic drugs in patients with pan-cancer. However, we have noted that a prognostic model containing eight genes, including IGF2BP3, for pediatric brain tumors has already been developed recently in a randomized controlled trial, which dramatically enhances the identification of those patients with a poorer prognosis by such gene signature (75). In the future, it is necessary to prospectively study the expression of IGF2BP3 and its significance in cancer immune infiltration, and to develop new drugs with higher anti-tumor activity targeting IGF2BP3.

Conclusion

In conclusion, as far as we know, this is the first systematic study to elucidate the role of IGF2BP3 in pan-cancer from various angles, including its expression pattern, diagnosis, survival prognosis, genetic mutation, TMB, MSI, tumor immune microenvironment, relevant signaling pathways, and drug sensitivity. Based on our findings, IGF2BP3 may serve as a biomarker for the clinical detection of

cancer. Our findings on the role of IGF2BP3 are prerequisites for clinical research and the practical application of IGF2BP3-based therapies.

Data availability statement

The original contributions presented in the study are included in the article/**Supplementary Material**. Further inquiries can be directed to the corresponding authors.

Ethics statement

The studies involving human participants were reviewed and approved by the Ethics Committee of Zhongshan Hospital of Fudan University (Shanghai, China). The patients/participants provided their written informed consent to participate in this study.

Author contributions

PC and JX performed the statistical analysis and drew the pictures. PC performed experiments to verify the expression of IGF2BP3 in glioma. JX, ZC, and SW performed the data analysis. PC: writing the article, critical revision of the article. XZ and TX contributed to the design of the study protocol. All authors contributed to the article and approved the submitted version.

References

- Dominissini D, Moshitch-Moshkovitz S, Schwartz S, Salmon-Divon M, Ungar L, Osenberg S, et al. Topology of the human and mouse m⁶A RNA methylomes revealed by m⁶A-seq. *Nature* (2012) 485(7397):201–06. doi: 10.1038/nature11112
- Wang X, Zhao BS, Roundtree IA, Lu Z, Han D, Ma H, et al. N(6)-methyladenosine modulates messenger RNA translation efficiency. *Cell* (2015) 161(6):1388–99. doi: 10.1016/j.cell.2015.05.014
- He L, Li H, Wu A, Peng Y, Shu G, Yin G. Functions of N6-methyladenosine and its role in cancer. *Mol Cancer* (2019) 18(1):176. doi: 10.1186/s12943-019-1109-9
- Yang Y, Hsu PJ, Chen YS, Yang YG. Dynamic transcriptomic m6A decoration: writers, erasers, readers and functions in RNA metabolism. *Cell Res* (2018) 28(6):616–24. doi: 10.1038/s41422-018-0040-8
- Bell JL, Wächter K, Mühleck B, Pazaitis N, Köhn M, Lederer M, et al. Insulin-like growth factor 2 mRNA-binding proteins (IGF2BPs): post-transcriptional drivers of cancer progression? *Cell Mol Life Sci* (2013) 70(15):2657–75. doi: 10.1007/s00018-012-1186-z
- Huang H, Weng H, Sun W, Qin X, Shi H, Wu H, et al. Recognition of RNA N6-methyladenosine by IGF2BP proteins enhances mRNA stability and translation. *Nat Cell Biol* (2018) 20(3):285–95. doi: 10.1038/s41556-018-0045-z
- Mancarella C, Scotlandi K. IGF2BP3 from physiology to cancer: Novel discoveries, unsolved issues, and future perspectives. *Front Cell Dev Biol* (2020) 7:363. doi: 10.3389/fcell.2019.00363
- Nielsen J, Christiansen J, Lykke-Andersen J, Johnsen AH, Wewer UM, Nielsen FC. A family of insulin-like growth factor II mRNA-binding proteins represses translation in late development. *Mol Cell Biol* (1999) 19(2):1262–70. doi: 10.1128/MCB.19.2.1262
- Lederer M, Bley N, Schleifer C, Hüttelmaier S. The role of the oncofetal IGF2 mRNA-binding protein 3 (IGF2BP3) in cancer. *Semin Cancer Biol* (2014) 29:3–12. doi: 10.1016/j.semcancer.2014.07.006
- Wang Z, Tong D, Han C, Zhao Z, Wang X, Jiang T, et al. Blockade of miR-3614 maturation by IGF2BP3 increases TRIM25 expression and promotes breast cancer cell proliferation. *EBioMedicine* (2019) 41:357–69. doi: 10.1016/j.ebiom.2018.12.061
- Endo I, Amatya VJ, Kushitani K, Kambara T, Nakagiri T, Fujii Y, et al. Insulin-like growth factor 2 mRNA binding protein 3 promotes cell proliferation of malignant mesothelioma cells by downregulating p27Kip1. *Front Oncol* (2022) 11:795467. doi: 10.3389/fonc.2021.795467
- Li W, Liu D, Chang W, Lu X, Wang YL, Wang H, et al. Role of IGF2BP3 in trophoblast cell invasion and migration. *Cell Death Dis* (2014) 5(1):e1025. doi: 10.1038/cddis.2013.545
- Hanniford D, Ulloa-Morales A, Karz A, Berzoti-Coelho MG, Moubarak RS, Sánchez-Sendra B, et al. Epigenetic silencing of CDR1as drives IGF2BP3-mediated melanoma invasion and metastasis. *Cancer Cell* (2020) 37(1):55–70. doi: 10.1016/j.ccell.2019.12.007
- Zheng ZQ, Li ZX, Guan JL, Liu X, Li JY, Chen Y, et al. Long noncoding RNA TINCR-mediated regulation of acetyl-CoA metabolism promotes nasopharyngeal carcinoma progression and chemoresistance. *Cancer Res* (2020) 80(23):5174–88. doi: 10.1158/0008-5472.CAN-19-3626
- Yang Z, Zhao F, Gu X, Feng L, Xu M, Li T, et al. Binding of RNA m6A by IGF2BP3 triggers chemoresistance of HCT8 cells via upregulation of ABCB1. *Am J Cancer Res* (2021) 11(4):1428–45.
- Li Z, Peng Y, Li J, Chen Z, Chen F, Tu J, et al. N6-methyladenosine regulates glycolysis of cancer cells through PDK4. *Nat Commun* (2020) 11(1):2578. doi: 10.1038/s41467-020-16306-5
- Li X, Ma S, Deng Y, Yi P, Yu J. Targeting the RNA m6A modification for cancer immunotherapy. *Mol Cancer* (2022) 21(1):76. doi: 10.1186/s12943-022-01558-0
- Li Y, Gu J, Xu F, Zhu Q, Chen Y, Ge D, et al. Molecular characterization, biological function, tumor microenvironment association and clinical significance of m6A regulators in lung adenocarcinoma. *Brief Bioinform* (2021) 22(4):bbaa225. doi: 10.1093/bib/bbaa225
- Yang Z, Wang T, Wu D, Min Z, Tan J, Yu B. RNA N6-methyladenosine reader IGF2BP3 regulates cell cycle and angiogenesis in colon cancer. *J Exp Clin Cancer Res* (2020) 39(1):203. doi: 10.1186/s13046-020-01714-8
- Ding WB, Wang MC, Yu J, Huang G, Sun DP, Liu L, et al. HBV/Pregenomic RNA increases the stemness and promotes the development of HBV-related HCC through reciprocal regulation with insulin-like growth factor 2 mRNA-binding protein 3. *Hepatology* (2021) 74(3):1480–95. doi: 10.1002/hep.31850

Funding

This research was funded by Program of Shanghai Committee of Science and Technology, China, grant number was 22S31902500.

Conflict of interest

The authors declare that the research was conducted in the absence of any commercial or financial relationships that could be construed as a potential conflict of interest.

Publisher's note

All claims expressed in this article are solely those of the authors and do not necessarily represent those of their affiliated organizations, or those of the publisher, the editors and the reviewers. Any product that may be evaluated in this article, or claim that may be made by its manufacturer, is not guaranteed or endorsed by the publisher.

Supplementary material

The Supplementary Material for this article can be found online at: <https://www.frontiersin.org/articles/10.3389/fimmu.2023.1071675/full#supplementary-material>

21. Yin H, He H, Shen X, Zhao J, Cao X, Han S, et al. miR-9-5p inhibits skeletal muscle satellite cell proliferation and differentiation by targeting IGF2BP3 through the IGF2-PI3K/Akt signaling pathway. *Int J Mol Sci* (2020) 21(5):1655. doi: 10.3390/ijms21051655
22. Wan W, Ao X, Chen Q, Yu Y, Ao L, Xing W, et al. METTL3/IGF2BP3 axis inhibits tumor immune surveillance by upregulating N6-methyladenosine modification of PD-L1 mRNA in breast cancer. *Mol Cancer* (2022) 21(1):60. doi: 10.1186/s12943-021-01447-y
23. Goldman MJ, Craft B, Hastie M, Repčeka K, McDade F, Kamath A, et al. Visualizing and interpreting cancer genomics data via the xena platform. *Nat Biotechnol* (2020) 38(6):675–78. doi: 10.1038/s41587-020-0546-8
24. Barretina J, Caponigro G, Stransky N, Venkatesan K, Margolin AA, Kim S, et al. The cancer cell line encyclopedia enables predictive modelling of anticancer drug sensitivity. *Nature* (2012) 483(7391):603–07. doi: 10.1038/nature11003
25. Ru B, Wong CN, Tong Y, Zhong JY, Zhong SSW, Wu WC, et al. TISIDB: an integrated repository portal for tumor-immune system interactions. *Bioinformatics* (2019) 35(20):4200–2. doi: 10.1093/bioinformatics/btz210
26. Cerami E, Gao J, Dogrusoz U, Gross BE, Sumer SO, Aksoy BA, et al. The cBio cancer genomics portal: an open platform for exploring multidimensional cancer genomics data. *Cancer Discovery* (2012) 2(5):401–04. doi: 10.1158/2159-8290.CD-12-0095
27. Gao J, Aksoy BA, Dogrusoz U, Dresdner G, Gross B, Sumer SO, et al. Integrative analysis of complex cancer genomics and clinical profiles using the cBioPortal. *Sci Signal* (2013) 6(269):p11. doi: 10.1126/scisignal.2004088
28. Fancello L, Gandini S, Pelicci PG, Mazzarella L. Tumor mutational burden quantification from targeted gene panels: major advancements and challenges. *J Immunother Cancer* (2019) 7(1):183. doi: 10.1186/s40425-019-0647-4
29. Boland CR, Goel A. Microsatellite instability in colorectal cancer. *Gastroenterology* (2010) 138(6):2073–87. doi: 10.1053/j.gastro.2009.12.064
30. Rooney MS, Shukla SA, Wu CJ, Getz G, Hacohen N. Molecular and genetic properties of tumors associated with local immune cytolytic activity. *Cell* (2015) 160(1–2):48–61. doi: 10.1016/j.cell.2014.12.033
31. Thorsson V, Gibbs DL, Brown SD, Wolf D, Bortone DS, Ou Yang TH, et al. The immune landscape of cancer. *Immunity* (2018) 48(4):812–30.e14. doi: 10.1016/j.immuni.2018.03.023
32. Yoshihara K, Shahmoradgoli M, Martínez E, Vegesna R, Kim H, Torres-García W, et al. Inferring tumour purity and stromal and immune cell admixture from expression data. *Nat Commun* (2013) 4:2612. doi: 10.1038/ncomms3612
33. Li T, Fu J, Zeng Z, Cohen D, Li J, Chen Q, et al. TIMER2.0 for analysis of tumor-infiltrating immune cells. *Nucleic Acids Res* (2020) 48(W1):W509–14. doi: 10.1093/nar/gkaa407
34. Yuan H, Yan M, Zhang G, Liu W, Deng C, Liao G, et al. CancerSEA: A cancer single-cell state atlas. *Nucleic Acids Res* (2019) 47(D1):D900–8. doi: 10.1093/nar/gky939
35. Warde-Farley D, Donaldson SL, Comes O, Zuberi K, Badrawi R, Chao P, et al. The GeneMANIA prediction server: biological network integration for gene prioritization and predicting gene function. *Nucleic Acids Res* (2010) 38(Web Server issue):W214–20. doi: 10.1093/nar/gkq537
36. Franz M, Rodriguez H, Lopes C, Zuberi K, Montojo J, Bader GD, et al. GeneMANIA update 2018. *Nucleic Acids Res* (2018) 46(W1):W60–4. doi: 10.1093/nar/gky311
37. Reinhold WC, Sunshine M, Liu H, Varma S, Kohn KW, Morris J, et al. CellMiner: a web-based suite of genomic and pharmacologic tools to explore transcript and drug patterns in the NCI-60 cell line set. *Cancer Res* (2012) 72(14):3499–511. doi: 10.1158/0008-5472.CAN-12-1370
38. Velasco MX, Kostis A, Penalva LOF, Hernández G. The diverse roles of RNA-binding proteins in glioma development. *Adv Exp Med Biol* (2019) 1157:29–39. doi: 10.1007/978-3-030-19966-1_2
39. Li W, Li N, Gao L, You C. Integrated analysis of the roles and prognostic value of RNA binding proteins in lung adenocarcinoma. *PeerJ* (2020) 8:e8509. doi: 10.7717/peerj.8509
40. Mueller-Pillasch F, Pohl B, Wilda M, Lacher U, Beil M, Wallrapp C, et al. Expression of the highly conserved RNA binding protein KOC in embryogenesis. *Mech Dev* (1999) 88(1):95–9. doi: 10.1016/s0925-4773(99)00160-4
41. Müller-Pillasch F, Lacher U, Wallrapp C, Micha A, Zimmerhack H, Hameister H, et al. Cloning of a gene highly overexpressed in cancer coding for a novel KH-domain containing protein. *Oncogene* (1997) 14(22):2729–33. doi: 10.1038/sj.onc.1201110
42. Wang T, Fan L, Watanabe Y, McNeill PD, Moulton GG, Bangur C, et al. L523S, an RNA-binding protein as a potential therapeutic target for lung cancer. *Br J Cancer* (2003) 88(6):887–94. doi: 10.1038/sj.bjc.6600806
43. Jeng YM, Chang CC, Hu FC, Chou HY, Kao HL, Wang TH, et al. RNA-Binding protein insulin-like growth factor II mRNA-binding protein 3 expression promotes tumor invasion and predicts early recurrence and poor prognosis in hepatocellular carcinoma. *Hepatology* (2008) 48(4):1118–27. doi: 10.1002/hep.22459
44. Pryor JG, Bourne PA, Yang Q, Spaulding BO, Scott GA, Xu H. IMP-3 is a novel progression marker in malignant melanoma. *Mod Pathol* (2008) 21(4):431–37. doi: 10.1038/modpathol.3801016
45. Li D, Yan D, Tang H, Zhou C, Fan J, Li S, et al. IMP3 is a novel prognostic marker that correlates with colon cancer progression and pathogenesis. *Ann Surg Oncol* (2009) 16(12):3499–506. doi: 10.1245/s10434-009-0648-5
46. Zhang J, Ji Q, Jiao C, Ren L, Zhao Y, Chen Y, et al. IGF2BP3 as a potential tissue marker for the diagnosis of esophageal high-grade intraepithelial neoplasia. *Oncotargets Ther* (2017) 10:3861–66. doi: 10.2147/OTT.S141179
47. Sasaki M, Sato Y. Insulin-like growth factor II mRNA-binding protein 3 (IMP3) is a marker that predicts presence of invasion in papillary biliary tumors. *Hum Pathol* (2017) 62:152–59. doi: 10.1016/j.humpath.2016.12.028
48. Kanzaki A, Kudo M, Ansai S, Peng WX, Ishino K, Yamamoto T, et al. Insulin-like growth factor 2 mRNA-binding protein-3 as a marker for distinguishing between cutaneous squamous cell carcinoma and keratoacanthoma. *Int J Oncol* (2016) 48(3):1007–15. doi: 10.3892/ijo.2016.3323
49. Lochhead P, Imamura Y, Morikawa T, Kuchiba A, Yamauchi M, Liao X, et al. Insulin-like growth factor 2 messenger RNA binding protein 3 (IGF2BP3) is a marker of unfavourable prognosis in colorectal cancer. *Eur J Cancer* (2012) 48(18):3405–13. doi: 10.1016/j.ejca.2012.06.021
50. Guan S, He Y, Su Y, Zhou L. A risk signature consisting of eight m6A methylation regulators predicts the prognosis of glioma. *Cell Mol Neurobiol* (2022) 42(8):2733–43. doi: 10.1007/s10571-021-01135-x
51. Hong W, Gu Y, Guan R, Xie D, Zhou H, Yu M. Pan-cancer analysis of the CASP gene family in relation to survival, tumor-infiltrating immune cells and therapeutic targets. *Genomics* (2020) 112(6):4304–15. doi: 10.1016/j.ygeno.2020.07.026
52. Zhu L, Wu W, Jiang S, Yu S, Yan Y, Wang K, et al. Pan-cancer analysis of the mitophagy-related protein PINK1 as a biomarker for the immunological and prognostic role. *Front Oncol* (2020) 10:569887. doi: 10.3389/fonc.2020.569887
53. Chromecki TF, Cha EK, Pummer K, Scherr DS, Tewari AK, Sun M, et al. Prognostic value of insulin-like growth factor II mRNA binding protein 3 in patients treated with radical prostatectomy. *BJU Int* (2012) 110(1):63–8. doi: 10.1111/j.1464-410X.2011.10703.x
54. Zhou AG, Owens CL, Cosar EF, Jiang Z. Clinical implications of current developments in genitourinary pathology. *Arch Pathol Lab Med* (2013) 137(7):887–93. doi: 10.5858/arpa.2012-0210-RA
55. Liu X, Wang P, Teng X, Zhang Z, Song S. Comprehensive analysis of expression regulation for RNA m6A regulators with clinical significance in human cancers. *Front Oncol* (2021) 11:624395. doi: 10.3389/fonc.2021.624395
56. Ito Y, Miyashiro I, Ito H, Hosono S, Chihara D, Nakata-Yamada K, et al. Long-term survival and conditional survival of cancer patients in Japan using population-based cancer registry data. *Cancer Sci* (2014) 105(11):1480–86. doi: 10.1111/cas.12525
57. Yantiss RK, Woda BA, Fanger GR, Kalos M, Whalen GF, Tada H, et al. KOC (K homology domain containing protein overexpressed in cancer): a novel molecular marker that distinguishes between benign and malignant lesions of the pancreas. *Am J Surg Pathol* (2005) 29(2):188–95. doi: 10.1097/01.pas.0000149688.98333.54
58. Li C, Rock KL, Woda BA, Jiang Z, Fraire AE, Dresser K. IMP3 is a novel biomarker for adenocarcinoma *in situ* of the uterine cervix: an immunohistochemical study in comparison with p16(INK4a) expression. *Mod Pathol* (2007) 20(2):242–47. doi: 10.1038/modpathol.3800735
59. Constantinidou A, Aliferis C, Trafalis DT. Targeting programmed cell death -1 (PD-1) and ligand (PD-L1): A new era in cancer active immunotherapy. *Pharmacol Ther* (2019) 194:84–106. doi: 10.1016/j.pharmthera.2018.09.008
60. Chen EX, Jonker DJ, Loree JM, Kennecke HF, Berry SR, Couture F, et al. Effect of combined immune checkpoint inhibition vs best supportive care alone in patients with advanced colorectal cancer: The Canadian cancer trials group CO.26 study. *JAMA Oncol* (2020) 6(6):831–8. doi: 10.1001/jamaoncol.2020.0910
61. Samstein RM, Lee CH, Shoushtari AN, Hellmann MD, Shen R, Janjigian YY, et al. Tumor mutational load predicts survival after immunotherapy across multiple cancer types. *Nat Genet* (2019) 51(2):202–06. doi: 10.1038/s41588-018-0312-8
62. Riaz N, Havel JJ, Makarov V, Desrichard A, Urba WJ, Sims JS, et al. Tumor and microenvironment evolution during immunotherapy with nivolumab. *Cell* (2017) 171(4):934–49. doi: 10.1016/j.cell.2017.09.028
63. Le DT, Durham JN, Smith KN, Wang H, Bartlett BR, Aulakh LK, et al. Mismatch repair deficiency predicts response of solid tumors to PD-1 blockade. *Science* (2017) 357(6349):409–13. doi: 10.1126/science.aan6733
64. Rizvi NA, Hellmann MD, Snyder A, Kvistborg P, Makarov V, Havel JJ, et al. Cancer immunology. mutational landscape determines sensitivity to PD-1 blockade in non-small cell lung cancer. *Science* (2015) 348(6230):124–28. doi: 10.1126/science.aaa1348
65. Sabari JK, Leonardi GC, Shu CA, Umeton R, Montecalvo J, Ni A, et al. PD-L1 expression, tumor mutational burden, and response to immunotherapy in patients with MET exon 14 altered lung cancers. *Ann Oncol* (2018) 29(10):2085–91. doi: 10.1093/annonc/mdy334
66. Li R, Han D, Shi J, Han Y, Tan P, Zhang R, et al. Choosing tumor mutational burden wisely for immunotherapy: A hard road to explore. *Biochim Biophys Acta Rev Cancer* (2020) 1874(2):188420. doi: 10.1016/j.bbcan.2020.188420
67. Shiao SL, Chu GC, Chung LW. Regulation of prostate cancer progression by the tumor microenvironment. *Cancer Lett* (2016) 380(1):340–48. doi: 10.1016/j.canlet.2015.12.022
68. Bailey P, Chang DK, Nones K, Johns AL, Patch AM, Gingras MC, et al. Genomic analyses identify molecular subtypes of pancreatic cancer. *Nature* (2016) 531(7592):47–52. doi: 10.1038/nature16965
69. Pagès F, Mlecnik B, Marliot F, Bindea G, Ou FS, Bifulco C, et al. International validation of the consensus immunoscore for the classification of colon cancer: a

prognostic and accuracy study. *Lancet* (2018) 391(10135):2128–39. doi: 10.1016/S0140-6736(18)30789-X

70. Wu J, Li L, Zhang H, Zhao Y, Zhang H, Wu S, et al. A risk model developed based on tumor microenvironment predicts overall survival and associates with tumor immunity of patients with lung adenocarcinoma. *Oncogene* (2021) 40(26):4413–24. doi: 10.1038/s41388-021-01853-y

71. van der Leun AM, Thommen DS, Schumacher TN. CD8+ T cell states in human cancer: insights from single-cell analysis. *Nat Rev Cancer* (2020) 20(4):218–32. doi: 10.1038/s41568-019-0235-4

72. Hinshaw DC, Shevde LA. The tumor microenvironment innately modulates cancer progression. *Cancer Res* (2019) 79(18):4557–66. doi: 10.1158/0008-5472.CAN-18-3962

73. Roberts PJ, Der CJ. Targeting the raf-MEK-ERK mitogen-activated protein kinase cascade for the treatment of cancer. *Oncogene* (2007) 26(22):3291–310. doi: 10.1038/sj.onc.1210422

74. Suvasini R, Shruti B, Thota B, Shinde SV, Friedmann-Morvinski D, Nawaz Z, et al. Insulin growth factor-2 binding protein 3 (IGF2BP3) is a glioblastoma-specific marker that activates phosphatidylinositol 3-kinase/mitogen-activated protein kinase (PI3K/MAPK) pathways by modulating IGF-2. *J Biol Chem* (2011) 286(29):25882–90. doi: 10.1074/jbc.M110.178012

75. Wang Y, Zhou C, Luo H, Cao J, Ma C, Cheng L, et al. Prognostic implications of immune-related eight-gene signature in pediatric brain tumors. *Braz J Med Biol Res* (2021) 54(7):e10612. doi: 10.1590/1414-431X2020e10612

Glossary

RBP	RNA-binding protein
m6A	N6-methyladenosine
METTL3	methyltransferase-like protein 3
METTL14	methyltransferase-like 14
WTAP	Wilms-tumour associated protein
FTO	fat mass and obesity-associated protein
ALKBH5	AlkB homolog 5
TCGA	The Cancer Genome Atlas
GTE _x	Genotype-Tissue Expression
CCL	Cancer Cell Line Encyclopedia
HPA	Human Protein Atlas
DEGs	differentially expressed genes
TPM	transcripts per million reads
FC	fold-change
OS	overall survival
DSS	disease-specific survival
PFI	progression-free interval
WHO	World Health Organization
PD	progressive disease
SD	stable disease
PR	partial response
CR	complete response
TMB	tumor mutational burden
MSI	microsatellite instability
PPI	protein–protein interaction
KEGG	Kyoto Encyclopedia of Genes and Genomes
GSEA	Gene Set Enrichment Analysis
EMT	epithelial–mesenchymal transition
ACC	adrenocortical carcinoma
BLCA	bladder urothelial carcinoma
BRCA	breast invasive carcinoma
CESC	cervical squamous cell carcinoma and endocervical adenocarcinoma
CHOL	cholangiocarcinoma
COAD	colon adenocarcinoma
DLBC	lymphoid neoplasm diffuse large B-cell lymphoma
ESCA	esophageal carcinoma
GBM	glioblastoma multiforme
HNSC	head and neck squamous cell carcinoma
KICH	kidney chromophobe

(Continued)

Continued

KIRC	kidney renal clear cell carcinoma
KIRP	kidney renal papillary cell carcinoma
LAML	acute myeloid leukemia
LGG	brain lower grade glioma
LIHC	liver hepatocellular carcinoma
LUAD	lung adenocarcinoma
LUSC	lung squamous cell carcinoma
MESO	mesothelioma
OV	ovarian serous cystadenocarcinoma
PAAD	pancreatic adenocarcinoma
PCPG	pheochromocytoma and paraganglioma
PRAD	prostate adenocarcinoma
READ	rectum adenocarcinoma
SARC	sarcoma
SKCM	skin cutaneous melanoma
STAD	stomach adenocarcinoma
TGCT	testicular germ cell tumors
THCA	thyroid carcinoma
THYM	thymoma
UCEC	uterine corpus endometrial carcinoma
UCS	uterine carcinosarcoma
UVM	uveal melanoma



OPEN ACCESS

EDITED BY

Catherine Sautes-Fridman,
U1138 Centre de Recherche des Cordeliers
(CRC) (INSERM), France

REVIEWED BY

Rachael Rowsell-Turner,
University of Rochester, United States
Aishwarya Gokuldass,
Amgen, United States

*CORRESPONDENCE

John A. Carucci
✉ John.carucci@nyulangone.org

SPECIALTY SECTION

This article was submitted to
Cancer Immunity
and Immunotherapy,
a section of the journal
Frontiers in Immunology

RECEIVED 31 October 2022

ACCEPTED 13 January 2023

PUBLISHED 30 January 2023

CITATION

Saeidi V, Doudican N and Carucci JA
(2023) Understanding the squamous cell
carcinoma immune microenvironment.
Front. Immunol. 14:1084873.
doi: 10.3389/fimmu.2023.1084873

COPYRIGHT

© 2023 Saeidi, Doudican and Carucci. This is
an open-access article distributed under the
terms of the [Creative Commons Attribution
License \(CC BY\)](#). The use, distribution or
reproduction in other forums is permitted,
provided the original author(s) and the
copyright owner(s) are credited and that
the original publication in this journal is
cited, in accordance with accepted
academic practice. No use, distribution or
reproduction is permitted which does not
comply with these terms.

Understanding the squamous cell carcinoma immune microenvironment

Vahide Saeidi, Nicole Doudican and John A. Carucci*

Section of Dermatologic Surgery, Ronald O. Perleman Department of Dermatology, New York
University Langone Medical Center, New York, NY, United States

Primary cutaneous squamous cell carcinoma (cSCC) is the second most common human cancer with a rising incidence of about 1.8 million in the United States annually. Primary cSCC is usually curable by surgery; however, in some cases, cSCC eventuates in nodal metastasis and death from disease specific death. cSCC results in up to 15,000 deaths each year in the United States. Until recently, non-surgical options for treatment of locally advanced or metastatic cSCC were largely ineffective. With the advent of checkpoint inhibitor immunotherapy, including cemiplimab and pembrolizumab, response rates climbed to 50%, representing a vast improvement over chemotherapeutic agents used previously. Herein, we discuss the phenotype and function of SCC associated Langerhans cells, dendritic cells, macrophages, myeloid derived suppressor cells and T cells as well as SCC-associated lymphatics and blood vessels. Possible role(s) of SCC-associated cytokines in progression and invasion are reviewed. We also discuss the SCC immune microenvironment in the context of currently available and pipeline therapeutics.

KEYWORDS

squamous cell carcinoma, tumor microenvironment, PD-1, tumor infiltrating lymphocytes, exhausted T cells, cytokines

1 Introduction

Cutaneous SCC (cSCC) is the second most frequent skin cancer in the United States (US) with 1.8 million new cases each year, and its global incidence rate has been reported to increase 3-7% annually (1, 2). cSCC lesions appear in regions that are most exposed to ultraviolet (UV); the head and the neck are the most common sites followed by the trunk and extremities (3).

UV radiation can alter the genome of epidermal cells and cause SCC development and subsequent metastasis, usually to nearby lymph nodes. A complex network of genes (TP53, CDKN2A, NOTCH1, NOTCH2, EGFR and TERT) and molecular pathways (RAS/RAF/MEK/ERK and PI3K/AKT/mTOR) are associated with the pathogenesis of cSCC (4). Also, recent findings identified EP300, PBRM1, USP28, and CHUK as four novel genes that are mutated in greater than 10% of cSCCs (5). The top three recurrently altered genes in metastatic cSCCs are TP53, CDKN2A, and NOTCH1/2 (6-8).

In addition to UV exposure ionizing radiation, fair skin, chronic immunosuppression, genetic conditions, the presence of chronic wounds or scars, smoking, chemical carcinogens, and human papillomavirus (HPV) infection are the other risk factors of cSCC development (9). The vast majority of cSCC cases are treated successfully by excision with clear margins (10, 11); however, these tumors can be aggressive and responsible for most of the ~15,000 non-melanoma skin cancer deaths in the United States each year (1). Patients with localized cSCC have a favorable prognosis with a 5-year survival rate of 99% following Mohs micrographic surgery (12, 13). Metastasis affects approximately 3.7%–5.2% of all SCC patients (14). The expected 5-year and 10-year survival rates in these patients decreases to 25–50% and 16%, respectively (11, 15–17).

Advanced cSCC is described as either a locally advanced disease that is untreatable by surgery or radiation therapy (RT), a metastatic disease with distant metastases, or large, multiple, and extracapsular nodal disease with a high risk of recurrence despite lymphadenectomy and radiation therapy (18). Cemiplimab, an immune checkpoint inhibitor, is the first medication approved in the United States for advanced cSCC (19). It is a human monoclonal antibody that inhibits the PD-1 pathway by blocking T-cell inactivation, thus assisting the immune system in fighting cancer cells (20) as illustrated in Figure 1. Cemiplimab exhibits an overall response rate of 50%, which is a significant improvement over conventional chemotherapy. It has been shown that cemiplimab has a significant antitumor function with long-lasting response, and acceptable safety profile in patients (19). Pembrolizumab is another PD-1 inhibitor, with a similar mechanism to cemiplimab, and has been recently approved in the United States for recurrent or metastatic cSCC that is incurable with surgery or radiation therapy (21). A case of metastatic cSCC treated with nivolumab, another PD-1 inhibitor, has been reported, and the patient exhibited a complete response to this treatment (22). In another case report, a patient with unresectable recurrent scalp

cSCC with meningeal invasion was successfully treated with nivolumab monotherapy (23).

Lymphocyte activation gene 3 (LAG3) is an inhibitory receptor that is expressed on CD4⁺, CD8⁺, regulatory T (T-reg) cell, natural killer cell, B cell, and other immune cells (24). LAG3 serves a negative regulatory role in cancer immunology by interacting with its ligands. Higher LAG3 expression has been reported in head and neck squamous cell carcinoma compared to normal tissues. Therefore, LAG3-targeting agents could represent another promising checkpoint inhibitor immunotherapy for these malignancies (25). Combining immunotherapy and radiotherapy is another cutting-edge method of treating cSCC (26). The trials of radiation therapy and cemiplimab in patients with skin cancer (NCT05574101) as well as radiotherapy in combination with atezolizumab (PD-L1 inhibitor) in locally advanced borderline resectable or unresectable cSCC (NCT05085496) are ongoing. Another ongoing trial is testing cetuximab (EGFR inhibitor) before surgery in the treatment of patients with aggressive locally advanced skin cancer (NCT02324608).

The efficacy of talimogene laherparepvec (oncolytic viral immunotherapy) and panitumumab (EGFR inhibitor) for the treatment of locally advanced or metastatic cSCC is being researched in another ongoing trial (NCT04163952).

The development and progression of non-melanoma skin cancer (NMSC) are significantly influenced by immune system function (27). An increased incidence of cSCC in immunocompromised solid organ transplant recipients indicates the critical role of the immune surveillance in host protection (28). The immune system recognizes cancer cells as abnormal and can eliminate them in some cases (29); however, tumor cells might evade immune surveillance through immunoediting processes (30). Cancer cells utilize several mechanisms to escape immune surveillance, including MHC loss and expression of immunosuppressive factors, such as IL-6, IL-10, TGF- β , prostaglandins, and Fas ligand (31, 32).

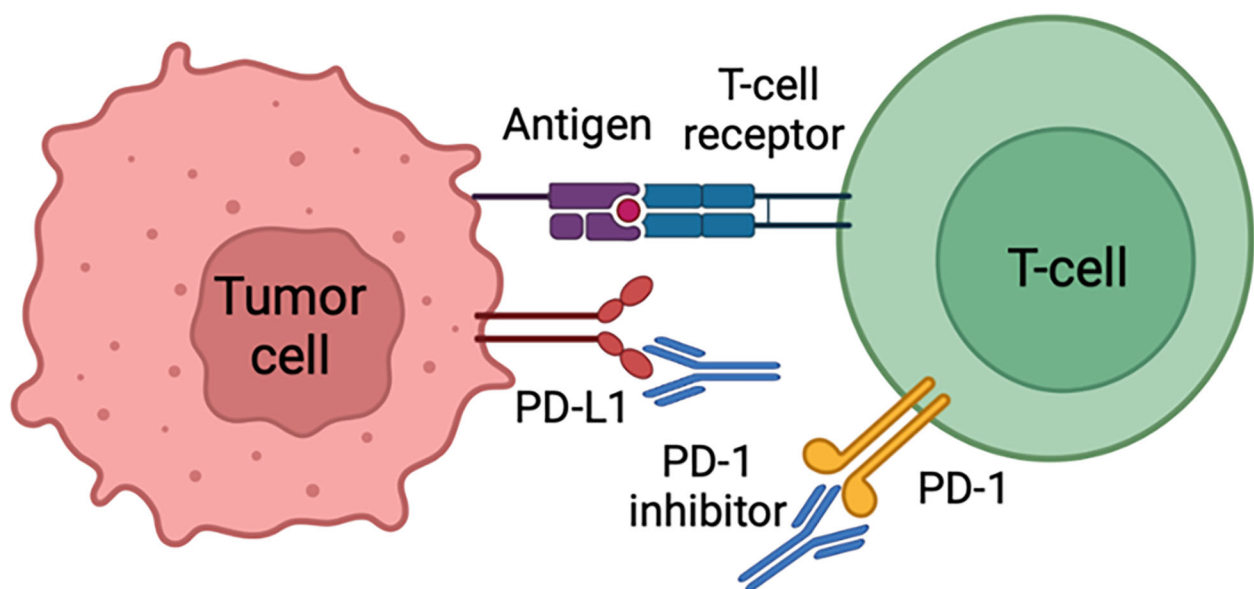


FIGURE 1

Cancer cells can evade immune surveillance by expressing PD-L1 protein that acts as a “stop sign” to inactivate T cells. PD-L1 attaches to PD-1 and B7.1 T cell receptors, both of which inactivate T cells. Cemiplimab prevents T cell inactivation and subsequently increases anti-cancer activity through PD-L1 blockade.

The tumor microenvironment is characterized as a combination of tumoral and non-tumoral cells at the dynamic interface of neoplasia (33). Although non-tumoral cells within the tumor microenvironment may have protective functions in limiting tumor progression, many studies show that they have also an important role in tumor growth and metastasis (34). Therefore, it is crucial to understand the features of the cSCC tumor-associated immune microenvironment in detail to develop reliable prognostic markers and new advanced treatments.

In this review, phenotype and functions of cSCC-associated Langerhans cells, dendritic cells, macrophages, myeloid-derived suppressor cells and T cells as well as cSCC-associated lymphatics and blood vessels are discussed. Moreover, the potential roles of cSCC-associated cytokines in progression and invasion of the tumor are described.

2 Myeloid-derived suppressor cells in SCC

Myeloid-derived suppressor cells (MDSCs) are pathologically activated neutrophils and monocytes with immunosuppressive activity. They participate in the regulation of immune responses in many pathological conditions, such as cancer, chronic infection, sepsis, and autoimmunity. Two major groups of MDSCs in humans include granulocytic/polymorphonuclear MDSCs (PMN-MDSCs) and monocytic MDSCs (M-MDSCs), which originate from the granulocytic and monocytic myeloid cell lineages, respectively (35). MDSCs are related to poor outcomes in cancer (36). It has been shown that high levels of circulating MDSC in patients with solid tumors, were related to poor overall survival (37).

In cancer patients, these cells express the common myeloid marker CD33 but not mature myeloid and lymphoid cell markers in cancer patients. In humans, MDSCs are identifiable as lineage (CD3, CD14, CD19, CD56)–negative, HLA-DR–negative, and CD33-positive or CD33⁺CD14[−]CD11b⁺ cells (38, 39).

The signals driving MDSCs development occur in two partially overlapping phases. Expansion of immature myeloid cells occurs in phase 1, and neutrophils and monocytes convert to pathologically activated MDSCs in phase 2 (38).

MDSCs are one of the major factors responsible for immune suppression in cancers that not only cause tumor progression but also result in the failure of immunotherapy (39). Arginase, nitric oxide (NO), and reactive oxygen species (ROS) have all been shown to play a role in MDSC-mediated T-cell suppression (40). MDSCs are critical producers of NO in SCC, which suppresses E-selectin expression on tumor vessels. Subsequently, the entry of skin homing T-cells into tumors are restricted, resulting in evasion of SCC from immune detection (41).

Clearly, a successful cancer immunotherapy will be possible if the immune suppressive factors can be eliminated from the body. As MDSCs are one of the major immune suppressive factors in cancers, the challenge of effectively and selectively targeting MDSCs remains (39). Medications that diminish NO production e.g., iNOS inhibitors, may be effective in the treatment of SCCs and their premalignant precursor lesions actinic keratoses through improvement of anti-

tumor immune responses (41). Based on earlier studies, all-trans retinoic acid (ATRA) promotes the differentiation of M-MDSCs into macrophages and DCs and apoptosis of PMN-MDSCs in both mice and humans (42–44). Concurrent use of ATRA therapy with CTLA-4 blockade was tested in melanoma patients and resulted in decrease in the number of circulating MDSCs. Therefore, targeting MDSCs in combination with immunotherapies may improve response rates and effectiveness in other skin cancers (45).

3 Tumor-associated macrophages

Macrophages are important tumor-infiltrating cells (46) contributing to different carcinogenesis stages, including initiation, growth, invasion, and metastasis (47, 48). More macrophages are present in SCC compared with normal skin (49). Macrophages surrounding and penetrating the tumor are termed tumor-associated macrophages (TAMs) (46).

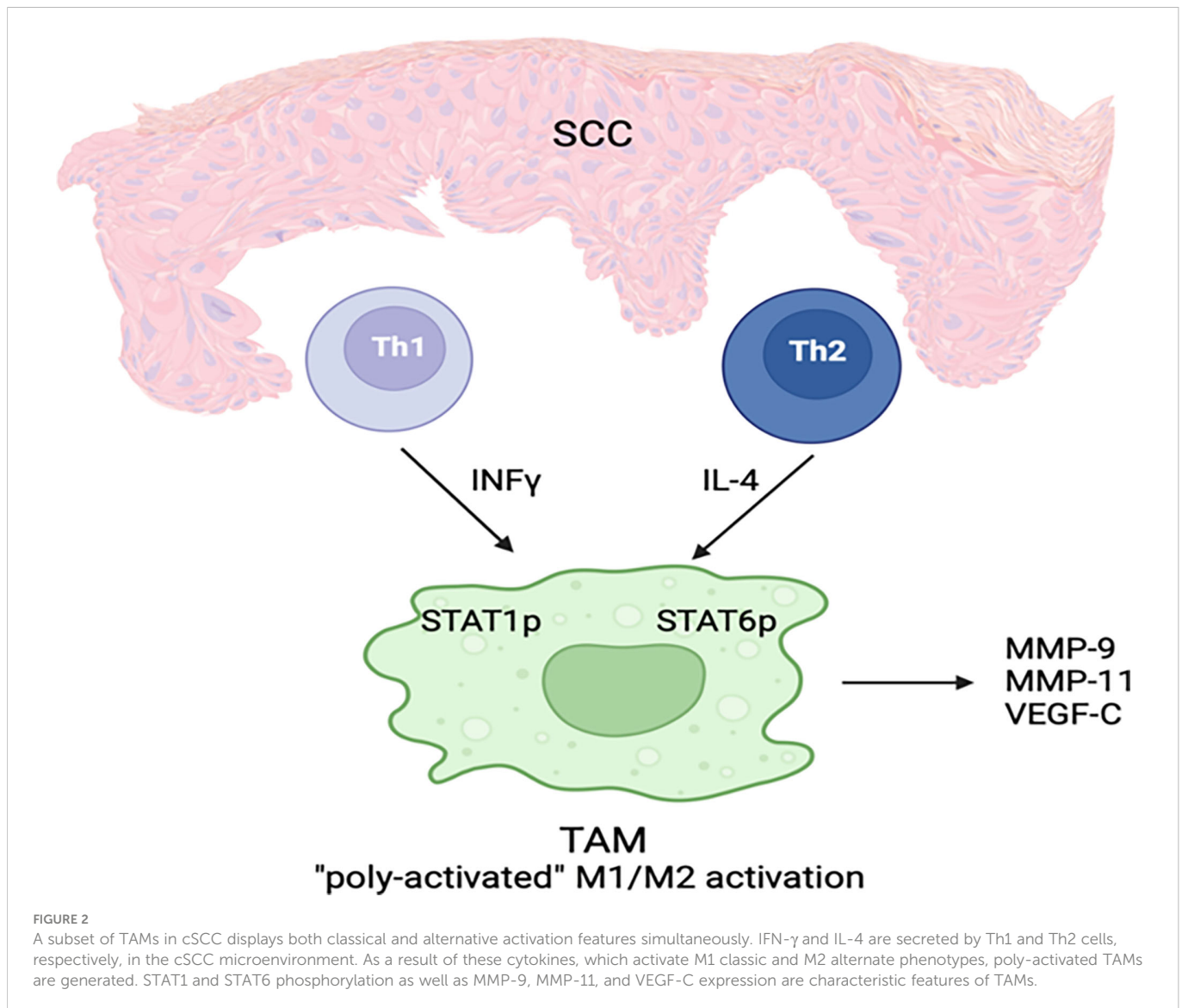
In response to tumors, macrophages display a polarized reaction defined by two different states: classically activated macrophage (M1) and alternatively activated macrophage (M2). M1 macrophages are activated by interferon- γ (IFN- γ), bacterial lipopolysaccharide (LPS), or tumor necrosis factor- α (TNF- α) and release interleukin 12 (IL-12) to prevent tumor growth. In contrast, M2 macrophages are activated by IL-4 and release IL-10, which contributes to tumor progression (27, 50–52).

Tumor-associated macrophages have many similar characteristics to alternatively activated macrophages (M2 macrophages) (46). Based on recent studies, macrophage activation in SCC is heterogenous and there are three types of TAMs: TAMs expressing M1 markers, TAMs expressing M2 markers and TAMs simultaneously expressing M1 and M2 (49) (Figure 2). It is believed that tumors can generate a dynamic microenvironment that alters the TAMs into macrophages that help tumor growth (53). Weaker classical macrophage activation in SCC cause TAMs to produce more tumorigenic growth factors (49). Increased TAM levels are associated with poor prognosis in various human malignancies (47, 48, 54).

Heterogeneous activation of TAMs in SCC suggests potential treatment strategies contributing to the induction of a more dominant M1 activation state with anti-cancer phenotype (27).

TAMs in SCC may produce matrix metalloproteinases (MMPs) that may aid tumor invasion. A positive correlation between MMP-9 (gelatinase B) and MMP-11 (stromelysin-3) proteins and increased tumor aggressiveness has been revealed (55–58). TAMs also contribute to lymphangiogenesis through vascular endothelial growth factor-C (VEGF-C) expression (59). It has been reported that enhanced lymph vessel density is related to increased risk of metastasis in the oral cavity SCC and melanoma (60, 61).

TAM densities and functional immunophenotypes differ in human cutaneous SCCs and BCCs, which can contribute to behavioral differences between these two tumors. It has been shown that SCCs express more TAM-associated markers (MMP-9, arginase-1, CD127 and CD40) compared with BCCs, and TAMs in SCC have a higher density and polarization state. Lactic acid levels are higher in SCCs compared with BCCs, and tumor-derived lactic acid is an important factor playing a role in TAM polarization in SCCs (62).



In fact, TAMs in SCC, due to weaker classical macrophage activation and higher production of tumorigenic growth factors, are unable to prevent tumor genesis and in fact they can even facilitate tumor growth; however, they contribute to tumor invasion and metastasis through production of high levels of MMPs, more dominant M2 activation and lymphangiogenic mediator (VEGF-C) expression (27).

CD200 (a known immunosuppressive surface protein) is overexpressed in stroma around cSCC, mainly by blood vessel endothelia. CD200 is also expressed on cSCC tumor cells (63). In addition, more CD200R⁺ cells are located in the cSCC microenvironment than normal skin, and CD200R was detected on macrophages and dendritic cells (28). Increased CD200 expression on tumor cells is associated with tumor progression and decreased patient survival (63, 64). Endothelial CD200 may inhibit aberrant diapedesis of macrophages during inflammation partly through downregulation of macrophage adhesion molecules. Hence, through this mechanism, CD200 may play a role in suppression of macrophage function (65). Moreover, binding of endothelial CD200 to CD200R on macrophages and dendritic cells inhibits

proinflammatory activation (66–70) and suppresses classic activation of macrophages; therefore, M2 cells become the predominant macrophage polarized state (71).

Anti-CD200 antibody (through blocking the CD200-CD200R interaction) has been shown to improve antitumor activity against CD200-expressing human tumors in a mouse model (72, 73). Thus, anti-CD200 therapies could represent effective treatments for aggressive SCCs (28).

4 Dendritic cells and Langerhans cells

Dendritic cells (DC) are antigen-presenting cells (APCs) that play an important role in linking the innate and adaptive immune systems (74). The ability of DCs to induce tumor-specific T-cell responses facilitates their vital role in cancer immune surveillance (75).

Three main subsets of cutaneous DCs in humans include Langerhans cells (LCs), myeloid DCs (mDCs), and plasmacytoid DCs (pDCs) (76). As Langerhans cells are found in the epidermis, they are the first APCs to encounter SCC (77). LCs from human SCC

can stimulate CD8⁺ or NK-cell-mediated response more efficiently than other DC subsets, resulting in a more robust proliferation of naive CD8⁺ T cells (78).

In addition to the primary role of DCs in initiating the cellular immunity, they are also involved in polarizing the naive CD4⁺ T cells towards a Th2 immune response through releasing type II cytokines, such as IL-4, IL-5, and IL-13 (79). Furthermore, it has been reported that LCs from SCC were more powerful inducers of allogeneic CD4⁺ and CD8⁺ T-cell proliferation and IFN- γ production compared to those from normal skin and eventually more potent in activating type 1 T-cell responses (77).

Tumor-induced dendritic cells dysfunction (29) and tumor-induced DC apoptosis (80–82) are two of major strategies used by tumors to escape immune surveillance.

Several studies have revealed that the number of both LCs and CD11c⁺ dermal DCs is markedly reduced in SCC lesions (83, 84) and the ability of the dermal myeloid DCs to activate T cells and stimulate the production of interferon (IFN)- γ is diminished (83, 85).

Higher levels of immunosuppressive cytokines, such as TGF- β , IL-10, IL-6 and VEGF-A, in the microenvironment of SCCs are

believed to be possible causes of mDCs suppression (83). IL-10 has the potential to inhibit the differentiation of monocytes to DC (86), weaken APC function of DCs (87, 88), suppress DCs' ability to activate T cells, and cause induction of antigen-specific anergy (89). Increased VEGF levels are related to decreased number of DCs in tumor lesion and in the peripheral blood of patients with various malignant tumors. This finding demonstrates the ability of VEGF to inhibit DC differentiation (90–92).

The presence of large numbers of pDCs is another distinguishing feature of the SCC tumor microenvironment (83). These cells facilitate tumor eradication through production of large quantities of IFN- α in response to foreign antigen. Moreover, pDCs can recognize, process, and cross-present foreign antigen to CD8⁺ T lymphocytes (93, 94). Despite lower antigen uptake by pDCs compared to mDCs, pDCs may still be effective in anti-tumor immune response (Figure 3) (95).

It can be concluded that DCs are desirable targets for tumor immunotherapy due to their capacity to link the innate and adaptive immune systems as well as their ability to initiate the immune response (74). In addition, human LCs have been shown to be

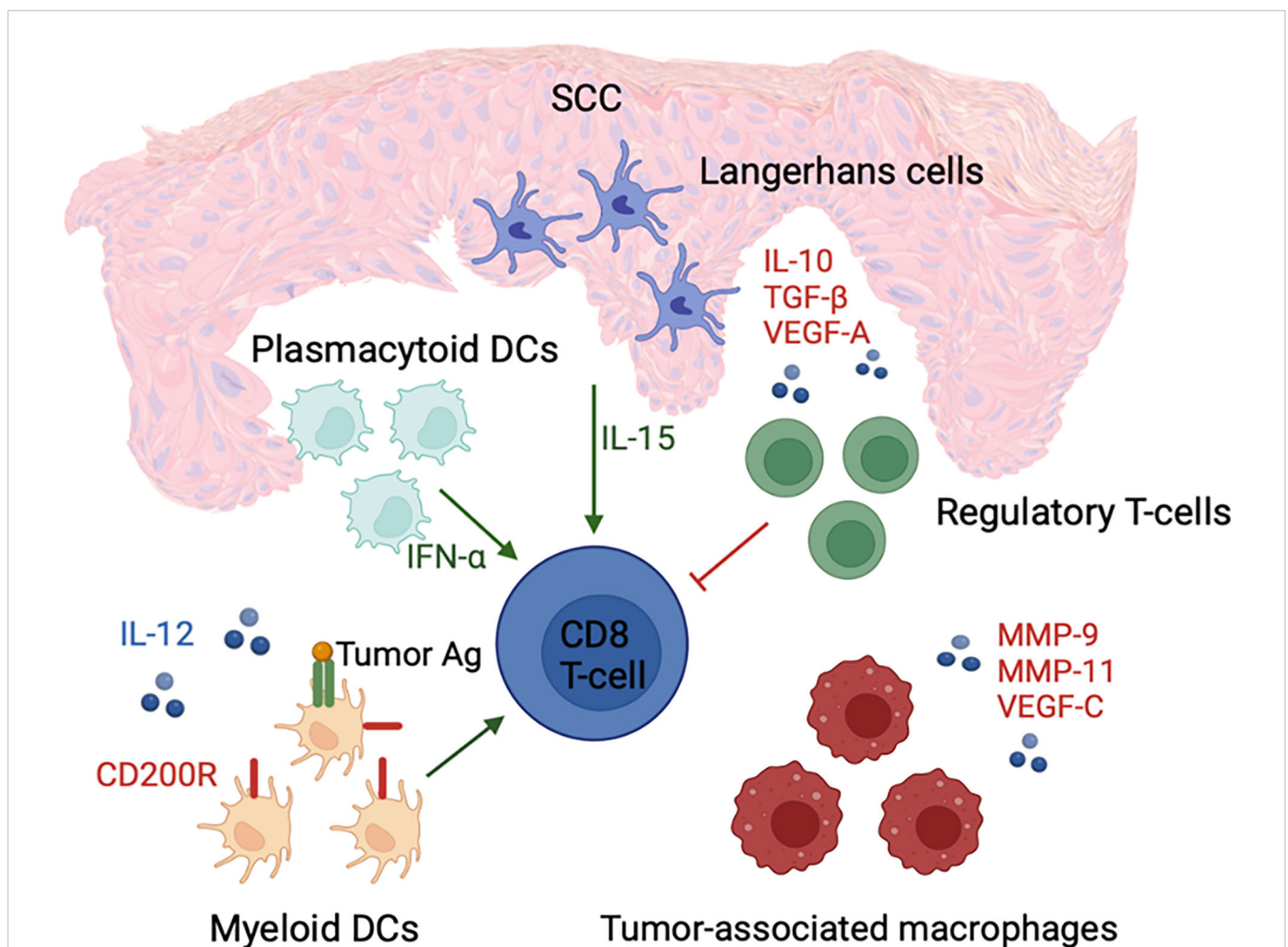


FIGURE 3

cSCC microenvironment is associated with an increased number of IFN- α -secreting pDCs and LCs with enhanced ability to activate CD8⁺ T cells, which potentially promote immunosurveillance. In contrast, an increased number of regulatory T cells; tumor-associated macrophages; and immune suppressive cytokines, such as IL-10, TGF- β , and VEGF-A, are present in the tumor microenvironment. These factors contribute to tumor growth and immune dysfunction through suppression of mDC and CD8⁺ T cell activity.

more potent inducers of type 1 T-cell response in the cSCC microenvironment. Hence, LCs can be used in DC-based cancer immunotherapy as a promising novel strategy in the treatment of skin malignancies (77).

5 T-lymphocytes

Numerous immune cells, including T-cells, are found in SCC lesions (96–98). Despite T cell infiltration into cutaneous SCC (cSCC), these cells are incapable of eradicating the tumor (99, 100).

It has been demonstrated that SCC and transplant-associated SCC (TSCC) microenvironments have significantly greater numbers of CD3⁺ and CD8⁺ T cells than normal skin. These cells accumulate predominantly in the peritumoral region and are less frequently noted within the tumoral region. The number of FOXP3⁺ T reg cells is increased in both SCC and TSCC compared to normal skin (101). Approximately more than 50% of the T cells infiltrating cSCCs from both immunocompetent and immunosuppressed patients are FOXP3⁺ T reg cells (97). These cells are CD4⁺ and lack CLA, CCR4, and CCR6 (skin resident T reg markers) (102). Moreover, these cells express markers of central memory T cells, such as L-selectin and CCR7. Given that T reg cells do not proliferate locally in tumors, recruitment from the blood may be the main mechanism responsible for significant presence of these cells in tumors (97).

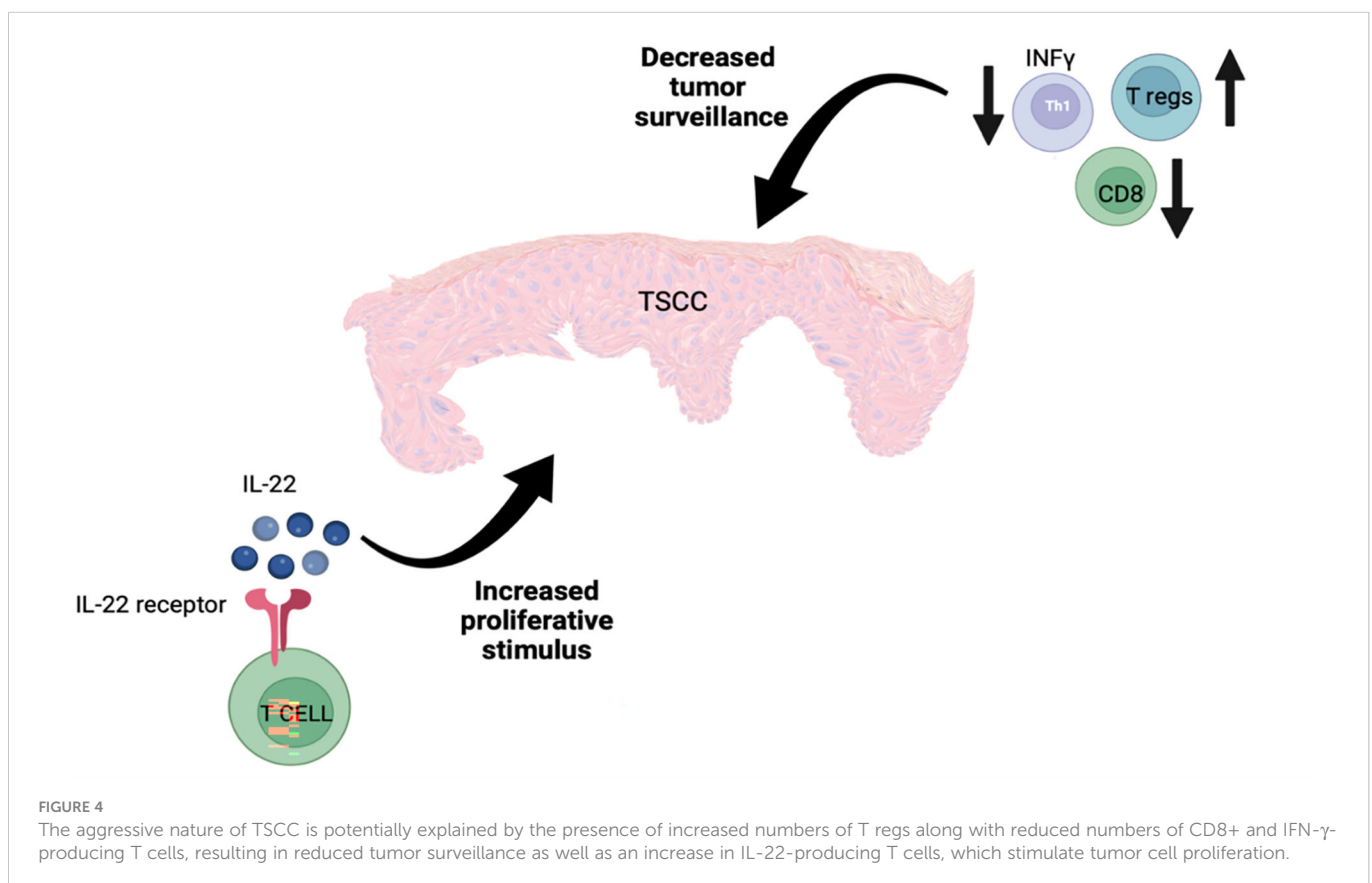
Although FOXP3⁺ T reg cells contribute to immune tolerance (103), which is important for preventing autoimmune diseases (104), they may suppress antitumor immunity (105, 106) and play a role in

immune evasion. Particularly, the immune response can be regulated by T reg cells by suppressing the proliferation and cytokine production of effector T cells (107, 108).

Based on several studies, the greater number of tumor infiltrating T regs is related to poor prognosis and lower survival rates in breast (109), ovarian (110, 111) and gastric carcinomas (105). T regs may contribute to cSCC metastasis and thus have potential prognostic significance (100). Some recent studies have identified CD8⁺ Tregs in cSCC (112) and other tumors (113) that exhibit even stronger regulatory activities compared to CD4⁺ Tregs (114). Given its ability to decrease the number of FOXP3⁺ T reg cells and inhibit T reg cell function, imiquimod could effectively inhibit the immunological destruction of cSCC (97).

TSCC has a distinct immune microenvironment that promotes tumor growth. There are fewer T cells, especially CD8⁺ T cells, in TSCC lesions in comparison to SCC lesions (101), and a decreased Tc/Treg ratio in TSCC has also been reported (112). Furthermore, an increased number of IL-22 producing CD8⁺ T cells and decreased number of CD4⁺ Th1 T cells have been revealed in TSCC lesions. Higher T regs and lower CD8⁺ T cells, which result in decreased immune surveillance, and increased exposure to IL-22, which enhances tumor proliferation, represent two main factors that contribute to the aggressive nature of TSCC (101) (Figure 4).

Compared to photodamaged skin, SCCs are associated with an increased number of CD4⁺ T-cells. However, compared to premalignant lesions, including intraepidermal carcinoma (IEC), SCCs may also be associated with fewer numbers of CD8⁺ T-cells. The ratio of CD4⁺ to CD8⁺ T-cells is significantly increased in SCC compared to IEC (115).



6 Lymphatic and blood vessels

The lymphatic vascular system is the main pathway for metastatic spread in SCCs. Various cancers can cause lymphangiogenesis, which is associated with increased expression of vascular endothelial growth factors as well as increased relative lymphatic vessel area (LVA) or lymphatic vessel density (LVD) (59, 116, 117). In this context, overexpression of genes related to lymphangiogenesis and increased LVD has been shown in cSCC compared to normal skin (118).

The risk of metastasis in SCCs is related to several variables, including tumor thickness, horizontal tumor size, and desmoplastic growth (11, 15–17). Tumor thickness has been shown to be the most accurate predictive factor for metastasis in SCCs. Metastatic SCCs are associated with increased lymphangiogenesis; however, the extent depends on the thickness of the tumor. It has been shown that greater tumor thickness in SCCs is accompanied by an increase in relative lymphatic vessel area and lymphatic vessel density (118). Despite clear excision margins in SCCs, increased dermal lymphangiogenesis can facilitate metastatic spread (59).

VEGF-C is a key lymphangiogenesis mediator (119). Increased VEGF-C levels in the tumor and the juxta-tumoral dermis of cSCC compared with normal skin have been reported, and it has been suggested that tumor-associated macrophages may play an important role in lymphangiogenesis through production of VEGF-C (59).

Podoplanin is a distinctive immunohistochemical marker of lymphatic endothelial cells. Overexpression of podoplanin in both tumor cells and stroma of cSCC have been reported (120). Additionally, a positive correlation is noted between the expression of podoplanin in intratumoral and peritumoral regions of cSCC and the Broder's tumor differentiation grades (121–123) as well as the depth of tumor invasion to the dermis based on the Clark's scale (124). According to several studies, increased podoplanin expression is associated with a higher mean of LVD in the SCC microenvironment (120, 124–126) and presence of LN metastasis in SCC patients (120, 121, 127, 128). Therefore, podoplanin could be used as a predictor of SCC prognosis given that increased podoplanin expression is related to poor prognosis and decreased survival in cSCC patients (120).

Most immune cells have their first contact with a tumor through endothelial cells of the local blood vessels (28). Endothelial cell integrity is believed to play an important role in tumors. Normal endothelial cells promote homeostasis, but dysfunctional endothelial cells can lead to cancer growth (129). Abnormal angiogenesis also contributes to tumor growth and promotes metastatic spread. The density of neovascularization in cSCC is positively correlated with deeper invasions and poorer tumor differentiation. As a result, SCC tumors with high angiogenic activity are classified as aggressive with poor prognosis (130). Podoplanin represents a potential target for antimetastatic therapy in cSCC. A cancer-specific monoclonal antibody against human podoplanin has been demonstrated to be an effective treatment strategy particularly in podoplanin-expressing malignancies (131).

7 Cytokines

Cytokines play an important role in tumor biology. It was previously thought that IFN- γ and other Th1 cytokines exhibit antitumor activity, whereas IL-4 and other Th2 cytokines have protumor function (132). However, based on recent studies, some cytokines, such as IFN- γ , have been shown to have pro-tumor or anti-tumor functions depending on the tumor type and tumor microenvironment (133).

High serum levels of proinflammatory cytokines, such as interleukin (IL)-1, IL-6, IL-8, and TNF- α , are often related to tumor growth and poor clinical prognosis in cancer patients (134–137). It has been suggested that the balance between multiple cytokines may contribute to the SCC pathogenesis (138). Several cytokines, including IL-6, IFN- γ , TGF- β and GM-CSF, play a role in keratinocyte proliferation and SCC development (139–143).

Significantly elevated serum IFN- γ levels have been reported in SCC patients compared with normal subjects, and higher IFN- γ levels in SCC patients are correlated with more advanced cancer stages. The combination of serum IFN- γ and TGF- β levels is more reliable for diagnosis of SCC, whereas measurement of serum IFN- γ alone is helpful in evaluating the SCC progression from early to middle stages (138).

Elevated serum IL-6 levels are associated with increased malignancy and poor prognosis in different types of tumors (144–146). It has been demonstrated that IL-6 is important in transforming benign tumors into malignant, invasive SCCs in the HaCaT cell model of skin carcinogenesis. A complex, reciprocally regulated cytokine network induced by IL-6 in the tumor cells, including inflammatory cytokines (MCP-1, GM-CSF, and IL-8) and angiogenic factor (VEGF), results in malignant and invasive tumor growth *in vivo* and stimulates tumor cell proliferation and migrations. These findings indicate that IL-6 could represent a great target for effective cSCC treatment (147).

IL-24 overexpression has been noted in invasive cSCC. IL-24 facilitates cSCC invasion (132) by increasing focal MMP-7 expression, and MMP-7 promotes cancer cell proliferation, migration, and invasion (148).

According to several reports, constitutive expression of G-CSF and GM-CSF together has been shown in SCCs (149–151). Through induction of cell proliferation, migration, and angiogenesis in cSCCs, G-CSF and GM-CSF contribute to tumor growth, invasion, and metastasis (149, 150, 152).

Transforming growth factor- β (TGF- β) signaling is mediated by several downstream proteins, such as Smad family proteins. This signaling pathway has a paradoxical role by acting as a tumor-suppressor or tumor-promoting factor in many types of cancers, such as SCC. In the early stages of SCC, TGF- β 1 and TGF- β RI act as tumor suppressors. However, in later stages, these proteins promote tumor growth. Smad2, TGF- β RII, and Smad4 are typically considered tumor suppressors in SCC (153).

IL-22 is produced by CD4⁺ helper T lymphocytes (Th), such as Th1, Th17, and Th22 as well as a subset of CD8⁺ cytotoxic T cells

(Tc22) (154–157). Significantly increased IL-22 is noted in the peritumoral regions of SCC and TSCC compared to normal skin. In transplant patients, overexpression of IL-22 and IL-22R facilitate tumor growth (101) and result in poorer prognosis (158). In addition to the role of IL-22 in cell proliferation, it can reduce IFN- γ production by Th1 cells as well as increase the production of immunosuppressive cytokines (159). It has been proposed that treating highly aggressive forms of SCCs in transplant patients by targeting the IL-22 pathway could represent an important, life-saving strategy (101).

8 Discussion

Skin malignancies are the most prevalent human cancers, and the immune system plays an important role in their development, progression, and eradication (160). There are approximately 1 million memory T cells/cm² in normal human skin, which is approximately twofold the number of T cells that exist in the entire circulation (161), indicating the importance of cutaneous immune surveillance as part of the immune system.

The immune microenvironment surrounding the cSCC is dynamic and contains contradictory forces that promote and suppress tumor growth (72, 162–165).

To summarize, the cSCC microenvironment has more Tregs and myeloid-derived suppressor cells that suppress immune responses and fewer mDCs with poor antigen-presenting function. The macrophages present in the cSCC microenvironment predominantly exhibit the M2 phenotype and promote tumor invasion and metastasis through producing MMPs and lymphangiogenic mediators. The SCC microenvironment is rich in IL-6, IFN- γ , TGF- β , GM-CSF, and

IL-24, which induce tumor growth and invasion. Moreover, increased dermal lymphangiogenesis facilitates metastatic spread. Overexpression of IL-22 and IL-22R accelerate tumor proliferation and subsequently result in poorer prognosis in transplant patients with cSCCs.

Author contributions

VS performed literature searches and composed initial draft of the manuscript. ND co-wrote initial draft and participated in all revisions. JAC conceived the original concept and provided multiple revisions of the manuscript. All authors contributed to the article and approved the submitted version.

Conflict of interest

JC has been the recipient of funding for investigator initiated basic science research from Regeneron and GlaxoSmithKline.

The remaining authors declare that the research was conducted in the absence of any commercial or financial relationships that could be construed as a potential conflict of interest.

Publisher's note

All claims expressed in this article are solely those of the authors and do not necessarily represent those of their affiliated organizations, or those of the publisher, the editors and the reviewers. Any product that may be evaluated in this article, or claim that may be made by its manufacturer, is not guaranteed or endorsed by the publisher.

References

1. The skin cancer foundation, in: *Our new approach to a challenging skin cancer statistic* (2021). Available at: <https://www.skincancer.org/blog/our-new-approach-to-a-challenging-skin-cancer-statistic/> (Accessed 18 October, 2022).
2. Lucas R, McMichael T, Smith W, Armstrong B. Solar ultraviolet radiation: Global burden of disease from solar ultraviolet radiation. *Environ Burden Dis Ser* (2006) 13).
3. Gray D, Suman V, Su W, Clay R, Harmsen W, Roenigk R. Trends in the population-based incidence of squamous cell carcinoma of the skin first diagnosed between 1984 and 1992. *Arch Dermatol* (1997) 133(6):735–40. doi: 10.1158/2159-8290.CD-11-0028
4. Di Nardo L, Pellegrini C, Di Stefani A, Del Regno L, Sollen P, Piccerillo A, et al. Molecular genetics of cutaneous squamous cell carcinoma: Perspective for treatment strategies. *J Eur Acad Dermatol Venereol* (2020) 34(5):932–41. doi: 10.1111/jdv.16098
5. Chang D, Shain AH. The landscape of driver mutations in cutaneous squamous cell carcinoma. *NPJ Genom Med* (2021) 6(1):61. doi: 10.1038/s41525-021-00226-4
6. Durinck S, Ho C, Wang NJ, Liao W, Jakkula LR, Collisson EA, et al. Temporal dissection of tumorigenesis in primary cancers. *Cancer Discov* (2011) 1(2):137–43. doi: 10.1158/2159-8290.CD-11-0028
7. Li YY, Hanna GJ, Laga AC, Haddad RI, Lorch JH, Hammerman PS. Genomic analysis of metastatic cutaneous squamous cell carcinoma. *Clin Cancer Res* (2015) 21(6):1447–56. doi: 10.1158/1078-0432.CCR-14-1773
8. Pickering CR, Zhou JH, Lee JJ, Drummond JA, Peng SA, Saade RE, et al. Mutational landscape of aggressive cutaneous squamous cell carcinoma. *Clin Cancer Res* (2014) 20(24):6582–92. doi: 10.1158/1078-0432.CCR-14-1768
9. Fu T, Aasi SZ, Hollmig ST. Management of high-risk squamous cell carcinoma of the skin. *Curr Treat Options Oncol* (2016) 17(7):34. doi: 10.1007/s11864-016-0408-2
10. Weinberg A, Ogle C, Shim E. Metastatic cutaneous squamous cell carcinoma: An update. *Dermatol Surg* (2007) 33(8):885–99. doi: 10.1111/j.1524-4725.2007.33190.x
11. Brantsch KD, Meisner C, Schonfisch B, Trilling B, Wehner-Caroli J, Rocken M, et al. Analysis of risk factors determining prognosis of cutaneous squamous-cell carcinoma: A prospective study. *Lancet Oncol* (2008) 9(8):713–20. doi: 10.1016/S1470-2045(08)70178-5
12. Lansbury L, Bath-Hextall F, Perkins W, Stanton W, Leonardi-Bee J. Interventions for non-metastatic squamous cell carcinoma of the skin: Systematic review and pooled analysis of observational studies. *BMJ* (2013) 347:f6153. doi: 10.1136/bmj.f6153
13. Hollestein LM, de Vries E, Nijsten T. Trends of cutaneous squamous cell carcinoma in the Netherlands: Increased incidence rates, but stable relative survival and mortality 1989–2008. *Eur J Cancer* (2012) 48(13):2046–53. doi: 10.1016/j.jejca.2012.01.003
14. Karia PS, Jambusaria-Pahlajani A, Harrington DP, Murphy GF, Qureshi AA, Schmults CD. Evaluation of American joint committee on cancer, international union against cancer, and Brigham and women's hospital tumor staging for cutaneous squamous cell carcinoma. *J Clin Oncol* (2014) 32(4):327–34. doi: 10.1200/JCO.2012.48.5326
15. Kwon S, Dong ZM, Wu PC. Sentinel lymph node biopsy for high-risk cutaneous squamous cell carcinoma: Clinical experience and review of literature. *World J Surg Oncol* (2011) 9:80. doi: 10.1186/1477-7819-9-80
16. Reschly MJ, Messina JL, Zaulyanov LL, Cruse W, Fenske NA. Utility of sentinel lymphadenectomy in the management of patients with high-risk cutaneous squamous cell carcinoma. *Dermatologic Surg* (2003) 29:135–40. doi: 10.1046/j.1524-4725.2003.29035.x
17. Rowe DE, Carroll RJ, Day C. Prognostic factors for local recurrence, metastasis, and survival rates in squamous cell carcinoma of the skin, ear, and lip. *Implications Treat Modality Selection. J Am Acad Dermatol* (1992) 26(6):976–90. doi: 10.1016/0190-9622(92)70144-5
18. Veness M, Morgan G, Palme C, Gebiski V. Surgery, and adjuvant radiotherapy in patients with cutaneous head and neck squamous cell carcinoma metastatic to lymph nodes: Combined treatment should be considered best practice. *Laryngoscope* (2005) 115(5):870–5. doi: 10.1097/01.MLG.0000158349.64337.ED

19. Keeping S, Xu Y, Chen CI, Cope S, Mojeibi A, Kuznik A, et al. Comparative efficacy of cemiplimab versus other systemic treatments for advanced cutaneous squamous cell carcinoma. *Future Oncol* (2021) 17(5):611–27. doi: 10.2217/fon-2020-0823
20. Villani A, Ocampo-Garza SS, Potestio L, Fabbrocini G, Ocampo-Candiani J, Ocampo-Garza J, et al. Cemiplimab for the treatment of advanced cutaneous squamous cell carcinoma. *Expert Opin Drug Saf* (2022) 21(1):21–9. doi: 10.1080/14740338.2022.1993819
21. *Keytruda® (Pembrolizumab) injection, for intravenous use*. NJ: Whitehouse Station: Merck & Co. I (2021).
22. Oro-Ayude M, Suh-Oh HJ, Sacristan-Santos V, Vazquez-Bartolome P, Florez A. Nivolumab for metastatic cutaneous squamous cell carcinoma. *Case Rep Dermatol* (2020) 12(1):37–41. doi: 10.1159/000505478
23. Fujimura T, Kambayashi Y, Tono H, Lyu C, Ohuchi K, Hashimoto A, et al. Successful treatment of unresectable recurrent cutaneous squamous cell carcinoma of the scalp with meningeal invasion with nivolumab monotherapy. *Dermatol Ther* (2020) 33(4):e13672. doi: 10.1111/dth.13672
24. Maruhashi T, Sugiura D, Okazaki IM, Okazaki T. Lag-3: From molecular functions to clinical applications. *J Immunother Cancer* (2020) 8(2). doi: 10.1136/jitc-2020-001014
25. Wang M, Du Q, Jin J, Wei Y, Lu Y, Li Q. Lag3 and its emerging role in cancer immunotherapy. *Clin Transl Med* (2021) 11(3):e365. doi: 10.1002/ctm.2.365
26. Alberti A, Bossi P. Immunotherapy for cutaneous squamous cell carcinoma: Results and perspectives. *Front Oncol* (2021) 11:727027. doi: 10.3389/fonc.2021.727027
27. Ovits CG, Carucci JA. Immune environment of cutaneous malignancies. In: AAGe al, editor. *Clinical and basic immunodermatology*. Switzerland: Springer International Publishing (2017). p. 741–55.
28. Belkin DA, Mitsui H, Wang CQ, Gonzalez J, Zhang S, Shah KR, et al. Cd200 upregulation in vascular endothelium surrounding cutaneous squamous cell carcinoma. *JAMA Dermatol* (2013) 149(2):178–86. doi: 10.1001/jamadermatol.2013.1609
29. Pinzon-Charry A, Maxwell T, Lopez JA. Dendritic cell dysfunction in cancer: A mechanism for immunosuppression. *Immunol Cell Biol* (2005) 83(5):451–61. doi: 10.1111/j.1440-1711.2005.01371.x
30. Mittal D, Gubin MM, Schreiber RD, Smyth MJ. New insights into cancer immunoediting and its three component phases elimination, equilibrium and escape. *Curr Opin Immunol* (2014) 27:16–25. doi: 10.1016/j.coi.2014.01.004
31. Seliger B. Novel insights into the molecular mechanisms of hla class I abnormalities. *Cancer Immunol Immunother* (2012) 61(2):249–54. doi: 10.1007/s00262-011-1153-9
32. Whiteside TL. Tumor-induced death of immune cells: Its mechanisms and consequences. *Semin Cancer Biol* (2002) 12(1):43–50. doi: 10.1006/scbi.2001.0402
33. van Kempen LC, Ruiter DJ, van Muijen GN, Coussens LM. The tumor microenvironment: A critical determinant of neoplastic evolution. *Eur J Cell Biol* (2003) 82(11):539–48. doi: 10.1078/0171-9335-00346
34. Elmusrati A, Wang J, Wang CY. Tumor microenvironment and immune evasion in head and neck squamous cell carcinoma. *Int J Oral Sci* (2021) 13(1):24. doi: 10.1038/s41368-021-00131-7
35. Bronte V, Brandau S, Chen SH, Colombo MP, Frey AB, Greten TF, et al. Recommendations for myeloid-derived suppressor cell nomenclature and characterization standards. *Nat Commun* (2016) 7:12150. doi: 10.1038/ncomms12150
36. Veglia F, Sanseviero E, Gabrilovich DI. Myeloid-derived suppressor cells in the era of increasing myeloid cell diversity. *Nat Rev Immunol* (2021) 21(8):485–98. doi: 10.1038/s41577-020-00490-y
37. Wang PF, Song SY, Wang TJ, Ji WJ, Li SW, Liu N, et al. Prognostic role of pretreatment circulating mdscs in patients with solid malignancies: A meta-analysis of 40 studies. *Oncotarget* (2018) 7(10):e1494113. doi: 10.1080/2162402X.2018.1494113
38. Condamine T, Mastio J, Gabrilovich DI. Transcriptional regulation of myeloid-derived suppressor cells. *J Leukoc Biol* (2015) 98(6):913–22. doi: 10.1189/jlb.4RI0515-204R
39. Nagaraj S, Gabrilovich DI. Myeloid-derived suppressor cells in human cancer. *Cancer J* (2010) 16(4):348–53. doi: 10.1097/PPO.0b013e3181eb3358
40. Gabrilovich D, Nagaraj S. Myeloid-derived suppressor cells as regulators of the immune system. *Nat Rev Immunol* (2009) 9:162–74. doi: 10.1038/nri2506
41. Gehad AE, Lichtman MK, Schmults CD, Teague JE, Calareso AW, Jiang Y, et al. Nitric oxide-producing myeloid-derived suppressor cells inhibit vascular e-selectin expression in human squamous cell carcinomas. *J Invest Dermatol* (2012) 132(11):2642–51. doi: 10.1038/jid.2012.190
42. Nefedova Y, Fishman M, Sherman S, Wang X, Beg AA, Gabrilovich DI. Mechanism of all-trans retinoic acid effect on tumor-associated myeloid-derived suppressor cells. *Cancer Res* (2007) 67:11021–8. doi: 10.1158/0008-5472.CAN-07-2593
43. Kusmartsev S, Cheng F, Yu B, Nefedova Y, Sotomayor E, Lush R, et al. All-Trans-Retinoic acid eliminates immature myeloid cells from tumor-bearing mice and improves the effect of vaccination. *Cancer Res* (2003) 63:4441–9.
44. Iclozan C, Antonia S, Chiappori A, Chen DT, Gabrilovich D. Therapeutic regulation of myeloid-derived suppressor cells and immune response to cancer vaccine in patients with extensive stage small cell lung cancer. *Cancer Immunol Immunother* (2013) 62(5):909–18. doi: 10.1007/s00262-013-1396-8
45. Tobin RP, Jordan KR, Robinson WA, Davis D, Borges VF, Gonzalez R, et al. Targeting myeloid-derived suppressor cells using all-trans retinoic acid in melanoma patients treated with ipilimumab. *Int Immunopharmacol* (2018) 63:282–91. doi: 10.1016/j.intimp.2018.08.007
46. Wang YC, He F, Feng F, Liu XW, Dong GY, Qin HY, et al. Notch signaling determines the M1 versus M2 polarization of macrophages in antitumor immune responses. *Cancer Res* (2010) 70(12):4840–9. doi: 10.1158/0008-5472.CAN-10-0269
47. Qian BZ, Pollard JW. Macrophage diversity enhances tumor progression and metastasis. *Cell* (2010) 141(1):39–51. doi: 10.1016/j.cell.2010.03.014
48. Noy R, Pollard JW. Tumor-associated macrophages: From mechanisms to therapy. *Immunity* (2014) 41(1):49–61. doi: 10.1016/j.immuni.2014.06.010
49. Pettersen JS, Fuentes-Duculan J, Suarez-Farinas M, Pierson KC, Pitts-Kiefer A, Fan L, et al. Tumor-associated macrophages in the cutaneous scc microenvironment are heterogeneously activated. *J Invest Dermatol* (2011) 131(6):1322–30. doi: 10.1037/jid.2011.9
50. Mills CD, Kincaid K, Alt JM, Heilman MJ, Hill AM. M-1/M-2 macrophages and the Th1/Th2 paradigm. *J Immunol* (2000) 164(12):6166–73. doi: 10.4049/jimmunol.164.12.6166
51. Trinchieri G. Interleukin-12 and the regulation of innate resistance and adaptive immunity. *Nat Rev Immunol* (2003) 3(2):133–46. doi: 10.1038/nri1001
52. Edwards JP, Zhang X, Frauwirth KA, Mosser DM. Biochemical and functional characterization of three activated macrophage populations. *J Leukoc Biol* (2006) 80(6):1298–307. doi: 10.1189/jlb.0406249
53. Gocheva V, Wang HW, Gadea BB, Shree T, Hunter KE, Garfall AL, et al. IL-4 induces cathepsin protease activity in tumor-associated macrophages to promote cancer growth and invasion. *Genes Dev* (2010) 24(3):241–55. doi: 10.1101/gad.1874010
54. Sica A, Mantovani A. Macrophage plasticity and polarization: *In vivo* veritas. *J Clin Invest* (2012) 122(3):787–95. doi: 10.1172/JCI59643
55. Pinto CA, Carvalho PE, Antonangelo L, Garippo A, Da Silva AG, Soares F, et al. Morphometric evaluation of tumor matrix metalloproteinase 9 predicts survival after surgical resection of adenocarcinoma of the lung. *Clin Cancer Res* (2003) 9(8):3098–104.
56. Buerger D, Weber T, Maurer GD, Mudduluru G, Medved F, Leupold JH, et al. Urokinase receptor, mmp-1 and mmp-9 are markers to differentiate prognosis, adenoma and carcinoma in thyroid malignancies. *Int J Cancer* (2009) 125(4):894–901. doi: 10.1002/ijc.24462
57. Shah SA, Spinale FG, Ikonomidis JS, Stroud RE, Chang EI, Reed CE. Differential matrix metalloproteinase levels in adenocarcinoma and squamous cell carcinoma of the lung. *J Thorac Cardiovasc Surg* (2010) 139(4):984–90. doi: 10.1016/j.jtcvs.2009.12.016
58. Zhao ZS, Chu YQ, Ye ZY, Wang YY, Tao HQ. Overexpression of matrix metalloproteinase 11 in human gastric carcinoma and its clinicopathologic significance. *Hum Pathol* (2010) 41(5):686–96. doi: 10.1016/j.humpath.2009.10.010
59. Moussai D, Mitsui H, Pettersen JS, Pierson KC, Shah KR, Suárez-Fariñas M, et al. The human cutaneous squamous cell carcinoma microenvironment is characterized by increased lymphatic density and enhanced expression of macrophage-derived vegf-c. *J Invest Dermatol* (2011) 131(1):229–36. doi: 10.1038/jid.2010.266
60. Boone B, Blokk W, De Bacquer D, Lambert J, Ruiter D, Brochez L. The role of vegf-c staining in predicting regional metastasis in melanoma. *Virchows Arch* (2008) 453(3):257–65. doi: 10.1007/s00428-008-0641-6
61. Sugiura T, Inoue Y, Matsuki R, Ishii K, Takahashi M, Abe M, et al. Vegf-c and vegf-d expression is correlated with lymphatic vessel density and lymph node metastasis in oral squamous cell carcinoma: Implications for use as a prognostic marker. *Int J Oncol* (2009) 34(3):673–80. doi: 10.3892/ijo_00000193
62. Jiang X, Wang M, Cyrus N, Yanez DA, Lacher RK, Rhebergen AM, et al. Human keratinocyte carcinomas have distinct differences in their tumor-associated macrophages. *Heliyon* (2019) 5(8). doi: 10.1016/j.heliyon.2019.e02273
63. Stumpfova M, Ratner D, Desciak EB, Eliezri YD, Owens DM. The immunosuppressive surface ligand Cd200 augments the metastatic capacity of squamous cell carcinoma. *Cancer Res* (2010) 70(7):2962–72. doi: 10.1158/0008-5472
64. Khan IZ, Del Guzzo CA, Shao A, Cho J, Du R, Cohen AO, et al. The Cd200-Cd200R axis promotes squamous cell carcinoma metastasis via regulation of cathepsin K. *Cancer Res* (2021) 81(19):5021–32. doi: 10.1158/0008-5472.CAN-20-3251
65. Ko YC, Chien HF, Jiang-Shieh YF, Chang CY, Pai MH, Huang JP, et al. Endothelial Cd200 is heterogeneously distributed, regulated and involved in immune cell-endothelium interactions. *J Anat* (2009) 214(1):183–95. doi: 10.1111/j.1469-7580.2008.00986.x
66. Hoek RM, Ruuls SR, Murphy CA, Wright GJ, Goddard R, Zurawski SM, et al. Down-regulation of the macrophage lineage through interaction with Ox2 (Cd200). *Science* (2000) 290(5497):1768–71. doi: 10.1126/science.290.5497.1768
67. Gorczynski RM, Cattral MS, Chen Z, Hu J, Lei J, Min WP, et al. An immunoadhesin incorporating the molecule ox-2 is a potent immunosuppressant that prolongs allo- and xenograft survival. *J Immunol* (1999) 163(3):1654–60.
68. Taylor N, McConachie K, Calder C, Dawson R, Dick A, Sedgwick JD, et al. Enhanced tolerance to autoimmune uveitis in Cd200-deficient mice correlates with a pronounced Th2 switch in response to antigen challenge. *J Immunol* (2005) 174(1):143–54. doi: 10.4049/jimmunol.174.1.143
69. Gorczynski RM, Yu K, Clark D. Receptor engagement on cells expressing a ligand for the tolerance-inducing molecule Ox2 induces an immunoregulatory population that inhibits alloreactivity in vitro and in vivo. *J Immunol* (2000) 165(9):4854–60. doi: 10.4049/jimmunol.165.9.4854
70. Koning N, van Eijk M, Pouwels W, Brouwer MS, Voehringer D, Huitinga I, et al. Expression of the inhibitory Cd200 receptor is associated with alternative macrophage activation. *J Innate Immun* (2010) 2(2):195–200. doi: 10.1159/000252803

71. Zhang S, Cherwinski H, Sedgwick JD, Phillips JH. Molecular mechanisms of Cd200 inhibition of mast cell activation. *J Immunol* (2004) 173(11):6786–93. doi: 10.4049/jimmunol.173.11.6786
72. Kretz-Rommel A, Qin F, Dakappagari N, Ravey EP, McWhirter J, Oltean D, et al. Cd200 expression on tumor cells suppresses antitumor immunity: New approaches to cancer immunotherapy. *J Immunol* (2007) 178(9):5595–605. doi: 10.4049/jimmunol.178.9.5595
73. Kretz-Rommel A, Qin F, Dakappagari N, Cofield R, Faas SJ, Bowdish KS. Blockade of Cd200 in the presence or absence of antibody effector function: Implications for anti-Cd200 therapy. *J Immunol* (2008) 180(2):699–705. doi: 10.4049/jimmunol.180.2.699
74. Yanofsky VR, Mitsui H, Felsen D, Carucci JA. Understanding dendritic cells and their role in cutaneous carcinoma and cancer immunotherapy. *J Immunol Res* (2013) 2013:624123. doi: 10.1155/2013/624123
75. Gottfried E, Kreutz M, Mackensen A. Tumor-induced modulation of dendritic cell function. *Cytokine Growth Factor Rev* (2008) 19(1):65–77. doi: 10.1016/j.cytogfr.2007.10.008
76. Zaba LC, Krueger JG, Lowes MA. Resident and "Inflammatory" dendritic cells in human skin. *J Invest Dermatol* (2009) 129(2):302–8. doi: 10.1038/jid.2008.225
77. Fujita H, Suarez-Farinas M, Mitsui H, Gonzalez J, Bluth MJ, Zhang S, et al. Langerhans cells from human cutaneous squamous cell carcinoma induce strong type 1 immunity. *J Invest Dermatol* (2012) 132(6):1645–55. doi: 10.1038/jid.2012.34
78. Klechevsky E, Morita R, Liu M, Cao Y, Coquery S, Thompson-Snipes L, et al. Functional specializations of human epidermal langerhans cells and Cd14+ dermal dendritic cells. *Immunity* (2008) 29(3):497–510. doi: 10.1016/j.immuni.2008.07.013
79. Banchereau J, Klechevsky E, Schmitt N, Morita R, Palucka K, Ueno H. Harnessing human dendritic cell subsets to design novel vaccines. *Ann N Y Acad Sci* (2009) 1174:24–32. doi: 10.1111/j.1749-6632.2009.04999.x
80. Esche C, Lokshin A, Shurin GV, Gastman BR, Rabinowich H, Watkins SC, et al. Tumor's other immune targets: Dendritic cells. *J Leukoc Biol* (1999) 66(2):336–44. doi: 10.1002/jlb.66.2.336
81. Pirtskhalaishvili G, Shurin GV, Esche C, Cai Q, Salup RR, Bykovskaia SN, et al. Cytokine-mediated protection of human dendritic cells from prostate cancer-induced apoptosis is regulated by the bcl-2 family of proteins. *Br J Cancer* (2000) 83:506–13. doi: 10.1054/bjoc.2000.1289
82. Pirtskhalaishvili G, Shurin GV, Gambotto A, Esche C, Wahl M, Yurkovetsky ZR, et al. Transduction of dendritic cells with bcl-xl increases their resistance to prostate cancer-induced apoptosis and antitumor effect in mice. *J Immunol* (2000) 165(4):1956–64. doi: 10.4049/jimmunol.165.4.1956
83. Bluth MJ, Zaba LC, Moussai D, Suarez-Farinas M, Kaporis H, Fan L, et al. Myeloid dendritic cells from human cutaneous squamous cell carcinoma are poor stimulators of T-cell proliferation. *J Invest Dermatol* (2009) 129(10):2451–62. doi: 10.1038/jid.2009.96
84. Galan A, Ko CJ. Langerhans cells in squamous cell carcinoma vs. pseudoeplitheliomatous hyperplasia of the skin. *J Cutan Pathol* (2007) 34(12):950–2. doi: 10.1111/j.1600-0560.2007.00741.x
85. Nestle FO, Burg G, Fähr J, Wrone-Smith T, Nickoloff BJ. Human sunlight-induced basal-cell carcinoma-associated dendritic cells are deficient in T cell Co-stimulatory molecules and are impaired as antigen-presenting cells. *Am J Pathol* (1997) 150(2):641–51.
86. Allavena P, Piemonti L, Longoni D, Bernasconi S, Stoppacciaro A, Ruco L, et al. IL-10 prevents the differentiation of monocytes to dendritic cells but promotes their maturation to macrophages. *Eur J Immunol* (1998) 28:359–69. doi: 10.1002/(SICI)1521-4141(199801)28:01<359::AID-IMMU359>3.0.CO;2-4
87. Buelens C, Verhasselt V, De Groote D, Thielemans K, Goldman M, Willems F. Interleukin-10 prevents the generation of dendritic cells from human peripheral blood mononuclear cells cultured with interleukin-4 and Granulocyte/Macrophage-colonystimulating factor. *Eur J Immunol* (1997) 27:756–62. doi: 10.1002/eji.1830270326
88. Enk AH, Angeloni VL, Udey MC, Katz SI. Inhibition of langerhans cell antigen-presenting function by il-10. A Role IL-10 Induction Tolerance. *J Immunol* (1993) 151(5):2390–8.
89. Steinbrink K, Jonuleit H, Muller G, Schuler G, Knop J, Enk A. Interleukin-10 treated human dendritic cells induce a melanomaantigen-specific anergy in Cd8(+) T cells resulting in a failure to lyse tumor cells. *Blood* (1999) 93:1634–42.
90. Lissoni P, Malugani F, Bonfanti A, Bucovec R, Secondino S, Brivio F, et al. Abnormally enhanced blood concentrations of vascular endothelial growth factor (Vegf) in metastatic cancer patients and their relation to circulating dendritic cells, il-12 and endothelin-1. *J Biol Regul Homeost* (2001) 15:140–44.
91. Takahashi A, Kono K, Ichihara F, Sugai H, Fujii H, Matsumoto Y. Vascular endothelial growth factor inhibits maturation of dendritic cells induced by lipopolysaccharide, but not by proinflammatory cytokines. *Cancer Immunol Immunother* (2004) 53(6):543–50. doi: 10.1007/s00262-003-0466-8
92. Saito H, Tsujitani S, Ikeguchi M, Maeta M, Kaibara N. Relationship between the expression of vascular endothelial growth factor and the density of dendritic cells in gastric adenocarcinoma tissue. *Br J Cancer* (1998) 78(12):1573–7. doi: 10.1038/bjc.1998.725
93. Hoeffel G, Ripoche AC, Matheoud D, Nascimbeni M, Escriviou N, Lebon P, et al. Antigen crosspresentation by human plasmacytoid dendritic cells. *Immunity* (2007) 27(3):481–92. doi: 10.1016/j.immuni.2007.07.021
94. Tel J, Schreibeit G, Sittig SP, Mathan TS, Buschow SI, Cruz LJ, et al. Human plasmacytoid dendritic cells efficiently cross-present exogenous ags to Cd8+ T cells despite lower Ag uptake than myeloid dendritic cell subsets. *Blood* (2013) 121(3):459–67. doi: 10.1182/blood-2012-06-435644
95. Tel J, Aarntzen EH, Baba T, Schreibeit G, Schulte BM, Benitez-Ribas D, et al. Natural human plasmacytoid dendritic cells induce antigen-specific T-cell responses in melanoma patients. *Cancer Res* (2013) 73(3):1063–75. doi: 10.1158/0008-5472.CAN-12-2583
96. Hussein MR, Ahmed RA. Analysis of the mononuclear inflammatory cell infiltrate in the non-tumorigenic, pre-tumorigenic and tumorigenic keratinocytic hyperproliferative lesions of the skin. *Cancer Biol Ther* (2005) 4(8):819–21. doi: 10.4161/cbt.4.8.1864
97. Clark RA, Huang SJ, Murphy GF, Mollet IG, Hijnjen D, Muthukuru M, et al. Human squamous cell carcinomas evade the immune response by down-regulation of vascular e-selectin and recruitment of regulatory T cells. *J Exp Med* (2008) 205(10):2221–34. doi: 10.1084/jem.20071190
98. Kosmidis M, Dziunycz P, Suarez-Farinas M, Muhleisen B, Schärer L, Lauchli S, et al. Immunosuppression affects Cd4+ mrna expression and induces Th2 dominance in the microenvironment of cutaneous squamous cell carcinoma in organ transplant recipients. *J Immunother* (2010) 33(5):538–46. doi: 10.1097/CJI.0b013e3181cc2615
99. Halliday GM, Patel A, Hunt MJ, Tefany FJ, Barnetson RS. Spontaneous regression of human Melanoma/Nonmelanoma skin cancer: Association with infiltrating Cd4+ T cells. *World J Surg* (1995) 19:352–8. doi: 10.1007/BF00299157
100. Lai C, August S, Albibas A, Behar R, Cho SY, Polak ME, et al. OX40+ regulatory T cells in cutaneous squamous cell carcinoma suppress effector T cell responses and associate with metastatic potential. *Clin Cancer Res* (2016) 22(16):4236–48. doi: 10.1158/1078-0432.CCR-15-2614
101. Zhang S, Fujita H, Mitsui H, Yanofsky VR, Fuentes-Duculan J, Pettersen JS, et al. Increased Tc22 and Treg/Cd8 ratio contribute to aggressive growth of transplant associated squamous cell carcinoma. *PLoS One* (2013) 8(5):e62154. doi: 10.1371/journal.pone.0062154
102. Clark RA, Kupper TS. IL-15 and dermal fibroblasts induce proliferation of natural regulatory T cells isolated from human skin. *Blood* (2007) 109(1):194–202. doi: 10.1182/blood-2006-02-002873
103. Yu P, Fu YX. Tumor-infiltrating T lymphocytes: Friends or foes? *Lab Invest* (2006) 86(3):231–45. doi: 10.1038/labinvest.3700389
104. Rutella S, Lemoli RM. Regulatory T cells and tolerogenic dendritic cells: From basic biology to clinical applications. *Immunol Lett* (2004) 94(1–2):11–26. doi: 10.1016/j.imlet.2004.04.015
105. Beyer M, Schultze JL. Regulatory T cells in cancer. *Blood* (2006) 108(3):804–11. doi: 10.1182/blood-2006-02-002774
106. Beyer M, Kochanek M, Giese T, Endl E, Weihrauch MR, Knolle PA, et al. In vivo peripheral expansion of naive Cd4+ Cd25high Foxp3+ regulatory T cells in patients with multiple myeloma. *Blood* (2006) 107(10):3940–9. doi: 10.1182/blood-2005-09-3671
107. Thornton AM, Shevach EM. Cd4+ Cd25+ immunoregulatory T cells suppress polyclonal T cell activation in vitro by inhibiting interleukin 2 production. *J Exp Med* (1998) 188(2):287–96. doi: 10.1084/jem.188.2.287
108. Ng WF, Duggan PJ, Ponchel F, Matarese G, Lombardi G, Edwards AD, et al. Human Cd4(+) Cd25(+) cells: A naturally occurring population of regulatory T cells. *Blood* (2001) 98(9):2736–44. doi: 10.1182/blood.v98.9.2736
109. Bates GJ, Fox SB, Han C, Leek RD, Garcia JF, Harris AL, et al. Quantification of regulatory T cells enables the identification of high-risk breast cancer patients and those at risk of late relapse. *J Clin Oncol* (2006) 24(34):5373–80. doi: 10.1200/JCO.2006.05.9584
110. Wolf D, Wolf AM, Rumpold H, Fiegl H, Zeimet AG, Muller-Holzner E, et al. The expression of the regulatory T cell-specific forkhead box transcription factor Foxp3 is associated with poor prognosis in ovarian cancer. *Clin Cancer Res* (2005) 11(23):8326–31. doi: 10.1158/1078-0432.CCR-05-1244
111. Curiel TJ, Coukos G, Zou L, Alvarez X, Cheng P, Mottram P, et al. Specific recruitment of regulatory T cells in ovarian carcinoma fosters immune privilege and predicts reduced survival. *Nat Med* (2004) 10(9):942–9. doi: 10.1038/nm1093
112. Frazzette N, Khodadadi-Jamayran A, Doudican N, Santana A, Felsen D, Pavlick AC, et al. Decreased cytotoxic T cells and tcr clonality in organ transplant recipients with squamous cell carcinoma. *NPJ Precis Oncol* (2020) 4:13. doi: 10.1038/s41698-020-0119-9
113. Zhang S, Wu M, Wang F. Immune regulation by Cd8(+) treg cells: Novel possibilities for anticancer immunotherapy. *Cell Mol Immunol* (2018) 15(9):805–7. doi: 10.1038/cmi.2018.170
114. Robb RJ, Lineburg KE, Kuns RD, Wilson YA, Raffelt NC, Olver SD, et al. Identification and expansion of highly suppressive Cd8(+)Foxp3(+) regulatory T cells after experimental allogeneic bone marrow transplantation. *Blood* (2012) 119(24):5898–908. doi: 10.1182/blood-2011-12-396119
115. Freeman A, Bridge JA, Maruthayanar P, Overgaard NH, Jung JW, Simpson F, et al. Comparative immune phenotypic analysis of cutaneous squamous cell carcinoma and intraepidermal carcinoma in immune-competent individuals: Proportional representation of Cd8+ T-cells but not Foxp3+ regulatory T-cells is associated with disease stage. *PLoS One* (2014) 9(10):e10928. doi: 10.1371/journal.pone.0110928
116. Sedivy R, Beck-Mannagetta J, Haverkamp C, Battistutti W, Honigschnabl S. Expression of vascular endothelial growth factor-c correlates with the lymphatic microvessel density and the nodal status in oral squamous cell cancer. *J Oral Pathol Med* (2003) 32(8):455–60. doi: 10.1034/j.1600-0714.2003.00168.x
117. Miyahara M, Tanuma J, Sugihara K, Semba I. Tumor lymphangiogenesis correlates with lymph node metastasis and clinicopathologic parameters in oral squamous cell carcinoma. *Cancer* (2007) 110(6):1287–94. doi: 10.1002/cncr.22900

118. Krediet JT, Kanitakis J, Bob A, Schmitter J, Krediet AC, Rowert J, et al. Prognostic value of the area and density of lymphatic vessels in cutaneous squamous cell carcinoma. *J Dtsch Dermatol Ges* (2016) 14(11):1114–21. doi: 10.1111/ddg.12880
119. Karpanen T, Egeblad M, Karkkainen MJ, Kubo H, Yla-Herttuala S, Jaattela M, et al. Vascular endothelial growth factor c promotes tumor lymphangiogenesis and intralymphatic tumor growth. *Cancer Res* (2001) 61(5):1786–90.
120. Neinaa YME, El-Ashmawy AA, Alshenawy HA, Dorgham WL. The prognostic value of podoplanin expression in nonmelanoma skin cancers: Correlation with lymphatic vessel density. *Am J Dermatopathol* (2020) 42(6):432–8. doi: 10.1097/DAD.0000000000001561
121. Kreppel M, Krakowezki A, Kreppel B, Drebber U, Wedemeyer I, Mauch C, et al. Podoplanin expression in cutaneous head and neck squamous cell carcinoma prognostic value and clinicopathologic implications. *J Surg Oncol* (2013) 107(4):376–83. doi: 10.1002/jso.23238
122. Hesse K, Satzger I, Schacht V, Köther B, Hillen U, Klode J, et al. Characterization of prognosis and invasion of cutaneous squamous cell carcinoma by podoplanin and e-cadherin expression. *Dermatology* (2016) 232(5):558–65. doi: 10.1159/000450920
123. Cañueto J, Cardenoso-Álvarez E, Cosano-Quero A, Santos-Briz Á, Fernández-López E, Pérez-Losada J, et al. The expression of podoplanin is associated with poor outcome in cutaneous squamous cell carcinoma. *J Cutan Pathol* (2017) 44(2):144–51. doi: 10.1111/cup.12859
124. Wojciechowska-Zdrojowy M, Szepietowski JC, Matusiak Ł, Dzięgiel P, Puła B. Expression of podoplanin in non-melanoma skin cancers and actinic keratosis. *Anticancer Res* (2016) 36(4):1591–7.
125. de Sousa SF, Gleber-Netto FO, de Oliveira-Neto HH, Batista AC, Nogueira Guimarães Abreu MH, de Aguiar MC. Lymphangiogenesis and podoplanin expression in oral squamous cell carcinoma and the associated lymph nodes. *Appl Immunohistochem Mol Morphol* (2012) 20(6):588–94. doi: 10.1097/PAI.0b013e31824bb3ea
126. Aiswarya A, Suresh R, Janardhanan M, Savithri V, Aravind T, Mathew L. An immunohistochemical evaluation of podoplanin expression in oral leukoplakia and oral squamous cell carcinoma to explore its potential to be used as a predictor for malignant transformation. *J Oral Maxillofac Pathol* (2019) 23(1):159. doi: 10.4103/jomfp.JOMFP_272_17
127. Kim HY, Rha KS, Shim GA, Kim JH, Kim JM, Huang SM, et al. Podoplanin is involved in the prognosis of head and neck squamous cell carcinoma through interaction with vegf-c. *Oncol Rep* (2015) 34(2):833–42. doi: 10.3892/or.2015.4070
128. Arimoto S, Hasegawa T, Takeda D, Saito I, Amano R, Akashi M, et al. Lymphangiogenesis and lymph node metastasis in oral squamous cell carcinoma. *Anticancer Res* (2018) 38(11):6157–62. doi: 10.21873/anticancer.12968
129. Franses JW, Baker AB, Chitalia VC, Edelman ER. Stromal endothelial cells directly influence cancer progression. *Sci Transl Med* (2011) 3(66):66ra5. doi: 10.1126/scitranslmed.3001542
130. Kakasheva-Mazhenkovska L, Bashkeska N, Crvenkova S, Gordana P, Milenkova L, Janevska V, et al. Correlation between microvessel density and morphological features in skin squamous cell carcinoma. *Pril (Makedon Akad Nauk Umet Odd Med Nauki)* (2017) 38(1):63–73. doi: 10.1515/prilozi-2017-0009
131. Yamada S, Ogasawara S, Kaneko MK, Kato Y. Lpmab-23: A cancer-specific monoclonal antibody against human podoplanin. *Monoclon Antib Immunodiagn Immunother* (2017) 36(2):72–6. doi: 10.1089/mab.2017.0001
132. Mitsui H, Suarez-Farinas M, Gulati N, Shah KR, Cannizzaro MV, Coats I, et al. Gene expression profiling of the leading edge of cutaneous squamous cell carcinoma: IL-24-Driven mmp-7. *J Invest Dermatol* (2014) 134(5):1418–27. doi: 10.1038/jid.2013.494
133. Zaidi MR, Merlino G. The two faces of interferon- Γ in cancer. *Clin Cancer Res* (2011) 17(19):6118–24. doi: 10.1158/1078-0432.CCR-11-0482
134. Lin WW, Karin M. A cytokine-mediated link between innate immunity, inflammation, and cancer. *J Clin Invest* (2007) 117(5):1175–83. doi: 10.1172/JCI31537
135. Lewis AM, Varghese S, Xu H, Alexander HR. Interleukin-1 and cancer progression: The emerging role of interleukin-1 receptor antagonist as a novel therapeutic agent in cancer treatment. *J Transl Med* (2006) 4:48. doi: 10.1186/1479-5876-4-48
136. Balkwill F. Tnf-alpha in promotion and progression of cancer. *Cancer Metastasis Rev* (2006) 25(3):409–16. doi: 10.1007/s10555-006-9005-3
137. Yuan A, Chen JJ, Yao PL, Yang PC. The role of interleukin-8 in cancer cells and microenvironment interaction. *Front Biosci* (2005) 10:853–65. doi: 10.2741/1579
138. Yamada S, Jinnin M, Kajihara I, Nakashima T, Aoi J, Harada M, et al. Cytokine expression profiles in the sera of cutaneous squamous cell carcinoma patients. *Drug Discovery Ther* (2016) 10(3):172–6. doi: 10.5582/ddt.2016.01032
139. Lathers DM, Young MR. Increased aberrance of cytokine expression in plasma of patients with more advanced squamous cell carcinoma of the head and neck. *Cytokine* (2004) 25(5):220–8. doi: 10.1016/j.cyt.2003.11.005
140. Skrinjar I, Brailo V, Vidovic-Juras D, Vucicevic-Boras V, Milenovic A. Evaluation of pretreatment serum interleukin-6 and tumour necrosis factor alpha as a potential biomarker for recurrence in patients with oral squamous cell carcinoma. *Med Oral Patol Oral Cir Bucal* (2015) 20(4):e402–7. doi: 10.4317/medoral.20373
141. Glick AB. The role of tgfb signaling in squamous cell cancer: Lessons from mouse models. *J Skin Cancer* (2012) 2012:249063. doi: 10.1155/2012/249063
142. Smith CW, Chen Z, Dong G, Loukinova E, Pegram MY, Nicholas-Figueroa L, et al. The host environment promotes the development of primary and metastatic squamous cell carcinomas that constitutively express proinflammatory cytokines il-1alpha, il-6, gm-csf, and kc. *Clin Exp Metastasis* (1998) 16(7):655–64. doi: 10.1023/a:1006559811429
143. Naganawa K, Takayama E, Adachi M, Mitsudo K, Iida M, Kamiya-Mizuno M, et al. Producing capabilities of interferon-gamma and interleukin-10 in peripheral blood from oral squamous cell carcinoma patients. *Open Dent J* (2015) 9:120–4. doi: 10.2174/18742106015090101020
144. Trikha M, Corringham R, Klein B, Rossi JF. Targeted anti-Interleukin-6 monoclonal antibody therapy for cancer: A review of the rationale and clinical evidence. *Clin Cancer Res* (2003) 9(13):4653–65.
145. Bachelot T, Ray-Coquard I, Menetrier-Caux C, Rastkha M, Duc A, Blay JY. Prognostic value of serum levels of interleukin 6 and of serum and plasma levels of vascular endothelial growth factor in hormone-refractory metastatic breast cancer patients. *Br J Cancer* (2003) 88(11):1721–6. doi: 10.1038/sj.bjc.6600956
146. Grivennikov S, Karin M. Autocrine il-6 signaling: A key event in tumorigenesis? *Cancer Cell* (2008) 13(1):7–9. doi: 10.1016/j.ccr.2007.12.020
147. Lederle W, Depner S, Schnur S, Obermueller E, Catone N, Just A, et al. IL-6 promotes malignant growth of skin scs by regulating a network of autocrine and paracrine cytokines. *Int J Cancer* (2011) 128(12):2803–14. doi: 10.1002/ijc.25621
148. Ii M, Yamamoto H, Adachi Y, Maruyama Y, Shinomura Y. Role of matrix metalloproteinase-7 (Matrilysin) in human cancer invasion, apoptosis, growth, and angiogenesis. *Exp Biol Med (Maywood)* (2006) 231(1):20–7. doi: 10.1177/153537020623100103
149. Mueller MM, Peter W, Mappes M, Huelsen A, Steinbauer H, Boukamp P, et al. Tumor progression of skin carcinoma cells in vivo promoted by clonal selection, mutagenesis, and autocrine growth regulation by granulocyte colony-stimulating factor and granulocyte-macrophage colony-stimulating factor. *Am J Pathol* (2001) 159(4):1567–79. doi: 10.1016/S0002-9440(10)62541-2
150. Mueller MM, Fusenig NE. Constitutive expression of G-csf and gm-csf in human skin carcinoma cells with functional consequence for tumor progression. *Int J Cancer* (1999) 83(6):780–9. doi: 10.1002/(sici)1097-0215(19991210)83:6<780::aid-ijcl4>3.0.co;2-c
151. Mann EA, Spiro JD, Chen LL, Kreutzer DL. Cytokine expression by head and neck squamous cell carcinomas. *Am J Surg* (1992) 164(6):567–73. doi: 10.1016/s0002-9610(05)80708-1
152. Obermueller E, Vosseler S, Fusenig NE, Mueller MM. Cooperative autocrine and paracrine functions of granulocyte colony-stimulating factor and granulocyte-macrophage colony-stimulating factor in the progression of skin carcinoma cells. *Cancer Res* (2004) 64(21):7801–12. doi: 10.1158/0008-5472.CAN-03-3301
153. Wu F, Weigel KJ, Zhou H, Wang XJ. Paradoxical roles of tgfbeta signaling in suppressing and promoting squamous cell carcinoma. *Acta Biochim Biophys Sin (Shanghai)* (2018) 50(1):98–105. doi: 10.1093/abbs/gmx127
154. Wolk K, Witte E, Witte K, Warszawska K, Sabat R. Biology of interleukin-22. *Semin Immunopathol* (2010) 32(1):17–31. doi: 10.1007/s00281-009-0188-x
155. Res PC, Piskin G, de Boer OJ, van der Loos CM, Teeling P, Bos JD, et al. Overrepresentation of il-17a and il-22 producing Cd8 T cells in lesional skin suggests their involvement in the pathogenesis of psoriasis. *PLoS One* (2010) 5(11):e14108. doi: 10.1371/journal.pone.0014108
156. Chung Y, Yang X, Chang SH, Ma L, Tian Q, Dong C. Expression and regulation of il-22 in the il-17-Producing Cd4+ T lymphocytes. *Cell Res* (2006) 16(11):902–7. doi: 10.1038/sj.cr.7310106
157. Nogral KE, Zaba LC, Shemer A, Fuentes-Duculan J, Cardinale I, Kikuchi T, et al. IL-22-Producing “T22” T cells account for upregulated il-22 in atopic dermatitis despite reduced il-17-Producing Th17 T cells. *J Allergy Clin Immunol* (2009) 123(6):1244–52.e2. doi: 10.1016/j.jaci.2009.03.041
158. Abikhair M, Mitsui H, Yanofsky V, Roudiani N, Ovits C, Bryan T, et al. Cyclosporine a immunosuppression drives catastrophic squamous cell carcinoma through il-22. *JCI Insight* (2016) 1(8):e86434. doi: 10.1172/jci.insight.86434
159. Curd LM, Favors SE, Gregg RK. Pro-tumour activity of interleukin-22 in hpafii human pancreatic cancer cells. *Clin Exp Immunol* (2012) 168(2):192–9. doi: 10.1111/j.1365-2249.2012.04570.x
160. Rangwala S, Tsai KY. Roles of the immune system in skin cancer. *Br J Dermatol* (2011) 165(5):953–65. doi: 10.1111/j.1365-2133.2011.10507.x
161. Clark RA, Chong B, Mirchandani N, Brinster NK, Yamanaka K, Dowgiert RK, et al. The vast majority of cla+ T cells are resident in normal skin. *J Immunol* (2006) 176(7):4431–9. doi: 10.4049/jimmunol.176.7.4431
162. Mellman I, Coukos G, Dranoff G. Cancer immunotherapy comes of age. *Nature* (2011) 480(7378):480–9. doi: 10.1038/nature10673
163. Rosenberg SA. Cancer immunotherapy comes of age. *Nat Clin Pract Oncol* (2005) 2(3):115. doi: 10.1038/npcn0101
164. Tamai H, Watanabe S, Zheng R, Deguchi K, Cohen PA, Koski GK, et al. Effective treatment of spontaneous metastases derived from a poorly immunogenic murine mammary carcinoma by combined dendritic-tumor hybrid vaccination and adoptive transfer of sensitized T cells. *Clin Immunol* (2008) 127(1):66–77. doi: 10.1016/j.clim.2007.12.001
165. Topalian SL, Weiner GJ, Pardoll DM. Cancer immunotherapy comes of age. *J Clin Oncol* (2011) 29(36):4828–36. doi: 10.1200/JCO.2011.38.0899



OPEN ACCESS

EDITED BY

Catherine Sautes-Fridman,
Institut national de la santé et de la
recherche médicale (INSERM) U1138
Centre de Recherche des Cordeliers (CRC),
France

REVIEWED BY

Wang Ma,
First Affiliated Hospital of Zhengzhou
University, China
Chao H. Huang,
University of Kansas Medical Center
Research Institute, United States

*CORRESPONDENCE

Athéna Crespin
✉ athena.crespin@hotmail.fr

[†]These authors contributed
equally to this work and share
last authorship

SPECIALTY SECTION

This article was submitted to
Cancer Immunity
and Immunotherapy,
a section of the journal
Frontiers in Oncology

RECEIVED 20 October 2022

ACCEPTED 14 February 2023

PUBLISHED 02 March 2023

CITATION

Crespin A, Le Bescop C, de Gunzburg J,
Vitry F, Zalcman G, Cervesi J and
Bandinelli P-A (2023) A systematic review
and meta-analysis evaluating the impact of
antibiotic use on the clinical outcomes of
cancer patients treated with immune
checkpoint inhibitors.
Front. Oncol. 13:1075593.
doi: 10.3389/fonc.2023.1075593

COPYRIGHT

© 2023 Crespin, Le Bescop, de Gunzburg,
Vitry, Zalcman, Cervesi and Bandinelli. This is
an open-access article distributed under the
terms of the [Creative Commons Attribution
License \(CC BY\)](#). The use, distribution or
reproduction in other forums is permitted,
provided the original author(s) and the
copyright owner(s) are credited and that
the original publication in this journal is
cited, in accordance with accepted
academic practice. No use, distribution or
reproduction is permitted which does not
comply with these terms.

A systematic review and meta-analysis evaluating the impact of antibiotic use on the clinical outcomes of cancer patients treated with immune checkpoint inhibitors

Athéna Crespin^{1*}, Clément Le Bescop¹, Jean de Gunzburg¹,
Fabien Vitry¹, Gérard Zalcman^{2,3}, Julie Cervesi^{1†}
and Pierre-Alain Bandinelli^{1†}

¹Da Volterra, Paris, France, ²Department of Thoracic Oncology and CIC1425, Institut du Cancer AP-HP, Nord, Hôpital Bichat-Claude Bernard, AP-HP, Université de Paris, Paris, France, ³U830 Institut National de la Santé et de la Recherche Médicale (INSERM) "Cancer, Heterogeneity, Instability and Plasticity" Curie Institute, Paris, France

Background: Immune checkpoint inhibitors (ICIs) have considerably improved patient outcomes in various cancer types, but their efficacy remains poorly predictable among patients. The intestinal microbiome, whose balance and composition can be significantly altered by antibiotic use, has recently emerged as a factor that may modulate ICI efficacy. The objective of this systematic review and meta-analysis is to investigate the impact of antibiotics on the clinical outcomes of cancer patients treated with ICIs.

Methods: PubMed and major oncology conference proceedings were systematically searched to identify all studies reporting associations between antibiotic use and at least one of the following endpoints: Overall Survival (OS), Progression-Free Survival (PFS), Objective Response Rate (ORR) and Progressive Disease (PD) Rate. Pooled Hazard Ratios (HRs) for OS and PFS, and pooled Odds Ratios (ORs) for ORR and PD were calculated. Subgroup analyses on survival outcomes were also performed to investigate the potential differential effect of antibiotics according to cancer types and antibiotic exposure time windows.

Results: 107 articles reporting data for 123 independent cohorts were included, representing a total of 41,663 patients among whom 11,785 (28%) received antibiotics around ICI initiation. The pooled HRs for OS and PFS were respectively of 1.61 [95% Confidence Interval (CI) 1.48-1.76] and 1.45 [95% CI 1.32-1.60], confirming that antibiotic use was significantly associated with shorter survival. This negative association was observed consistently across all cancer types for OS and depending on the cancer type for PFS. The loss of survival was particularly strong when antibiotics were received shortly before or after ICI initiation. The pooled ORs for ORR and PD were respectively of 0.59 [95% CI 0.47-0.76] and 1.86 [95% CI 1.41-2.46], suggesting that antibiotic use was significantly associated with worse treatment-related outcomes.

Conclusion: As it is not ethically feasible to conduct interventional, randomized, controlled trials in which antibiotics would be administered to cancer patients treated with ICIs to demonstrate their deleterious impact *versus* control, prospective observational studies and interventional trials involving microbiome modifiers are crucially needed to uncover the role of microbiome and improve patient outcomes. Such studies will reduce the existing publication bias by allowing analyses on more homogeneous populations, especially in terms of treatments received, which is not possible at this stage given the current state of the field. In the meantime, antibiotic prescription should be cautiously considered in cancer patients receiving ICIs.

Systematic review registration: <https://www.crd.york.ac.uk/prospero/>, identifier CRD42019145675.

KEYWORDS

systematic review, meta-analysis, cancer, antibiotics, microbiome, microbiota, immune checkpoint inhibitors, immunotherapies

1 Introduction

Cancer immunotherapy targeting immune checkpoints has revolutionized cancer management and resulted in significant improvement in patient outcomes in a large array of cancers (1). Currently approved immune checkpoint inhibitors (ICIs) include monoclonal antibodies targeting programmed cell death protein 1 (anti-PD-1) and its ligand (anti-PD-L1), as well as cytotoxic T-lymphocyte-associated protein 4 (anti-CTLA-4). Furthermore, numerous molecules targeting other immune checkpoints are currently being evaluated in clinical trials and could soon enrich the list of authorized ICIs. Besides, the indications of approved products are increasingly expanded to new cancer types and earlier lines of treatment¹.

This significant and steadily increasing use of ICIs and the variation of response between patients warrant attention to the factors that mitigate their efficacy. Only between 15 and 60% of patients, depending on cancer types, do respond to ICI treatment (1, 2), which leaves a wide range of patients who do not fully benefit from ICIs. In non-small cell lung cancer (NSCLC), one of the first cancers for which ICIs were authorized, only 15 to 30% of patients seem to achieve a durable benefit from ICIs (1, 3, 4).

In recent years, the gut microbiome has been increasingly discussed as playing a crucial role in the education and development of major components of the host's immune system, and therefore in a certain number of health conditions and diseases (5). The role of the gut microbiome in modulating or predicting the effectiveness of ICIs has also been highlighted in recent papers (6–8). Several studies have identified gut bacteria that could be associated with good or poor clinical response in the fecal

microbiome of cancer patients treated with ICIs. They have even shown that fecal microbiota transplantation (FMT) from patients responding to ICIs into germ-free or antibiotic-treated mice modulated the response of mice tumors to ICI treatment (6–8).

Cancer patients are particularly vulnerable to bacterial infections and antibiotics (ABX) are often used in the clinical practice. ABX are known to induce profound changes to the gut microbiome and to disrupt the balance between the various bacterial groups, genera and species normally found in each healthy individual. Microbiome disruption, called dysbiosis, can last for several weeks or even months after ABX intake (9, 10), and alter key functions of the microbiome (11). The relationship between ABX use and ICI efficacy is therefore increasingly studied in clinical practice. ABX exposure was notably shown in numerous retrospective and prospective studies to adversely influence the clinical outcomes of patients suffering from different types of cancer treated with ICIs (12–14). Sixteen meta-analyses were published on the subject and consistently concluded on a damaging impact of ABX use on the clinical outcomes of cancer patients treated with ICIs (15–30), yet only 48 cohorts (12,794 patients) were included in the most comprehensive meta-analysis (23), leaving a large part of the literature unexploited.

By including in the present meta-analysis a total of 107 articles reporting clinical data based on ABX exposure on 123 independent cohorts, for a total of 41,663 patients, we aimed to exhaustively cover the literature of the field and to provide novel analyses that were not performed in previously published meta-analyses. In particular, the impact of ABX use on treatment-related outcomes such as Objective Response Rate (ORR) and Progressive Disease (PD) rate has been poorly investigated to date, with few articles included in the meta-analyses having performed such analyses. Also, the potential differential effect of ABX use depending on the cancer type has not been investigated in as many cancer types as possible, and, for instance, the impact of ABX use in urothelial

¹ Cancer Research Institute. <https://www.cancerresearch.org/scientists/immuno-oncology-landscape/pd-1-pd-l1-landscape>

carcinoma (UC), in which ICIs are increasingly used, has never been conclusively examined. Hopefully, our findings will help improve the understanding of the links between ABX use and ICI efficacy, optimize individualized clinical care during cancer immunotherapy and benefit patient prognosis.

This meta-analysis aims to answer the following questions: is the use of ABX before and/or during an anti-PD-L(1)-based treatment associated with a modification of the response to treatment and survival in cancer patients? Are there elements related to the cancer, the ABX therapy itself and/or the time window of ABX exposure relative to ICI initiation that could modulate this impact and help physicians issue best practice recommendations?

2 Materials and methods

2.1 Registration

The meta-analysis protocol was submitted to the International Prospective Register of Systematic Reviews CRD42019145675URL : <https://www.crd.york.ac.uk/prospero/> and the research work was conducted according to the Preferred Reporting Items for Systematic Reviews and Meta-Analyses (PRISMA) guidelines (31).

2.2 Data sources and literature search strategy

A systematic literature search was performed using MEDLINE (through PubMed) and a comprehensive query (Figure 1) in order to retrieve all relevant studies published until September 15, 2022 and reporting data on the associations between ABX use and the clinical outcomes of cancer in patients treated with anti-PD-(L)1-based treatments. In order to include the largest possible patient population, no filters for language (although the query was submitted in English) or year of publication were applied.

Besides, proceedings of major oncology conferences held between 2017 and 2022 were also screened to identify unpublished studies that could be included, thus minimizing publication bias, using the following keywords: antibiotic, antibiotics, antimicrobial, antimicrobials, anti-infective, anti-infectives. Such conferences were the European Lung Cancer Congress (ELCC) and the World Conference on Lung Cancer (WCLC), as well as annual meetings from the American Association for Cancer Research (AACR), the American Society of Clinical Oncology (ASCO), the European Society for Medical Oncology (ESMO), the International Association for the Study of Lung Cancer (IASLC) and the Society for Immunotherapy of Cancer (SITC). Any relevant article references were also screened for additional studies.

2.3 Study selection

Studies were included in the present meta-analysis if they fulfilled the following criteria: 1) study subjects were patients diagnosed with any type of cancer and treated with anti-PD-(L)1 agents, either as monotherapy or in combination with other anticancer treatments, 2) ABX-exposed patients received ABX before and/or after the initiation of and/or during immunotherapy, regardless of ABX class, route of administration and duration of use, 3) ABX-unexposed patients (the control group) did not receive ABX within the defined timeframes, and 4) studies provided data, suitably formatted for inclusion, on the associations between ABX use and at least one outcome retained for this meta-analysis, namely Overall Survival (OS), Progression-Free Survival (PFS), ORR and PD.

If several studies were redundant (*i.e.* they reported data on overlapping patient populations, which was identified by looking at patient recruitment centers and study periods), the most recent study was selected for inclusion in the meta-analysis.

The literature screening was independently conducted by two reviewers who consulted with a third author to resolve any discrepancy.

```
(immunotherapy[Title/Abstract] OR immunotherapies[Title/Abstract] OR immunotherapeutic[Title/Abstract] OR
immunotherapeutics[Title/Abstract] OR ICI[Title/Abstract] OR ICIs[Title/Abstract] OR CPI[Title/Abstract] OR "immune-checkpoint
inhibitor"[Title/Abstract] OR "immune checkpoint inhibitor"[Title/Abstract] OR "immune-checkpoint blockade"[Title/Abstract] OR
"immune checkpoint blockade"[Title/Abstract] OR ICB[Title/Abstract] OR ICBs[Title/Abstract] OR nivolumab[Title/Abstract] OR
opdivo[Title/Abstract] OR pembrolizumab[Title/Abstract] OR keytruda[Title/Abstract] OR atezolizumab[Title/Abstract] OR
tecentriq[Title/Abstract] OR avelumab[Title/Abstract] OR bavencio[Title/Abstract] OR durvalumab[Title/Abstract] OR
imfinzi[Title/Abstract] OR ipilimumab[Title/Abstract] OR yervoy[Title/Abstract] OR cemiplimab[Title/Abstract] OR
libtayo[Title/Abstract] OR toripalimab[Title/Abstract] OR TopAlliance[Title/Abstract] OR sintilimab[Title/Abstract] OR
Innovent[Title/Abstract] OR camrelizumab[Title/Abstract] OR dostalimab[Title/Abstract] OR tislelizumab[Title/Abstract] OR "PD-
1"[Title/Abstract] OR PD1[Title/Abstract] OR "PD-L1"[Title/Abstract] OR "PD-(L)1"[Title/Abstract] OR PDL1[Title/Abstract] OR
"CTLA-4"[Title/Abstract] OR CTLA4[Title/Abstract] OR "AMP-124"[Title/Abstract] OR "AMP-514"[Title/Abstract] OR "STI-
A1110"[Title/Abstract] OR "TSR-042"[Title/Abstract] OR "RG-7446"[Title/Abstract] OR "BMS-936559"[Title/Abstract] OR "MEDI-
4736"[Title/Abstract] OR "MSB-0020718C"[Title/Abstract] OR "AUR-012"[Title/Abstract] OR "STI-A1010"[Title/Abstract])
AND
(antibiotic*[Title/Abstract] OR antimicrobial*[Title/Abstract] OR "anti-infective"[Title/Abstract] OR "anti-
infectives"[Title/Abstract] OR macrolide*[Title/Abstract] OR fluoroquinolone*[Title/Abstract] OR quinolone*[Title/Abstract] OR
"beta-lactam"[Title/Abstract] OR "beta-lactams"[Title/Abstract] OR cephalosporin*[Title/Abstract] OR
tetracycline*[Title/Abstract] OR penicillin*[Title/Abstract] OR aminoglycoside*[Title/Abstract] OR cycline*[Title/Abstract] OR "co-
medication"[Title/Abstract] OR comedication*[Title/Abstract] OR "concurrent medication"[Title/Abstract] OR "concomitant
medication"[Title/Abstract] OR "concurrent drug"[Title/Abstract] OR "concomitant drug"[Title/Abstract] OR "co-
medications"[Title/Abstract] OR "concurrent medications"[Title/Abstract] OR "concomitant medications"[Title/Abstract] OR
"concurrent drugs"[Title/Abstract] OR "concomitant drugs"[Title/Abstract])
```

FIGURE 1
Literature query used on PubMed.

2.4 Data extraction

Using a standardized data extraction spreadsheet, the following data were collected from each of the included study, when available: first author's name, publication year, publication type (full-text article, poster or abstract), country, patient and cancer characteristics (*i.e.* number of patients included, histology, cancer stage, Eastern Cooperative Oncology Group performance score (ECOG PS)), immunotherapy characteristics (ICI type, treatment scheme and line of treatment), ABX treatment characteristics (number of ABX users, ABX exposure time window (TW), indication, class, route of administration and duration of use) and outcomes of interest based on ABX exposure. Authors were contacted when crucial data, such as the number of ABX users, were missing in a study.

For OS and PFS, Hazard Ratios (HRs) and their 95% Confidence Intervals (CI) were included in the meta-analysis when reported as such in the studies and estimated from Kaplan-Meier curves with the Tierney et al. approach (32) when not, with the estimations performed independently in duplicate by two reviewers to ensure consistency of the results. In case of discrepancy, another estimation was performed by a third author and if the results remained inconclusive, the estimations were not included in the meta-analysis.

Regardless of the outcome, results yielded by multivariate analyses were preferred over results yielded by univariate analyses, when available, for inclusion in the meta-analysis. When results were available on multiple ABX exposure time windows in a given study, pre-defined criteria of selection were applied to include the largest number of qualitative results and to make the most relevant analyses possible (see the complete methodology in Supplementary Figure 1).

2.5 Quality assessment

As the majority of the studies included had a retrospective design, a quality assessment was independently performed by two reviewers using the Newcastle-Ottawa scale (NOS), a star-based system that rates non-randomized studies based on the three following domains: selection of the study groups, comparability of the study groups and ascertainment of the outcomes.

2.6 Data analyses

2.6.1 Pooled analyses

OS and PFS are respectively defined as time from immunotherapy initiation until death by any cause or loss to follow up (for OS) or until radiological evidence of progressive disease or loss to follow-up (for PFS). One of the aims of the meta-analysis was to evaluate the impact of ABX use on the survival and survival without cancer progression of cancer patients treated with ICIs by calculating pooled HRs for OS and PFS along with their 95% CI across all cohorts.

ORR and PD are treatment-related outcomes, with ORR representing the number of patients experiencing a complete or partial response, and PD equated, for the purpose of the meta-analysis, with the number of patients experiencing cancer progression. One of the aims of the meta-analysis was to assess the association between ABX use and response to treatment by calculating pooled Odds Ratios (ORs) for ORR and PD along with their 95% CI across all cohorts.

2.6.2 Subgroup analyses

In order to minimize between-study heterogeneity and to determine factors influencing the impact of ABX use on survival and treatment-related outcomes, several subgroup analyses were conducted, subject to an acceptable number of cohorts per group. As the number of studies reporting data on treatment-related outcomes was relatively small, the subgroup analyses were restricted to survival outcomes.

2.6.2.1 Subgroup analyses according to the cancer type

A cancer type formed a separate category if at least four cohorts of patients with that cancer type were available with data on both OS and PFS according to ABX exposure. An "Other" category was created to group cancers for which less than four cohorts of patients with that type of cancer reported data on survival outcomes, while an "Aggregated" category was defined to group cohorts having pooled patients suffering from various types of cancer.

2.6.2.2 Subgroup analyses according to the antibiotic exposure time window

Five ABX exposure TWs relative to ICI initiation were selected, based on the TWs defined in the included studies and with the assumption of a stronger impact of ABX when taken around ICI initiation: [-60 days; 0], [-30 days; 0], [-60 days; 60 days], [-90 days; 120 days] and "undefined" (noted hereafter [-∞; ∞]), Day 0 being the day of initiation of the treatment with ICIs, *i.e.* the day of the first administration of immunotherapy. Of note, a patient included in the TW [-60 days; 0] may have taken ABX only in an unspecified short period included in this TW (for example, between -15 and -10 days before ICI initiation).

2.6.3 Focus on non-small cell lung cancer

Lung cancers are responsible for the largest number of cancer-related deaths worldwide². About 80% to 85% of all lung cancers are NSCLC. As NSCLC was one of the first cancers for which ICIs were approved³, it is the cancer for which the literature is the most comprehensive, with nearly half of the patients included in the meta-analysis suffering from NSCLC (and just as many studies focusing on this cancer type). For comparison, the second most represented cancer in this literature, namely UC, represents less than 15% of all patients and cohorts included. NSCLC was therefore the subject of a focus in the present meta-analysis, and some analyses were

² Global Cancer Observatory. <https://gco.iarc.fr/>

³ Cancer Research Institute. <https://www.cancerresearch.org/scientists/immuno-oncology-landscape/pd-1-pd-l1-landscape>

performed exclusively on the NSCLC patient population, allowing to minimize heterogeneity between studies. Thus, in addition to pooled HRs for OS and PFS and pooled ORs for ORR and PD, subgroup analyses were performed on survival outcomes according to the following ABX exposure TWs: [-60 days; 60 days], [-45 days; 45 days], [-90 days; 120 days] and $]-\infty; \infty]$, Day 0 being the day of initiation of the treatment with ICIs. In addition, NSCLC studies were analyzed in more detail to bring out information on the baseline characteristics of NSCLC patients (histology, ECOG PS, PD-L1 expression), on the immunotherapy treatment (anti-PD-(L)1 scheme and agent, and treatment line) and on the use of ABX (ABX class, cause of prescription and route of administration).

2.7 Random-effect model

All calculations of HRs and ORs were performed using the inverse variance-weighted average method according to a random-effect model, to best accommodate the high heterogeneity expected from the included studies and measured using the Higgins and Thompson statistic I^2 . For survival outcomes, a value of $HR > 1$ indicated that ABX use was negatively associated with the considered outcome, while a 95% CI > 1 indicated that the association was statistically significant. For treatment-related outcomes, a value of OR for ORR < 1 indicated that ABX use was negatively associated with treatment response, and the association was statistically significant if the 95% CI was inferior to 1. On the contrary, a value of OR for PD > 1 indicated that ABX was associated with an increased odd of cancer progression, while a 95% CI > 1 indicated that the association was statistically significant. For all analyses, a p-value ≤ 0.05 was considered to be statistically significant.

2.8 Publication bias and sensitivity analysis

One weakness of a meta-analysis is that it relies on the available published literature and can be affected by publication bias, which occurs when the results of a study have an impact on the decision to publish the study. For example, it is known that researchers are less likely to publish their study when their working hypothesis is not met (in our case, if antibiotics do not impact patient outcomes). Publication bias was assessed for pooled HRs for OS and PFS and pooled ORs for ORR and PD through the generation of funnel plots that were analyzed for asymmetry using Begg and Egger tests. If a publication bias was detected, its impact on the meta-analysis results was assessed *via* a trim-and-fill approach. A sensitivity analysis was also conducted to assess the risk of one individual study biasing the results using the leave-one-out approach.

All analyses were performed using R version 3.6.1 and the meta package (33, 34).

3 Results

3.1 Study selection

The literature search conducted on PubMed initially retrieved 2,036 hits, of which 1,950 were excluded based on their title or

abstract, leaving a total of 86 candidate studies for full-text reading. 20 studies were consequently discarded due to different reasons, including redundancy and/or overlapping cohorts, and the reporting of outcomes other than the ones retained for this meta-analysis. An additional 30 relevant studies were extracted from the screening of major oncology conference proceedings, and 11 were further identified by reviewing the references of relevant articles in the field. 67 articles published in peer-reviewed journals, 25 posters and 15 abstracts were ultimately included in the meta-analysis, representing a total of 107 articles (7, 12–14, 35–137), issued between 2017 and 2022, and reporting data on 123 independent cohorts. The results of the literature search process are displayed in Figure 2.

As shown in Supplementary Table 1, the included studies had Newcastle-Ottawa scale scores ranging from 3 to 8, with a median at 6. The missing criteria were generally item D (demonstration that outcome of interest was not present at start of study), G (adequate duration of follow-up) and H (loss to follow-up rate), and the lowest scores were mainly attributed to the abstracts. Of note, low scores do not necessarily correspond to poor-quality studies but rather to a lack of sufficient information.

3.2 Characteristics of studies and patients included

Baseline characteristics of studies and patients included are displayed in Supplementary Table 2. The very large majority of studies were retrospective analyses of patient medical records (some of which were entered into prospectively-maintained databases); only 6 studies reported prospective observational clinical trial data (13, 43, 81, 101, 110, 114).

Overall, a total of 41,663 patients diagnosed with cancer and treated with an anti-PD-(L)1-based treatment were included in the meta-analysis, among whom 11,785 (28%) were administered ABX in varying timeframes around ICI initiation.

The United States of America (USA) and Europe were the continents providing most cohorts and patients (34% of cohorts and 47% of patients for the USA, 29% of cohorts and 22% of patients for Europe), followed by Asia (22% and 9% of cohorts and patients, respectively). Within Europe, France and Spain produced most cohorts and included most patients (31% and 55% of cohorts and patients for France, respectively, and 29% and 14% for Spain).

The very large majority of patients included in the meta-analysis had a locally advanced or metastatic cancer. The number of patients enrolled in the studies ranged from 31 to 3,634, with the largest cohorts including NSCLC patients. In terms of number of patients (and of cohorts), NSCLC was by far the most represented cancer, with 40% of the 41,663 patients suffering from this cancer (and 41% of the cohorts including NSCLC patients), followed by UC (14% of patients, 12% of cohorts), melanoma (13% of patients, 7% of cohorts), renal cell carcinoma (RCC) (8% of patients, 7% of cohorts) and hepatocellular carcinoma (HCC) (4% of patients, 7% of cohorts). The remaining cohorts included patients suffering from cancer types less represented in this immuno-oncology literature, namely head and neck cancer, esophagogastric/gastric cancer, gynecologic cancers, cutaneous squamous cell carcinoma,

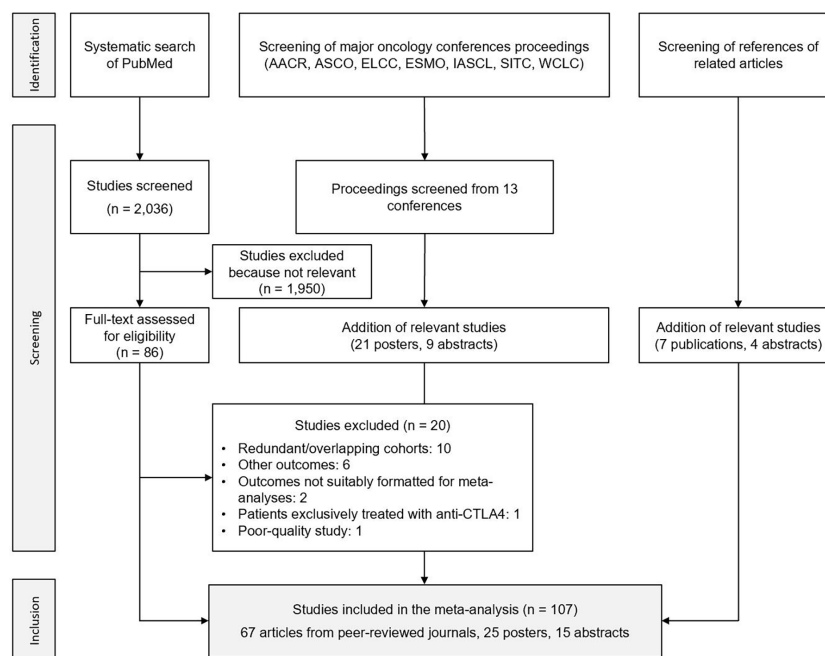


FIGURE 2

Flowchart of the search process. AACR, American Association for Cancer Research; ASCO, American Society of Clinical Oncology; ELCC, European Lung Cancer Congress; ESMO, European Society for Medical Oncology; IASCL, International Association for the Study of Lung Cancer; SITC, Society for Immunotherapy of Cancer; WCLC, World Conference on Lung Cancer.

Hodgkin lymphoma, colorectal cancer and sarcoma (each of these cancer types representing less than 3% of all patients and cohorts). Finally, 18 cohorts (16% of all patients) grouped patients suffering from various cancer types, of which NSCLC was once again the most represented cancer type (37%), followed by melanoma (29%).

The studies included were largely heterogeneous in terms of reported immunotherapy and ABX treatment characteristics, but from the review of this literature, patients seemed to be predominantly treated with anti-PD-1 monotherapy, nivolumab and pembrolizumab being the most represented ICI agents. The line of treatment greatly differed between studies, but the largest cohorts included patients receiving immunotherapy as first-line treatment for locally advanced or metastatic cancers. All studies selected varying time windows of exposure to ABX, some of them being strictly defined and very narrow around ICI initiation ([−14 days; 14 days] in Ahmed J. et al. (123)), other being broader and less defined (“after ICI initiation” in Masini et al. (131)). β -lactams and fluoroquinolones were the most used ABX in this patient population, and ABX were mostly administered *via* oral route. More detailed information on patient characteristics, anticancer treatment and antibiotic therapy is available for NSCLC patients in section 3.6.1.

3.3 Impact of antibiotic use on survival outcomes across all cancer types

3.3.1 Global analyses

112 and 80 cohorts reported data on OS and PFS based on ABX exposure, respectively, representing 40,236 patients and 12,564

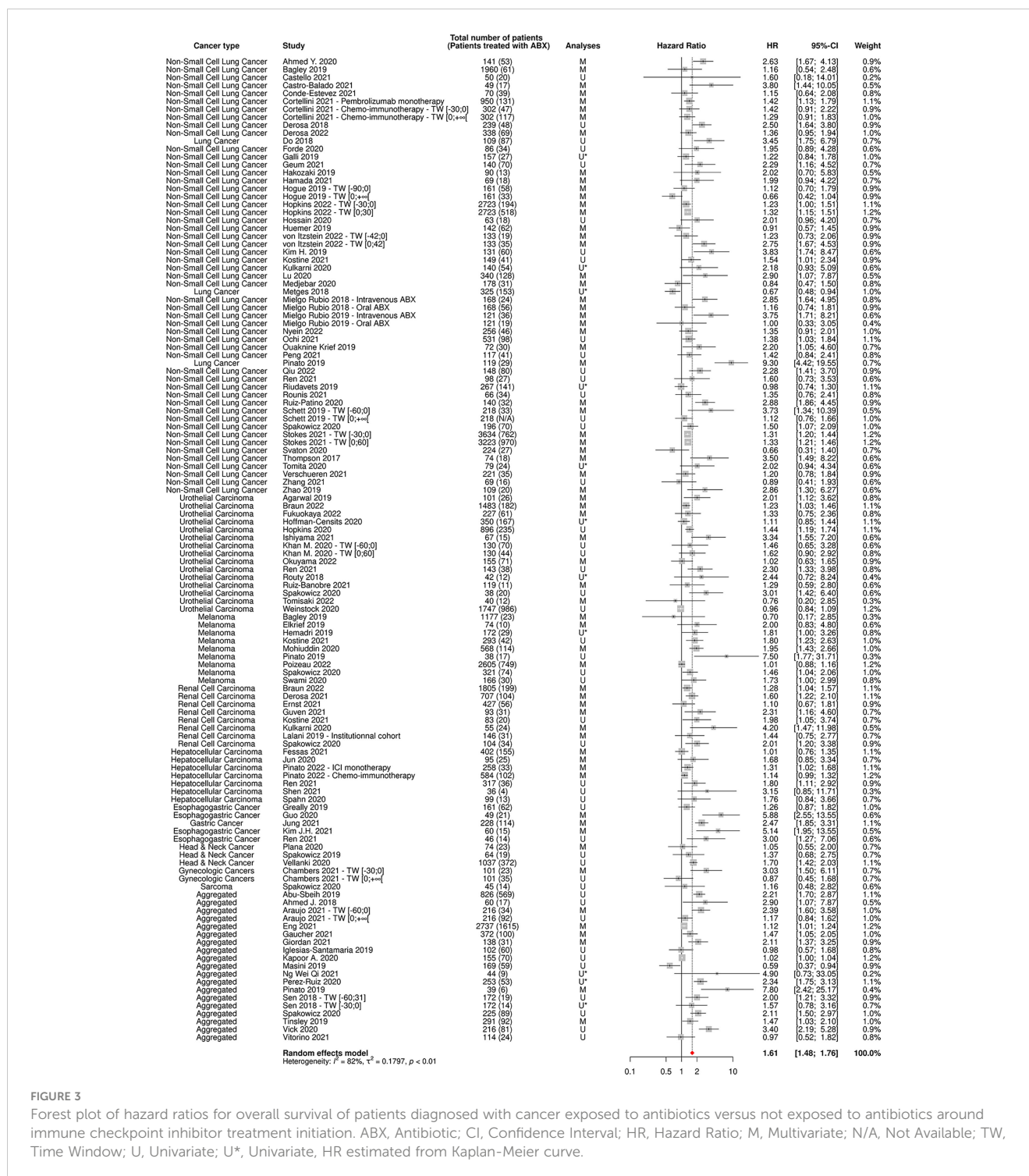
ABX users (31%) for OS and 20,318 patients and 6,223 ABX users (31%) for PFS.

The random-effect model yielded respective HRs for OS and PFS of 1.61 [95% CI 1.48–1.76] and 1.45 [95% CI 1.32–1.60] (Figures 3, 4) across all cancer types and ABX exposure time windows, suggesting that ABX use is significantly associated with reduced survival and survival without progression of cancer patients treated with ICIs. When excluding HRs calculated from univariate analyses, to keep uniquely cohorts having controlled for confounding factors, the association between ABX and survival outcomes remained very highly significant, with HRs for OS and PFS being respectively of 1.64 [95% CI 1.44–1.90] and 1.62 [1.39–1.89] (Figures 5, 6). Of note, the design of the study (prospective or retrospective) did not appear to have exerted an impact on the results (data not shown).

As expected, the heterogeneity factor was substantial in these global analyses (I^2 of 82% for OS, I^2 of 74% for PFS), due to the high variability observed between studies, notably in terms of type of cancer and ABX exposure time window.

3.3.2 Impact of antibiotic use on survival outcomes according to the cancer type

As shown in Table 1, ABX were negatively associated with OS across all cancer types, and this association was particularly pronounced in NSCLC and RCC patients, with HRs for OS being of 1.60 [95% CI 1.40–1.83] and 1.65 [95% CI 1.24–2.19], respectively. ABX use was also significantly associated with a decreased PFS in patients suffering from NSCLC, RCC, and from less represented cancers. Even though ABX use was not statistically



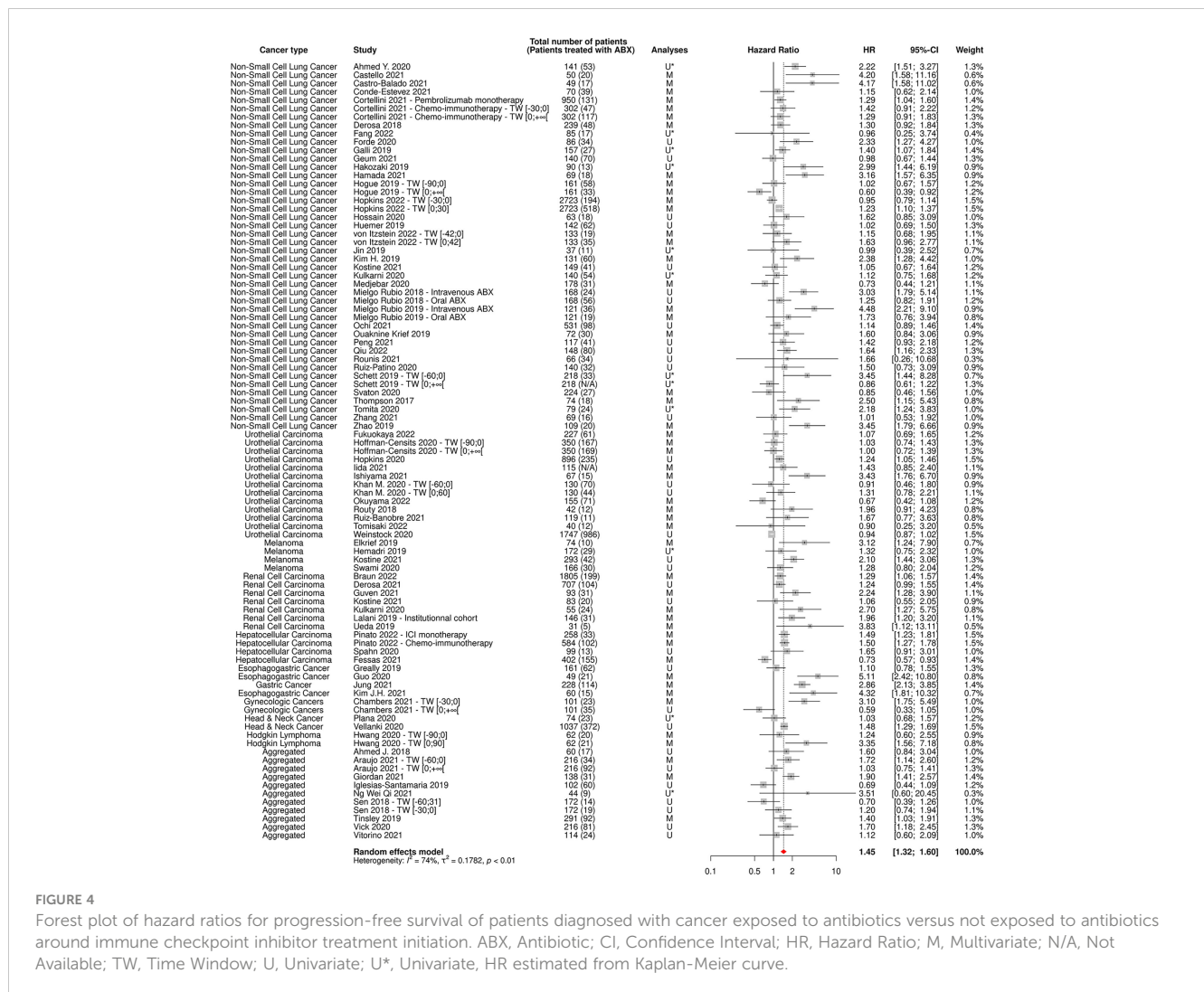
associated with a decreased PFS in patients suffering from UC, melanoma and HCC, the HRs superior to 1 and the 95% CI close to statistical significance (notably for UC and melanoma) suggest a clinically meaningful trend towards a similar negative association in these cancer types.

As shown in the forest plots available in [Supplementary Figures 2, 3](#), the I^2 value remained high ($> 50\%$) for most cancer types, which was expected given the large number of factors that can induce heterogeneity, such as the diversity of histological subtypes

among each cancer type and differential cancer management, for example.

3.3.3 Impact of antibiotic use on survival outcomes according to the exposure time window

As shown in [Table 2](#), the negative association between ABX use and survival outcomes was most pronounced when ABX were received in the one or two months preceding or following the



initiation of immunotherapy, with the HR for OS reaching the high value of 2.24 [95% CI 1.66-3.03] in the [-30 days; 0] TW. It appears that the TW of ABX exposure relative to the date of initiation of the ICI treatment has an impact on the observed clinical outcomes, with ABX taken long before or after the initiation of the ICI initiation having a less pronounced impact on patient outcomes, compared with ABX taken just before or just after ICI initiation.

As shown in the forest plots available in [Supplementary Figures 4, 5](#), heterogeneity remained high ($I^2 > 50\%$) for most TWs.

3.4 Impact of antibiotic use on treatment-related outcomes across all cancer types

44 and 38 cohorts reported data on ORR and PD based on ABX exposure, respectively, representing 7,854 patients and 1,997 ABX users (25%) for ORR and 6,142 patients and 1,654 ABX users (27%) for PD.

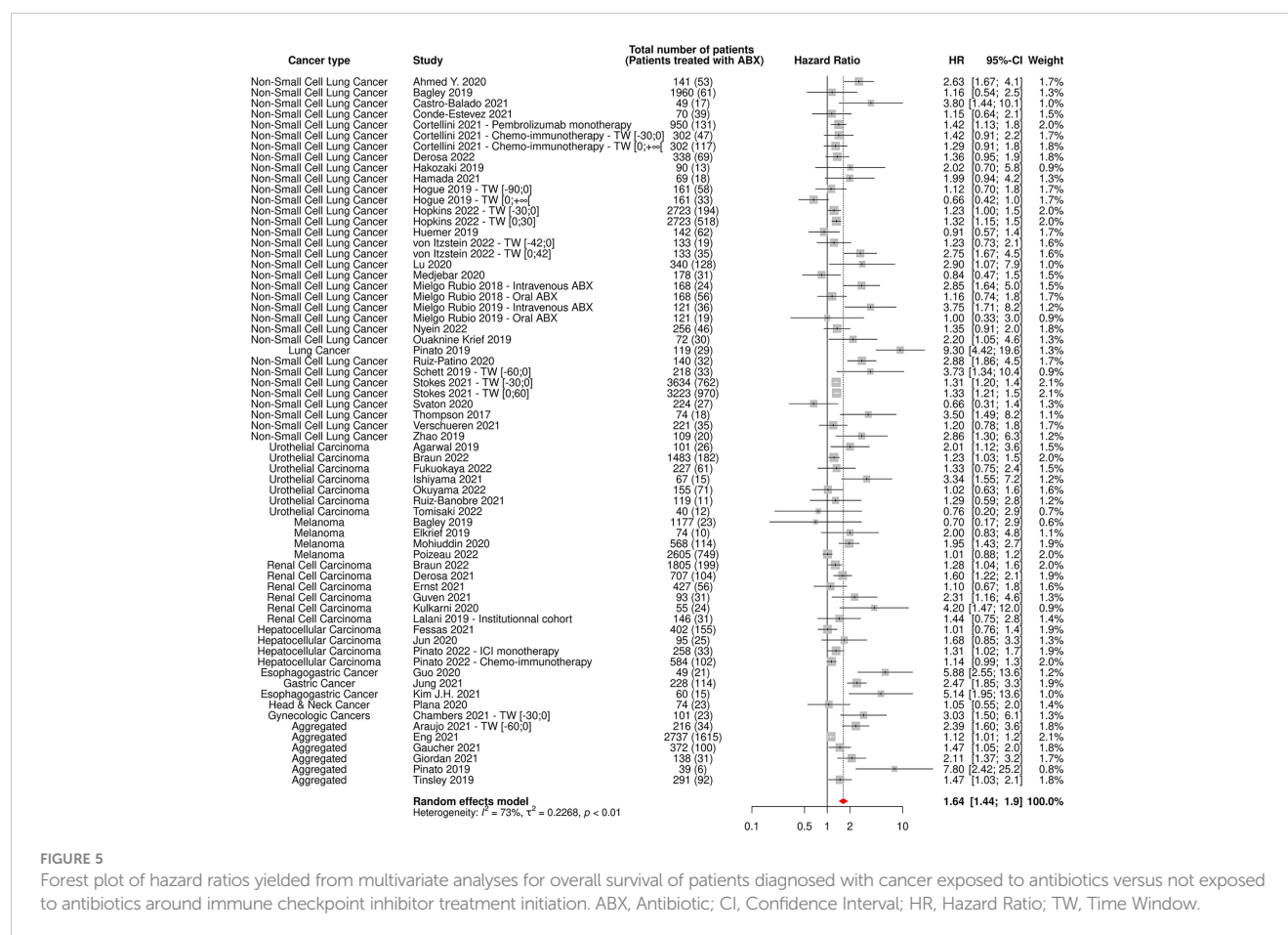
The random-effect model yielded ORs for ORR and PD of 0.59 [95% CI 0.47-0.76] and 1.86 [95% CI 1.41-2.46], respectively ([Figures 7, 8](#)), suggesting that ABX use was significantly and

negatively associated with impaired response to treatment among cancer patients receiving ABX, with both a reduced odd of response and an increased odd of cancer progression among ABX users.

As expected, the heterogeneity factor was substantial (I^2 of 57% for ORR, I^2 of 74% for PD) in these analyses.

3.5 Publication bias and sensitivity analysis

Funnel plots for OS, PFS, ORR and PD are available in [Supplementary Figures 6–9](#). Begg and/or Egger tests indicate the existence of publication bias, as suggested by asymmetrical funnel plots, in global analyses associating ABX use with OS, PFS, ORR and PD (OS: p-value for Begg test: 0.7280, p-value for Egger test < 0.0001; PFS: p-value for Begg test: 0.0042, p-value for Egger test < 0.0001; ORR: p-value for Begg test: 0.0012, p-value for Egger test: 0.0014; PD: p-value for Begg test: 0.6212, p-value for Egger test: 0.0509). However, the trim-and-fill approach implemented indicated that the publication bias was unable to significantly affect the results for OS, PFS and PD, and that antibiotic use remained significantly associated with decreased OS (HR 1.44 [95% CI 1.30-1.59]) and PFS (HR 1.38



[95% CI 1.24-1.54]), and increased PD (OR 1.58 [95% CI 1.18-2.12]). On the contrary, the suggested deleterious impact of ABX treatment on the ORR did not remain statistically significant (OR 0.78 [95% CI 0.59-1.03]), although a clear trend for an impaired response still persisted. Besides, the sensitivity analysis performed using the leave-one-out-approach demonstrated that no single study was able to significantly influence the pooled HRs for OS and PFS, as well as the pooled ORs for ORR and PD (data not shown), supporting the reliability of the results.

3.6 Impact of antibiotic use on NSCLC patient clinical outcomes

3.6.1 Characteristics of NSCLC patients, immunotherapy and antibiotic treatment

A total of 50 independent cohorts including 16,529 patients (46% in the USA, 22% in Europe) suffering from NSCLC were included in the meta-analysis, of whom 5,022 (30%) were given ABX in the three months prior to ICI initiation and/or during immunotherapy.

The reported data on NSCLC patient characteristics, anticancer treatment and antibiotic therapy were largely heterogeneous between studies.

Pooling the 38 NSCLC cohorts reporting histologic data (10,561 patients), non-squamous cell carcinoma and squamous cell carcinoma accounted for 62% and 17% of histological subtypes, respectively. According to the 32 cohorts reporting performance status scores (6,323 patients), 87% of NSCLC patients had an ECOG PS equal to 0 or 1, with one-third of these patients having an ECOG PS of 0 and two-thirds having an ECOG PS of 1. Regarding expression of PD-L1 protein at tumor cell surface, as expressed by the Tumor Proportion Score (TPS), a TPS $\geq 50\%$ was the most represented PD-L1 expression level among NSCLC patients, accounting for 45% of the 4,413 patients included in the 20 cohorts reporting such data, corresponding to an over-representation of this level of PD-L1 expression compared to the 30% rate usually observed (138, 139).

Among the 38 cohorts documenting treatments in more detail (representing 6,652 patients), the vast majority of patients (90%) received an anti-PD-(L)1-based treatment as monotherapy. Nivolumab, pembrolizumab (both anti-PD-1 agents) and atezolizumab (anti-PD-L1) respectively accounted for 40%, 31% and 28% of the molecules received (reported in 31 cohorts for 10,728 patients). 70% of patients were treated with anti-PD-(L)1-based treatments as first-line (22 cohorts, 5,651 patients).

β -lactams, fluoroquinolones and macrolides were the most represented classes used by NSCLC patients, accounting

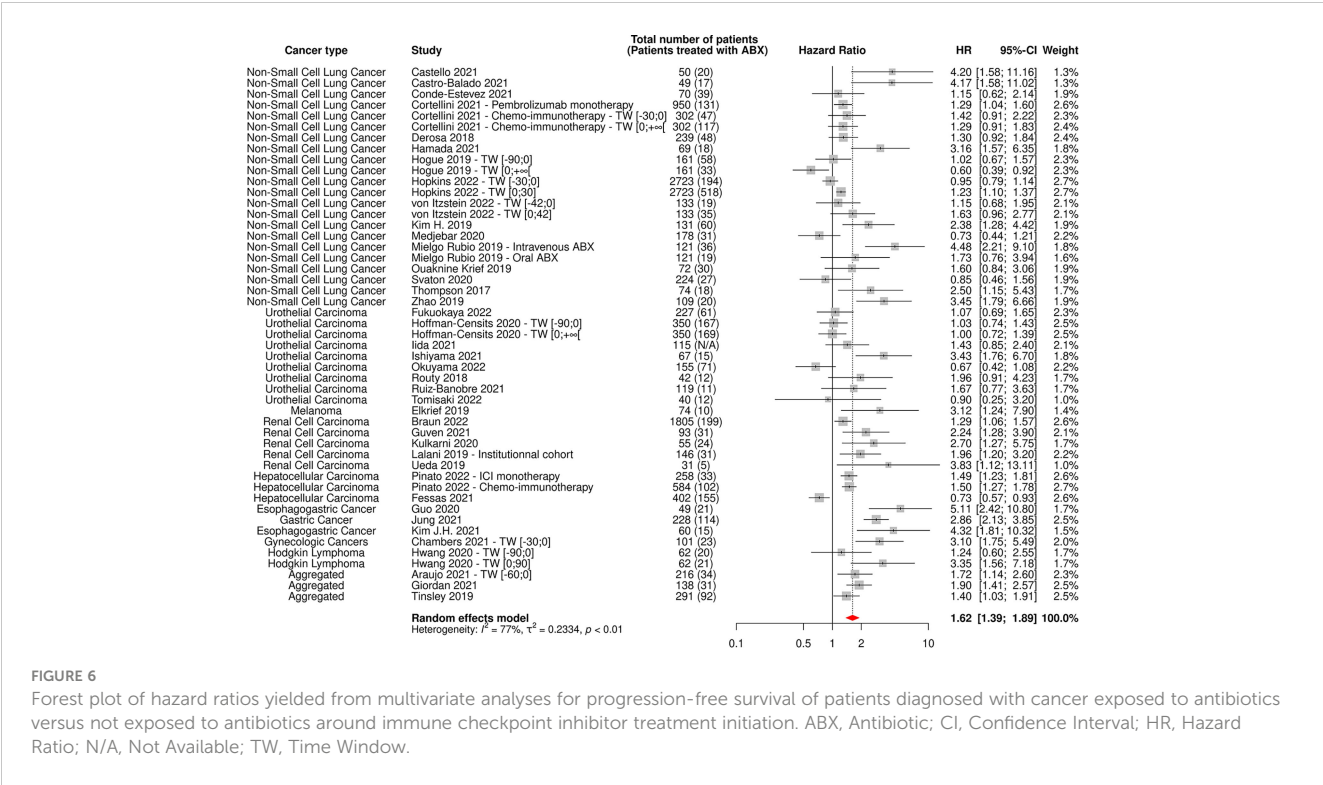


TABLE 1 Table of hazard ratios for overall survival and progression-free survival of patients diagnosed with cancer and exposed to antibiotics versus not exposed to antibiotics around immune checkpoint inhibitor treatment initiation, according to the cancer type.

Cancer Type	Number of Cohorts Included for OS	Pooled Number of Patients for OS (Number of ABX Users, % of ABX users)	Pooled HR OS [95% CI]	Number of Cohorts Included for PFS	Pooled Number of Patients for PFS (Number of ABX Users, % of ABX users)	Pooled HR PFS [95% CI]
Non-Small Cell Lung Cancer	47 cohorts (55 HR values)	16,163 (4,913, 30%)	1.60 [1.40-1.83]	37 cohorts (44 HR values)	8,421 (2,363, 28%)	1.47 [1.27-1.70]
Urothelial Carcinoma	14 cohorts (15 HR values)	5,454 (1,950, 36%)	1.45 [1.18-1.80]	11 cohorts (13 HR values)	3,804 (1,853, 49%)	1.18 [0.94-1.49]
Melanoma	9 cohorts	5,414 (1,088, 20%)	1.65 [1.16-2.34]	4 cohorts	705 (111, 16%)	1.72 [0.95-3.10]
Renal Cell Carcinoma	8 cohorts	3,420 (499, 15%)	1.65 [1.24-2.19]	7 cohorts	2,920 (414, 14%)	1.65 [1.14-2.38]
Hepatocellular Carcinoma	7 cohorts	1,791 (368, 21%)	1.35 [1.04-1.75]	4 cohorts	1,343 (303, 23%)	1.25 [0.69-2.30]
Other Cancers	10 cohorts (11 HR values)	1,865 (712, 38%)	1.92 [1.27-2.91]	8 cohorts (10 HR values)	1,772 (706, 40%)	1.88 [1.13-3.11]
Aggregated	17 cohorts (19 HR values)	6,129 (3,034, 50%)	1.67 [1.29-2.17]	9 cohorts (11 HR values)	1,353 (362, 27%)	1.28 [0.99-1.66]
Pooled	112 cohorts (124 HR values)	40,236 (12,564, 31%)	1.61 [1.48-1.76]	80 cohorts (93 HR values)	20,318 (6,223, 30%)	1.45 [1.32-1.60]

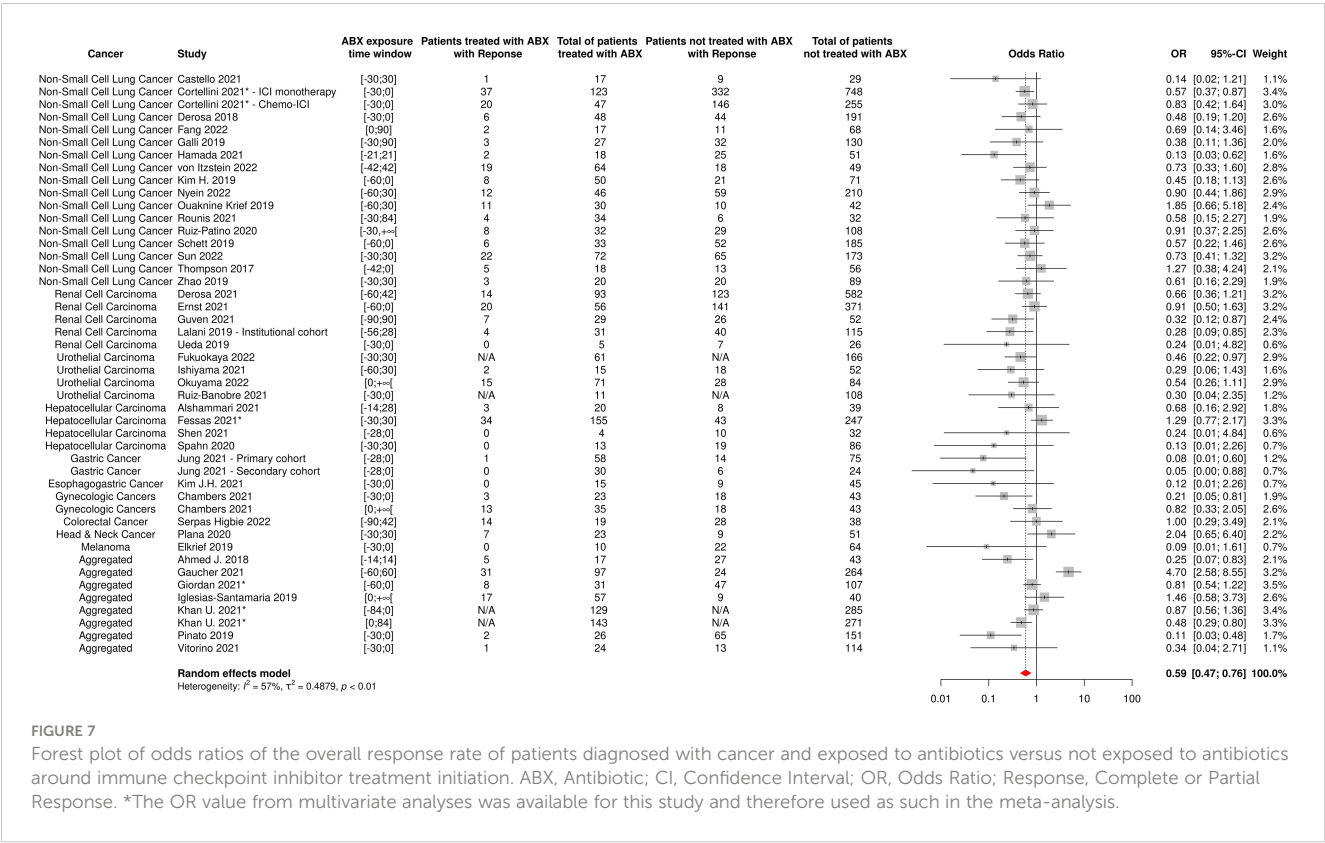
Statistically significant deleterious effect. Non statistically significant effect.
ABX, Antibiotic; CI, Confidence Interval; HR, Hazard Ratio; OS, Overall Survival; PFS, Progression-Free Survival.

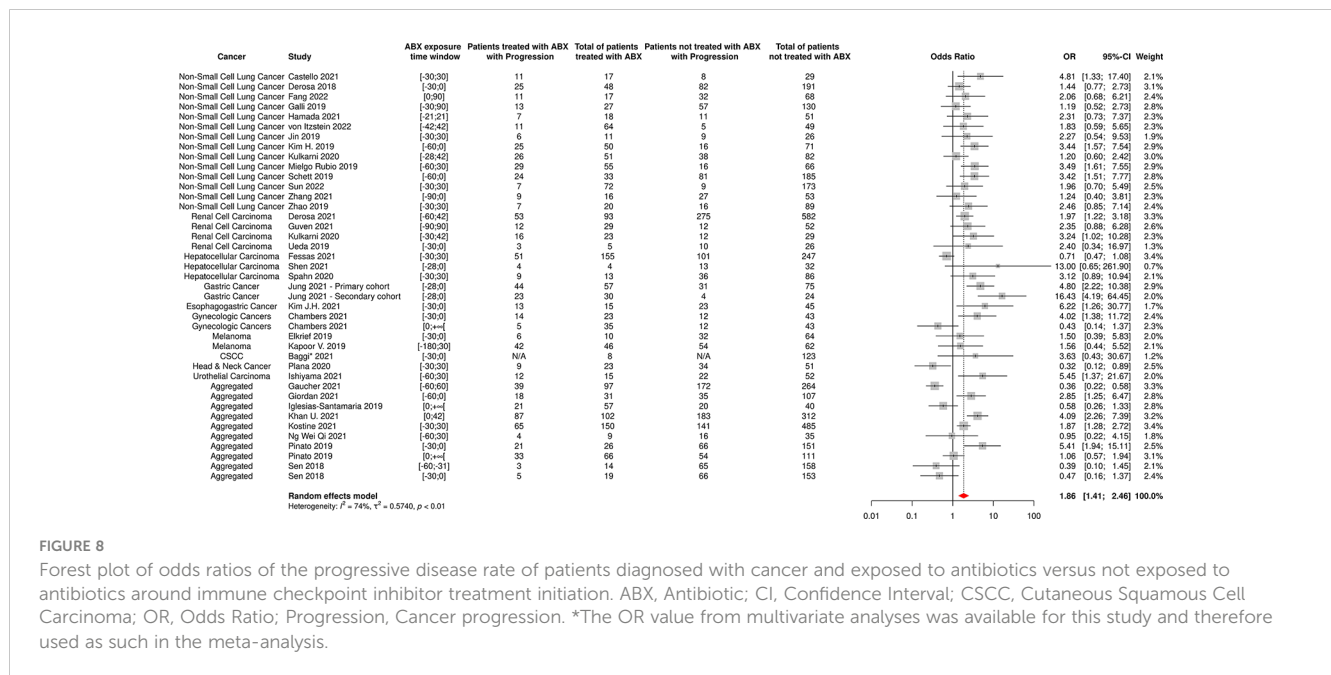
TABLE 2 Table of hazard ratios for overall survival and progression-free survival of patients diagnosed with cancer and exposed to antibiotics versus not exposed to antibiotics around immune checkpoint inhibitor treatment initiation, according to the antibiotic exposure time window.

Time Window of Exposure to ABX in Relation to ICI Treatment Initiation (Days)	Number of Cohorts Included for OS	Pooled Number of Patients for OS (Number of ABX users, % of ABX users)	Pooled HR OS [95% CI]	Number of Cohorts Included for PFS	Pooled Number of Patients for PFS (Number of ABX users, % of ABX users)	Pooled HR PFS [95% CI]
[-60; 0]	14 cohorts	5,055 (1,003, 20%)	1.72 [1.36-2.18]	10 cohorts	1,457 (333, 23%)	1.60 [1.14-2.23]
[-30; 0]	19 cohorts	9,539 (1,599, 17%)	2.24 [1.66-3.03]	14 cohorts	5,364 (658, 12%)	1.77 [1.33-2.35]
[-60; 60]	61 cohorts (63 HR values)	21,855 (5,009, 23%)	1.68 [1.53-1.85]	43 cohorts (45 HR values)	12,705 (3,264, 26%)	1.59 [1.39-1.82]
[-90; 120]	9 cohorts	4,139 (1,235, 30%)	1.26 [1.02-1.57]	9 cohorts (10 HR values)	1,113 (430, 39%)	1.34 [1.02-1.76]
]-∞; ∞[19 cohorts	7,000 (2,007, 29%)	1.33 [1.03-1.73]	14 cohorts	4,185 (959, 23%)	1.02 [0.84-1.24]

Statistically significant deleterious effect. Non statistically significant effect.
ABX, Antibiotic; CI, Confidence Interval; HR, Hazard Ratio; ICI, Immune Checkpoint Inhibitor; OS, Overall Survival; PFS, Progression-Free Survival.

respectively for 52%, 27% and 14% of ABX prescriptions within the 23 cohorts documenting ABX use (1,531 ABX prescriptions). This was not unexpected considering the relatively broad spectrum of antimicrobial activity of these ABX classes, which are often used for oncology patients. In the 19 cohorts reporting the indication for ABX use (917 prescriptions), more than half (51%) of the prescriptions were indicated to treat respiratory tract infections including suspected pneumonia. Finally, the oral route was the most





represented route of administration and accounted for 66% of the 537 prescriptions documented in 12 cohorts, which was expected as most of these patients are treated in the community setting.

3.6.2 Impact of antibiotic use on clinical outcomes of NSCLC patients

As previously mentioned, ABX use was significantly associated with impaired OS and PFS of NSCLC patients, as reported by the HRs respectively measured at 1.60 [95% CI 1.40-1.83] and 1.47 [95% CI 1.27-1.70] (Table 1 and Supplementary Figures 2, 3).

Similarly to the results obtained in the global analyses grouping all cancer types, excluding studies reporting only univariate analyses did not substantially change the results, with HRs being of 1.62 [95% CI 1.34-2.0] for OS and 1.51 [95% CI 1.18-1.93] for PFS, respectively (Supplementary Figures 10, 11). Of note, the most examined potential confounding factors for OS were, in this order, ECOG PS, age, sex, treatment line, smoking status/history, histology, other co-medications, cancer stage at diagnosis and presence of central nervous system metastases. The factors were broadly the same for PFS. Among the potential confounding factors, ECOG PS, histology and use of other co-medications were the factors with the greatest impact on OS and PFS (data not shown).

As shown in Table 3 and Figures 9, 10, OS and PFS were particularly reduced in patients treated with ABX within the weeks preceding or following ICI initiation, whereas the suggested damaging impact was not statistically significant when ABX were taken in timeframes more distant to immunotherapy start.

17 and 14 cohorts reported data on ORR and PD based on ABX exposure, respectively, representing 3,296 NSCLC patients and 696 ABX users (21%) for ORR and 1,803 NSCLC patients and 499 ABX users (28%) for PD. The random-effect models yielded ORs for ORR and PD of 0.65 [95% CI 0.50-0.86] and 2.09 [95% CI 1.61-

2.70], respectively, confirming significantly impaired response to treatment among NSCLC patients having received ABX around ICI initiation (Figures 11, 12).

3.6.3 Publication bias and sensitivity analysis

Funnel plots for OS, PFS, ORR and PD are available in Supplementary Figures 12–15 and suggested, again, some level of asymmetry. Begg and Egger tests both suggested the existence of publication bias in global analyses associating ABX use with survival outcomes (OS: p-value for Begg test: 0.0062, p-value for Egger test: 0.0047; PFS: p-value for Begg test: 0.0020, p-value for Egger test: 0.0037), but not in global analyses associating ABX use and treatment-related outcomes (ORR: p-value for Begg test: 0.2165, p-value for Egger test: 0.3866; PD: p-value for Begg test: 0.7016, p-value for Egger test: 0.3909). The trim-and-fill approach implemented indicated that such publication bias was unable to significantly affect the results for OS and PFS, with HRs being respectively re-calculated at 1.43 [95% CI 1.23-1.67] and 1.40 [95% CI 1.20-1.64]. In addition, the sensitivity analysis performed using the leave-one-out-approach demonstrated for all four outcomes that no single study was able to significantly influence the results, validating their reliability (data not shown).

4 Discussion

With the increasing use of immune checkpoint inhibitors in cancer care, considerable efforts have been made to identify factors that may alter their effectiveness, and ABX use has recently emerged as one of them, as demonstrated by numerous retrospective and prospective studies (7, 12–14, 35–137) and several meta-analyses (15–30) published on the topic. Our meta-analysis stands out from the others in that it included more than three-fold the number of

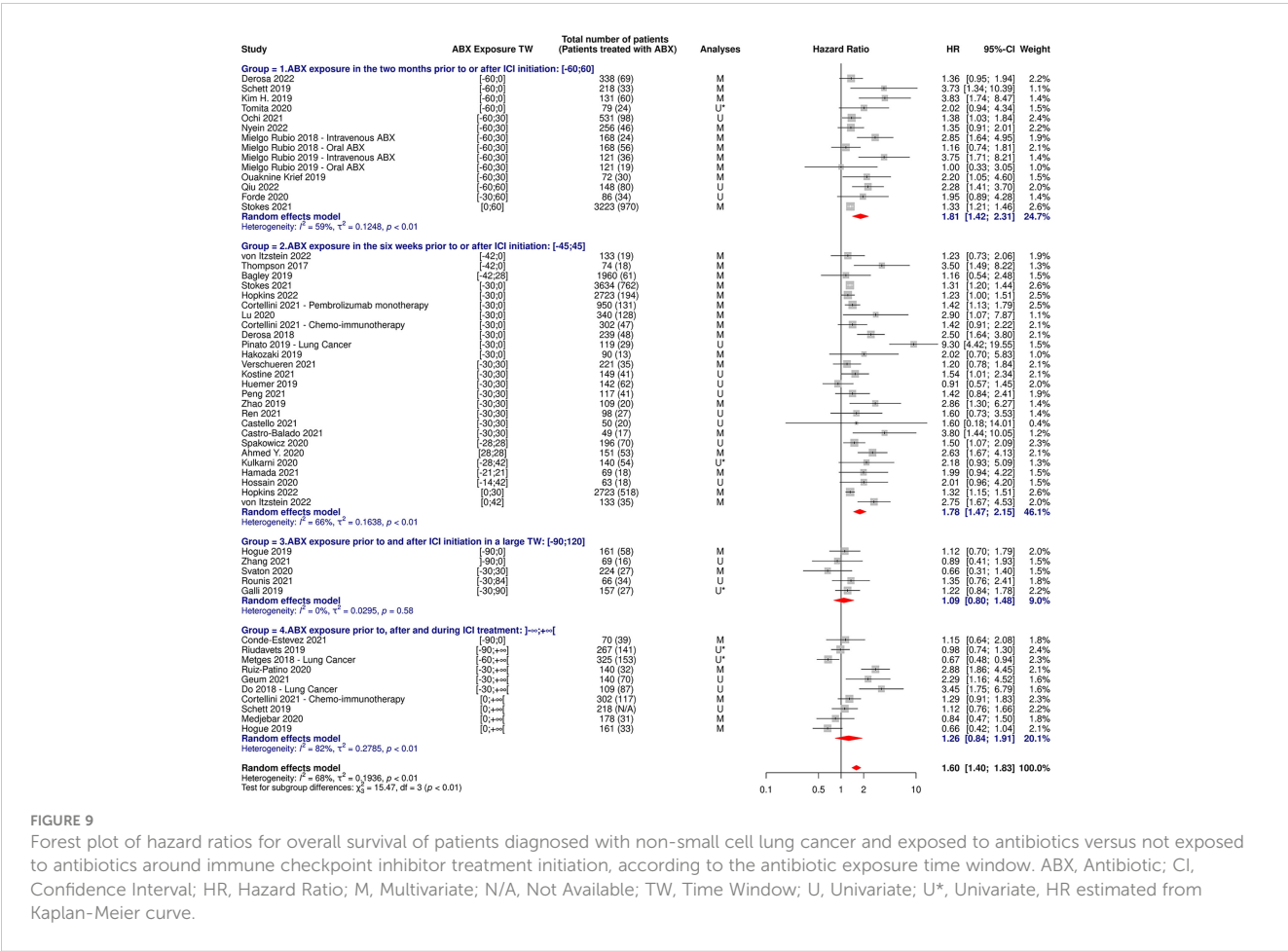
TABLE 3 Table of hazard ratios for overall survival and progression-free survival of patients diagnosed with non-small cell lung cancer and exposed to antibiotics versus not exposed to antibiotics around immune checkpoint inhibitor treatment initiation, according to the antibiotic exposure time window.

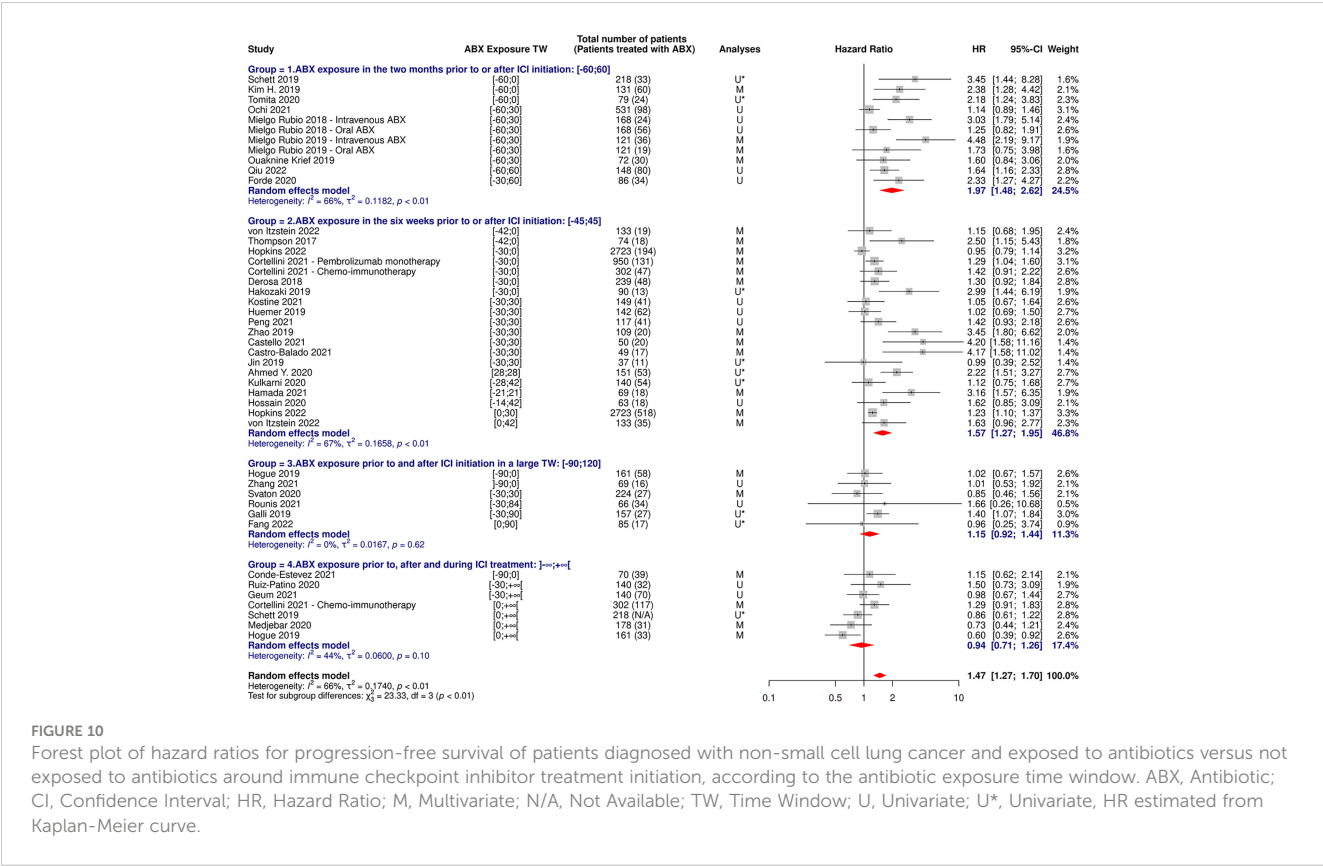
Time Window of Exposure to ABX in Relation to ICI Treatment Initiation (Days)	Number of Cohorts Included for OS	Pooled Number of Patients for OS (Number of ABX users, % of ABX users)	Pooled HR OS [95% CI]	Number of Cohorts Included for PFS	Pooled Number of Patients for PFS (Number of ABX users, % of ABX users)	Pooled HR PFS [95% CI]
[-60; 60]	12 cohorts (14 HR values)	5,372 (1,579, 29%)	1.81 [1.42-2.31]	9 cohorts (11 HR values)	1,554 (494, 32%)	1.97 [1.48-2.62]
[-45; 45]	23 cohorts (26 HR values)	12,286 (2,500, 20%)	1.78 [1.47-2.15]	18 cohorts (20 HR values)	5,577 (1,368, 25%)	1.57 [1.27-1.95]
[-90; 120]	5 cohorts	677 (162, 24%)	1.09 [0.80-1.48]	6 cohorts	762 (179, 23%)	1.15 [0.92-1.44]
]-∞; ∞[10 cohorts	1,910 (703, >37%)	1.26 [0.84-1.91]	7 cohorts	1,209 (322, 27%)	0.94 [0.71-1.26]

Statistically significant deleterious effect. Non statistically significant effect.
ABX, Antibiotic; CI, Confidence Interval; HR, Hazard Ratio; ICI, Immune Checkpoint Inhibitor; OS, Overall Survival; PFS, Progression-Free Survival.

patients compared with the most comprehensive published meta-analysis so far (23), allowing to perform reliable subgroup analyses evaluating the potential differential association of ABX use with outcomes depending on the cancer type and on the ABX exposure

time window. The numbers of cohorts and patients included in our meta-analysis were also sufficient to explore the impact of ABX use on short-term treatment-related outcomes, namely ORR and PD, which has been relatively understudied to date. Response-based

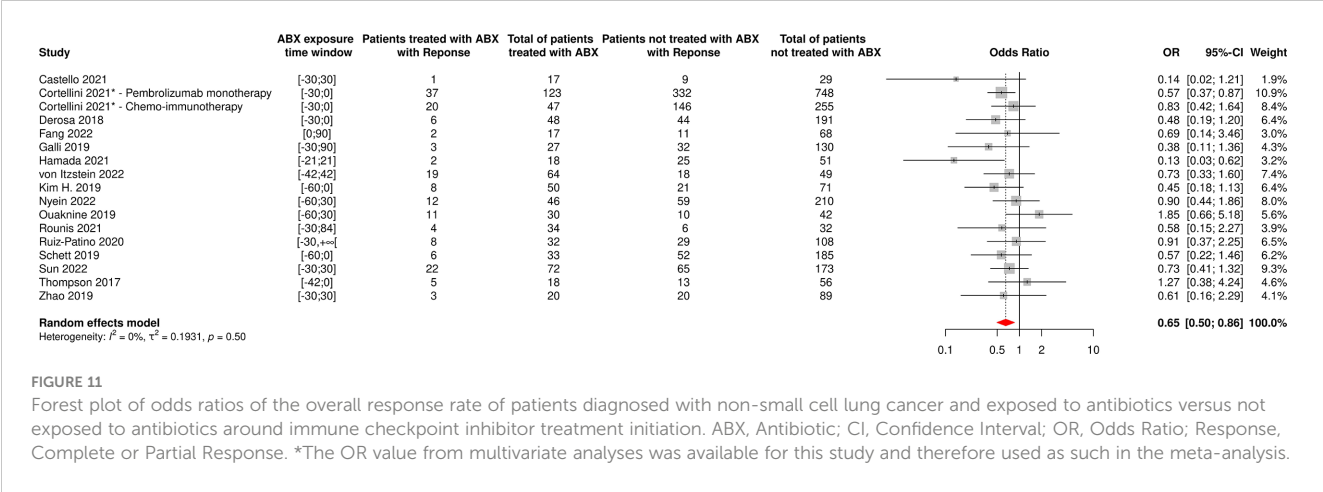




endpoints, such as ORR and PD, although investigator-assessed, are likely to be less affected by the patient inherent state of health, or subsequent lines of therapy, than overall survival outcome. Furthermore, such outcomes closely reflect the anti-tumor effect of the treatment (shrinkage *versus* escape *versus* growth of the tumor). Demonstrating a deleterious impact of antibiotics on response-based endpoints could therefore be an interesting way to dispose of possible confounding factors (such as the occurrence of a severe infection requiring an antibiotic treatment), that may be

associated with a poorer prognosis without being directly related to the impact of ABX use on the gut microbiome. For all these reasons, our analyses provide some novel insights that may be useful in clarifying the specific settings in which ABX should be prescribed in cancer patients treated with ICIs.

Using a random-effect model, we firstly demonstrated that ABX use was associated with impaired survival outcomes in the entire cancer patient population receiving ICIs, which was subsequently confirmed by the analyses of publication bias and sensitivity, that



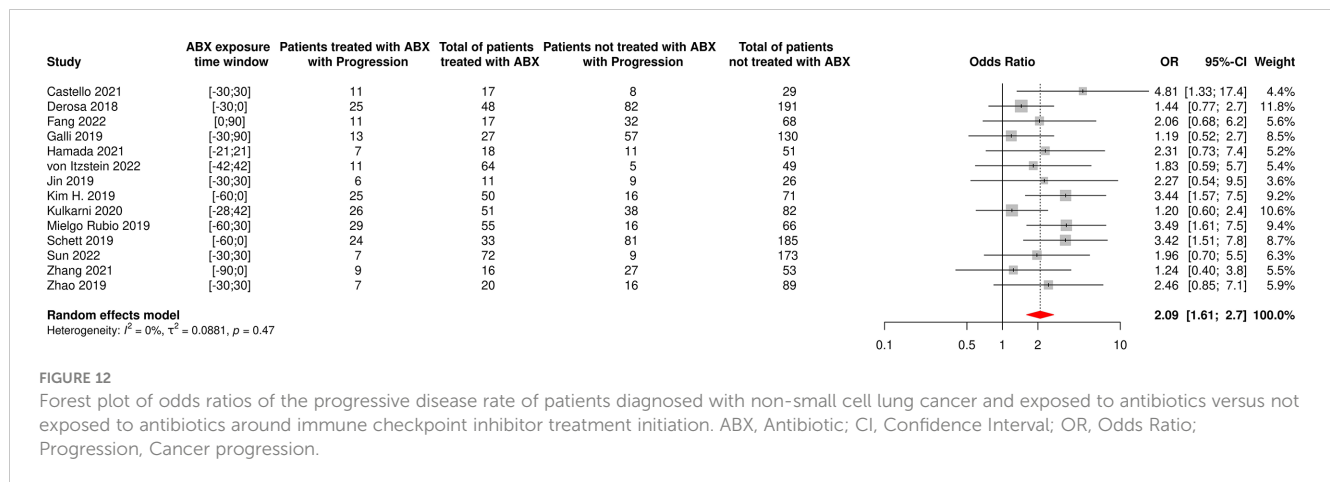


FIGURE 12

Forest plot of odds ratios of the progressive disease rate of patients diagnosed with non-small cell lung cancer and exposed to antibiotics versus not exposed to antibiotics around immune checkpoint inhibitor treatment initiation. ABX, Antibiotic; CI, Confidence Interval; OR, Odds Ratio; Progression, Cancer progression.

confirmed the reliability and the robustness of the results, and which is in accordance with the meta-analyses previously published on the subject (15–30). Exclusion of cohorts not having performed multivariate analyses further showed that this suggested deleterious impact persisted despite adjustment for confounding factors, suggesting that ABX use is an independent predictor factor for OS and PFS. The negative association of ABX and OS held across all cancer types investigated, namely NSCLC, UC, melanoma, RCC and HCC, with the strongest effects observed in NSCLC and RCC patients. However, the association with PFS was not significant in melanoma, UC and HCC patients (although close to statistical significance, and clinically meaningful for melanoma and UC). These differential effects are likely explained in part by the fewer numbers of cohorts included in each category for PFS, but it also could be caused by heterogeneity between cancers and patients as well as different modalities of ABX use. NSCLC patients are, for example, particularly prone to lung infections due to smoking that impairs local epithelial immunity and cilia-induced mucus clearance (140). Nevertheless, the publication of more and more articles showing a negative association between ABX and outcomes in more and more types of cancer, in patients not specifically affected by respiratory infections, seems to suggest a common effect to a large part of cancer types. The deleterious impact of ABX did not seem to vary according to the route of administration, suggesting that it is not related to the severity of the underlying infection. Strikingly, ABX were strongly associated with decreased survival outcomes when taken in the few weeks prior to or following ICI initiation for patients suffering from all types of cancer and especially for NSCLC patients. The association between ABX use, OS and PFS seems to depend from the TW of ABX exposure relative to the date of initiation of the ICI treatment: ABX taken long before or after ICI start have a less pronounced impact on patient outcomes, compared with ABX taken just before or just after ICI initiation. This result supports the hypothesis of an involvement of the gut microbiome, as patients having received ABX near ICI initiation probably have a highly dysbiotic microbiome at the time of starting ICI. Finally, ABX were negatively associated to treatment-related outcomes, with a decreased odd of response

and an increased odd of cancer progression in patients suffering from all types of cancer and notably in NSCLC patients. These results remained significant following publication bias and sensitivity analyses, except for the OR for ORR of patients diagnosed with any type of cancer (although a clear trend for an impaired response persisted), confirming that ABX are also negatively associated with the response to ICI treatment. ABX prophylaxis is now recommended in cancer patients receiving chemotherapy who are at high risk of grade 4 neutropenia and sepsis, and for whom the standard of care is now concomitant chemotherapy and ICIs. The results of this meta-analysis plead for caution in using such routine ABX prophylaxis when ICIs are considered. However, our analysis included a minority of studies dedicated to chemo-immunotherapy treatment and the indication for prophylactic ABX should be balanced with the risk of life-threatening neutropenia, taking into account individual characteristics (age, comorbidities, previous grade 4 neutropenia events, etc.) (141).

This systematic review and meta-analysis work certainly cannot discuss causality between ABX use and impaired clinical outcomes of cancer patients treated with ICIs, nor can it elucidate the underlying mechanisms involved. It can only show an association between ABX use and reduced ICI efficacy, and growing evidence in the literature and in the clinic suggest an involvement of the intestinal microbiome and ABX-induced dysbiosis. A high gut microbiome diversity at baseline was for example significantly associated with favorable clinical outcomes in several studies on NSCLC and melanoma patients (49, 56, 142). Our team recently demonstrated that FMT from ABX-treated healthy volunteers into germ-free mice altered the response of tumor-bearing mice to anti-PD-1 treatment, whereas FMT from healthy individuals having received both ABX and an ABX-adsorbent delivered to the colon that acted to protect the intestinal microbiome against dysbiosis was able to preserve ICI efficacy in the same mouse model (143). Besides, two recent clinical trials conducted in patients whose metastatic melanoma was refractory to a previous treatment with anti PD-(L)1 monoclonal antibodies suggested that FMT from other patients whose cancer responded to the same

immunotherapy enabled to overcome the resistance of their tumor to PD-(L)1 blockade (144, 145). The mechanisms by which the gut microbiome impacts response to immunotherapy remain largely debated, but two types of non-mutually exclusive conjectures are being discussed: an adjuvant effect and non-antigen specific improvement of the anti-tumor response by an increased “immune tonus” on one hand (146), and an antigenic effect with improvement of anti-tumor immune response by antigenic mimicry and cross reactivity with phage or bacterial encoded antigens, on the other hand (147). Interestingly, the damaging impact of ABX on the clinical outcomes of cancer patients treated with ICIs, that remains to be proved, could also be exerted on the outcomes of patients treated with other types of cancer immunotherapy. In a recent retrospective study including 228 patients suffering from hematological cancers and treated with Chimeric Antigenic Receptor – T cells (CAR-T) therapy, ABX use in the four weeks preceding treatment initiation was indeed associated to worse survival and increased neurotoxicity (148). In another retrospective study presentation at ESMO 2022, ABX use in the three weeks prior to CAR-T therapy initiation was also associated to impaired survival outcomes and increased cancer progression (149). Changes in the composition of the gut microbiome was also associated to clinical outcomes. The intestinal microbiome, through its complex interplay with the immune system, could therefore be crucial for response to cancer immunotherapy in most cancers, making personalized patient management and microbiome research essential.

Several inherent limitations to our meta-analysis are worth mentioning. First, a meta-analysis depends in part on the studies included, and most of them, in this case, were retrospective and therefore heterogeneous and incomplete in terms of reported data. Heterogeneity was very high in most of our analyses, although we attempted to mitigate it by performing subgroup analyses. Besides, the potential differential impact of ABX use could not be evaluated according to patient and treatment baseline characteristics such as PD-L1 expression or line of treatment, due to the lack of cohorts having reported such data, whereas these factors might have been of importance. Similarly, too few studies reported detailed data according to ABX treatment characteristics (duration of use, ABX class and route of administration) on patient outcomes, thus making it impossible to refine results in this regard. Further research in the field shall investigate the differential impact of ABX classes or treatment schemes. Besides, some TWs may have been overlapping without the authors’ knowledge. For example, a patient exposed to ABX in the 30 days prior to ICI initiation could have received ABX in the 30 days following treatment start and only be included in the first category. In addition, the retrospective design made it impossible to characterize the microbiome of patients before and during ICI treatment. Second, statistical analyses demonstrated the existence of publication bias within the literature, which we attempted to mitigate by including unpublished studies such as conference proceedings abstracts and by performing analyses that confirmed that publication bias could not affect most of our results. Third, the studies have included patients whose cancer characteristics and immunotherapy treatment are no longer the most representative of the real-world setting. Indeed, studies

mainly included patients treated with ICI as single agent, which no longer corresponds to standard of care, for most oncology indications, as ICIs are now mainly given in combination with chemotherapy or other treatment modalities. The impact of ABX use on patients treated with such combinations deserves to be further investigated, as only a few articles have investigated this matter (41, 52, 82) and do not allow to draw clear conclusions. Besides, nivolumab was the most represented ICI agent used in the papers included in this meta-analysis, whereas it has been largely supplanted by pembrolizumab in clinical practice since 2017. There was also an over-representation of high PD-L1 expressors (PD-L1 expression $\geq 50\%$) in the cohorts included in the meta-analysis compared to the real-world setting in link with the large number of single ICI agent studies. Fourth, ABX intake could not be the cause of worse outcomes but simply a marker of a degraded state in a patient, even though the performance of multivariate analyses precisely aims at adjusting for patient baseline characteristics. Finally, other medical interventions (e.g. prior radiotherapy), patient care and other co-medications besides ABX, such as proton pump inhibitors and steroids, may also play a role in modulating ICI efficacy, and were not necessarily captured in the included studies. A meta-analysis evaluating the impact of proton pump inhibitor use on the clinical outcomes of 15,957 cancer patients treated with ICIs effectively concluded that their usage was negatively associated with survival outcomes (150). A negative association between steroid use and survival outcomes was also reported in another meta-analysis including 4,045 cancer patients receiving ICIs, suggesting the value of further studying the role of other co-medications (151).

In summary, this study demonstrated that ABX use around ICI initiation was negatively associated to survival and treatment-related outcomes of cancer patients, particularly when ABX were taken shortly before or after ICI start, suggesting that ABX prescription should be cautiously considered in cancer patients receiving an anti-PD-(L)1-based treatment. Future larger, prospective observational, multicentric studies evaluating changes of the intestinal microbiome and patient outcomes during immunotherapy, and interventional, controlled, randomized trials involving microbiome modifiers such as FMT or microbiome protectors, are crucially needed to explore the hypothesis of an involvement of the microbiome, elucidate the mechanisms at stake and restore the effectiveness of immunotherapies to improve patient care. It is only through such studies, which will put an end to the current publication bias by allowing analyses on more homogeneous populations, that we will be able to definitively conclude whether or not antibiotics have a deleterious impact on the clinical outcomes of cancer patients, and take the appropriate measures to improve the treatment of these patients.

Data availability statement

The original contributions presented in the study are included in the article/Supplementary Material. Further inquiries can be directed to the corresponding author.

Author contributions

AC, CL, JC, and P-AB designed the study, ran the systematic search, collected the data, and performed the analyses. AC, CL, JG, FV, GZ, JC, and P-AB discussed the results and critically reviewed the manuscript. All authors contributed to the article and approved the submitted version.

Acknowledgments

We would like to thank Dr. Renaud Buffet for his excellent comments and suggestions.

Conflict of interest

The authors declare that this study received funding from Da Volterra, France. The funder was involved in the study design, collection, analysis, interpretation of data, the writing of this article, and the decision to submit it for publication.

AC, FV, and JC are employees of Da Volterra. CL and P-AB are employees of Da Volterra and may have owned or received shares of Da Volterra, during the study period. JG and GZ are consultants for Da Volterra and report receiving consulting fees from Da Volterra.

References

- Ribas A, Wolchok JD. Cancer immunotherapy using checkpoint blockade. *Science* (2018) 359:1350–5. doi: 10.1126/science.aar4060
- Das S, Johnson DB. Immune-related adverse events and anti-tumor efficacy of immune checkpoint inhibitors. *J Immunother Cancer* (2019) 7:306. doi: 10.1186/s40425-019-0805-8
- Mazieres J, Drilon A, Lusque A, Mhanna L, Cortot AB, Mezquita L, et al. Immune checkpoint inhibitors for patients with advanced lung cancer and oncogenic driver alterations: results from the IMMUNOTARGET registry. *Ann Oncol* (2019) 30:1321–8. doi: 10.1093/annonc/mdz167
- Lo Russo G, Moro M, Sommariva M, Cancila V, Boeri M, Centonze G, et al. Antibody-Fc/FcR interaction on macrophages as a mechanism for hyperprogressive disease in non-small cell lung cancer subsequent to PD-1/PD-L1 blockade. *Clin Cancer Res* (2019) 25:989–99. doi: 10.1158/1078-0432.CCR-18-1390
- Zheng D, Liwinski T, Elinav E. Interaction between microbiota and immunity in health and disease. *Cell Res* (2020) 30:492–506. doi: 10.1038/s41422-020-0332-7
- Matson V, Fessler J, Bao R, Chongswat T, Zha Y, Alegre M-L, et al. The commensal microbiome is associated with anti-PD-1 efficacy in metastatic melanoma patients. *Science* (2018) 359:104–8. doi: 10.1126/science.aao3290
- Routy B, Le Chatelier E, Derosa L, Duong CPM, Alou MT, Daillière R, et al. Gut microbiome influences efficacy of PD-1-based immunotherapy against epithelial tumors. *Science* (2018) 359:91–7. doi: 10.1126/science.aan3706
- Gopalakrishnan V, Spencer CN, Nezi L, Reuben A, Andrews MC, Karpinetz TV, et al. Gut microbiome modulates response to anti-PD-1 immunotherapy in melanoma patients. *Science* (2018) 359:97–103. doi: 10.1126/science.aan4236
- Sullivan A, Edlund C, Nord CE. Effect of antimicrobial agents on the ecological balance of human microflora. *Lancet Infect Dis* (2001) 1:101–14. doi: 10.1016/S1473-3099(01)00066-4
- Willing BP, Russell SL, Finlay BB. Shifting the balance: antibiotic effects on host-microbiota mutualism. *Nat Rev Microbiol* (2011) 9:233–43. doi: 10.1038/nrmicro2536
- Andremont A, Cervesi J, Bandinelli P-A, Vitry F, de Gunzburg J. Spare and repair the gut microbiota from antibiotic-induced dysbiosis: state-of-the-art. *Drug Discovery Today* (2021) 26:2159–63. doi: 10.1016/j.drudis.2021.02.022
- Stokes WA, Behera M, Jiang R, Gutman D, Giuste F, Burns A, et al. Effect of antibiotic therapy on immunotherapy outcomes for non-small cell lung cancer:

JG reports having owned shares of Da Volterra, during the study period. GZ reports having received grants, personal fees, and nonfinancial support from ROCHE; personal fees from MSD; personal fees and non-financial support from Bristol-Myers Squibb, Inventiva, Sanofi-Regeneron and Astra-Zeneca Pharmaceuticals; and non-financial support from Pfizer, AbbVie, and Da Volterra, outside of the submitted work.

Publisher's note

All claims expressed in this article are solely those of the authors and do not necessarily represent those of their affiliated organizations, or those of the publisher, the editors and the reviewers. Any product that may be evaluated in this article, or claim that may be made by its manufacturer, is not guaranteed or endorsed by the publisher.

Supplementary material

The Supplementary Material for this article can be found online at: <https://www.frontiersin.org/articles/10.3389/fonc.2023.1075593/full#supplementary-material>

Analysis from the veterans health administration database. *J Clin Oncol* (2021) 39:9017–7. doi: 10.1200/JCO.2021.39.15_suppl.9017

13. Rounis K, Makrakis D, Papadaki C, Monastirioti A, Vamvakas L, Kalbakis K, et al. Prediction of outcome in patients with non-small cell lung cancer treated with second line PD-1/PDL-1 inhibitors based on clinical parameters: Results from a prospective, single institution study. *PloS One* (2021) 16:e0252537. doi: 10.1371/journal.pone.0252537

14. Mohiuddin JJ, Chu B, Facciabene A, Poirier K, Wang X, Doucette A, et al. Association of antibiotic exposure with survival and toxicity in patients with melanoma receiving immunotherapy. *J Natl Cancer Inst* (2021) 113:162–70. doi: 10.1093/jnci/djaa057

15. Huang X-Z, Gao P, Song Y-X, Xu Y, Sun J-X, Chen X-W, et al. Antibiotic use and the efficacy of immune checkpoint inhibitors in cancer patients: a pooled analysis of 2740 cancer patients. *Oncoimmunology* (2019) 8:e1665973. doi: 10.1080/2162402X.2019.1665973

16. Wilson BE, Routy B, Nagrial A, Chin VT. The effect of antibiotics on clinical outcomes in immune-checkpoint blockade: a systematic review and meta-analysis of observational studies. *Cancer Immunol Immunother* (2020) 69:343–54. doi: 10.1007/s00262-019-02453-2

17. Lurienne L, Cervesi J, Duhalde L, de Gunzburg J, Andremont A, Zalcman G, et al. NSCLC immunotherapy efficacy and antibiotic use: A systematic review and meta-analysis. *J Thorac Oncol* (2020) 15:1147–59. doi: 10.1016/j.jtho.2020.03.002

18. Xu H, Xu X, Wang H, Ge W, Cao D. The association between antibiotics use and outcome of cancer patients treated with immune checkpoint inhibitors: A systematic review and meta-analysis. *Crit Rev Oncol Hematol* (2020) 149:102909. doi: 10.1016/j.critrevonc.2020.102909

19. Petrelli F, Iaculli A, Signorelli D, Ghidini A, Dottorini L, Perego G, et al. Survival of patients treated with antibiotics and immunotherapy for cancer: A systematic review and meta-analysis. *J Clin Med* (2020) 9:E1458. doi: 10.3390/jcm9051458

20. Yang M, Wang Y, Yuan M, Tao M, Kong C, Li H, et al. Antibiotic administration shortly before or after immunotherapy initiation is correlated with poor prognosis in solid cancer patients: An up-to-date systematic review and meta-analysis. *Int Immunopharmacol* (2020) 88:106876. doi: 10.1016/j.intimp.2020.106876

21. Huang L, Chen X, Zhou L, Xu Q, Xie J, Zhan P, et al. Antibiotic exposure windows and the efficacy of immune checkpoint blockers in patients with cancer: a meta-analysis. *Ann Palliat Med* (2021) 10:2709–22. doi: 10.21037/apm-20-2076

22. Wu Q, Liu J, Wu S, Xie X. The impact of antibiotics on efficacy of immune checkpoint inhibitors in malignancies: A study based on 44 cohorts. *Int Immunopharmacol* (2021) 92:107303. doi: 10.1016/j.intimp.2020.107303
23. Tsikalas-Vafea M, Belani N, Vieira K, Khan H, Farmakiotis D. Use of antibiotics is associated with worse clinical outcomes in patients with cancer treated with immune checkpoint inhibitors: A systematic review and meta-analysis. *Int J Infect Dis* (2021) 106:142–54. doi: 10.1016/j.ijid.2021.03.063
24. Yu Y, Zheng P, Gao L, Li H, Tao P, Wang D, et al. Effects of antibiotic use on outcomes in cancer patients treated using immune checkpoint inhibitors: A systematic review and meta-analysis. *J Immunother* (2021) 44:76–85. doi: 10.1097/CJI.0000000000000346
25. Chen H, Han K-D, He Z-J, Huang Y-S. How to choose a survival period? the impact of antibiotic use on OS or PFS in NSCLC patients treated with immune checkpoint inhibitors: A systematic review and meta-analysis. *Technol Cancer Res Treat* (2021) 20:1–12. doi: 10.1177/1530338211033498
26. Derosa L, Routy B, Desilets A, Daillère R, Terrisse S, Kroemer G, et al. Microbiota-centered interventions: The next breakthrough in immuno-oncology? *Cancer Discovery* (2021) 11:2396–412. doi: 10.1158/2159-8290.CD-21-0236
27. Huo G-W, Zuo R, Song Y, Chen W-D, Chen W-M, Chong D-Q, et al. Effect of antibiotic use on the efficacy of nivolumab in the treatment of advanced/metastatic non-small cell lung cancer: A meta-analysis. *Open Med (Wars)* (2021) 16:728–36. doi: 10.1515/med-2021-0272
28. Jiang S, Geng S, Chen Q, Zhang C, Cheng M, Yu Y, et al. Effects of concomitant antibiotics use on immune checkpoint inhibitor efficacy in cancer patients. *Front Oncol* (2022) 12:823705. doi: 10.3389/fonc.2022.823705
29. Zhou J, Huang G, Wong W-C, Hu D-H, Zhu J-W, Li R, et al. The impact of antibiotic use on clinical features and survival outcomes of cancer patients treated with immune checkpoint inhibitors. *Front Immunol* (2022) 13:968729. doi: 10.3389/fimmu.2022.968729
30. Zhang L, Chen C, Chai D, Li C, Guan Y, Liu L, et al. The association between antibiotic use and outcomes of HCC patients treated with immune checkpoint inhibitors. *Front Immunol* (2022) 13:956533. doi: 10.3389/fimmu.2022.956533
31. 2020 PRISMA guidelines. Available at: <https://www.prisma-statement.org/> (Accessed October 10, 2022).
32. Tierney JF, Stewart LA, Ghersi D, Burdett S, Sydes MR. Practical methods for incorporating summary time-to-event data into meta-analysis. *Trials* (2007) 8:16. doi: 10.1186/1745-6215-8-16
33. R Core Team. *R: a language and environment for statistical computing*. Vienna: R Foundation for Statistical Computing. Available at: <https://www.R-project.org/> (Accessed October 10, 2022).
34. Schwarzer G. Meta: an R package for meta-analysis. *R News* (2007) 7:40–5.
35. Ahmed Y, Calvert P. Antibiotics and response to immunotherapy: real-world experience. In: *Regular and young investigator award abstracts*. BMJ Publishing Group Ltd (2020). p. A435.2–A436. doi: 10.1136/jitc-2020-SITC2020.0728
36. Bagley SJ, Dhopeswarkar N, Narayan V, Meropol NJ, Mamtani R, Boursi B. Impact of antibiotics (ABX) on overall survival (OS) in patients (pts) with advanced non-small-cell lung cancer (aNSCLC) and melanoma (aMel) treated with first-line immune checkpoint inhibition (ICI). *J Clin Oncol* (2019) 37:e20643–3. doi: 10.1200/JCO.2019.37.15_suppl.e20643
37. Castello A, Rossi S, Toschi L, Lopci E. Impact of antibiotic therapy and metabolic parameters in non-small cell lung cancer patients receiving checkpoint inhibitors. *J Clin Med* (2021) 10:1251. doi: 10.3390/jcm10061251
38. Castro Balado A, Touris Lores M, Álvarez Sánchez R, Bernárdez Ferrán B, López Montero E, Mosquera Torre A, et al. 4CPS-301 association of antibiotics and proton pump inhibitors on clinical activity of firstline pembrolizumab for non-small cell lung cancer: 2 years of real world data. In: *Section 4: Clinical pharmacy services*. British Medical Journal Publishing Group (2021). p. A65.2–A65. doi: 10.1136/ehp-pharm-2021-eahpconf.133
39. Conde-Estévez D, Monge-Escartín I, Ríos-Hoyo A, Monzonis X, Echeverría-Esnal D, Moliner L, et al. Prognostic factors and effect on survival of immune-related adverse events in patients with non-small-cell lung cancer treated with immune checkpoint blockade. *J Chemother* (2021) 33:32–9. doi: 10.1080/1120009X.2020.1849488
40. Cortellini A, Di Maio M, Nigro O, Leonetti A, Cortinovis DL, Aerts JG, et al. Differential influence of antibiotic therapy and other medications on oncological outcomes of patients with non-small cell lung cancer treated with first-line pembrolizumab versus cytotoxic chemotherapy. *J Immunother Cancer* (2021) 9:e002421. doi: 10.1136/jitc-2021-002421
41. Cortellini A, Ricciotti B, Facchinetti F, Alessi JMV, Venkatraman D, Dall'Olio FG, et al. Antibiotic-exposed patients with non-small-cell lung cancer preserve efficacy outcomes following first-line chemo-immunotherapy. *Ann Oncol* (2021) 32:1391–9. doi: 10.1016/j.annonc.2021.08.1744
42. Derosa L, Hellmann MD, Spaziano M, Halpenny D, Fidelle M, Rizvi H, et al. Negative association of antibiotics on clinical activity of immune checkpoint inhibitors in patients with advanced renal and non-small-cell lung cancer. *Ann Oncol* (2018) 29:1437–44. doi: 10.1093/annonc/mdy103
43. Derosa L, Routy B, Thomas AM, Iebba V, Zalcman G, Friard S, et al. Intestinal akkermansia muciniphila predicts clinical response to PD-1 blockade in patients with advanced non-small-cell lung cancer. *Nat Med* (2022) 28:315–24. doi: 10.1038/s41591-021-01655-5
44. Do TP, Hegde AM, Cherry CR, Stroud CRG, Sharma N, Cherukuri SD, et al. Antibiotic use and overall survival in lung cancer patients receiving nivolumab. *J Clin Oncol* (2018) 36:e15109–9. doi: 10.1200/JCO.2018.36.15_suppl.e15109
45. Fang C, Fang W, Xu L, Gao F, Hou Y, Zou H, et al. Distinct functional metagenomic markers predict the responsiveness to anti-PD-1 therapy in Chinese non-small cell lung cancer patients. *Front Oncol* (2022) 12:837525. doi: 10.3389/fonc.2022.837525
46. Forde C, Gregory R, Scott JA, Campbell L, Scullin P. Antibiotic use in advanced non-small cell lung cancer (NSCLC) patients receiving immune checkpoint inhibitors across the northern Ireland cancer network. *Lung Cancer* (2020) 139:S54. doi: 10.1016/S0169-5002(20)30152-5
47. Galli G, Triulzi T, Proto C, Signorelli D, Imbimbo M, Poggi M, et al. Association between antibiotic-immunotherapy exposure ratio and outcome in metastatic non small cell lung cancer. *Lung Cancer* (2019) 132:72–8. doi: 10.1016/j.lungcan.2019.04.008
48. Geum MJ, Kim C, Kang JE, Choi JH, Kim JS, Son ES, et al. Broad-spectrum antibiotic regimen affects survival in patients receiving nivolumab for non-small cell lung cancer. *Pharm (Basel)* (2021) 14:445. doi: 10.3390/ph14050445
49. Hakoziaki T, Okuma Y, Omori M, Hosomi Y. Impact of prior antibiotic use on the efficacy of nivolumab for non-small cell lung cancer. *Oncol Lett* (2019) 17:2946–52. doi: 10.3892/ol.2019.9899
50. Hamada K, Yoshimura K, Hirasawa Y, Hosonuma M, Murayama M, Narikawa Y, et al. Antibiotic usage reduced overall survival by over 70% in non-small cell lung cancer patients on anti-PD-1 immunotherapy. *Anticancer Res* (2021) 41:4985–93. doi: 10.21873/anticancer.15312
51. Hogue C, Kuzel T, Borgia J, Marwaha G, Bonomi P, Fidler MJ, et al. Impact of antibiotic usage on survival during checkpoint inhibitor treatment of non-small cell lung cancer (NSCLC). *J Thorac Oncol* (2019) 14:S735. doi: 10.1016/j.jtho.2019.08.1574
52. Hopkins AM, Badaoui S, Kichenadasse G, Karapetis CS, McKinnon RA, Rowland A, et al. Efficacy of atezolizumab in patients with advanced NSCLC receiving concomitant antibiotic or proton pump inhibitor treatment: Pooled analysis of five randomized control trials. *J Thorac Oncol* (2022) 22(00093–4):S1556–0864. doi: 10.1016/j.jtho.2022.02.003
53. Hossain T, Htut S, Pathmanathan S, Fletcher J, Pandey R, Lui A, et al. Do antibiotics reduce survival in patients with advanced non-small cell lung cancer treated with immunotherapy? *Asia Pac J Clin Oncol* (2020) 16:29–47. doi: 10.1111/ajco.13417
54. Huemer F, Lang D, Westphal T, Gampenrieder SP, Hutarew G, Weiss L, et al. Baseline absolute lymphocyte count and ECOG performance score are associated with survival in advanced non-small cell lung cancer undergoing PD-1/PD-L1 blockade. *J Clin Med* (2019) 8:E1014. doi: 10.3390/jcm8071014
55. von Itzstein MS, Gonugunta AS, Sheffield T, Homsy J, Dowell JE, Koh AY, et al. Association between antibiotic exposure and systemic immune parameters in cancer patients receiving checkpoint inhibitor therapy. *Cancers* (2022) 14:1327. doi: 10.3390/cancers14051327
56. Jin Y, Dong H, Xia L, Yang Y, Zhu Y, Shen Y, et al. The diversity of gut microbiome is associated with favorable responses to anti-programmed death 1 immunotherapy in Chinese patients with NSCLC. *J Thorac Oncol* (2019) 14:1378–89. doi: 10.1016/j.jtho.2019.04.007
57. Kim H, Lee JE, Hong SH, Lee MA, Kang JH, Kim I-H. The effect of antibiotics on the clinical outcomes of patients with solid cancers undergoing immune checkpoint inhibitor treatment: a retrospective study. *BMC Cancer* (2019) 19:1100. doi: 10.1186/s12885-019-6267-z
58. Kostine M, Mauric E, Tison A, Barnette T, Barre A, Nikolski M, et al. Baseline co-medications may alter the anti-tumoural effect of checkpoint inhibitors as well as the risk of immune-related adverse events. *Eur J Cancer* (2021) 157:474–84. doi: 10.1016/j.ejca.2021.08.036
59. Kulkarni AA, Ebadi M, Zhang S, Meybodi MA, Ali AM, DeFor T, et al. Comparative analysis of antibiotic exposure association with clinical outcomes of chemotherapy versus immunotherapy across three tumour types. *ESMO Open* (2020) 5:e000803. doi: 10.1136/esmoopen-2020-000803
60. Lu P-H, Tsai T-C, Chang JW-C, Deng S-T, Cheng C-Y. Association of prior fluoroquinolone treatment with survival outcomes of immune checkpoint inhibitors in Asia. *J Clin Pharm Ther* (2021) 46:408–14. doi: 10.1111/jcpt.13298
61. Medjebbar S, Truntzer C, Perrichet A, Limagne E, Fumet J-D, Richard C, et al. Angiotensin-converting enzyme (ACE) inhibitor prescription affects non-small-cell lung cancer (NSCLC) patients response to PD-1/PD-L1 immune checkpoint blockers. *Oncimmunology* (2020) 9:1836766. doi: 10.1080/2162402X.2020.1836766
62. Metges J-P, Michaud E, Deniel Lagadec D, Marhuenda F, Chaslerie A, Grude F. Impact of anti-infectious and corticosteroids on immunotherapy: Nivolumab and pembrolizumab follow-up in a French study. *J Clin Oncol* (2018) 36:e15157–7. doi: 10.1200/JCO.2018.36.15_suppl.e15157
63. Mielgo-Rubio X, Chara L, Sotelo-Lezama M, Lopez Castro R, Rubio-Martínez J, Velastegui A, et al. MA10.01 antibiotic use and PD-1 inhibitors: Shorter survival in lung cancer, especially when given intravenously. Type of infection also matters. *J Thorac Oncol* (2018) 13:S389. doi: 10.1016/j.jtho.2018.08.395
64. Mielgo-Rubio XM, Aguado C, Sereno M, Chara LE, Cabezon L, Velastegui A, et al. P1.04-16 early antibiotic use affects the efficacy of first line immunotherapy in lung cancer patients but route of administration seems to be decisive. *J Thorac Oncol* (2019) 14:S445. doi: 10.1016/j.jtho.2019.08.919

65. Nyein AF, Bari S, Hogue S, Zhao Y, Maller B, Sha S, et al. Effect of prior antibiotic or chemotherapy treatment on immunotherapy response in non-small cell lung cancer. *BMC Cancer* (2022) 22:101. doi: 10.1186/s12885-022-09210-2
66. Ochi N, Ichihara E, Takigawa N, Harada D, Inoue K, Shibayama T, et al. The effects of antibiotics on the efficacy of immune checkpoint inhibitors in patients with non-small-cell lung cancer differ based on PD-L1 expression. *Eur J Cancer* (2021) 149:73–81. doi: 10.1016/j.ejca.2021.02.040
67. Ouaknine Krief J, Helly de Tauriers P, Dumenil C, Neveux N, Dumoulin J, Giraud V, et al. Role of antibiotic use, plasma citrulline and blood microbiome in advanced non-small cell lung cancer patients treated with nivolumab. *J Immunother Cancer* (2019) 7:176. doi: 10.1186/s40425-019-0658-1
68. Peng K, Chen K, Teply BA, Yee GC, Farazi PA, Lyden ER. Impact of proton pump inhibitor use on the effectiveness of immune checkpoint inhibitors in advanced cancer patients. *Ann Pharmacother* (2022) 56:377–86. doi: 10.1177/10600280211033938
69. Pinato DJ, Howlett S, Ottaviani D, Urus H, Patel A, Mineo T, et al. Association of prior antibiotic treatment with survival and response to immune checkpoint inhibitor therapy in patients with cancer. *JAMA Oncol* (2019) 5:1774–8. doi: 10.1001/jamaoncol.2019.2785
70. Qiu H, Ma Q-G, Chen X-T, Wen X, Zhang N, Liu W-M, et al. Different classes of antibiotics exhibit disparate negative impacts on the therapeutic efficacy of immune checkpoint inhibitors in advanced non-small cell lung cancer patients. *Am J Cancer Res* (2022) 12:3175–84.
71. Ren Z-G, Gao Y, Wei C, Li X, Liu S, Zhang J, et al. 968P association between use of antibiotics (ATB) and clinical outcomes with tislelizumab (tisle) monotherapy. *Ann Oncol* (2021) 32:S835. doi: 10.1016/j.annonc.2021.08.1353
72. Riudavets M, Mosquera J, Campelo RG, Serra J, Anguera G, Gallardo P, et al. P2.04-52 impact of corticosteroids and antibiotics on efficacy of immune-checkpoint inhibitors in patients with advanced non-small cell lung cancer. *J Thorac Oncol* (2019) 14:S728. doi: 10.1016/j.jtho.2019.08.1557
73. Ruiz-Patiño A, Barrón F, Cardona AF, Corrales L, Mas L, Martín C, et al. Antibiotics impair immune checkpoint inhibitor effectiveness in Hispanic patients with non-small cell lung cancer (AB-CLICaP). *Thorac Cancer* (2020) 11:2552–60. doi: 10.1111/1759-7714.13573
74. Schett A, Rothschild SI, Curioni-Fontecedro A, Krähenbühl S, Früh M, Schmid S, et al. Predictive impact of antibiotics in patients with advanced non small-cell lung cancer receiving immune checkpoint inhibitors: Antibiotics immune checkpoint inhibitors in advanced NSCLC. *Cancer Chemother Pharmacol* (2020) 85:121–31. doi: 10.1007/s00280-019-03993-1
75. Spakowicz D, Hoyd R, Muniak M, Husain M, Bassett JS, Wang L, et al. Inferring the role of the microbiome on survival in patients treated with immune checkpoint inhibitors: causal modeling, timing, and classes of concomitant medications. *BMC Cancer* (2020) 20:383. doi: 10.1186/s12885-020-06882-6
76. Sun M, Ji H, Xu N, Jiang P, Qu T, Li Y. Real-world data analysis of immune checkpoint inhibitors in stage III-IV adenocarcinoma and squamous cell carcinoma. *BMC Cancer* (2022) 22:762. doi: 10.1186/s12885-022-09843-3
77. Svaton M, Zemanova M, Zemanova P, Kultán J, Fischer O, Skrickova J, et al. Impact of concomitant medication administered at the time of initiation of nivolumab therapy on outcome in non-small cell lung cancer. *Anticancer Res* (2020) 40:2209–17. doi: 10.21873/anticancer.14182
78. Thompson J, Szabo A, Arce-Lara C, Menon S. P1.07-008 microbiome & immunotherapy: Antibiotic use is associated with inferior survival for lung cancer patients receiving PD-1 inhibitors. *J Thorac Oncol* (2017) 12:S1998. doi: 10.1016/j.jtho.2017.09.926
79. Tomita Y, Ikeda T, Sakata S, Saruwatari K, Sato R, Iyama S, et al. Association of probiotic clostridium butyricum therapy with survival and response to immune checkpoint blockade in patients with lung cancer. *Cancer Immunol Res* (2020) 8:1236–42. doi: 10.1158/2326-6066.CIR-20-0051
80. Verschueren MV, van der Welle CMC, Tonn M, Schramel FMNH, Peters BJM, van de Garde EMW. The association between gut microbiome affecting concomitant medication and the effectiveness of immunotherapy in patients with stage IV NSCLC. *Sci Rep* (2021) 11:23331. doi: 10.1038/s41598-021-02598-0
81. Zhang F, Ferrero M, Dong N, D'Auria G, Reyes-Prieto M, Herreros-Pomares A, et al. Analysis of the gut microbiota: An emerging source of biomarkers for immune checkpoint blockade therapy in non-small cell lung cancer. *Cancers* (2021) 13:2514. doi: 10.3390/cancers13112514
82. Zhao S, Gao G, Li W, Li X, Zhao C, Jiang T, et al. Antibiotics are associated with attenuated efficacy of anti-PD-1/PD-L1 therapies in Chinese patients with advanced non-small cell lung cancer. *Lung Cancer* (2019) 130:10–7. doi: 10.1016/j.lungcan.2019.01.017
83. Agarwal A, Pond GR, Curran C, Nassar A, Nuzzo PV, Kumar V, et al. Impact of concurrent medications on outcomes with PD1/PD-L1 inhibitors for metastatic urothelial carcinoma. *J Clin Oncol* (2019) suppl 7S. abstr 435. doi: 10.1200/JCO.2019.37.7_SUPPL.435
84. Braun A, Deng M, Handorf EA, Abbosh P. Association of antibiotic therapy and treatment efficacy in urothelial cell carcinoma patients receiving immune checkpoint inhibitors. *J Clin Oncol* (2022) 40:4578–8. doi: 10.1200/JCO.2022.40.16_suppl.4578
85. Fukuoka Y, Kimura T, Komura K, Uchimoto T, Nishimura K, Yanagisawa T, et al. Effectiveness of pembrolizumab in patients with urothelial carcinoma receiving proton pump inhibitors. *Urol Oncol* (2022) 40:346.e1–8. doi: 10.1016/j.urolonc.2022.02.020
86. Hoffman-Censits JH, Harshman LC, Metcalf M, Abou Alaiwi S, Meyer CS, Yang E, et al. Real-world evidence of the impact of prior antibiotic exposure on immune checkpoint inhibitor outcomes in patients with metastatic urothelial cancer. *J Clin Oncol* (2020) 38:452–2. doi: 10.1200/JCO.2020.38.6_suppl.452
87. Hopkins AM, Kichenadasse G, Karapetis CS, Rowland A, Sorich MJ. Concomitant antibiotic use and survival in urothelial carcinoma treated with atezolizumab. *Eur Urol* (2020) 78:540–3. doi: 10.1016/j.eururo.2020.06.061
88. Iida K, Nagai T, Nozaki S, Etani T, Naiki T, Nakane A, et al. Proton pump inhibitor use is a negative prognostic factor for metastatic urothelial carcinoma progression in pembrolizumab-treated patients. *J Urol* (2021) 206. doi: 10.1097/JU.0000000000002062.15
89. Ishiyama Y, Kondo T, Nemoto Y, Kobari Y, Ishihara H, Tachibana H, et al. Antibiotic use and survival of patients receiving pembrolizumab for chemotherapy-resistant metastatic urothelial carcinoma. *Urol Oncol* (2021) 39:834.e21–834.e28. doi: 10.1016/j.urolonc.2021.05.033
90. Khan MS, Radakovich N, Ornstein M, Gupta S. 778P concomitant antibiotic use and its effect on immune-checkpoint inhibitor efficacy in patients with advanced urothelial carcinoma. *Ann Oncol* (2020) 31:S597. doi: 10.1016/j.annonc.2020.08.850
91. Okuyama Y, Hatakeyama S, Numakura K, Narita T, Tanaka T, Miura Y, et al. Prognostic impact of proton pump inhibitors for immunotherapy in advanced urothelial carcinoma. *BJUI Compass* (2022) 3:154–61. doi: 10.1002/bco2.118
92. Ruiz-Bañobre J, Molina-Díaz A, Fernández-Calvo O, Fernández-Núñez N, Medina-Colmenero A, Santomé L, et al. Rethinking prognostic factors in locally advanced or metastatic urothelial carcinoma in the immune checkpoint blockade era: a multicenter retrospective study. *ESMO Open* (2021) 6:100090. doi: 10.1016/j.esmoop.2021.100090
93. Tomisaki I, Harada M, Minato A, Nagata Y, Kimuro R, Higashijima K, et al. Impact of the use of proton pump inhibitors on pembrolizumab effectiveness for advanced urothelial carcinoma. *Anticancer Res* (2022) 42:1629–34. doi: 10.21873/anticancer.15638
94. Weinstock C, Bandaru P, Fernandes LL, Chang E, Girvin A, Tang S, et al. Impact of timing of antibiotic use on clinical outcomes in patients with urothelial cancer treated with immune checkpoint inhibitors (ICIs). *J Clin Oncol* (2020) 38:5045–5. doi: 10.1200/JCO.2020.38.15_suppl.5045
95. Elkrief A, El Raichani L, Richard C, Messaoudene M, Belkaid W, Malo J, et al. Antibiotics are associated with decreased progression-free survival of advanced melanoma patients treated with immune checkpoint inhibitors. *Oncoimmunology* (2019) 8:e1568812. doi: 10.1080/2162402X.2019.1568812
96. Hemadri A, Lin H, Lin Y, Rose A, Sander C, Najjar Y, et al. Association of medication (Med) and antibiotic (Abx) use with response and survival in advanced melanoma (MEL) receiving PD-1 inhibitors, in: *Proceedings from ASCO*; Chicago (2019).
97. Kapoor V, Runnels J, Boyce T, Pankratz VS, Rixe O. Effect of antibiotic exposure in patients with metastatic melanoma treated with PD-1 inhibitor or CTLA-4 inhibitor or a combination of both. *J Clin Oncol* (2019) 37:e14141–1. doi: 10.1200/JCO.2019.37.15_suppl.e14141
98. Poizeau F, Kerbrat S, Balusson F, Tattevin P, Revest M, Cattoir V, et al. The association between antibiotic use and outcome among metastatic melanoma patients receiving immunotherapy. *J Natl Cancer Inst* (2022) 114(5):686–94. doi: 10.1093/jnci/djac019
99. Swami U, Chennamadhavuni A, Borchering N, Bossler AD, Mott SL, Garje R, et al. Multivariable analysis of 169 cases of advanced cutaneous melanoma to evaluate antibiotic exposure as predictor of survival to anti-PD-1 based immunotherapies. *Antibiot Basel* (2020) 9:E740. doi: 10.3390/antibiotics9110740
100. Braun A, Deng M, Handorf EA, Abbosh P. Association of antibiotic therapy and treatment efficacy in patients with renal cell carcinoma receiving immune checkpoint inhibitors. *J Clin Oncol* (2022) 40:4556–6. doi: 10.1200/JCO.2022.40.16_suppl.4556
101. Derosa L, Alves Costa Silva C, Daban C, Colomba E, Negrier S, Chevreau C, et al. (2021). Antibiotic (ATB) therapy and outcome from nivolumab (N) in metastatic renal cell carcinoma (mRCC) patients (pts): Results of the GETUG AFU 26 NIVOREN multicentric phase II study, in: *Proceedings from ESMO*, .
102. Ernst MS, Abou Alaiwi S, Dizman N, Labaki C, Vitale Nuzzo P, Adib E, et al. The impact of antibiotic (Ab) exposure on clinical outcomes in patients with metastatic renal cell carcinoma (mRCC) treated with immune checkpoint inhibitors (ICI) or VEGF targeted therapy (VEGT-TT): Results from the international mRCC DataBase consortium (IMDC), in: *Proceedings from ASCO*; Chicago (2021).
103. Guven DC, Acar R, Yekeduz E, Bilgetekin I, Baytemur NK, Erol C, et al. The association between antibiotic use and survival in renal cell carcinoma patients treated with immunotherapy: a multi-center study. *Curr Probl Cancer* (2021) 45:100760. doi: 10.1016/j.cuprob.2021.100760
104. Lalani A-KA, Xie W, Braun DA, Kaymakalan M, Bossé D, Steinharter JA, et al. Effect of antibiotic use on outcomes with systemic therapies in metastatic renal cell carcinoma. *Eur Urol Oncol* (2020) 3:372–81. doi: 10.1016/j.euo.2019.09.001
105. Ueda K, Yonekura S, Ogasawara N, Matsunaga Y, Hoshino R, Kurose H, et al. The impact of antibiotics on prognosis of metastatic renal cell carcinoma in Japanese patients treated with immune checkpoint inhibitors. *Anticancer Res* (2019) 39:6265–71. doi: 10.21873/anticancer.13836

106. Alshammari K, Alsugheir F, Aldawoud M, Alolayan A, Algarni MA, Sabatin F, et al. Association between antibiotic exposure and survival in patients with hepatocellular carcinoma treated with nivolumab. *J Clin Oncol* (2021) 39:e16186–6. doi: 10.1200/JCO.2021.39.15_suppl.e16186
107. Fessas P, Naeem M, Pinter M, Marron TU, Szafron D, Balcar L, et al. Early antibiotic exposure is not detrimental to therapeutic effect from immunotherapy in hepatocellular carcinoma. *Liver Cancer* (2021) 10:583–92. doi: 10.1159/000519108
108. Jun T, Dharmapuri S, Marron TU, Sung MW, Ang C. Effect of baseline medications on response to immunotherapy in hepatocellular carcinoma. *J Clin Oncol* (2020) 38:484–4. doi: 10.1200/JCO.2020.38.4_suppl.484
109. Pinato DJJ, Li X, Mishra-Kalyani PS, D'Alessio A, Fulgenzi CAM, Wei G, et al. Antibiotic therapy and association with oncological outcomes from targeted and immune-based therapy in hepatocellular carcinoma (HCC). *J Clin Oncol* (2022) 40:4089–9. doi: 10.1200/JCO.2022.40.16_suppl.4089
110. Shen Y-C, Lee P-C, Kuo Y-L, Wu W-K, Chen C-C, Lei C-H, et al. An exploratory study for the association of gut microbiome with efficacy of immune checkpoint inhibitor in patients with hepatocellular carcinoma. *J Hepatocell Carcinoma* (2021) 8:809–22. doi: 10.2147/JHC.S315696
111. Spahn S, Roessler D, Pompilia R, Gabernet G, Gladstone BP, Horger M, et al. Clinical and genetic tumor characteristics of responding and non-responding patients to PD-1 inhibition in hepatocellular carcinoma. *Cancers* (2020) 12:E3830. doi: 10.3390/cancers12123830
112. Grealley M, Chou JF, Chatila WK, Margolis M, Capanu M, Hechtman JF, et al. Clinical and molecular predictors of response to immune checkpoint inhibitors in patients with advanced esophagogastric cancer. *Clin Cancer Res* (2019) 25:6160–9. doi: 10.1158/1078-0432.CCR-18-3603
113. Guo J-C, Lin C-C, Lin C-Y, Hsieh M-S, Kuo H-Y, Lien M-Y, et al. Neutrophil-to-lymphocyte ratio and use of antibiotics associated with prognosis in esophageal squamous cell carcinoma patients receiving immune checkpoint inhibitors. *Anticancer Res* (2019) 39:5675–82. doi: 10.21873/anticancer.13765
114. Jung M, Kim CG, Shin S-J, Hong M, Cheol Chung H, Sun Young Rha S, et al. Association between prior antibiotic administration and outcomes of programmed cell death 1 protein blockade or chemotherapy in patients with advanced gastric cancer, in: Proceedings from ESMO (2021).
115. Kim JH, Ahn B, Hong S-M, Jung H-Y, Kim DH, Choi KD, et al. Real-world efficacy data and predictive clinical parameters for treatment outcomes in advanced esophageal squamous cell carcinoma treated with immune checkpoint inhibitors. *Cancer Res Treat* (2022) 54:505–16. doi: 10.4143/crt.2020.1198
116. Plana M, Cefarelli G, Guillén P, Esteve A, Oliva M, Gonzalez A, et al. 949P impact of antibiotic use and derived neutrophil to lymphocyte ratio (dNLR) in patients with recurrent/metastatic head and neck squamous cell cancer (R/M HNSCC) treated with immunotherapy. *Ann Oncol* (2020) 31:S675. doi: 10.1016/j.annonc.2020.08.1064
117. Vellanki PJ, Marur S, Bandaru P, Mishra-Kalyani PS, By K, Girvin A, et al. Evaluation of the correlation between antibiotic use and survival in patients with recurrent or metastatic head and neck squamous cell carcinoma (R/M HNSCC) treated with immune checkpoint inhibitors (ICIs). *J Clin Oncol* (2020) 38:6509–9. doi: 10.1200/JCO.2020.38.15_suppl.6509
118. Serpas Higbie V, Rogers J, Hwang H, Qiao W, Xiao L, Dasari A, et al. Antibiotic exposure does not impact immune checkpoint blockade response in MSI-H/dMMR metastatic colorectal cancer: A single-center experience. *Oncologist* (2022) 27(11):952–7. doi: 10.1093/oncolo/oyac162
119. Baggi A, Quagliaro P, Rubatto M, Depenni R, Guida M, Ascierto PA, et al. Real world data of cemiplimab in locally advanced and metastatic cutaneous squamous cell carcinoma. *Eur J Cancer* (2021) 157:250–8. doi: 10.1016/j.ejca.2021.08.018
120. Chambers LM, Michener CM, Rose PG, Reizes O, Yao M, Vargas R. Impact of antibiotic treatment on immunotherapy response in women with recurrent gynecologic cancer. *Gynecol Oncol* (2021) 161:211–20. doi: 10.1016/j.ygyno.2021.01.015
121. Hwang SR, Higgins A, Castillo Almeida NE, LaPlant B, Maurer MJ, Ansell SM, et al. Effect of antibiotic use on outcomes in patients with Hodgkin lymphoma treated with immune checkpoint inhibitors. *Leuk Lymphoma* (2021) 62:247–51. doi: 10.1080/10428194.2020.1827250
122. Abu-Sbeih H, Herrera LN, Tang T, Altan M, Chaftari A-MP, Okhuysen PC, et al. Impact of antibiotic therapy on the development and response to treatment of immune checkpoint inhibitor-mediated diarrhea and colitis. *J Immunother Cancer* (2019) 7:242. doi: 10.1186/s40425-019-0714-x
123. Ahmed J, Kumar A, Parikh K, Anwar A, Knoll BM, Puccio C, et al. Use of broad-spectrum antibiotics impacts outcome in patients treated with immune checkpoint inhibitors. *Oncoimmunology* (2018) 7:e1507670. doi: 10.1080/2162402X.2018.1507670
124. Araujo Ha, Moniz CMV, Braghioroli OFM, Mak MP, Uratani LF, Dahmer Tiecher R, et al. Proton pump inhibitors and antibiotics impact on toxicities and clinical outcomes in cancer patients treated with immunotherapy. *J Clin Oncol* (2021) 39:2652–2. doi: 10.1200/JCO.2021.39.15_suppl.2652
125. Eng L, Sutradhar R, Niu Y, Liu N, Liu Y, Kaliwal Y, et al. Impact of antibiotic (ATB) exposure prior to immune checkpoint inhibitor (ICI) treatment on overall survival (OS): A population-based study. *J Clin Oncol* (2021) 39:303–3. doi: 10.1200/JCO.2020.39.28_suppl.303
126. Gaucher L, Adda L, Séjourné A, Joachim C, Guillaume C, Poulet C, et al. Associations between dysbiosis-inducing drugs, overall survival and tumor response in patients treated with immune checkpoint inhibitors. *Ther Adv Med Oncol* (2021) 13:1–23. doi: 10.1177/17588359211000591
127. Giordan G, Salleron J, Vallance C, Moriana C, Clement-Duchene C. Impact of antibiotics and proton pump inhibitors on efficacy and tolerance of anti-PD-1 immune checkpoint inhibitors. *Front Immunol* (2021) 12:716317. doi: 10.3389/fimmu.2021.716317
128. Iglesias-Santamaria A. Impact of antibiotic use and other concomitant medications on the efficacy of immune checkpoint inhibitors in patients with advanced cancer. *Clin Transl Oncol* (2020) 22:1481–90. doi: 10.1007/s12094-019-02282-w
129. Kapoor A, Noronha V, Patil VM, Joshi A, Menon N, Mahajan A, et al. Concomitant use of antibiotics and immune checkpoint inhibitors in patients with solid neoplasms: retrospective data from real-world settings. *Ecancermedicalscience* (2020) 14:1038. doi: 10.3332/ecancer.2020.1038
130. Khan U, Ho K, Hwang EK, Peña C, Brouwer J, Hoffman K, et al. Impact of use of antibiotics on response to immune checkpoint inhibitors and tumor microenvironment. *Am J Clin Oncol* (2021) 44:247–53. doi: 10.1097/COC.0000000000000813
131. Masini C, Berselli A, Romagnani A, Bonelli C, Fantinel E, Pagano M, et al. Results of an Italian CORE-IMMUNO study: Safety and clinical-related biomarkers as predictors of immunotherapy (IT) benefit in real-world treatment of various advanced tumors (ATs). *J Clin Oncol* (2019) 37:e14156–6. doi: 10.1200/JCO.2019.37.15_suppl.e14156
132. Ng Wei Qi K, Bird B, Murphy C, O' Connor D, Cook J. (2021). Efficacy of pembrolizumab with concomitant use of antibiotics, in: *Proceedings from ESMO*, .
133. Pérez-Ruiz E, Jiménez-Castro J, Berciano-Guerrero M-A, Valdivia J, Estalella-Mendoza S, Toscano F, et al. Impact of intestinal dysbiosis-related drugs on the efficacy of immune checkpoint inhibitors in clinical practice. *Clin Transl Oncol* (2020) 22:1778–85. doi: 10.1007/s12094-020-02315-9
134. Sen S, Carmagnani Pestana R, Hess K, Viola GM, Subbiah V. Impact of antibiotic use on survival in patients with advanced cancers treated on immune checkpoint inhibitor phase I clinical trials. *Ann Oncol* (2018) 29:2396–8. doi: 10.1093/annonc/mdy453
135. Tinsley N, Zhou C, Tan G, Rack S, Lorigan P, Blackhall F, et al. Cumulative antibiotic use significantly decreases efficacy of checkpoint inhibitors in patients with advanced cancer. *Oncologist* (2020) 25:55–63. doi: 10.1634/theoncologist.2019-0160
136. Vick E, Abuali I, Ludvigsen S, Kelleher A, Moore N, Arias N, et al. Antibiotic administration prior to immunotherapy leads to poor overall survival across multiple malignancies. In: *Late-breaking abstracts*. BMJ Publishing Group Ltd (2020). p. A464–5. doi: 10.1136/jitc-2020-SITC2020.0774
137. Vitorino M, Batista MV, Tiago T, Baptista de Almeida S, Freitas R, Silva M. (2021). Prior antibiotic use in immunotherapy treated patients - the experience of a community hospital, in: *Proceedings from ELCC*, .
138. Gelatti ACZ, Cordeiro de Lima VC, Freitas H, Werutsky G, Gaiger AM, Klock C, et al. Real-world prevalence of PD-L1 expression among tumor samples from patients with non-small-cell lung cancer. *Clin Lung Cancer* (2020) 21:e511–5. doi: 10.1016/j.clcc.2020.04.007
139. Dietel M, Savelov N, Salanova R, Micke P, Bigras G, Hida T, et al. Real-world prevalence of programmed death ligand 1 expression in locally advanced or metastatic non-small-cell lung cancer: The global, multicenter EXPRESS study. *Lung Cancer* (2019) 134:174–9. doi: 10.1016/j.lungcan.2019.06.012
140. Rabe KF, Watz H. Chronic obstructive pulmonary disease. *Lancet* (2017) 389:1931–40. doi: 10.1016/S0140-6736(17)31222-9
141. Taplitz RA, Kennedy EB, Bow EJ, Crews J, Gleason C, Hawley DK, et al. Antimicrobial prophylaxis for adult patients with cancer-related immunosuppression: ASCO and IDSA clinical practice guideline update. *J Clin Oncol* (2018) 36:3043–54. doi: 10.1200/JCO.18.00374
142. Peters BA, Wilson M, Moran U, Pavlick A, Izsak A, Wechter T, et al. Relating the gut metagenome and metatranscriptome to immunotherapy responses in melanoma patients. *Genome Med* (2019) 11:61. doi: 10.1186/s13073-019-0672-4
143. Messaoudene M, Saint-Lu N, Sablier-Gallis F, Ferreira S, Le Bescop C, Ponce M, et al. 1663MO DAV132 prevents antibiotic-induced intestinal microbiota dysbiosis and maintains anti-PD-1 efficacy: A proof-of-concept in tumor-bearing mice transplanted with human feces. *Ann Oncol* (2022) 33:S1303. doi: 10.1016/j.annonc.2022.07.1743
144. Davar D, Dzutsev AK, McCulloch JA, Rodrigues RR, Chauvin J-M, Morrison RM, et al. Fecal microbiota transplant overcomes resistance to anti-PD-1 therapy in melanoma patients. *Science* (2021) 371:595–602. doi: 10.1126/science.abf3363
145. Baruch EN, Youngster I, Ben-Betzalel G, Ortenberg R, Lahat A, Katz L, et al. Fecal microbiota transplant promotes response in immunotherapy-refractory melanoma patients. *Science* (2021) 371:602–9. doi: 10.1126/science.abb5920
146. Sepich-Poore GD, Zitvogel L, Straussman R, Hasty J, Wargo JA, Knight R. The microbiome and human cancer. *Science* (2021) 371:eabc4552. doi: 10.1126/science.abc4552
147. Zitvogel L, Kroemer G. Cross-reactivity between microbial and tumor antigens. *Curr Opin Immunol* (2022) 75:102171. doi: 10.1016/j.coi.2022.102171
148. Smith M, Dai A, Ghilardi G, Amelsberg KV, Devlin SM, Pajarillo R, et al. Gut microbiome correlates of response and toxicity following anti-CD19 CAR T cell therapy. *Nat Med* (2022) 28:713–23. doi: 10.1038/s41591-022-01702-9
149. Elinav E. Host microbiome interactions in health and disease, in: *Proceedings from ESMO*; Paris (2022).

150. Chen B, Yang C, Dragomir MP, Chi D, Chen W, Horst D, et al. Association of proton pump inhibitor use with survival outcomes in cancer patients treated with immune checkpoint inhibitors: a systematic review and meta-analysis. *Ther Adv Med Oncol* (2022) 14:1–18. doi: 10.1177/17588359221111703

151. Petrelli F, Signorelli D, Ghidini M, Ghidini A, Pizzuttilo EG, Ruggieri L, et al. Association of steroids use with survival in patients treated with immune checkpoint inhibitors: A systematic review and meta-analysis. *Cancers* (2020) 12:546. doi: 10.3390/cancers12030546



OPEN ACCESS

EDITED BY

Catherine Sautes-Fridman,
INSERM U1138 Centre de Recherche des
Cordeliers (CRC), France

REVIEWED BY

Monika Holubová,
Charles University, Czechia
Jennifer D. Wu,
Northwestern University, United States

*CORRESPONDENCE

Anahid Jewett

✉ ajewett@mednet.ucla.edu

RECEIVED 27 December 2022

ACCEPTED 31 March 2023

PUBLISHED 01 May 2023

CITATION

Kaur K, Chen P-C, Ko M-W, Mei A,
Senior E, Malarkannan S, Kos J and
Jewett A (2023) Sequential therapy with
supercharged NK cells with either
chemotherapy drug cisplatin or anti-PD-1
antibody decreases the tumor size and
significantly enhances the NK function in
Hu-BLT mice.

Front. Immunol. 14:1132807.

doi: 10.3389/fimmu.2023.1132807

COPYRIGHT

© 2023 Kaur, Chen, Ko, Mei, Senior,
Malarkannan, Kos and Jewett. This is an
open-access article distributed under the
terms of the [Creative Commons Attribution
License \(CC BY\)](https://creativecommons.org/licenses/by/4.0/). The use, distribution or
reproduction in other forums is permitted,
provided the original author(s) and the
copyright owner(s) are credited and that
the original publication in this journal is
cited, in accordance with accepted
academic practice. No use, distribution or
reproduction is permitted which does not
comply with these terms.

Sequential therapy with supercharged NK cells with either chemotherapy drug cisplatin or anti-PD-1 antibody decreases the tumor size and significantly enhances the NK function in Hu-BLT mice

Kawaljit Kaur¹, Po-Chun Chen¹, Meng-Wei Ko¹, Ao Mei²,
Emanuela Senior^{1,3,4}, Subramaniam Malarkannan^{2,5},
Janko Kos^{3,4} and Anahid Jewett^{1,6*}

¹Division of Oral Biology and Medicine, The Jane and Jerry Weintraub Center for Reconstructive Biotechnology, University of California School of Dentistry, Los Angeles, CA, United States,

²Laboratory of Molecular Immunology and Immunotherapy, Blood Research Institute, Versiti,

Milwaukee, WI, United States, ³Department of Biotechnology, Jožef Stefan Institute, Ljubljana, Slovenia,

⁴Faculty of Pharmacy, University of Ljubljana, Ljubljana, Slovenia, ⁵Department of Microbiology and

Immunology, Medical College of Wisconsin, Milwaukee, WI, United States, ⁶The Jonsson Comprehensive Cancer Center, University of California, Los Angeles (UCLA) School of Dentistry and Medicine, Los Angeles, CA, United States

Introduction and methods: In this study we report that sequential treatment of supercharged NK (sNK) cells with either chemotherapeutic drugs or check-point inhibitors eliminate both poorly differentiated and well differentiated tumors *in-vivo* in humanized-BLT mice.

Background and results: sNK cells were found to be a unique population of activated NK cells with genetic, proteomic, and functional attributes that are very different from primary untreated or IL-2 treated NK cells. Furthermore, NK-supernatant differentiated or well-differentiated oral or pancreatic tumor cell lines are not susceptible to IL-2 activated primary NK cell-mediated cytotoxicity; however, they are greatly killed by the CDDP and paclitaxel in *in-vitro* assays. Injection of one dose of sNK cells at 1 million cells per mouse to aggressive CSC-like/poorly differentiated oral tumor bearing mice, followed by an injection of CDDP, inhibited tumor weight and growth, and increased IFN- γ secretion as well as NK cell-mediated cytotoxicity substantially in bone marrow, spleen and peripheral blood derived immune cells. Similarly, the use of check point inhibitor anti-PD-1 antibody increased IFN- γ secretion and NK cell-mediated cytotoxicity, and decreased the tumor burden *in-vivo*, and tumor growth of resected minimal residual tumors from hu-BLT mice when used sequentially

with sNK cells. The addition of anti-PDL1 antibody to poorly differentiated MP2, NK-differentiated MP2 or well-differentiated PL-12 pancreatic tumors had different effects on tumor cells depending on the differentiation status of the tumor cells, since differentiated tumors expressed PD-L1 and were susceptible to NK cell mediated ADCC, whereas poorly differentiated OSCSCs or MP2 did not express PD-L1 and were killed directly by the NK cells.

Conclusions: Therefore, the ability to target combinatorially clones of tumors with NK cells and chemotherapeutic drugs or NK cells with checkpoint inhibitors at different stages of tumor differentiation may be crucial for successful eradication and cure of cancer. Furthermore, the success of check point inhibitor PD-L1 may relate to the levels of expression on tumor cells.

KEYWORDS

NK cells, supercharged NK cells, cytotoxicity, IFN- γ , chemotherapeutic, Hu-BLT, checkpoint inhibitor

Introduction

Cancer is the second leading cause of mortality globally (1, 2). Because of limited efficacy, and undesirable toxicities of current cancer therapies, there is an urgent need to improve the clinical outcomes in cancer patients (3–5). Despite intense research and improvement in therapeutic regimens, diagnosis of many cancers at the later stages of the disease remains associated with poor prognosis (2). With the rapid advances in the immunotherapy approaches in cancer, there is now greater focus on development of cell-based immunotherapies. More recently, clinical trials on cancer immunotherapies have demonstrated that immunotherapy is an effective treatment modality for many types of malignancies including metastatic melanoma, lung cancer, and bladder cancer (6–10). Effectors of the immune system are thought to shape the survival and maturation of tumor cells and also in the elimination of cancer. Hence, while surgery in combination with chemotherapy and radiotherapy is considered a fundamental therapeutic strategy and the standard of care in many solid tumors, immunotherapy alone or in combination with other therapies is now playing an important role in the treatment of various malignancies. The ultimate goal of immunotherapies is to assist the immune system to eradicate the cancer cells, and it appears that immunotherapy is on the way to transform terminal cancer to perhaps a more manageable chronic disease, and ultimately cure the patients from the disease if underlying mechanisms of immune activation and function are clearly delineated and the role of each immune subset clarified in the shaping of the tumors (11).

Heterogeneity in tumor cells necessitates treatment strategies which target all the different clones of tumor cells, and restores the function of immune cells in patients to prevent recurrences and the generation of new cancers. Thus, combinatorial treatments with immunotherapy may be required to target tumor cells at different stages of differentiation. We have shown in many previous publications that natural killer cells (NK) cells target cancer stem cells (CSCs)/poorly

differentiated tumors whereas well differentiated tumors are not susceptible to primary NK cell effects, but they are susceptible to CD8+ T cell function, chemotherapy, radiation and antibody therapy (12). Not too many treatment strategies other than NK cells are capable of targeting CSCs, or poorly differentiated tumors, primarily due to their lack of or much lower expression of MHC-class I (13). We have shown recently that cannabinoids are potentially other factors that can target the CSCs/poorly differentiated oral and pancreatic tumors (14). However, radiation (15–18) and chemotherapy (12, 16–19) were unsuccessful in targeting CSCs. We have also shown that NK cell-mediated ADCC was significantly higher against PD-L1 and MICA/B expressing differentiated tumors as compared to their CSCs (20). It is conceivable that CAR-T and CAR-NK cells generated to high expressing surface receptors on CSCs/poorly differentiated tumors can achieve similar outcomes as NK cells; however, down-modulation or loss of those receptors on these cells may make these CARs ineffective and promote tumor growth and expansion, whereas the more a cell mutates and loses surface receptors, the better it is targeted by the NK cells (21). Indeed, NK cell-based clinical trials have demonstrated not only the safety but also the efficacy in decrease in tumor relapse rate (22–25).

NK cells mediate direct cytotoxicity as well as antibody-dependent cellular cytotoxicity (ADCC) (26). Two effector functions of NK cells that are crucial for the elimination of the tumors are NK cell-mediated cytotoxicity and secretion of cytokines which lead to direct killing of CSCs, and NK cell-mediated differentiation of tumors respectfully (27). IFN- γ and TNF- α secreted by NK cells play a crucial role in differentiating CSCs/undifferentiated tumors (28). We have shown previously that differentiated tumors are favorable targets of chemotherapy, thus, NK cells could assist chemotherapy in eradication of tumors (12, 29). Also, combining NK cell immunotherapy with checkpoint inhibitors such as anti-PD1 have shown promising results (26, 30).

In this study, we demonstrate the differences between the primary and supercharged NK cells (sNK) based on their

genetics, proteomics and functional attributes, demonstrating the uniqueness of sNK cells not only for their increased cycling and significant rate of expansion, but also their superior function and their unique transcriptional profile on single cell RNAseq analysis level. The *in-vivo* studies revealed how the combination of sNK cells with chemotherapy or sNK cells with anti-PD1 antibody reduce tumor burden and either restore or increase IFN- γ secretion, and cytotoxic function of NK cells in various tissue compartments of oral and pancreatic tumor-bearing humanized-BLT (hu-BLT) mice. We also provide some underlying mechanisms governing such *in vivo* observations in a series of *in vitro* studies.

Results

Unique attributes of supercharged NK cells in comparison to primary NK cells

In our previous studies as well in this study, we demonstrate the superior ability of osteoclasts (OCs) to condition NK cells for greater expansion and heightened function (Figure S1) (31). Here, we compared cell expansion, IFN- γ secretion, and NK cell-mediated cytotoxicity of untreated, IL-2 treated NK, IL-2+anti-CD16mAbs treated NK, and IL-2+anti-CD16mAbs+sAJ2 treated NK cells with

IL-2+anti-CD16mAbs+sAJ2+OCs treated NK cells, and found higher cell expansion and increased function in the presence of OCs (Figure 1). Probiotic bacteria, sAJ2 is a combination of 7-8 different strains, and is prepared as described previously (32). Due to their unusually high expansion rate and potent function, we coined IL-2 +anti-CD16mAbs+sAJ2+OCs treated NK cells as supercharged NK (sNK) cells to differentiate them from all the other NK cell subsets that we had tested in our laboratory throughout the last 30 years (28). To further understand the differences between IL-2 treated primary NK (NK+IL-2) cells and sNK cells, we performed single-cell RNA sequencing. In the analysis of NK+IL-2 and sNK cells, we also integrated untreated NK cells derived from donor PBMC to help characterize the NK cell subsets. By studying untreated NK, NK+IL-2, and sNK cells, we were able to identify 4 transcriptionally unique NK cell clusters (Figure 2A). All 4 clusters have a consistent expression of NK cell genetic markers (*IL2RB*, *CD7*, *NKG7*). Among the 4 clusters, Cluster 1 has the highest expression of *IL7R* and *NCAM1*, resembling the transcriptional signature of previously characterized CD56^{bright} NK cells (33). Cluster 3 has a comparably higher expression of genes related to cytotoxicity (*GZMB*, *PRF1*) and *FCGR3A*, which are identified as the genetic signature of cytotoxic CD56^{dim} NK cells. The gene expression pattern of cluster 2 follows a subset of transitional NK cells between CD56^{bright} and CD56^{dim} NK cells. When the single-cell clusters are split by the three conditions, cluster 4 is shown to be exclusive in untreated

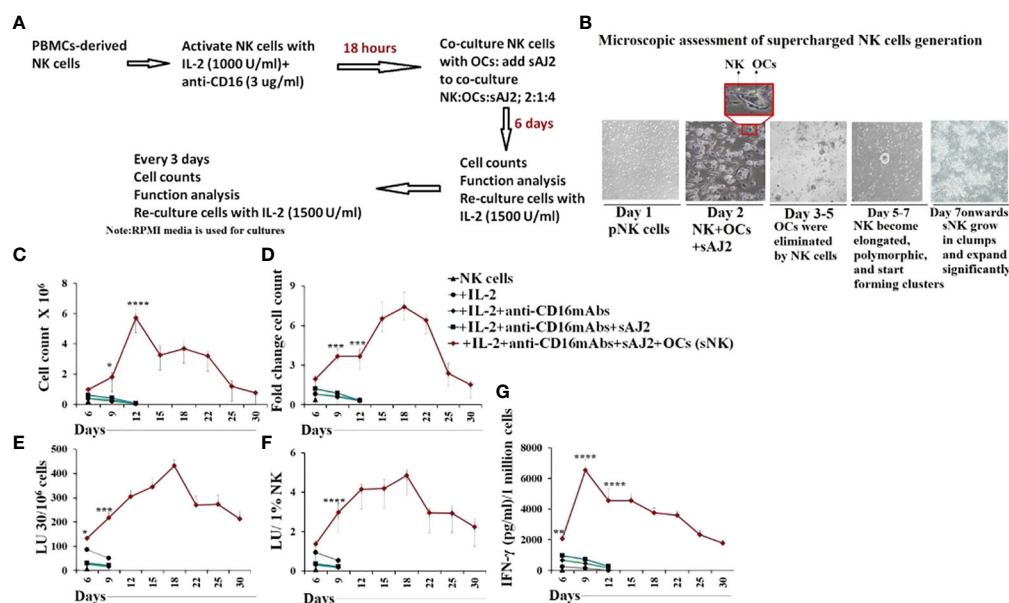


FIGURE 1

Osteoclasts induced higher cell expansion, increased cytokine secretion and cytotoxicity in NK cells in comparison to IL-2, IL-2+anti-CD16mAbs and IL-2+anti-CD16mAbs+sAJ2 treatments. Osteoclasts (OCs) were generated as described in the Materials and Methods section. NK cells (0.5×10^6 cells/2ml) were treated with a combination of IL-2 (1000 U/ml) and anti-CD16mAb (3 µg/ml) for 18 hours before they were co-cultured with OCs and treated with sAJ2 (2:1:4: NK : OCs:sAJ2). NK cells were counted on days 6, 9, 12, 15, 18, and onwards until cells are expanding (Average: 24–36 days) (A, B). NK cells (0.5×10^6 cells/2ml) were left untreated, or treated with IL-2 (1000 U/ml), or a combination of IL-2 (1000 U/ml) and anti-CD16mAb (3 µg/ml), or a combination of IL-2 (1000 U/ml), anti-CD16mAb (3 µg/ml), and sAJ2 (2:4:NK:sAJ2), or a combination of IL-2 (1000 U/ml), anti-CD16mAb (3 µg/ml), sAJ2, and OCs (2:1:4: NK : OCs:sAJ2). NK cells were counted on the days shown in the Figure (C), and the fold change based on the initial cell count of 0.5×10^6 cells/2 mL were determined every 3 days as shown in the figure (D). NK cell-mediated cytotoxicity against oral squamous cell carcinoma stem cell line (OSCCs) was determined on the days shown in the figure using a standard 4-hour ⁵¹Cr release assay. The lytic units 30/10⁶ cells were determined using the inverse number of NK cells required to lyse 30% of OSCCs $\times 100$ (E). Lytic units per 1% NK cells were determined based on the percentages of CD16+/CD56+ NK cells in the cultures obtained by flow cytometric analysis (F). The supernatants were harvested from the cultures on the days shown in the Figure E to determine IFN- γ secretion using single ELISA, and the levels were adjusted based on the number of cells (G). Averages and std. dev of three independent experiments are shown in Figure 1. ****(p value < 0.0001), *** (p value 0.0001–0.001), ** (p value 0.001–0.01), * (p value 0.01–0.05).

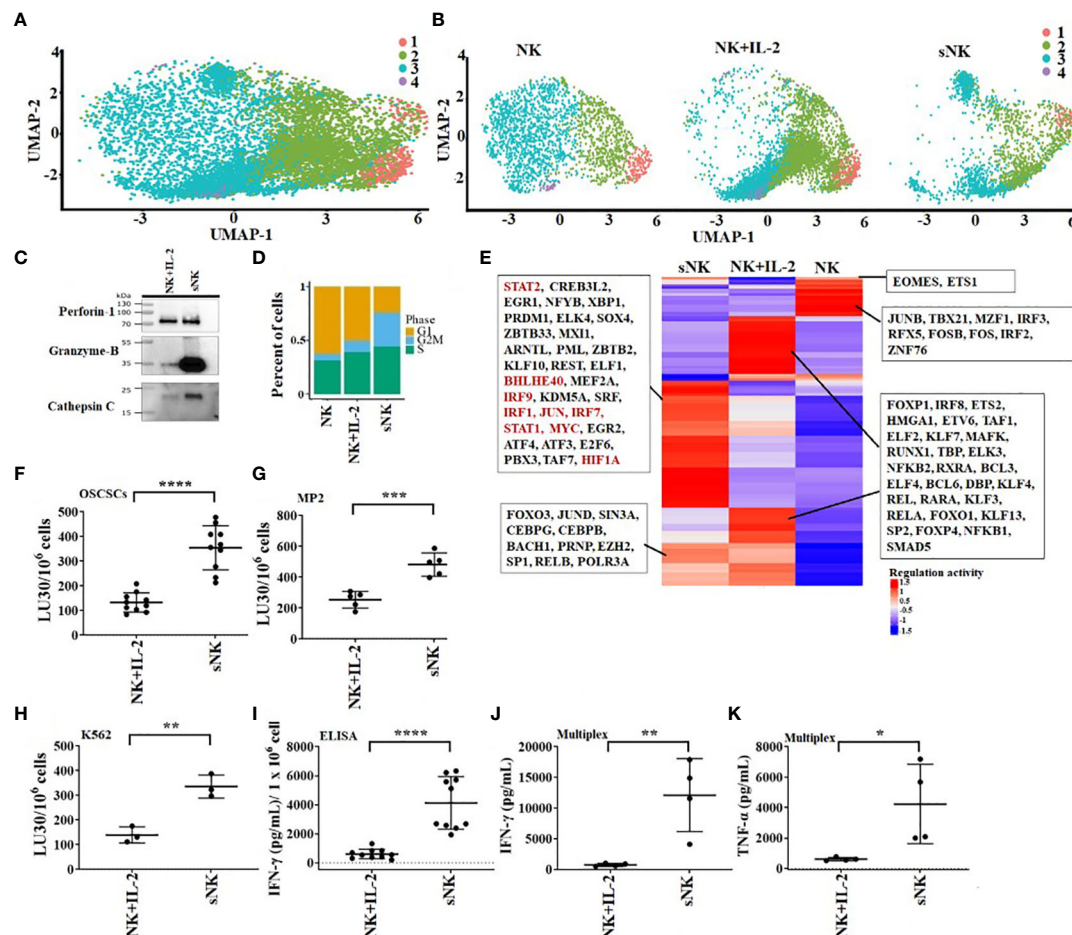


FIGURE 2

OC-expanded supercharged NK cells exhibit higher levels of cytotoxic granules, increased cytotoxicity and augmented secretion of cytokines when compared to primary activated NK cells. OCs were generated as described in the Materials and Methods section. NK cells (0.5×10^6 cells/ 2ml) from healthy individuals were treated with a combination of IL-2 (1000 U/ml) and anti-CD16 mAbs (3 μ g/ml) overnight before they were cultured with OCs and sAJ2 at a ratio of 2:1:4 (NK:OCs:sAJ2). Untreated NK cells, IL-2 treated NK cells, and super-charged NK (sNK) cells are used to construct single-cell cDNA libraries for sequencing. UMAP of all of the samples combined (A) or separated (B) are shown. Colors represent different UMAP clusters indicating genetically distinct NK cell subsets. Western blot of protein expression of granzyme B, cathepsin C, and perforin-1 in sNK vs. IL-2 treated primary NK cells derived from the same donor is shown in figure (C). Loading control can be found in Figure S1A. Each cell is assigned a cell-cycle score based on gene markers of different phases. The percentage of cells in each phase is represented in the bar-plot for untreated NK cells, IL-2 treated NK cells, and sNK cells (D). SCENIC is used to analyze the regulon activity in each condition. Each row of the heatmap represents a regulon, with some highlighted in the box (E). On day 14 of cultures, another set of NK cells were purified from healthy donors and were treated with IL-2 (1000 U/ml) overnight. Cytotoxicity of day 15 sNK cells and overnight IL-2 treated primary NK cells was determined using standard 4-hour ^{51}Cr release assay against OSCSCs (F), MP2 (G), and K562 (H). The Lytic units (LU) 30/10⁶ cells were determined using the inverse number of NK cells required to lyse 30% of OSCSCs (n=10) (F) or MP2 (n=5) \times 100 (G) or K562 (n=3) \times 100 (H). Primary NK cells were treated with IL-2 as described in Figure 1F, and the supernatants were harvested from day 15 sNK cells or IL-2 treated primary NK cells after an overnight incubation and were used to determine IFN- γ secretion using single ELISA. The amounts of IFN- γ secretion were adjusted based on 1×10^6 cells (n=10) (I). Primary NK cells were treated with IL-2 as described in Figure 1F, and the supernatants were harvested from day 15 expanded sNK cells or IL-2 treated primary NK cells after an overnight incubation, and they were used to determine IFN- γ (J) and TNF- α (K) using multiplex cytokine arrays (n=4). ****(p value < 0.0001), *** (p value 0.0001–0.001), ** (p value 0.001–0.01), * (p value 0.01–0.05).

NK cells (Figure 2B). We have also analyzed the expression of the main effector molecules in NK cell cytotoxic granules: perforin-1, granzyme B and cathepsin C (cathepsin C is responsible for the activation of granzyme B) (32). A significantly higher expression of granzyme B and cathepsin C in the presence of slightly decreased perforin was seen in sNK cells in comparison to primary IL-2 treated NK cells (Figures 2C, S2A). Through the cell-cycle score analysis on the single-cell RNA sequencing result, a considerably higher amount of sNK cells is assigned to the G2M phase, indicating a more active proliferation program in the sNK cells compared to untreated and NK+IL-2 cells (Figure 2D). Also, by performing SCENIC analysis on the sequencing

data, a distinct regulon network is utilized in the sNK cells compared to either untreated or NK+IL-2 cells. Among the predicted regulon activities, sNK cells have upregulated regulon activities associated with NK cell survival (STAT2, IRF9) and effector functions (IRF1, JUN, STAT1, HIF1A) (Figure 2E) (27, 34–37). When assessed NK cell-mediated cytotoxicity of IL-2 treated primary NK and sNK cells against oral squamous carcinoma stem cells (OSCSCs), Mia PaCa-2 (MP2), and K562 cell lines, significantly higher cytotoxicity was mediated by sNK cells in comparison to NK+IL-2 cells (Figures 2F–H). We also observed higher secretion of IFN- γ and TNF- α by sNK cells in comparison to primary NK cells treated with IL-2 (Figures 2I–K,

S2B). These results exhibited higher anti-cancer activity of sNK cells in comparison to primary activated NK cells.

Differentiated oral and pancreatic tumors are more susceptible to chemotherapeutic drugs in comparison to their stem-like counterparts

Our previous findings have demonstrated that differentiated tumors were more sensitive to chemotherapeutic drugs in comparison to CSCs/poorly differentiated tumors (12). Here, we determined the extent of cell death of oral cancer stem-like cells (OSCSCs), NK-diff-OSCSCs, CSCs/poorly differentiated pancreatic cancer MP2, and differentiated pancreatic cancer PL12 and NK-diff-MP2 with or without the treatments with chemotherapeutic drugs cisplatin (CDDP) and paclitaxel (Figure 3). We observed higher cell death induced by CDDP (Figures 3A, C, S3) and paclitaxel (Figures 3B, D) against differentiated tumors in comparison to their CSCs/poorly differentiated counterparts. Thus, differentiation of tumors by the NK cells is an important step not only in curtailing the tumor growth, but more importantly in the response to chemotherapy drugs.

sNK cell immunotherapy alone or in combination with CDDP greatly inhibited tumor growth in hu-BLT mice

We used humanized-BLT (hu-BLT) mice model to demonstrate the efficacy of combinational treatment with sNK cells and chemotherapy against human oral CSCs/poorly differentiated tumors. Hu-BLT mice were generated by surgically implanting pieces of human fetal liver and thymus tissues under the renal capsule of NSG mice, followed by tail vein IV injection of same-donor CD34⁺ hematopoietic cells to support full reconstitution of the human bone marrow (38–40). In this study, hu-BLT mice after human immune cell reconstitution were surgically with human OSCSCs in oral cavity followed by IV injections of sNK cells and CDDP sequentially as depicted in Figure (Figure 4A). Upon sacrifice, the tumors were harvested and weighed. sNK cells alone or sNK cells combined with CDDP treated mice had smaller tumors in comparison to untreated mice with tumor (Figure 4B). Next, we dissociated tumors and recovered single cells to determine tumor cell counts. Tumors from tumor implanted mice treated with sNK cells alone or sNK cells combined with CDDP treated mice had significantly lower numbers of tumor cells as compared to tumor alone implanted mice (Figure 4C). When the same numbers of dissociated tumor cells from hu-BLT mice were cultured, significantly lower tumor cell expansion was seen in tumors from sNK cells alone or sNK cells combined with CDDP treated mice as compared to untreated tumors from tumor-bearing mice until day 14–19, after which the tumor growth rate gradually increased and at day 30 the tumor cultures were terminated. Even though the levels of tumor growth approached the levels seen with tumor alone implanted mice, we could still see a higher decrease in tumor growth with sNK+CDDP group as compared to sNK group, and

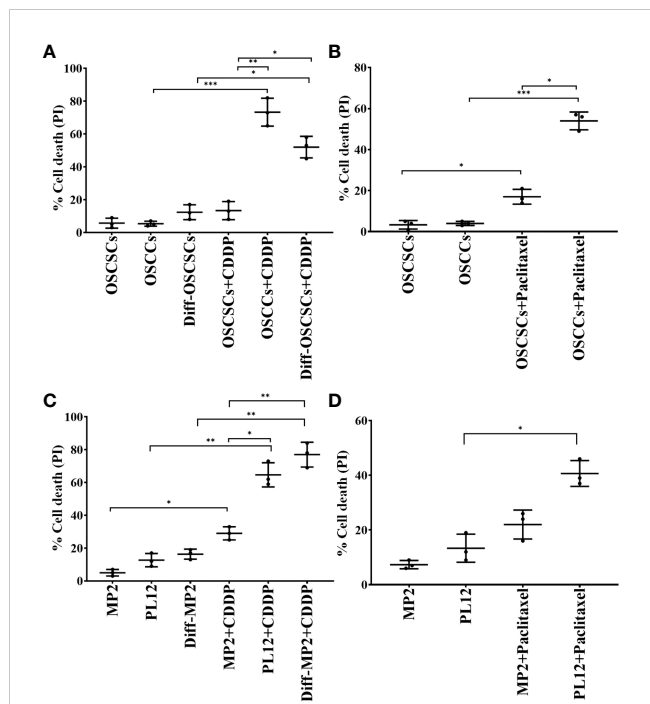


FIGURE 3

Increased susceptibility of differentiated oral and pancreatic tumor cell lines to chemotherapeutic drugs in comparison to their stem-like counterparts. OSCSCs were differentiated using supernatants from IL-2 (1000 U/ml) and anti-CD16 mAbs (3 µg/ml) treated primary NK cells as described in Materials and Methods section. OSCSCs, OSCCs and NK-diff-OSCSCs were treated with cisplatin (60 µg/ml) for 18–20 hours, after which, the cells were stained with propidium iodide (PI) to determine percent cell death using flow cytometric analysis (n=3) (A). OSCSCs and OSCCs were treated with paclitaxel (40 µg/ml) for 18–20 hours, after which, the cells were stained with PI to determine percent cell death using flow cytometric analysis (n=3) (B). MP2 cells were treated with supernatants from IL-2 (1000 U/ml) and anti-CD16 mAbs (3 µg/ml) treated primary NK cells in order to induce differentiation as described in the Materials and Methods section. MP2, PL12, and NK-diff-MP2 cells were treated with cisplatin (60 µg/ml) for 18–20 hours, after which, the cells were stained with PI to determine percentage of cell death using flow cytometric analysis (n=3) (C). MP2 and PL12 tumor cells were treated with paclitaxel (40 µg/ml) for 18–20 hours, after which, the cells were stained with PI to determine percent cell death using flow cytometric analysis (n=3) (D). *** (p value 0.0001–0.001), ** (p value 0.001–0.01), * (p value 0.01–0.05).

both groups had on average less growth when compared to those from tumor alone implanted mice (Figure 4D). When the dissociated tumors of hu-BLT mice were used as targets for primary IL-2 activated NK cells in Cr-release assay, tumors from sNK cells alone or sNK cells combined with CDDP treated mice were killed much less when compared to untreated tumor-bearing mice (Figure 4E). In addition, there was statistically significant differences in the resistance of tumor cells to NK cell-mediated cytotoxicity dissociated from sNK+CDDP group as compared to sNK group, and both these groups had highly significant decreases in cytotoxicity when compared to those obtained from tumor alone implanted hu-BLT mice (Figure 4E). Our previous studies have demonstrated that CSCs/poorly-differentiated tumors grow at higher rate and are excellent targets of NK cell-mediated cytotoxicity, whereas differentiated tumors grow slow and are

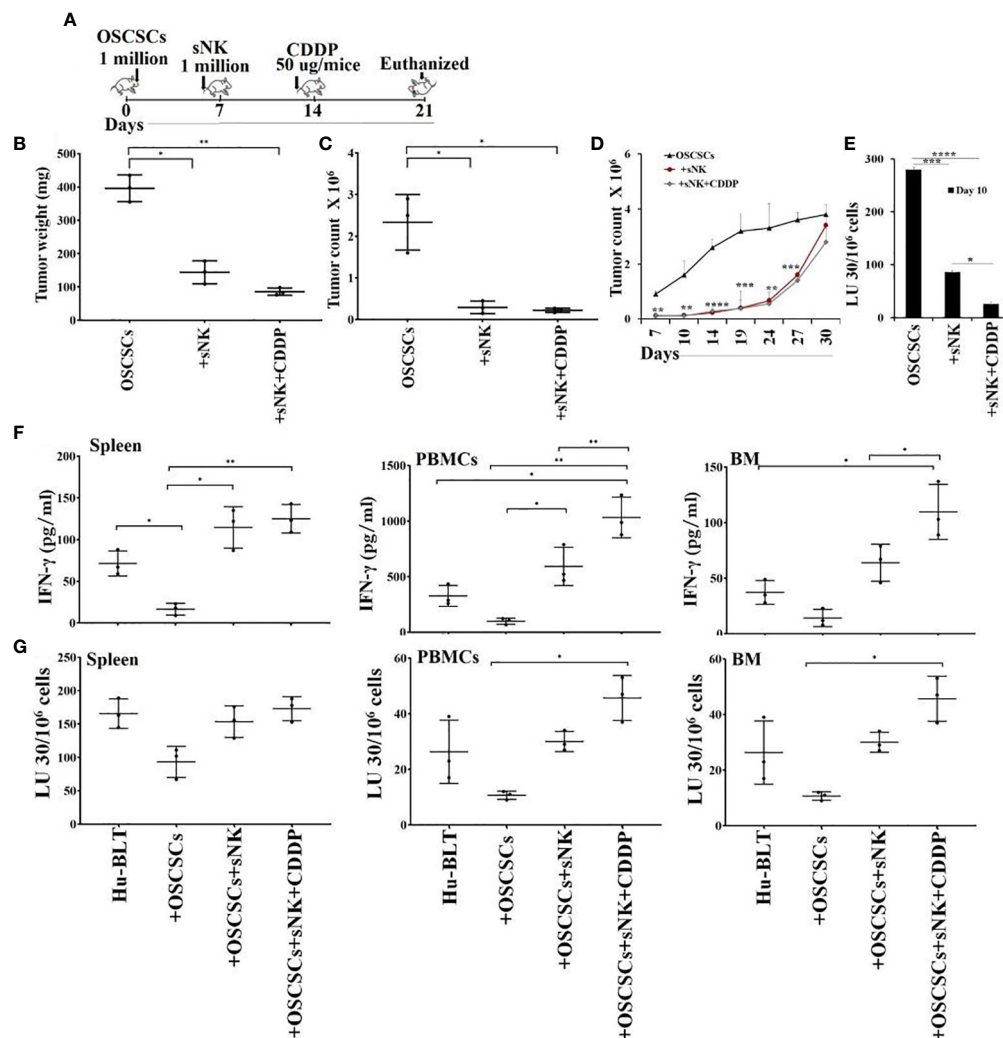


FIGURE 4

Cisplatin mediated decrease in tumor growth when used sequentially with sNK cell treatment in tumor implanted hu-BLT mice, and increased NK cell-mediated cytotoxicity by immune effectors derived from spleen, bone marrow and peripheral blood. Hu-BLT mice were orthotopically implanted with 1×10^6 human OSCSCs into the floor of the mouth. One week after the tumor implantation, mice received supercharged NK (sNK) cells via tail-vein injection, and one week after sNK cell injection, mice received CDDP (50 µg/mice) via tail vein injection. The disease progression was monitored for another week (A). Hu-BLT mice were implanted with OSCSC tumors and were injected with sNK cells and CDDP sequentially as depicted in Figure 4A. At the end of experiment, hu-BLT mice were sacrificed; the tumors were harvested and weighed (n=3) (B). Hu-BLT mice were implanted with OSCSC tumors and, were injected with sNK cells and CDDP sequentially as depicted in Figure 4A. At the end of the experiment, hu-BLT mice were sacrificed; the tumors were harvested, and the single-cells were obtained as described in the Materials and Methods section. Tumor cells were counted microscopically (n=3) (C). Tumor cells were counted microscopically (n=3) (C). Hu-BLT derived tumors were cultured at 1.5×10^5 / ml at the initiation of the cultures. On day 3, unattached cells were removed and fresh media was added. Tumors were detached and counted on days 7, 10, 14, 19, 24, 27, and 30, each time 1×10^5 / ml cells were cultured (n=3) (D). NK cells (1×10^6 /ml) from healthy human donors were treated with IL-2 (1000 U/ml) for 18 hours before they were added to ⁵¹Cr labeled hu-BLT derived tumors at various effector to target ratios. NK-mediated cytotoxicity was determined using 4-hour ⁵¹Cr release assay. The lytic units (LUs) 30/10⁶ cells were determined using inverse number of NK cells required to lyse 30% of the tumor-cells x 100 (n=2 per each experimental condition) (E). Hu-BLT mice were implanted with OSCSC tumors and were injected with sNK cells and CDDP sequentially as shown in Figure 4A. At the end of the experiment, hu-BLT mice were sacrificed. Spleens, peripheral blood, and bone marrow were harvested and single cell suspensions were obtained and cultured (1×10^6 /ml) with IL-2 (1000 U/ml) for 7 days. On day 7, the supernatants were harvested and the secretions of IFN-γ were determined using single ELISA (n=3) (F). Spleens, peripheral blood, and bone marrow cells were cultured (1×10^6 /ml) with IL-2 (1000 U/ml) for 7 days. On day 7, cells were used as effectors against OSCSCs using standard 4-hour ⁵¹Cr release assay. The Lytic units (LU) 30/10⁶ cells were determined using the inverse number of cells required to lyse 30% of OSCSCs x 100 (n=3) (G). ****(p value < 0.0001), *** (p value 0.0001–0.001), ** (p value 0.001–0.01), * (p value 0.01–0.05).

resistant to NK cell-mediated cytotoxicity (13, 41–43). Results shown in Figures 4D, E indicates that tumors from sNK cells alone or sNK cells combined with CDDP treated mice exhibited characteristics of differentiated tumors. In addition, when all the floating immune cells were removed by changing the media from tumor cultures throughout the days of 7–27 the differentiated nature

of tumor cells grown from sNK cells or sNK in combination with CDDP gradually reverted to their CSC/poorly differentiated tumors, and their growth rate gradually increased and approached to those grown from tumor alone implanted BLT mice (Figures 4D). We have previously shown that reversion of NK differentiated tumors occurs after two weeks in culture without immune cells, and it

correlates with the decreased MHC class I expression on tumor cells (44).

Sequential treatment with sNK cell immunotherapy and CDDP exhibited increased IFN- γ secretion and NK cell-mediated cytotoxicity by bone marrow, PBMCs and splenocytes of hu-BLT mice

We then assessed IFN- γ secretion and NK cell-mediated cytotoxicity of splenocytes, peripheral blood and bone marrow derived cells of tumor-bearing hu-BLT mice with or without treatments. We observed suppression of both secretion of IFN- γ (Figures 4F, S4, S5A) and NK cell-mediated cytotoxicity (Figures 4G, S5B) in tumor-bearing untreated mice in comparison to those obtained from healthy mice without tumor implantation. Increase or restoration of IFN- γ secretion and NK cell-mediated cytotoxicity by bone marrow, splenocytes and PBMCs were seen in sNK cell injected tumor-bearing mice, and both these functions were further increased with the combination of sNK cells and CDDP treatment of tumor implanted mice when compared to those with tumor alone implanted mice (Figures 4F, G, S4, S5). CDDP alone injected mice either did not increase or increased slightly the secretion of IFN- γ in cells dissociated from spleen, peripheral blood, and BM (Figure S4).

Differentiated tumors expressed higher levels of PD-L1 and were more susceptible to NK cell-mediated ADCC in the presence of anti-PD-L1 as compared to their stem-like counterparts

Our previous studies have shown that CSCs/poorly-differentiated tumors are excellent targets of direct NK cell-mediated cytotoxicity, whereas their differentiated counterparts are significantly more resistant (13, 41–43). We have also shown previously that differentiated tumors have higher surface expression of MICA/MICB and are susceptible to ADCC mediated by the primary NK cells in the presence of anti-MICA/MICB antibody, even though NK cells are not able to kill these tumors directly (20). Here, we evaluated NK cell-mediated cytotoxicity against untreated stem-like (OSCSCs and MP2) and untreated or anti-PD-L1 antibody treated differentiated tumors (NK-Diff-OSCSCs, OSCCs, NK-Diff-MP2, and PL12) (Figure 5A–F). We demonstrate that NK cells mediated direct cytotoxicity of OSCSCs (Figure 5A) and MP2 (Figure 5D) tumors, whereas susceptibility to NK cell-mediated cytotoxicity was substantially and significantly lower against NK-diff-OSCSCs (Figures 5B, S6A), OSCCs (Figure 5C, S6A), NK-diff-MP2 (Figures 5E, S6B), and PL12 (Figure 5F, S6B) tumors when compared to OSCSCs and MP2 cells. NK cell-mediated cytotoxicity was increased against anti-PDL1-treated NK-diff-OSCSCs (Figure 5B), OSCCs (Figure 5C), NK-diff-MP2 (Figure 5E), and PL12 (Figure 5F) tumors. In accordance, higher surface expression of PD-L1 was seen on NK-diff-OSCSCs and OSCCs (Figure 5G) and NK-diff-MP2 and PL-12 (Figure 5H) tumors in comparison to their

stem-like counterparts. Differentiated tumors also expressed higher surface expression of MHC-class I (Figures S7B, C). We also assessed surface expression of PD-L1 on NK cells (Figure S7A). The results indicated that both IL-2 and IL-2+anti-CD16mAb treatment elevated the expression of PD-L1 on NK cells (Figure S7A). Taken together, the data indicated that differentiated tumors express higher PD-L1 on their surface, and treatment of these cells with anti-PD-L1 antibody mediate ADCC in the presence of NK cells. However, poorly differentiated tumors are devoid of this surface antigen and therefore NK cells may become inactivated in the presence of anti-PD-L1 antibody treatment since activated NK cells exhibit PD-L1 on the surface.

Anti-PD1 antibody induced higher IFN- γ secretion from NK cells in the presence of stem-like tumors in comparison to differentiated tumors

We have previously demonstrated that NK cells secrete higher levels of IFN- γ when co-cultured with CSCs/poorly differentiated tumors in comparison to differentiated tumors (42). In our current study, we co-cultured stem-like/poorly differentiated (MP2 and OSCSCs) and their differentiated counterparts (NK-Diff-MP2 and NK-Diff-OSCSCs) with NK cells with or without anti-PD1 treatment (Figures 6, S7). Lower secretion of IFN- γ was found when NK cells were co-cultured with NK-diff-OSCSCs (Figures 6A, S8) and NK-diff-MP2 (Figure 6B) in comparison to the cultures with their stem-like counterparts. Anti-PD1 treated NK cells without tumors showed slightly increased levels of IFN- γ secretion, however, the highest effect of anti-PD1 treatment was seen when NK cells were co-cultured with OSCSCs (Figures 6A, S8) or MP2 (Figure 6B) cells in comparison to those co-cultured with their NK-differentiated counterparts.

sNK cell immunotherapy alone or in combination with anti-PD1 antibody inhibited tumor growth in hu-BLT mice and significantly improved immune function of hu-BLT mice

Hu-BLT mice were surgically implanted with human MP2 tumors followed by injections of sNK cells and anti-PD1 sequentially as depicted in Figure 7A. Upon sacrifice, the tumors were harvested and weighed, and the results were compared to tumor bearing mice in the absence of treatments. sNK cells alone or sNK cells combined with anti-PD1 antibody injected mice had smaller tumors in comparison to untreated tumor implanted mice (Figures 7B, S9A). Anti-PD1 antibody alone treated mice had smaller tumors compared to untreated tumor-bearing mice but the size was larger in comparison to either sNK treated or sNK + anti-PD1 antibody treated group (Figure 7B). Tumors were then dissociated and counted and the numbers were adjusted to 1.5×10^5 per well. Tumor growth were slightly with anti-PD1 alone treatment, and was much less with sNK cells alone or sNK cells combined with anti-PD1 treatments when compared to untreated tumor implanted

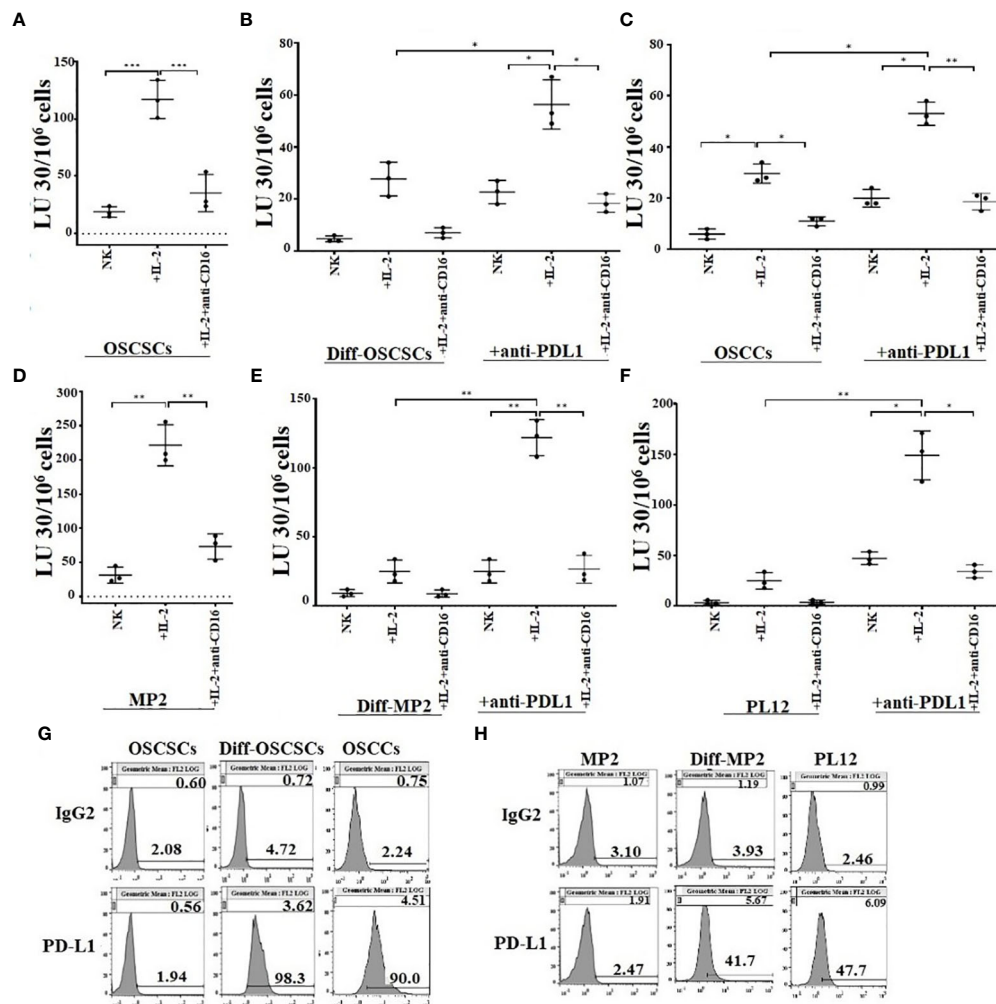


FIGURE 5

Differentiated tumors expressed higher levels of PD-L1 on their surface and were more susceptible to NK cell-mediated cytotoxicity when compared to their stem-like counterparts in the presence of anti-PDL1. Purified NK cells (1×10^6 cells/ml) from healthy individuals were left untreated, or treated with IL-2 (1000 U/ml), or treated with IL-2 (1000 U/ml) and anti-CD16 mAbs ($3 \mu\text{g}/\text{mL}$) for 18 hours and were used as effectors in chromium release assay. OSCSCs were differentiated using IL-2 (1000 U/ml) and anti-CD16 mAbs ($3 \mu\text{g}/\text{mL}$) treated NK cell supernatants as described in Materials and Methods section. OSCSCs (A), NK-differentiated-OSCSCs (B), and differentiated OSCCs (C), were labeled with ^{51}Cr for an hour. NK-differentiated-OSCSCs (B), and differentiated OSCCs (C), ^{51}Cr -labeled tumor cells were then left untreated or treated with anti-PDL1 ($5 \mu\text{g}/\text{mL}$) for 30 minutes. The unbound antibodies were washed away, and the cytotoxicity against the tumor cells was determined using a standard 4-hour ^{51}Cr release assay. The Lytic units (LU) $30/10^6$ cells were determined using the inverse number of NK cells required to lyse 30% of tumors $\times 100$ ($n=3$) (A–C). The surface expression of PD-L1 was analyzed on tumor cells using flow cytometry. IgG2 isotype control antibodies were used as controls (G). Purified NK cells (1×10^6 cells/ml) from healthy individuals were left untreated, or treated with IL-2 (1000 U/ml) or treated with IL-2 (1000 U/ml) and anti-CD16 mAbs ($3 \mu\text{g}/\text{mL}$) for 18 hours and they were used as effectors in chromium release assay. MP2 cells were differentiated using IL-2 (1000 U/ml) and anti-CD16 mAbs ($3 \mu\text{g}/\text{mL}$) treated NK cell supernatants as described in Materials and Methods section. MP2 (D), NK-differentiated MP2 (E), and differentiated PL12 (F) were labeled with ^{51}Cr for an hour. NK-differentiated MP2 (E), and differentiated PL12 (F) ^{51}Cr -labeled tumor cells were then left untreated or treated with anti-PDL1 ($5 \mu\text{g}/\text{mL}$) for 30 minutes. The unbound antibodies were washed away, and the cytotoxicity against the tumor cells was determined using a standard 4-hour ^{51}Cr release assay. The Lytic units (LU) $30/10^6$ cells were determined using the inverse number of NK cells required to lyse 30% of tumors $\times 100$ ($n=3$) (D, E, F). The surface expression of PD-L1 was analyzed on tumor cells using flow cytometry. IgG2 isotype control antibodies were used as controls (H). ***(p value 0.0001–0.001), **(p value 0.001–0.01), *(p value 0.01–0.05).

mice (Figures 7C). When the same numbers of dissociated tumor cells from hu-BLT mice were cultured, significantly lower tumor cell expansion was seen in tumors from sNK cells alone or sNK cells combined with anti-PD-1 antibody treated mice as compared to those from untreated tumor-bearing mice until day 14–18, after which the tumor growth rate gradually increased and approached to those obtained from tumor alone implanted mice, and at day 27 the tumor cultures were terminated. Even though the levels of tumor growth gradually approached the levels seen with tumor alone

implanted mice at the days 18–24, we could still see a lower tumor growth with sNK+anti-PD-1 antibody treated group as compared to sNK treated group, and both groups had on average lower growth when compared to those from tumor alone implanted mice (Figures 7D, S9B). Tumors dissociated from anti-PD-1 antibody group exhibited a lower rate of tumor growth when compared to the tumor alone implanted group but the levels of tumor growth were higher than those obtained from either the sNK treated or the sNK +anti-PD-1 antibody treated group (Figures 7D, S8B). In addition,

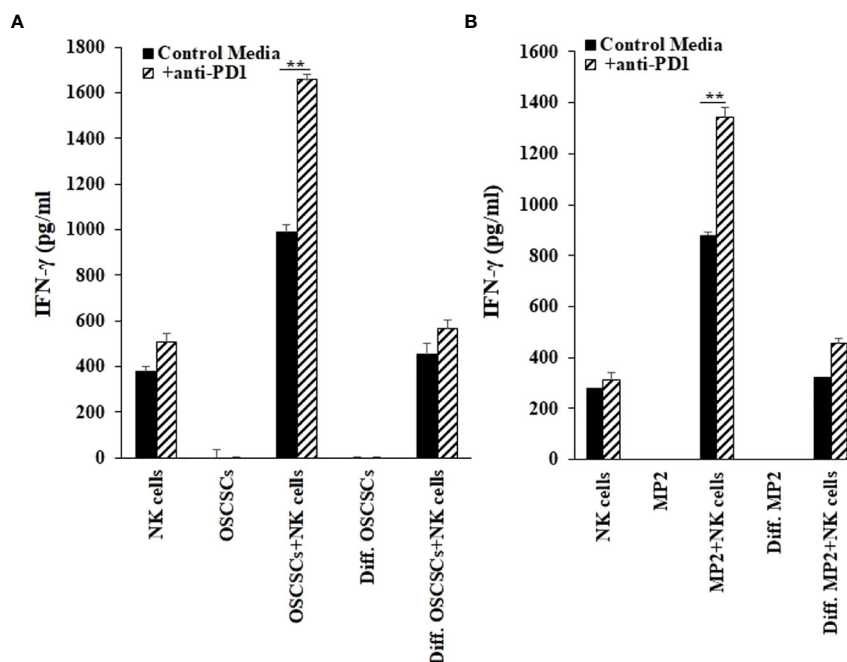


FIGURE 6

Increased IFN- γ secretion by NK cells in the presence of cancer stem cells and anti-PD1. OSCSCs were differentiated using IL-2 (1000 U/ml) and anti-CD16 mAbs (3 μ g/ml) treated NK cell supernatants as described in the Materials and Methods section. NK cells of healthy individuals were treated with IL-2 (1000 U/ml) for 18–20 hours before they were co-cultured with tumor cells (NK: tumors; 1:1), and treated with anti-PD1 (500 ng/ml) antibody. On day 3 of co-culture, the supernatants were harvested and the secretion of IFN- γ was determined using single ELISAs (A). MP2 cells were treated with IL-2 (1000 U/ml) and anti-CD16 mAbs (3 μ g/ml) treated NK cell supernatants to induce differentiation as described in the Materials and Methods section. NK cells of healthy individuals were treated with IL-2 (1000 U/ml) for 18–20 hours before they were added to tumor cells (NK: tumors; 1:1), and were treated with anti-PD1 (500 ng/ml) antibody. On day 3 of co-culture, the supernatants were harvested and the secretion of IFN- γ was determined using single ELISA (B). **(p value 0.001–0.01).

when all the floating immune cells were removed by changing the media every three days from tumor cultures throughout the days of 7–27 the differentiated nature of tumor cells grown from sNK cells or sNK in combination with anti-PD-1 gradually reverted to their CSC/poorly differentiated tumors, and their growth rate gradually increased and approached to those grown from tumor alone implanted BLT mice (Figure 7D).

Sequential treatment with sNK cells and anti-PD1 augmented IFN- γ secretion and NK cell-mediated cytotoxicity by immune cells of spleen, peripheral blood, and bone marrow of tumor bearing hu-BLT mice

We observed suppression of both secretion of IFN- γ (Figures 7E, G, H, S10A, S11A) and NK cell-mediated cytotoxicity (Figures 7F, S10B, S11B) in tumor-bearing hu-BLT mice in comparison to those from healthy mice. Restoration or increased IFN- γ secretion and NK cell-mediated cytotoxicity were seen in tumor-bearing mice injected with sNK cells alone or anti-PD1 alone, and both of these functions were further increased with the combination of sNK cells and anti-PD1 antibody injection in tumor bearing mice (Figures 7E–H, S9, S10). It is important to note that the levels of IFN- γ secretion were comparable between sNK cells treated mice and anti-PD-1 treated mice; however, the NK cell

mediated cytotoxicity was much higher in sNK treated tumor bearing mice than in the presence of anti-PD-1 treated tumor bearing mice (Figures 7E–H, S10, S11). The combination of both sNK and anti-PD-1 treatment significantly elevated IFN- γ secretion when compared to each treatment alone and increased cytotoxicity more than those seen in the presence of sNK treatment alone (Figures 7E–H, S10, S11). Taken together, these results indicated that sequential treatment of sNK cells with anti-PD-1 antibody is capable of increasing cytotoxic function in tumor-implanted hu-BLT mice and significantly augmented the secreted IFN- γ in immune cells from bone marrow, spleen and peripheral blood.

Discussion

NK cells are indispensable for the treatment of cancer due to their many important functions. We have come a long way in understanding the mechanisms underlying activation and increased function of NK cells, however, we still do not have a cure or even successful treatment for aggressive cancers. Most problems stem from not having the full understanding of NK function in cancer patients, and many underlying mechanisms of NK cell function still await clarifications. The mere fact that NK cells are specialized to target CSCs/poorly differentiated aggressive tumors, should place these cells at the top of any treatment strategies. Indeed, the function of NK cells found to be compromised in many if not all

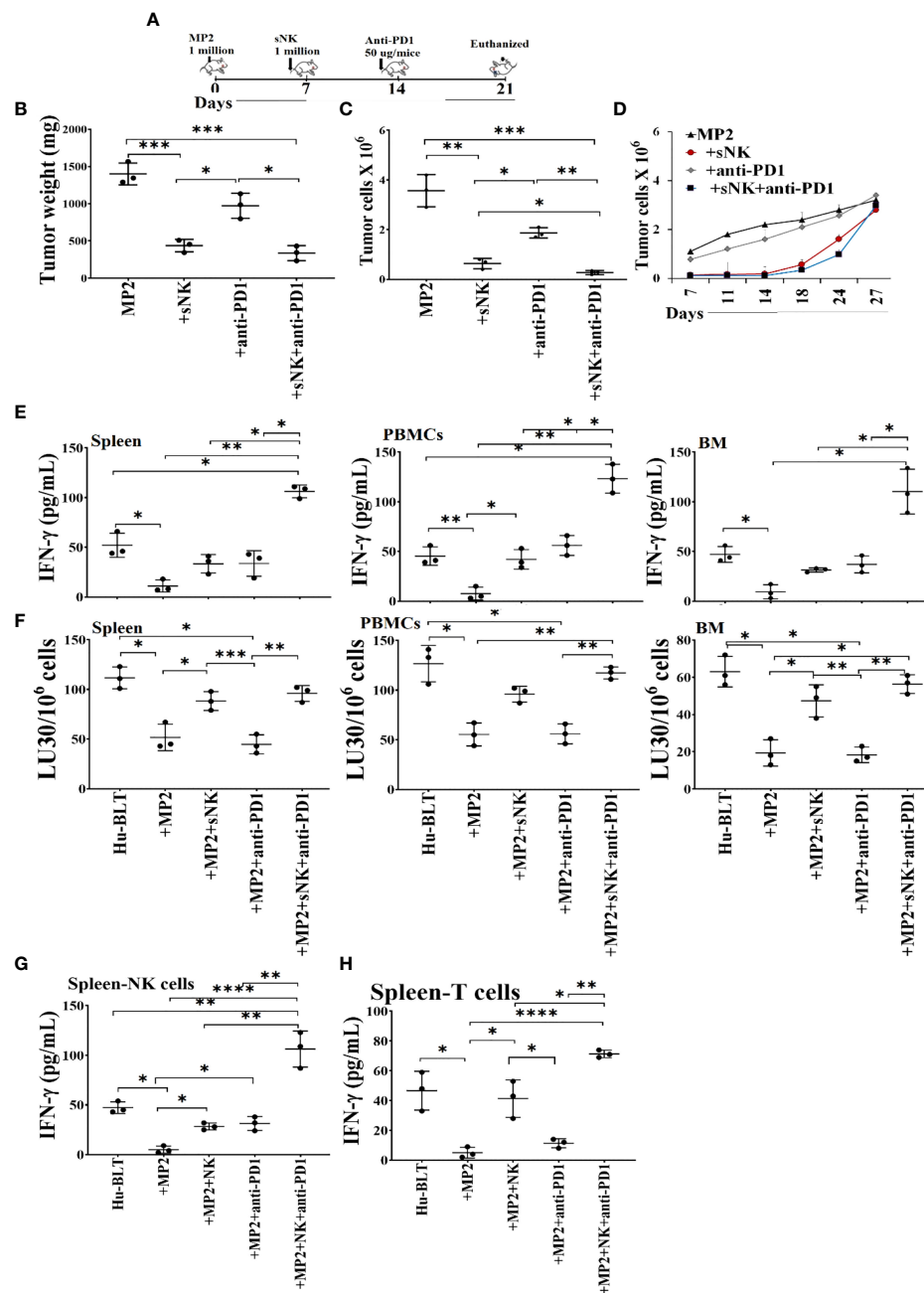


FIGURE 7

Combination of sNK cells and anti-PD1 antibody halted the growth of MP2 tumors, and increased IFN- γ secretion and cytotoxic function by PBMCs, splenocytes and bone marrow derived immune cells from hu-BLT mice. Hu-BLT mice were orthotopically injected with 1×10^6 human MP2 tumors in the pancreas. One week after the tumor implantation, mice received supercharged NK (sNK) cells *via* tail-vein injection, and one week after sNK cell injection, mice received anti-PD1 (50 μ g/mice) antibody *via* tail vein. The disease progression was monitored for another week (A). Hu-BLT mice were implanted with MP2 tumors and were injected with sNK cells and anti-PD1 antibody as depicted in Figure 7A. At the end of the experiment, hu-BLT mice were sacrificed and the tumors were harvested and weighed (n=3) (B). Hu-BLT mice were implanted with MP2 tumors and were injected with sNK cells and anti-PD1 antibody as depicted in Figure 7A. At the end of the experiment, hu-BLT mice were sacrificed and the tumors were harvested and single-cells were isolated as described in Materials and Methods section. Tumor cells were counted microscopically (n=3) (C). Hu-BLT derived tumors were cultured at 0.15×10^6 /ml at the initiation of the tumor cultures, and the cell growth were determined on the days shown in the Figure. Statistical analysis is shown for sNK or sNK+anti-PD1 antibody group vs. untreated group (n=3) (D). Hu-BLT mice were implanted with MP2 tumors and, were injected with sNK cells and anti-PD1 antibody as depicted in Figure 7A. At the end of the experiment, hu-BLT mice were sacrificed and the spleens, peripheral blood, and bone marrow were harvested, and single cell suspensions were prepared and cultured in the presence of IL-2 (1000 U/ml) for 7 days. On day 7, the supernatants were harvested and the secretion of IFN- γ was determined using single ELISA (n=3) (E). Splenocytes, and peripheral blood and bone marrow derived immune cells were cultured in the presence of IL-2 (1000 U/ml) for 7 days. On day 7, cells were used as effectors against OSCSCs using standard 4-hour ⁵¹Cr release assay. The Lytic units (LU) 30/10⁶ cells were determined using the inverse number of cells required to lyse 30% of OSCSCs x 100 (n=3) (F). NK (G) and CD3+ T (H) cells were purified from the spleen and cultured in the presence of IL-2 (1000 U/ml for NK cultures; and 100 U/ml for T cell cultures) for 7 days. On day 7, the supernatants were harvested and the secretion of IFN- γ was determined using single ELISA (n=3) (G, H). ****(p value < 0.0001), *** (p value 0.0001–0.001), ** (p value 0.001–0.01), * (p value 0.01–0.05).

cancer patients provide the rationale for the induction and progression of cancer since NK cells eliminate the clones that seed the cancer (28, 45, 46). In addition, loss of NK cell function at the preneoplastic stage of tumorigenesis before the establishment of pancreatic cancer is a testament to the crucial roles that NK cells play in suppression of cancer (47, 48). Moreover, NK cells differentiate tumors through the production of IFN- γ and TNF- α leading to decreased expansion and progression of cancer, in addition to the conditioning of T cells to target tumor cells. In this regard, sNK cells with exceptional expansion and functional capabilities, select CD8⁺ T cells and expand their numbers and function allowing the formation of memory/effector cells (45). Indeed, successful eradication of cancer is partly dependent on formation of tumor specific memory/effector CD8⁺ T cells, and tumors infiltrated by CD8⁺ T cells were shown to have a much better prognosis in patients (49). When comparing the function of primary IL-2 activated NK cells or IL-2+anti-CD16mAb or IL-2 +anti-CD16mAb+sAJ2 treated NK cells with sNK cells, many significant differences could be seen on genetic as well as protein and functional levels (Figure 1 and manuscript in prep) (28). Briefly, sNK cells are a unique population of NK cells with completely distinct profiles from those of untreated and IL-2 treated NK cells at the RNA seq analysis at the single cell level based on UMAP and regulon profiles, and in terms of cell cycle analysis, granule content and functional capabilities (Figure 2). When comparing to primary NK cells treated with different treatment strategies (Figure 1A) or those cultured with K562 or OSCSCs or MP2 or PBMCs (Figure S1), sNK cells proliferated up to 27–34 days, mediated much higher cytotoxicity and secreted much higher levels of IFN- γ whereas the primary NK cells after day 6 of culture lost their expansion capability and had minimal function (Figure 1). Having generated such a unique and potent population of NK cells, we aimed at understanding their effect in combination with other therapeutic modalities. Furthermore, by better understanding sNK cell function, we were able to establish combinatorial therapies to successfully treat cancer in hu-BLT mice. In this regard, we demonstrated two different treatments that can be combined with sNK cells not only restore or further activate the NK cells but also provide a strategy to augment the efficacy of the treatment with other treatment modalities to successfully eradicate all different subpopulations of tumor cells in the tumor microenvironment. In this case, we have previously shown that NK cell-differentiated tumors become susceptible to chemotherapeutic drugs (12). Indeed, treatment of tumor cells with supernatants from sNK cells not only increased the differentiation antigens such as MHC-class I, CD54, PDL-1 but it also curtailed their growth and made the tumors susceptible to chemotherapeutic drugs in *in vitro* experiments published previously and shown in here (12) (Figures 3, S3, S6). Furthermore, combining sNK cell treatment with chemotherapy drugs augmented the targetability of tumor cells by the chemotherapeutic drugs *in vivo*, as evidenced by the *in vitro* data. To validate our *in vitro* observations reported previously and in here, and to test the premise that sNK cells treated tumors become targetable by the chemotherapeutic drugs *in vivo*, we performed experiments in hu-BLT mice by first targeting and differentiating tumors with sNK cells (Figure 4) (12) followed by the

use of chemotherapy drugs to target the differentiated tumors. In this paper, we showed that one dose of 1×10^6 sNK cell injection not only kills but also differentiates tumors in tumor bearing hu-BLT mice, allowing chemotherapy drugs to target the remaining tumors, thereby decreasing the tumor load, and also augmenting the secretion of IFN- γ by the NK cells from humanized mice. Such combinatorial treatments will establish a circular pattern in which sNK cells will increase the effectiveness of chemotherapeutic drugs in targeting tumors but also the chemotherapy drugs will increase the function of sNK cells to target more tumors. Thus, these treatment strategies should be able to remove the heterogenous nature of tumor cells, allowing restoration of NK cell function in cancer patients to prevent cancer recurrences. When tumors were resected and single cells were prepared and cultured, tumors from OSCSC implanted mice grew and proliferated at a much higher rate than those cultured either from sNK injected or sNK+CDDP treated tumor implanted mice (Figure 4D). Tumor growth was much less in sNK and sNK+CDDP treated tumor implanted mice until day 24 after which they started to increase their growth potential and the growth rate became closer to the tumors resected from tumor alone implanted mice. Coincided with increase in tumor growth was the decrease in MHC-class I expression on the tumor cells since the differentiated tumors were not supplied by either sNK cells or their supernatants, therefore, the tumors reverted to the poorly differentiated/CSC stage at the end of cultures. The reversion could be due to de-differentiation of the tumors or selection of tumors with CSCs/poorly differentiated phenotype which has much lower MHC class I expression. Indeed, in our previous paper we established that all the tumors initially exhibited differentiated phenotype and later lost the differentiation antigens and became poorly differentiated tumors (12, 13). Thus, those results argued for the de-differentiation of tumors rather than selection (13). In addition, when day 10 tumor cultures were tested in cytotoxicity against fresh IL-2 activated primary NK cells, those that were obtained from tumor implanted and sNK or sNK+CDDP injected mice had much lower susceptibility to NK cell mediated cytotoxicity when compared to those cultured from tumor alone implanted mice, indicating the increased differentiation and acquisition of MHC-class I antigens in these cultures. Interestingly, in this assay we could see significant differences in the decreases of cytotoxicity between sNK and sNK +CDDP tumor cultures, indicating higher differentiation stage of sNK+CDDP tumor cultures as compared to sNK tumor cultures (Figure 4E) (13, 41–43). In agreement with our studies, previous work from other labs demonstrated cisplatin mediated up-regulation of NK cell cytotoxicity through suppression of AR, and upregulation of ULBP-2 in the HCC tumor model (50). In addition, Low-dose cisplatin administration prevented suppression of NK cell activity in patients with gastrointestinal cancer (51). Finally, the use of combination of cisplatin and natural killer cells overcame cisplatin resistance in ovarian cancer (52).

Check-point inhibitors such as anti-PD-1 and anti-PD-L1 are becoming standard of care for many cancers; however, even though they work for certain cancer types and in certain cancer patients, not all cancer patients benefit from such treatments. To increase the effectiveness of both NK cells and anti-PD-1 therapy we sequentially

we sequentially treated the tumor bearing hu-BLT mice with sNK cells and anti-PD-1 therapy and found such treatment to not only prevent and remove most of tumors from the mice but also it augmented the function of immune cells by increasing the secretion of IFN- γ when both treatments were used in mice. Indeed, anti-PD-1 treatment of NK cells in the presence of CSC/poorly differentiated tumors augmented the secretion of IFN- γ by the NK cells, indicating that NK cells are capable of activation through PD-1 surface receptors similar to those of T cells (Figures 6, 7G, S7). Indeed, sequential treatment of tumor bearing hu-BLT mice with sNK cells and anti-PD-1 antibody increased the release in IFN- γ by the immune effectors notably both the NK cells and T cells and halt the tumor growth and expansion (Figures 7G, H). Similar to the *in vivo* experiments with sNK+CDDP treatment, when tumors were resected from the sNK+anti-PD-1 treated mice, and single cells were prepared and cultured, tumors from MP2 implanted mice grew and proliferated at a much higher rate than those cultured either from sNK injected or sNK+anti-PD-1 treated and tumor implanted mice (Figure 7D). Tumor growth was much less in sNK and sNK+ anti-PD-1 treated and tumor implanted mice until day 18-24, after which they started to increase their growth potential and the growth rate became closer to the tumors resected from tumor alone implanted mice at day 27. Coinciding with the increase in tumor growth was the decrease in MHC-class I expression on the tumor cells since the differentiated tumors were not supplied by either sNK cells or their supernatants, therefore, the tumors reverted to the poorly differentiated/CSC stage at the end of the cultures. The reversion could be due to de-differentiation of the tumors or selection of tumors with poorly differentiated/CSC phenotype as stated above. In accordance with our studies, adoptive transfer of *ex vivo* IL-2-activated NK cells combined with anti-PD-1 resulted in tumor growth inhibition in a xenograft gastric cancer model (53). In another study, PD-1 and PD-L1 blockade induced a strong NK cell response that was found to be indispensable for the full therapeutic effect of immunotherapy (54). In addition, the authors showed that PD-1 was expressed on NK cells within transplantable, spontaneous, and genetically induced mouse tumor models. Furthermore, PD-1 expression was higher on NK cells with a more activated phenotype with no evidence of exhausted phenotype.

However, one has to take precaution in interpreting the *in vivo* data because the heterogeneity of tumor cells in terms of their differentiation stage may make the results very difficult to interpret. This could be one reason why certain cancer patients are able to benefit from the checkpoint inhibitors and yet others do not. For instance, the use of anti-PD-L1 antibody can have completely different effect on NK cells depending on the stage of differentiation of tumor cells, as seen in our study (Figure 5). If competent NK cells have infiltrated tumors with a higher fraction of CSCs/poorly differentiated tumors, they should be able to eliminate these tumors in direct cytotoxicity (Figure 5). In addition, higher expression of PD-L1 on tumor-activated NK cells may make NK cells themselves to become susceptible to ADCC, and decrease in the cytotoxic function of NK cells. On the other hand, if the tumor phenotype is tilted towards a well-differentiated phenotype, this may increase effectiveness of NK cells in mediating ADCC since tumor cells will be upregulating PD-L1 and becoming susceptible to NK cell-mediated ADCC effect, whereas such tumors are not, or are less

susceptible to direct cytotoxicity by the primary NK cells as seen in our studies (Figure 5). Therefore, when such therapies fail in patients, one has to not only understand the nature of NK cells but also what type of tumors NK cells are targeting.

Finally, in this paper we present two different combinatorial therapies that will likely be successful in patients. There are many others such as combination of NK cells with CD8+ T cells, NK cells with radiotherapy, NK cells with virotherapy, NK cells with bacterial therapy, etc. All of these different scenarios are under investigation in our laboratory and should provide exciting treatment strategies for cancer therapy in the future.

Materials and methods

Cell lines, reagents, and antibodies

Oral squamous carcinoma stem cells (OSCSCs) and oral squamous cell carcinoma (OSCCs) were isolated from patients with tongue tumors at UCLA (13, 42, 55). NK cells, OSCSCs, and OSCCs were cultured in RPMI 1640 (Invitrogen by Life Technologies, CA), supplemented with 10% fetal bovine serum (FBS) (Gemini Bio-Products, CA). Recombinant IL-2 was obtained from NIH-BRB. Antibodies to CD16 were purchased from Biolegend (San Diego, CA). Antibodies used for flow cytometry – IgG2, MHC-class I, and B7H1 (PD-L1) were purchased from Biolegend (San Diego, CA). MIA PaCA-2 (MP2), PL12, and Capan human pancreatic cancer cell lines were provided by Dr. Nicholas Cacalano (UCLA, School of Medicine, CA, USA), and were cultured in DMEM supplemented with 10% FBS. Cisplatin and Paclitaxel were purchased from Ronald Reagan Pharmacy at UCLA. ELISA kits for IFN- γ were purchased from Biolegend (San Diego, CA), and multiplex analysis kit was purchased from Millipore (Billerica, MA). Propidium iodide (PI) and chromium-51 was purchased from PeproTech (Cranbury, NJ, USA) and Perken Elmer (Waltham, MA, USA), respectively. Chromium Single cell 3' Reagent kit v3, Cat#1000075 was purchased from 10X Genomics (Pleasanton, CA, USA).

Purification of human NK cells and monocytes

Written informed consents, approved by UCLA Institutional Review Board (IRB), were obtained from healthy individuals, and all procedures were approved by the UCLA-IRB. Peripheral blood was separated using ficoll-hypaque centrifugation, after which the white layer, containing peripheral blood mononuclear cells (PBMCs) was harvested. NK cells and monocytes were negatively selected from PBMCs using the EasySep[®] Human NK cell enrichment and EasySep[®] Human monocytes enrichments kits, respectively, purchased from Stem Cell Technologies (Vancouver, BC, Canada). Purified NK cells and monocytes were stained with anti-CD16 and anti-CD14, respectively, to measure purity using flow cytometric analysis. Samples showing greater than 95% purity were used for the study.

NK cell supernatant collection and stem cell differentiation

Purified NK cells were activated with rh-IL-2 (1000 U/ml) and anti-CD16 mAb (3 µg/ml) for 18–20 hours before the supernatant was harvested, and was used in differentiation of OSCSCs, and MP2 cells. The supernatant volume was determined based on IFN-γ required, and was accessed by ELISA specific to IFN-γ. Differentiation of OSCSCs and MP2 cells were conducted with an average total amount of 2000 pg and 5000 pg, respectively, over the course of 5 days. On day 0, 1×10^6 tumor cells were cultured, on day 1 unattached tumor cells were removed and attached tumor cells were treated with NK cell supernatants on days 1, 2, 3 and 4. On day 5, tumor cells were rinsed with 1 X PBS, detached and used for experiments.

Generation of osteoclasts and supercharged NK cells

To generate osteoclasts (OCs), monocytes were cultured in alpha-MEM media supplemented with M-CSF (25 ng/mL) and RANKL (25 ng/mL) for 21 days, media was replenished every three days. Human purified NK cells were activated with rh-IL-2 (1000 U/ml) and anti-CD16 mAb (3 µg/ml) for 18–20 hours before they were co-cultured with OCs and sAJ2 (OCs : NK:sAJ2; 1:2:4) in RPMI 1640 medium containing 10% FBS. Probiotic bacteria, AJ2 is a combination of seven to eight different strains of gram-positive probiotic bacteria (*Streptococcus thermophiles*, *Bifidobacterium longum*, *Bifidobacterium breve*, *Bifidobacterium infantis*, *Lactobacillus acidophilus*, *Lactobacillus plantarum*, *Lactobacillus casei*, and *Lactobacillus bulgaricus*) selected for their superior ability to induce optimal secretion of both pro-inflammatory and anti-inflammatory cytokines in NK cells (32). The medium was refreshed every three days with RPMI containing rh-IL-2 (1500 U/ml).

Western blot analysis

Cells were washed twice with an ice-cold PBS and lysed in NP-40 lysis buffer supplemented with protease inhibitor cocktail (APEX-BIO). Lysates were centrifuged at 16000g at 4°C for 20 minutes to obtain post-nuclear cell fraction. Protein concentration was determined with Pierce BCA protein assay kit (ThermoFisher Scientific). Non-reducing SDS-PAGE was performed, and separated proteins were transferred to nitrocellulose membrane. Membranes were blocked for 1 hour in 5% non-fat dry milk in PBS. Membranes were incubated in primary antibodies overnight at 4°C and HRP conjugated secondary antibodies for 1h at room temperature. Bands were visualized with Clarity Max Western ECL substrate (BioRad). Images were acquired with ChemiDoc ML imaging System (Biorad). The following primary antibodies were used: mouse anti-granzyme B (sc-8022, Santa Cruz Biotechnology), mouse anti-cathepsin C (sc-74590, Santa Cruz Biotechnology), mouse anti-perforin-1 (sc-136994, Santa Cruz Biotechnology). We used anti-mouse HRP conjugated secondary antibodies (405306 BioLegend). Stain free technology (BioRad) was used for loading control.

Single-cell RNA sequencing

Single-cell RNA sequencing was performed using a 10X Chromium machine. Single-cell cDNA libraries were prepared using the 10X Chromium Single cell 3' Reagent kit v3 and sequenced via Illumina Novaseq 6000 (Illumina) to a depth of around 30 thousand reads per cell. Raw data from each sample were demultiplexed and aligned to a custom reference genome (GRCh38), and UMI counts were quantified using 10X Genomics CellRanger software (v3.0.0) with default parameters. Single-cell clustering and cell-cycle scoring are performed using the Seurat package (v3.0). Single-cell regulatory network inference and clustering (SCENIC) is done by using the SCENIC R package (1.2.0) with the hg38 database (<https://resources.aertslab.org/cistarget/>).

Tumor implantation in hu-BLT mice

Animal research was performed under the written approval of the UCLA Animal Research Committee (ARC) in accordance with all federal, state, and local guidelines. Combined immunodeficient NOD.CB17-Prkdcscid/J and NOD.Cg-Prkdcscid Il2rgtm1Wjl/SzJ (NSG lacking T, B, and NK cells) were purchased from Jackson Laboratory. Humanized-BLT (hu-BLT; human bone marrow/liver/thymus) mice were prepared on NSG background as previously described (38, 56). To establish orthotopic tumors, mice were first anesthetized with isoflurane in combination with oxygen, and 1×10^6 human OSCSCs and MP2 tumor cells suspended in 10 µl HC Matrigel were then injected directly into the floor of their mouths and pancreas, respectively. One week after tumor implantation mice received 1×10^6 OC-expanded supercharged NK cells via tail vein injection. One week after NK injections, mice received CDDP (50 µg/mice) or anti-PD1 (50 µg/mice) via tail vein injection. One week later, mice were euthanized, and tumors, bone marrow, spleen, and peripheral blood were harvested.

Cell isolation and cell cultures of tumors and immune cells of hu-BLT mice

The oral and pancreatic tumors harvested from hu-BLT mice were immediately cut into 1 mm³ pieces and placed into a digestion buffer containing 1 mg/ml collagenase II (oral tumor) or collagenase IV (pancreatic tumor), 10 U/ml DNase I, and 1% bovine serum albumin (BSA) in DMEM media, and incubated for 20 minutes at 37°C oven on a 150 rpm shaker. After digestion, the sample were filtered through 40 µm cell strainer and centrifuged at 1500 rpm for 10 minutes at 4°C. The pellet was re-suspended in DMEM media and cells were counted. To obtain single-cell suspensions from BM, femurs were cut at both ends and flushed by using RPMI 1640 media; afterwards, BM cells were filtered through a 40 µm cell strainer. To obtain single-cell suspensions from spleen, the spleens were minced, and the samples were filtered through a 40 µm cell strainer and centrifuged at 1500 rpm for 5 minutes at 4°C. The pellets were re-suspended in ACK buffer for 2–5 mins to remove the red blood cells followed by re-suspension in RPMI media and centrifugation at 1500 rpm for 5 minutes at 4°C. PBMCs

were isolated from peripheral blood using Ficoll-Hypaque centrifugation of heparinized blood specimens. The buffy coats containing PBMCs were harvested, washed, and re-suspended in RPMI 1640 medium. Cells obtained from each tissue sample were treated with IL-2 (1000 U/ml) and cultured in RPMI 1640 medium containing 10% FBS for 7 days.

Surface staining and cell death analysis

Staining was performed by labeling the cells with antibodies as described previously (43, 57, 58). The percentage of dead cells was determined by propidium iodine (PI) (100 µg/ml) staining using flow cytometric analysis. Flow cytometric analysis was performed using Attune NxT flow cytometer (Thermo Fisher Scientific, Waltham, MA) and FlowJo v10.4 (BD, Oregon, USA) were used for analysis. For selected experiments Beckman Coulter Epics XL cytometer (Brea, CA) was also used, and the results were analyzed in the FlowJo vX software (Ashland, OR).

Enzyme-linked immunosorbent assays and multiplex cytokine assay

Single ELISAs were performed as previously described (43). To analyze and obtain the cytokine and chemokine concentration, a standard curve was generated by either two- or three-fold dilutions of recombinant cytokines provided by the manufacturer. For multiple cytokine array, the levels of cytokines were determined by multiplex assay, which was conducted as described in the manufacturer's protocol for each specified kit. Analysis was performed using a Luminex multiplex instrument (MAGPIX, Millipore, Billerica, MA), and data was analyzed using the proprietary software (xPONENT 4.2, Millipore, Billerica, MA).

⁵¹Cr release cytotoxicity assay

The ⁵¹Cr release cytotoxicity assay was performed as previously described (59). Briefly, different ratios of effectors and ⁵¹Cr-labeled target cells were incubated for four hours. After which, the supernatants were harvested from each sample, and the released radioactivity was counted using the gamma counter. The percentage specific cytotoxicity was calculated as follows:

$$\% \text{cytotoxicity} = \frac{\text{Experimental cpm} - \text{spontaneous cpm}}{\text{Total cpm} - \text{spontaneous cpm}}$$

LU 30/10⁶ was calculated by using the inverse of the number of effector cells needed to lyse 30% of target cells × 100.

Statistical analyses

Prism-9 software was used for statistical analysis. An unpaired or paired, two-tailed Student's t-test was performed for experiments with two groups. One-way ANOVA with a Bonferroni post-test was used to compare different groups for experiments with more than two

groups. Duplicate or triplicate samples were used for assessment. The following symbols represent the levels of statistical significance within each analysis: ****(p value < 0.0001), *** (p value 0.0001–0.001), ** (p value 0.001–0.01), * (p value 0.01–0.05).

Data availability statement

The data presented in the study are deposited in the NCBI GEO repository, accession number GSE226160.

Ethics statement

The studies involving human participants were reviewed and approved by UCLA Institutional Review Board (IRB). The patients/participants provided their written informed consent to participate in this study. The animal study was reviewed and approved by UCLA Animal Research Committee (ARC).

Author contributions

KK generated and analyzed data, wrote, reviewed and edited the manuscript. P-CC, M-WK, AM, ES generated supporting data and edited manuscript. SM, JK reviewed and edited manuscript. AJ oversaw the studies, conceptualization of the report, reviewed and edited the report, and acquired funding. All authors contributed to the article and approved the submitted version.

Funding

This research was funded by the Slovenian Research Agency, grant numbers P4-0127, J4-1776 to JK.

Conflict of interest

The authors declare that the research was conducted in the absence of any commercial or financial relationships that could be construed as a potential conflict of interest.

Publisher's note

All claims expressed in this article are solely those of the authors and do not necessarily represent those of their affiliated organizations, or those of the publisher, the editors and the reviewers. Any product that may be evaluated in this article, or claim that may be made by its manufacturer, is not guaranteed or endorsed by the publisher.

Supplementary material

The Supplementary Material for this article can be found online at: <https://www.frontiersin.org/articles/10.3389/fimmu.2023.1132807/full#supplementary-material>

References

- Fitzmaurice C, Allen C, Barber RM, Barregard L, Bhutta ZA, Brenner H, et al. Global, regional, and national cancer incidence, mortality, years of life lost, years lived with disability, and disability-adjusted life-years for 32 cancer groups, 1990 to 2015: A systematic analysis for the global burden of disease study. *JAMA Oncol* (2017) 3(4):524–48. doi: 10.1001/jamaoncol.2016.5688
- Lo Russo G, Imbimbo M, Garassino MC. Is the chemotherapy era in advanced non-small cell lung cancer really over? maybe not yet. *Tumori* (2016) 2016(3):223–5. doi: 10.5301/tj.5000479
- Maroof H, Hassan ZM, Mobarez AM, Mohamadabadi MA. Lactobacillus acidophilus could modulate the immune response against breast cancer in murine model. *J Clin Immunol* (2012) 32(6):1353–9. doi: 10.1007/s10875-012-9708-x
- Hassan Z. Anti-cancer and biotherapeutic potentials of probiotic bacteria. *J Cancer Sci Ther* (2019) 11:009–13. doi: 10.4172/1948-5956.1000575
- Górska A, Przysupski D, Niemczura MJ, Kulbacka J. Probiotic bacteria: A promising tool in cancer prevention and therapy. *Curr Microbiol* (2019) 76(8):939–49. doi: 10.1007/s00284-019-01679-8
- Liu E, Marin D, Banerjee P, Macapinlac HA, Thompson P, Basar R, et al. Use of CAR-transduced natural killer cells in CD19-positive lymphoid tumors. *N Engl J Med* (2020) 382(6):545–53. doi: 10.1056/NEJMoa1910607
- Terranova-Barberio M, Pawlowska N, Dhawan M, Moasser M, Chien AJ, Melisko ME, et al. Exhausted T cell signature predicts immunotherapy response in ER-positive breast cancer. *Nat Commun* (2020) 11(1):3584. doi: 10.1038/s41467-020-17414-y
- Chen EX, Jonker DJ, Loree JM, Kennecke HF, Berry SR, Couture F, et al. Effect of combined immune checkpoint inhibition vs best supportive care alone in patients with advanced colorectal cancer: The Canadian cancer trials group CO.26 study. *JAMA Oncol* (2020) 6(6):831–8. doi: 10.1001/jamaoncol.2020.0910
- Rosenberg SA, Restifo NP. Adoptive cell transfer as personalized immunotherapy for human cancer. *Sci (New York N.Y.)* (2015) 348(6230):62–8. doi: 10.1126/science.aaa4967
- Sharma P, Allison JP. The future of immune checkpoint therapy. *Science* (2015) 348(6230):56–61. doi: 10.1126/science.aaa8172
- Emens LA, Jonker DJ, Loree JM, Kennecke HF, Berry SR, Couture F, et al. Cancer immunotherapy: Opportunities and challenges in the rapidly evolving clinical landscape. *Eur J Cancer* (2017) 81:116–29. doi: 10.1016/j.ejca.2017.01.035
- Kozłowska AK, Topchyan P, Kaur K, Tseng HC, Teruel A, Hiraga T, et al. Differentiation by NK cells is a prerequisite for effective targeting of cancer stem cells; poorly differentiated tumors by chemopreventive and chemotherapeutic drugs. *J Cancer* (2017) 8(4):537–54. doi: 10.7150/jca.15989
- Tseng HC, Arasteh A, Paranjpe A, Teruel A, Yang W, Behel A, et al. Increased lysis of stem cells but not their differentiated cells by natural killer cells; de-differentiation or reprogramming activates NK cells. *PLoS One* (2010) 5(7):e11590. doi: 10.1371/journal.pone.0011590
- Ko M-W, Breznik B, Senjor E, Jewett A. Synthetic cannabinoid WIN 55,212–2 inhibits growth and induces cell death of oral and pancreatic stem-like/poorly differentiated tumor cells. *Adv Cancer Biol - Metastasis* (2022) 5:100043. doi: 10.1016/j.adcanc.2022.100043
- Rycak K, Tang DG. Cancer stem cells and radioresistance. *Int J Radiat Biol* (2014) 90(8):615–21. doi: 10.3109/09553002.2014.892227
- Chang JC. Cancer stem cells: Role in tumor growth, recurrence, metastasis, and treatment resistance. *Medicine* (2016) 95(1 Suppl 1):S20–S25. doi: 10.1097/MD.00000000000004766
- Steinbichler TB, Dudás J, Skvortsov S, Ganswindt U, Riechelmann H, Skvortsova II, et al. Therapy resistance mediated by cancer stem cells. *Semin Cancer Biol* (2018) 53:156–67. doi: 10.1016/j.semcancer.2018.11.006
- Prieto-Vila M, Takahashi RU, Usuba W, Kohama I, Ochiya T. Drug resistance driven by cancer stem cells and their niche. *Int J Mol Sci* (2017) 18(12):2574. doi: 10.3390/ijms18122574
- Kaur K, Topchyan P, Kozłowska AK, Ohanian N, Chiang J, Maung PO, et al. Super-charged NK cells inhibit growth and progression of stem-like/poorly differentiated oral tumors in vivo in humanized BLT mice; effect on tumor differentiation and response to chemotherapeutic drugs. *Oncoimmunology* (2018) 7(5):e1426518. doi: 10.1080/2162402X.2018.1426518
- Kaur K, Safaie T, Ko MW, Wang Y, Jewett A. ADCC against MICA/B is mediated against differentiated oral and pancreatic and not stem-like/poorly differentiated tumors by the NK cells; loss in cancer patients due to down-modulation of CD16 receptor. *Cancers (Basel)* (2021) 13(2):239. doi: 10.3390/cancers13020239
- Pan K, Farrukh H, Chittepudi VCSR, Xu H, Pan C-x, Zhu Z. CAR race to cancer immunotherapy: from CAR T, CAR NK to CAR macrophage therapy. *J Exp Clin Cancer Res* (2022) 41(1):119. doi: 10.1186/s13046-022-02327-z
- Ciurea SO, Schafer JR, Bassett R, Denman CJ, Cao K, Willis D, et al. Phase I clinical trial using mBIL21 ex vivo-expanded donor-derived NK cells after haploidentical transplantation. *Blood* (2017) 130(16):1857–68. doi: 10.1182/blood-2017-05-785659
- Hallner A, Bernson E, Hussein BA, Ewald Sander F, Brune M, Aurelius J, et al. The HLA-b -21 dimorphism impacts on NK cell education and clinical outcome of immunotherapy in acute myeloid leukemia. *Blood* (2019) 133(13):1479–88. doi: 10.1182/blood-2018-09-874990
- Björklund AT, Carlsten M, Sohlberg E, Liu LL, Clancy T, Karimi M, et al. Complete remission with reduction of high-risk clones following haploidentical NK-cell therapy against MDS and AML. *Clin Cancer Res* (2018) 24(8):1834–44. doi: 10.1158/1078-0432.CCR-17-3196
- Ishikawa T, Okayama T, Sakamoto N, Ideno M, Oka K, Enoki T, et al. Phase I clinical trial of adoptive transfer of expanded natural killer cells in combination with IgG1 antibody in patients with gastric or colorectal cancer. *Int J Cancer* (2018) 142(12):2599–609. doi: 10.1002/ijc.31285
- Cichocki F, Bjordahl R, Gaidarova S, Mahmood S, Abujarour R, Wang H, et al. iPSC-derived NK cells maintain high cytotoxicity and enhance in vivo tumor control in concert with T cells and anti-PD-1 therapy. *Sci Transl Med* (2020) 12(568):568. doi: 10.1126/scitranslmed.aaz5618
- Geary CD, Krishna C, Lau CM, Adams NM, Gearty SV, Pritykin Y, et al. Non-redundant ISGF3 components promote NK cell survival in an auto-regulatory manner during viral infection. *Cell Rep* (2018) 24(8):1949–1957 e6. doi: 10.1016/j.celrep.2018.07.060
- Kaur K, Cook J, Park SH, Topchyan P, Kozłowska A, Ohanian N, et al. Novel strategy to expand super-charged NK cells with significant potential to lyse and differentiate cancer stem cells: Differences in NK expansion and function between healthy and cancer patients. *Front Immunol* (2017) 8:297. doi: 10.3389/fimmu.2017.00297
- Nandi M, Pal S, Ghosh S, Chakraborty BC, Dey D, Baidya A, et al. CD8(+)/CD28(-) T cells: key cytotoxic players impacting disease pathogenesis in chronic HBV infection. *Clin Sci (Lond)* (2019) 133(17):1917–34. doi: 10.1042/CS20190369
- Benson DM Jr, Bakan CE, Mishra A, Hofmeister CC, Efebera Y, Becknell B, et al. The PD-1/PD-L1 axis modulates the natural killer cell versus multiple myeloma effect: a therapeutic target for CT-011, a novel monoclonal anti-PD-1 antibody. *Blood* (2010) 116(13):2286–94. doi: 10.1182/blood-2010-02-271874
- Tseng HC, Kanayama K, Kaur K, Park SH, Park S, Kozłowska A, et al. Bisphosphonate-induced differential modulation of immune cell function in gingiva and bone marrow in vivo: Role in osteoclast-mediated NK cell activation. *Oncotarget* (2015) 6(24):20002–25. doi: 10.18632/oncotarget.4755
- Bui VT, Tseng HC, Kozłowska A, Maung PO, Kaur K, Topchyan P, et al. Augmented IFN-gamma and TNF-alpha induced by probiotic bacteria in NK cells mediate differentiation of stem-like tumors leading to inhibition of tumor growth and reduction in inflammatory cytokine release; regulation by IL-10. *Front Immunol* (2015) 6:576. doi: 10.3389/fimmu.2015.00576
- Yang C, Siebert JR, Burns R, Gerbec ZJ, Bonacci B, Rymaszewski A, et al. Heterogeneity of human bone marrow and blood natural killer cells defined by single-cell transcriptome. *Nat Commun* (2019) 10(1):3931. doi: 10.1038/s41467-019-11947-7
- Duncan GS, Mittrucker HW, Kagi D, Matsuyama T, Mak TW. The transcription factor interferon regulatory factor-1 is essential for natural killer cell function in vivo. *J Exp Med* (1996) 184(5):2043–8. doi: 10.1084/jem.184.5.2043
- Gotthardt D, Sexl V. STATs in NK-cells: The good, the bad, and the ugly. *Front Immunol* (2016) 7:694. doi: 10.3389/fimmu.2016.00694
- Ni J, Wang X, Stojanovic A, Zhang Q, Wincher M, Buhler L, et al. Single-cell RNA sequencing of tumor-infiltrating NK cells reveals that inhibition of transcription factor HIF-1alpha unleashes NK cell activity. *Immunity* (2020) 52(6):1075–1087 e8. doi: 10.1016/j.immuni.2020.05.001
- Aibar S, Gonzalez-Blas CB, Moerman T, Huynh-Thu VA, Imrichova H, Hulselman G, et al. SCENIC: single-cell regulatory network inference and clustering. *Nat Methods* (2017) 14(11):1083–6. doi: 10.1038/nmeth.4463
- Shimizu S, Hong P, Arumugam B, Pokomo L, Boyer J, Koizumi N, et al. A highly efficient short hairpin RNA potentially down-regulates CCR5 expression in systemic lymphoid organs in the hu-BLT mouse model. *Blood* (2010) 115(8):1534–44. doi: 10.1182/blood-2009-04-215855
- Vatakis DN, Bristol GC, Kim SG, Levin B, Liu W, Radu CG, et al. Using the BLT humanized mouse as a stem cell based gene therapy tumor model. *J Vis Exp* (2012) 70:e4181. doi: 10.3791/4181
- Kozłowska AK, Kaur K, Topchyan P, Jewett A. Adoptive transfer of osteoclast-expanded natural killer cells for immunotherapy targeting cancer stem-like cells in humanized mice. *Cancer Immunology Immunotherapy* (2016) 65(7):835–45. doi: 10.1007/s00262-016-1822-9
- Jewett A, Man Y-G, Tseng H-C. Dual functions of natural killer cells in selection and differentiation of stem cells; role in regulation of inflammation and regeneration of tissues. *J Cancer* (2013) 4(1):12–24. doi: 10.7150/jca.5519
- Tseng HC, Bui V, Man YG, Cacalano N, Jewett A. Induction of split anergy conditions natural killer cells to promote differentiation of stem cells through cell-cell contact and secreted factors. *Front Immunol* (2014) 5:269. doi: 10.3389/fimmu.2014.00269
- Jewett A, Bonavida B. Target-induced inactivation and cell death by apoptosis in a subset of human NK cells. *J Immunol* (1996) 156(3):907–15. doi: 10.4049/jimmunol.156.3.907
- Tseng H. C., Cacalano A., Jewett A. A. Tseng, H.C., N. Cacalano, and A. Jewett. Split anergized Natural Killer cells halt inflammation by inducing stem cell

differentiation, resistance to NK cell cytotoxicity and prevention of cytokine and chemokine secretion. *Oncotarget* (2015) 6(11):58947–59. doi: 10.18632/oncotarget.3250

45. Kaur K, Ko MW, Ohanian N, Cook J, Jewett A. Osteoclast-expanded supercharged NK-cells preferentially select and expand CD8+ T cells. *Sci Rep* (2020) 10(1):20363. doi: 10.1038/s41598-020-76702-1

46. Kaur K, Ko MW, Chen F, Jewett A. Defective NK cell expansion, cytotoxicity, and lack of ability to differentiate tumors from a pancreatic cancer patient in a long term follow-up: implication in the progression of cancer. *Cancer Immunol Immunother* (2022) 71(5):1033–47. doi: 10.1007/s00262-021-03044-w

47. Kaur K, Chang HH, Topchyan P, Cook JM, Barkhordarian A, Eibl G, et al. Deficiencies in natural killer cell numbers, expansion, and function at the pre-neoplastic stage of pancreatic cancer by KRAS mutation in the pancreas of obese mice. *Front Immunol* (2018) 9:1229. doi: 10.3389/fimmu.2018.01229

48. Kaur K, Chang HH, Cook J, Eibl G, Jewett A. Suppression of gingival NK cells in precancerous and cancerous stages of pancreatic cancer in KC and BLT-humanized mice. *Front Immunol* (2017) 8:1606. doi: 10.3389/fimmu.2017.01606

49. van der Leun AM, Thommen DS, Schumacher TN. CD8(+) T cell states in human cancer: insights from single-cell analysis. *Nat Rev Cancer* (2020) 20(4):218–32. doi: 10.1038/s41568-019-0235-4

50. Shi L, Lin H, Li G, Sun Y, Shen J, Xu J, et al. Cisplatin enhances NK cells immunotherapy efficacy to suppress HCC progression via altering the androgen receptor (AR)-ULBP2 signals. *Cancer Lett* (2016) 373(1):45–56. doi: 10.1016/j.canlet.2016.01.017

51. Ishikawa K, Shimoda K, Shiraishi N, Adachi Y, Kitano S. Low-dose cisplatin-5-fluorouracil prevents postoperative suppression of natural killer cell activity in patients with gastrointestinal cancer. *Jpn J Clin Oncol* (1998) 28(6):374–7. doi: 10.1093/jjco/28.6.374

52. Choi SH, Jung D, Kim KY, An HJ, Park KS. Combined use of cisplatin plus natural killer cells overcomes immunoresistance of cisplatin resistant ovarian cancer. *Biochem Biophys Res Commun* (2021) 563:40–6. doi: 10.1016/j.bbrc.2021.05.066

53. Abdolahi S, Ghazvinian Z, Muhammadnejad S, Ahmadvand M, Aghdaei HA, Ebrahimi-Barough S, et al. Adaptive NK cell therapy modulated by anti-PD-1 antibody in gastric cancer model. *Front Pharmacol* (2021) 12:733075. doi: 10.3389/fphar.2021.733075

54. Hsu J, Hodgins JJ, Marathe M, Nicolai CJ, Bourgeois-Daigneault MC, Trevino TN, et al. Contribution of NK cells to immunotherapy mediated by PD-1/PD-L1 blockade. *J Clin Invest* (2018) 128(10):4654–68. doi: 10.1172/JCI99317

55. Tseng HC, Inagaki A, Bui VT, Cacalano N, Kasahara N, Man YG, et al. Differential targeting of stem cells and differentiated glioblastomas by NK cells. *J Cancer* (2015) 6(9):866–76. doi: 10.7150/jca.11527

56. Vatakis DN, Koya RC, Nixon CC, Wei L, Kim SG, Avancena P, et al. Antitumor activity from antigen-specific CD8 T cells generated in vivo from genetically engineered human hematopoietic stem cells. *Proc Natl Acad Sci U.S.A.* (2011) 108(51):E1408–16. doi: 10.1073/pnas.1115050108

57. Jewett A, Cavalcanti M, Bonavida B. Pivotal role of endogenous TNF-alpha in the induction of functional inactivation and apoptosis in NK cells. *J Immunol* (1997) 159(10):4815–22. doi: 10.4049/jimmunol.159.10.4815

58. Jewett A, Bonavida B. Interferon-alpha activates cytotoxic function but inhibits interleukin-2-mediated proliferation and tumor necrosis factor-alpha secretion by immature human natural killer cells. *J Clin Immunol* (1995) 15(1):35–44. doi: 10.1007/BF01489488

59. Jewett A, Wang MY, Teruel A, Poupak Z, Bostanian Z, Park NH. Cytokine dependent inverse regulation of CD54 (ICAM1) and major histocompatibility complex class I antigens by nuclear factor kappaB in HEp2 tumor cell line: effect on the function of natural killer cells. *Hum Immunol* (2003) 64(5):505–20. doi: 10.1016/S0198-8859(03)00039-9

Frontiers in Immunology

Explores novel approaches and diagnoses to treat immune disorders.

The official journal of the International Union of Immunological Societies (IUIS) and the most cited in its field, leading the way for research across basic, translational and clinical immunology.

Discover the latest Research Topics

[See more →](#)

Frontiers

Avenue du Tribunal-Fédéral 34
1005 Lausanne, Switzerland
frontiersin.org

Contact us

+41 (0)21 510 17 00
frontiersin.org/about/contact

